THE UNIVERSITY OF CALGARY

Investigations into μ-hydrido bridged carbocations

by

Christoph Taeschler

A DISSERTATION
SUBMITTED TO THE FACULTY OF GRADUATE STUDIES
IN PARTIAL FULFILLMENT OF THE REQUIREMENTS FOR THE
DEGREE OF DOCTOR OF PHILOSOPHY

DEPARTMENT OF CHEMISTRY

CALGARY, ALBERTA
JUNE 1999

Abstract

This Dissertation describes experimental and theoretical aspects of μ-hydrido bridged carbocations, focusing on the bicyclo[3.3.3]undecyl and tricyclo[5.3.1.$1^{3,9}$]dodecyl systems. Also described are results involving the classical mono and dications of these systems.

An analysis of approaches to the synthesis of a μ-H bridged bicyclo[3.3.3]undecyl cation showed that the most promising way would be to generate the dication and to introduce a hydride between the two cation centers. This process could be done via an external hydride delivery or via internal hydride delivery.

Precursors needed for the external hydride delivery involved a twelve step synthesis in the bicyclic system and an eight step synthesis for the tricyclic system. Many of the intermediates were already known; however, most of the steps have been modified.

The bicyclo[3.3.3]undeca-1,5-diyl and tricyclo[5.3.1.$1^{3,9}$]dodeca-5,9-diyl dications were prepared from their dichloride precursors and the NMR spectra were compared with high level *ab initio* calculations.

Preparation of the bicyclic and tricyclic dications led to the discovery of three different rearrangement reactions. The bicyclo[3.3.3]undeca-1,5-diyl dication was found to rearrange into the 2,7-dimethylbicyclo[3.3.1]nona-2,7-diyl and then into the 3,7-dimethylbicyclo[3.3.1]nona-3,7-diyl dication with associated energy barriers of 16.0 and 17.4 kcal/mol; the tricyclo[5.3.1.$1^{3,9}$]dodec-5-yl cation rearranged into the 2-ethyl-2-adamantyl cation with a barrier of 16.0 kcal/mol, and the 9-ethylbicyclo[3.3.1]non-9-yl cation into the 5-ethylbicyclo[4.3.0]undec-1-yl cation and then into the 2-methyl-2-decalyl cation with barriers of 12.2 and 15.4 kcal/mol.

The reduction of the bicyclic and tricyclic dications with hydride donors such as isopentane, sodium borohydride or hydrogen gas was unsuccessful and resulted in the formation of the classical monocations.

The internal hydride delivery was first attempted on the 3-methoxy substituted bicyclo[3.3.3]undecyl system, and the fourteen step synthesis leading to the dihydroxy derivative was unsuccessful at the last step.

The synthesis of an isobutyl substituted tricyclo[5.3.1.$1^{3,9}$]dodecane as a precursor for

internal hydride delivery was completed to the tricyclo[5.3.1.$1^{3,9}$]dodecan-7-ol stage, but was stopped due to the results of *ab initio* calculations, which predicted the internal hydride shift to possess an energy barrier of 75.5 kcal/mol.

Acknowledgments

First, I wish to express my sincerest gratitude to my supervisor Dr. T. S. Sorensen for his guidance and patience, and especially for allowing me to pursue my own ideas to a large extent.

I am grateful to Dr. R. Yamdagni, Dr. Q. Wu and Ms. D. Fox for their technical assistance, to Dr. A. Rauk for providing computer capacity, Dr. S. Wolff and Dr. S. Patchkovskii for their help with compiling Gaussian 94 and Gaussian 98, Mr. M. Toonen for manufacturing sophisticated glass apparatus, Dr. Parvez for solving the x-ray crystal structure presented in this Dissertation and to Ms. G. Prihodko for her administrative guidance.

I wish to express my thanks to the past and present members of the Sorensen lab group, Dr. F. Sun, Dr. D. Simion, Mr. G. Carelse, Mr. B. Surridge, Mr. B. Watson, Mr. J. Willson, and Mr. T. Vickers for making the work in our lab a pleasant experience.

I also thank my friends Dan Wehrli, Tina Böck, Marco Passafaro, Irene Passafaro, Brian Dyck, Pat Gladstone, Grant Carelse, Blair Surridge, Steve Wolff, Colette Sims, Brian Hausermann, Dani Hausermann, Ian Hunt, Vivian Mozol, Katsumasa Nakajima, Suanne Nakajima, Kazik Minksztym, Gabriel Sung, Jerry Taylor, Ziad Moussa, Joey Payne, Denise Baron, Neil Andersen, Brian Keay, Lou Somlai, Katrin Köhler, Larry Lee, Preston Chase, Lisa Knight, Kathleen Tremblay, James Blackwell, Sue , Craig Mckinnon, Kevin Cook and Bryon Carpenter, for their encouragement and fruitful discussions.

Finally, I would like to acknowledge the Department of Chemistry for financial support.

für meine Eltern

Marie-Theres Taeschler-Gemperle

Marcel Taeschler

Table of Contents

List of Tables

List of Figures

List of Abbreviations

Å	Angstrom
AIBN	2,2'-azobis(2-methylpropionitrile)
B3LYP	Becke's three parameter functional, where the non-local correlation is provided by the correlation functional of Lee, Yang and Parr.
bp.	boiling point
br	broad
°C	degrees Celsius
calc.	calculated
cm^{-1}	reciprocal centimetres-wavenumbers
^{13}C NMR	carbon-13 nuclear magnetic resonance
COSY	H-H two dimensional correlation NMR spectroscopy
d	doublet
DBU	1,8-diazabicyclo[5.4.0]undec-7-ene
dd	doublet of doublets
ddd	doublet of doublet of doublets
dddd	doublet of doublet of doublet of doublets
DMF	N,N-dimethylformamide
DMSO	dimethylsulfoxide
dt	doublet of triplets
Et	ethyl
exp.	experimental
g	grams
GC	gas chromatography
h	hours
$H^{\cdot}$	proton
HETCOR	heteronuclear two dimensional correlation NMR spectroscopy
^{1}H NMR	hydrogen nuclear magnetic resonance

hv	light
High res. MS	high resolution mass spectrum
Hz	Hertz
IR	infrared spectroscopy
i	iso
imag.	imaginary
J	Joules
J	coupling constant
k	kilo
LDA	lithium diisopropylamide
lit.	literature
M	molar
m	multiplet
$M^{\cdot}$	molecular ion
m/z	mass to charge ratio
Me	methyl
*m*CPBA	*m*-chloroperoxybenzoic acid
MP2	second order Møller-Plesset perturbation method
mg	milligrams
MHz	mega Hertz
min.	minutes
mL	millilitres
µL	microlitres
mmol	millimoles
mol	moles
mp.	melting point
MS	mass spectrometry
NBS	N-bromosuccinimide
Nu:	nucleophile

Ph	phenyl
ppm	parts per million
q	quartet
ref.	reference
rf	reflux
RB	round bottom
RT	room temperature
s	singlet for NMR spectroscopy; strong for IR spectroscopy
SCF	self consistent field
t	triplet
THF	tetrahydrofuran
TLC	thin layer chromatography
TMS	trimethylsilyl
Ts	p-toluenesulfonyl
UV	ultraviolet spectrum
ZPE	zero point vibrational energy

MISCELLANEOUS SYMBOLS

δ	chemical shift in ppm downfield from tetramethylsilane

CHAPTER I

Introduction

This dissertation is concerned with theoretical and experimental aspects of compounds suitable for the construction of μ-hydrido bridged carbocations. The field of carbocation chemistry makes use of specialized techniques and principles not common to every organic chemist. Therefore, in addition to general background information, the introduction also discusses all the relevant techniques and principles necessary for generating and observing carbocations

1.1 Definitions

Carbocations are positively charged organic molecules, in which at least one carbon atom bears a positive charge. The coordination numbers vary considerably, and range from one to six. Examples are the one coordinated ethinyl cation **1**[1] and the tricyclic dication **2**[2] containing 4 six coordinated centers.

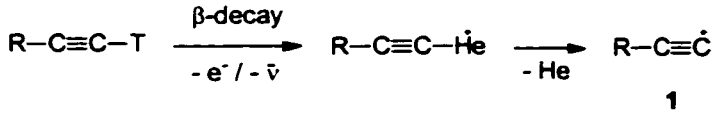

1

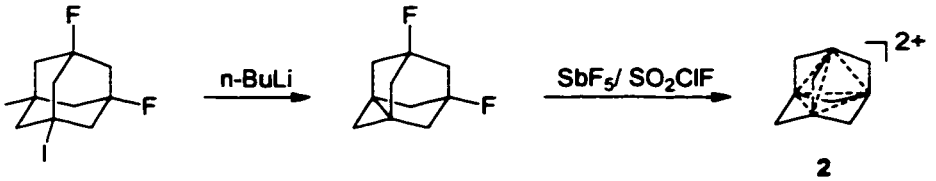

2

Most known carbocations however, are three to five (**3** - **5**) coordinated and include many key reactive intermediates in a variety of reactions ranging from enzymatic biotransformations to the largest petroleum refining processes.

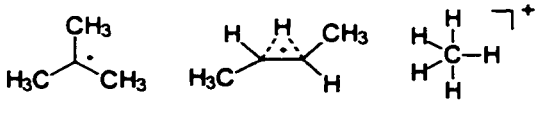

3 **4** **5**

According to Olah[3], three coordinated carbocations (e.g. **3**) are termed carbenium ions and the five coordinated (e.g. **5**) as carbonium ions (in some older literature, the term carbonium ion has been used for carbenium ions or just as a general term for positively charged carbon compounds and this has led to some confusion). The term carbocation is now widely used as a generic description for a positively charged carbon compound. Commonly, the trivalent or three coordinated carbocations are also referred to as classical and the four or higher coordinated carbocations as nonclassical. However, the distinction between classical and nonclassical cations can involve very subtle interpretive differences of an experimental result and this led to the nonclassical ion debate.[4]

This dissertation will follow the combined efforts of Brown and Schleyer and use the term classical carbocation for a positively charged species which can be appropriately described using only two center two electron bonds. A nonclassical carbocation will be considered as a species requiring electron deficient bonds (e.g. a three center two electron bond) for its adequate description. Other terms such as carbonium ion or carbenium ion will be avoided.

The naming of carbocations according to IUPAC rules can be categorized in the following two examples.

1. Carbocations formally derived by the addition of a proton to a neutral molecule. The name of the parent hydride is altered by replacing the final "e" by the suffix "-ium" for mono cations or "-diium" for dications etc.

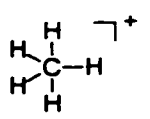

Methanium

Benzenium

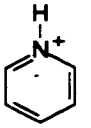

Pyridin-1-ium

2. Carbocations formally derived by the removal of a hydride ion (H^-) from the parent molecule. The suffix "ylium" is used in the same way as the suffix "yl" with radicals. Alternatively, the radical name can be used followed by "cation" as a separate word.

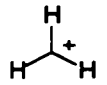

Methylium
Methyl cation

Cyclohexane-1,1-bis(ylium)
Cyclohexylidene dication

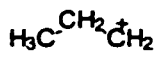

Propylium
Propyl cation

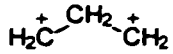

Propane-1,3-bis(ylium)
Propane-1,3-diyl dication

Cyclopropenylium
Cyclopropenyl cation

1.2 Historical Development[5]

The origins of carbocation chemistry were laid in the late 19th century when the discovery and preparation of synthetic dyes by Perkin, Hofmann and others[6] initiated the search for new theoretical explanations.

Arrhenius developed a theory about ionic dissociation of inorganic compounds in the 1880s.[7] These fundamental new ideas revolutionized the field of chemistry and in 1899 Stieglitz[8] announced the first carbocation as a reaction intermediate. Initially not accepted by the chemical community, these ideas were later awarded with the Nobel Prize for Arrhenius in 1903 and for Ostwald in 1909.[9]

In 1901 Norris[10] and Kehrman[11] independently reported the formation of an intensely yellow or orange colored solution by the treatment of triphenyl carbinol with conc. sulfuric acid or triphenylchloromethane with aluminum chloride, respectively.

Conductivity and molar freezing point depression measurements provided further proof for the salt like character of triphenylmethyl carbinol in sulfuric acid. Later, Hammett,[12] Hantzsch[13] determined that four charged particles were formed.

$$(C_6H_5)_3COH + 2\,H_2SO_4 \rightleftharpoons (C_6H_5)_3C^+ + H_3O^+ + 2\,HSO_4^- \qquad (1)$$

In 1922 Meerwein and Van Emster[14] found that reaction conditions expected to favor the

formation of carbocations accelerated the rearrangement of camphene hydrochloride into isobornyl chloride, a reaction first discovered by Wagner[15] in 1899. They then proposed the involvement of a cationic intermediate rather than a migration of the chlorine atom and laid the foundation for the modern concept of carbocationic intermediates.

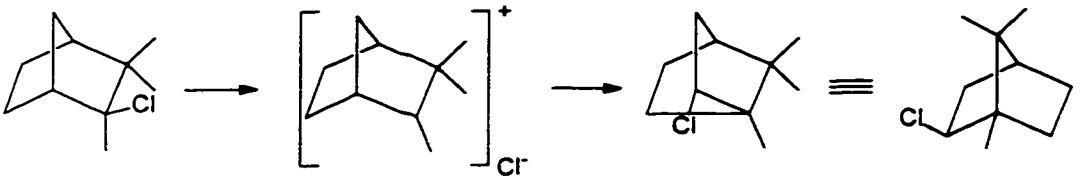

(2)

Further developments of the concept involving reactive carbocation intermediates were carried out by Hughes and Ingold[16] who introduced in the 1920s the theory of nucleophilic substitution at a saturated carbon and also polar elimination reactions, later termed S_N1, S_N2 and E1.

Freudenberg proposed in 1927 the first nonclassical carbocation structure[17] as a transition state structure in a 1,2-phenyl shift reaction and illustrated this with Bohr-Sommerfeld orbits represented by ellipses, each supposed to be occupied by one electron (Figure 1).

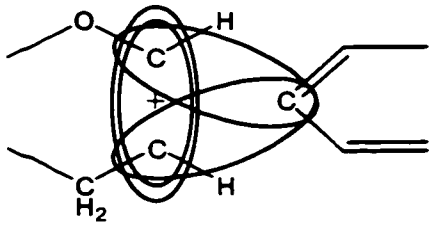

Figure 1: Freudenberg's representation of a nonclassical structure in **1927.**

Mainly based on the work of Meerwein, Whitmore generalized the concept of carbocationic intermediates in a series of papers starting with the famous article " The Common Basis of Intramolecular Rearrangements" spanning the theory of an entire field.[18]

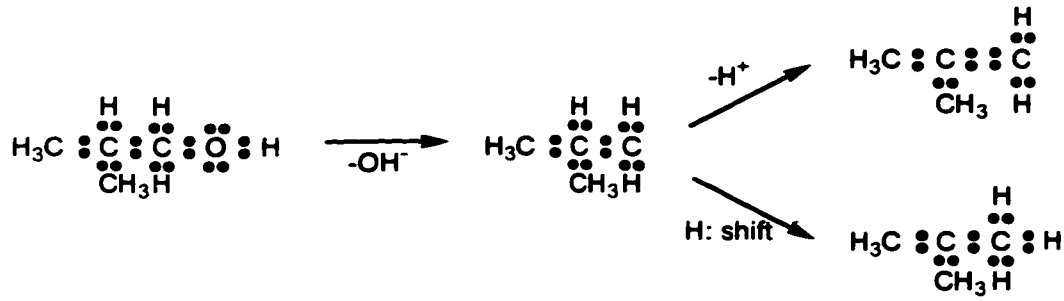

Figure 2: Designation according to Whitmore **1932.**

In the 1930s, carbocations were considered to be extremely reactive species since they could not be observed directly in solution. Many chemists therefore disputed the concept of cationic intermediates and consistently doubted the existence of carbocations. The prestigious *Journal of the American Chemical Society* did not accept any article containing the notation R_3C^+ and Whitmore for example was never allowed to publish his structures according to his rationale.

In 1939, Wilson and coworkers[19] solved Meerwein's stereochemical problem of the bornyl-isobornyl rearrangement, by using radioactive Cl^- isotopes. The absence of significant incorporation of radioactivity led to the proposal of an ion pair mechanism, involving the nonclassical structure **6**.

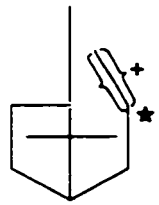

6

A bridged bromonium ion intermediate was suggested by Roberts and Kimbal in 1937 as an explanation for the stereospecifity of trans brominations in alkenes. Winstein and coworkers extended this theory to nucleophilic substitution reactions having a similar stereochemical behavior, and these observations evolved into the concept of neighboring group participation, also termed anchimeric assistance (Figure 3).

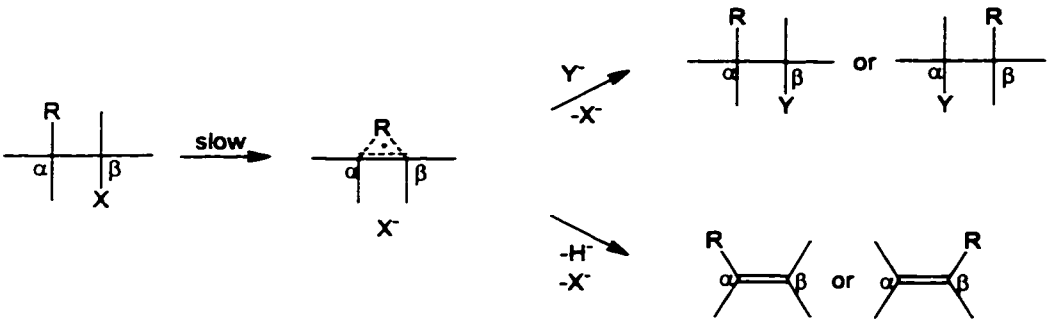

Figure 3: Anchimeric assistance according to Winstein **1948**.

In search of observable cations, Meerwein prepared a series of oxonium ions,[20] known as Meerwein salts; however, no acyl or alkyl cation salts were obtained. In 1943, Seel[21] prepared acetylium tetrafluoroborate by the reaction of acetyl fluoride and boron trifluoride.

$$H_3COF + BF_3 \rightleftharpoons CH_3CO^+ BF_4^- \qquad (3)$$

During the period from 1933 to 1959, great efforts were devoted toward the preparation of observable alkyl cations by numerous researchers (Brown,[22] Wetyproroch,[23] Olah,[24] Fairbrother,[25] Rosenbaum,[26] Finch and Symons[27]). However, all the experiments were unsuccessful and spectroscopic observation of carbocations remained reserved for gas phase mass spectrometric studies[28] until the early 1960s.

Known from Pearson's studies[29] concerning Friedel-Crafts acylations, a mixture of acylation and alkylation products is obtained if pivaloyl chloride and aluminum chloride are reacted with benzene. Olah continued this study[30] and finally discovered the formation of a stable t-butyl cation solution upon reaction of pivaloyl fluoride with antimony pentafluoride.[31]

$$(CH_3)_3CCOF + SbF_5 \rightleftharpoons (CH_3)_3CCO^+ SbF_6^- \xrightarrow[-CO]{} (CH_3)_3C^+ SbF_6^- \qquad (4)$$

In 1964 a detailed report on alkyl cations including NMR and IR spectra was published by Olah.[32] In the same year Hogeveen and Brouwer also reported the observations of alkyl cations.[33]

These results finally proved the existence of long lived alkyl cations since alternative descriptions, such as a rapidly exchanging Lewis acid - Lewis base complex, could be ruled out.

The acidic environment necessary for the formation of observable carbocations was characterized by Gillespie and coworkers in 1968. They defined acids stronger than 100 % sulfuric acid as superacid[34] after a term invented by Conant,[35] who used it to describe acids stronger than usual mineral acids in his studies in 1927 on protonated carbonyl compounds.

The still questionable participation of σ-bonds in the stabilization of carbocations prompted Schleyer, Saunders and Olah to investigate and directly observe the 2-norbornyl cation, and a long and intense debate followed.[4] After nearly three decades of controversy, sophisticated NMR studies conducted by Saunders, Myhre and Koch[36] and high-level *ab initio* calculations by Schleyer and Sieber[37] proved particularly definitive in favor of the symmetrical nonclassical structure.

The field of stable carbocation chemistry evolved explosively after Olah's discovery and a large variety of carbocations were characterized, rearrangements explored and the fundamental principles of this chemistry firmly established.

In order to illustrate some of the more recent examples of this carbocation chemistry, a few highlights have been chosen and are outlined in the following paragraphs.

Hogeveen and Kwant[38] prepared the unusual pyramidal hexamethyl dication **7** from a variety of different precursors.

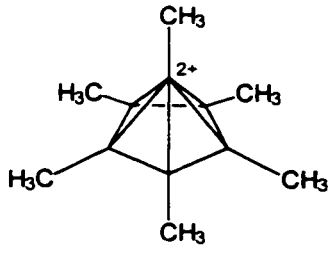

7

Low temperature NMR experiments confirmed the proposed structure **7**. The ^{13}C NMR chemical shifts of the five-membered ring carbons had a value of 126.3 ppm and the apical

carbon had the very high field shift of 2.0 ppm. These shifts could only be explained with the nonclassical structure **7**.

Early studies from Prelog[39] and Cope[40] implied the involvement of μ-hydrido bridged carbocations in dihydroxylation reactions of medium sized carbocyclic alkenes. However, it was not until 1978 that the first μ-hydrido bridged carbocation could be spectroscopically observed. Sorensen and coworkers[41] successfully prepared the μ-hydrido bridged carbocation **8** in superacidic medium at low temperature (this topic is expanded in Section 1.8, page 52, since this thesis involves further developments in this area).

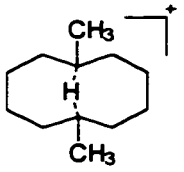

8

The first total synthesis of the dodecahedrane **9** by Paquette and coworkers[42] enabled Olah and his research group[43] to prepare the cations **10** and **11**.

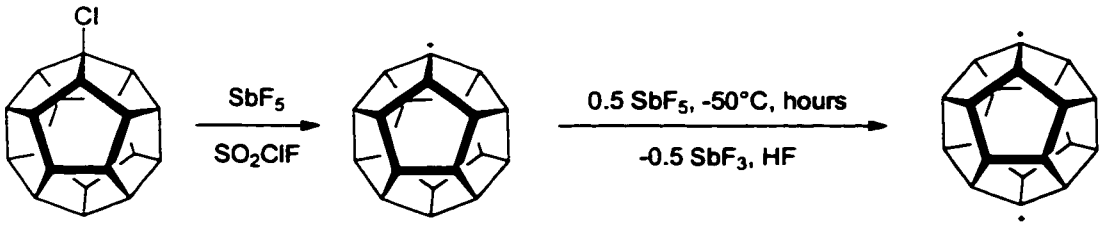

9 **10** **11**

The exceptional ^{13}C NMR chemical shifts of the cationic carbons (363.9 ppm for **10** and 379.2 ppm for **11**) can be rationalized with help of *ab initio* calculations, which predict cation **11** to be sp^3 hybridized. The value of 379.2 ppm for the dication **11** is still the lowest field chemical shift ever measured for a "pure" organic compound.

Currently, over 100 articles on carbocation chemistry are published every year, making it a still interesting and challenging field. The results of theses studies continue to expand our fundamental understanding of chemistry and have had a major impact on synthetic organic chemistry.[44]

1.3 Chemical Behavior

The reactivity of carbocations is controlled by electronic or structural effects of the atoms near the positively charged carbon(s). Electronic effects of substituents on carbocations are determined by their electron donating or accepting ability. Charge stabilization can occur via electron donating substituents, sharing the charge amongst a number of carbons (conjugation), and via solvation from solvents, destabilization occurs usually through having electron withdrawing substituents near the positively charged carbon.

While stabilization through a π-type interaction or conjugation has been accepted since the 1920's and is now a firmly established concept, the participation of σ-bonds in stabilizing carbocations has only been accepted relatively recently and the details of these interactions are the subject of many current carbocation studies.[45] C-C or C-H Hyperconjugation is the most important stabilizing interaction in alkyl cations, the main class described in this project, and various types of hyperconjugative interaction are illustrated below.

If a neighboring C-H bond is properly aligned with the p-orbital of the cation, substantial overlap occurs and stabilization through hyperconjugation can be achieved. In a similar way, this type of interaction also occurs with neighboring C-C bonds (see Figure 4).

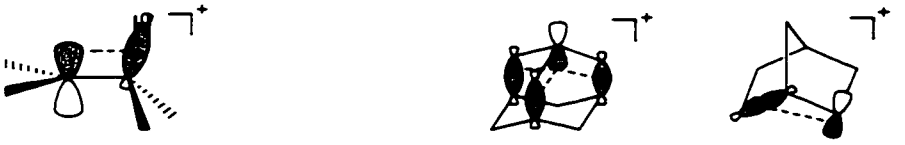

C-H Hyperconjugation

C-C Hyperconjugation

Figure 4: Examples of C-H and C-C hyperconjugation.

Carbocations are substantially stabilized by solvation.[46] Tertiary alkyl halides for example have been estimated to dissociate 10^{80} times faster in polar protic solvents than in the gas phase.[47] Gold and Abraham estimated a solution energy for the *tert*-butyl cation in water of at least 50 kcal/mol.[48]

Structural effects are mainly determined by the geometry of the cation center. In the ideal case, a simple tertiary carbocation adopts a planar trigonal sp^2 geometry. Cyclic alkanes however, can force angle deviations from this ideal geometry and as a result destabilize the

carbocation.

The bicyclic carbocations resulting from dissociation of compounds **12** to **15** are even more geometrically restrained and the positively charged carbon cannot attain the desired planarity. The influence of these geometric restraints on the bridgehead reactivity of various polycyclic compounds has been studied by Schleyer and Bingham.[49] The following series shows that increased geometric strain at the bridgehead position is paralleled by a decrease in the relative solvolysis rate.

12 1.0 **13** 3×10^{-3} **14** 10^{-8} **15** 10^{-14}

Figure 5: Approximate relative solvolysis rates for some bicyclic compounds. X = Cl, Br, or Ts.

In many cases, the implementation of a given strain on a carbocation center is lessened because of a change in other interactions, which are stabilizing. Thus, a geometrically restrained cation can actually be energetically more stable than a cation with a planar sp^2 geometry. For example, the 1-adamantyl cation is about 4 kcal/mol more stable than the geometrically unstrained *tert*-butyl cation, according to gas phase experiments.[50]

1.4 Stability

Carbocations in general are highly reactive and their stability compared to "normal" isolable compounds is very low in terms of temperature and environment. Most carbocations are only observable in either the gas phase or in a specially designed super acidic environment, which is characterized by an extremely low nucleophilicity.[51] The measurement of all the required thermodynamic data has proven to be difficult, and so there are various ways to describe carbocation stability.[52]

These can be divided into three different categories.

1. pK_a stability
2. thermodynamic energetic stability
3. kinetic stability

1.4.1 pK_a Stability

One way to describe the stability of carbocations is to determine the least "drastic" environment needed to prepare the cation. For this purpose the following reaction can be considered.

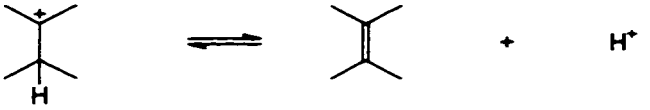

The alkene is the base in this example and the stability of the cation (expressed as a pK_a value, where $pK_a = -\log K_a$) can in principle be calculated by measuring the acid strength (or activity) of the solution needed for the protonation of the alkene, and the ratio of alkene / carbocation, as shown below:

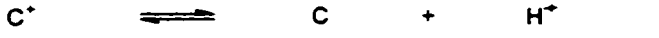

(5)

$$K_a = \frac{\alpha_C \ \alpha_{H^+}}{\alpha_{C^+}} = \frac{[C]\gamma_C \ \alpha_{H^+}}{[C^+]\gamma_{C^+}} \qquad \textbf{(6)}$$

α = activity
γ = activity coefficient
C = alkene
C^+ = carbocation

In general, extremely strong acids are needed to achieve protonation of an alkene to a measurable extent. In order to characterize the "acidity" of such strongly acidic solutions, Hammett defined the H_o acidity function by using different aniline derivatives as indicators.[53]

Rearrangement of equation **(6)** yields the acidity function according to Hammett.

$$H_O = -\log h_o \equiv -\log\left\{K_a \frac{[C^+]}{[C]}\right\} = -\log \frac{a_{H^+}\, \gamma_C}{\gamma_{C^+}} \qquad (7)$$

Table 1 illustrates the acidities of some acid systems.

Table 1: H_o acidity function values for some selected acid systems.

Acid system	H_o value	Acid system	H_o value
H_2SO_4 50% in H_2O [a]	-3	HSO_3Cl [b]	-13.8
H_2SO_4 90% in H_2O [a]	-9.2	HSO_3F [d]	-15.1
H_2SO_4 98% in H_2O [a]	-10.4	HSO_3F + 10 mol % SbF_5 [d]	-18.9
H_2SO_4 100% in H_2O [a]	-11.9	HSO_3F + 90 mol % SbF_5 [d]	-26.5
H_2SO_4 + 10 mol % SO_3 [b]	-13.9	HF 100% [e]	-11.5
$H_2S_2O_7$ [b]	-14.4	HF + 1 mol % SbF_5 [e]	-20.5
$HClO_4$ [c]	~ -13.0	HF + 80 mol % SbF_5 [e]	~ -30

[a] ref.[54] [b] ref.[55] [c] ref.[56] [d] ref.[55, 57, 58] [e] ref.[57, 59]

Some carbocation substrates cannot undergo an elimination reaction and a pK_a stability of the above type cannot be defined. In these cases the ionization equilibrium of a protonated alcohol has been considered as an alternative to the H_o definition, leading to the H_R acidity function and the related pK_{R^+} scale.[60]

$$ROH + H^+ \rightleftharpoons R^+ + H_2O \qquad (8)$$

$$H_R \equiv pK_{R^+} - \log\frac{[R^+]}{[ROH]} = -pK_{ROH} - \log\frac{[R^+]}{[ROH]} \qquad (9)$$

Table 2: pK_{R^+} values for some triphenylmethyl cations.[61]

Compound	pK_{R^+} value
Tris(4-nitrophenyl)methyl cation	-16.27
4-Nitrophenyldiphenylmethyl cation	-9.15
Triphenylmethyl cation	-6.63
4-Methoxyphenyldiphenylmethyl cation	-3.40
Tris(4-methoxyphenyl)methyl cation	+0.82
Tris(4-aminophenyl)methyl cation	+7.57

Basicity measurements using the H_o scale have often yielded inconsistent values (non-thermodynamic). This has led to the definition of a variety of different acidity functions, each one usually applicable to a given type of base.[62] All of these functions are variations of the

Hammett acidity function H_o, trying to specify a thermodynamic proton activity, which will apply to the particular system.

A pK_a "stability" is exclusively a condensed phase property, mainly because all the measurements are connected with the proton activity. Corresponding gas phase measurements would not consider the abovementioned equilibrium reactions but rather the proton affinity, which is discussed below (see Section 1.4.2, page 14).

1.4.2 Thermodynamic Stability of Carbocations

A thermodynamic stability scale for carbocations can take many forms. One of the simplest definitions involves high level *ab initio* calculations on a series of isomeric carbocations, the most stable cation being that one with the lowest -E value. A similar approach is possible using semi-empirical calculations, the most negative heat of formation corresponding to the most stable carbocation. However, total energies and heats of formation are not necessarily very relevant as a practical manifestation of carbocation stability, as measured by other criteria. For example, the 1-adamantyl cation and the tricyclopropylmethyl cation are isomeric ($C_{10}H_{15}^+$), with the 1-adamantyl cation expected to be much more stable on the calculated global potential energy surface, while the tricyclopropylmethyl cation would be expected to have considerably more stability as measured using hydride affinity values, expected solvolysis rates etc.

In the following sections, a number of these latter measures of cation stability are discussed, e.g. hydride affinities, proton affinities, ionization potentials, rates of solvolysis or dissociation enthalpies.

Measuring the electron beam energy or the irradiation energy necessary to convert a neutral molecule into a cationic species in the gas phase allows one to measure the appearance potential AP (corresponding to the energy change of the reaction, ΔE_{Rxn}), which is the sum of the reaction enthalpy ΔH_{Rxn} and the excess energies of A^+ and $B^\cdot$, $\sum E_e$, of the reaction **(18)** (see Section 1.5.1, page 24).

$$AP = \Delta E_{Rxn} = \Delta H_{Rxn} + RT + \sum E_e \approx \Delta H_{Rxn} + \sum E_e \qquad \textbf{(10)}$$

The heat of formation of the cation $\Delta H_{f(A^+)}$ can then be derived as follows.

$$\Delta H_{f(A^+)} = AP + \Delta H_{f(AB)} - \Delta H_{f(B^\bullet)} - \sum E_e \qquad (11)$$

The determination of the excess energies $\sum E_e$ of the different particles has proven to be a problem, and the corresponding heats of formation have an uncertainty of about 2 kcal/mol.[63]

Ionizing radicals gives access to ionization potentials. Together with the heat of formation of the in situ generated radical one can determine the gas phase heat of formation of the corresponding carbocation (see also reaction **(19)** Section 1.5.1 , page 25).

$$\Delta H_{f(R^+)} = \Delta H_{f(R^\bullet)} + IP \qquad (12)$$

$\Delta H_{f(R^+)}$ = heat of formation of the carbocation
$\Delta H_{f(R^\bullet)}$ = heat of formation of the radical
IP = Ionization potential

The enthalpy change of reaction **(13)** is defined as the proton affinity (PA) of B and the change in free energy as the gas phase basicity (GB),[64] which in turn are a measure of the cation stability.

$$B + H^+ \rightleftharpoons BH^+ \qquad (13)$$

$$PA = \Delta H_{diss} = \Delta H_{f(BH^+)} - \Delta H_{f(H^+)} - \Delta H_{f(B)}$$
$$GB = \Delta G_{diss} = \Delta G_{f(BH^+)} - \Delta G_{f(H^+)} - \Delta G_{f(B)} \qquad (14)$$

ΔH_{diss} = dissociation enthalpy of reaction **(13)**
$\Delta H_{f(BH^+)}$ = heat of formation of the BH^+
$\Delta H_{f(H^+)}$ = heat of formation of H^+
$\Delta H_{f(B)}$ = heat of formation of B
$\Delta G_{f(BH^+)}$, etc. are the corresponding free energies

The hydride ion affinity (HIA) is a very practical value for comparing gas phase and condensed phase thermochemical data. The enthalpy change in reaction **(15)** is defined as the hydride ion affinity (HIA), which is the sum of the heat of formation of the associated cation R^+ ($\Delta H_{f(R^+)}$) , the hydride anion H^- ($\Delta H_{f(H^-)}$) and the hydrocarbon RH ($\Delta H_{f(RH)}$) , whose values

are usually obtainable by appearance potential or ionization potential measurements.

$$RH \rightleftharpoons R^{+} + H^{-} \quad \textbf{(15)}$$

$$HIA = \Delta H_{f(R^{-})} + \Delta H_{f(H^{-})} - \Delta H_{f(RH)} \quad \textbf{(16)}$$

Table 3 gives some gas phase thermochemical data for selected examples.

Table 3: Thermodynamic data for selected carbocations in the gas phase.[52a, 65]

carbocation R^{+}	ΔH_{R+}	$D_{(R-H)}$	$IP_{R\cdot}$	HIA_{R+}	ΔH_{RH}	GB_{olefin}	PA_{olefin}	ΔH_{olefin}	olefin
CH_3^{+}	261	104	226.9	312	-17.9				
$CH_3CH_2^{+}$	219	98.0	193.3	273	-20.2		163.5	12.5	ethene
$CH_3CH_2CH_2^{+}$	208	97.9	186.8	266	-24.8	176.5	184.9	4.9	propene
$CH_3CH^{+}CH_3$	192	94.5	174.1	247.4	-24.8	176.5	184.9	4.9	propene
$CH_3CH_2CH_2CH_2^{+}$	201	100.5	184.7	265	-30.4				
$(CH_3)_3C^{+}$	164.0	92.5	154.5	229.6	-32.4	188.3	196.9	-4.3	$(CH_3)_2C{=}CH_2$
	226	89	186	256	4.9				
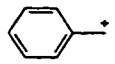	213	85	167.6	234					
	266	99.2	206.4	287	12.5				
	179			218	-6	200.9	209.3	21	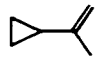
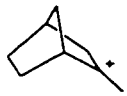	172			224.1	-19.6	199	207	12	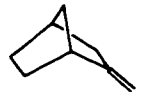
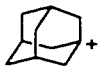	158	98.5		224.3					
	167.5	96.0		233.8					
	198.2	94.9	172.3	249.8	-18.4				
	168.0			226.5	-25.3	190.4	198.6	-0.6	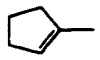
	200.7	81.7	161.4	225.7	8.2		200	31.9	
	257	81.1	193.9	258	31.9				

A broad range of thermochemical data in the condensed phase is available through the work

of Arnett and coworkers.[66] Calorimetric measurement of the ionization energy of organic halides RX and alcohols ROH in superacids has yielded valuable data on condensed phase carbocation stabilities and has allowed a comparison of these results with the corresponding gas phase measurements.

$$R{-}X + 2\,SbF_5 \xrightarrow[SO_2ClF]{} R^+ + Sb_2F_{10}X^-$$

$$R{-}OH + HOSO_2F\text{-}SbF_5 \xrightarrow[SO_2ClF]{} R^+ + H_3O^+ + SO_3F\text{-}SbF_5^-$$

The dissolution of a sample of solid RX in a SO_2ClF solution of SbF_5 involves a number of different energy factors. Since the carbocations produced usually are only stable at a relatively low temperature, all of the measurements were conducted at -60°C. Cooling the RX (solid) from 25°C to -60°C involves the heat energy change, $\Delta H_{Heat} = \int_{213K}^{298K} C_{p,RX}\, dT$, where $C_{p,RX}$ represents the molar heat capacity. Dissolving the solid material on the other hand involves the heat of solution ΔH_S, followed by complexation of the dissolved RX by the superacid, which forms the hypothetical alkyl halide - acid complex, and the complexation enthalpy is shown as $\Delta H_{compl.}$. Finally, the heat of ionization ($\Delta H_{R+,ionization}$) results from the separation of the halide - acid complex into the corresponding ions R^+ and HAX^-.

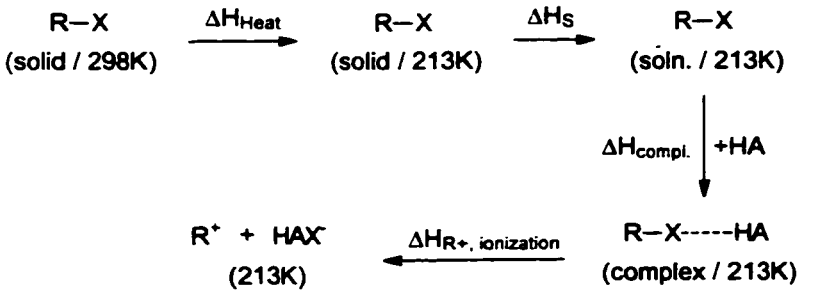

However, control experiments[67] showed that the observed enthalpy ($\Delta H_{obs} = \Delta H_{Heat} + \Delta H_S + \Delta H_{compl.} + \Delta H_{R+,ionization}$) depends only on structural changes which have a direct influence on

the stability of the cation R^+. In other words, the enthalpies ΔH_{Heat}, ΔH_S and $\Delta H_{compl.}$ are relatively constant for a variety of different cations and the differences in ΔH_{obs} are almost exclusively due to changes in $\Delta H_{f(R+)}$. Therefore, the measured ΔH_{obs} values are a useful criterion for determining the stability of carbocations.

Table 4: Ionization enthalpies of some alcohols in a mixture of SbF_5, FSO_3H and SO_2ClF [66] and for comparison, the corresponding gas-phase hydride ion affinities.

alcohol	cation	ΔH_{obs}	HIA
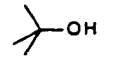		-35.5	230.6
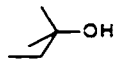	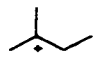	-40.3	229.1
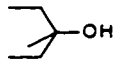	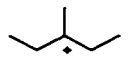	-36.7	226.8
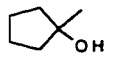	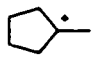	-38.3	225.8
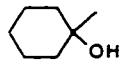	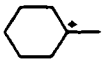	-37.8	227.2
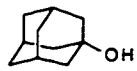		-31.0	224.3
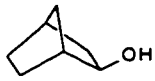		-34.6	231.1
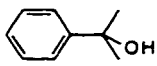	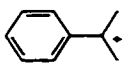	-40.3	220
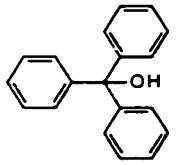	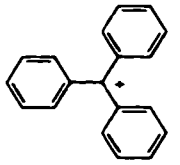	-49.0	

Solvolysis reactions can also be used to derive a stability criteria for carbocations.[68] In solvolysis reactions proceeding according to an S_N1 mechanism, one can correlate the reaction rate with the stability of the corresponding carbocation, since the first step is rate-determining, and the transition-state should ressemble the carbocation intermediate (Figure 6).[69]

Variable solvation[46, 70] or neighboring group participation (i.e. anchimeric effect)[71] are factors in the stabilization of a carbocation intermediate. However, a same solvent comparison can be made in some cases and in the examples shown here anchimeric effects are probably

not large.

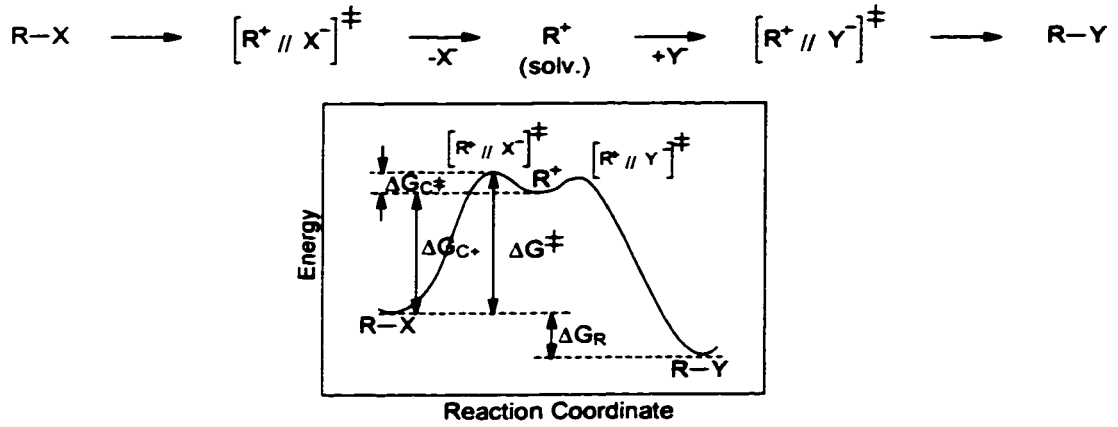

Figure 6: Free energy profile for an S_N1 reaction (carbocation as a reactive intermediate).

The nature of the leaving group can have a large influence on the reaction rate of solvolysis reactions.[72] In most cases, a comparison of rates of solvolysis reactions and gas phase stabilities of the corresponding carbocations show very good to excellent correlation.[66]

A particularly useful group are compounds with bridgehead halides, whose solvolysis reactions follow a pure S_N1 mechanism, since the backside of the reaction center in question is blocked. The relative stabilities of the associated carbocations have been estimated from strain energy calculations. Comparison of the calculated stabilities with the corresponding rates of solvolysis shows a good correlation[49, 73] (Figure 7).

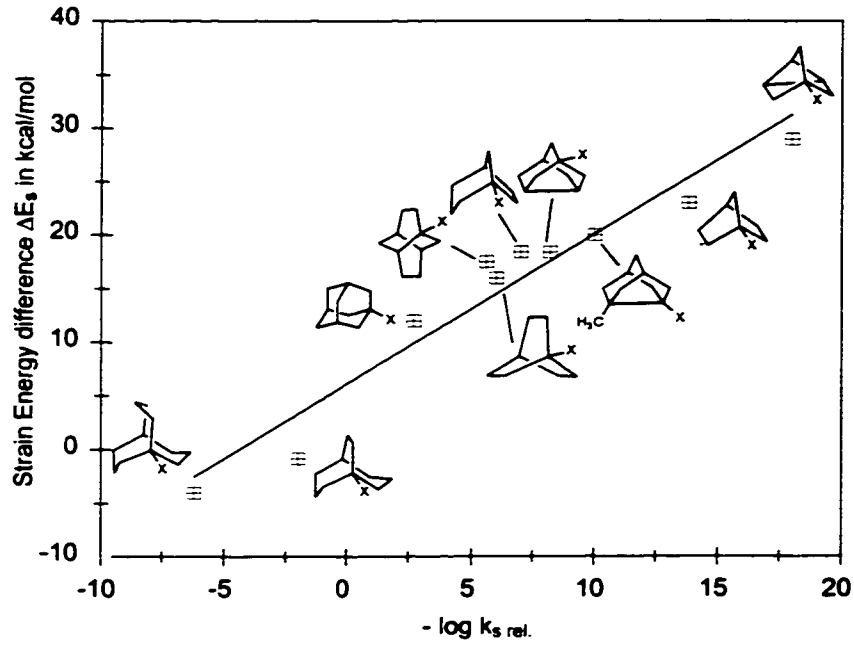

Figure 7: Correlation of the Hydrocarbon-Carbocation Strain Energy difference and the relative rate of solvolysis of the corresponding alcohols and halides.[73]

These findings indicate that the solvation energy in a specific solvent system is constant for a variety of different carbocations and the relative rate of solvolysis can be used to estimate the relative stability of carbocations.

Despite the good general correlation of measurements in the gas phase and in the condensed phase, there are still many cases where important differences occur. For example, the tendency of larger alkyl substituents to be more stabilizing than their smaller homologs in the gas phase is reversed in solution. This behavior has been explained as involving the less effective solvation of carbocations with big substituents because of steric hindrance.

Despite the enormous amount of thermochemical data available for the estimation of carbocation stabilities, the measurements are often difficult and experimentally demanding. It is important to control as many of the variables as possible when making comparisons between different methods.

Scheme 1 summarizes the different energy terms important to carbocation stability considerations.

Scheme 1: Thermochemical terms for carbocations. BDE = bond dissociation energy, $\Delta H_{f(a)}$ = heat of formation of the alkane, $\Delta H_{f(o)}$ = heat of formation of the olefin, XA = halide affinity, for the explanation of the other terms see text.

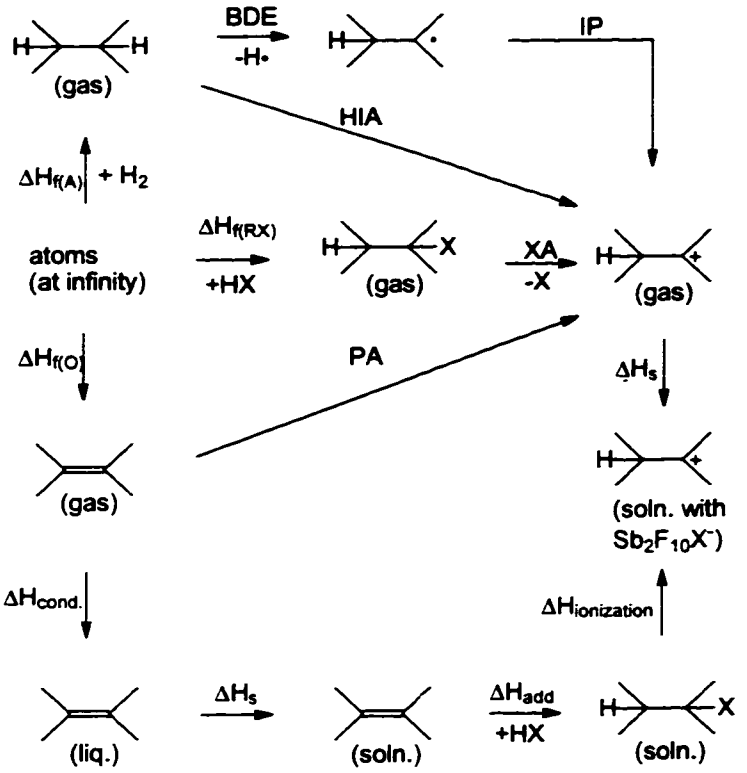

1.4.3 Kinetic Stability

The third category of stability is kinetic stability, which reflects mainly how easily a particular carbocation rearranges, i.e. the height of various transition-states barriers.

For example, the secondary 2-propyl cation, generated from isopropyl fluoride and SbF_5, is observable via NMR spectroscopy in the condensed phase at -60°C.[74] No other rearranged cation can be observed even over a long period of time. The related 2-butyl cation on the other hand was found to undergo a facile rearrangement to the thermodynamically more stable *tert*-

butyl cation.

Another example is the comparison of the cyclopentyl and the cyclohexyl cation. The 5 membered cation **16** can be prepared in a SO_2ClF / SbF_5 solution at -78°C without any significant rearrangement or decomposition, despite its very high heat of formation (191.4 kcal/mol).[75]

16

The NMR data recorded in solution[76] at -78°C and at -203°C as a solid,[77] reveal very rapid 1,2-hydride shifts. The solution ^{13}C NMR shows only one carbon signal at 99 ppm, representing an average of all the different environments. The solid-state NMR spectrum at -203°C however freezes out the hydride shifts and the individual ^{13}C NMR signals at 320, 71 and 28 ppm can be observed.[77] The associated energy barrier of this process was narrowed down to a value of less than 4.5 kcal/mol.

On the other hand, the very similar secondary cyclohexyl cation with a heat of formation of 175 kcal/mol[75] has never been observed in the condensed phase. All attempts to produce the cation in super acidic media result in the formation of the 8 kcal/mol more stable methylcyclopentyl cation.[78] However, more recent gas phase experiments have been successful in the detection of this secondary cation.[79] Saunders and coworkers have prepared different isotopically labeled methylcyclopentyl cations and measured the activation energies for proton scrambling (15.4 kcal/mol), and for carbon scrambling (18.2 kcal/mol).[80]

Scheme 2: Proposed mechanism for proton and carbon scrambling in the methylcyclopentyl cation.

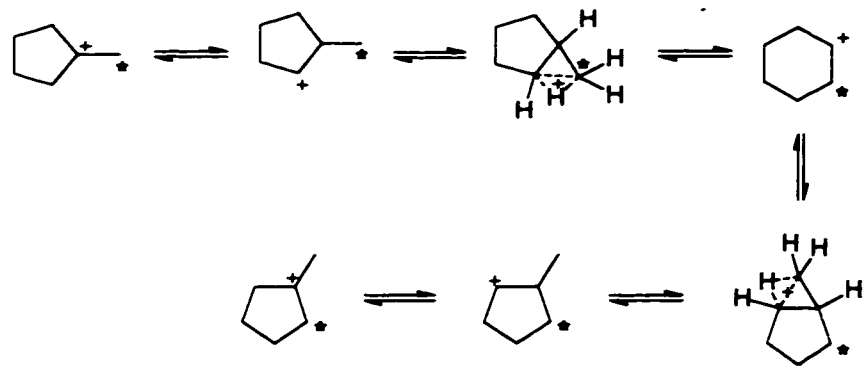

The carbon scrambling logically involves the secondary cyclohexyl cation as an intermediate and the activation energy for the rearrangement of the secondary cyclohexyl cation back into the *tert*-methylcyclopentyl cation was calculated to be about 10 kcal/mol using the energy barrier for the carbon scrambling and the heats of formation of the two carbocations in question[80] (see Scheme 2).

1,2-Hydride shifts are in general very rapid. Similarily, 1,3- and 1,5-hydride shifts can also be extremely fast, if the geometric arrangement is appropriate. In molecules such as the substituted cyclohexyl **17** and the bicyclo[3.3.1]nonyl cation **18**, hydride shifts proceed very fast with an energy barrier of only 10.5[81] and 3.5 kcal/mol[82] respectively.

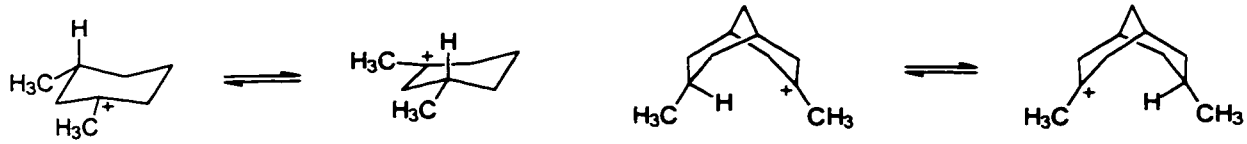

17 **18**

Intermolecular hydride shifts have also been shown to proceed in a very facile manner, with hydride exchange from isobutane to *tert*-butyl cation requiring an activation energy of only 3.6 kcal/mol.[83]

As illustrated by the above examples, carbocation rearrangements involving alkyl cations can be categorized into three groups.

1) Hydride shifts: These rearrangements proceed very rapidly if the atoms involved (and the corresponding orbitals) are properly aligned (see Figure 8). This usually means that there is a substantial overlap of the p orbital of the cation and the C-H bond, so that the C-H bond is already weakened before much movement of the H has occurred.

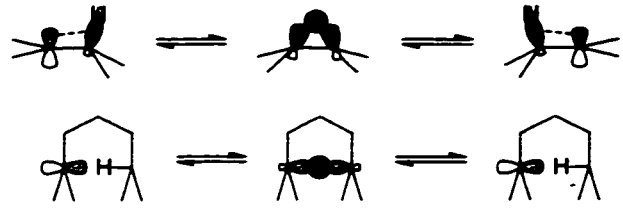

Figure 8: Participating orbitals in hydride shifts.

Typical energy barriers of 2 - 10 kcal/mol are usually observed if the H-shift takes place between carbons of the same carbocation type (i. e. *tert-* - *tert-*)

2) "Classical" 1,2-Wagner-Meerwein shifts. Again, properly aligned orbitals facilitate this alkyl shift and typical energy barriers have been found to be only slightly larger than the corresponding hydride shifts.

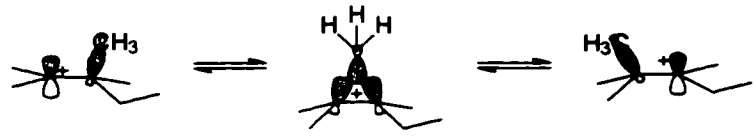

3) Rearrangement involving protonated cyclopropane structures.

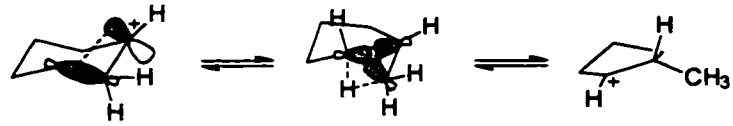

These reactions often involve a route which avoids the intermediacy of an actual primary cation intermediate or transition state, and the overall barriers typically range from 15 to 30 kcal/mol.

Brouwer and coworkers introduced the terminology of A- or B- type rearrangement reactions,[84] which refer to non-branching and branching reaction types, respectively. The above mentioned categories 1 and 2 would correspond to A-type reactions and generally involve less drastic reaction conditions than the B-type reactions corresponding to category 3.

1.5 Formation of Observable Carbocations

The formation of reactive species such as carbocations requires a large thermodynamic driving force. Once generated, the environment needs to be inert enough to support a carbocation life-time sufficient for the observation. An inert environment for carbocations is characterized by the presence of a very weakly nucleophilic counterion and solvent.

In the gas phase, carbocations can be generated as "isolated" species using high energy electron beams or photo irradiation as the thermodynamic driving force for their generation and the only environment the cation center has is in the molecule itself. Any rearrangement fragmentation reactions are intrinsic to the cation itself, at least in low pressure situations. An advantageous aspect of gas phase cation chemistry is the fact that the produced particles can be "observed" within a very short time of their generation (10^{-7}s). These factors allow one to "observe" carbocations which are extremely electrophilic (CH_3^-) or very prone to rearrange (secondary cyclohexyl cation).

1.5.1 Gas Phase

Irradiation of a neutral molecule AB in the gas phase[85, 52a] with either an electron beam or electromagnetic energy results in a transfer of energy into AB, which can then lose one (electromagnetic irradiation) or two electrons (electron beam) to form a cation radical. This process occurs according to the Frank-Condon principle, within a time frame of approx. 10^{-15} s.

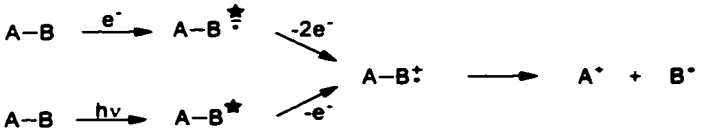

(18)

The dissociation of the cation radical can involve a much longer time period, up to 10^{-5} s.[86] This presents a problem for very reactive carbocations such as primary propyl or butyl cations, which rearrange into their more stable secondary or tertiary isomers in less than 10^{-6} s. One can get around this problem by irradiation of *in situ* generated radicals, since this directly generates the cation, and this allows one to observe extremely reactive primary carbocations.[87] This process has a time frame of about 10^{-15} s.

$$R\cdot \xrightarrow{h\nu} R^{+} + e^{-} \qquad \textbf{(19)}$$

The energy of the irradiation can be adjusted to the energy level required to achieve ionization of the free radical and this provides additional information about the stability of the cation (compare Section 1.4.2, page 13).

Ion molecule reactions can be carried out with high pressure mass spectroscopy (10^{-3} Torr) or with ion cyclotron resonance spectroscopy (ICR).[88, 89, 52a] These techniques keep the ions in the generation chamber for a relatively long time, which allows them to collide with other molecules as they undergo reaction.

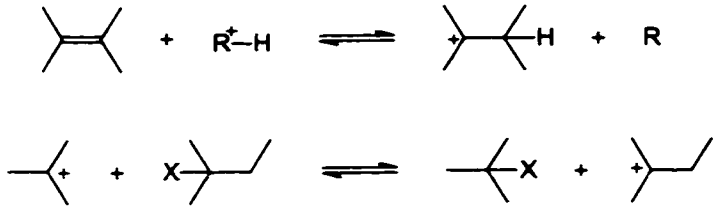

Equilibrium measurements of proton, hydride or halide transfer reactions allows one to measure relative thermochemical data to an accuracy of ± 0.1 kcal/mol[52a, 52b] (see also Section 1.4.2, page 14).

1.5.2 Condensed Phase

In comparison with the gas phase generation of carbocations, the production of condensed phase carbocations puts extreme restrictions on the kind of medium one can use, and on the thermodynamics involved in forming the free cation-anion pair. In addition, low temperatures are also an essential requirement.

1.5.2.1 Solvent

An appropriate solvent for the observation of long lived carbocations needs to possess a relatively large polarity in order to ionize and solvate the charged species. In addition to that, the basicity or nucleophilicity must be extremely low so as to not initiate substitution or elimination reactions. Initially, pure superacids such as mixtures of SbF_5 and HF or HSO_3F, or even neat SbF_5 were used to prepare carbocations.[31, 32] Later, solvents such as HF, SO_2, SO_2ClF and SO_2F_2 were used to dilute the superacid mixtures.

Sulfuryl chloridefluoride (SO_2ClF) has a boiling point of 7°C and a freezing point of -125°C. Its viscosity is very low, comparable to ether, over the whole liquid range. The polarity is relatively high and polar compounds such as carbocations are reasonably soluble.

Sulfuryl fluoride (SO_2F_2) is a very stable and inert compound, boiling at -55°C and melting at -135°C. However, its polarity is relatively low and in conjunction with superacids, the carbocations formed often crystallize out of solution at low temperature. Commonly, a mixture of sulfuryl fluoride and sulfuryl chloridefluoride are employed for NMR experiments conducted at very low temperature (down to -150°C).

Hydrogen fluoride exists as a volatile liquid with a bp. of 19°C and a melting point of -83.4°C. The relatively high bp. and the very low viscosity of 0.256 cP at 0°C (0.772 cP at -62.5°C) results from its ability to form linear hydrogen bridged oligomers. At -73°C, this liquid has a very high dielectric constant of 175 (84 at 0°C), which makes it an excellent solvent for carbocation studies. The biggest disadvantage is its incompatibility with glass and specially designed fluoropolymers have to be used to handle such solutions.[90]

Sulfur dioxide is a colorless, pungent gas with moderate toxicity. Its low viscosity as a liquid between -10°C and -75.5°C, its reasonably large polarity, and its ready availability and

low cost have made it a commonly used solvent. However, extremely reactive carbocations such as the secondary propyl cation have been found to O-alkylate SO_2.[91] It appears that SO_2ClF and SO_2F_2 are less nucleophilic than SO_2.

Fluorosulfonic acid is a mobile liquid with a bp. of 162.7°C and a mp. of -89.0°C. The viscosity is 1.56 cP at 25°C (comparable to water), and its density is 1.726 g/ml.[92] The high polarity of this solvent makes it very useful for preparing carbocations, but one cannot carry out solution-phase observations lower than *ca.* -100°C. Table 5 summarizes some physical properties of the most important solvents used for the preparation of stable carbocations.

Table 5: Physical properties of selected solvents for carbocation preparation chemistry.

Property	HF	SO_2	HSO_3H	SO_2ClF	SO_2F_2
mp. [°C]	-83.4	-75.5	-89	-125.7	-135.8
bp. [°C]	19.5	-10.0	163	7.1	-55.4
viscosity [cP]	0.256 (0°C)	0.403 (0°C)	1.56 (25°C)		
dielectricity	84 (0°C)	15.4	150[a]		
constant	175 (-73°C)				

[a] value estimated according equivalent conductivities by Gillespie.[93]

1.5.2.2 Lewis Acid systems

In a similar way to the arbitrary definition of a Brønsted superacid being stronger than 100% H_2SO_4,[34] Lewis superacids are defined as those stronger than anhydrous aluminum trichloride.[94] Despite the somewhat contradictory order of the acid strength of various Lewis acids, as measured in the older literature by a variety of different methods,[94] a relative order is now well established. Electrochemical measurements in anhydrous hydrogen fluoride revealed the following qualitative Lewis acid strengths:[95]

$$SbF_5 > AsF_5 > TaF_5 > BF_3 > NbF_5 > PF_5 > TiF_4$$

Neat boron trifluoride at low temperatures, first used by Seel[21] in 1943, led to the formation of acetylium tetrafluorborate salts when reacted with acetyl fluoride. Attempts to prepare alkyl cations using this Lewis acid, initially by Meerwein[20] and later by Olah[96] resulted in the formation of polarized complexes. In the reaction of *tert*-butyl fluoride and boron trifluoride, polymeric materials were isolated, indicating an equilibrium of the polarized complex, the

ionized cation and anion species, and 2-methyl-2-propene and HBF_4, with the latter alkene then polymerizing in the presence of some of the cation.

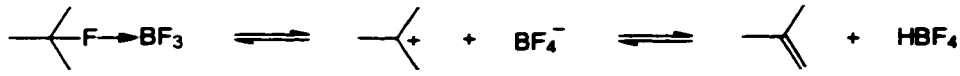

Mixtures of boron trifluoride and hydrogen fluoride are used as catalysts in many industrial Friedel-Crafts reactions, with the advantage of an easy removal of the volatile catalyst.[97] Furthermore, this mixture is also used in conjunction with hydrogen as a system for ionic hydrogenations.[98] Acidity measurements of a 7 % (mol/mol) solution of BF_3 in HF yielded an H_o value of -16.6[99] (for the definition of H_o see Section 1.4.1, page 11).

Arsenic pentafluoride is a colorless gas at room temperature with a boiling point of -53°C. As a liquid, it is largely a monomeric covalent compound with a high coordinating ability for halides. It has been used for a few halide cation preparations,[100] but has not found extended use in carbocation chemistry, possibly due to its potentially high toxicity.

Tantalum and niobium pentafluorides show very similar properties (tantalum pentafluoride being slightly stronger). They are both thermally stable white solids, which can be prepared by direct fluorination of the corresponding metals. However, they are much less soluble in HF or FSO_3H solvents compared to antimony pentafluoride and are therefore somewhat limited for use in the preparation of observable carbocations. Tantalum pentafluoride dissolves only to the extent of 0.6 % in HF at 0°C, the solution having an H_o value of -18.85.[101] On the other hand, the high redox potential and the low volatility of these Lewis acids are valuable properties for the preparation of catalysts for alkane alkylations and aromatic protonation reactions.[102]

The strongest Lewis acid known today[103] is antimony pentafluoride, which melts at 7°C and has a boiling point of 142.7°C. The pure liquid at 20°C has a viscosity of 460cP, which is similar to that of glycerol. In the absence of moisture, it can be handled in glass without any appreciable attack. It is a powerful oxidizing reagent with moderate fluorinating ability and reacts violently with water to form a hydrate ($SbF_5 \cdot 2H_2O$), which dissolves in more water to a clear and colorless solution.

Its preparation can be accomplished by direct fluorination of antimony or by the halogen

exchange of antimony pentachloride with anhydrous hydrogen fluoride.[104] The commercial product often contains some HF, which reduces the viscosity drastically. For purification, it can conveniently be distilled in high vacuum at room temperature or at normal pressure at elevated temperature. The thermal stability is sufficient to keep a sample at 250°C over several hours without any sign of decomposition.

Anhydrous solvents such as HF, SO_2, FSO_3H, $HOSO_2CF_3$, SO_2ClF and SO_2F_2 form clear solutions with SbF_5 in any ratio. Addition of SbF_5 to a pure acid produces a drastic increase in the acidity. Solutions of SbF_5 in HF or HSO_3F reach H_o values of nearly -30 (see Table 1, page 12)

The high solubility of SbF_5 in conjunction with the strength of this Lewis acid make it the best candidate for studying carbocations, using a variety of different methods (see Section 1.6 page 33). Antimony pentafluoride at room temperature forms oligomeric cisoid structures, in which each antimony is surrounded by six fluorine atoms in an octahedral arrangement.[105] In carbocation solutions the antimony fluoride counter anion is mainly the mono- to trimeric species **19 - 21**, depending on the SbF_5 excess used.

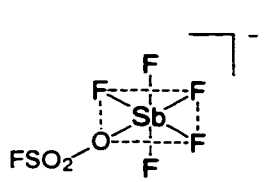

20

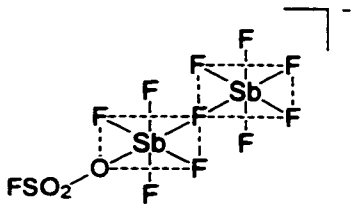

21

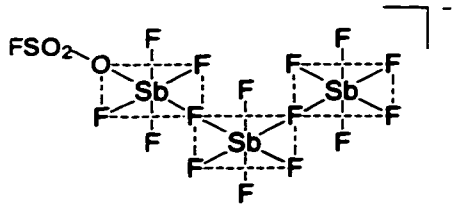

22

Fluorine NMR experiments of Magic Acid using different HSO_3F / SbF_5 molar ratios revealed that in solutions with up to 40 % SbF_5, the mono anion **19** is the most abundant counter anion, from 40 to about 60 % it is the dimer **20** and above 60 % the trimer **21**.[106]

However, even the strongest systems such as 10 % HSO_3F / 90 % SbF_5 or 20 % HF / 80 % SbF_5 still have limitations and many cations "observable" in the gas phase are too "electrophilic" to be observed in the condensed phase in these media. For example, the "naked" proton, considered as the "ultimate" electrophile, would require environments with an H_o value of -50 to -60, according to thermochemical gas-phase data.[56, 107] In fact, the unsolvated proton in the gas phase is so reactive, that it is able to protonate helium to form HeH^+.[108]

1.5.2.3 Techniques for Stable Carbocation Preparation

Olah and coworkers were the first to develop techniques for the preparation of solutions of stable alkyl carbocations.[109] The method of Olah consists of mixing a precooled solution of the cation precursor (mostly alcohol or chloride) in SO_2 or SO_2ClF with a cooled mixture of superacid using vortex stirring techniques. Typical temperatures for the generation of cations are -78°C (dry ice / acetone) or -116°C (N_2 / ethanol), depending on the nature of the generated cation.

An apparatus for the generation of carbocation solutions using syringe techniques was suggested by Kelly and Brown.[110]

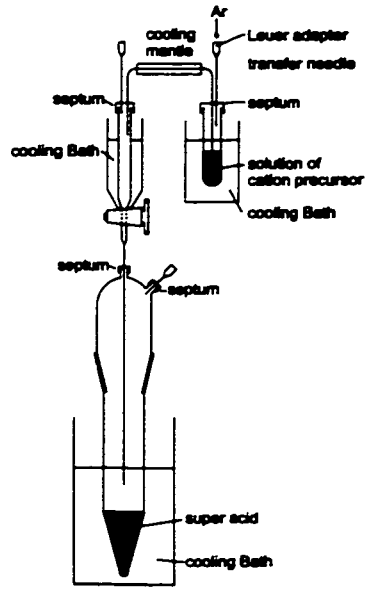

Figure 9: Apparatus designed by Kelly and Brown[110] for the generation of carbocation solutions.

For the generation of very thermally labile cations, the use of standard cooling baths such as dry ice / acetone (-78°C) or ethanol slush (-116°C) is not sufficient. In these cases 2-methylbutane (mp. -150°C) can be cooled with a stream of cold nitrogen, whose temperature can be regulated by heating a pool of liquid nitrogen. Ahlberg and Engdahl designed the following apparatus for the generation of a carbocation solution directly in an NMR tube.[111]

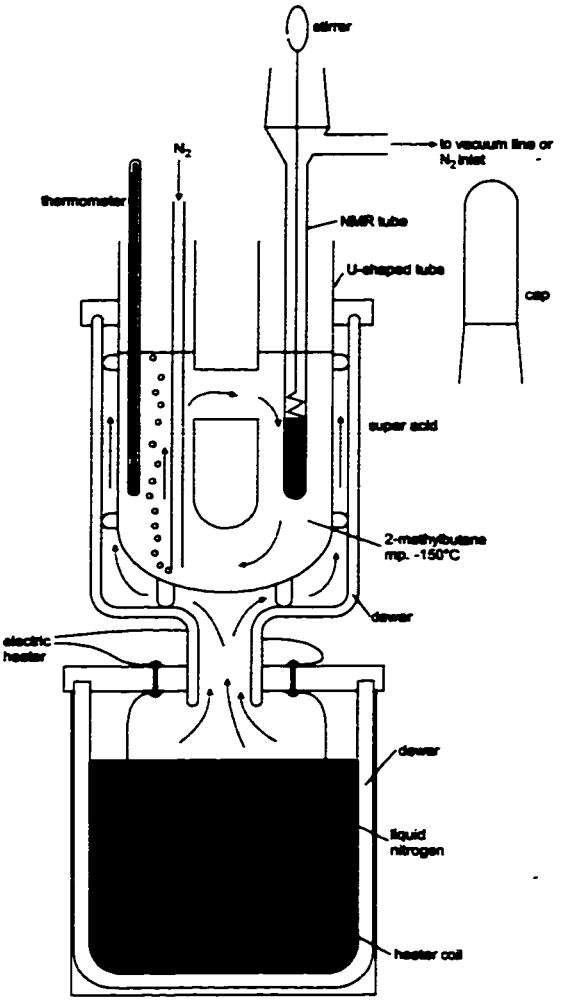

Figure 10: Apparatus designed by Ahlberg and Engdahl[111] for the prepartaion of carbocation solutions as low as to -150°C.

Since the ionization reaction is relatively exothermic (typically 30 to 40 kcal/mol for alcohols and 20 to 30 kcal/mol for chlorides) it is very difficult to prepare carbocation solutions without having transient "hot spots" developing in the sample. In the case of a thermally-labile carbocation, some rearrangement can therefore occur during the preparation stage. This problem is quite variable, so that some preparation attempts are more successful than others. Even when the cation generation is conducted at a temperature 30 to 50°C below the temperature where a rearrangement becomes rapid, this local heating can cause a significant amount of the initially formed cation species to rearrange. The protonation of alkenes for the generation of carbocations is often accompanied by polymerization reactions,

which result from having carbocations and alkenes in the same solution. Using conventional mixing techniques, these side reactions are extremely difficult to avoid.[112] Saunders and coworkers, however, have developed a method which allowed them to suppress competitive side reactions efficiently.

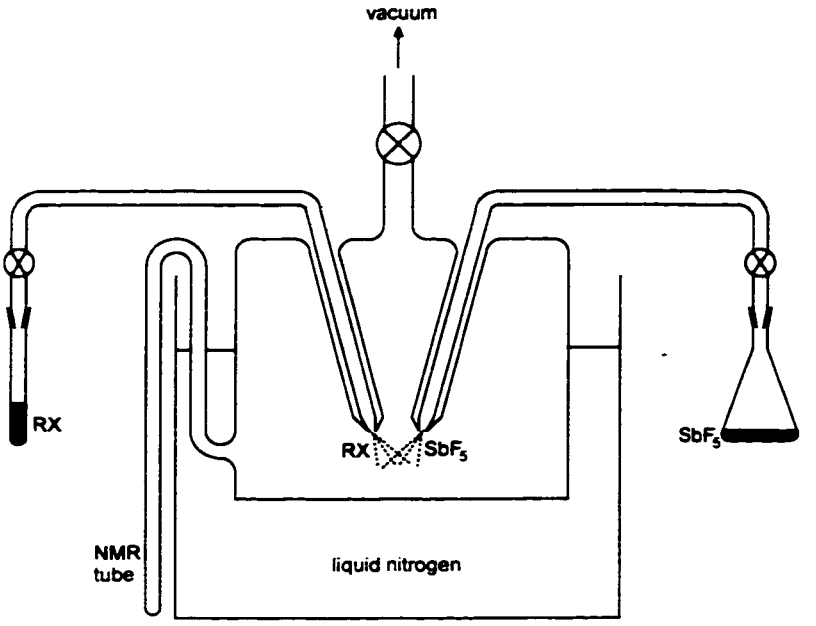

Figure 11: Apparatus for the generation of NMR samples using a matrix condensation technique developed by Saunders.[113]

Their procedure was to condense SbF_5 and the carbocation precursor simultaneously onto a surface of sulfuryl chloridefluoride or fluorosulfonic acid at cryogenic temperatures.[113] In this way, a matrix of superacid and starting material was produced, which could then be melted by warming the matrix to the desired temperature (i. e. -150°C to -120°C).

For the most reactive carbocations, these again were produced using matrix condensation techniques, but the resulting solid was then directly used for solid state NMR measurements. In order to load a CPMAS spinner with the solid sample at cryogenic temperatures and under an inert atmosphere a two piece setup was suggested,[114] as shown in Figure 12.

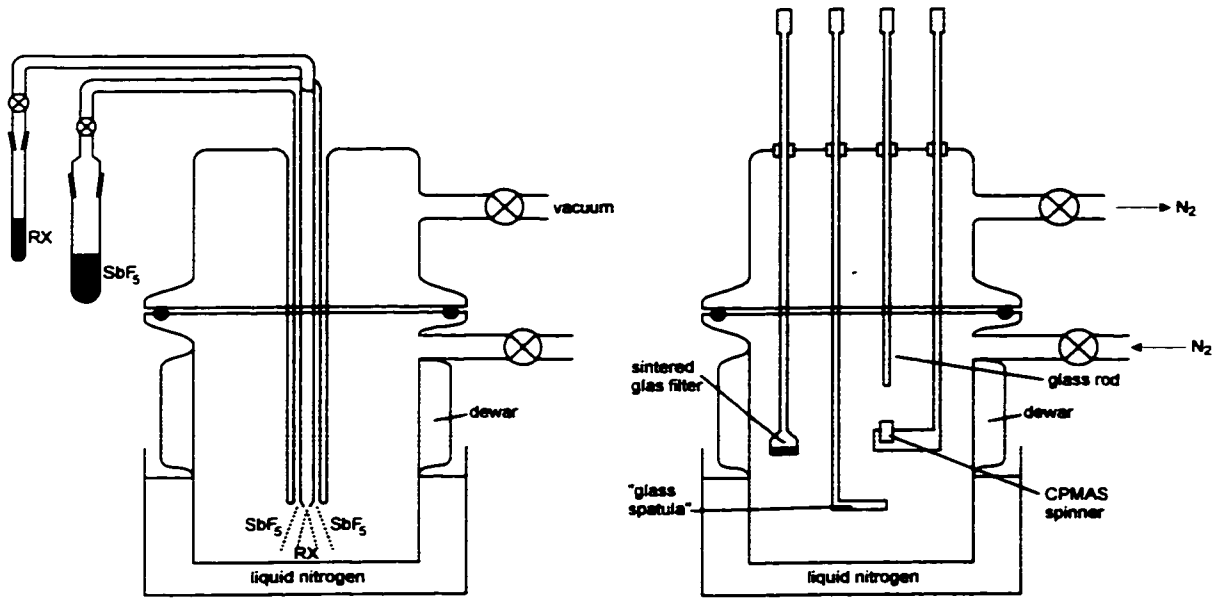

Figure 12: Apparatus developed by Vančik and Sunko for the preparation of solid state NMR samples at cryogenic temperatures.[114]

1.6 Observation Methods

1.6.1 Conductometry

Heterolytic dissociation of a neutral species forms ions, which are electrolytes and therefore capable of conducting electricity. Thus, conductivity measurements can be used to estimate the dissociation equilibrium into ions and the methods can also be used to probe ion-pair formation.

$$R{-}X \rightleftharpoons R^{+} + X^{-} \quad \text{or} \quad R^{+}//\,X^{-}$$

For example, sulfur dioxide solutions of triphenylmethyl halides show some dissociation into ions, as determined from conductivity measurements. The protonation behavior of alcohols, esters, anhydrides among other classes of compounds have been investigated by this method, using sulfuric acid, chlorosulfonic acids and hydrogen halides.[115]

1.6.2 Cryoscopy

A melting point depression depends on the molal concentration of dissolved particles and the cryoscopic constant of the solvent used. Ionization of a neutral compound, dissolved in an appropriate solvent, generates a larger number of particles and therefore increases the molal freezing point depression. For example, dissolution of an alcohol in strong acid can result in complete ionization, which forms four particles for every molecule of alcohol.

The very large cryoscopic constant of 6.12 K kg mol^{-1} and a convenient mp. of 10.37°C have made sulfuric acid very useful, and this solvent has been used extensively for the study of stabilized carbocations such as triphenylmethyl.[116] Less stabilized carbocations can be measured in the more acidic fluorosulfonic acid, which has a mp. of -88.98°C and a cryoscopic constant of 3.98 K kg mol^{-1}.[117] However, many alkyl carbocations require a much more acidic environment, which can only be obtained by preparing mixtures of the strong acids HF or HSO_3F with Lewis acids such as SbF_5. The latter forms oligomers in solution, whose molecular weight depends on the nominal SbF_5 concentration. Molal freezing point depression measurements therefore become unreliable in this type of system.

1.6.3 UV Spectroscopy

Despite initial reports of a UV absorption of alkyl cations at approximately 270nm, it was later shown that these carbocations do not posses any absorption bands above 210nm. The measured absorption could be traced to the formation of small amounts of substituted allyl cations.

Conjugated carbocations show characteristic UV absorptions, and the individual data for these has been summarized by Olah, Pittman and Symons.[118]

1.6.4 NMR Spectroscopy

NMR spectroscopy is by far the most important method for the observation of carbocations in solution or in the solid state. Chemical shifts, coupling constants, line broadening, temperature dependence of chemical shifts, use in measuring reaction rates, solid state NMR spectroscopy and nutation NMR spectroscopy have successfully been used for the exploration of structure and reactivity aspects as well as for the rearrangement pathways of a variety of different carbocations.[98]

1.6.4.1 Chemical Shift

The chemical shift of a hydrogen mainly depends on the diamagnetic shielding properties of its environment and is therefore a sensitive indication of the charge borne by this hydrogen. The secondary hydrogen of the isopropyl cation for example has a chemical shift of 13.5 ppm with the methyl hydrogens found at 4.5 ppm.[119] Typical chemical shifts of α-protons in alkyl cations are in the range of 4 to 4.5 ppm, with β-protons from 1.3 to 2 ppm (see Figure 13 for the definition of α or β position).

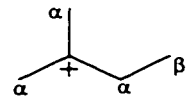

α - methyl hydrogens: 3.7 ppm
α - methylene hydrogens: 4.2 ppm
β - methyl hydrogens: 1.6 ppm

Figure 13: Hydrogen chemical shifts of the isopentyl cation.

The interpretation of ^{13}C-chemical shifts is more difficult, because a substantial paramagnetic deshielding is the largest contributor to the chemical shift of any given carbon, and this chemical shift parameter is not directly related to the charge density experienced by the carbon. According to Olah, Spiesecke and Nelson,[120] carbocations with similar hybridization and substitution relationships show relatively constant paramagnetic deshielding, with the chemical shift changes being a direct consequence of the charge variations of the particular carbon. The positively charged carbons in carbocations are found at very low fields compared to the values in related hydrocarbons. The distinct chemical shift behavior of different carbocations allows one to arrange them into four groups:

1. Classical alkyl cations:

The main stabilization of this class of carbocations occurs via C-H or C-C hyperconjugation but in some examples partial bridging (2-alkyl-2-norbornyl cation) or other unique types of delocalization exist, such as in the cyclopropylcarbinyl cations. These latter two species represent borderline cases which show some similarity to nonclassical cations or to the π-conjugated cation group. The positively charged carbon atom of a typical classical alkyl cation has a chemical shift of approximately 330 ppm. The following examples are illustrative (see Table 6).

Table 6: Selected carbocations and their corresponding chemical shifts.[121]

Compound	δ ^{13}C in ppm	Compound	δ ^{13}C in ppm
	321		337
	335		320
	335		379
	336		286

Some alkyl cations undergo reversible hydride or alkyl shift reactions, which are fast in terms of the NMR time scale (see also below, page 40). As a result of this, one can only observe an averaged signal at an unusual position. However, at very low temperatures it is usually possible to freeze out these reactions and one can then find typical chemical shift values for the cationic carbon in the range of 330 ppm (see Table 7 for examples).

Table 7: ^{13}C NMR data of equilibrating systems.[122]

carbocation	activation barrier $\Delta G^{\neq}$ [kcal/mol]	δ ^{13}C [ppm] averg. C1 / C2 / T [°C]	δ ^{13}C [ppm]; static C1 / C2 / T [°C]
	3.1	198 / 198 / -70	335 / 59 / -145
	3.5	197 / 197 / -80	330 / 55 / -108
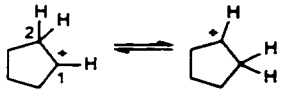	< 4.5	99 / 99 / -80	320 / 71 / -203
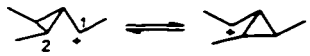	< 5	137 / 137 / -70	232 / 88 / -154

Many of the carbocations associated with this dissertation are classical alkyl cations and the carbon chemical shift of the C^+ is expected to be in the range of 330 ppm.

2. π-Conjugated cations:

Carbocations with substituents allowing conjugation experience significant stabilization by distributing the charge over two or more carbons.

Table 8: Selected conjugated carbocations and their corresponding chemical shifts.[123]

Compound	δ ^{13}C in ppm	Compound	δ ^{13}C in ppm
	231 / 147		319
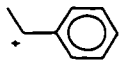	230	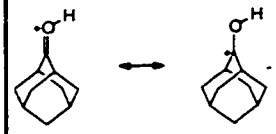	257
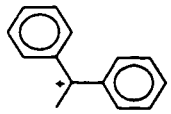	201	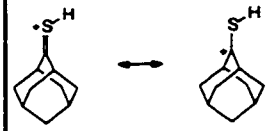	286
	285		

Electron donation involving π-type interactions can also occur in heteroatom substituted carbocations. Particularly stabilizing are nitrogen and oxygen stubstituents but even an

electronegative fluorine substituent has a stabilizing effect on a carbocation center if the electron demand is large. The chemical shift of the cationic carbon atom of various heteroatom substituted cations are given in Table 8.

3. Aromatic carbocations:

Cyclic carbocations stabilized through aromatization show an exceptional stability. Well known examples are the dibenzotropylium and tricyclopropylcyclopropenyl cations. Figure 14 shows relevant carbon chemical shifts.

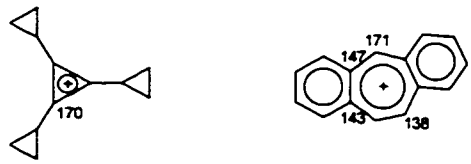

Figure 14: ^{13}C NMR shifts of aromatic carbocations.

4. Nonclassical carbocations

Carbocations possessing four or more coordination sites are considered nonclassical. The change of the total chemical shift sum comparing the cation with the corresponding hydrocarbon is in general considerably smaller for nonclassical than for classical carbocations. This smaller difference has also been used as a criterion to distinguish between classical and nonclassical carbocations.[124] However, rather than a strict separation between these two groups of carbocations, numerous examples with various degrees of nonclassical character were found.

Some of the unusual chemical shifts found in nonclassical cations are shown in Table 9.

Table 9: Examples of chemical shifts in some nonclassical carbocations.

carbocation	δ ^{13}C [ppm]	compound	δ ^{13}C [ppm]
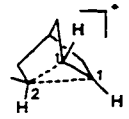	C1: 125 C2: 21	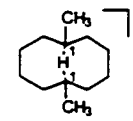	C1: 142
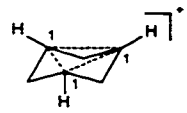	C1: 5	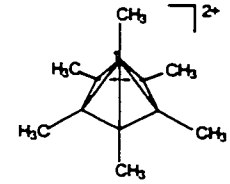	C1: 2

1.6.4.2 Coupling Constants

The magnitude of the ^{13}C-^{1}H coupling constant reflects the hybridization of the corresponding C-H bond, revealing valuable geometrical information of the particular carbon center in question. The empirical formula **(20)** allows one to calculate the s-character of the carbon under consideration (typical value for an sp^3 C-H: 124 Hz, and for an sp^2 C-H: 172 Hz).[125]

$$^{1}J_{CH} = 570 \cdot s_C - 18.4\,Hz \qquad \textbf{(20)}$$

$^{1}J_{CH}$ = ^{13}C-^{1}H coupling constant in Hz
s_C = s character of the carbon atom in %

However, the number of NMR observable carbocations possessing a C-H bond with the cation center is very limited. One example is the classical isopropyl cation, whose C^+-H coupling constant was measured as 169 Hz, reflecting the profound sp^2 character of the cation center. The nonclassical μ-hydrido bridged carbocation group is another class of compounds with C-H bonds to positively charged carbon centers (partial formal bond), for which C-H coupling constants provide valuable geometrical information (see also Section 1.8, page 54). Values in the range of 35 to 40 Hz were found to be typical for the μ-hydrido C-H-C bond.

Another typical feature of carbocations in terms of NMR coupling constants is the presence of relatively large ^{4}J H-H long range coupling as shown in Figure 15. While these couplings are usually too small to be observed in neutral compounds such as hydrocarbons, a value of 4 to 6 Hz is often observed in carbocations.

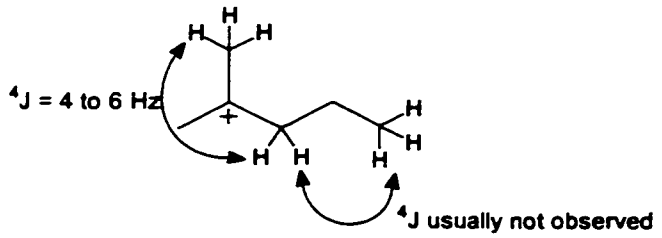

Figure 15: ^4J Couplings in carbocations.

1.6.4.3 NMR Line Broadening

NMR measurements of two interconverting compounds show separate sets of signals if the exchange rate is slow (*ca.* 10 s^{-1} or less). An increased exchange rate causes the individual signal pairs (e. g. one particular carbon atom in one compound and the same carbon atom in the rearranged compound) to collapse and finally to form a peak at the averaged position (see Figure 16 for an illustration).

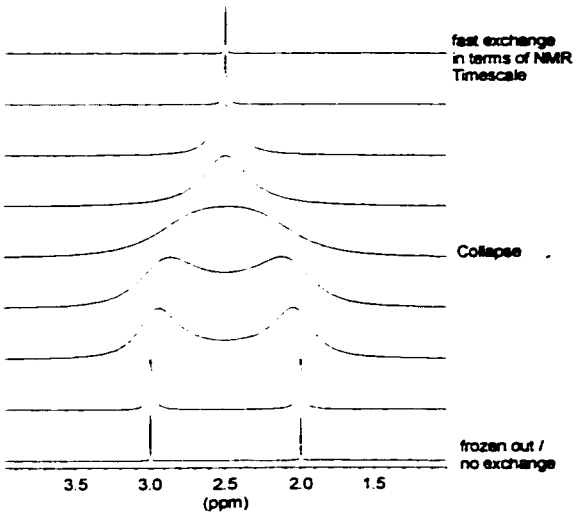

Figure 16: Typical NMR spectra of two exchanging spins at different rates.

At the point of signal collapse or coalescence, the exchange rate can be estimated according to equation **(21)**, in which ν_{AB} represents the frequency difference of the two exchanging signals.

$$k_{ex} = \frac{\pi}{\sqrt{2}} \nu_{AB} \qquad \textbf{(21)}$$

More accurate results can be obtained by line shape analysis of the experimentally obtained spectra.[126] Using this NMR technique, energy barriers of reversible exchange reactions with values as low as *ca.* 6 kcal/mol can be measured. Since the cation center C^+ possesses an empty orbital, carbocations are particularly prone to rearrangement reactions, with many examples known.

1.6.4.4 Temperature Dependance of Chemical Shifts for Rapidly Equilibrating Systems

If an equilibrium involves two compounds with different heats of formation, the concentration of each individual compound becomes temperature dependant. Since the resulting NMR signal consists of a weighted average of the two chemical shifts, a change in concentration as a result of a temperature variation can cause the averaged chemical shift to change accordingly.

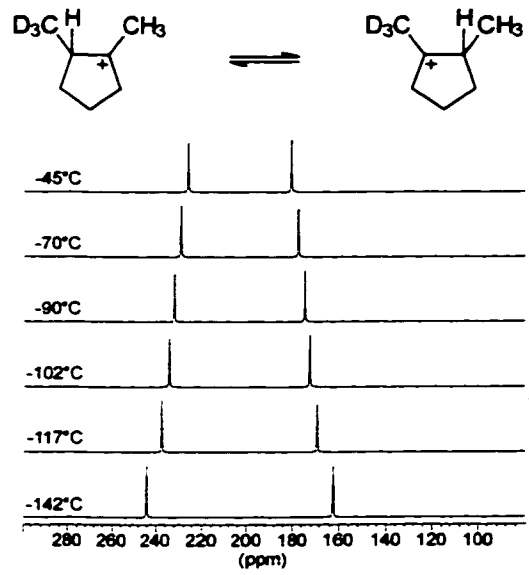

Figure 17: Isotopic perturbation of the dimethylcyclopentyl cation according to Saunders and coworkers.[127]

Many equilibrium systems however involve "two" structures with identical heat of formation (degenerate equilibria), thus a change in temperature has no effect on the averaged chemical shift. In this case, one can use Saunder's isotopic perturbation method.[127] Isotopic desymmetrization causes the two initially equivalent compounds to become different in terms of heats of formation and to therefore show temperature dependent chemical shifts (an example is shown in Figure 17).

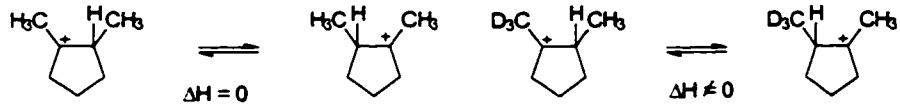

This technique is important for distinguishing between a rapid equilibrating system or a static structure, if the barrier for the exchange reaction is too low to be frozen out using NMR spectroscopy.

1.6.4.5 Reaction Rate Measurements

Irreversible rearrangement reactions can also be followed by NMR spectroscopy. Most of these rearrangement reactions are first order reactions, illustrated by equation **(22)**.

$$A \longrightarrow B \qquad (22)$$

The associated energy barrier can be calculated using the transition state theory.

$$\Delta G^{\#} = -RT\, ln\frac{k_R \cdot h}{k_B \cdot T} \qquad (23)$$

k_R = rate constant
k_B = Boltzmann constant
h = Planck constant

A temperature of -150°C is the lowest feasible temperature for preparing carbocation solutions, and for measuring them with conventional NMR spectrometers. From equation **(23)**, and using a cation preparation time in the order of minutes, then the lowest possible $\Delta G^{\#}$ that can be measured is approximately 10 kcal/mol.

However, in observing cation systems with low rearrangement barriers, two other aspects become important. First, thermally labile carbocations need to be generated at a temperature which is 30°C to 40°C below the temperature where the rearrangement becomes rapid (see Section 1.5.2.3, page 31). Second, at temperatures as low as -150°C, only dilute concentrations of the carbocation in a superacid - SO_2ClF - SO_2F_2 solution can be prepared and even these mixtures can become viscous, causing the absorption peaks to become broad and weak.

1.6.4.6 Solid State NMR Spectroscopy

The development of cross-polarization and magic-angle spinning techniques (CPMAS) allow one to record ^{13}C NMR spectra of solids with sufficient resolution to recognize the individual signals of many carbocations. Yannoni, Myhre and Fyfe have obtained solid state spectra at temperatures as low as 5K.[128]

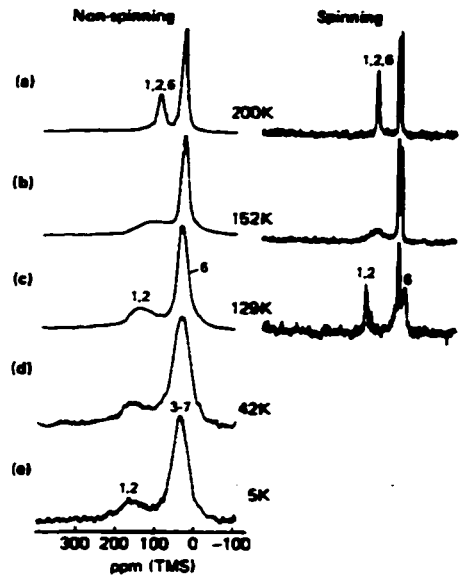

Figure 18: Variable temperature CPMAS NMR of the norbornyl cation.[128]

The availability of NMR data at such low temperatures is useful for the detection of very low energy degenerate rearrangement processes. For example, the absence of any low field peak at ca. 330 ppm for the 2-norbornyl cation at 5 K (see Figure 18) showed with high certainty that this species was a symmetrical nonclassical cation and this result helped to end the controversy about this system (see Section 1.2, page 7). Another example is the cyclopentyl cation, whose rapid 1,2 hydride shifts could be frozen out at cryogenic temperatures using solid state NMR techniques (see Table 7, page 37).

1.6.4.7 Nutation NMR Spectroscopy

In solids, two magnetic nuclei in close proximity experience a dipolar coupling, which is not canceled through fast tumbling of the molecule as in solution NMR. This dipolar coupling depends on the distance between the two nuclei and with appropriate pulse sequences, eliminating the J-coupling through bonds, generates a "Pake" doublet. Comparing the doublet shape with calculated spectra allows one to measure the distances between the two nuclei. The advantages of this method, called nutation spectroscopy, are that polycrystalline compounds can be used at cryogenic temperatures.[129]

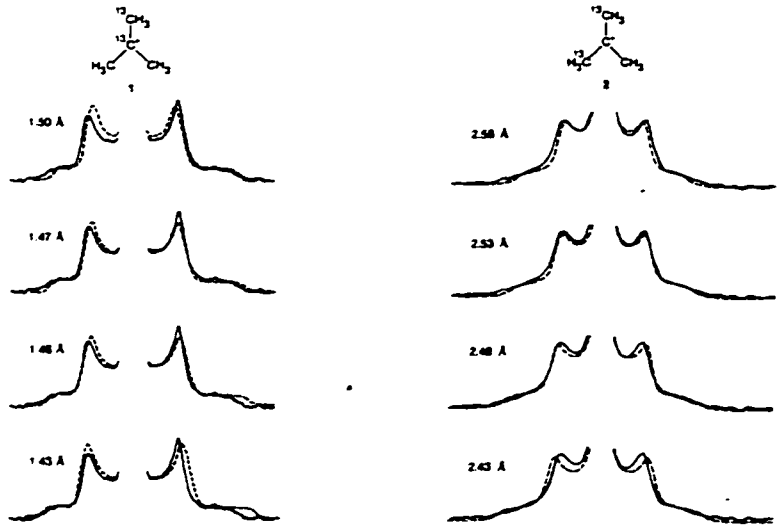

Figure 19: Determination of C-C bond length in the *tert*-butyl cation using nutation NMR techniques.[130]

Using various ^{13}C enriched carbocations, Yannoni and coworkers[130] measured the C-C bond distance and the C-C-C angle of the *tert*-butyl cation (see Figure 19), which agree well with the theoretically computed values.

1.6.5 IR and Raman Spectroscopy

The first reported IR spectrum of a carbocation was published by Olah and coworkers and involved the *tert*-butyl cation.[131] Later, the IR spectra of stabilized cations such as the tropylium, cyclopropylcarbinyl and triarylmethyl cations were reported.[132] Substantial technical difficulties were found preparing concentrated samples and in recording the spectra, and this prevented this method from becoming popular in the field of carbocation chemistry.

The development of fast computers, allowing one to calculate accurate vibrational frequencies for reasonably large molecules (10 to 15 "heavy", non hydrogen atoms), greatly increased the attractiveness of IR spectroscopy in this field. A further step was achieved when Craig and coworkers[133] designed a technique to record IR spectra of polycrystalline carbocations. This method was then further perfected by Sunko and coworkers who used Saunders molecular beam technique to produce a carbocation matrix film on a CsI plate,

suitable for recording IR spectra.[134]

IR spectroscopy can be extremely helpful in distinguishing between a fast equilibrium process and a static structure, due to the shorter time scale of IR spectroscopy (10^{-13} s) compared to NMR spectroscopy.

1.6.6 Mass Spectroscopy

The only direct information mass spectroscopic techniques provide are the molecular weight and the abundance of cationic species, *ca.* 10^{-7} to 10^{-10}s after their generation by electron impact or electromagnetic irradiation. However, using graduated irradiation energies can yield information about the stability of cations in the gas phase. High pressure mass spectroscopy allows one to perform ion molecule reactions which provides information about the relative stability of carbocations through proton, hydride or halogen transfer reactions (see also Section 1.5, page 24). Ion cyclotron resonance spectroscopy can keep the generated cations in a specially designed chamber for up to about 1 s, which is useful for studying a variety of different ion molecule reactions.[135]

The drawback of this spectroscopy is the difficulty of deriving structural information, which is only available in a limited way through various advanced techniques.

1.6.7 ESCA

Core electron spectroscopy for chemical analysis, called ESCA, utilizes high energy x-ray beams to initiate core electron emission from a particular atom.[136] The ionization process takes in the order of 10^{-16} s, which like IR spectroscopy, provides "instantaneous" structural information.

The "binding" energy of the 1s electrons in a carbon atom (280 to 290 eV, corresponding to *ca.* 6500 to 6700 kcal/mol) depends slightly on its chemical environment. However the differences between various neutral hydrocarbons are rather small and the resolution of ESCA spectroscopy does not allow one to distinguish between the carbons of hydrocarbons such as ethane, ethene or ethyne. Larger binding differences of the 1s electrons are observed in positively charged carbon atoms when compared to neutral ones. For example, the *tert*-butyl

cation has approximately a 4 eV (92 kcal/mol) higher binding energy than the corresponding carbon of the neutral hydrocarbon.

Table 10 illustrates the binding energy (E_b) of 1s electrons in some selected compounds.[137]

Table 10: ESCA energies of some selected compounds.[137]

compound	E_b [eV]	ΔE_b [a] [eV]
	290.6	
	290.7	
	291.2	
	289.8	3.9
		4.3
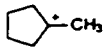		4.2
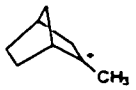		3.7
		1.5

[a] ΔE_b = ESCA energy difference of between the cation and the corresponding hydrocarbon.

1.6.8 X-Ray Crystallography

Due to the high reactivity of carbocations, the generation of single crystals suitable for x-ray crystallography is an extremely difficult task. Highly stabilized carbocations, such as the triphenylmethyl cation **22** or the substituted cyclopropenylium cation **23**, are stable at room temperature and were the first carbocations to be analyzed by x-ray crystallography.

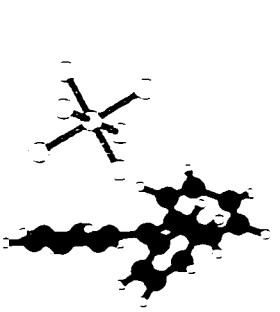

22

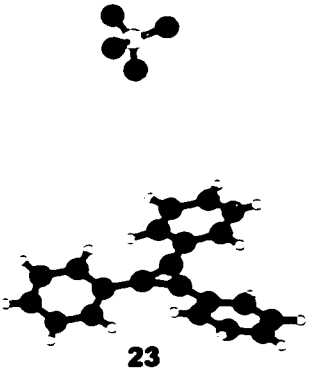

23

In general, relatively stable (stable at -25°C) carbocation salts can be obtained as hexafluoroantimonates by reacting the corresponding alkylfluoride with antimony pentafluoride in 1,2,2-trichloro-1,2,2-trifluoroethane.[138]

Alternatively, alkyl chlorides can be reacted with antimony pentafluoride in HF. However, these systems usually require a working temperature of -70°C. The solubility of carbocations in freons is relatively low and addition of these solvents to a concentrated superacid solution of a carbocation can be used to initiate crystallization.[139]

X-ray crystallographic data on alkyl cations stabilized only by C-C or C-H hyperconjugation is rare, hence only a few of these structures have been determined. Two examples are the $Sb_2F_{11}^-$ salts of *tert*-butyl cation **24**[140] and the trimethyladamantyl cation **25**.[141]

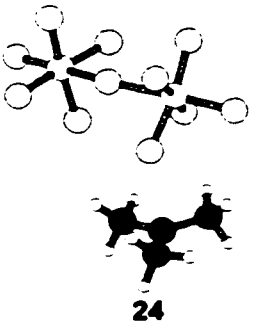

24

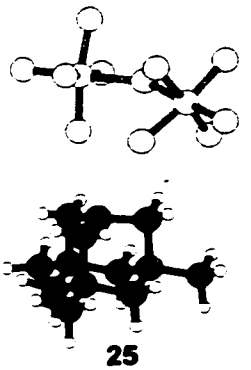

25

The availability of a crystal structure of the norbornyl derivative **26**[142] provides one with valuable information about the much argued nonclassical character of these systems, as determined from NMR experiment and *ab initio* calculations.

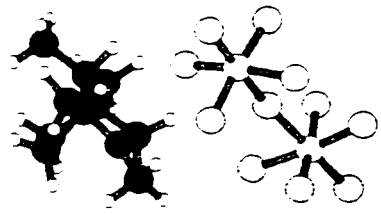

26

1.7 Calculation Methods

Molecular orbital calculations became routine in the 1970's after the development of a gradient based algorithm by Pulay,[143] allowing one to optimize molecular geometries. However, it was quickly recognized that accurate calculations required an enormous amount of computer power. The availability of high performance computers have improved tremendously during the past five years and it is now possible to calculate relatively large systems (10 to 15 atoms of second row elements) at levels adequate to achieve good agreement with experimental data. However, computing power requirement still represents a major problem, because it is desirable to calculate bigger systems at even higher levels of theory.

Attempts to reduce the demand for computer power has led to the introduction of various approximations using a variety of calculation methods. The presently available calculation methods can be divided into three groups.

1. molecular mechanics calculations

2. semiempirical calculations

3. *ab initio* calculations

The fastest method for calculating molecular structures is the molecular mechanics method.[144] This method uses parameters such as optimal bond distances, bond angles etc. for each atom to arrange the geometry of particular molecule in a way to minimize the deviation of these parameters. However, this method does not calculate molecular orbitals, and therefore properties such as the energy and shape of the HOMO or LUMO, NMR chemical shifts etc., cannot be obtained. The output from these calculations usually consists of a "strain" energy and an optimized geometry.

Relatively fast for calculating molecular orbital properties are the semiempirical methods. These methods use experimental data in the evaluation of the energy. The availability of various different parameter sets provides the possibility of calculating molecular orbital properties for a large variety of compounds, and for achieving a reasonably good agreement with experimental data.[145]

The most universal type of calculations are the *ab initio* calculations, whose accuracy mainly depend on the level of the approximations made.[146] One limitation involves the basis set used, which defines the "flexibility" of the electrons in the molecule under consideration. The use of more basis functions however results in a large increase in computer time needed for the calculation. A second type of approximation is in the treatment of electron correlation, which describes interactions between electrons. The simplest case is Hartree-Fock theory, which considers only a single assignment of electrons to orbitals (single electron configuration), neglecting the electron correlation energy completely.

For the inclusion of electron correlation energies, different methods have been suggested, of which Møller-Plesset perturbation methods and density functional theories are most frequently used. The designation MP2 or MP3 corresponds to the extent of which the Rayleigh-Schrödinger perturbation expansions are considered.[147] However, the use of MP2 methods is extremely expensive in terms of computing power, which increases to the 4^{th} order of the number of basis functions. Density functional theories include correlation energy by using an electron gas, described with different functionals of the density.[148] The advantage of this method is the speed, which is of the same order as a Hartree-Fock calculation. Becke[149] combined the Hartree-Fock method with selected functionals, constructing very accurate

calculation methods, and involving reasonably economical computer power. The most frequently used method of this kind is the Becke3LYP variant.

Table 11: Suggested protocol for the *ab initio* calculations at various levels of theory.

Basis set	Correlation method			
	HF	MP2	MP3	MP4
STO 3G				
3-21G				
6-31G*				
6-311+G**				

In order to find a proper balance between the size of the basis set, the calculation method, and the time demand on a computer, a variety of different basis sets and methods have been applied to specific systems[150] whose calculation results could be compared to experimental values. The outcome of this investigation suggested that one could improve Hartree-Fock calculations up to the 6-31G* basis set.[151] Further increase of the basis set size does not result in a significant improvement of the calculation results, which is known as the Fock limit. Using at least a basis set of 6-31G*, one can then use a variety of different correlation methods to achieve more accurate calculation results (see Table 11).

In this dissertation the following protocol was used for calculating structures.

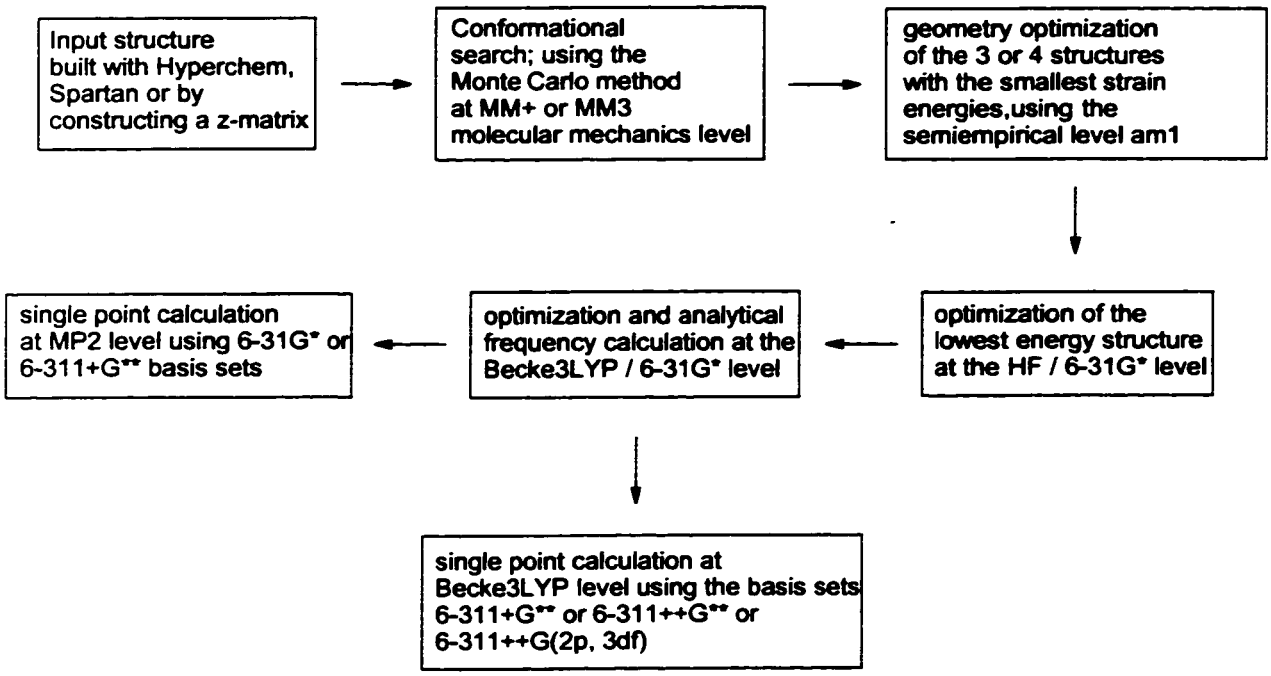

1.8 μ-Hydrido Bridged Carbocations

In 1952, Cope and Prelog independently reported the occurrence of transannular shifts in the dihydroxylation reaction of cyclooctene.[152]

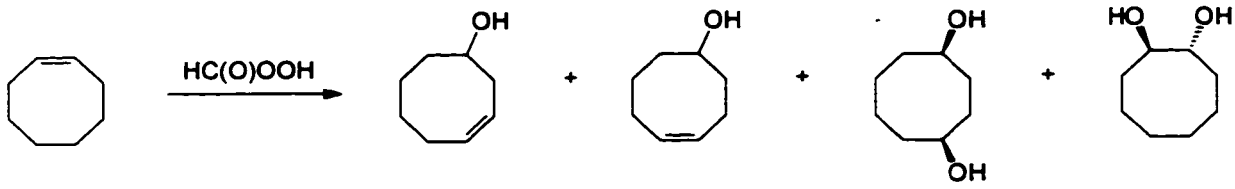

Deuterium labeling experiments by Cope and Roberts[153] showed that both 1,3- and 1,5-hydride shifts occur. Initially, the stereospecifity of the formation of the cis 1,4-diol could not be explained by a "normal" 1,5-hydride shift. Later, a μ-hydrido bridged species was suggested to be involved.[154]

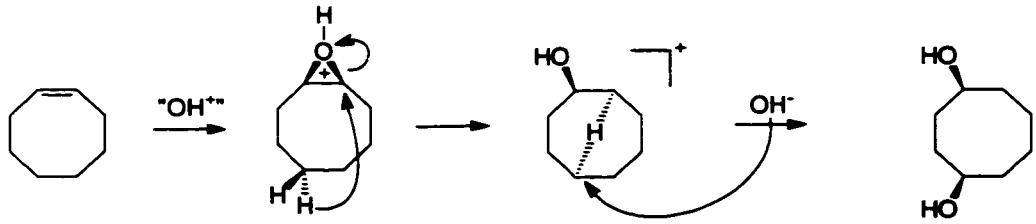

First thought to be transition states, μ-hydrido bridged carbocations were later shown to be intermediates and the first spectroscopic evidence for the existence of a μ-H carbocation was published in 1978.[41, 155]

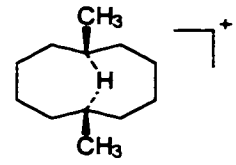

8

In the following few years a variety of different μ-hydrido bridged carbocations were prepared, revealing that certain structural requirements have to be met in order to obtain an observable μ-hydrido bridged carbocation.[156]

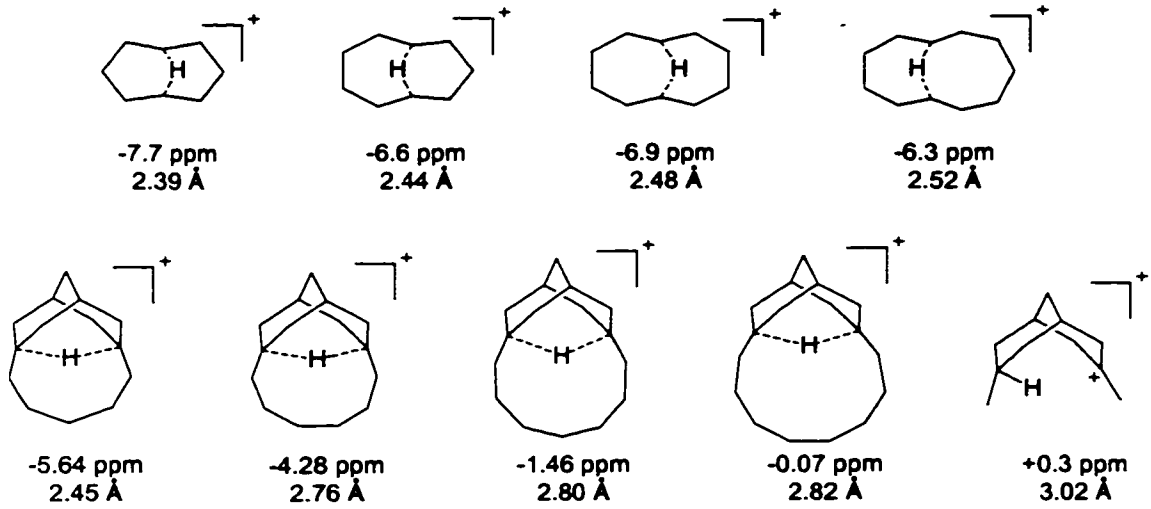

Figure 20: A series of secondary and tertiary μ-hydrido bridged carbocations with the experimental chemical shift of the μ-hydrogen and the calculated bridgehead distance (this work) at Becke3LYP / 6-31G*.[156]

Studies on a series of secondary and tertiary systems with various bridgehead distances showed that the latter need to be in the range of 2.4 to 2.5 Å. Larger bridgehead distances result in the formation of classical cations, usually involving rapid equilibrating hydride shifts. The lower series of tertiary μ-H cations illustrated in Figure 20 show a gradual change from a stable μ-hydrido bridged carbocation (bridgehead distance 2.45 Å) to a system involving rapid hydride shifts (bridgehead distance 3.02 Å). This gradation can also be followed by observing the change in the NMR shift of the μ-hydrogen. The more distinct the μ-H bond is,

the higher field the chemical shift, which reachs a maximum in the cyclooctyl system of -7.7 ppm (see Figure 20).

Proof for the μ-H bridged species possessing a single energy minimum rather than a double well minimum, as in a rapidly equilibrating system, was obtained using IR spectroscopy, a consideration of C-H coupling constants, Saunders' isotopic perturbation criterion and the Altman-Forsén test. IR stretching frequencies of the μ-hydrogen are distinctly different from the usual 2 center - 2 electron bonded hydrogens. The μ-hydrido bridged bicyclo[4.4.4]tetradecyl cation, for example, showed a value of 2113 cm^{-1}, which agreed rather well with the theoretically predicted value of 2019 cm^{-1}.[157] Symmetrically bonded μ-hydrogens should exhibit an equal coupling to both bonded bridgehead carbons and with a much smaller coupling constant than for an alkane C-H bond (J = 120 to 125 Hz). For most of the μ-H cation structures, coupling constants of 35 to 40 Hz, which are distinctly different from the expected 60 to 65 Hz for a rapidly equilibrating species (average of 120 to 125 Hz for the saturated C-H bond and 0 Hz for the no bond).[82] Another useful method to distinguish between a system with a double well energy potential (rapidly equilibrating system) and a single well potential is Saunders' isotopic perturbation method (see also Section 1.6.4.4, page 42).

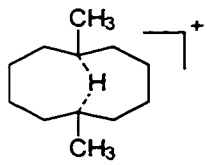

8

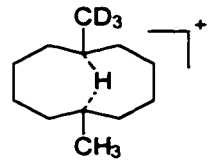

27

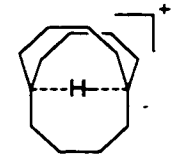

28

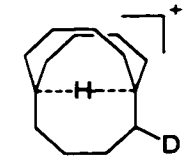

29

Using this method the μ-H cations **27** and **29**, for example, showed a chemical shift difference for the bridgehead carbons compared to their parent systems of only 0.6 or 0.8 ppm and no temperature dependance could be measured, indicating a static structure rather than rapidly equilibrating structures.

Theoretical treatment of these μ-hydrido bridged species revealed a large discrepancy between the calculated μ-H chemical shifts and the experimentally measured values. Calculations at an MP2/6-31G** // HF/6-311G** (GIAO-CPHF) level predicted -10.06 ppm for the μ-H of cation **28** compared to the experimental value of -3.46 ppm.[158] Cioslowski

suggested that large vibrational motions of the μ-H hydrogen at 298 K, as a result of a very flat energy profile for the movements of this hydrogen, was a likely cause for the discrepancy, since calculated structures assume frozen positions for all atoms at 0 K.[159]

McMurry and coworkers have prepared a series of μ-H bridged bicyclic cations, where the bicyclic bridges were [6.4.2], [6.3.3], [5.4.4] and [4.4.4]. They observed relatively large differences in the μ-H chemical shifts in these structures, and proposed that the C-H-C bond angle was the critical factor in determining the differences. This correlation was based on semi-empirical AM1 calculations of the cation geometries, and is shown in Figure 21.[157b]

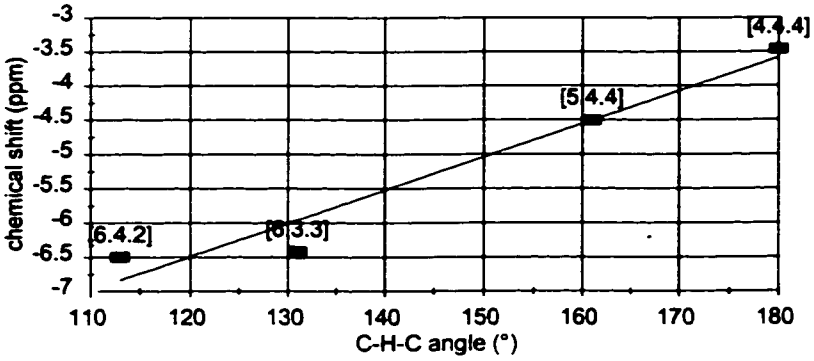

Figure 21: Correlation of the calculated C-H-C bond angle (AM1) vs. the experimental chemical shift of the μ-hydrogen.[157b]

Considering the stability of these cations, it was found that secondary μ-H carbocations were thermally extremely labile. The cyclooctyl system for example rearranges into the methylcycloheptyl cation at -150°C within minutes. A number of tertiary bridged cations on the other hand proved to be much more stable, and solutions of tricyclo[7.3.1.$1^{3,11}$]tetradecyl or the bicyclo[4.4.4]tetradecyl cations were found to be unchanged after keeping them at room temperature for several hours.[82, 157] The stability in terms of acidity also showed exceptional values, and the tricyclic cation was found to have a pK_a value of -1.00 and the bicyclic +4.75.

Extending the idea to a carbocyclic system with an even closer bridgehead distance to form should result in the formation of a hyperstable μ-H cation (stable at room temperature and possessing a pK_a value of greater than 7). This idea led then to the initial project goal of this dissertation - to synthesize a μ-hydrido bridged cation in a bicyclo[3.3.3]undecyl carbocyclic framework.

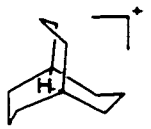

30

1.9 Scope of this Dissertation

As mentioned, the original aim of this project was to prepare a μ-hydrido bridged cation with a bicyclo[3.3.3]undecyl framework **30**.

All the known μ-hydrido bridged carbocations have been prepared by the same approach, which consists of having a carbocyclic system possessing a C=C double bond and a C-H bond in close proximity, and protonating the double bond to generate a cation. The hydrogen in close proximity then instantly interacts with the cation center to form the μ-H bridged structure.

Due to the small size of the [3.3.3] bicyclic system, a different approach was needed (for a discussion of the different approaches, see Section 2.1, page 58). The initial intention was to generate the dication **31** and hope that the large charge repulsion between the two close cation centers would allow a hydride shift from the 3 position of the ring to form the desired μ-hydrido bridged cation **32**.

31 **32**

The attempted preparation of the dication **31** involved a long linear synthesis of the corresponding dihydroxy hydrocarbon skeleton, but this was ultimately unsuccessful at the last step. As a consequence of this, other approaches to the formation of this μ-hydrido bridged

bicyclo[3.3.3]undecyl structure were formulated. One of these involved the attempted preparation of the bishomoadamantyl cation **33**.

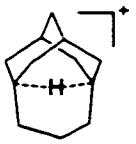

33

The synthesis of the bicyclic and tricyclic cations, as potential precursors for μ-H bridged cations, led to the discovery of three different rearrangement reactions.

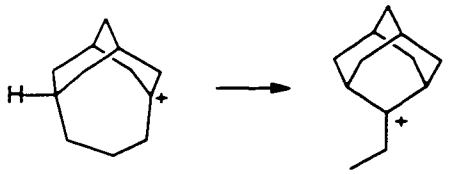

34 **35**

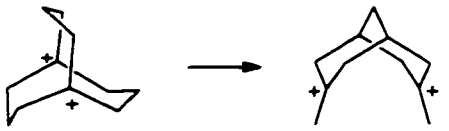

36 **37**

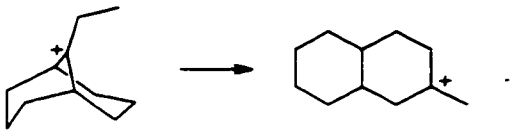

38 **39**

The theoretical and experimental exploration of these rearrangements was then studied in detail and the results are described in Sections 2.2.3.1 through 2.2.3.3.

All of the experimental details are described in one experimental section, and some details of theoretical calculations are summarized in Appendix A. Appendix B contains details on the x-ray structure of tricyclo[5.3.1.$1^{3,9}$]dodecane-5,9-diol, the precursor of dication **40**.

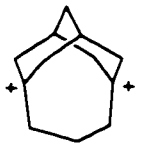

40

Chapter II

Bicyclo[3.3.3]undecyl and Tricyclo[5.3.1.1^{3,9}]dodecyl systems

2.1 Possible Routes to Bicyclo[3.3.3]undecyl and Tricyclo[5.3.1.1^{3,9}]dodecyl μ-H cations

In principle there are three different routes for the construction of a μ-H bridged cation (see Figure 22).

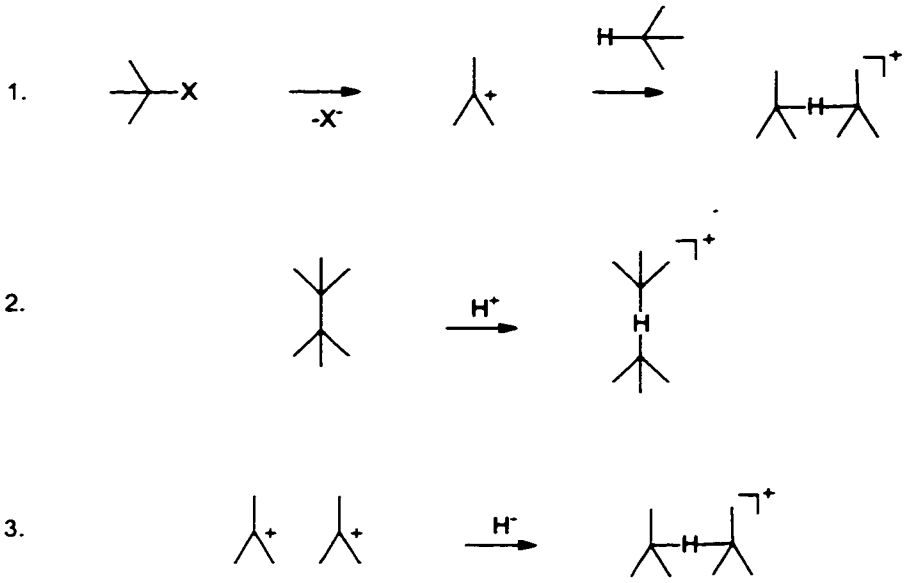

Figure 22: Three principal approaches for the production of a μ-H bridged cation.

The first approach consists of the generation of an "ordinary" carbocation, which can be accomplished by various means, in a skeleton having an appropriate C-H bond in close proximity, which then causes an immediate interaction to form a μ-H bond. A completely different method is pictured in the second approach, in which a C-C bond is protonated to form the desired cation. The third principal approach is the reduction of a dication with a hydride to form the μ-H bridged monocation.

Considering the target molecules **30** and **33**, their close resemblance is obvious (see Figure 23).

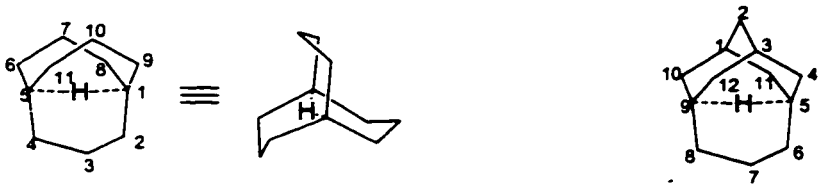

30 **33**

Figure 23: Bicyclo[3.3.3]undecyl and tricyclo[5.3.1.1^{3,9}]dodecyl μ-H bridged cations.

Applying the above approaches to the bicyclo[3.3.3]undecyl or tricyclo[5.3.1.1^{3,9}]-dodecyl systems results in the five following possible routes leading to **30** and **33**.

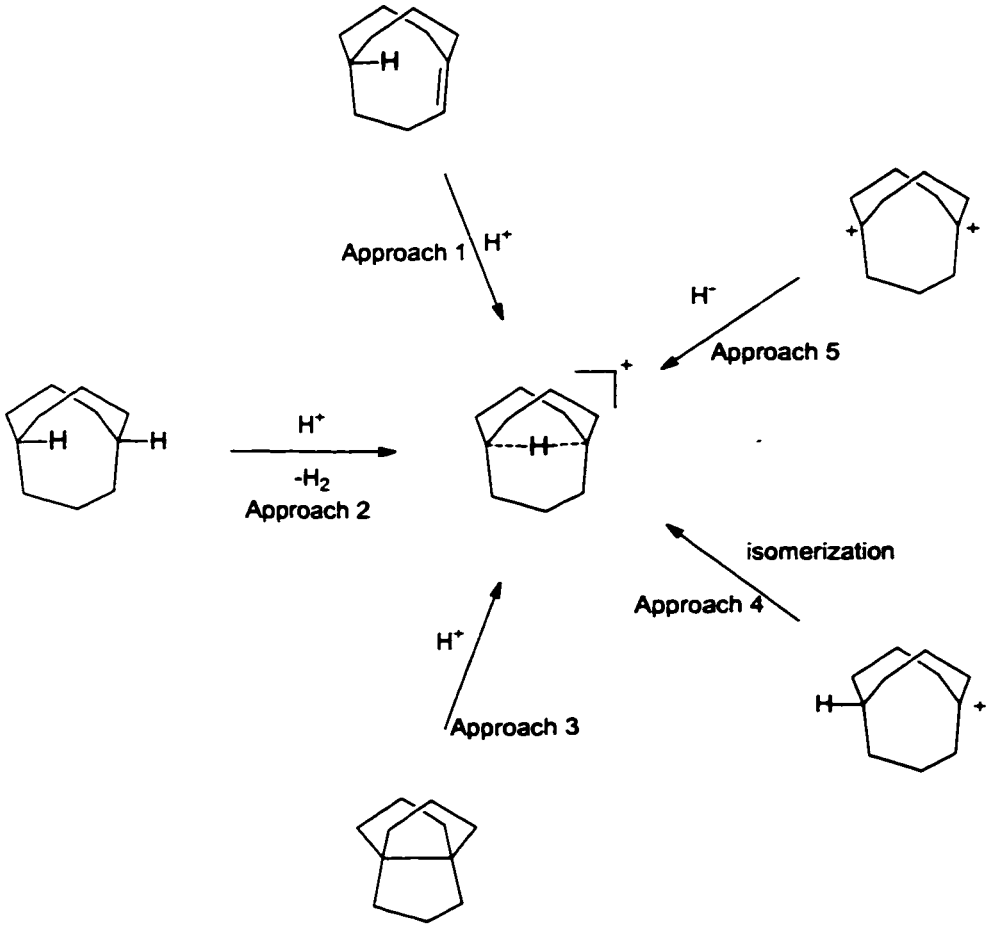

Figure 24: Five possible approaches to bicyclo[3.3.3]undecyl and tricyclo[5.3.1.1^{3,9}]dodecyl μ-H bridged cations (In order to simplify Figure 24 the bicyclo[3.3.3]undecyl system is representative for both target systems).

2.1.1 Approach 1 and 2

The possible approaches 1 and 2 are closely related and are most conveniently discussed together. These approaches have been used for the generation of all known μ-H bridged carbocations prepared to date.[156] Applying these approaches to the two target molecules **30** and **33** leads to the precursors *in*-bicyclo[3.3.3]undec-1-ene **41**, *in-out*-bicyclo[3.3.3]-undecane **42**, *in*-tricyclo[5.3.1.$1^{3,9}$]dodec-1-ene **43** or *in-out*-tricyclo[5.3.1.$1^{3,9}$]dodecane **44**.

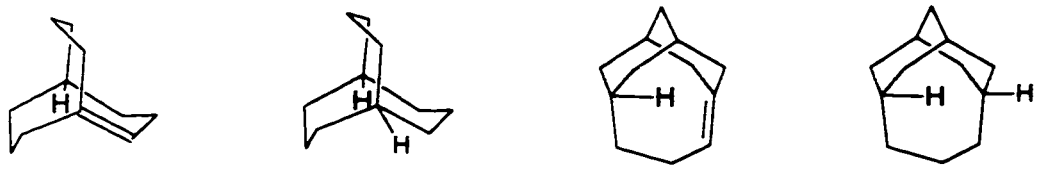

41 **42** **43** **44**

Protonation of the alkenes **41** and **43** would then generate the corresponding bridgehead cations **45** and **46**, which would instantly undergo interaction with the *in*-hydrogen to form the corresponding μ-hydrido bridged cations **30** and **33**.

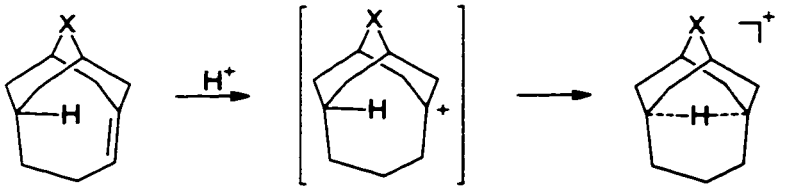

X = CH_2: **43**
X = – : **41**

X = CH_2: **46**
X = – : **45**

X = CH_2: **33**
X = – : **30**

Treatment of the in-out alkanes **42** and **44** with super acids would protonate the tertiary out-hydrogen producing **47** and **48**. The loss of dihydrogen, representing the reversed reaction of an ionic hydrogenation, would again generate the bridgehead cations **45** and **46**, which, as before, would instantly form the μ-H bridged structures **30** and **33**.

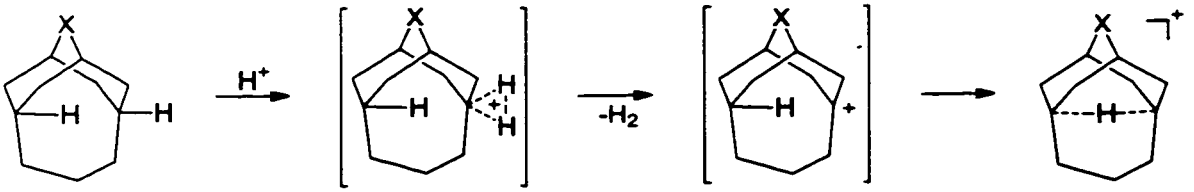

X = CH_2: **44**
X = – : **42**

X = CH_2: **48**
X = – : **47**

X = CH_2: **46**
X = – : **45**

X = CH_2: **33**
X = – : **30**

The most closely related known examples of **30** and **33** are the bicyclo[4.4.4]tetradecyl-1,6-μ-hydrido bridged cation **28** [157b] and the tricyclo[7.3.1.1^{7,11}]tetradecyl μ-H bridged cation.[82]

The generation of *in*-bicyclo[4.4.4]tetradec-1-ene was accomplished by a McMurry coupling of the aldehyde ketone **49**, prepared from decalin in a six step procedure.

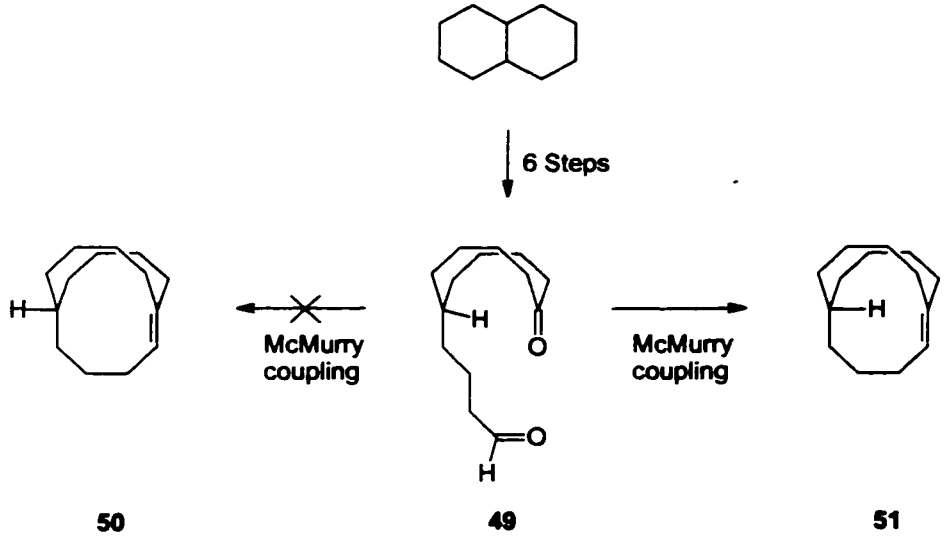

The McMurry coupling yielded exclusively the *in*-alkene **51**, which was calculated (Becke3LYP / 6-31G*, this work) to be 11.0 kcal/mol more stable than the corresponding *out*-isomer **50**. However, the imposed strain of the *in*-hydrogen of smaller bicylic compounds increases significantly and the formation of the *out*-bicyclo[3.3.3]undec-1-ene is favorable by 38.9 kcal/mol (B3LYP / 6-31G*, this work) compared to the corresponding *in*-isomer **41**, making the preparation of **41**, using the above route, very unlikely.

Turning to tricyclo systems, the *in*-alkene **53** has been prepared by a McMurry coupling route in about 20 % yield from the ketoaldehyde **52**, which was produced from 2-adamantanone in a nine step procedure.[82]

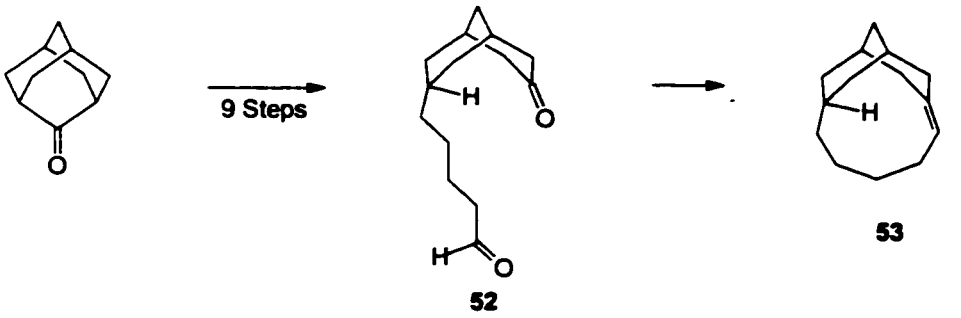

52 53

Ring closure of **52** to produce an *out*-tricycloalkene is prevented by the C_1 bridge of the bicyclo[3.3.1]nonyl unit in this ketoaldehyde. However, attempts to ring close the next smaller homolog **54** were not successful.

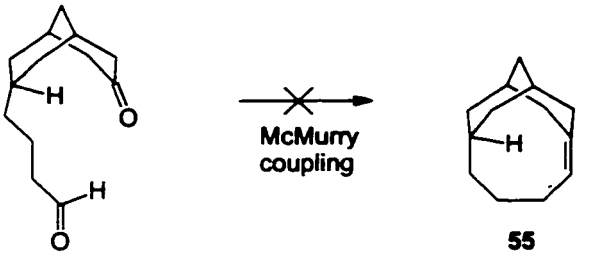

54 55

Calculating the energies of the *in*- and *out*-isomers of the tricyclo[5.3.1.$1^{3,9}$]dodec-1-ene revealed that the *in*-isomer is 46.8 kcal/mol (Becke3LYP / 6-31G*, this work) higher in energy. The corresponding energy difference in the tricyclo[6.3.1.$1^{6,10}$]tridecyl and in the tricyclo[7.3.1.$1^{7,11}$]tetradecyl systems was calculated to be 26.4 and 7.0 kcal/mol respectively. Since the formation of tricyclo[6.3.1.$1^{6,10}$]tridec-1-ene **55** has been reported to be unsuccessful, and since the *in*-tricyclo[5.3.1.$1^{3,9}$]dodec-1-ene **43** is expected to be even less likely to form by this route, this approach was not considered to be feasible.

The formation of the μ-H bridged cation **28** by a C-H protonation followed by loss of hydrogen has been shown to be an unexpectedly facile process, presumably due to a large stabilization of the bridgehead cation through μ-H bridging.[160]

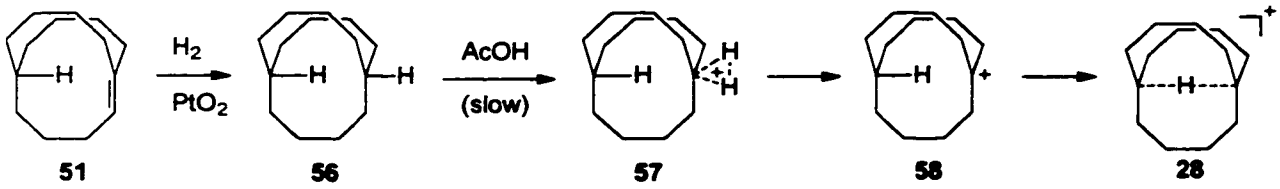

In this route to the target molecules **30** and **33**, one would have to synthesize the *in-out* hydrocarbons **42** and **44**. In these alkanes, calculations show that the *in-out* vs. the *out-out* energy difference is about 10 kcal/mol less than in the corresponding alkenes. However, they are still very strained and there is no obvious synthetic route to these *in-out*-bicycloalkanes. The results of the calculations carried out in this work, and involving these alkanes and alkenes, are summarized in Table 12.

Table 12: Energies of different *in- out*-isomers at the B3LYP / 6-31G* and the MM3 level of theory.

Structure	B3LYP / 6-31G* [Hartree]	ZPE [kcal/mol]	$H°_{298}$- $H°_0$ [kcal/mol]	$S°_{298}$ [cal/mol K]	MM3 [kcal/mol]	rel. E[a] (reference) [kcal/mol]
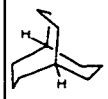 **59**	-431.20918311	184.6	6.6	92.8	44.4 (exp. 27.2)	
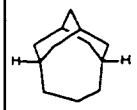 **61**	-469.324663775	190.1	6.5	92.9	45.2	
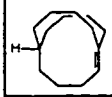 **50**	-547.898295833	224.9	8.8	108.3	57.1	
 **51**	-547.907998664	224.2	8.7	108.1	49.0	-6.8 (**50**)
 **63**	-546.720619343	211.4	7.7	101.2	42.3	
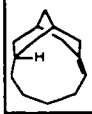 **53**	-546.708796227	211.0	7.7	101.2	48.3	7.0 (**63**)
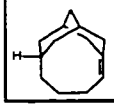 **64**	-507.401470969	193.1	7.1	96.8	46.5	

Structure		B3LYP / 6-31G* [Hartree]	ZPE [kcal/mol]	$H°_{298}$- $H°_0$ [kcal/mol]	$S°_{298}$ [cal/mol K]	MM3 [kcal/mol]	rel. E[a] (reference) [kcal/mol]
	**55**	-507.359036873	192.8	7.1	97.1	70.8	26.4 (**64**)
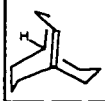	**60**	-429.966762397	170.0	6.5	91.7	45.5	
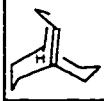	**41**	-429.904796999	169.2	6.5	91.8	85.8	38.1 (**60**)
	**42**	-431.157506928	185.2	6.7	93.7	72.6	32.0 (**59**)
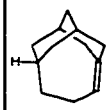	**62**	-468.090121432	174.8	6.2	90.2	42.3	
	**43**	-468.015560140	174.1	6.2	90.2	89.9	46.1 (**62**)
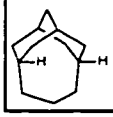	**44**	-469.269009474	189.9	6.5	92.2	77.1	34.7 (**61**)

[a] values obtained using the formula HF + 0.98 *(ZPE + ($H°_{298}$-$H°_0$)) - 0.98 * 298.15 * $S°_{298}$ and comparing the result with the result obtained for the reference compound.

A further complication is the fact that even the *out-out*-alkanes possess a large steric strain (approx. 30 kcal/mol from Benson group equivalents[161] or approx 50 kcal/mol total strain from MM3 calculations [a]). The additional strain in the *in*-isomer leads to a very large total strain energy (85 - 90 kcal/mol).

[a]The Benson group equivalents also possess a "strain" and the use of these equivalents leads to strain values significant lower than the MM3 calculated total strain, which uses hypothetically isolated atoms with ideal angles and bond lengths as the reference base.

2.1.2 Approach 3

The third type of approach involves the protonation of the quaternary C-C single bond in a [3.3.3]propellane or in a tetracyclo[5.3.1.$1^{3,9}$.$0^{3,7}$]dodecane.

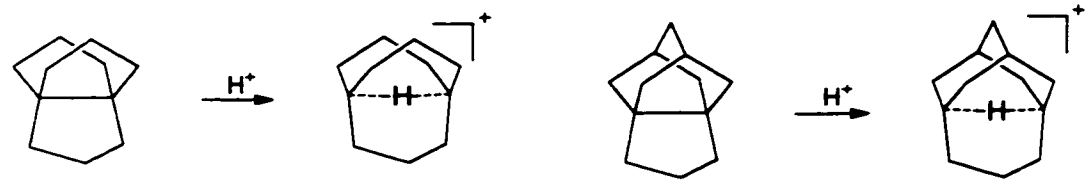

65 30 66 33

Protonation and deprotonation of a C-C bond (both processes should follow the same mechanism, but in an opposite direction) has been proposed to play a key role in the acid catalyzed isomerization or homologation reactions of small alkanes and has been subject to intensive research.[162] Both, C-H and C-C single bond protonation processes are now widely accepted to occur in superacidic media.

However, the known tricyclo[7.3.1.$1^{3,11}$]tetradecyl system shows no sign of exchange of the μ-H with deuterium in a trifluoroacetic acid / D_2O solution, while protons at the β-positions were exchanged instantly.[82]

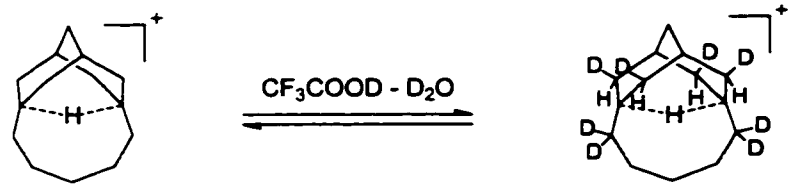

67 68

In a similar way, the bicyclo[4.4.4]undecyl μ-H bridged cation **28** also experiences fast exchange of the β-hydrogens, but there is no sign of μ-H exchange.[157]

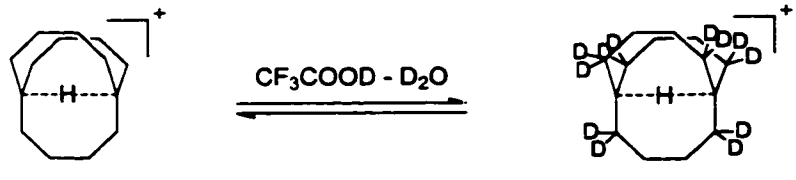

28 69

Furthermore, deprotonation reactions of the μ-H cation **67** yielded only bridgehead alkenes and in no case has any of the tetracyclo[7.3.1.1.^{3,11}0^{3,9}]tetradecane **71** been observed, [82] even though the formation of a C-C bond giving **71** can be calculated to be 25.7 kcal/mol more favorable than the formation of alkene **53** (major product) (see Table 13).

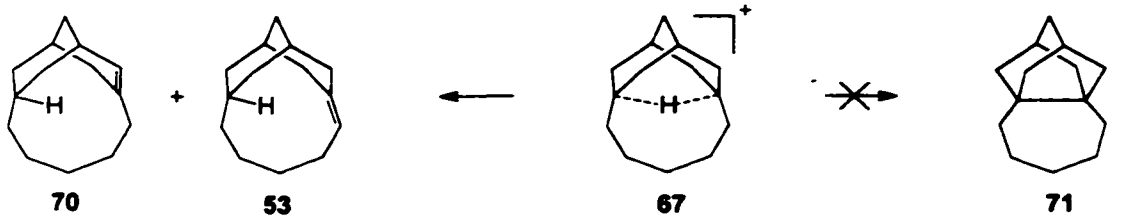

70 **53** **67** **71**

These comparisons are much more dramatic when one applies them to cations **30** and **33**. In these cases, the C-C bond formation is calculated to produce alkane products **65** and **66**, which are 74.3 and 68.2 kcal/mol lower in energy than the corresponding alkenes **41** and **43** (see Figure 25). It can be argued on thermodynamic grounds alone that the C-C protonation of alkanes **65** and **66** would be beyond the capability of even the strongest superacid (H_o = -30, see Section, 1.5.2.2, page 29).

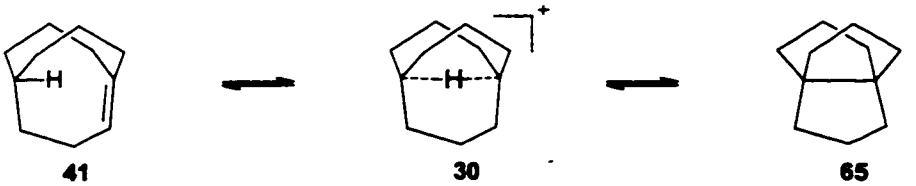

41 **30** **65**

Energies according to B3LYP / 6-31G* (kcal/mol) 0 -74.3

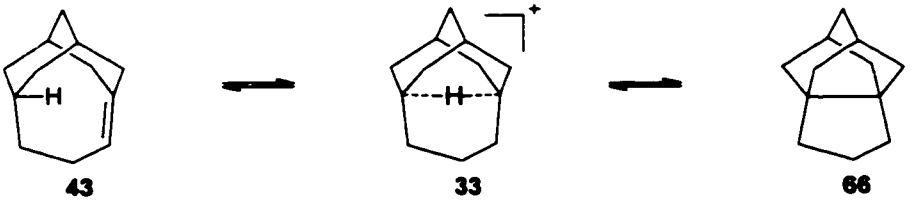

43 **33** **66**

Energies according to B3LYP / 6-31G* (kcal/mol) 0 -68.2

Figure 25: Relative free energies of bicyclic and tricyclic *in*-alkenes and alkanes.

The H-D exchange studies discussed above show that μ-H cations are much more readily deprotonated to alkenes than to alkanes. Since the mechanisms of protonation and deprotonation reactions should follow the same pathway, this implies that C-C alkane protonation has a much higher activation barrier, than a C=C protonation. Taken together with the above thermodynamic discussion, it would appear that the C-C protonation of **65** and **66** to give **30** and **33** is an "impossible reaction".

Table 13: Calculated energies of small multicyclo compounds at B3LYP / 6-31G*.

Structure	HF [Hartree]	ZPE [kcal/mol]	$H°_{298}-H°_0$ [kcal/mol]	$S°_{298}$ [cal/mol K]	rel. energy (ref.) [kcal/mol]
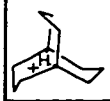 **28**	-430.328443502	176.5	6.5	91.7	
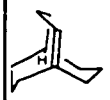 **51**	-429.904796999	169.2	6.5	91.8	
 **65**	-430.024267762	169.8	6.3	90.8	-74.3 (**51**)
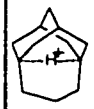 **33**	-468.435649632	181.2	6.2	90.1	
 **43**	-468.01556014	174.1	6.2	90.2	
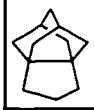 **66**	-468.125526707	174.8	5.9	88.6	-68.2 (**43**)
 **67**	-547.088676565	216.8	7.8	101.2	
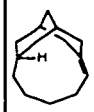 **53**	-546.708796227	211.0	7.8	101.2	
 **71**	-546.751093125	211.4	7.3	98.3	-25.7 (**53**)

An explanation for the high energy barrier for deprotonation of the C-H-C proton in μ-H cations can be found by considering the frontier orbitals involved in this type of structure.

As illustrated in Section 3.1, page 181, a linear C-H-C bond possesses a non-bonding LUMO orbital, which one needs to attack with a base in order to abstract the proton. Due to the linear arrangement of the C-H-C atoms, the abstraction of the proton can only occur in a perpendicular direction. Since the nodal plane of the 3c-2e LUMO is also perpendicular to the C-H-C axis intersecting the hydrogen, the orbital interaction of the HOMO of the approaching base and the LUMO of the 3c-2e bond is symmetry forbidden (the overlap is zero).

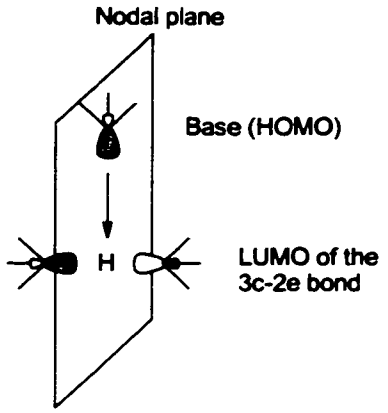

Figure 26: Orbitals involved in a proton abstraction of a μ-H bond.

In summary, the results of the present calculations and the experimental work from Sorensen, McMurry and coworkers[157, 82] clearly illustrate that direct protonation of an appropriate C-C single bond to form μ-H bridged carbocations is not a promising approach and was not further considered in this project.

2.1.3 Approach 4

The μ-hydrido bridged cations **30** and **33** are isomeric with the corresponding classical out-cations **78** and **34**, respectively, and approach 4 considers the possibilities for an isomerization reaction, leading to the respective μ-H cations.

A very related example of such an isomerization is the electrochemical oxidation of 1,6-diazabicyclo[4.4.4]tetradecane **72**, which was found to induce the migration of a bridge

hydrogen atom into the cavity of the bicyclic structure to form a symmetrical hydrogen bond (see Scheme 3).[163]

Scheme 3: 1,5-Hydrogen shift in 1,6-diazabicyclo[4.4.4]tetradecane.

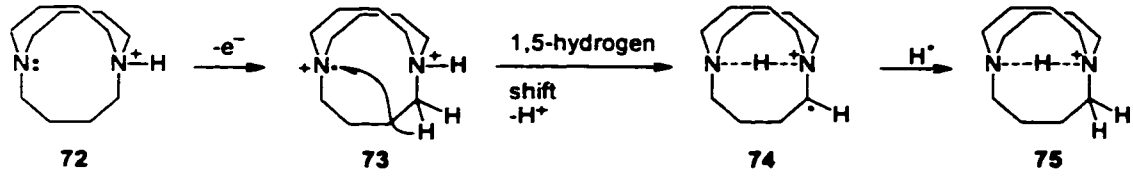

Despite the difference between the formation of a μ-H bridged carbocation (3c-2e bond), and the formation of the 3c-4e bond in **75**, this example illustrates the potential of this approach.

Using this approach for the bicyclo[3.3.3]undecyl or tricyclo[5.3.1.$1^{3,9}$]dodecyl systems, there are two aspects one has to consider.

Thermodynamical consideration of the *in- out*-isomerism of the monocations was explored with high level *ab initio* calculations at a B3LYP / 6-31G* or MP2(Full) / 6-311+G** level of theory. At the B3LYP level, the μ-hydrido bridged cations were found to be moderately higher in free energy than the corresponding classical *out*-isomers and values of 5.9 kcal/mol for the bicyclo[3.3.3]undecyl and 17.0 kcal/mol for the tricyclo[5.3.1.$1^{3,9}$]dodecyl system were calculated (see Figure 27).

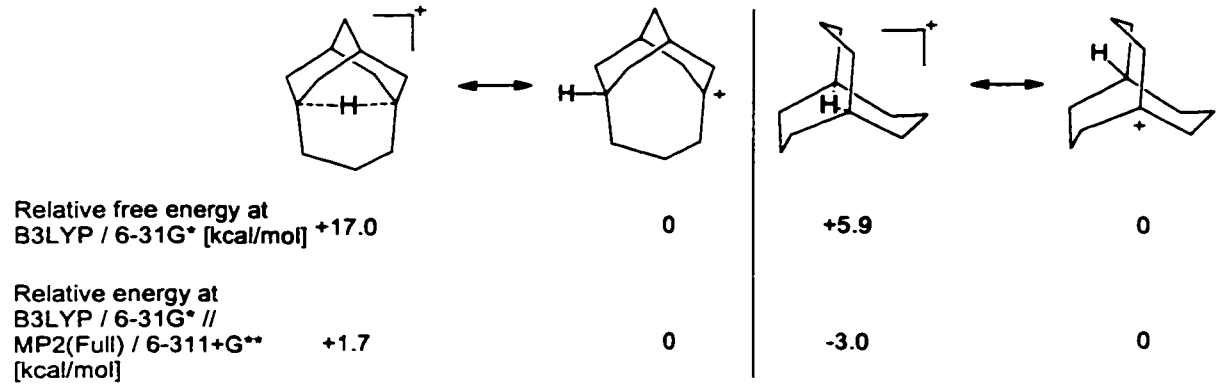

Figure 27: B3LYP / 6-31G* and MP2(Full) / 6-311+G** relative free energies and relative energies, respectively, for the *in- out-* isomerism of the bicyclo[3.3.3]undecyl and tricyclo[5.3.1.$1^{3,9}$]dodecyl systems.

However, μ-hydrido bond energies appear to be underestimated at the B3LYP / 6-31G* level and single point calculations of the B3LYP / 6-31G* optimized geometry at an MP2(Full) / 6-311+G** level, significantly lowered the relative energy of the μ-H cation structure compared to the *out*-isomers. The bicyclo[3.3.3]undecyl μ-H bridged cation **30** was found to be 3.0 kcal/mol more stable than the classical *out*-bicyclo[3.3.3]undec-1-yl cation **78** and the tricyclo[5.3.1.$1^{3,9}$]dodecyl μ-H bridged cation **33** 1.7 kcal/mol less stable than the *out*-tricyclo[5.3.1.$1^{3,9}$]dodec-1-yl cation **34**. The similar energy of the *in*- and *out*- isomers suggests that isomerization is feasible on thermodynamic grounds.

A second consideration is whether there is a reasonable mechanism by which the isomerization could take place.

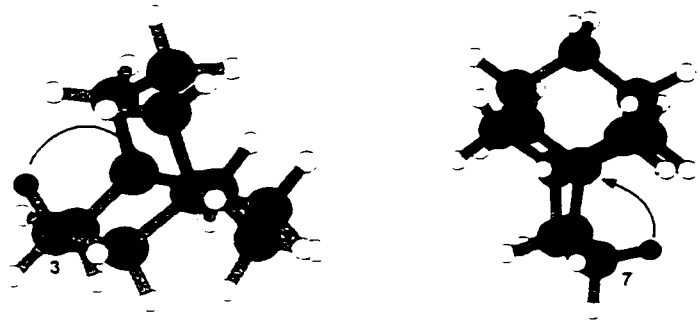

78 **34**

Figure 28: Possible bridge hydrogens (solid black) to shift into the cavity of the polycyclic structures.

The migration of a hydrogen at the 3 or 7 position of the bicyclo[3.3.3]undecyl or tricyclo[5.3.1.$1^{3,9}$]dodecyl system (see Figure 28) respectively involves the secondary cations **76** and **77**, which were calculated to be 51.2 or 64.5 kcal/mol higher than the classical out-isomers **78** and **34** (see Figure 29).

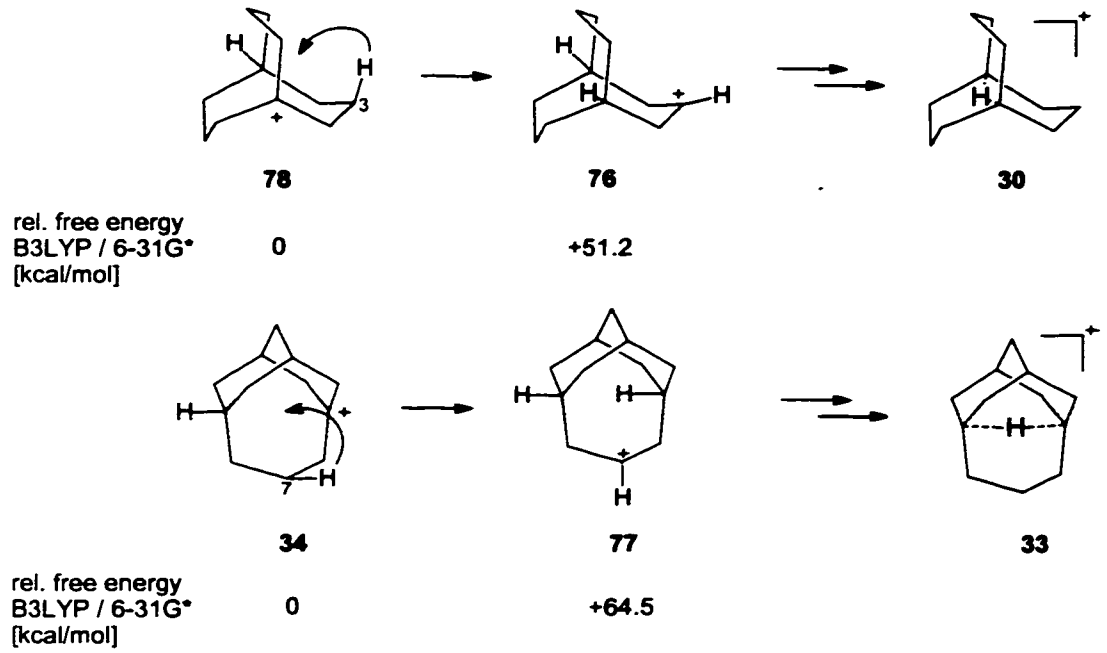

Figure 29: Calculated relative free energies of some involved intermediates in bridge hydrogen shifts of the bicyclo[3.3.3]undecyl and the tricyclo[5.3.1.$1^{3,9}$]dodecyl systems.

Despite the favorable thermodynamic aspects of the final μ-H cations, the very high relative free energy calculated for the intermediates **76** or **77** make this approach unlikely to occur. Detailed computational results are summarized in Table 14.

Table 14 : Calculated energies of multicyclo monocations at B3LYP / 6-31G* and MP2(Full) / 6-311+G** // B3LYP / 6-31G*.

Structure	HF [Hartree]	ZPE [kcal/mol]	$H°_{298}$-$H°_0$ [kcal/mol]	$S°_{298}$ [cal/mol K]	$G°_{298}$ [hartrees]	rel. energy (ref.) [kcal/mol]
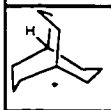 **78**	-430.338749812 -429.0657448[a]	177.3	6.7	93.0	-430.09466806	
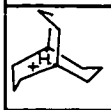 **30**	-430.328443502 -429.0705573[a]	176.5	6.5	91.7	-430.0853259482	5.9 (**78**) -3.0 (**78**)[a]
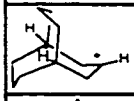 **76**	-430.255002643	175.7	6.4	91.0	-430.0130048001	51.2 (**78**)
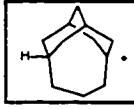 **34**	-468.455106111 -467.0880564[a]	176.5	6.5	91.7	-468.2119885572	

Structure	HF [Hartree]	ZPE [kcal/mol]	$H°_{298}-H°_{0}$ [kcal/mol]	$S°_{298}$ [cal/mol K]	$G°_{298[}$ [hartrees]	rel. energy (ref.) [kcal/mol]
 33	-468.435649632 -467.0854119[a]	181.2	6.2	90.1	-468.1849673489	17.0 (34) 1.7 (34)[a]
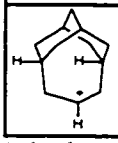 77	-468.356341354	180.0	6.9	95.8	-468.1091391243	64.5 (34)

[a] single point calculations at MP2(Full) / 6-311+G** of B3LYP / 6-31G* optimized geometries.

2.1.4 Approach 5

The final approach describes the possible reduction of a dication with a hydride. The highly electrophilic cavity of the bicyclo[3.3.3]undeca-1,5-diyl dication or tricyclo[5.3.1.$1^{3,9}$]dodeca-5,9-diyl dication could attract a hydride ion (or equivalent) to form the desired μ-hydrido bridged cations.

A thermodynamic consideration of the *in- vs. out*-isomers of the bicyclo[3.3.3]undecyl or the tricyclo[5.3.1.$1^{3,9}$]dodecyl systems shows that these have very similar energies, (see Section 2.1.3, page 69), so on thermodynamic grounds this route is also feasible.

One difficulty in this type of approach involves the preparation of the corresponding dications, due to the very close proximity of the two cation centers. The smallest observable alicyclic alkyl dication is the 2,5-dimethylhexyl-2,5-diyl dication with a calculated (B3LYP / 6-31G*) separation of the cation centers of 3.96 Å, while in the bicyclo[3.3.3]undeca-1,5-diyl or tricyclo[5.3.1.$1^{3,9}$]dodeca-5,9-diyl dications, the cation center separations are only 2.80 Å and 2.81 Å (B3LYP / 6-31G*), respectively, and the latter therefore experience a significantly higher repulsion energy. However, Olah and coworkers have already prepared the bicyclo[3.3.3]undeca-1,5-diyl dication[183] and it is therefore conceivable that the related tricyclo[5.3.1.$1^{3,9}$]dodeca-5,9-diyl dication should also be capable of preparation.

Considering the orbital interaction of such a possible reduction of a dication, this reaction is symmetry allowed and should therefore proceed without an intrinsically large energy barrier as illustrated in Figure 30.

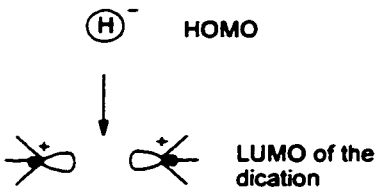

Figure 30: Orbital interactions of the reduction of a dication with a hydride ion.

The reduction of a dication with a hydride can in principle occur in two possible ways.

1. external delivery of the hydride

2. internal delivery of the hydride

The external delivery of a hydride requires hydride donors, which also must be stable under superacidic conditions, which are necessary to prepare the dication in the first place. Some appropriate hydride donors under these conditions might be hydrogen, sodium borohydride or alkanes such as isopentane.

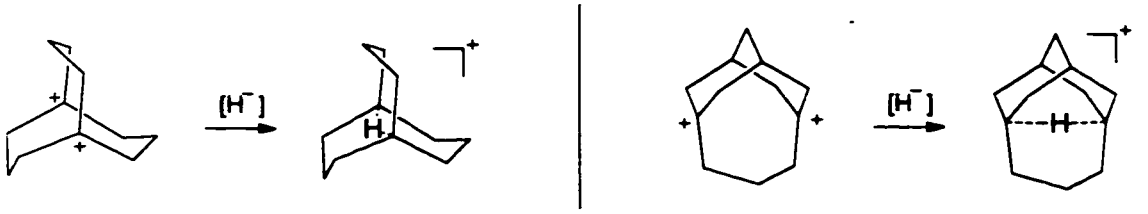

The internal hydride delivery corresponds to a dication rearrangement. As in the approach 4 (Section 2.1.3, page 70) the hydride with the closest proximity to the dication cavity would be located in the 3 position of the bicyclo[3.3.3]undecyl system or in the 7 position of the tricyclo[5.3.1.$1^{3,9}$]dodecyl system as illustrated below.

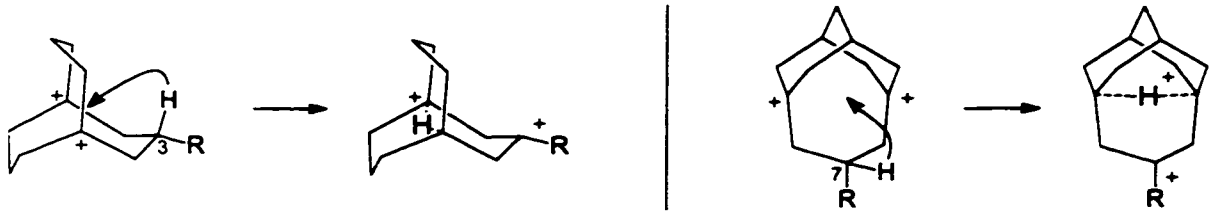

A cation stabilizing substituent in the R position should facilitate the hydride shift. *Ab initio* calculations at a B3LYP / 6-31G* level of theory on bicyclic and tricyclic systems with a variety of different R substituents showed that the most promising candidates would be the isobutyl or methoxy substituents, with some examples favoring the μ-H bridged structure by up to 11.75 kcal/mol (see Table 15 for detailed computational results of substituted bicyclic and tricyclic systems).

Table 15: Calculated energies of substituted bicyclo[3.3.3]undecyl and tricyclo[5.3.1.$1^{3,9}$]dodecyl dications at B3LYP / 6-31G*.

Structure	HF [Hartree]	ZPE [kcal/mol]	$H°_{298}-H°_{0}$ [kcal/mol]	$S°_{298}$ [cal/mol K]	$G°_{298[}$ [hartrees]	rel. energy (ref.) [kcal/mol]
 **36**	-429.294393323	168.46	6.73	93.29	-429.064241256	
 **79**	-429.239412648	165.59	6.70	93.58	-429.013920371	31.58 (**36**)
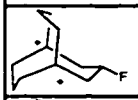 **80**	-528.50933698	163.26	7.27	97.94	-528.288613578	
 **81**	-528.483610999	161.83	7.09	97.91	-528.265400485	14.57 (**80**)
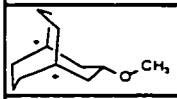 **31**	-543.823394827	188.63	8.49	106.91	-543.565319640	
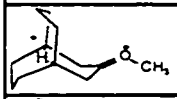 **32**	-543.834674365	188.31	8.31	108.18	-543.577972469	-7.94 (**31**)
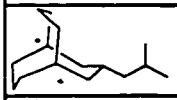 **82**	-586.565323229	239.23	10.26	120.79	-586.231929315	
 **83**	-586.58184013	238.07	10.14	121.24	-586.250648235	-11.75 (**82**)
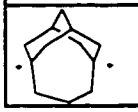 **40**	-467.412217343	172.64	6.16	89.78	-467.174767693	

Structure	HF [Hartree]	ZPE [kcal/mol]	$H°_{298}-H°_{0}$ [kcal/mol]	$S°_{298}$ [cal/mol K]	$G°_{298[}$ [hartrees]	rel. energy (ref.) [kcal/mol]
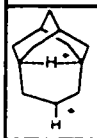 **84**	-467.348594894	170.43	6.41	91.42	-467.114992838	37.51 (**40**)
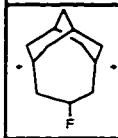 **85**	-566.627797225	167.52	6.68	94.17	-566.399598412	
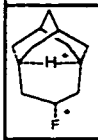 **86**	-566.593044463	166.59	6.82	95.75	-566.366801125	20.58 (**85**)
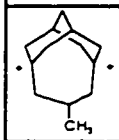 **87**	-506.733773266	190.11	7.12	96.59	-506.470722584	
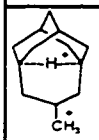 **88**	-506.698386164	188.33	7.34	98.58	-506.438704293	20.09 (**87**)
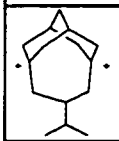 **89**	-585.367309487	225.73	8.80	109.64	-585.052093353	
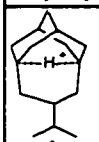 **90**	-585.357935806	224.92	9.14	113.19	-585.045108782	4.38 (**89**)
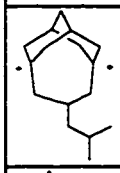 **91**	-624.683296009	243.60	10.14	120.88	-624.343293819	
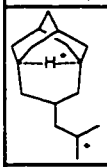 **92**	-624.690394087	242.72	9.92	120.50	-624.351942600	-5.43 (**91**)
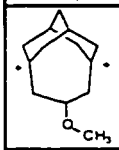 **93**	-581.94033684	192.83	8.46	107.09	-581.675831260	

Structure	HF [Hartree]	ZPE [kcal/mol]	$H°_{298}-H°_{0}$ [kcal/mol]	$S°_{298}$ [cal/mol K]	$G°_{298}$ [hartrees]	rel. energy (ref.) [kcal/mol]
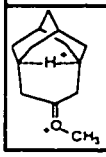 **94**	-581.944420155	193.00	8.05	105.87	-581.679740933	-2.45 (**93**)

Considering the fact that the bicyclo[3.3.3]undeca-1,5-diyl dication **36** has been prepared, and the high probability that the related tricyclo[5.3.1.$1^{3,9}$]dodeca-5,9-diyl dication **40** could be prepared, together with the calculations that show the in and out- isomers to possess similar energies, makes this type of approach the most promising route to prepare the target molecules **30** and **33**. Therefore, it was decided to follow this approach.

2.2 External Delivery of a Hydride

This section discusses the synthesis of the starting materials for the generation of the dications **36** and **40** (Section 2.2.1, page 77 and Section 2.2.2, page 83) and comments on the generation of these dications (Section 2.2.3, page 91) as well as the reduction of these cations with various hydride donors (Section 2.2.4, page 157). Along the way, three different rearrangements were discovered, and these were investigated in detail. The results associated with these three rearrangements are discussed in this section as well (Section 2.2.3.1, page 110, Section 2.2.3.2, page 129 and Section 2.2.3.3, page 142).

2.2.1 Synthesis of the Bicyclo[3.3.3]undecyl system

Bicyclo[3.3.1]nonan-9-one **100** is a well-known starting material for a variety of bicyclic compounds and is one of the key intermediates for the preparation of the bicyclo[3.3.3]undecyl system. There are a number of reported syntheses; the most direct methods are an Organic Synthesis preparation [164] starting from 9-BBN (9-borabicyclo[3.3.1]nonan) (78 - 83 % yield) and the reaction of 1,5-cyclooctadiene with $Ni(CO)_4$ (60 %).[165] The 9-BBN method employs syringe techniques, and is moderately costly (9-BBN, nBuLi, dichloromethyl methyl ether). The latter method is unattractive because of the toxicity of $Ni(CO)_4$. The 1964 six step synthesis of Foote and Woodward,[166] starting from the cyclohexanone enamine **95** and acrolein, has been the most used route in the older literature but an overall yield of only *ca.* 20 % and difficulties in purifying intermediates are the drawbacks of this method.

Using the same starting materials as the Foote and Woodward synthesis, pure bicyclo[3.3.1]nonan-9-one was prepared in this work in a three step sequence (Scheme 4) with an overall yield of 47 % without purification of any intermediates.

Scheme 4: Synthesis of bicyclo[3.3.1]nonan-9-one.

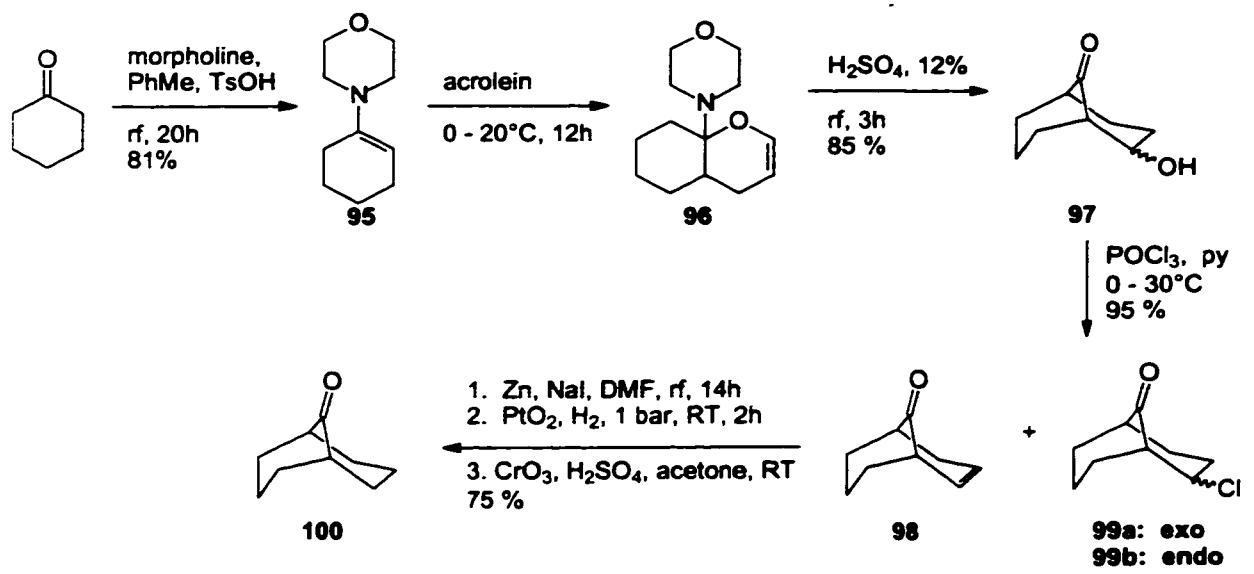

The reaction of enamine **95**[167] with acrolein is known[168] to first give **96**, but ultimately 2-N-morpholinobicyclo[3.3.1]nonan-9-one is formed. This latter compound was used by Foote and Woodward but the removal of the morpholino group is troublesome. One can verify the *in situ* formation of **96**, from **95** and acrolein, by means of an ^{1}H NMR spectrum of a sample of the crude mixture, focusing on the alkene hydrogens. Cope *et. al.*,[169] and Allan *et. al.*[170], have described the mild hydrolysis of **96** to the respective keto-aldehyde, and the subsequent aldol condensation to give an epimeric mixture of **97**. We have modified this procedure to give **97** in a one pot process from **95**, using a 12 % aqueous H_2SO_4 solution for the combined hydrolysis-aldol condensation step. The overall yield is much improved since isolation of the labile keto aldehyde is avoided. The crude alcohol **97** was used directly for the next step (purity > 95 % by GC and ^{1}H NMR). The replacement of the hydroxyl group in **97** by chlorine, using $POCl_3$-pyridine, results in a mixture of **98** and **99**, as also reported by Allan *et. al.*[170] Premixing the pyridine-$POCl_3$, using an excess of pyridine, and then adding

97, gave the best results. Various attempts to reduce the formation of **98** were unsuccessful[a], so **98** and **99** were directly used in the zinc reduction step, a modification of the method of Fujimoto *et. al.*.[171] In the work-up of this final reaction, a room temperature-atmospheric pressure PtO_2 / H_2 hydrogenation was carried out on the mixture of **98** and **100**. This reaction is rapid in methanol, but is accompanied by ca. 5 % of ketone reduction, which was reversed with a small amount of Jones reagent. The crude off-white crystalline product **100** has an estimated 99.5 % purity by GC and the ^1H NMR spectrum is identical to that obtained from recrystallized material, m.p. 152-154 °C (crude), reported,[165] 155 - 158.5 °C.

Bicyclo[3.3.3]undecane was first synthesized by Leonard and coworkers[172] by a two fold Tiffeneau-Demjanov ring expansion of bicyclo[3.3.1]nonan-9-one. The first ring expansion could be carried out by simply adding *in situ* generated diazomethane to **100** forming bicyclo[3.3.2]decan-9-one **101**. Attempts to further ring expand **101** using diazomethane under a variety of different conditions and with addition of Lewis acids, such as $BF_3 \cdot Et_2O$ resulted in no detectable reaction.[173] This unusual behavior can be explaned by the large steric strain contained in the bicyclo[3.3.3]undecyl system.

The strain energy of bicyclo[3.3.3]undecane has been measured experimentally as 27.2 kcal/mol,[174] which is in very good agreement with the 26.1 kcal/mol calculated at a B3LYP / 6-31G* level of theory using the homodesmic reaction **(24)** (this work):

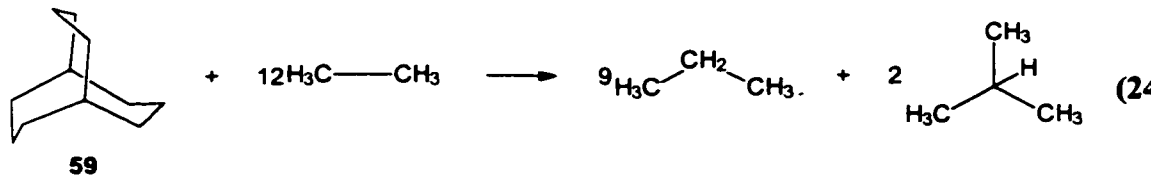

59 **(24)**

---

[a] Chloride **99a** has been shown to undergo aqueous (NaOH) base-induced elimination whereas isomer **99b** gives mainly a ring-opened cyclooctenecarboxylic acid under the same conditions. We also find that only the exo chloride **99a** is dehydrochlorinated by t-butoxide. The OH and Cl replacement in my work requires temperatures of at least 20°C and several hours reaction time. It is possible therefore that **99a** is the source of alkene **98** via a slow reaction with the excess pyridine. Alternatively, the elimination may occur via the initially formed phosphate ester of the exo alcohol.

The total strain energy according to Molecular Mechanics Calculations using the MM3 force field was found to be 44.4 kcal/mol[a] (see Table 16).

Table 16. MM3 strain energy of the bicyclo[3.3.3]undecane.[175]

MM3 strain in kcal/mol			
Total Strain Energy	44.4285	Gradient	0.0704
Stretching	1.1528	Torsion-Stretch	-0.3592
Bending	13.6463	Bend-Bend	0.5597
Torsion	12.6441	VdW Energy	16.2442
Stretch-Bend	0.5406	Bond Moments	0.0000

The bicyclic ketone **100** proved to be inert to a variety of nucleophiles and the formation of the needed amino alcohol **105** was accomplished by a sequence of a Wittig type reaction, epoxidation with mCPBA, nucleophilic ring opening of the epoxide with sodium azide and reduction of the azide with catalytic hydrogenation. The second Tiffeneau-Demjanov ring expansion was then carried out in aqueous solution with acetic acid and sodium nitrite.

Scheme 5: Synthesis of the bicyclo[3.3.3]undecane **59** according to Leonard *et. al.*[172]

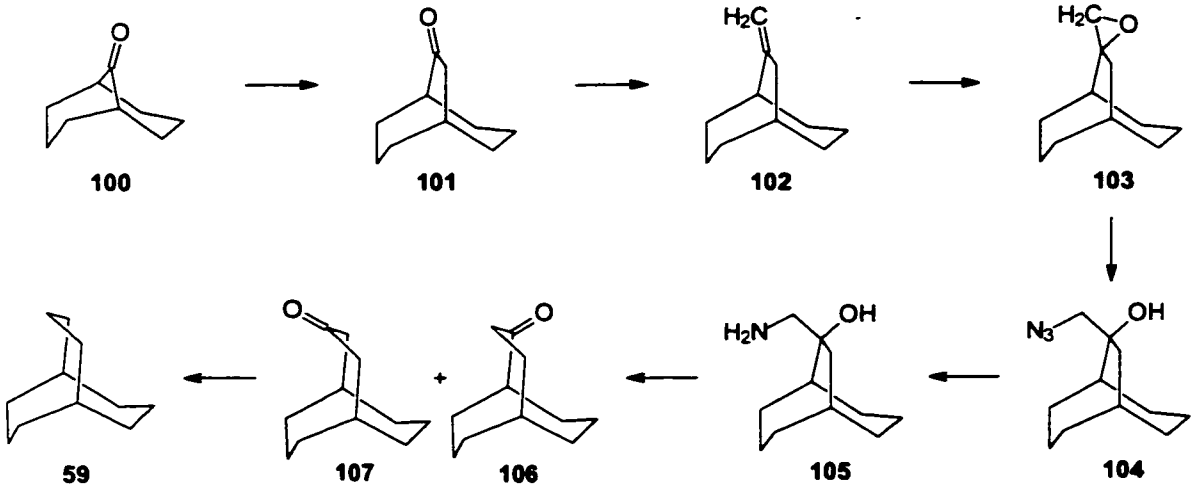

[a] The large difference between the experimentally measured strain energy and the Molecular Mechanics calculated value is mainly due to using different reference points.

More recently, Wayne and Snyder[176] used trimethylsilyl cyanide in the presence of zinc chloride to convert the ketone **101** into 9-cyano-9-trimethylsiloxybicyclo[3.3.2]decane followed by LAH reduction to form the amino alcohol **105**.

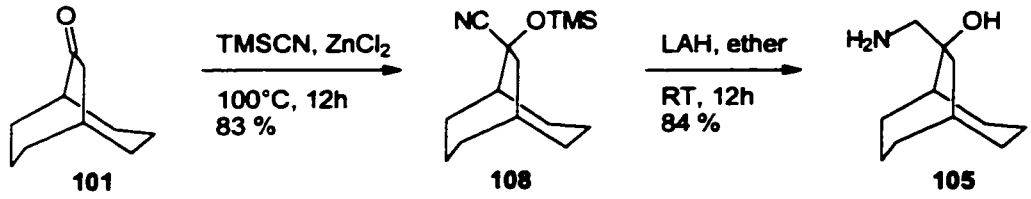

The synthesis employed in this work followed closely the pathway of Leonard, but for preparation of the amino alcohol **105** the method of Wayne and Snyder was employed.

The first ring expansion of bicyclo[3.3.1]nonan-9-one **100** was carried out by a dropwise addition of a methanol solution of Diazald® (Aldrich product) to a mixture of **100** and potassium hydroxide in water - methanol at 0°C. It was found that extending the addition period of the Diazald® solution from the 4 hours used by Leonard to 20 h increased the yield from the published 60 % to 72%. An even slower addition or the use of a larger excess of Diazald® did not result in a significant improvement of the yield. The resulting crude mixture consisted of bicyclo[3.3.2]dodecan-9-one **101** and bicyclol[3.3.1]nonan-9-one **100**, whose separation via column chromatography was troublesome.

Heating a mixture of the ketone **101**, zinc chloride and TMSCN to 100°C for 12 hours produced the cyanide **108**, which was reduced to the amino alcohol **105** with LAH in ether according to the procedure of Wayne and Snyder.[176] The second ring expansion was accomplished by dissolving the amino alcohol **105** in an aqueous solution of acetic acid and dropwise addition of a sodium nitrite solution over a period of 30 min. The resulting solution was stirred at ambient temperature for 4 hours before it was heated to 90°C for 3h. According to the method of Leonard, the reaction mixture obtained after the addition of the sodium nitrite solution was immediately heated to 90°C, but in this work an additional stirring period at room temperature was found to improve the yields from 47 % to 87 %. Application of the Wolff-Kishner reduction according to Nagata and Itazaki[177] was found to be the best method of reducing the ketones **106** and **107** to the alkane manxane (bicyclo[3.3.3]undecane **59**) in 91 %

yield.

Hydrogen NMR spectra of manxane solutions in chloroform-*d* were found to be temperature dependent, which is associated with a flipping process of the three bridges.

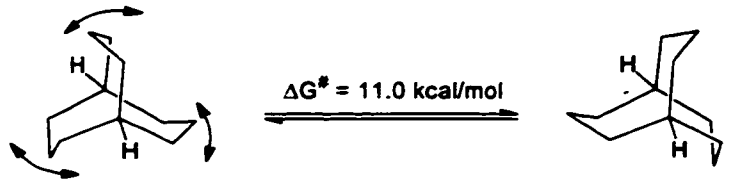

59 59

Figure 31: Flipping process of the bridges in bicyclo[3.3.3]undecane.

Using line shape analysis techniques, the associated energy barrier for this process was measured to be 11.0 kcal/mol ± 0.2 kcal/mol, which was in good agreement with the estimated value of 11 ± 2 kcal/mol by Parker and Schleyer.[178]

The facile oxidation of the bridgehead positions of bicyclo[3.3.3]undecane **59** was first recognized by Parker and coworkers who obtained mono and diperoxides upon bubbling air through a pentane solution for 2 h.[179] However, attempts to reproduce this functionalization reaction yielded only traces of the oxidized products. Irradiation using a sunlamp and extended periods (2 - 4 weeks) of bubbling air through pentane or hexane solutions of **59** were required to yield the desired peroxides. Later, it was found that exposure of the solid alkane to air or pure oxygen resulted in a much higher reaction rate. Exposure of the solid alkane as a film on the surface of a round bottom flask to oxygen for 2 days formed a mixture consisting predominantly of the bicyclo[3.3.3]undecan-1-ol **109**, mono and di peroxide as well as small amounts of the diol **110**. Exhaustive oxidation by exposing the solid bicyclo[3.3.3]undecane **59** to oxygen for 3 weeks resulted mainly in the formation of bicyclo[3.3.3]undecane-1,5-diperoxide, which was reduced with sodium borohydride to yield the desired diol **110**.

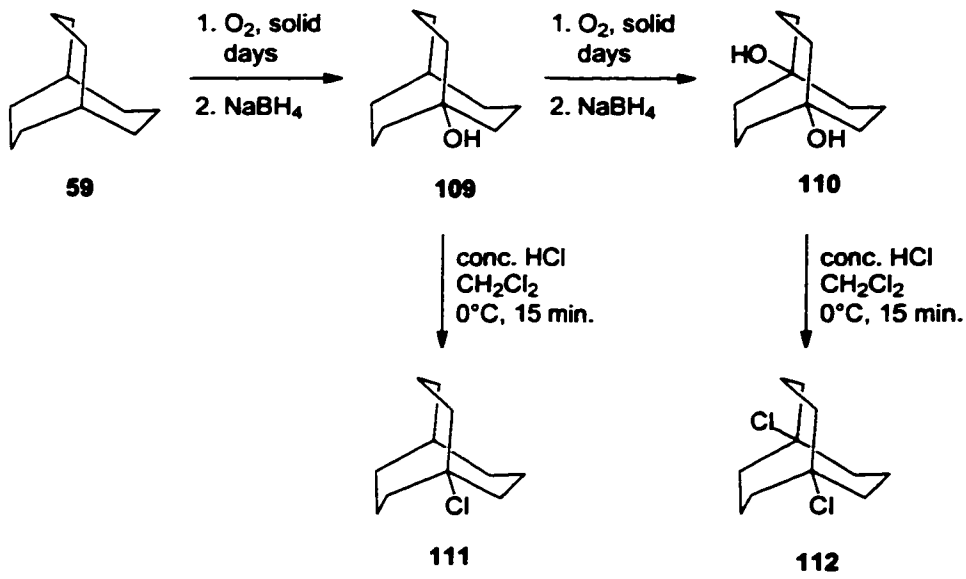

Stirring a solution of the mono alcohol **109** or diol **110** in dichloromethane with conc. hydrochloric acid at 0°C for 15 min. formed pure chlorides **111** and **112**. This procedure was found to be superior to the treatment of the alcohols with thionyl chloride, as reported by Parker and coworkers.[179] The thermal stability of these tertiary chlorides is rather low and storing them at room temperature for 1 day causes significant decomposition.

2.2.2 Synthesis of the Tricyclo[5.3.1.$1^{3,9}$]dodecyl system

Tricyclo[5.3.1.$1^{3,9}$]dodecane **61** is known and has been synthesized by Sasaki and Tabushi via a two fold Tiffeneau-Demjanov ring expansion of 2-adamantanone by two cycles of HCN addition, reduction with LAH to the amino alcohol and reaction with sodium nitrite in acidic solution, forming tricyclo[4.3.1.$1^{3,7}$]undecan-2-one **115**[180] in 48 % to 85 % yield and tricyclo[5.3.1.$1^{3,7}$]dodecan-2-one **118**[181] in 15 % yield from **115**. Another method for the preparation of **115** makes use of a selective C-H insertion of dichlorocarbene followed by a hydrolytic rearrangement[182] producing the desired ketone in 63 % yield from adamantane.

Similar to the bicyclo[3.3.3]undecyl system the tricyclo[5.3.1.$1^{3,9}$]dodecyl system has a high ring strain, which has a large effect on the reaction chemistry of this skeleton. According to B3LYP / 6-31G* calculations the strain energy was estimated as 24.2 kcal/mol using the

homodesmic reaction **(25)**.

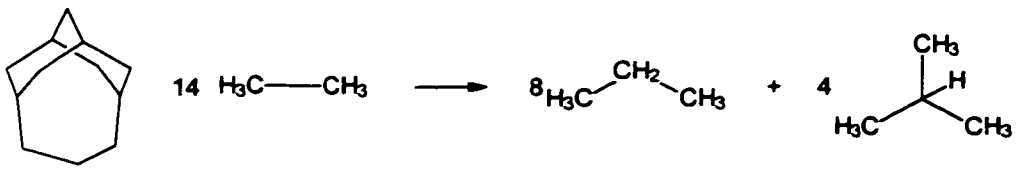

61 **(25)**

Molecular Mechanics calculations with the MM3 force field predict the total strain to be 45.2 kcal/mol (Table 17). This result is analogous to that of the bicyclo[3.3.3]undecyl system and the discrepancy between the homodesmic reaction number and the MM3 strain energy can be largely attributed to having different reference points (see Footnote [a] on page 80).

Table 17. MM3 strain energy of the tricyclo[5.3.1.$1^{3,9}$]dodecane[175]

MM3 strain in kcal/mol			
Strain Energy	45.2291	Gradient	0.1887
Stretching	1.3196	Torsion-Stretch	-0.4225
Bending	10.6499	Bend-Bend	0.4050
Torsion	16.2772	VdW Energy	16.5528
Stretch-Bend	0.4472	Bond Moments	0.0000

In this project, the dichlorocarbene insertion procedure was slightly modified in the preparation of ketone **115**, which was then used for the second ring expansion using TMSCN addition followed by LAH reduction to obtain the amino alcohol **117** (Scheme 6).

Scheme 6: Synthesis of the tricyclo[5.3.1.$1^{3,9}$]dodecane by a two fold ring expansion of 2-adamantanone.

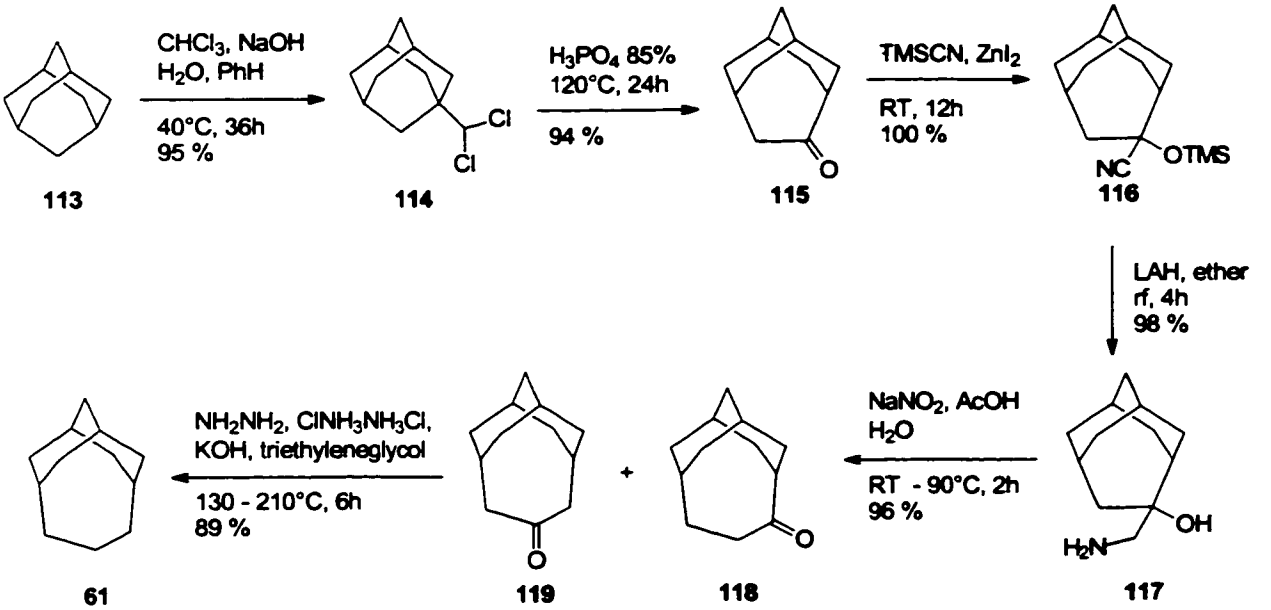

Dropwise addition of chloroform to a mechanically stirred mixture of adamantane **113**, sodium hydroxide solution (50 %) and benzene over a period of 36 hours yielded a mixture of adamantane and dichloromethyladamantane **114**. Despite the formation of a black solid, which is most likely due to polymerization of the *in situ* generated dichlorocarbene, the yield of the reaction can be as high as 95 %, based on consumed adamantane. Separation of the mixture, consisting of adamantane **113** and dichloromethyladamantane **114** can best be achieved by sublimation, which becomes burdensome with large scale reactions (larger than 10 g). The low polarity of both **113** and **114** makes a separation via silica gel column chromatography impossible.

However, adamantane was found to be inert in the next step, allowing one to use the unseparated mixture of **113** and **114** as starting materials for the preparation of the tricyclo[4.3.1.$1^{3,8}$]undecanone **115**. Heating the reaction mixture of **113** and **114** in 85 % phosphoric acid to 120°C for an extended period of time (24 h) converted 69 % of the dichloride **114** into homoadamantanone **115**, producing a mixture with adamantane and dichloromethyladamantane. Purification of the homoadamantanone **115** at this stage was facile and column chromatography on silica gel yielded pure **115** in 94 % yield based on consumed starting material. Increasing the reaction temperature substantially increases the reaction rate, but the yield is lowered due to the formation of white insoluble impurities (sparingly soluble in hexanes, not soluble in any other common solvent).

Lewis acid (ZnI_2) catalyzed addition of TMSCN to the ketone **115** was completed in 12 h at room tempreature to quantitatively yield the cyanide **116**, which was reduced with LAH in refluxing ether within 4 hours. Dissolving the amino alcohol **117** in an excess of aqueous acetic acid and adding sodium nitrite solution induced the second ring expansion, to produce a mixture of the isomeric ketones **118** and **119**, in the ratio 96 : 4.

Reduction of the tricyclo[5.3.1.$1^{3,9}$]dodecyl ketones **118** and **119** was accomplished via a Wolff-Kishner reaction,[177] which was found to be superior to a sodium borohydride reduction of the corresponding tosyl hydrazone[181] in terms of number of steps and yield (89 % vs. 65 %).

The hydrogen and the carbon NMR spectra of **61** were found to possess a temperature dependence, which can be attributed to a flipping process of the single flexible bridge (C6 -

C7 - C8) in the tricyclo[5.3.1.1^{3,9}]dodecane hydrocarbon (see Figure 33).

Figure 32: Ring flip of the C6-C7-C8 bridge in the bicyclo[5.3.1.1^{3,9}]dodecane **61**.

Using the carbon NMR spectra in the temperature range of 240 K to 280 K and line shape analysis techniques, the associated energy barrier for this flipping process was measured as 13.1 ± 0.1 kcal/mol. This value is slighty higher than the corresponding energy for the bicyclo[3.3.3]undecane (11.0 ± 0.2 kcal/mol), which can be attributed to having a more rigid framework in the tricyclic hydrocarbon compared to the bicyclic structure. A more rigid structure would imply that large-angle strain, experienced by the carbon framework in the transition state of this flipping process, involves a larger energy change, hence a larger energy barrier would be observed.

Similar to bicyclo[3.3.3]undecane, tricyclo[5.3.1.1^{3,9}]dodecane **61** is readily oxidized with oxygen at room temperature. However, two different bridgehead positions with tertiary hydrogens are present in the tricyclic system, presenting two possible sites for an oxidation reaction.

The oxidation of the solid alkane **61** proceeds without the need for a light source. Furthermore, no "initiation" period was observed and the products are formed in a relatively constant reaction rate. Partial oxidation of the alkane formed a crude mixture consisting of starting material, mono alcohol **120**, diol **121** and only minor amounts of peroxides. This implies that initially formed peroxides must experience a homolytic O-O bond cleavage and a hydrogen atom abstraction to form the alcohol. The following proposed mechanism describes these reaction types (Scheme 7).

Scheme 7: Proposed mechanism for the oxidation of tricyclo[5.3.1.1^{3,9}]dodecane.

Initiation:

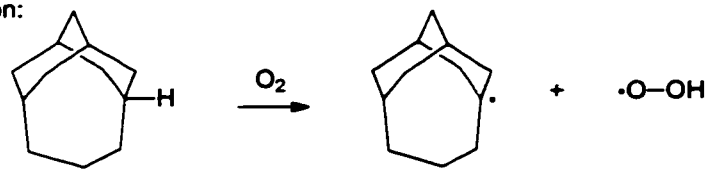

61 **122**

Propagation:

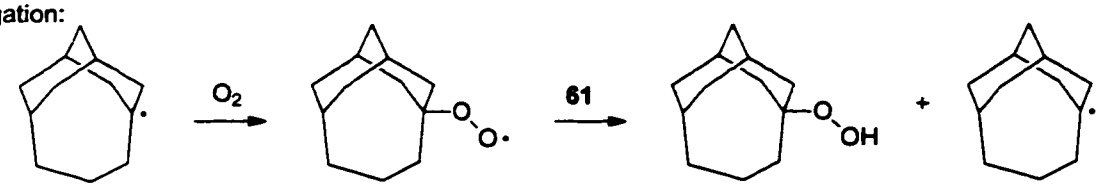

122 **124** **123** **122**

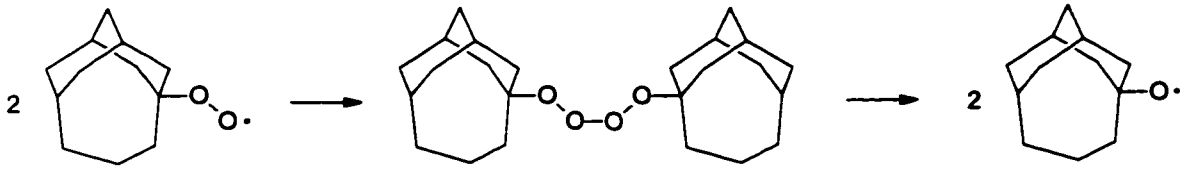

124 **125** **126**

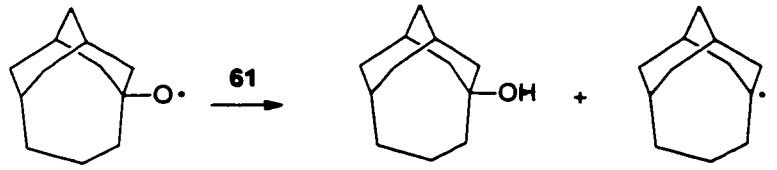

126 **120** **122**

Termination:

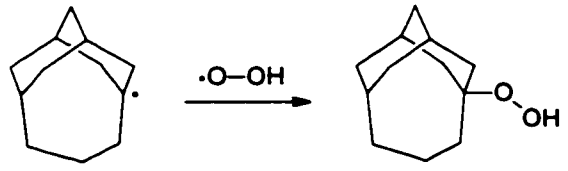

122 **123**

Ab initio calculations at a B3LYP / 6-31G* level of theory of the homodesmic reactions **(26)** and **(27)** allow one to compare the two radicals **122** and **127**.

127 61 (26)

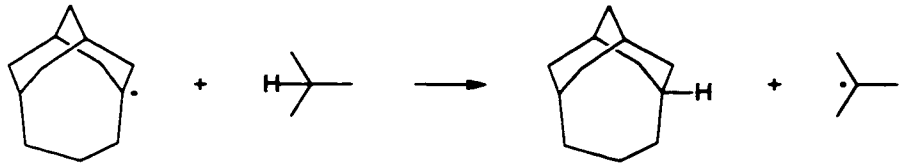

122 61 (27)

The radical **122** was calculated to be 8.1 kcal/mol more stable than **127**, explaining the selectivity of this oxidation reaction (no alcohol or peroxide groups could be observed at the 1 or 3 position of the tricyclo[5.3.1.$1^{3,9}$]dodecyl system). In comparison with the tertiary butyl radical, species **122** is 5.9 kcal/mol more stable, which explains the high reactivity of the bridgehead hydrogens at the 5 and 9 position of the tricyclo[5.3.1.$1^{3,9}$]dodecyl system.

Table 18: Calculated energies of bicyclo[3.3.3]undecyl and tricyclo[5.3.1.$1^{3,9}$]dodecyl radicals at B3LYP / 6-31G*.

Structure		HF [Hartree]	ZPE [kcal/mol]	$H°_{298}$-$H°_0$ [kcal/mol]	$S°_{298}$ [cal/mol K]	$G°_{298}$ [hartrees]
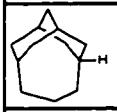	**61**	-469.324663775	190.09	6.52	92.90	-469.0608633082
	**122**	-468.675421683	181.05	6.56	94.30	-468.4263388422
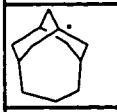	**127**	-468.663397395	181.55	6.51	94.05	-468.4134887244
		-158.458811657	83.06	4.16	72.09	-158.3561657284
		-157.79832092	73.60	4.59	77.45	-157.7122812697

The diol **121** forms colorless tetragonal crystals, of which an x-ray crystal structure was obtained.

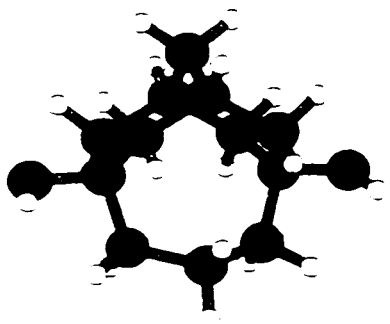

121

Figure 33: X-ray crystal structure of the tricyclo[5.3.1.$1^{3,9}$]dodecane-5,9-diol.

The geometrical parameters of this diol (see Table 19) indicate that all C-C-C angles involving bridge carbons (that is all carbons but C6') are unusual large, which confirms the steric strain involved in the tricyclo[5.3.1.$1^{3,9}$]dodecyl framework. Furthermore, one of the hydrogens, bonded to the C3 carbon is relatively close to the cavity within this tricyclic structure, and this would be a potential candidate for a possible migration in the case of intramolecular hydride delivery (see Section 2.3, page 164).

Table 19: Some geometrical parameters from the x-ray crystal structure of tricyclo[5.3.1.$1^{3,9}$]dodeca-5,9-diol **121** (see Figure 33 for the numbering system).

Atoms	Bond length [Å]	Atoms	Angle [°]
O1 - C1	1.454	O1 - C1 - C2	104.1
C1 - C2	1.535	C2 - C1 - C4	112.8
C1 - C4	1.539	C2' - C1 - C4	112.8
C2 - C3	1.526	C3 - C2 - C1	118.5
C3 - C6	1.548	C6' - C5 - C4*	108.1

Preparation of the dichloride **129** was accomplished by treating a solution of the corresponding alcohol in dichloromethane with conc. hydrochloric acid at 0°C for 15 min. Filtration and evaporation of the dichloromethane by using a stream of nitrogen at 0°C produced solid **129**, which was immediately used for subsequent reactions, since

decomposition into a complex mixture occurred within one to two hours at room temperature.

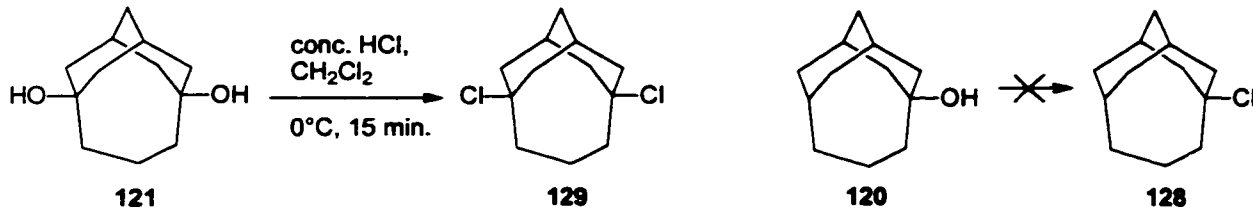

121 **129** **120** **128**

Several attempts to prepare the monochloride **128** in a similar way were not successful and resulted in the formation of a complex mixture. Using the method of Parker and coworkers[179] (thionyl chloride / chloroform) also only resulted in the formation of a complex mixture.

2.2.3 Generation of the Bicyclo[3.3.3]undecyl and Tricyclo[5.3.1.1^{3,9}]dodecyl cations

Bridgehead carbocations in small multicyclic compounds are often destabilized due to geometrical restrictions, which prevent the cation from attaining a favorable sp^2 geometry, and additionally, because of limited flexibility of the α hydrogens the cation cannot obtain an optimal configuration for hyperconjugative overlap. However, the unique geometry and the large ring strain in the bicyclo[3.3.3]undecyl or tricyclo[5.3.1.1^{3,9}]dodecyl systems greatly favor an sp^2 geometry at the bridgehead positions, thus stabilizing the formation of the corresponding carbocation (see Figure 34).

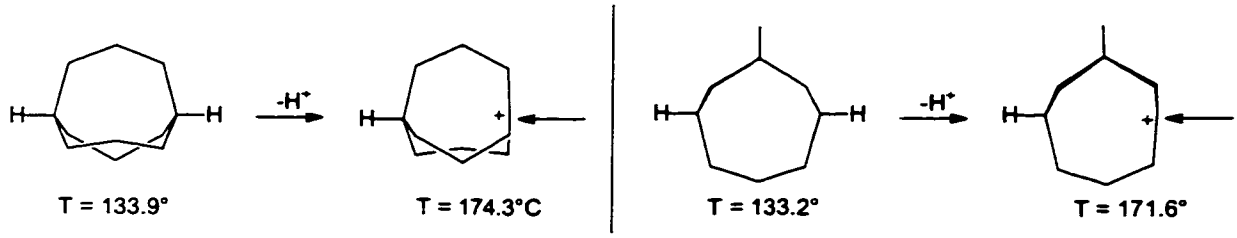

Figure 34: Comparison of the improper torsion angle at the bridgehead position of the alkane and the monocation of the bicyclo[3.3.3]undecyl and the tricyclo[5.3.1.1^{3,9}]dodecyl systems.

An estimate of this stabilizing effect can be obtained by comparing the *tert*-butyl cation - *tert*-butane pair with the multicyclic monocation - alkane pairs. The following homodesmic reactions were considered in this work using a B3LYP / 6-31G* level of theory.

59 78 **(28)**

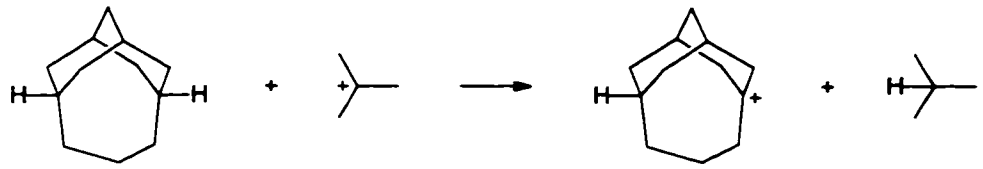

61 34 **(29)**

These calculations yield a free energy change for reaction **(28)** of -19.5 kcal/mol and -20.3 kcal/mol for reaction **(29)**.

Considering the geometrical arrangement of the α-hydrogens and of the α-β C-C bonds (see Figure 35), it becomes obvious that C-C hyperconjugation rather than C-H hyperconjugation must make the major contribution to the stabilization of the monocations **78** and **34**.

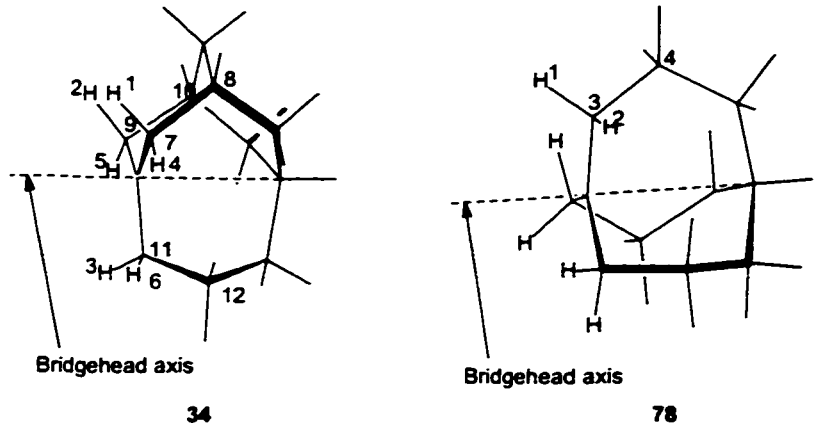

34 78

Figure 35: B3LYP / 6-31G* calculated geometries of the bicyclo[3.3.3]undecyl and tricyclo[5.3.1.$1^{3,9}$]dodecyl cations.

The best arrangement for optimal hyperconjugation involves a parallel alignment of the interacting bond with the p-type-orbital of the cation carbon, which corresponds to a torsion angle with either 0 or 180° to the bridgehead axis illustrated in Figure 35.

The B3LYP / 6-31G* optimized geometry of the bicyclo[3.3.3]undecyl cation **78** shows torsional angles between the bridgehead axis and hydrogen 1 of 37°, indicating that hyperconjugation is expected to be effective, but not optimal. The C-H bond of hydrogen 2 is almost perpendicular to the bridgehead axis and is expected to make no significant contribution to the hyperconjugative stabilization of this cation. The C3-C4 bond showed a torsion angle to the bridgehead axis of 27°, which suggests that this interaction should be even more significant than for hydrogen 1.

The tricyclo[5.3.1.$1^{3,9}$]dodecyl monocation **34**, shown in Figure 35, shows torsional angles between the bridgehead axis and the hydrogens 1, 2 and 3 of 40°, 45° and 31°, respectively, indicating that the C-H hyperconjugation of H3 is expected to be larger than for H1 or H2. The torsional angle of the bridgehead axis to carbons 8, 10 and 12 was measured as 26°, 31° and 32°. Thus, one would expect that the C9-C10 bond of **34** would undergo the most efficient hyperconjugative interaction.

The exceptional thermodynamic stability of **78** and **34**compared to the *tert*-butyl cation

explains the facile dissociation of the corresponding chlorides. The 1-chloro-bicyclo[3.3.3]undecane, for example, has been shown to be 10^4 times more reactive in hydrolysis reactions in aqueous ethanol than the *tert*-butyl system.[179] Attempts to prepare the tricyclic chloride **128** at 0°C resulted in the formation of a complex mixture (see Section 2.2.2, page 89), which can now be explained by the facile dissociation of this chloride, followed by other reactions.

Despite the large stabilization of the bicyclo[3.3.3]undecyl and the tricyclo[5.3.1.$1^{3,9}$]dodecyl cations, the formation of the dications **36** and **40** with a close proximity of the two cation centers, is expected to cause a very large repulsion energy. In order to quantify the magnitude of this repulsion energy, the following homodesmic reactions of the monocations **78** and **34** and the *tert*-butyl cation were considered at a B3LYP / 6-31G* level of theory.

78 **36** **(30)**

34 **40** **(31)**

The expected high repulsion energy is clearly reflected in the two strongly endothermic reactions **(30)** and **(31)**, with calculated free energies of + 89.0 and + 88.7 kcal/mol. In an attempt to estimate the stabilization of the dications **36** and **40** through strain relief, the tertiary dication **130**, with a fixed cation center separation of 2.81 Å (cation center separation in the bicyclic dication **36** is 2.80 Å and in the tricyclic cation **40** is 2.81 Å), was compared to the multicyclic dications **36** and **40**.

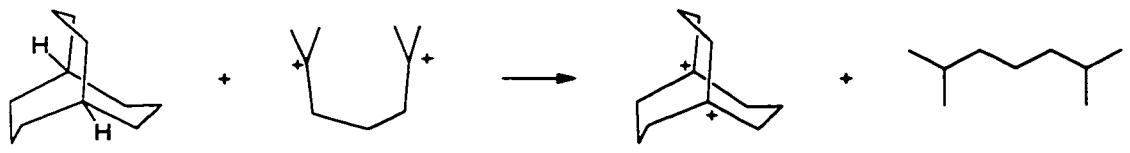

59 **130** **36** **131** **(32)**

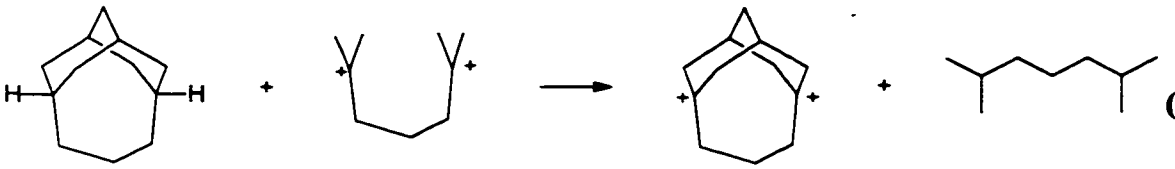

Despite the incorporation of some error due to additional steric interactions of the methyl groups in the dication **130**, the homodesmic reactions **(32)** and **(33)** illustrate that stabilization through angle strain relief is in the order of 21.0 kcal/mol for the bicyclo[3.3.3]undeca-1,5-diyl dication and 22.2 kcal/mol for the tricyclo[5.3.1.$1^{3,9}$]dodeca-5,9-diyl dication.

The bicyclo[3.3.3]undecyl mono and dication have already been prepared by Olah and coworkers;[183] however, no experimental details were given.

In this work the bicyclo[3.3.3]undec-1-yl monocation **78** was prepared either by dissolving a CD_2Cl_2 solution of the alcohol **109** in a solution of SbF_5 and FSO_3H in SO_2ClF at -116°C or adding a solution of the chloride **111** in CD_2Cl_2 to a solution of SbF_5 in SO_2ClF.

At very low temperatures (-116°C), the ^1H NMR spectra are consistent with a C_3-symmetry axis, which produces axial and equatorial type hydrogens in the three bridges, and these show different chemical shifts. Warming the monocation solution to 211 K caused a collapse of two of the NMR peaks at 3.9 and 2.8 ppm, showing that a ring flipping conformational change was occuring (Figure 36). The rate for this process was measured as 10.5 ± 0.3 kcal/mol. In the previous work of Olah,[183] this conformational flip was not seen.

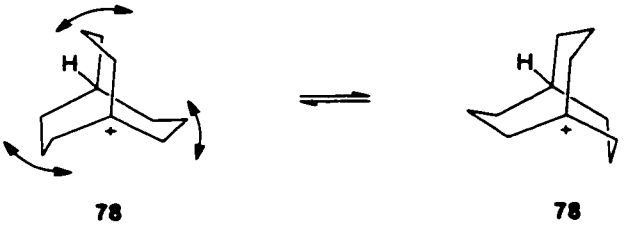

Figure 36: Flipping process of the C_3-bridges of the bicyclo[3.3.3]undecyl cation.

Upon further heating, the cation sample experiences decomposition into a complex mixture. At 232 K within a time period of 25 min. decomposition peaks became noticeable and at 242 K, 70 % of the monocation had decomposed within 25 min., corresponding to an activation energy of 17 ± 0.3 kcal/mol.

The best results for the preparation of the bicyclo[3.3.3]undeca-1,5-diyl dication **40** were obtained by dissolving the dichloride **129** in a solution of SbF_5 in SO_2ClF at -116°C, resulting in the formation of a clear, slightly yellow solution of the cation. In some cases, the addition of a small amount of CD_2Cl_2 was used to obtain a lock signal in the NMR spectrometer. In these cases, using typically 15 mg of the dichloride with 100 mg SbF_5 in 1.8 mL of SO_2ClF and 0.2 mL CD_2Cl_2, a metastable solution was formed at -116°C. The sample could be maintained at this temperature for several hours without any noticeable change. However upon warming to -80 to -70°C (189 to 200 K) most of the dication irreversibly precipitated. Generation of the dication at -78°C in the concentrations described above, formed initially a clear yellowish solution, from which most of the dication precipitated as fine white crystals after a time period of *ca.* 1 min. Addition of fluorosulfonic acid only slightly increased the solubility of the dication. Using a much more concentrated SbF_5 solution in SO_2ClF (300 mg SbF_5 in 0.4 mL SO_2ClF) finally prevented precipitation of the dication. On maintaining these dication solutions at -73°C (200 K) for 20 min., small amount of decomposition product was noted. At -52°C (221 K) 80 % of the dication decomposed within 20 min., corresponding to an activation energy for decomposition of 15.4 ± 0.5 kcal/mol.

Interestingly, the absence of the small amount of CD_2Cl_2 in the dication solution had a dramatic effect on the behavior upon heating, resulting in a well defined rearrangement (see Section 2.3.3.1 page 110).

The observation of dynamic NMR behavior as a result of the flipping process previously discussed was somewhat difficult, since significant decomposition was occurring at the ^1H NMR coalescence temperature of -62°C (211 K). Nevertheless, the energy barrier for the flipping process was measured as 9.4 ± 0.5 kcal/mol using line shape analysis techniques.

Comparing the energy barrier for this bridge flipping process in the alkane, the monocation and the dication of the bicyclo[3.3.3]undecyl system one sees a gradual decrease of the energy barrier from the 11.0 kcal/mol in the hydrocarbon to 10.5 kcal/mol in the monocation and 9.4 kcal/mol in the dication. This decrease can be explained by a smaller amount of angle strain in the transition state implied by the sp^2 hybridized bridgehead centers compared to the sp^3 hybridized bridgehead centers of the hydrocarbon (see Figure 37).

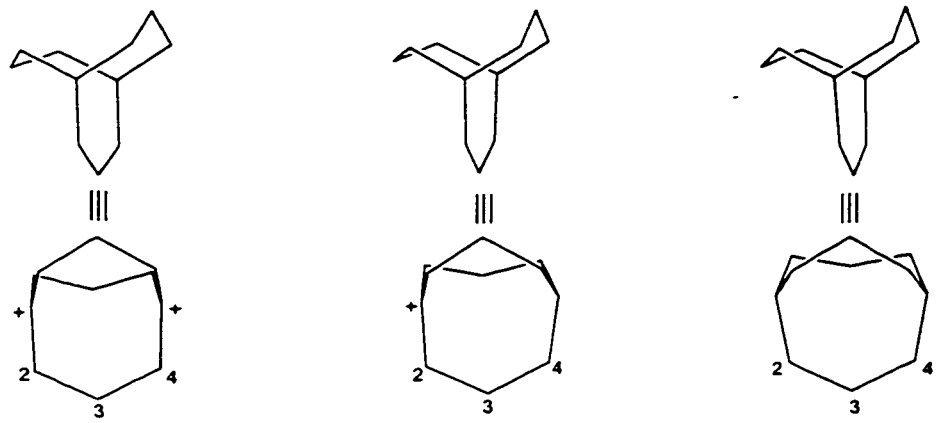

36 **78** **59**

increasing angle strain of the C2-C3-C4 bridge

Figure 37: Transition states for the C_3-bridge flipping process in the bicyclo[3.3.3]undecyl system.

An interesting property of the bicyclo[3.3.3]undecyl cations **34** and **40** is the ^{13}C NMR chemical shift behavior. The positive carbocation carbon chemical shift of the monocation **34** was measured as 357.5 ppm and in the dication **40** as 347.0 ppm. Since the geometry of the charged cation center is practically identical in the mono or the dication, one would expect that the stabilization through relief of angle strain as well as hyperconjugation to be very similar in both cations. Hence, the paramagnetic shielding effect of the cation center is expected to be very similar and the difference of the chemical shift should be a result of different charge densities around the cation centers. Naively, one might have expected the dication to show the lower field chemical shift, but if one examines the LUMO orbitals of the mono cation **78** and the dication **36** (see Figure 38) one can see that the charge is more localized in the monocation.

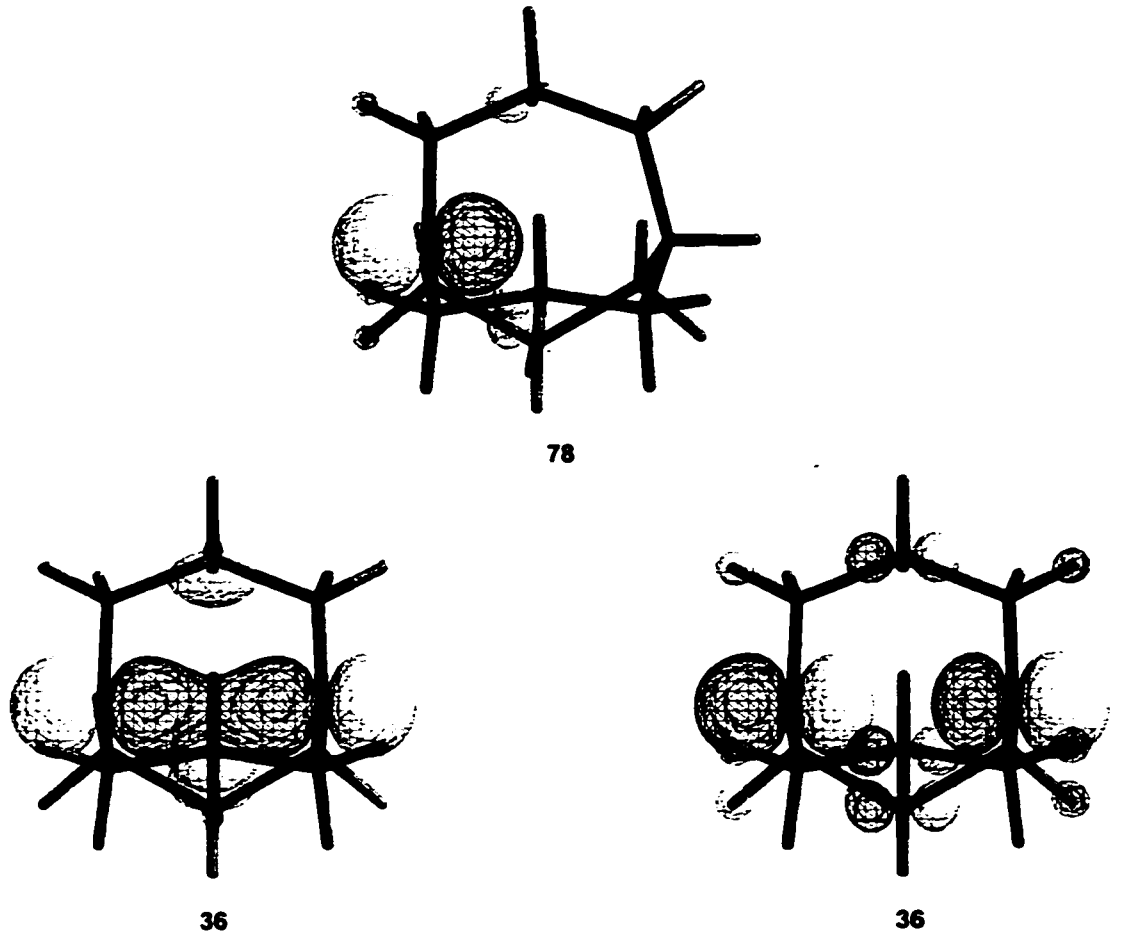

Figure 38: LUMO and LUMO + 1 orbitals of the monocation **78** and the dication **36**.

Furthermore, the calculated Mulliken charges (B3LYP / 6-31G*), normalized to one in the monocation and two in the dication, quantify the local charge at the corresponding cation center in question and values of 0.32 and 0.27 were obtained for the monocation **34** and the dication **40** at a B3LYP / 6-31G* level of theory.

This unexpected property of the monocation having a lower field ^{13}C chemical shift than the dication could be reproduced theoretically using *ab initio* calculations. The B3LYP / 6-31G* optimized geometries of the bicyclic monocation **78** and dication **36** were used for the GIAO NMR calculations at an MP2(Full) / 6-31G* level of theory. The experimental and theoretical spectral comparisons are shown in Figures 39 and 40.

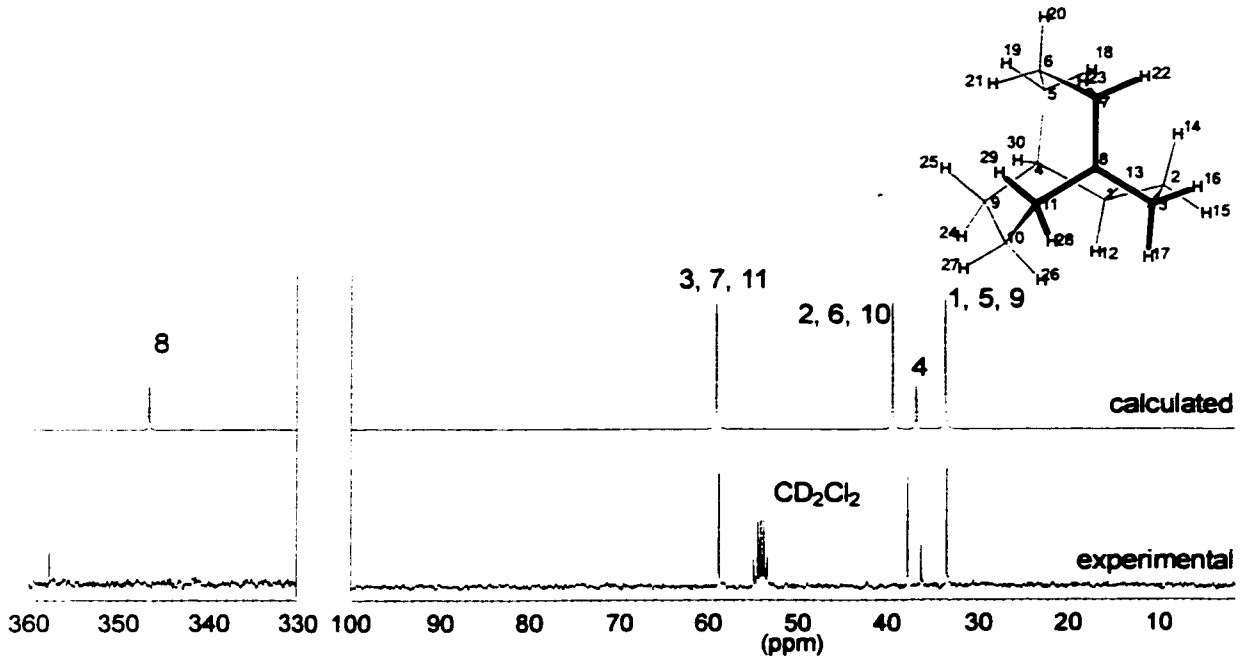

Figure 39: Experimental (bottom) and calculated (MP2(Full) / 6-31G* // B3LYP / 6-31G*) (top) NMR spectra of the bicyclo[3.3.3]undecyl cation **78**.

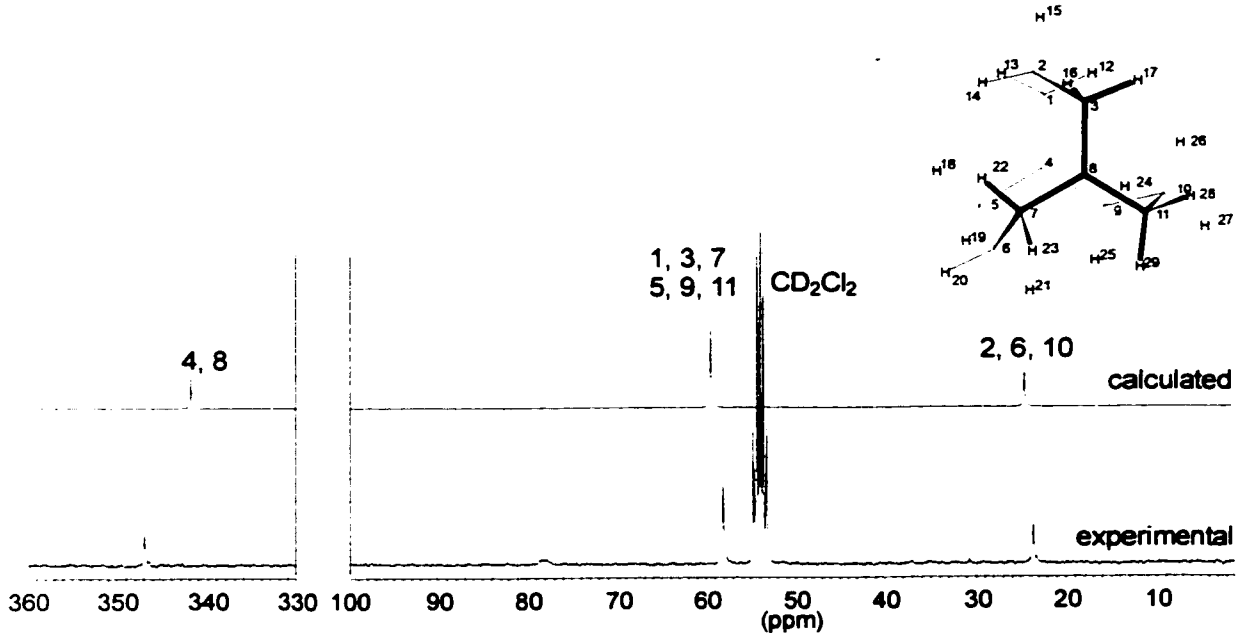

Figure 40: Experimental (bottom) and calculated (MP2(Full) / 6-31G* // B3LYP / 6-31G*) (top) NMR spectra of the bicyclo[3.3.3]undecyl dication **36**.

The experimental high field ^{13}C signals show excellent agreement with the calculated gas-phase values, with deviations of approximately 2 ppm. The cationic centers however, show a slightly higher deviation which could be caused by solvation effects, which should have a larger influence on the charged atoms. Nevertheless, the theoretically calculated ^{13}C chemical shift for the cation center in the monocation was predicted to be lower field than the corresponding shift in the dication, which is in agreement with the experimental observations.

Attempts to generate the tricyclo[5.3.1.$1^{3,9}$]dodec-1-yl cation in superacid solutions from the alcohol **120** under conditions used for the generation of related bicyclo[3.3.3]undecyl monocation were not successful (the corresponding chloride was not available as starting material see Section 2.2.2 , page 90). Instead of the expected tricyclo[5.3.1.$1^{3,9}$]dodec-1-yl cation, a pure solution of 2-ethyl-2-adamantyl cation **35** was obtained.

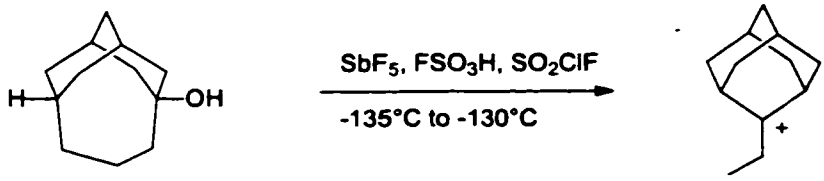

120 **35**

Lowering the temperature at which the alcohol **120** was ionized, to -135°C to -130°C, still resulted in the formation of cation **35** and no tricyclo[5.3.1.$1^{3,9}$]dodecyl cation **34** was formed (at this low temperature, the superacid mixture consisting of SbF_5, FSO_3H and SO_2ClF becomes very viscous, and it freezes if cooled further to *ca.* -140°C).

Since the ionization of alcohols in super acid solution is strongly exothermic (see Section 1.4.2, page 17) local heating was thought to be the reason for the complete rearrangement of the monocation **34** into the ethyladamantyl cation **35**. Alternatively, the protonation of an alkene to generate a carbocation is less exothermic and such a reaction should result in smaller local heating effects than for the ionization of the alcohol.

At temperatures of *ca.* -140°C (partially frozen superacid mixture) addition of a tricyclic bridgehead alkene **62** solution to the superacid solution produced a mixture of the desired tricyclo[5.3.1.$1^{3,9}$]dodec-1-yl cation **34** and the rearranged cation **132**.

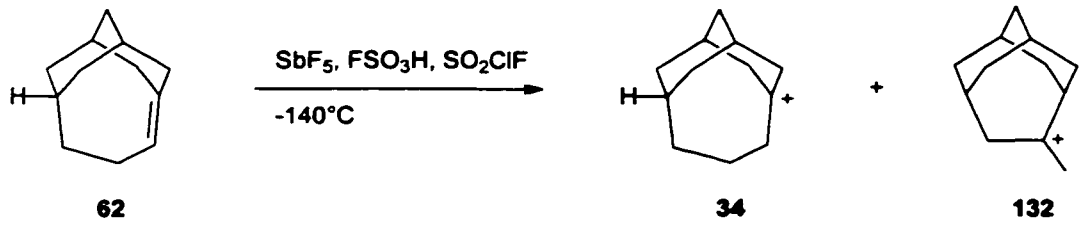

62 34 132

The preparation of the pure cation **132** was achieved by ionization of 6-methyltricyclo[4.3.1.$1^{3,8}$]undecan-6-ol **133** in superacid at -135°C, allowing one to assign all of the ^{13}C NMR signals of this cation.

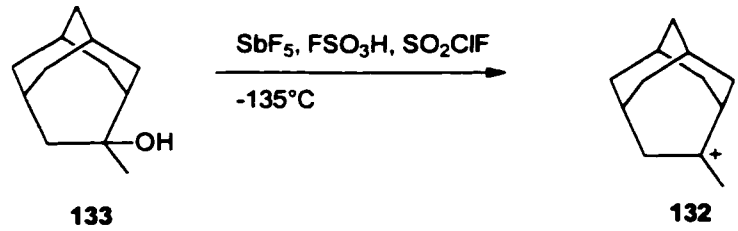

133 132

The carbon NMR of the cation **34** showed 12 signals with a C^+ chemical shift of 335.5 ppm. This chemical shift is distinctly different from the value found in the related bicyclo[3.3.3]undecyl monocation **78** (357.2 ppm), suggesting that structural and electronic effects must be rather different in these two systems.

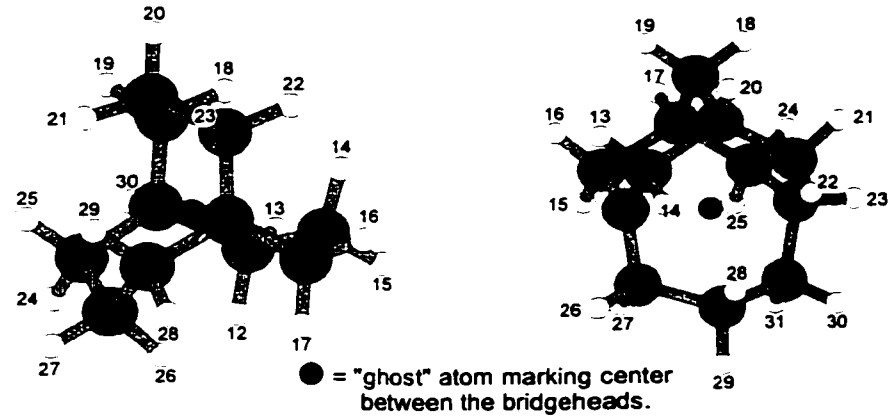

Figure 41: B3LYP / 6-31G* optimized geometries of the bicyclo[3.3.3]undecyl cation **78** and the tricyclo[5.3.1.$1^{3,9}$]dodecyl cation **34**.

The B3LYP / 6-31G* optimized structural features of cations **78** and **34** are summarized

in Table 20.

Table 20: Geometrical parameters of B3LYP / 6-31G* optimized structures **78** and **34**.

geometrical feature	bicyclo cation **78** (C_3 symmetry)		tricyclo cation **34**	
C^+-αC bond length [Å]	C8-C11	1.466	1.471 / 1.457 / 1.466	C2-C10 / C2-C3 / C2-C1
αC-βC bond length [Å]	C11-C10	1.575	1.556 / 1.611 / 1.605	C10-C11 / C3-C4 / C1-C6
αC-H bond length [Å]	C11-H28 / C11-H29	1.101 / 1.092	1.105 / 1.097 / 1.096 1.093 / 1.091 / 1.092	C10-H26 / C1-H13 / C3-H16 C10-H27 / C1-H14 / C3-H16
bridgehead axes - αC - βC torsion angle [°]	αH: H28 / H29	37.3 / 82.9	30.8 / 34.9 / 40.0 86.0 / 87.8 / 85.2	α-H: H26 / H13 / H16 α-H: H27 / H14 / H15
bridgehead axes - αC - βC torsion angle [°]	βC-αC: C10-C11	27.3	32.3 / 30.7 / 26.3	βC-αC: C11-C10 / C6-C1 / C4-C3
improper torsion angle at the C^+	C3-C8-C7-C11	174.3	171.5	C1-C2-C3-C10
distance to center between bridgeheads (ghost atom) [Å]	C10	2.092	2.104 / 2.049 / 2.041	C4 / C21 / C28

While the bicyclic monocation **78** has a C_3-symmetry and all the three bridges contribute the same amount of stabilization through C-H and C-C hyperconjugation, the tricyclic cation **34** shows slight differences between the three bridges. The two bridges in the adamantane-like substructure (C3-C4-C9 and C1-C6-C7) show shorter αC-C^+ bonds and longer αC-βC bonds than the C10-C11-C12 bridge, indicating that C-C hyperconjugation is more effective in the adamantane-like substructure, with the C3-C4-C9 bridge possessing the strongest C-C hyperconjugation. This property can be explained by the effect of the C5 CH_2 group in closing up the distance between carbons 4 and 6, which then results in a smaller torsion angle between the C2-C8 axis and the C3-C4 or C1-C6 bonds, respectively, as well as a smaller distance

between the carbons 4 or 6 and a line drawn between the bridgehead carbons. A smaller torsion angle and a closer proximity of the carbon atoms in question forms a geometry with more efficient overlap of the LUMO orbital (see Figure 35 and 42) and the corresponding C-C bonds, which in turn increases the C-C hyperconjugation. The difference between the two bridges in the adamantane-like substructure can be explained by a deformation of the LUMO orbital by the C-C and C-H hyperconjugation of the C10-C11-C12 bridge. This deformation forces the LUMO orbital to be slightly bent towards the C3-C4-C9 bridge, which in turn reflects a more extensive hyperconjugation (see orbitals in Figure 42 for the monocation **34** and Figure 46 for the dication **40**)

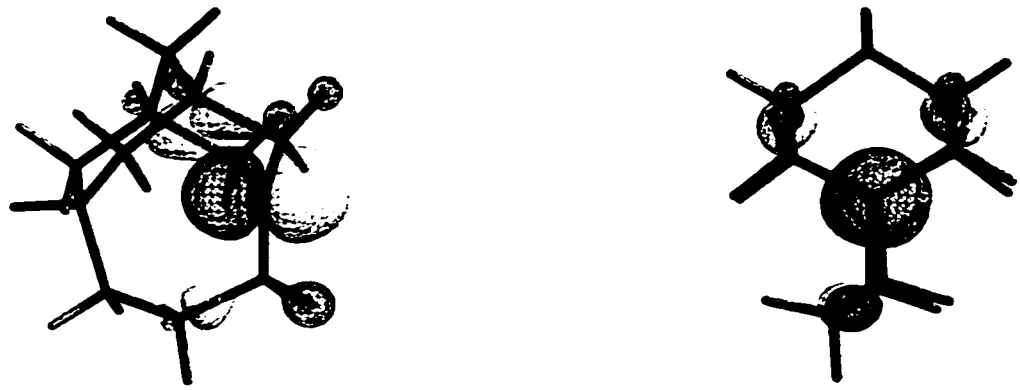

Figure 42: LUMO orbital of the tricyclo[5.3.1.$1^{3,9}$]dodecyl cation **34** at B3LYP / 6-31G*.

One can see a rather distinct difference between the orbital lobe sizes on the two bridges in the adamantane substructure (top two C_3 bridges in Figure 42) and the other bridge. The corresponding coefficients on the α-hydrogens, illustrating the strength of the C-H hyperconjugation, show the opposite trend and it appears that C-C and C-H hyperconjugation on an individual bridge are balanced out.

At this point it seems appropriate to mention that the shape of the LUMO orbital of a carbocation shows two important features. First, the coefficients of the LUMO indicate the most electrophilic regions, which is where a possible attack by a base or a nucleophile is expected to occur. Second, the strength and location of stabilizing interactions can be recognized from various lobe sizes. The latter feature is not a direct consequence of the LUMO

orbital and is easily misunderstood. Therefore, this principle is explained in somewhat greater detail in the following paragraph.

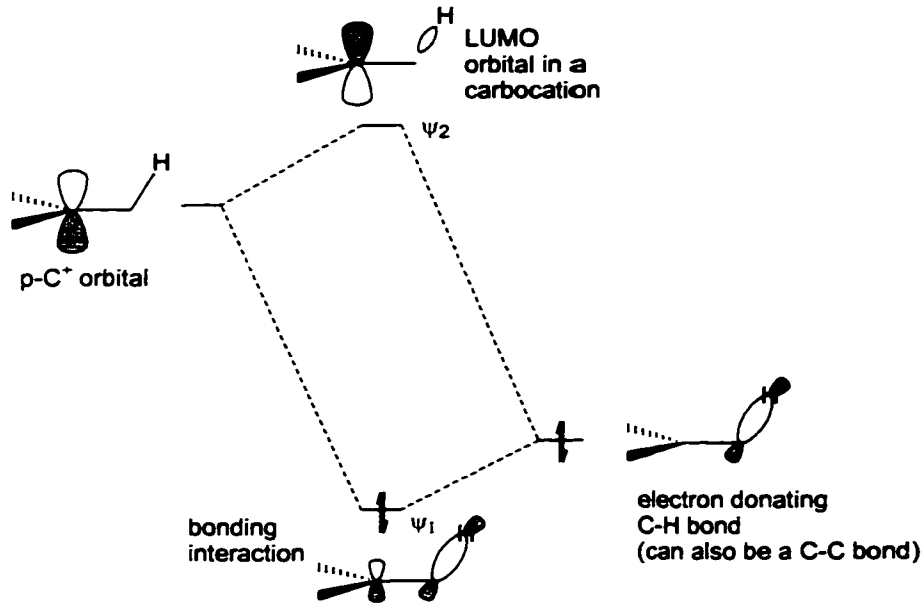

Figure 43: Hyperconjugation interaction between the p-orbital of a carbocation center (p-C^+) and a C-H bond.

Electron donation (stabilization) in most alkyl carbocations involve C-C or C-H bonds (hyperconjugation), which donate a small amount of their total electron density. A bonding interaction (in-phase interaction) between a p type orbital of a carbocation center (p-C^+) and a C-H bond (C-H- hyperconjugation) forms a new orbital (ψ_1 in Figure 43) with a lower energy than the original C-H bond. This interaction is the direct cause for the associated stabilization. However, in all but the smallest carbocations, these low-lying bonding orbitals are very complex (unlike the simple picture in Figure 43) and it is therefore difficult to identify the contribution made by this hyperconjugative interaction. Since every bonding interaction also has an antibonding counterpart, it is usually much easier to examine the LUMO orbital (ψ_2) to see these hyperconjugative interactions.

Ab initio GIAO NMR calculations at an MP2(Full) / 6-31G* level of theory on the B3LYP / 6-31G* optimized geometry of **34** were in good agreement with the experimentally measured data, as shown in Figure 44.

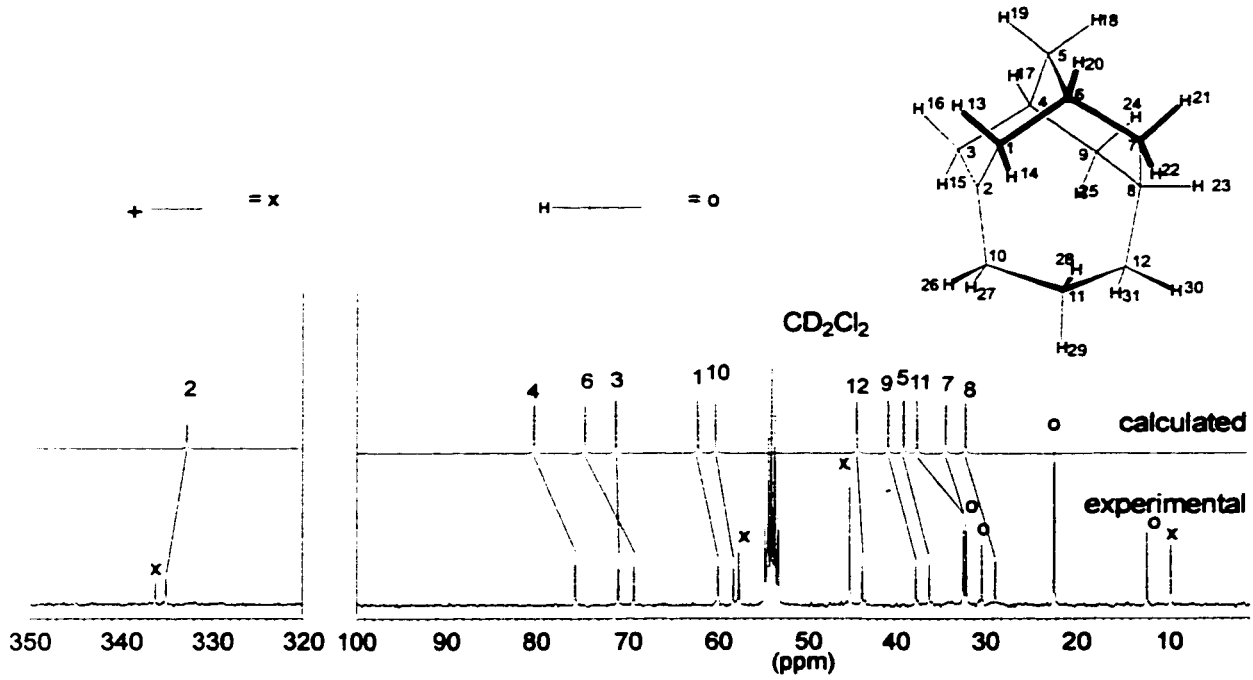

Figure 44: Calculated (MP2(Full) / 6-31G* // B3LYP / 6-31G*, top) and experimental (bottom) ^{13}C NMR spectra of tricyclo[5.3.1.$1^{3,9}$]dodec-1-yl cation, isopentyl cation and 2-methylpentane.

The cleanest spectra of the tricyclo[5.3.1.$1^{3,9}$]dodecyl monocation **34** were obtained by reducing the dication **40** with 2-methylpentane (see Section 2.2.3.2, page 132). The chemical shift of the cation carbon of **34** was calculated as 332.6 ppm and agreed very well with the experimental value of 335.1 ppm. A large difference in the chemical shift of the β-carbons in this system confirmed the distinct differences of the C-H versus C-C hyperconjugation in the three different bridges (C4: calc. 79.8 ppm, exp. 75.5 ppm, C6: calc. 74.1 ppm, exp. 69.2 ppm, C 11: calc. 36.8 ppm, exp. 32.2 ppm).

Comparing these values with the bicyclic monocation **78** (C^+: calc. 346.5 ppm, exp. 357.5, βC: calc. 39.3 ppm, exp. 37.5 ppm) one sees a large difference in these chemical shifts, confirming the distinct nature of these two systems.

The 12 individual signals in the ^{13}C NMR spectrum of **34** at temperatures lower than -60°C indicate that no symmetry is present in the molecule. Hence, the possible ring flip of the bridge C10-C11-C12 must be slow compared to the NMR time scale.

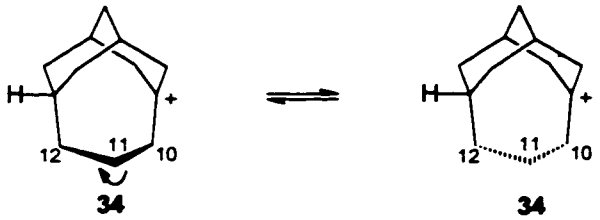

Attempts to measure the associated energy barrier for this process by warming **34** above -60°C resulted in irreversible rearrangement into the 2-ethyl-2-adamantyl cation (see Section 2.2.3.2, page 129), preventing one from measuring the energy barrier for a possible ring flip process.

Tricyclo[5.3.1.$1^{3,9}$]dodeca-5,9-decyl dication **40** was prepared by addition of a CD_2Cl_2 solution of the tricyclic dichloride **129** to a solution of SbF_5 in SO_2ClF at -116°C. NMR experiments at -105°C (168 K) revealed a species with eight different ^{13}C signals containing one absorption at 327.8 ppm, which is in accordance with the static geometry of the dication **40**.

Considering the ring flip process of the bicyclo[3.3.3]undecyl system, the associated energy barrier varies less than 2 kcal/mol comparing the alkane **59** with the dication **36**. By analogy, one would expect the energy barrier for the corresponding process in the tricyclo[5.3.1.$1^{3,9}$]dodecyl system to behave similarly and an energy barrier for this process in the dication of *ca.* 11 kcal/mol would be expected. NMR experiments at -105°C therefore are expected to reveal the frozen out or static structure, which is in agreement with the observed spectrum.

Furthermore, the extensive C-C hyperconjugation, observed in the monocation **34**, should also be present in the two adamantane like bridges of the tricyclo[5.3.1.$1^{3,9}$]dodecyl dication **40** and all but two carbon signals are expected to possess a relatively low field chemical shift. This indeed was the case with the observed ^{13}C NMR spectrum, which showed two CH signals at 72.1 and 67.1 ppm respectively as well as 3 CH_2 groups at 65.9, 60.1 and 57.4 ppm and two high field CH_2's at 35.1 and 27.6 ppm.

Theoretically calculated NMR shifts at a MP2(Full) / 6-31G* // B3LYP / 6-31G* level using the GIAO method were in good agreement with the experimental data (see Figure 45).

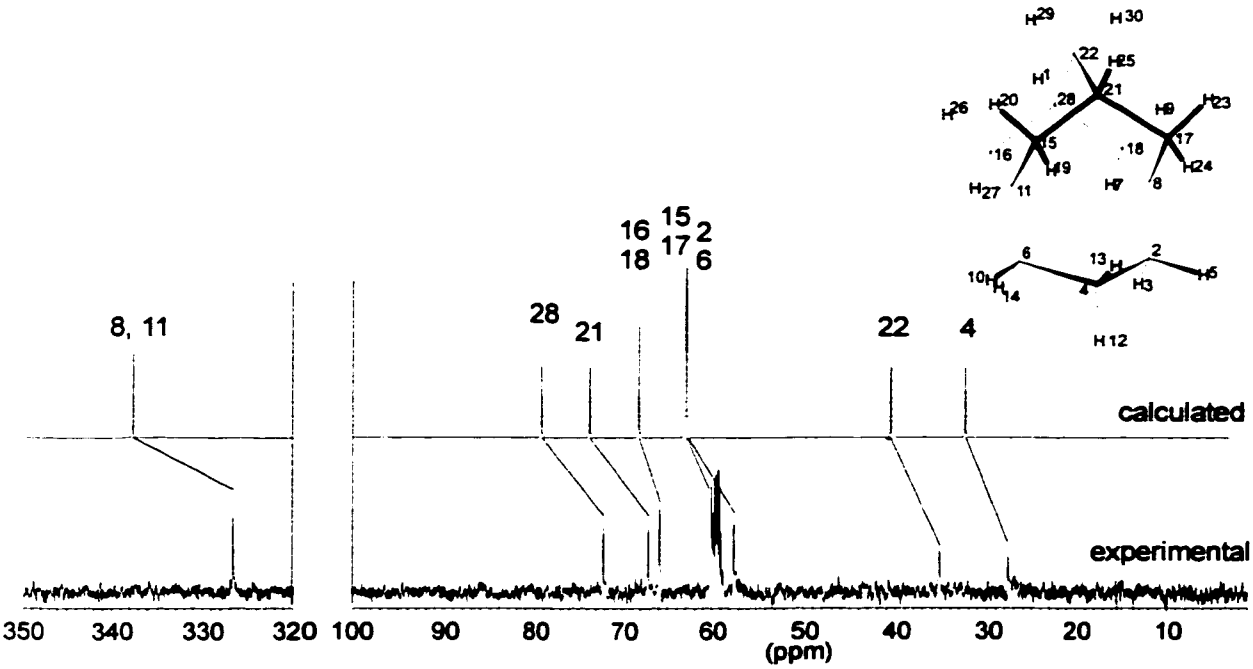

Figure 45: Experimental (bottom) and calculated (MP2(Full) / 6-31G* // B3LYP / 6-31G*) (top) ^{13}C NMR spectra of the tricyclo[5.3.1.$1^{3,9}$]dodeca-1,5-diyl dication **40**.

The chemical shift of the cation centers, 327.8 ppm, had a higher field chemical shift than the corresponding value for the monocation **34** (335.1 ppm). Although the theoretical prediction is for the opposite trend, the corresponding values differ only by a few ppm. These deviations most likely result from different solvation effects. Slightly different concentrations of the cation or SbF_5 in a sample solution can cause chemical shift changes of the C^+ carbon by several ppm. Hence, the deviation of the calculated and experimentally measured values can at least partially be attributed to solvent effects.

The higher chemical shift of the cation centers in the dication **40** compared to the cation center in the monocation **34** parallels the findings in the bicyclo[3.3.3]undecyl system and can be explained by the positive charge of the dication being spread out over a larger space, dispersing the positive charge on the cation centers (see also Section 2.2.3, page 96).

The Mulliken charges of the cation centers were calculated (B3LYP / 6-31G*) to 0.296 in the monocation (normalized to 1.00) and 0.266 in the dication (normalized to 2.00). The LUMO and LUMO+1 orbitals are given in Figure 46.

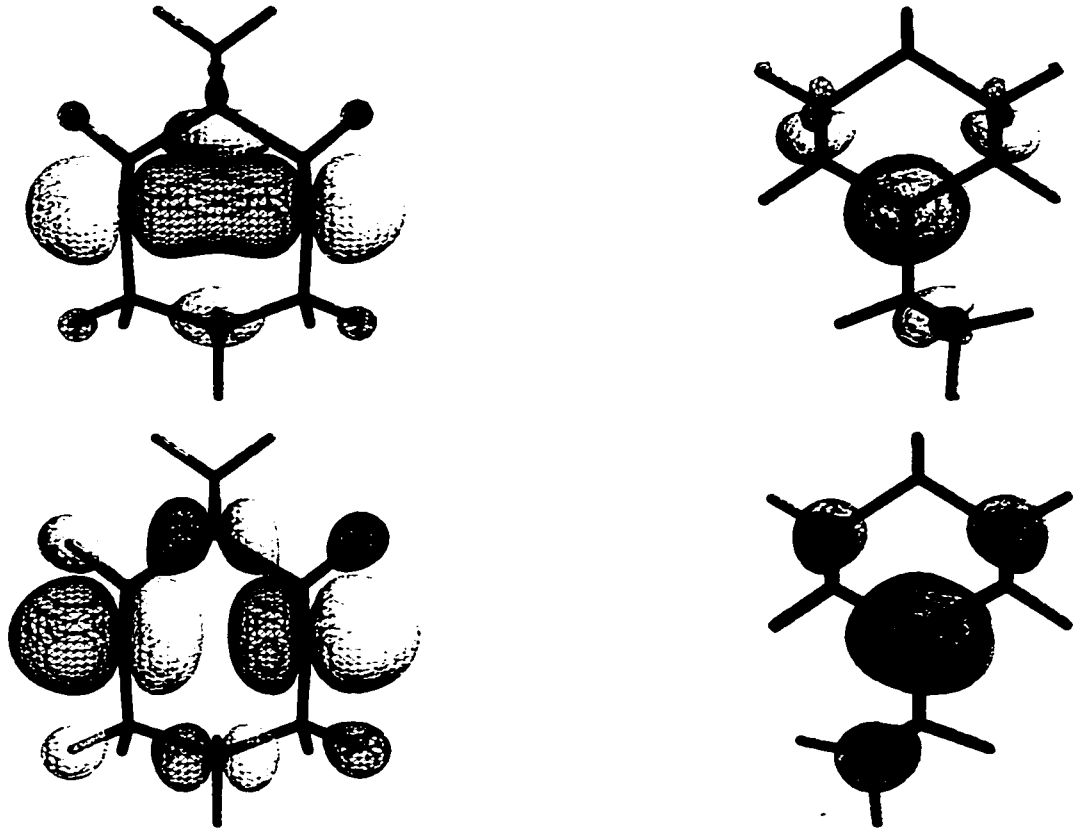

Figure 46: LUMO and LUMO+1 orbitals of the tiryclo[5.3.1.$1^{3,9}$]dodec-1.5-diyl dication **40** at B3LYP / 6-31G*.

The two p type orbitals of the cation centers interact with each other and produce an in-phase interaction, resulting in the formation of the LUMO and an out of phase interaction in the formation of the LUMO + 1 orbital. As in the monocation (see Section 2.2.3, page 101), stabilization of the dication through hyperconjugation forms a bonding and an antibonding interaction with the electron accepting orbital. In this case, however, there are two electron accepting orbitals, the LUMO and the LUMO + 1, which both interact with other bonds in the molecule. The LUMO orbital shows a relatively large component involving the α - β C-C bond and only minor contribution from the α C-H bonds. The LUMO + 1 orbital has about an equal contribution from the α C-H and the α - β C-C bond. Since the LUMO + 1 orbital possesses a higher energy than the LUMO orbital, the hyperconjugation interaction is expected to be stronger in the LUMO than in the LUMO + 1. Since the C-C hyperconjugation has a larger

contribution in the LUMO orbital, the stabilization of the dication through C-C hyperconjugation is therefore expected to be larger than that from C-H hyperconjugation.

A comparison of the geometrical features of cations **36** and **40** was carried out and the results are summarized in Table 21.

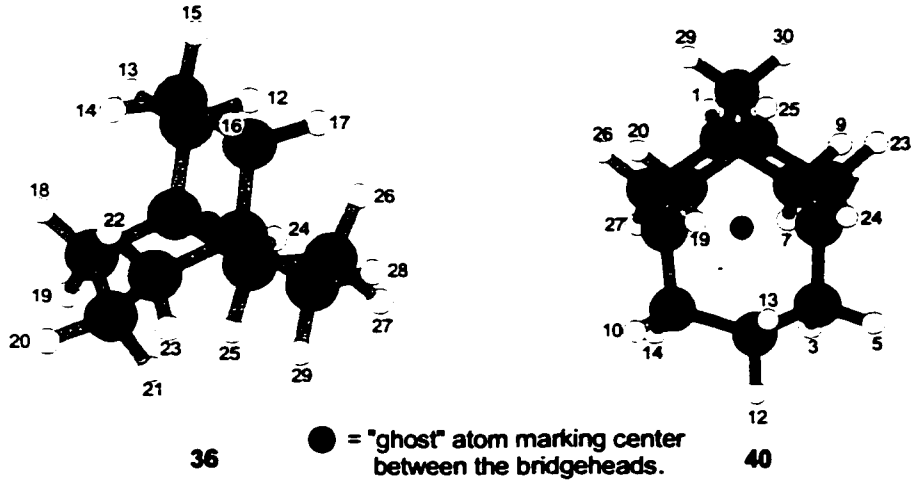

36 **40**

Figure 47: Optimized geometries of the dications **36** and **40** at the B3LYP / 6-31G* level of theory.

Table 21: Geometrical parameters of B3LYP / 6-31G* optimized structures **36** and **40** (see Figure 47 for the numbering system).

geometrical feature	bicyclic cation **36** (C_3 symmetry)		tricyclic cation **40**	
C$^+$-αC bond length [Å]	C8-C11	1.475	1.475 / 1.476 / 1.473	C2-C10 / C2-C3 / C2-C1
αC-βC bond length [Å]	C11-C10	1.577	1.572 / 1.595 / 1.597	C10-C11 / C3-C4 / C1-C6
αC-H bond length [Å]	C11-H28 / C11-H29	1.103 / 1.093	1.104 / 1.100 / 1.100 1.093 / 1.092 / 1.092	C6-H10 / C15-H20 / C16-H26 C6-H14 / C15-H19 / C16-H27
bridgehead axis - αC - βC torsion angle [°]	αH: H28 / H29	37.7 / 82.1	36.0 / 35.1 / 35.4 83.2 / 86.2 / 86.5	α-H: H10 / H20 / H26 α-H: H14 / H19 / H27

geometrical feature	bicyclic cation **36** (C_3 symmetry)		tricyclic cation **40**	
bridgehead axis - αC - βC torsion angle [°]	βC-αC: C10-C11	26.3	28.0 / 30.2 / 30.2	βC-αC: C4-C6 / C21-C15 / C28-C16
improper torsion angle at the C^+	C3-C8-C7-C11	171.7°	169.7°	C1-C2-C3-C10
cation center separation [Å]	C8-C4	2.796	2.813	C8-C11
distance to center between bridgeheads (ghost atom) [Å]	C10	2.089	2.094 / 2.055 / 2.051	C4 / C21 / C28

Comparing the properties of the two dications **36** and **40** only small geometrical differences in terms of bond distances and torsional angles were noted from the calculated structures. The biggest difference is in the distances of the carbon centers C21 and C28 of **40** to the center of the dication cavity (marked with a black dot in Figure 46; ghost atom) compared to the carbon center C10 - ghost atom in the bicyclic dication **36**. The smaller distances in the tricyclic dication **40** are in agreement with a stronger C-C hyperconjugation in the tricyclic structure, which would explain the experimental NMR data for the C21 and C28 carbons, which were found to be at a relatively low field position compared to the carbon C4 (see Figure 45). However, these differences in C-C or C-H hyperconjugation are not as large as in the monocation, which is also reflected in the sizes of the LUMO orbital lobes (see Figures 46 and 42).

Investigating the thermal stability of the dication **40**, one finds that the solution is stable up to -78°C for 15 min. without significant decomposition. Maintaining the cation solution at -63°C (210 K) for 10 min. causes approximately 90 % of the dication to decompose into a complex mixture, which corresponds to an activation energy of 14.5 ± 0.4 kcal/mol.

2.2.3.1 Rearrangement of the Bicyclo[3.3.3]undecyl dication

Maintaining a solution of bicyclo[3.3.3]undecyl dication in SO_2ClF at -78°C (absence of CD_2Cl_2) for an extended time period (12 h) caused a significant amount of the dication **36** to rearrange. Measuring the rate for the corresponding rearrangement at -52°C revealed that 36 % of **36** rearranged after 30 min., corresponding to an activation energy of 16.0 ± 0.4 kcal/mol. The initially formed rearrangement product showed 13 low field protons in the ^1H NMR spectrum, all of these assignable to an alpha position relative to the cation center, as well as two different C^+ signals at 329.3 ppm and 323.6 ppm in the ^{13}C NMR. DEPT experiments identified two overlapping methyl groups (peak areas determined using an inverse gated ^{13}C NMR spectrum), five methylene groups and two methine groups. The combination of this data allows one to propose the two possible candidates **134** and **135** for this first rearrangement product.

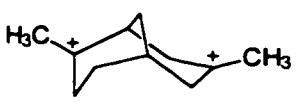

134

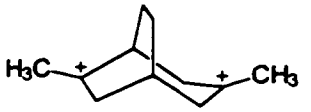

135

Using *ab initio* calculations at a B3LYP / 6-31G* level of theory, the ground state energy of **135** was calculated to be 5.0 kcal/mol higher than for **134**, suggesting that proposed structure **134** is the first observable intermediate.

Table 22: Calculated energies of possible intermediates in the rearrangement of bicyclo[3.3.3]undeca-1,5-diyl dication at B3LYP / 6-31G*.

Structure	HF [Hartree]	ZPE [kcal/mol]	$H°_{298}$-$H°_0$ [kcal/mol]	$S°_{298}$ [cal/mol K]	$G°_{298}$ [Hartree]	rel. energy (ref.) [kcal/mol]
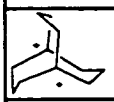 **36**	-429.294393323	168.46	6.73	93.29	-429.064241257	0
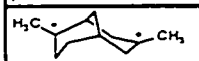 **134**	-429.323166043	165.50	7.44	99.50	-429.099413003	-22.07 (**36**)
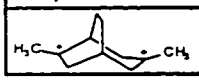 **135**	-429.313157785	164.91	7.71	102.82	-429.091437375	-17.07 (**36**)

Further support for this structure was gained by comparing the theoretically predicted ^{13}C

NMR shifts (B3LYP / 6-31G*) with the experimental values (see Table 23). From this comparison, structure **134** can be assigned to the first observable intermediate with a high degree of certainty.

Table 23: Calculated and experimental ^{13}C NMR shifts of the two dications **134** and **135**.

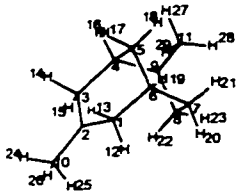 **134**			exp. values δ (ppm)	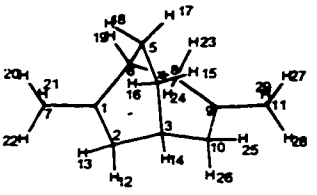 **135**		
atom number	calc. value: δ (ppm)	difference to exp. values		difference to exp. values	calc. value: δ (ppm)	atom number
1 (CH_2)	63.16	4.1	59.1	4.97	64.07	2 (CH_2)
2 (C^+)	321.80	-7.5	329.3	6.47	335.77	1 (C^+)
3 (CH_2)	55.92	1.9	54.0	-14.7	39.29	5 (CH_2)
4 (CH)	64.26	1.2	65.4	-5.8	59.59	6 (CH)
5 (CH_2)	57.47	-0.2	57.7	2.22	59.92	8 (CH2)
6 (CH)	35.48	2.7	32.8	2.78	35.58	3 (CH)
7 (CH_2)	64.09	-1.3	63.1	3.01	66.11	10 (CH_2)
8 (CH_2)	51.51	-2.5	54.0	-27.68	26.32	4 (CH_2)
9 (C^+)	310.19	-13.4	323.6	2.88	326.48	9 (C^+)
10 (CH_3)	46.11	-0.7	46.8	0.18	46.92	7 (CH_3)
11 (CH_3)	46.28	-0.6	46.9	2.06	48.96	11 (CH_3)

In measuring the rearrangement rate for the formation of **134** from **36** by maintaining the sample at -52°C for 30 min., a second rearrangement product could also be observed. After about 30 min. at -46°C, most of the initial dication **36** had disappeared and the first rearrangement product **134** became the main component of the reaction solution. Raising the temperature to - 41°C and maintaining it there for 30 min. caused 32 % of **134** to rearrange into the second product. This reaction rate corresponds to an energy barrier of 17.4 ± 0.4 kcal/mol. The formation and disappearance of the various dications in this reaction mixture can be followed by ^{13}C NMR spectroscopy, illustrated in Figure 48.

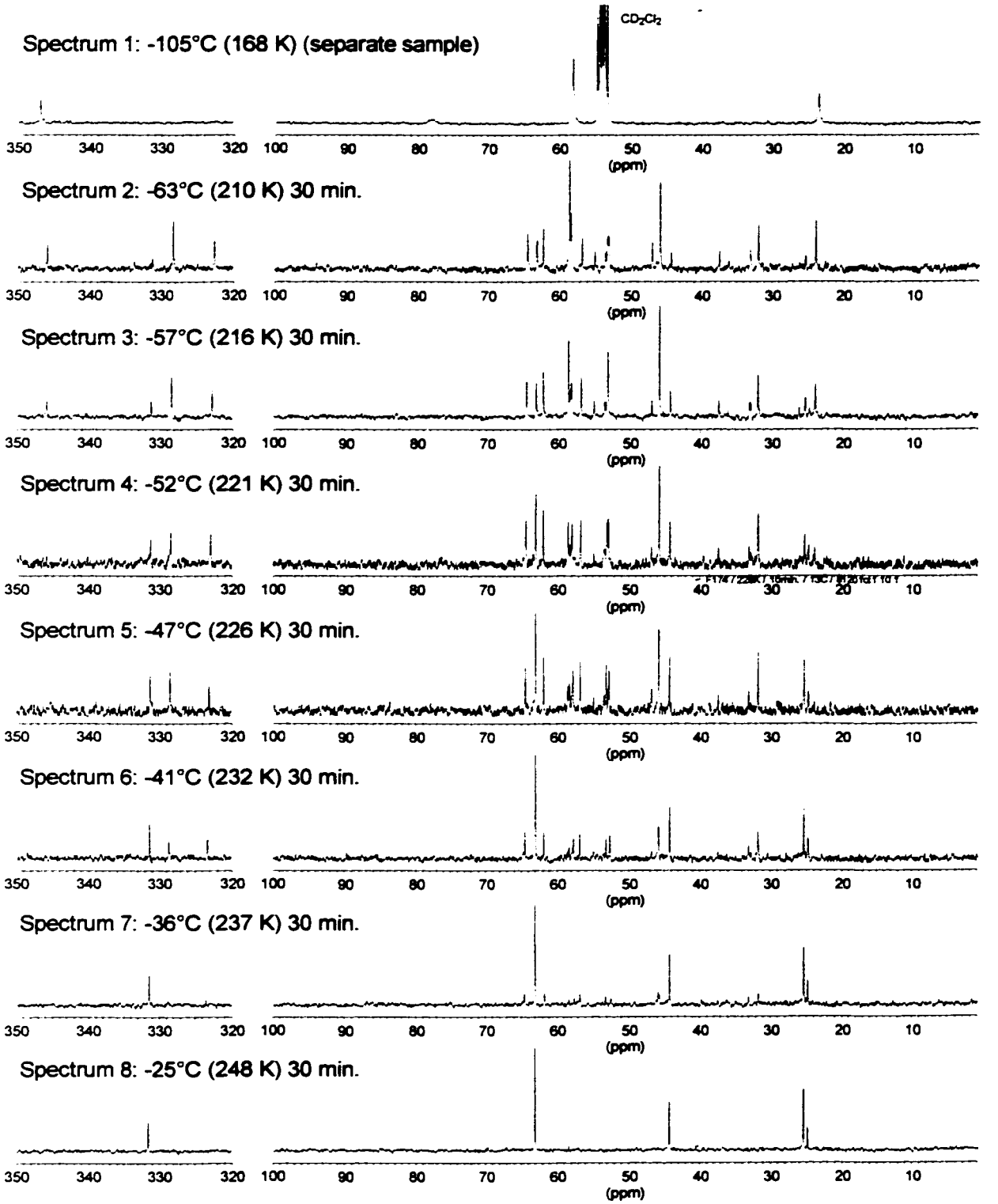

Figure 48: A series of ^{13}C NMR spectra showing the progress of the rearrangement of the bicyclo[3.3.3]undeca-1,5-diyl dication.

Eventually a relatively clean solution of the second rearrangement product was formed, which proved to be thermally quite stable. Only about 40 % of this cation had decomposed into a complex mixture after storing the sample at -18°C for one week. The ^{1}H NMR spectrum of this second product showed a low field doublet (4 H) at 4.6 ppm, a doublet of doublets (4 H) at 4.3 ppm and a quintet (6 H) at 3.7 ppm. Higher field singlets were found at 3.1 and 2.3 ppm, each of area two.

The ^{13}C NMR spectrum showed only five signals, whose relative areas could be determined using inverse gated broadband decoupling techniques. The five signals were measured at 332.3 ppm (two quaternary carbons), 64.0 (four methylene carbons), 45.3 (two methyl carbons), 27.3 (two methine carbons) and 26.7 (one methylene carbon). The presence of four identical methylene groups in a molecule with a total of 11 carbons requires one to have at least two planes of symmetry. Arrangement of two more pairs of identical carbons (one pair C^{+} and one pair CH) and a single CH_2 in a system with two planes of symmetry leaves only one possible structure, 3,7-dimethylbicyclo[3.3.1]nona-3,7-diyl dication **37**, for the second rearrangement product .

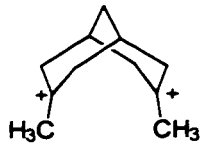

37

Ab initio calculations at a MP2(Full) / 6-31G* // B3LYP / 6-31G* level of theory were used to compare the experimentally obtained ^{13}C NMR spectrum with the theoretically predicted chemical shifts (see Figure 49).

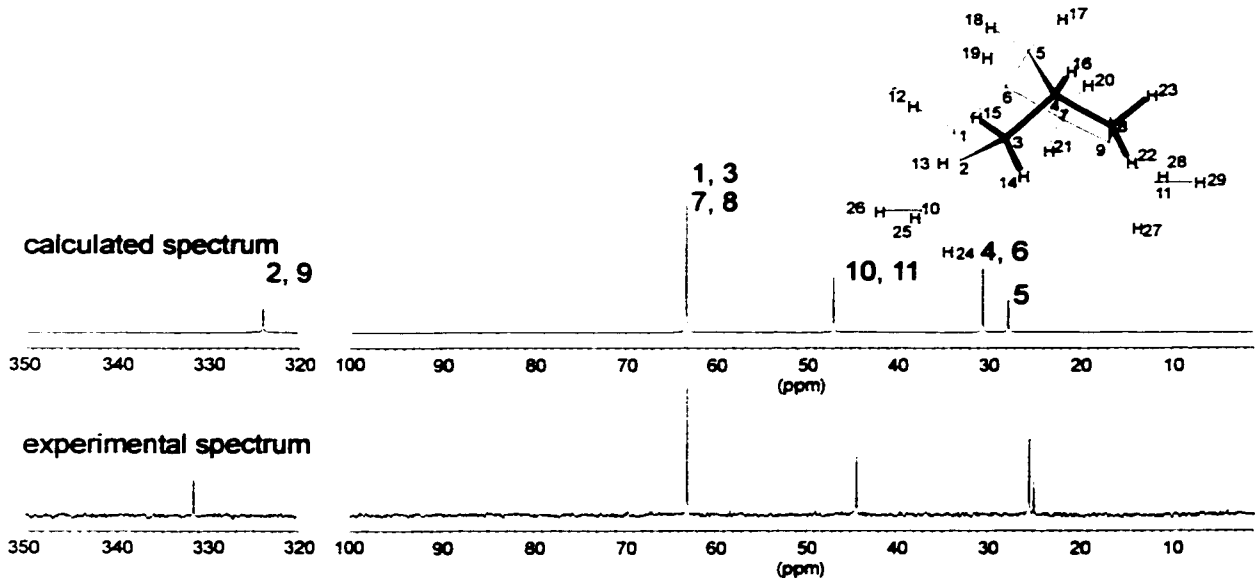

Figure 49: Comparison of the experimentally measured and the calculated (B3LYP / 6-31G*) ^{13}C NMR spectrum of 3,7-dimethylbicyclo[3.3.1]nona-3,7-diyl dication **37**.

Quite good agreement between the theoretically predicted and experimentally measured chemical shifts were obtained, confirming the proposed structure **37** as the second rearrangement product.

The optimized (B3LYP / 6-31G*) geometry of **37** (see Table 24 for selected parameters) reveals a bicyclo[3.3.1]nonyl structure with a very large torsion angle of the methyl groups to the bridgehead methines. This unusual geometry, resembling the transition state of a flipping process of the C3 bridges in the bicyclo[3.3.1]nonyl system, can be attributed to the large repulsion energy of the two cation centers.

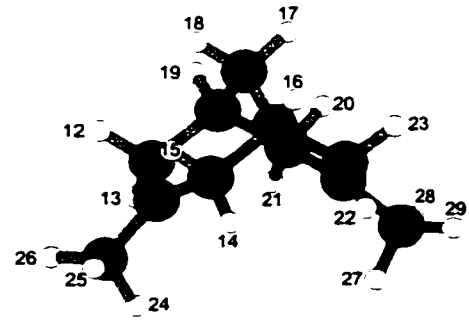

37

Table 24: Geometrical parameters of B3LYP / 6-31G* optimized structures of dication **37** (C_{2v}).

geometrical feature		
C^+-αC bond length [Å]	C2-C10 / C2-C1	1.467 / 1.474
αC-βC bond length [Å]	C1-C6	1.548
αC-H bond length [Å]	C1-H12 / C10-H24 C1-H13 / C10-H25	1.114 / 1.111 1.101 / 1.095
bridgehead axis - αC - βC torsion angle [°]	C4-C3-C2-C9	35.7
αC-C^+- αC - βC torsion angle [°]	C10-C2-C3-C4	167.8
improper torsion angle at the C^+	C1-C2-C3-C10	176.8
cation center separation [Å]	C2-C9	3.579
distance of βC to C^+ [Å]	C4-C2	2.586

The considerably larger separation of the two cation centers in **37**, relative to **36** (3.58 Å vs. 2.81 Å) is expected to be the main driving force for the rearrangement, in which dication **37** was calculated to be 26.9 kcal/mol more stable than dication **36**, using a B3LYP / 6-31G* level of theory. This value is close to the calculated (B3LYP / 6-31G*) energy difference (27.0 kcal/mol) between the two 2,5-dimethylhepta-2,5-diyl dication structures **130** and **136**. In the latter, the cation structure was fully optimized to give a C^+ - C^+ separation of 5.21 Å, while structure **130** was optimized with the cation centers being restricted to a 2.81Å distance.

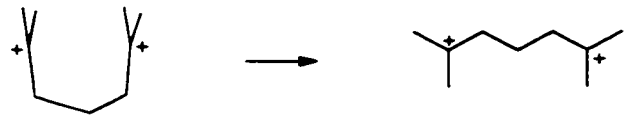

130 **136**

An interesting feature of dication **37** is the ^{13}C NMR chemical shift of the bridgehead carbons (C4, C6), which show very little sign of being involved in C-C hyperconjugation.

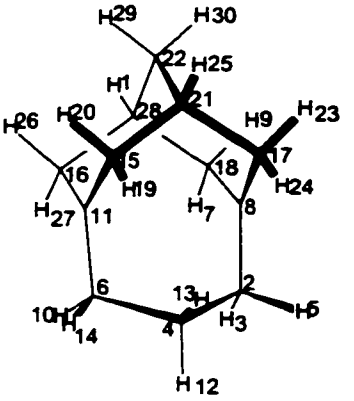

40

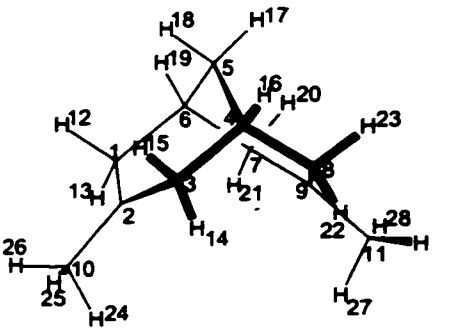

37

A comparison of **37** with the related tricyclic dication **40** illustrates the dependance of C-C hyperconjugation, as reflected in the chemical shift of the affected carbons (e.g. C4 / C6 in **37** and C21 C28 in **40**), and the distance between these and the corresponding C^+ carbon (2.59 Å in **37** and 2.49 Å in **40**).

In the tricyclic dication **40**, C21 and C28 had chemical shifts of 67.1 and 72.1 ppm, respectively, while in the dication **37**, C4 and C6 were observed at 26.3 ppm (see Figure 48).

Off-setting the lack of C-C hyperconjugation in **37** is a much stronger C-H hyperconjugation (in comparison to **40**). This interaction is visible in plots of the LUMO and LUMO + 1 orbitals of **37**.

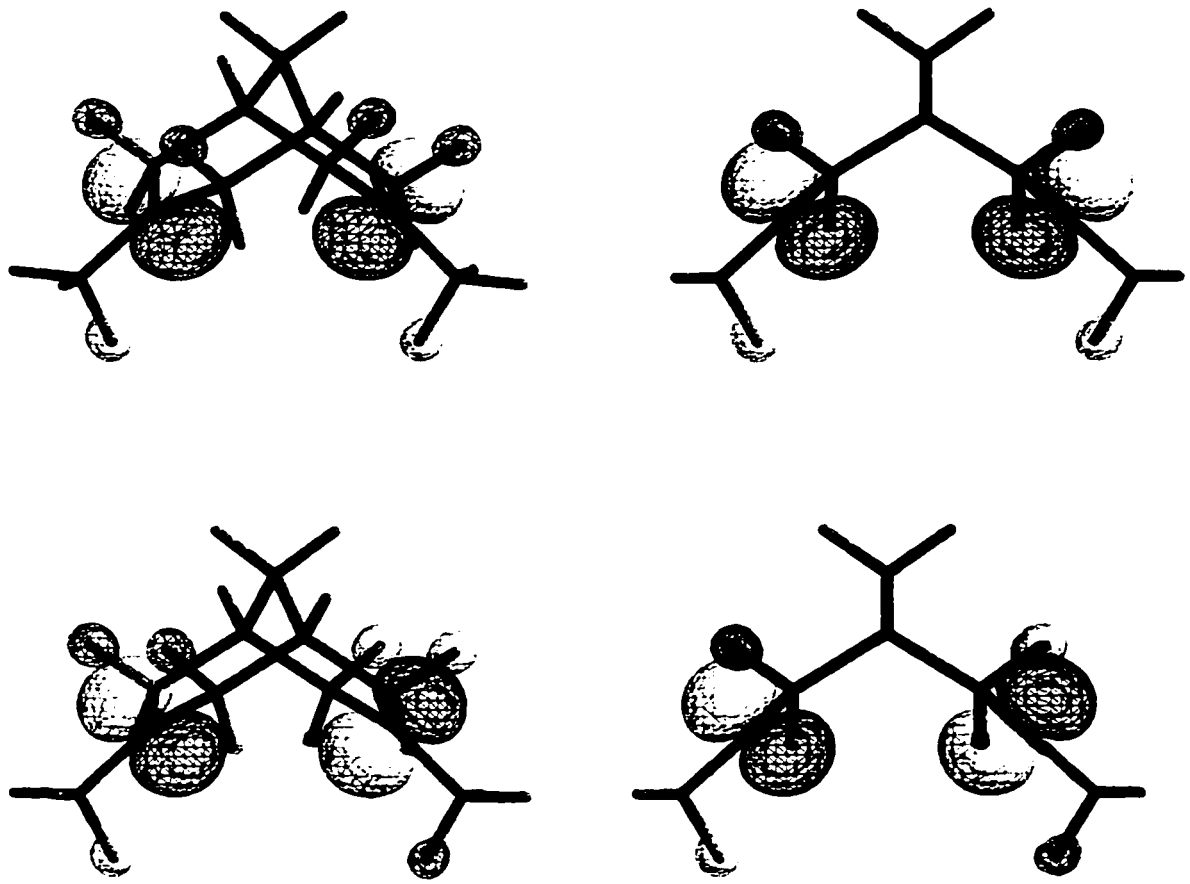

Figure 50: LUMO (top) and LUMO + 1 (bottom) orbitals of the 3,7-dimethylbicyclo[3.3.1]nona-3,7-diyl dication **37**.

In considering a possible mechanism for the rearrangement of dication **36** into **37**, it becomes clear that the first step must be a 1,2 hydride shift in the bicyclo[3.3.3]undecyl dication (see Scheme 8). The only other plausible first step is a ring contraction which would result in the formation of a primary carbocation (or protonated cyclopropane), both high energy intermediates, so this reaction is unlikely to occur.

Scheme 8: Proposed reaction mechanism for the rearrangement of the bicyclo[3.3.3]undecyl dication **36** (numbers in brackets are the relative free energies according to B3LYP / 6-31G* calculations referenced to the dication **36**).

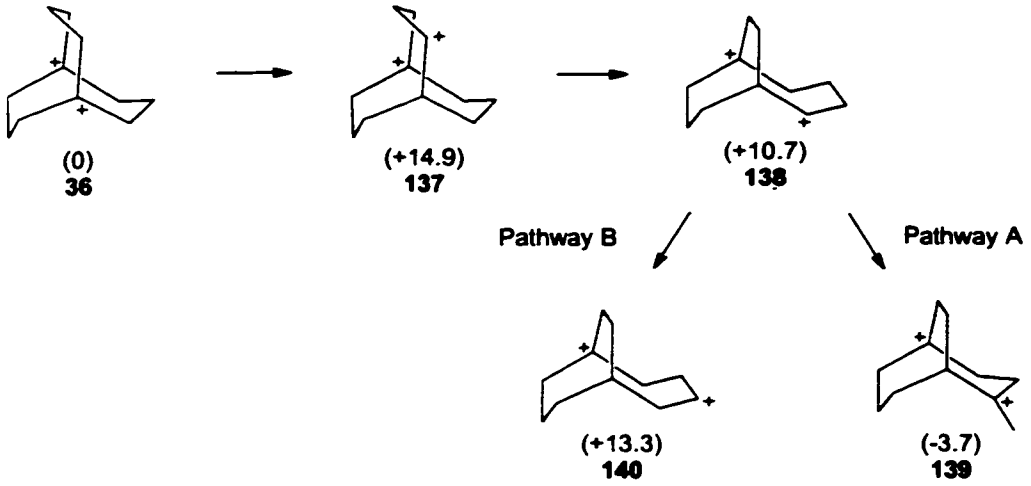

Ab initio calculations at the B3LYP / 6-31G* level of theory show the secondary cation **137** to possess a relative free energy of 14.9 kcal/mol (relative to the bicyclo[3.3.3]undecyl dication **36** as zero). A 1,2-alkyl shift of either bridge would form the secondary cation **138** with a relative free energy of 10.7 kcal/mol. At this point two reasonable pathways leading to the first observable rearrangement intermediate **134** are proposed.

Scheme 9: Pathway A of the bicyclo[3.3.3]undecyl dication rearrangement. Values in brackets correspond to relative free energies according to B3LYP / 6-31G* calculations referenced to the dication **36**.

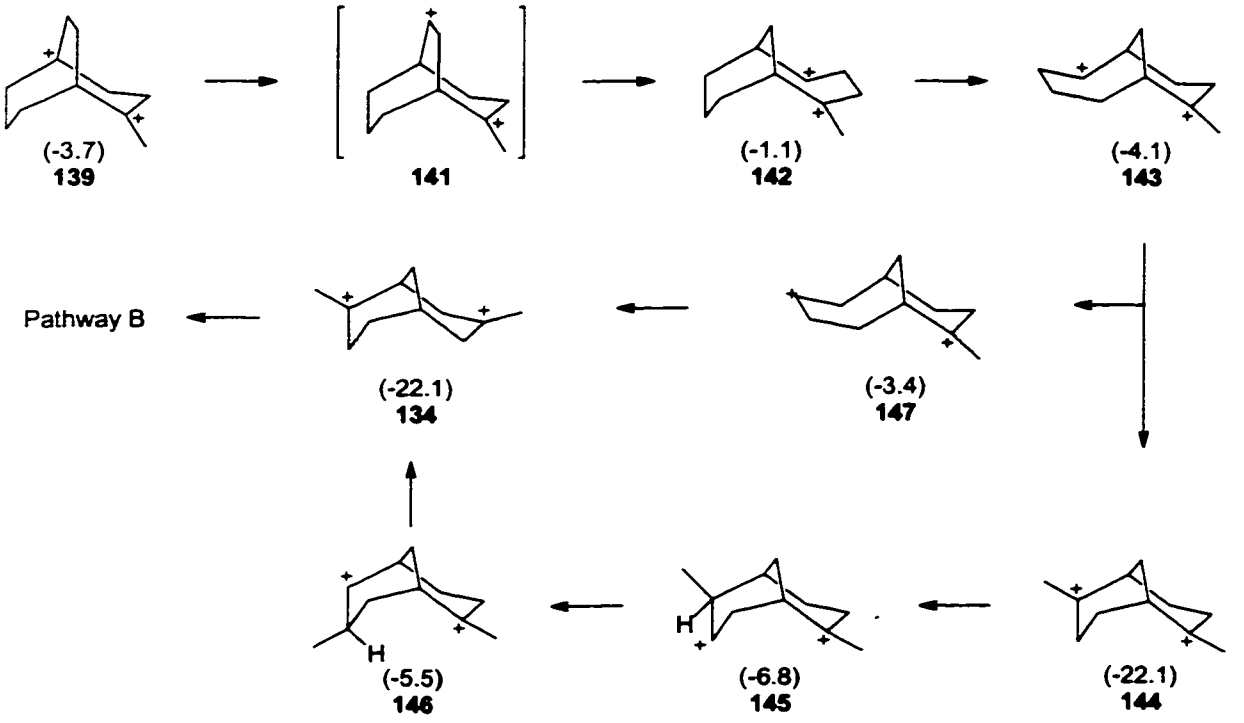

The first proposed pathway (pathway A) consists of an initial ring contraction of the intermediate **138** to the methyl substituted bicyclo[3.3.2]decyl dication **139** with a relative free energy of -3.7 kcal/mol. A 1,2 hydride shift from the C_2 bridge to the bridgehead in **139** would form the secondary cation **141** which was not a ground state according to calculations at the B3LYP / 6-31G* level of theory. Attempts to optimize the geometry of **141** led to the structure **142**, which was found to be 1.1 kcal/mol lower in energy than the initial bicyclo[3.3.3]undeca-1,5-diyl dication **36**. Rearranging **142** by a 1,2 alkyl shift of the C_1 bridge leads to the bicyclo[4.3.1]decyl cation **143** (rel. free energy: -4.1 kcal/mol) from which either a 1,2 hydride shift (intermediate **147** with a rel. free energy of -3.4 kcal/mol), followed by a ring contraction would lead to the first observable cation **134**, or one could have an initial ring contraction of **143** to form **144** (-22.1 kcal/mol) followed by series of hydride and methyl shifts involving intermediates **145** and **146** to also form the first observable cation **134**.

Starting from the intermediate **138** the second pathway (Pathway B) (see Scheme 10)

follows a route involving intermediates **140** (+13.3 kcal/mol), **148** (+0.0 kcal/mol), **149** (-0.3 kcal/mol) and **150** (-0.5 kcal/mol). From the proposed intermediate **150** two different routes would lead to the final rearrangement product **37**. The first route would be a hydride shift followed by a ring contraction involving the secondary cation intermediate **151**, with a relative free energy of -6.9 kcal/mol compared to **36**. This route however would not involve the first observed intermediate **134** and it is therefore not the most promising pathway variation. The second route would be a ring contraction of the intermediate **150** to form the first observable intermediate, which could then undergo a hydride - methyl - hydride shift sequence to form the final 3,7-dimethylbicyclo[3.3.1]nona-3,7-diyl dication. Only the first intermediate **152** was found to be a ground state according to B3LYP / 6-31G* calculations, possessing a relative free energy of -11.9 kcal/mol. Attempts to optimize the geometry of **153** at the same calculation level resulted in the formation of **37**.

Scheme 10: Pathway B of the bicyclo[3.3.3]undeca-1,5-diyl dication rearrangement. Relative free energies compared to the dication **36** are given in brackets.

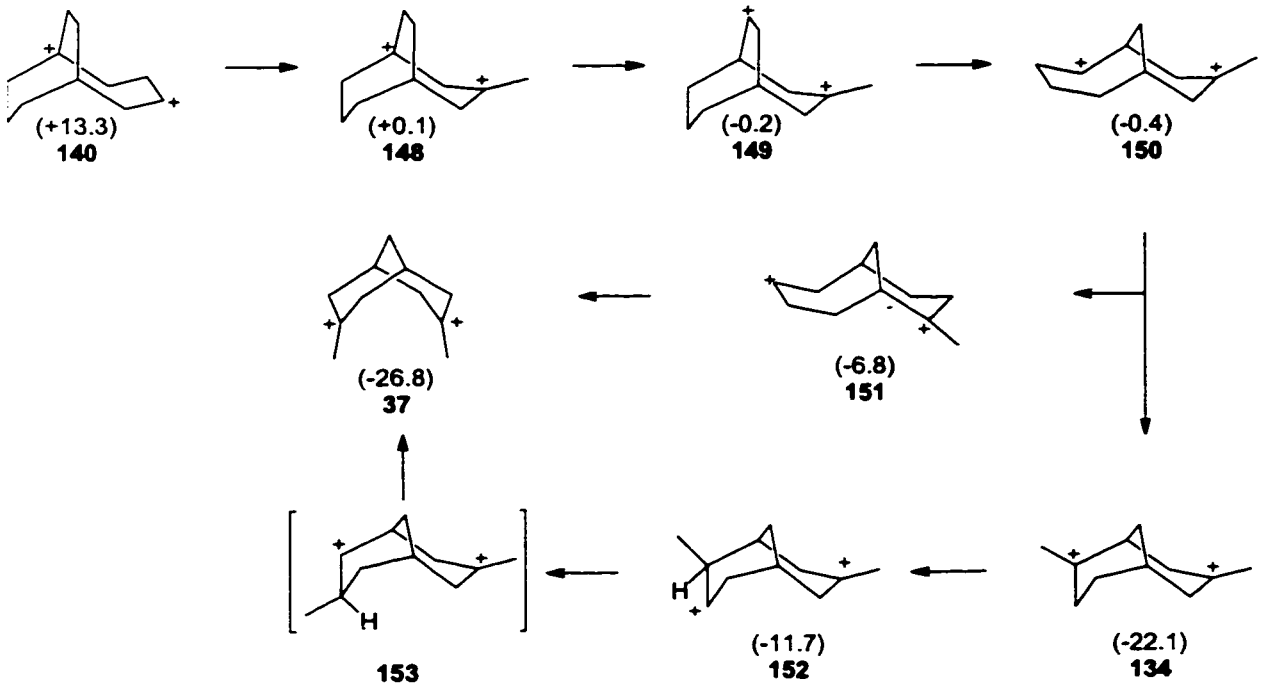

Considering that all the reaction steps are hydride or alkyl shifts, which are expected to

possess similar transition states with similar energy barriers, pathway A involving the intermediate **145** would be the most probable reaction cascade, since all the intermediates involved have relatively low free energies. The second route in pathway A consisting of the intermediates **144**, **145** and **146** is expected to be a less probable reaction route, since the intermediate **144** was calculated to possess an almost identical relative free energy to the experimentally observed dication **134**, and a reaction mechanism involving this intermediate should have resulted in a detectable concentration of this cation at some point in the rearrangement cascade.

Table 25 summarizes the calculation results on all of the intermediates under discussion.

Table 25: Calculated energies of possible intermediates in the rearrangement of bicyclo[3.3.3]undeca-1,5-diyl dication at B3LYP / 6-31G*.

Structure	HF [Hartree]	ZPE [kcal/mol]	$H°_{298}$-$H°_0$ [kcal/mol]	$S°_{298}$ [cal/mol K]	$G°_{298}$[[hartrees]	rel. energy (ref.) [kcal/mol]
 **36**	-429.294393323	168.46	6.73	93.29	-429.0642412567	0
 **137**	-429.269760524	168.17	6.93	94.88	-429.040479246	14.91
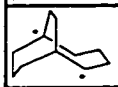 **138**	-429.275879291	168.08	7.03	96.24	-429.04722044	10.68
 **139**	-429.296996849	167.40	7.28	98.54	-429.070087202	-3.67
 **142**	-429.291385363	166.60	7.39	99.36	-429.065922695	-1.06
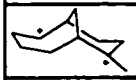 **143**	-429.296188693	166.40	7.34	98.67	-429.070795295	-4.11
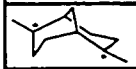 **144**	-429.323117598	165.67	7.55	100.49	-429.099389063	-22.06
 **145**	-429.299751023	166.47	7.61	101.38	-429.075080897	-6.80
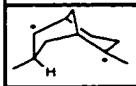 **146**	-429.29987096	165.71	7.69	101.83	-429.073052616	-5.53
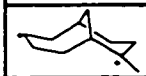 **147**	-429.295138467	166.42	7.28	98.28	-429.069629551	-3.38
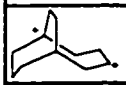 **140**	-429.269899735	167.06	7.07	96.60	-429.042930401	13.37
 **148**	-429.288838503	166.21	7.38	99.57	-429.064106794	0.08

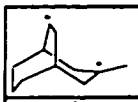	**149**	-429.29025852	166.34	7.23	97.49	-429.064577486	-0.21
	**150**	-429.287733611	165.14	7.41	99.97	-429.064813509	-0.36
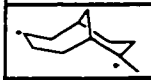	**151**	-429.298569431	165.24	7.35	98.97	-429.075102311	-6.82
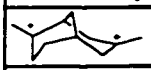	**134**	-429.323166043	165.50	7.44	99.50	-429.099413003	-22.07
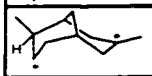	**152**	-429.304063093	165.04	7.83	104.94	-429.082951953	-11.74
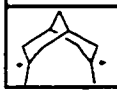	**37**	-429.329015847	164.58	7.51	100.32	-429.106970612	-26.81

In order to obtain conclusive evidence for the identity of the 3,7-dimethyl-bicyclo[3.3.1]nona-3,7-diyl dication **37**, it was synthesized via a more straightforward route.

The synthetic strategy for the "direct" generation of dication **37** was to prepare a dimethyl substituted bicyclo[3.3.1]nonane system with two functionalities in place suitable for ionization in superacid solutions.

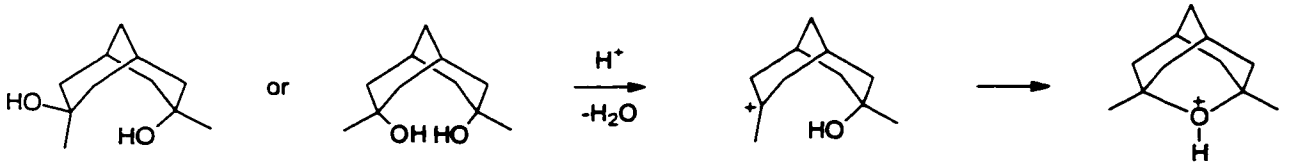

154 **155** **156** **157**

Possible precursors **154** and **155** would be expected to form the protonated ether **157**, by analogy to the known reaction of the diene **158** to form the substituted adamantane derivative **161** in acidic solutions.[184]

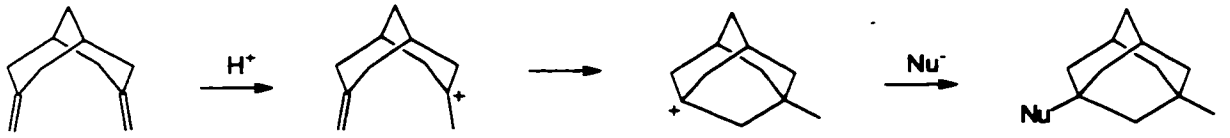

158 **159** **160** **161**

Less likely to form such adamantane-like structures would be the precursor **162** . Ionization of the tertiary position in superacid solution is expected to occur very rapidly, while the primary chloride would probably initially form a Lewis acid complex, species **163**.

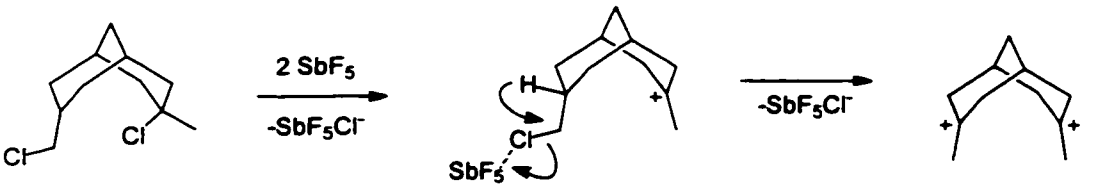

162 **163** **37**

Eventually, the second ionization could be facilitated by a simultaneous hydride shift to generate **37**.

The synthesis of the precursor **162** was attempted starting from adamantane. The electrophilic introduction of two chlorine substituents to give **164** was carried out according to a literature procedure.[185]

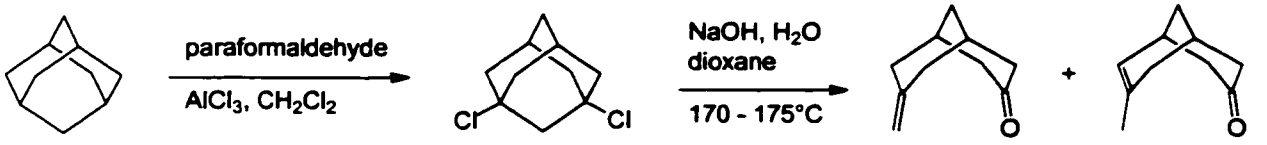

113 **164** **165** **166**

The ketones **165** and **166** were obtained as a mixture, via a Grob fragmentation of **164** at 170 to 175°C. According to McKervey *et. al.*[185] the Grob fragmentation of **164** under identical reported conditions resulted in the formation of the pure **165**. In related work Stephanov and coworkers [186] found that attempted hydrogenation of 3,7-dimethylidenebicyclo[3.3.1]nonane **158** with Raney nickel catalyst led to formation of the isomeric dienes **167** and **168**.

158 **167** **168**

Similar observations were published by Kimoto and coworkers,[187] who found that ketone **165** was isomerized upon attempted hydrogenation with PtO_2 / H_2 in acetic acid.

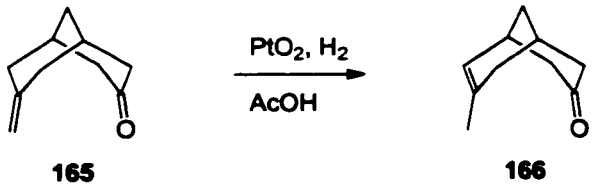

165 **166**

The Grob fragmentation reaction carried out in this work was conducted in a stainless steel apparatus and traces of noble metals from previous hydrogenation reactions could have been present on the surface of the reactor, explaining the formation of the **165** and **166** mixture.

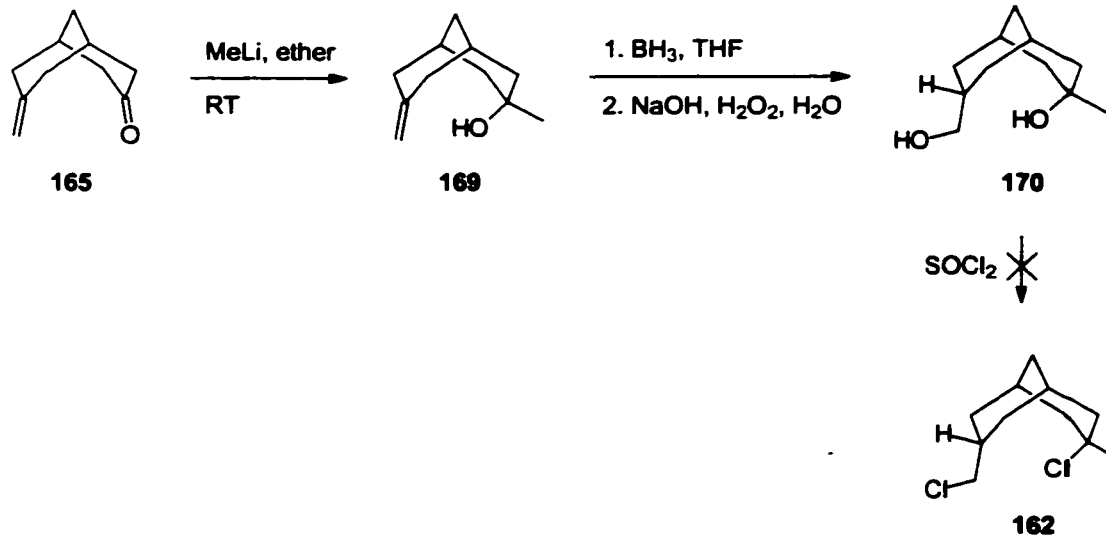

165 **169** **170** **162**

Treatment of the ketone **165** with methyl lithium in ether resulted in the formation of the tertiary alcohol **169** in only 7 % yield, the rest being the recovered starting material **165**. Refluxing the reaction solution of the ketone **165** and methyllithium had no influence on the yield. This result can be explained by a competitive enolization reaction of the carbonyl group, with methyllithium acting as a base, as shown below.

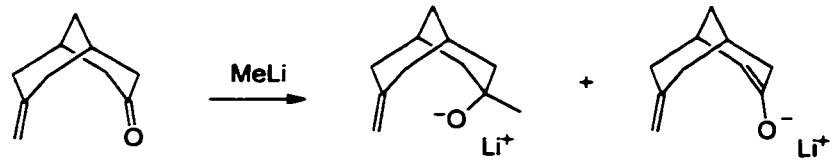

165 7 % **171** 93% **172**

Nevertheless, repeated cycles of methyllithium addition to an etheral solution of the ketone **165** could be used to increase the overall yield of the tertiary alcohol, which was then separated using column chromatography. Hydroboration followed by alkaline oxidation formed the diol **170**. However, attempts to convert the diol **170** into the desired dichloride **162** using thionyl chloride resulted in the formation of a complex mixture.

Since diol **170** was available, an ionization of this was attempted using a mixture of SbF_5 -

FSO_3H in SO_2ClF at -116°C. However, the resulting solution consisted of a mixture of the protonated ether **173** and the dication **174** in a 1 : 0.6 ratio. Increasing the temperature to -52°C (221 K) for 78 min. caused about 80 % of the cation mixture to decompose. No formation of the dication **37** could be observed.

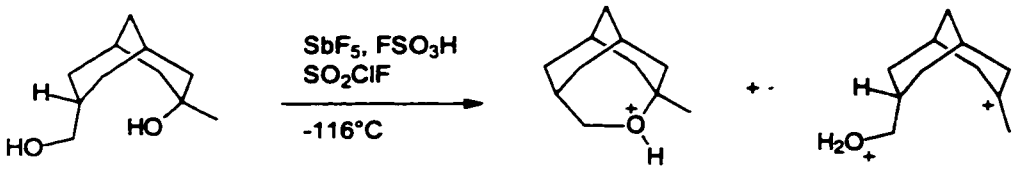

170 **173** **174**

Another approach to dication **37** would be the treatment of the chloride **175** with Magic Acid solution. The possible cationic cyclization of the alkene **175** to **176** is expected to be considerably less favorable than the corresponding reaction of the alkene **158** due to the larger ring strain in **176** as well as an unfavorable steric interaction between the two methyl groups.

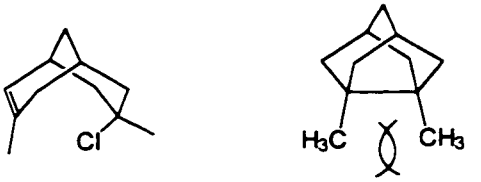

175 **176**

Reaction of ketone **166** with methyllithium once again involved a competition with an enolization side reaction, however, the ratio was found to be more favorable towards the formation of the desired tertiary alcohol **179**.

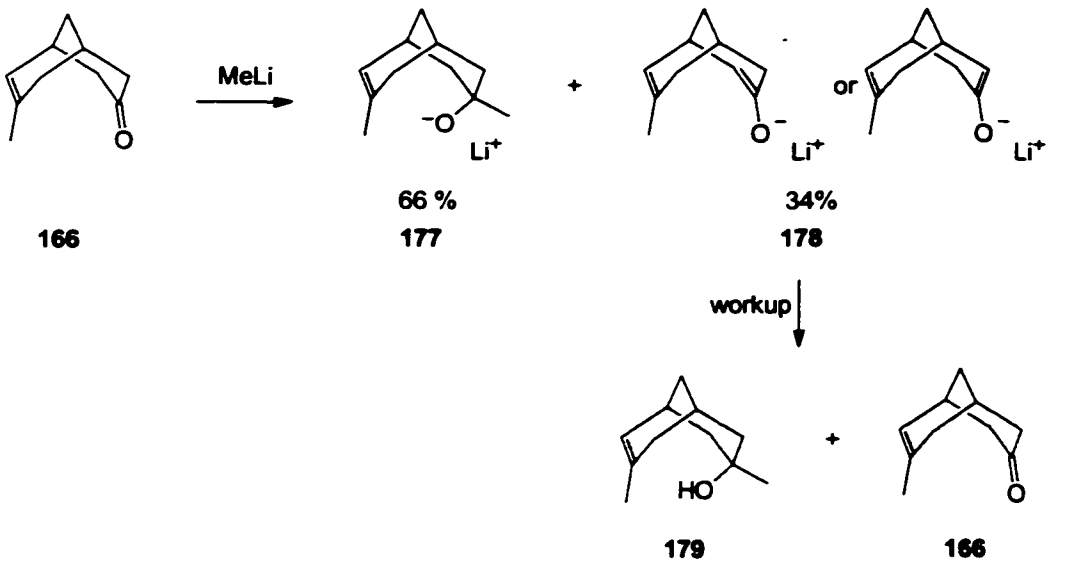

Attempts to convert **179** into the corresponding chloride **175** either with thionyl chloride or with conc. HCl (this reaction also had the prospect of forming a dichloride, which would also be an appropriate precursor) resulted in the formation of a complex mixture. Having no access to the chloride **175**, the ionization of the alcohol **179** was attempted in superacid solution, in the hope that the rate for the protonation of the alcohol group would be comparable to the protonation of the double bond, which might then allow the formation of some 3,7-dimethylbicyclo[3.3.1]nona-3,7-diyl dication **37**.

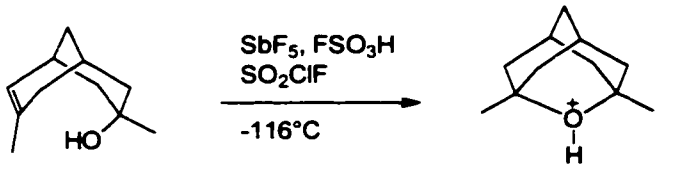

However, the solution contained as the sole product, O-protonated 1,3-dimethyl-2-oxatricyclo[3.3.1.$1^{3,7}$]decane **157**, which showed no sign of decomposition after several hours at -52°C.

The final successful approach to **37** involved protonation of the dienes **167** and **168**.

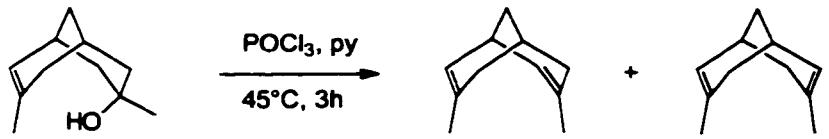

179 167 168

The preparation of these starting materials, as a mixture, was accomplished by treating the advanced intermediate **179** with a mixture of $POCl_3$ - pyridine.

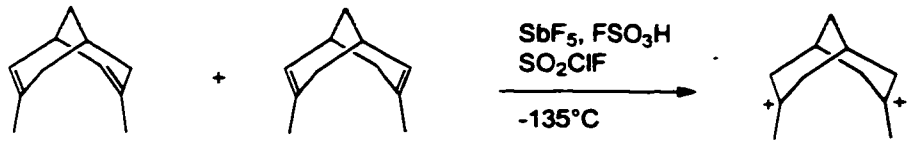

167 168 37

Addition of a precooled (-78°C) SbF_5 - FSO_3H solution in SO_2ClF to an NMR tube containing a thin film of the dialkenes **167** and **168** at -135°C finally formed the desired dication **37**, whose spectral data were in accordance with the spectra obtained by the rearrangement of **36** (see Figure 51 and 52). The cation solution formed from dienes **167** and **168** was not entirely clean, but all of the peaks assigned to cation **37** were visible.

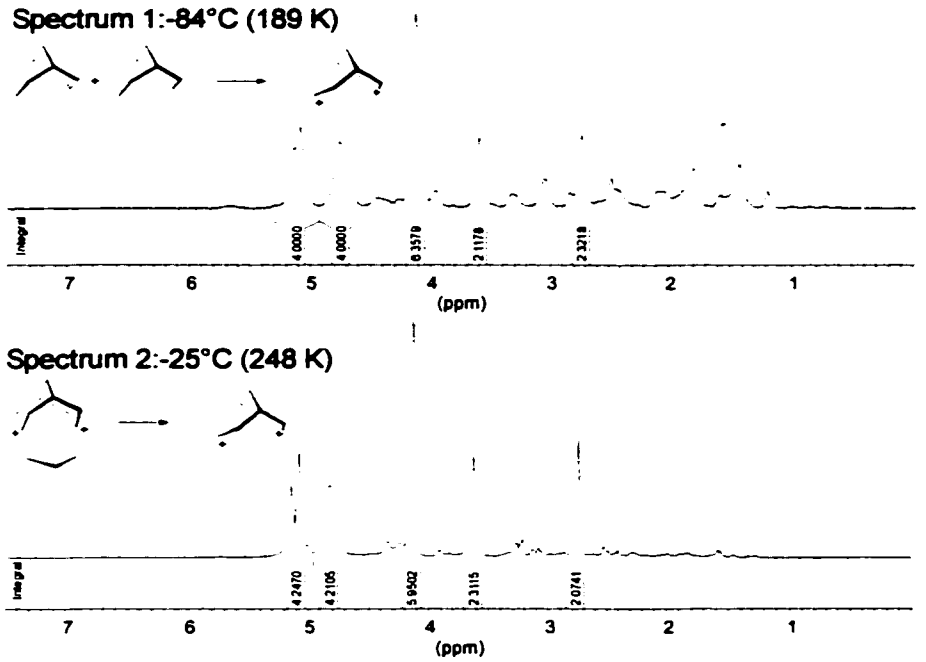

Figure 51: ^{1}H NMR spectra of the 3,7-dimethylbicyclo[3.3.1]nona-3,7-diyl dication **37** generated from the alkenes **167** and **168** (top) or obtained by rearrangement of the dication **36** (bottom).

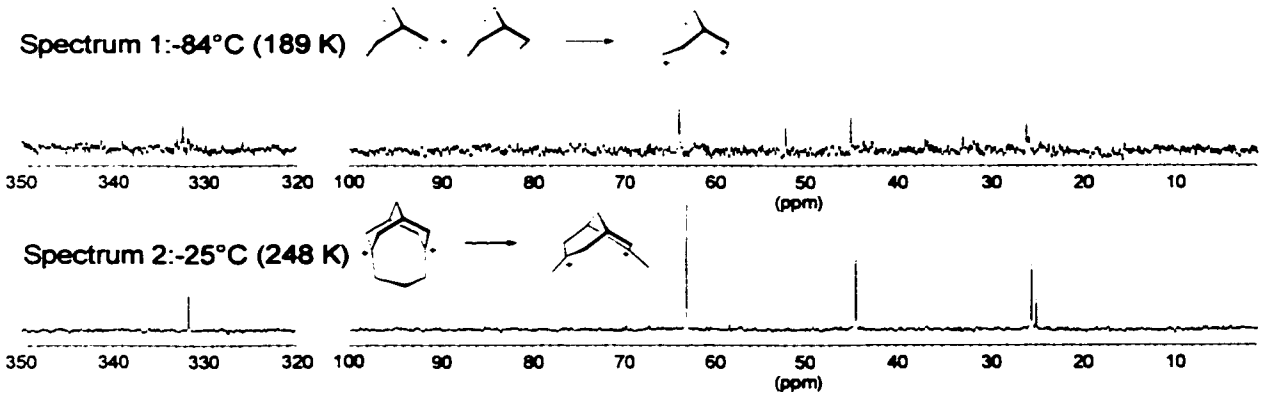

Figure 52: ^{13}C NMR spectra of the 3,7-dimethylbicyclo[3.3.1]nona-3,7-diyl dication **37** generated from the alkenes **167** and **168** (top) or obtained by the rearrangement of the dication **36** (bottom).

2.2.3.2 Rearrangement of the Tricyclo[5.3.1.1^{3,9}]dodecyl monocation

Attempts to generate the tricyclo[5.3.1.1^{3,9}]dodecyl monocation **34** by adding the alcohol **120** to superacid solutions resulted in the formation of a rearranged cation species, which was identified as 2-ethyl-2-adamantyl cation **35** by comparing the NMR data with those of authentic 2-ethyl-2-adamantyl cation generated from the alcohol **180** (see Figure 53 and 54).

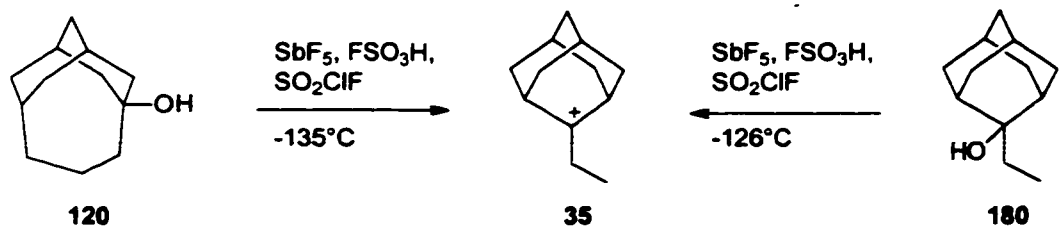

120 **35** **180**

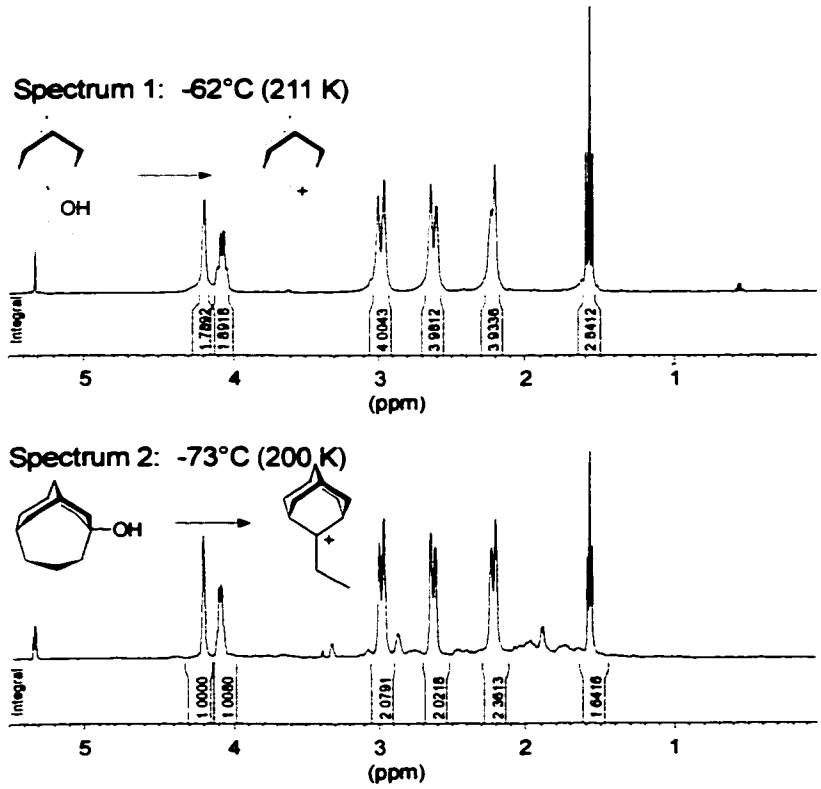

Figure 53: ^{1}H NMR spectrum of 2-ethyl-2-adamantyl cation **35** prepared from 2-ethyl-2-adamantanol **180** (Spectrum 1) and from tricyclo[5.3.1.1^{3,9}]dodecan-5-ol **120** (Spectrum 2).

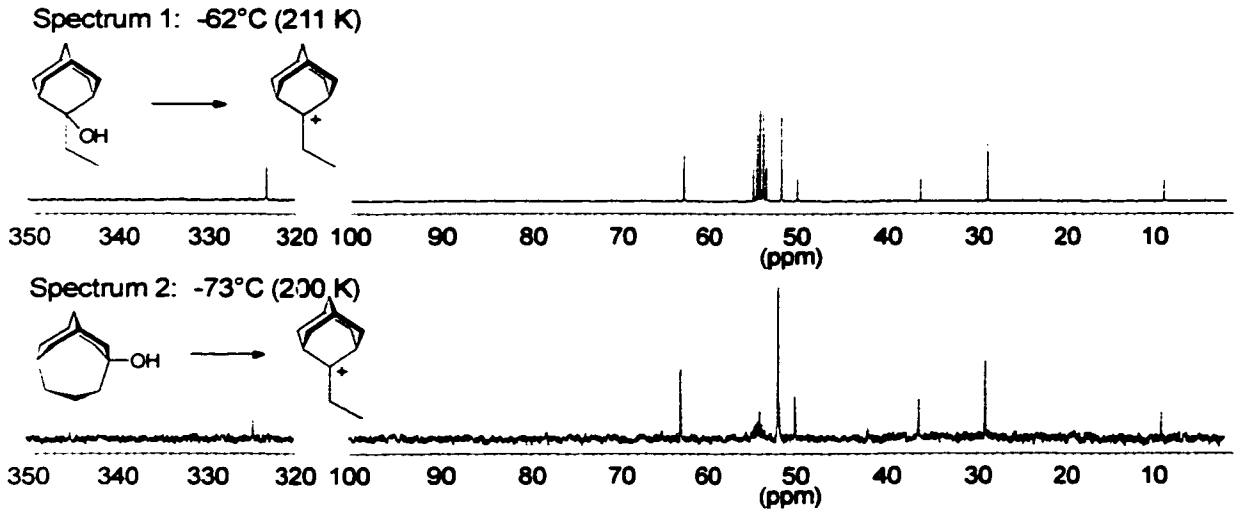

Figure 54: ^{13}C NMR spectra of 2-ethyl-2-adamantyl cation **35** prepared from 2-ethyl-2-adamantanol **180** (Spectrum 1) and from tricyclo[5.3.1.1^{3,9}]dodecan-5-ol **120** (Spectrum 2).

The most successful way to generate the tricyclic monocation **34** directly from a neutral species was the protonation of alkene **62** with superacid at -140°C, which however did not result in the formation of a pure solution of **34** but as a mixture of **34** and **132** (see also Section 2.2.3, page 99), as shown in Figures 55 and 56.

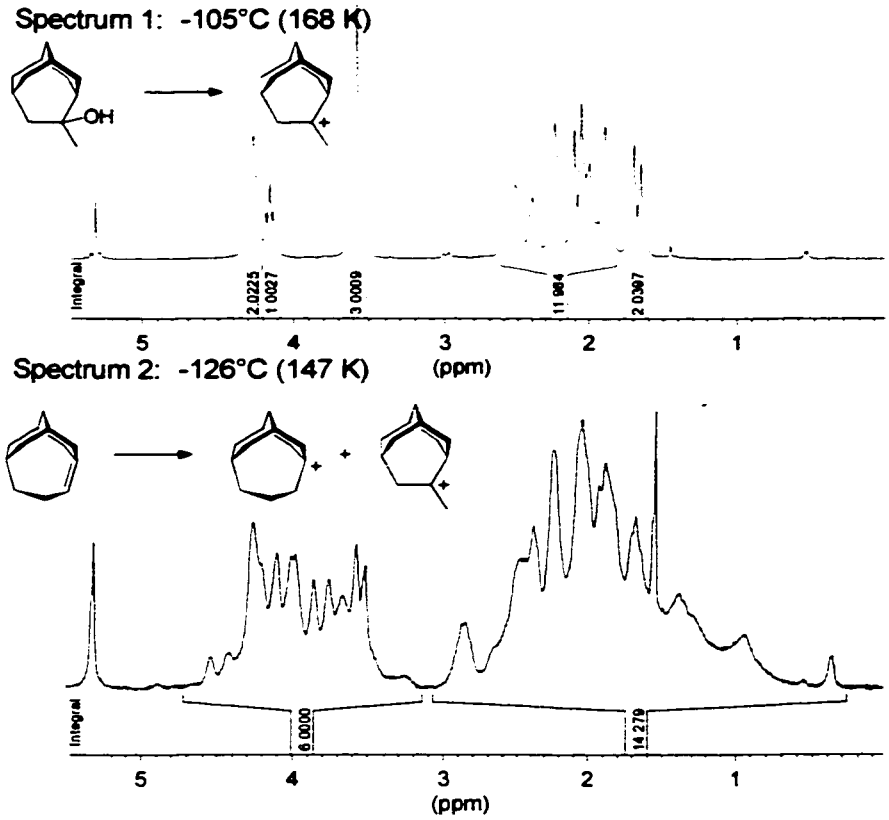

Figure 55: ^{1}H NMR spectra of the pure 6-methyltricyclo[4.3.1.1^{3,8}]undec-6-yl cation **132** (top) and as a mixture with the tricyclo[5.3.1.1^{3,9}]dodec-5-yl cation **34** (bottom).

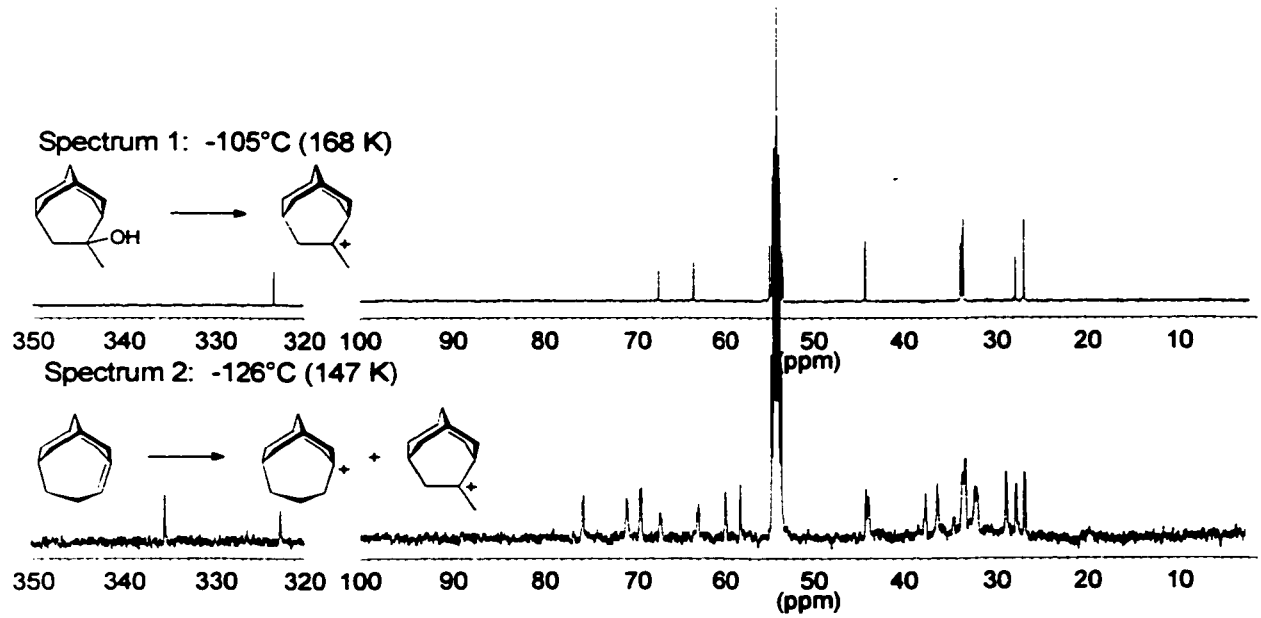

Figure 56: ^{13}C NMR spectra of the pure 6-methyltricyclo[4.3.1.1^{3,8}]undec-6-yl cation **132** (top) and as a mixture with the tricyclo[5.3.1.1^{3,9}]dodec-5-yl cation **34** (bottom).

Warming this solution to -62°C (211 K) for 10 min. formed a relatively clean solution of the 2-ethyl-2-adamantyl cation **35**. The observation of the intermediate cation **132** strongly suggests that a two step rearrangement reaction is involved in the formation of the adamantyl cation. In order to investigate each step of this rearrangement reaction, the preparation of pure sample solutions of the cations **34** and **132** was required.

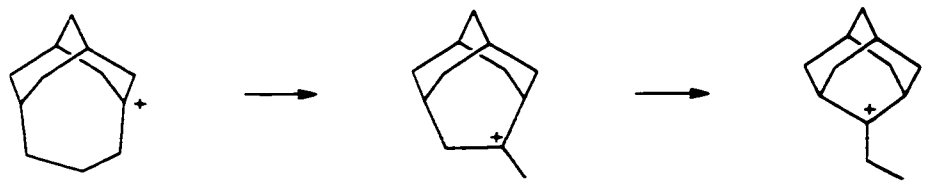

34 **132** **35**

A pure sample of the tricyclo[4.3.1.$1^{3,8}$]dec-5-yl cation **132** could be prepared by ionizing the alcohol **133** in superacid solution at a temperature of -135°C (see section 2.2.3, page 99), and this preparation then allows one not only to measure the energy barrier for the subsequent rearrangement, but also to assign the ^{13}C NMR signals of the **34** / **132** cation mixture, obtained from the protonation of the tricyclic alkene **62**. The energy barrier for the rearrangement of **132** into **35** was measured by warming the cation solution to -73°C (200 K) for 10 min., during which time 28 % of **132** rearranged, corresponding to an activation barrier of 14.4 ± 0.3 kcal/mol.

The generation of a pure solution of the tricyclo[5.3.1.$1^{3,9}$]dodecyl cation proved difficult and the cleanest solutions were obtained indirectly by the reduction of the tricyclic dication **40** with isopentane, resulting in the formation of a solution containing **34**, and the isopentyl cation as well as isopentane. Gradual warming of this cation solution brought about the formation of the 2-ethyl-2-adamantyl cation, which became apparent at -52°C (211 K). During a 10 min. period at -41°C (222 K), 33 % of **34** rearranged into **35**, corresponding to an activation barrier of 16.0 ± 0.7 kcal/mol. No detectable concentration of the homoadamantyl cation **132** could be observed during the rearrangement process. Figure 57 illustrates the changes in the ^{1}H NMR spectra in the temperature range of -94°C (179 K) to -41°C (232 K) and Figure 58 shows the carbon NMR spectra before and after the rearrangement process.

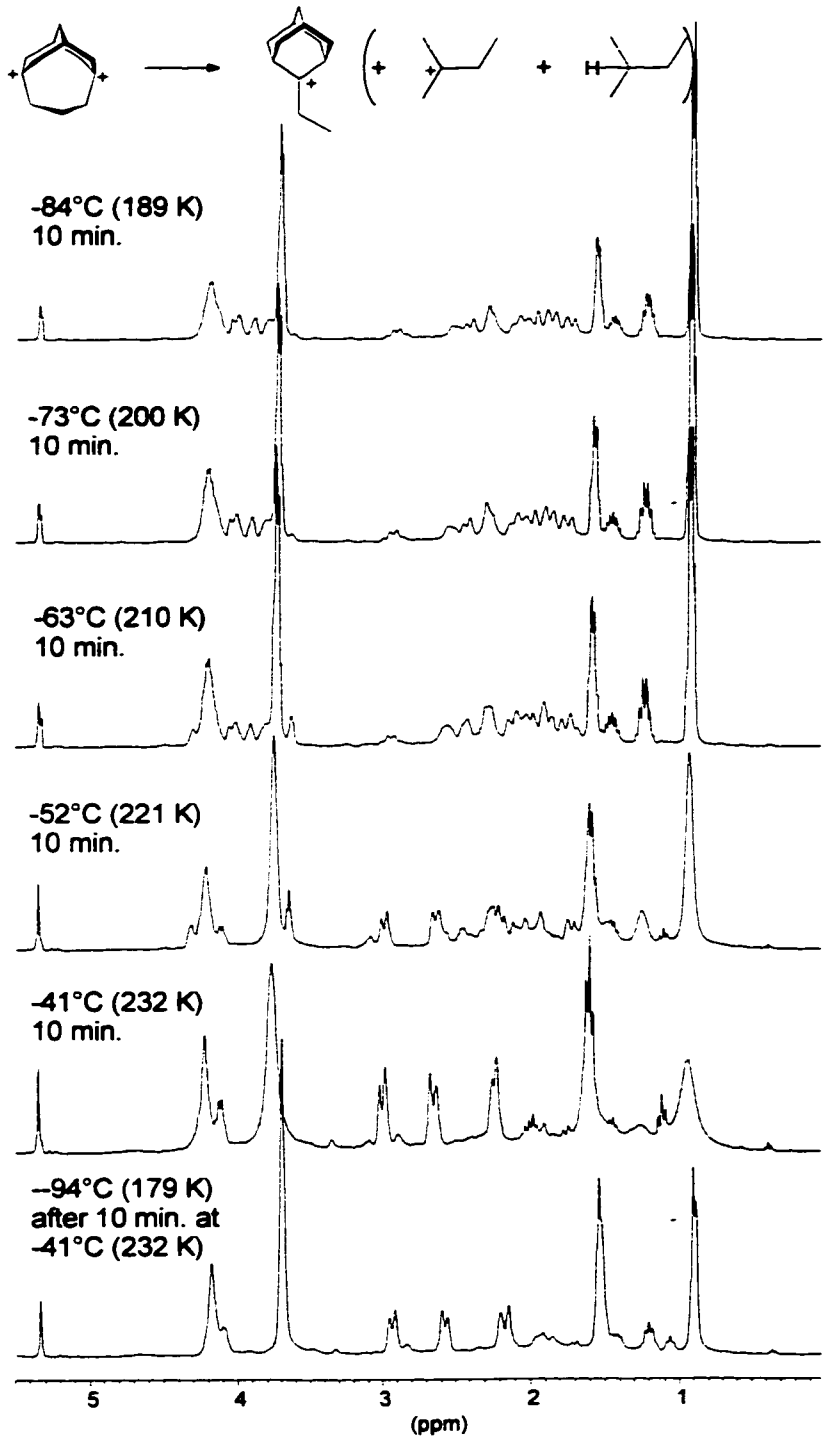

Figure 57: ^{1}H NMR spectra of the mixture of the monocation **34**, isopentyl cation and isopentane in a temperature range from -94°C (179 K) to -41°C (232 K).

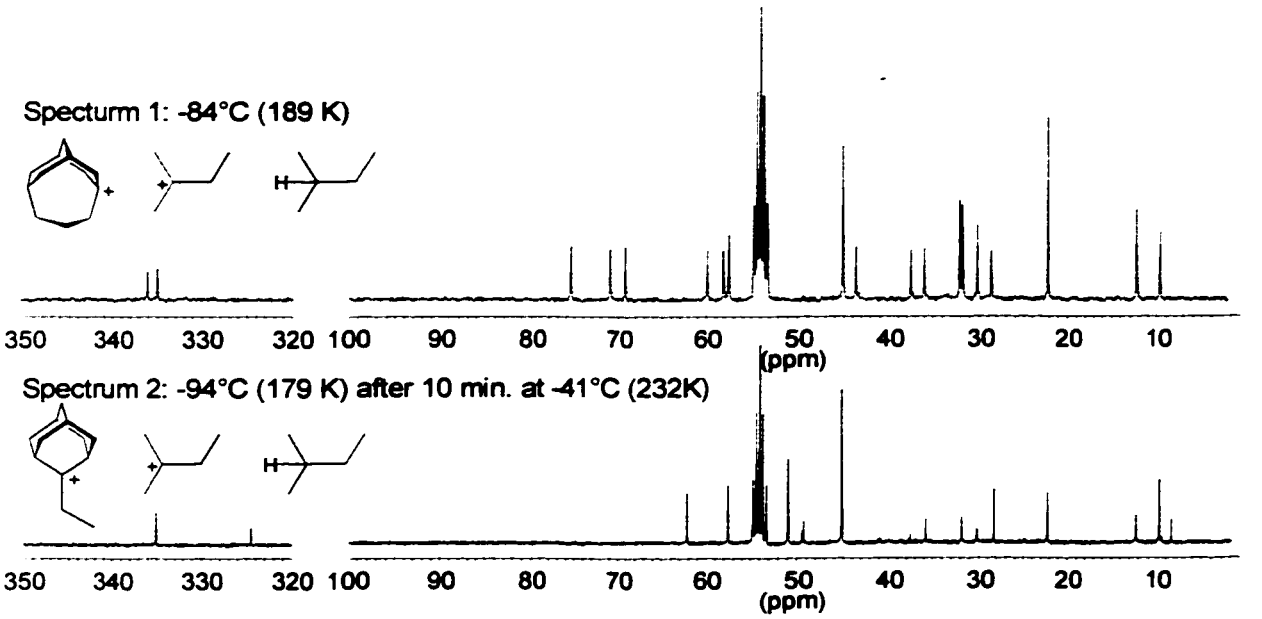

Figure 58: ^{13}C NMR spectra of the mixture of the monocation **34** isopentyl cation and isopentane in a temperature range from -94°C (179 K) to -41°C (232 K).

Initially, the mechanism associated with the **34** → **132** rearrangement was considered to directly involve the tricyclic cation **132** (pathway A in Scheme 11), since it is observed as the initial rearrangement product in the experiments for the preparation of the tricyclic cation **34** and in addition to that, **132** also rearranges into the the 2-ethyl-2-adamantyl cation **34**.

Scheme 11:Proposed mechanisms for the rearrangement of the tricyclo[5.3.1.$1^{3,9}$]dodec-5-yl cation **34**.

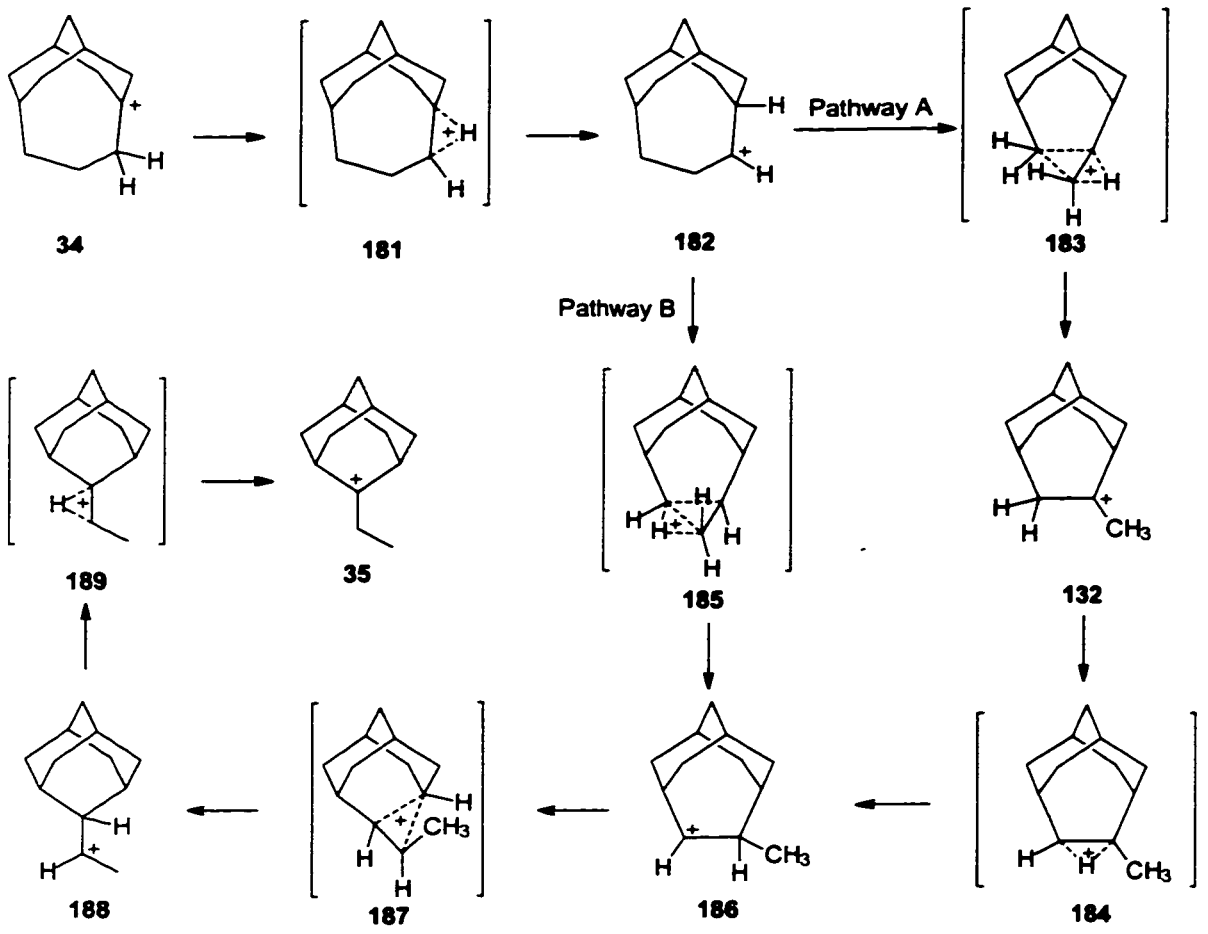

However, high level *ab initio* calculations at the B3LYP / 6-31G* level show the free energy of transition state **183** to be 33.2 kcal/mol higher than that of the starting cation **34**.

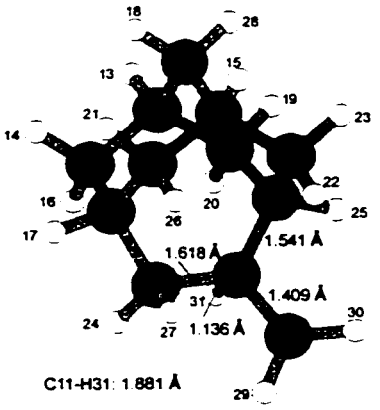

Transition state **183**

The transition state **183** has a developing C-C bond between C10 and C12 of only 1.618 Å and the C11-C12 bond being broken has already reached a length of 2.497 Å, indicating that the carbon framework for the ring-contracted species **132** is already nearly in place. The developing methyl group (C11), however, corresponds closely to a primary carbocation, and this center (C11) experiences only a relatively small stabilizing interaction with hydrogen H31 (C11-H21: 1.881 Å). This pronounced character of a primary carbocation explains the high relative free energy of 33.2 kcal/mol for this transition state. Despite the possibility that this energy barrier is overestimated due to the limited basis set being used in calculations, as well as a limited electron correlation treatment, a discrepancy of 17.2 kcal/mol between the experimental value of 16.0 ± 0.7 kcal/mol and the calculated value suggests that the rearrangement reaction follows a different pathway.

A much lower energy barrier (23.5 kcal/mol) was calculated for transition state **185** (B3LYP / 6-31G*), which can be described as a π-complex of a secondary carbocation and a C=C double bond, or more precisely an edge-protonated cyclopropane species..

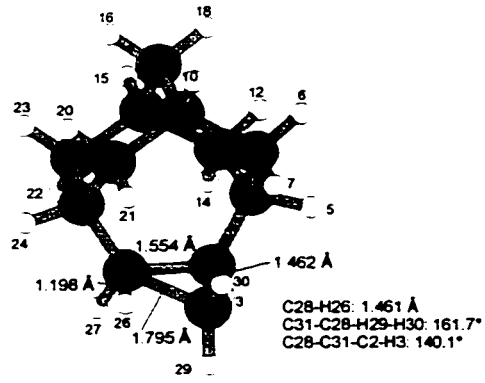

185

Considering the TS as a π-complex, the carbons C31 and C28 represent sp^2-like centers with a distance between them of 1.462 Å. The improper torsional angles on C28 and C31 are large, 161.7° (C31-C28-H29-H30) and 140.1° (C28-C31-C2-H3). The two remaining bonds lengths in the cyclopropyl substructure are calculated as 1.554 Å (C25-C31) and 1.795 Å (C25-C28), indicating that the developing C25-C31 bond has almost completely formed, but the C25-C28 bond being broken is still quite strong. The migrating hydrogen H26 has a distance to C25 of 1.198 Å and to C28 of 1.461 Å, which indicates that the migration is still in a relatively early

stage. This transition state directly leads to the secondary cation **182** without the direct involvement of the tertiary tricyclic cation **132**. However, a facile 1,2-hydride shift of the secondary cation **186**, with a calculated energy barrier of only 2.9 kcal/mol, would lead to **132**, explaining its presence in the protonation reaction of the alkene **?**. In the formation of the 2-ethyl-2-adamantyl cation **35** a second ring contraction is involved and a corner protonated cyclopropane transition state **187** with a relative free energy (B3LYP / 6-31G*) of 10.2 kcal/mol compared to the starting tricyclo cation **34**, or 15.1 kcal/mol compared to the homoadamantyl cation **132**, was located in the calculations. The latter value can be directly compared to the experimentally measured activation energy of the rearrangement of the separately generated cation **132**, which was measured as 14.4 ± 0.3 kcal/mol.

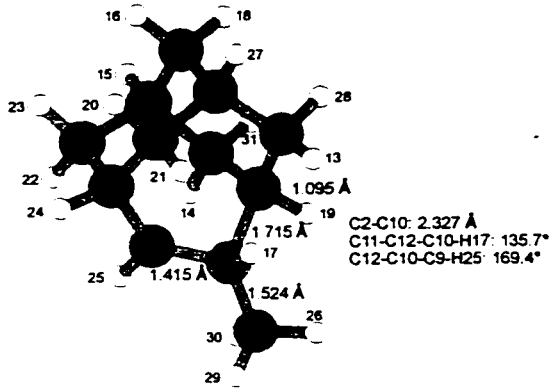

187

The bond lengths in the cyclopropane-like substructure of transition state **187** were 1.415 Å (C10-C12), 1.715 Å (C2-C12) and 2.327 Å (C10-C12), the last one being the developing C-C bond, indicating a rather early transition state. The remaining step of the proposed reaction mechanism consists of a simultaneous rotation of the ethyl group and a 1,2-hydride shift (structure **189**), with a calculated energy barrier (B3LYP / 6-31G*) of 3.8 kcal/mol from the starting secondary cation **188**.

The transition states involved in these rearrangement reactions all show significant σ-bond delocalization, which is known to require calculation methods with electron correlation and the use of large basis sets including polarization functions.[146] Hence, expanding the basis sets from 6-31G* to 6-311++G** or 6-311++G(3df, 2p) and using a more sophisticated electron correlation method such as MP2(fc), should result in calculated energies closer to the

experimental values. However, due to the massive amount of computer power needed for conducting these calculations, only single point calculations based on the B3LYP / 6-31G* optimized geometries could be performed, and these involved either a B3LYP / 6-311++G(3df, 2p) procedure or a MP2(fc) / 6-311++G** level of theory. Figure 59 illustrates the relative energies of all transition states and intermediates involved in the rearrangement (see Scheme 11) at both a B3LYP / 6-31G* and a MP2(fc) / 6-311++G** // B3LYP / 6-31G* level of theory.

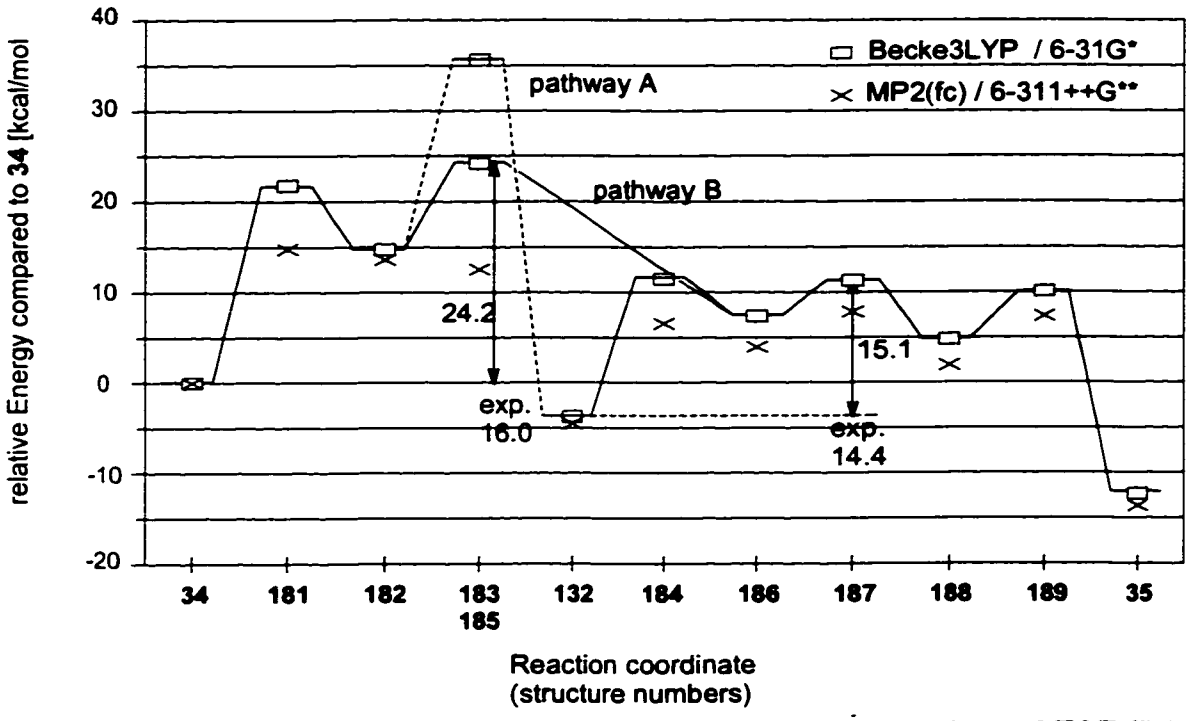

Figure 59: Calculated relative free energies at a B3LYP / 6-31G* or relative energies at a MP2(Full) / 6-311++G** // B3LYP / 6-31G* level of theory.

All of the relative energies at the MP2(fc) level were lower than the corresponding values at the B3LYP / 6-31G* level, with the structures possessing the largest amount of σ-delocalization showing the most significant decreases. The transition state **185** showed the largest change between the two calculational levels and the relative energy at the MP2(fc) / 6-311++G** level was calculated as 12.3 cal/mol compared to 23.5 kcal/mol at the B3LYP / 6-31G* level. Since other transition states did not experience such a dramatic change between these two levels, the rate determining step at the MP2 (fc) / 6-311++G** level was predicted

to be the first hydride shift (transition state **181**; 14.8 kcal/mol), while at the B3LYP / 6-31G* level, the edge-protonated cyclopropane structure **185** was calculated to be the rate determining transition state. The situation is somewhat different for the species involved in the rearrangement of the homoadamantyl cation **132**. At both levels, B3LYP /6-31G* and MP2(fc) / 6-311++G** // B3LYP /6-31G*, the structure **187** was found to be the rate limiting transition state.

A comparison of the experimental and calculated energy barriers is shown in Table 26 (the details of all calculated values are given in Table 27).

Table 26: Experimental and calculated activation energies for the rearrangement of tricyclo[5.3.1.$1^{3,9}$]dodec-5-yl cation **34** and tricyclo[4.3.1.$1^{3,8}$]undec-5-yl cation **132** into the 2-ethyl-2-adamantyl cation **35**.

Method	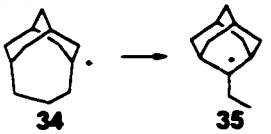 **34** **35**	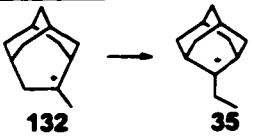 **132** **35**
experiment [kcal/mol]	16.0 ± 0.7	14.4 ± 0.3
B3LYP / 6-31G* [kcal/mol]	23.4	15.3
B3LYP / 6-31G* (free energy) [kcal/mol]	23.5	15.1
B3LYP / 6-311++G(3df, 2p) // B3LYP / 6-31G* [kcal/mol]	22.1	15.0
MP2(fc) / 6-311++G** // B3LYP / 6-31G* [kcal/mol]	14.8	12.3

Table 27: Calculation results of transition states and intermediates involved in the rearrangement of tricyclo[5.3.1.1^{3,9}]dodec-5-yl cation **34**.

Structure	B3LYP / 6-31G*[a] imag. freq.[b] rel. energy [c]	ZPE	$H°_0$-$H°_{298}$	S	G_{298} [hartrees] rel. free energy [d] rel. free energy [e]	B3LYP / 6-311++G(3df,2p) rel. energy [f] rel. energy [g]	MP2(fc) / 6-311++G** rel. energy[h] rel. energy[i]
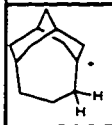 **34**	-468.455106111 0	181.67	6.61	93.59	-468.204632877 0	-468.59522926 0	-467.0894808 0
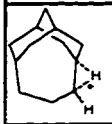 **181**	-468.421326368 -813.4[b] 21.20[c]	180.13	6.28	90.78	-468.172469133 20.18[d]	-468.563809603 19.72[f]	-467.065908 14.79[h]
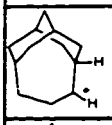 **182**	-468.431765313 14.65[c]	181.45	6.62	93.34	-468.181511248 14.51[d]	-468.572812289 14.07[f]	-467.0677862 13.61[h]
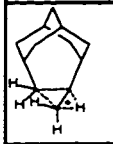 **183**	-468.398120726 -460.7[b] 35.76[c]	179.41	6.57	94.55	-468.151693521 33.22[d]	-468.540269204 34.49[f]	-467.0366427 33.16[h]
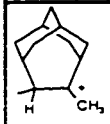 **132**	-468.461503674 -4.01[c]	180.53	6.46	92.37	-468.212482201 -4.93[d] 0	-468.60252305 -4.58[f] 0[g]	-467.0966328 -4.49[h] 0[i]
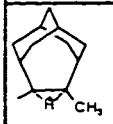 **184**	-468.437050895 -492.1[b] 11.33[c]	179.61	6.58	92.97	-468.189564179 9.46[d] 14.38	-468.579145675 10.09[f] 14.67[g]	-467.0790751 6.53[h] 11.02[i]
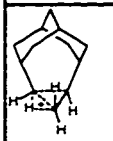 **185**	-468.417744162 -506.3[b] 23.44[c]	181.05	6.11	89.64	-468.167184495 23.50[d]	-468.560053629 22.07[f]	-467.0695251 12.52[h]
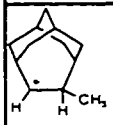 **186**	-468.442771222 7.74[c]	180.78	6.94	95.73	-468.194172612 6.56[d] 11.49[e]	-468.583758813 7.20[f] 11.77[g]	-467.0832183 3.93[h] 8.42[i]
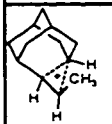 **187**	-468.437638784 -163.4[b] 10.96[c]	180.58	6.48	92.14	-468.188404744 10.18[d] 15.11[e]	-468.578547587 10.47[f] 15.04[g]	-467.0770085 7.83[h] 12.31[i]
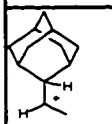 **188**	-468.44657179 5.36[c]	180.58	6.99	96.54	-468.198589827 3.79[d] 8.72[e]	-468.587623699 4.77[f] 9.35[g]	-467.0864095 1.93[h] 6.42[i]

Structure	B3LYP / 6-31G*[a] imag. freq.[b] rel. energy [c]	ZPE	H°_0-H°_{298}	S	G_{298} [hartrees] rel. free energy[d] rel. free energy [e]	B3LYP / 6-311++G(3df,2p) rel. energy[f] rel. energy [g]	MP2(fc) / 6-311++G** rel. energy[h] rel. energy[i]
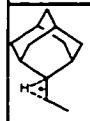 **189**	-468.43921829 -78.4[b] 9.97[c]	179.24	6.53	93.16	-468.192457141 7.64[d] 12.57[e]	-468.581036622 8.91[f] 13.48[g]	-467.077783 7.34[h] 11.83[i]
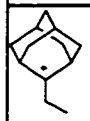 **35**	-468.473324282 -11.43[c]	181.13	7.05	98.23	-468.22517677 -12.89[d] -7.97[e]	-468.613568332 -11.51[f] -6.93[g]	-467.1112353 -13.65[h] -9.16[i]

[a]SCF energy of the fully optimized geometry at B3LYP / 6-31G*. [b]single imaginary frequency in cm^{-1}. [c]relative SCF energy in kcal/mol at B3LYP / 6-31G* of fully optimized geometries, referenced to **34**. [d]relative free energy (298 K) in kcal/mol at B3LYP / 6-31G* of fully optimized geometries, referenced to **34**. The ZPE, the thermal correction for the enthalpy as well as the entropy were scaled with the factor 0.98.[188] [e]relative free energy in kcal/mol (298 K) at B3LYP / 6-31G* of fully optimized geometries referenced to **34**. The ZPE, the thermal correction for the enthalpy as well as the entropy were scaled with the factor 0.98.[188] [f]relative SCF energy in kcal/mol at B3LYP / 6-311++G(3df, 2p) of B3LYP / 6-31G* optimized geometries, referenced to **34** [g] relative SCF energy in kcal/mol at B3LYP / 6-311++G(3df, 2p) of B3LYP / 6-31G* optimized geometries, referenced to **132**. [h]relative MP2 energy in kcal/mol at MP2(fc) / 6-311++G** of B3LYP / 6-31G* optimized geometries, referenced to **34**. [i]relative MP2 energy in kcal/mol at MP2(fc) / 6-311++G** of B3LYP / 6-31G* optimized geometries, referenced to **132**.

2.2.3.3 Rearrangement of the 9-Ethylbicyclo[3.3.1]nonyl cation

Considering the facile rearrangement reactions of the bicyclo[3.3.3]undecyl dication **36** and the tricyclo[5.3.1.$1^{3,9}$]dodecyl monocation **34**, which both require an initial 1,2-hydride shift of a bridge hydrogen onto the bridgehead cation center, one might expect the bicyclo[3.3.3]undecyl cation **78** to behave correspondingly, and follow the same rearrangement cascade as observed for the tricyclic monocation **34**.

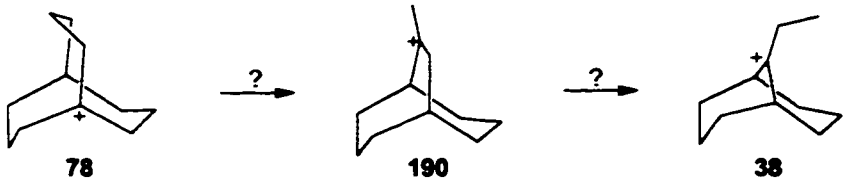

78 **190** **38**

However, no formation of either **190** or **38** could be observed at temperatures ranging from -105°C (168 K) to -41°C (232K), at which temperature decomposition into a complex mixture became rapid. In order to probe the transition state involved in a 1,2-hydride shift to the bridgehead carbon, the methyl substituted bicyclic alcohol **191** was prepared and ionized in superacidic solutions at -116°C.

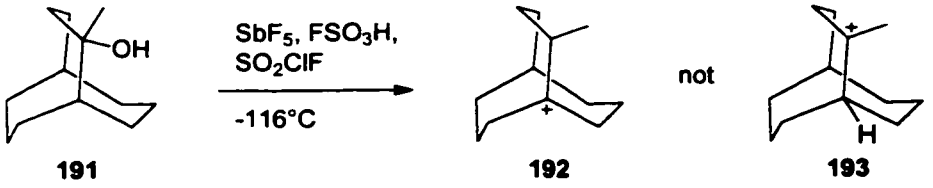

191 **192** **193**

Instead of the expected tertiary cation **193**, the bridgehead cation **192** was observed, possessing a carbon NMR chemical shift of 361.6 ppm. The facile formation of **192** indicates that the 1,2-hydride shift of the bridgehead hydrogen in **193** must be a low energy process and that the bridgehead cation **192** is thermodynamically more stable than the tertiary cation **193**. In analogy to the tricyclic system, a single ring contraction in **78** would lead to the methyl substituted bicyclo[3.3.2]decyl cation. Hence the direct generation of this cation was attempted. The preparation of 9-methylbicyclo[3.3.2]decan-9-ol by reaction of the ketone **101** using Grignard or methyllithium reagents was troublesome and yielded under different conditions (several hours reflux in THF) only a mixture of starting material and the reduced bicyclo[3.3.2]undecan-9-ol **194**.

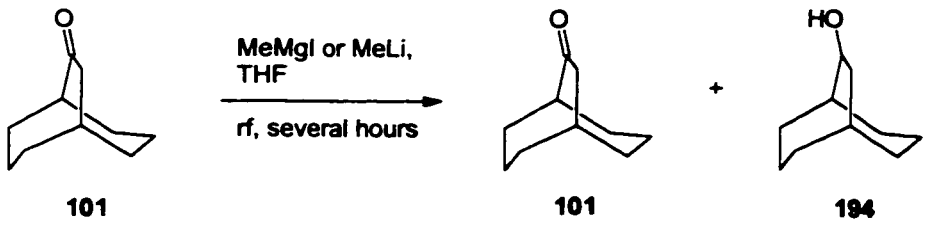

This exceptionally low reactivity of the carbonyl group in **101** can be explained by a blocking effect of the carbonyl carbon by the axial hydrogens of the two C_3 bridges as illustrated in Figure 60.

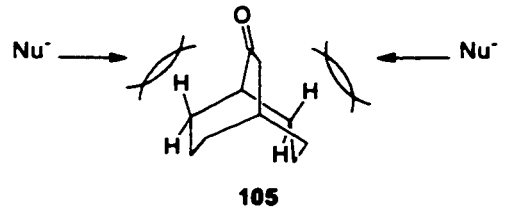

Figure 60: Blocking of an approaching nucleophile by axial hydrogens in bicyclo[3.3.2]decan-9-one **101**.

Treatment of the ketone **101** with the Lombardo reagent[189] quantitatively yielded the alkene **102**, which was protonated in superacidic solution at -135°C. However, none of the expected cation **190** was obtained. Instead, a mixture of two rearranged, but as yet unidentified cations was produced, and these decompose into a complex mixture when the temperature was maintained at -63°C (210 K) for 1h.

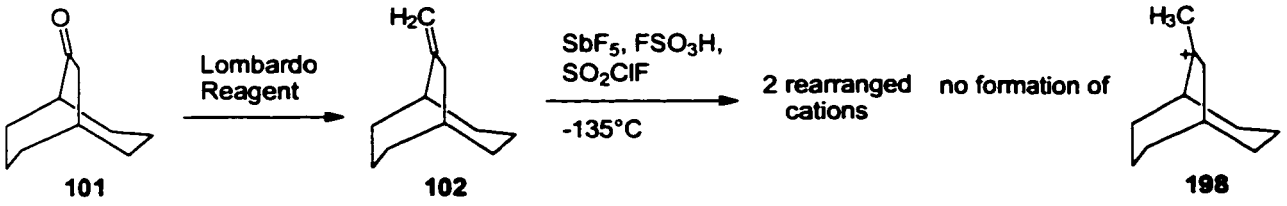

Based on the rearrangement products of the tricyclo[5.3.1.$1^{3,9}$]dodecyl cation **34**, the next rearrangement product of **78** after **190**, would be the 9-ethylbicyclo[3.3.1]non-9-yl cation **38**. However, experiments for the preparation of this cation directly from either the chloride **196** or the alcohol **195** in superacidic solutions revealed that cation **38** easily undergoes further rearrangement reactions. Maintaining the solution at -105°C (168 K) for 1h caused 83 % of the

symmetrical bicyclic cation **38** to rearrange into a species with 11 different types of carbons (1 C^+, 2 CH, 7 CH_2, 1 CH_3) and 5 low field protons between 3.2 and 4.4 ppm, as well as 14 high field protons (see Figures 61 and 62). The rearrangement energy barrier was measured as 12.2 ± 0.6 kcal/mol.

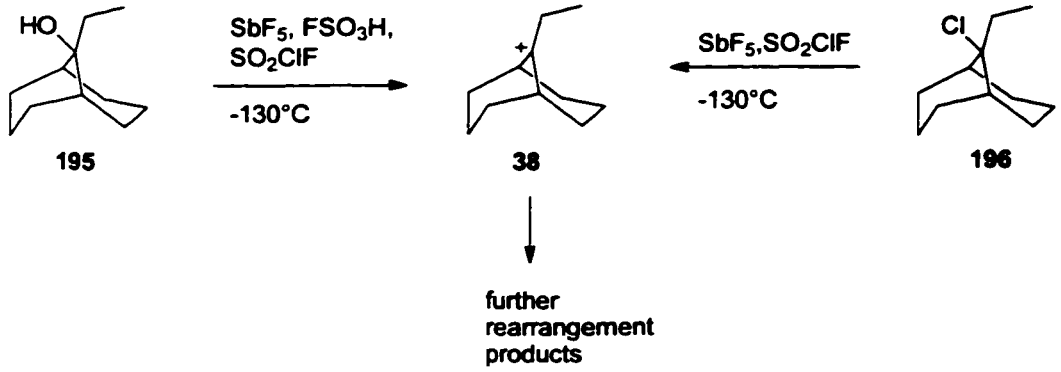

The rearrangement of cation **38** is closely related to a previously reported rearrangement of 9-methylbicyclo[3.3.1]non-9-yl cation **199**, which was reported by Sorensen and Kirchen[190] to rearrange into an unknown species at similar temperatures. A comparison of the carbon and the hydrogen NMR spectra of these rearrangement products shows that they have the same basic structure.

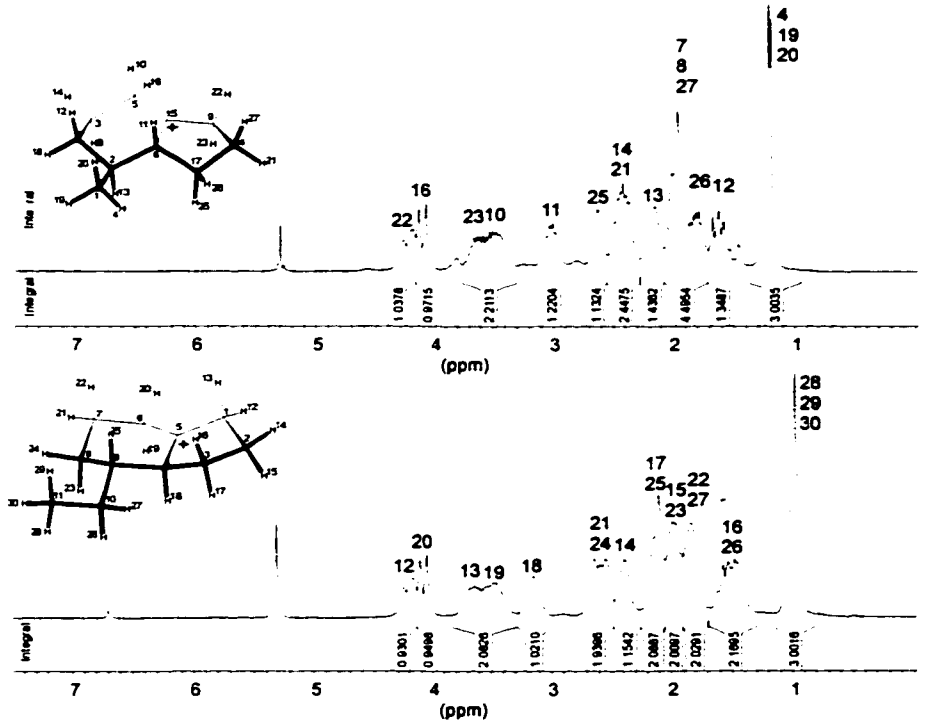

Figure 61: Hydrogen NMR spectra of the first rearrangement cation from 9-methylbicyclo[3.3.1]non-9-yl cation **199** and 9-ethylbicyclo[3.3.1]non-9-yl cation **38**.

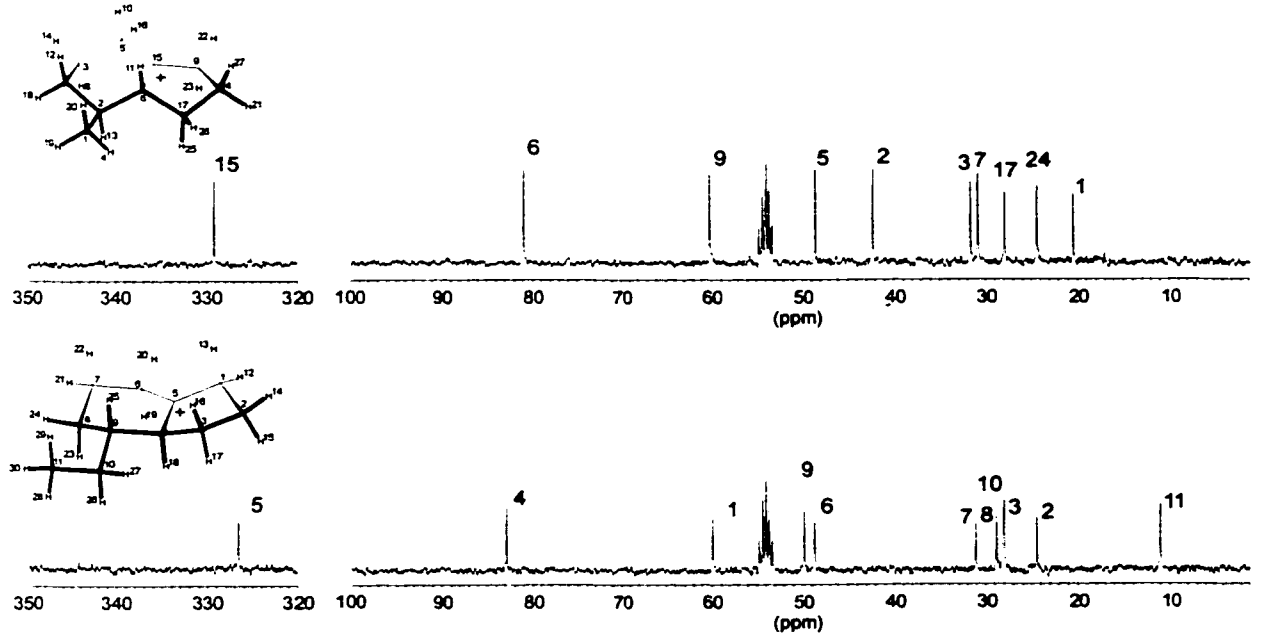

Figure 62: Carbon NMR spectra of the first rearrangement product of the 9-methylbicyclo[3.3.1]non-9-yl cation **199** (top) and 9-ethylbicyclo[3.3.1]non-9-yl cation **38** (bottom).

For simplicity reasons and shorter calculation times, the methyl derivative was chosen for the structure elucidation of this first rearrangement product, the assumption being that the ethyl analog will have the same structure, except for a methyl *vs.* ethyl-group. The combination of the hydrogen and carbon NMR data allows one to propose two possible structures, **200** and **201** .

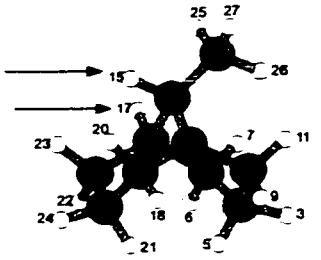

200

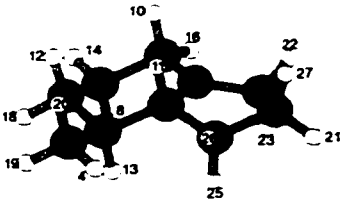

201

Using HETCOR and COSY 2D-NMR spectroscopy, the structure **200** was ruled out as a possible candidate due to an inappropriate chemical shift for H15 (H15 would have to possess a chemical shift of 2.2 ppm, which would be unusual for an α hydrogen) as well as an unreasonable coupling pattern for H15 and H17 (H15 shows coupling to H6, while H17 shows no sign of coupling to either H6 or H7 (see Figure 61 and the HETCOR / COSY spectra in section 5.4.28, page 255). The structure **201** was found to accommodate all of the coupling patterns as well as the chemical shifts, and all the peaks in the carbon as well as in the hydrogen spectrum could be assigned (see Figure 61 and 62).

Further supporting information for structure **201** was collected using *ab initio* calculations. The theoretically calculated NMR shifts (MP2(Full) / 6-31G* // B3LYP / 6-31G*) of the two possible species **200** and **201** were compared to the experimental data, showing that cation **201** was a better match with the experimental data than was the bridgehead cation **199** (see Table 28).

Table 28: Calculated and experimental ^{13}C NMR chemical shifts of the two cations **200** and **201**.

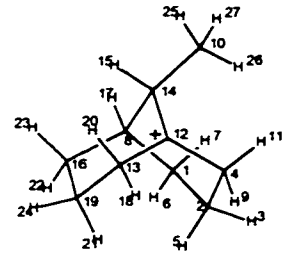 **200**			exp. values δ (ppm)	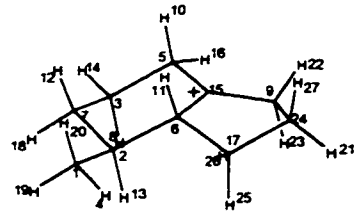 **201**		
atom number	calc. value: δ (ppm) [a]	difference from exp. values		difference from exp. values	calc. value: δ (ppm) [a]	atom number
1 (CH_2)	27.2	3.1	24.1	2.6	26.8	24 (CH_2)
2 (CH_2)	60.3	0.1	60.2	2.4	62.6	9 (CH_2)
4 (CH_2)	48.7	18.2	30.5	2.7	33.2	17 (CH_2)
8 (CH)	117.1	36.5	80.6	-1.3	79.3	6 (CH)
10 (CH_3)	17.8	-2.4	20.2	2.2	22.4	1 (CH_3)
12 (C^+)	304.5	-26.8	331.3	10.6	341.9	15 (C^+)
13 (CH_2)	54.4	23.0	31.4	1.2	32.6	7 (CH_2)
14 (CH)	89.8	47.8	42.0	6.2	48.2	2 (CH)
16 (CH_2)	34.0	6.4	27.6	3.9	31.5	3 (CH_2)
19 (CH_3)	58.2	9.7	48.5	2.2	50.7	5 (CH_3)

[a]NMR shifts were calculated on a MP2(Full) / 6-31G* level of theory using B3LYP / 6-31G* optimized geometries and referenced to a calculated TMS value.

The energies of cations **200** and **201** were also calculated (B3LYP / 6-31G*) and cation **201** was found to be 7.4 kcal/mol lower than **200** (free energy at B3LYP / 6-31G*; see Table 31 for details), supporting the results of the NMR calculations as well as the experimental data derived from 2D-NMR spectra. Hence, the first observable intermediate in the rearrangement of the 9-methylbicyclo[3.3.1]non-9-yl cation **199** can be identified as **201** with a high certainty.

The related rearrangement reaction of the 9-ethylbicyclo[3.3.1]non-9-yl cation **38** was investigated in a similar way and the experimental 2D NMR spectra (HETCOR, COSY; see section 5.4.29, page 258) confirmed cation **202** to be the observed intermediate. Supporting data were obtained from theoretical NMR calculations of the intermediate **202**, which showed

good agreement with the experimental NMR.

38 **202**

The results of the *ab initio* NMR calculation (B3LYP / 6-31G*) are summarized in Table 29.

Table 29: Calculated and experimental ^{13}C NMR chemical shifts of cation **202**.

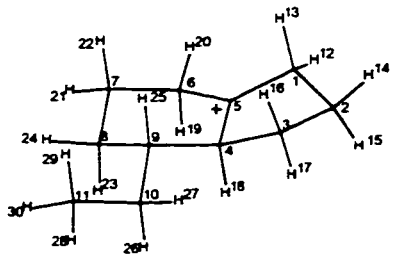

atom number	calc. value: δ (ppm) [a]	difference from exp. values	exp. values δ (ppm)
1 (CH_2)	60.9	1.0	59.9
2 (CH_2)	26.3	1.9	24.4
3 (CH_2)	32.1	4.1	28.0
4 (CH)	78.8	-4.1	82.9
5 (C^+)	332.2	5.5	326.7
6 (CH_2)	50.4	1.7	48.7
7 (CH_2)	35.4	4.3	31.1
8 (CH_2)	30.6	1.7	28.9
9 (CH)	60.5	10.7	49.8
10 (CH_2)	32.6	4.5	28.1
11 (CH_3)	13.6	2.6	11.0

[a] NMR shifts were calculated at a B3LYP / 6-31G* level of theory, referenced to a calculated TMS value.

An interesting feature of these rearrangement products **201** and **202** is the unusually low

field chemical shift of the tertiary α-carbon (80.6 ppm for C6 in **201** and 82.9 ppm for C4 in **202**) . Looking at the LUMO orbital of the cation **201**, one sees relatively large lobes on the hydrogens H10, H11 and H23 (for the numbering of atoms, see Table 28) indicating relatively strong C-H hyperconjugation. Much less pronounced are the C-C hyperconjugative interactions, indicated by the relatively small lobes on the C-C bonds C2-C6 and C3-C5. The exceptionally low field chemical shift of the C6 carbon can be explained by a combination of the strong C-H hyperconjugation, C-C hyperconjugation (C2-C6), as well as multiple alkyl substitution effects. The rather large ^{13}C chemical shift difference between the two CH_2 groups C9 (60.2 ppm) and C5 (48.5 ppm) can be attributed to a more efficient C-H hyperconjugation involving both C-H bonds of C9, compared to the single interaction of the C5-H10 bond. This difference also shows up in a plot of the LUMO orbital for this cation, where the C9 CH_2 has a larger lobe (see Figure 63).

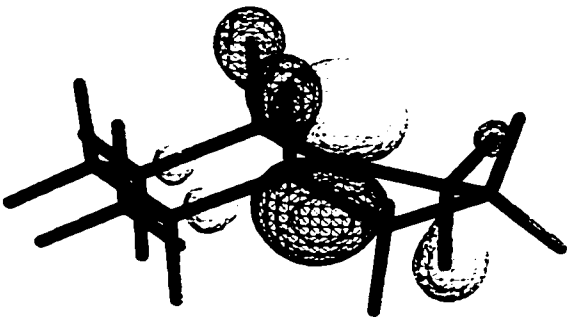

Figure 63: LUMO orbital of cation **201** at the B3LYP / 6-31G* level of theory.

The ethyl and methyl substituted cations **201** and **202** behaved very differently when the solutions of each were allowed to warm up to about -70°C. While a solution of **201** decomposed into a mixture of at least 6 different classical and nonclassical cations at temperatures above -63°C (210 K), the 5-ethylbicyclo[4.3.0]non-1-yl cation **202** experienced a well defined rearrangement reaction. Maintaining a corresponding sample solution at -73°C (200 K) for 1h converted 67 % of **202** into the known trans 2-methyl-2-decalyl cation **39** , which was identified by a comparison of ^{13}C NMR signals with the literature values[191] (see Table 30). The energy barrier for this second rearrangement reaction was measured as 15.4 ±

0.6 kcal/mol.

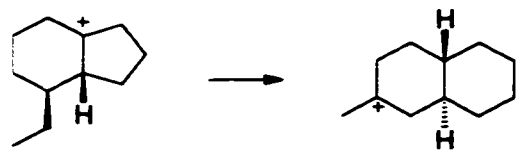

208 43

Table 30: Comparison of the ^{13}C NMR shifts of the 2-methyl-2-decalyl cation **39** according to Sorensen and Kirchen[191] and the second rearrangement product of the 9-ethylbicyclo[3.3.1]non-9-yl cation **38**.

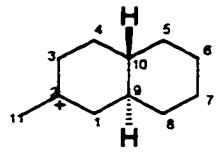

39

atom number	cation **39** from the rearrangement reaction at -73°C	literature values [191] of cation **39** at -90°C	differences
1 (CH_2)	65.2	64.4	0.8
2 (C^+)	325.8	324.9	0.9
3 (CH_2)	58.7	58.1	0.6
4 (CH_2)	40.6	39.3	1.3
5 (CH_2)	35.2	34.5	0.7
6 (CH_2)	32.0	31.6	0.4
7 (CH_2)	26.3	25.8	0.5
8 (CH_2)	25.9	25.5	0.4
9 (CH)	53.6	50.3	3.3
10 (CH)	40.7	39.9	0.8
11 (CH_3)	44.1	43.2	0.9

[a] NMR shifts were calculated at a B3LYP / 6-31G* level of theory, referenced to a calculated TMS value.

Ab initio calculations were used to determine the energies of all of the significant intermediates involved in the following proposed mechanisms, and these are shown in Scheme 12.

12 Proposed mechanism for the rearrangement of the 6-methylbicyclo[3.3.1]non-9-yl cation **199**. Values in brackets represent the relative free energy in kcal/mol at the B3LYP / 6-31G* level of theory using a scale factor of 0.98 for the ZPE , the thermal enthalpy correction, as well as the entropy.

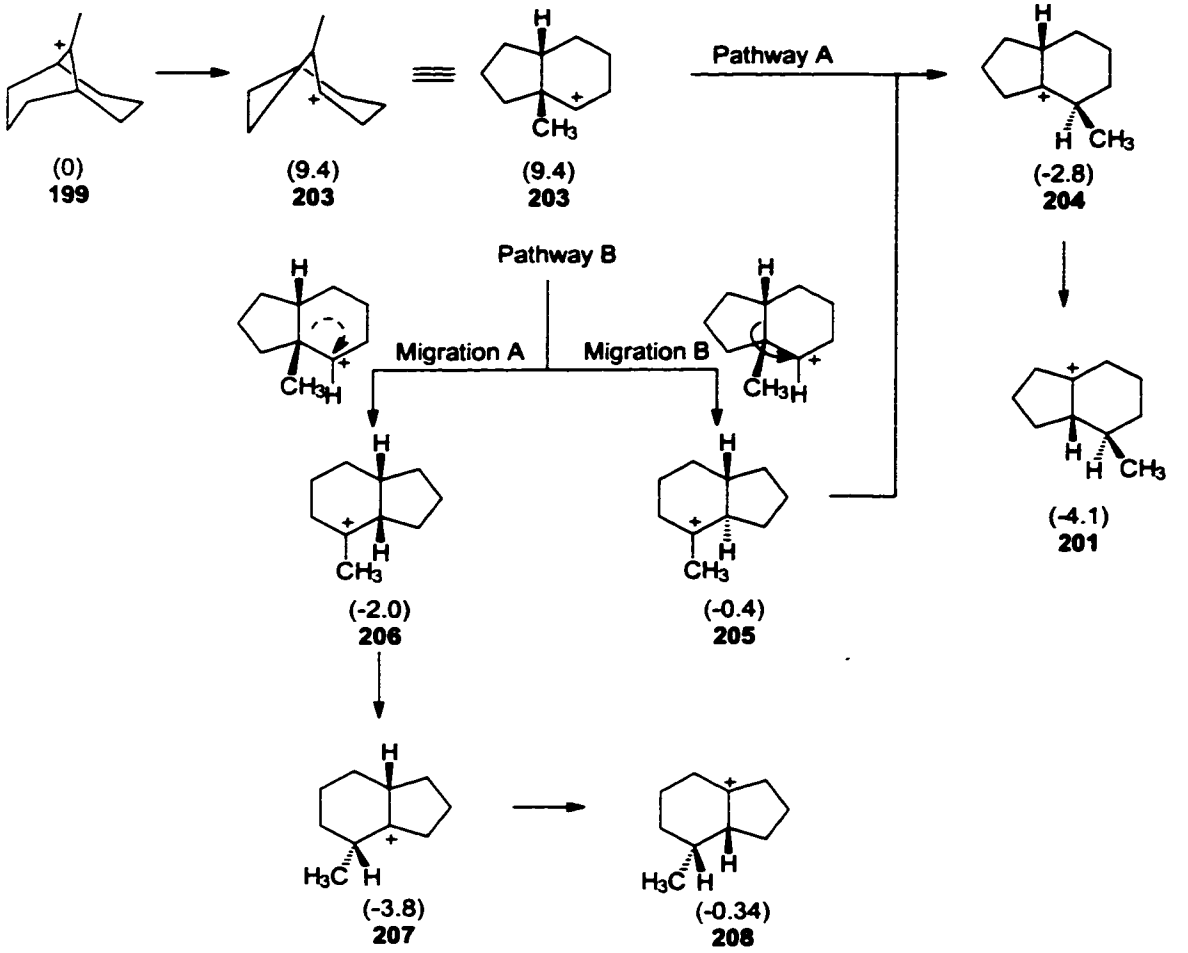

Bicyclo[3.3.1]nonyl cation systems are known to undergo a facile 1,2 alkyl shift of the C_1 bridge.[166, 192] The secondary cation **203** is therefore expected to be easily formed with a relatively low energy barrier. The most direct route to the observed cation **201** (Pathway A) could involve a methyl and a hydride shift forming **201** via the tertiary alkyl cation **204**. Alternatively, a "ring-rearrangement" of the secondary cation **203**, forming the new bond according to Migration B in Figure 64, would generate **205**, which could be transformed into the observed cation **201** after two hydride shifts (Pathway B in Scheme 12).

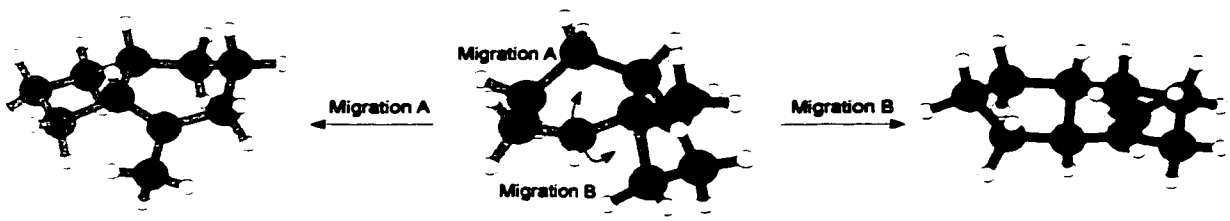

Figure 64: Two migration possibilities for the secondary cation **203**.

The "ring-rearrangement" in Figure 64 could also proceed according to Migration B, which represents a way for cis / trans isomerization of the bicyclo[4.3.0]nonyl framework to occur. Further elaboration of this pathway would form cation **207** with a very similar calculated relative free energy (B3LYP / 6-31G*) to the observed cation **201** (0.3 kcal/mol). Since none of this cation was observed, the energy barrier for the "ring-rearrangement" is expected to be significant larger than the competing alkyl shift mechanism which proceeds via intermediate **204** (Pathway A).

The reaction mechanism for the rearrangement of the related ethyl substituted system **38** into cation **202** is expected to follow the same reaction mechanism as for the methyl system and this is illustrated in Scheme 13 as "first rearrangement step".

13 Proposed mechanism for the rearrangement of the 9-ethylbicyclo[3.3.1]non-9-yl cation **38**. The values in brackets represent relative free energies according to B3LYP / 6-31G* calculations. A scale factor of 0.98 was applied to the ZPE, the thermal correction of the enthalpy from 0K to 298 K and the entropy.

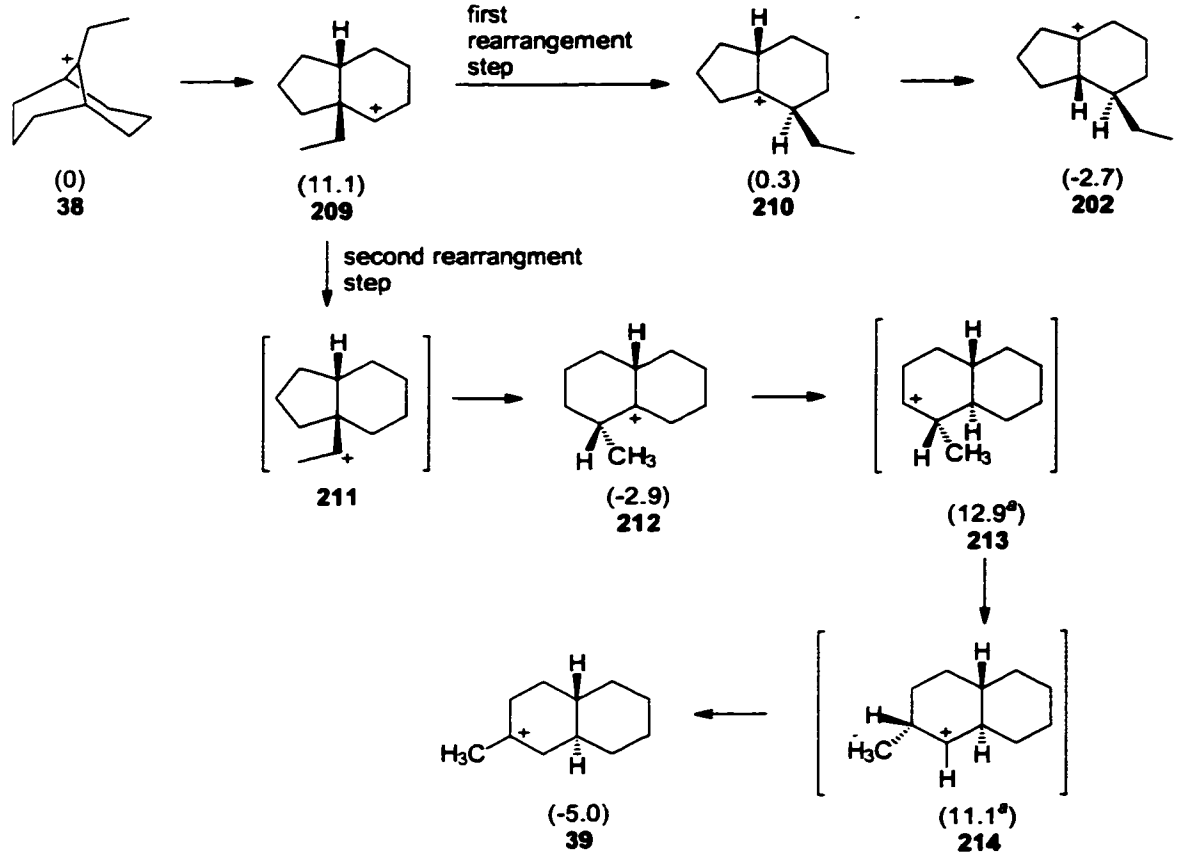

The second rearrangement step in Scheme 13 requires the formation of a secondary cation center in the ethyl group at some point. The best geometrical arrangement for this hydride shift appears to be the secondary cation **209** , in which the hydride exchanging carbons are only separated by 2.55 Å according to B3LYP / 6-31G* calculations (see Figure 65). The involvement of the cation **211** would be in agreement with the fact that the methyl derivative **203** does not follow a similar rearrangement reaction, which would require a primary carbocation species.

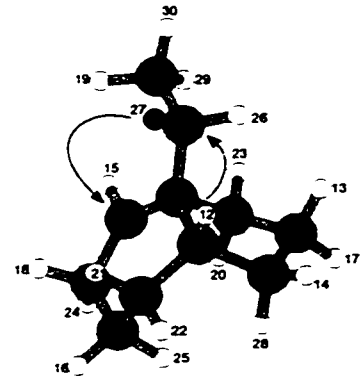

Figure 65: Geometry of the 1-ethylbicyclo[4.3.0]non-2-yl cation **209** (B3LYP / 6-31G*).

The secondary cation **211** formed no ground state minimum according to B3LYP / 6-31G* calculations. Attempts to optimize the geometry of this structure, obtained at the semiempirical level AM1 as a ground state, produced only the tertiary cation **212**, suggesting that the secondary cation **211** represents a saddle point on the reaction surface for a simultaneous hydride shift of H27 to C5 and an alkyl shift of C4 to C9 as illustrated in Figure 65.

The optimized geometry of **212** shows a favorable alignment of the cation center and H5, suitable for a 1,3 hydride shift, leading to the secondary cation **213**. A 1,2 methyl shift followed by a 1,2 hydride shift would then form the thermodynamically most favorable methyl substituted decalyl cation **39**.

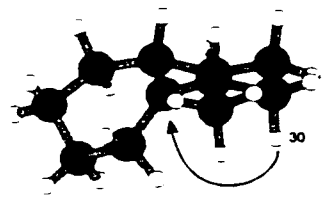

212

The two secondary cations **213** and **214**, also did not represent ground states at a B3LYP / 6-31G* level of theory. However, attempts to optimize these geometries revealed an extremely flat energy profile associated with the hydride shift reactions. Since such flat energy profiles require the calculation algorithms to perform numerous optimization steps for a

relatively small change in geometry and energy, individual optimization cycles can be used to provide approximate energies. The energy values given for structure **213** and **214** were derived in this way.

Table 31: Calculation results on the intermediates involved in the rearrangement of 9-methylbicyclo[3.3.1]non-9-yl cation **199** and 9-ethylbicyclo[3.3.1]non-9-yl cation **38**.

Structure		B3LYP / 6-31G* [hartrees]	ZPE [kcal/mol]	$H°_0$-$H°_{298}$ [kcal/mol]	S [cal/mol K]	G_{298} [hartrees][a]	rel. free energy (ref.)[b]
	**199**	-391.038429911	158.12	6.54	93.19	-390.824662156	0.00
	**200**	-391.035940601	158.52	6.43	91.59	-390.820978019	2.31 (**199**)
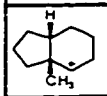	**203**	-391.022785111	157.67	6.62	93.31	-390.809657777	9.42 (**199**)
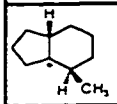	**204**	-391.040627674	156.96	6.69	94.62	-390.829113320	-2.79 (**199**)
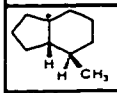	**201**	-391.041429473	156.37	6.73	95.40	-390.831124467	-4.06 (**199**)
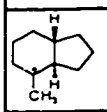	**205**	-391.035548937	156.35	6.72	95.37	-390.825289374	-0.39 (**199**)
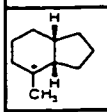	**206**	-391.039983813	157.61	6.72	95.50	-390.827822822	-1.98 (**199**)
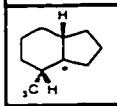	**207**	-319.041430385	156.54	6.70	95.01	-390.830727718	-3.81 (**199**)
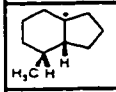	**208**	-391.035771396	156.43	6.65	94.76	-390.825204696	-0.34 (**199**)
	**38**	-430.354087781	176.38	7.44	101.36	-430.114202760	0.00 (**38**)
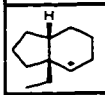	**209**	-430.336079966	175.77	7.45	100.01	-430.096497908	11.11(**38**)
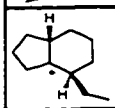	**210**	-430.350794068	174.83	7.55	102.66	-430.113756041	0.28 (**38**)
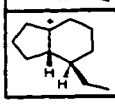	**202**	-430.354834079	174.38	7.61	102.95	-430.118554831	-2.73 (**38**)

Structure	B3LYP / 6-31G* [hartrees]	ZPE [kcal/mol]	H°_0-H°_{298} [kcal/mol]	S [cal/mol K]	G_{298} [hartrees][a]	rel. free energy (ref.)[b]
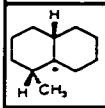 **212**	-430.358133473	175.67	7.34	99.98	-430.118874101	-2.93 (**38**)
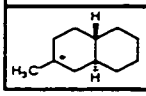 **39**	-430.362287876	175.91	7.24	98.66	-430.122195799	-5.02 (**38**)

[a]Free energy values were calculated by using a scale factor of 0.98 for the ZPE, the thermal correction of the enthalpy from 0 K to 298 K and the entropy. [b]relative free energy in kcal/mol.

2.2.4 Ionic Hydrogenation

2.2.4.1 Introduction

Catalytic hydrogenation is one of the best studied reactions of organic chemistry and the development of more specialized catalysts is still being pursued, to obtain wider activity and selectivity patterns. Alternatively, ionic activation can be used to induce a reduction reaction, forming another set of methods with unique activity and selectivity.[193, 194] However, only few methods are known compared to the huge variety in catalytic hydrogenation.

Ionic hydrogenation requires the generation of a relatively stable cation, whose lifetime is sufficiently long to capture a hydride from an appropriate hydride donor.[193, 194, 195]

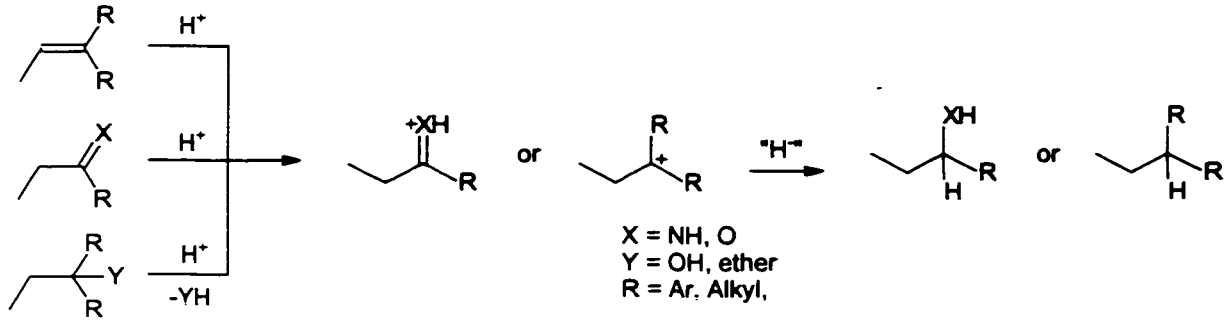

Common reaction conditions call for the use of trifluoroacetic acid as the proton source and silanes as the source of hydride.[196] This hydrogenating pair can be used to reduce functional groups such as C=C, C=O, C=N, C-OH, C-Hal or cyclopropyl.[193] These functional groups can only be reduced, if the corresponding carbocation is sufficiently long lived to capture a hydride from the silane. This implies the following requirements for the hydrogenating pair:

1. The acid and the hydride donor must not react.
2. The product formed must be stable under the reaction conditions.
3. The acid must be strong enough to generate a carbocation with a reasonable lifetime.
4. Abstraction of the hydride from its donor must be thermodynamically favorable.

Using superacidic media, one has the prospect of generating less stabilized carbocations

with an almost indefinite lifetime; however, the choice of appropriate hydride donors is very limited. In addition to that, hydrocarbons are known to react with superacidic media even at relatively low temperatures. In fact under superacidic conditions the reverse pathway of the ionic hydrogenation (see below) is usually observed[197] and this reaction has been investigated extensively.[3, 198]

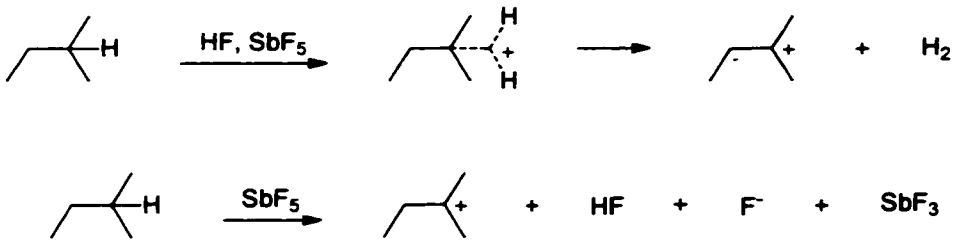

The relatively strong oxidizing nature of antimony pentafluoride has been recognized in experiments connected with the protonation of hydrocarbons. It was found that increasing the SbF_5 content in either HF or FSO_3H mixtures also increases the oxidative character of the corresponding solution. Since many carbocations require a relatively large concentration of SbF_5 to form a stable solution, finding potential hydride donors (reducing reagents) for superacidic solution work is of critical importance.

The ionic hydrogenation of alkyl cations in superacid solutions with hydrogen gas was first investigated by Hogeveen and coworkers.[199] The result of these investigations indicated that temperatures above -10°C and relatively high pressures of hydrogen (15 atm.) were necessary to obtain a reasonable reaction rate. The necessity of high temperatures above -10°C for these ionic hydrogenations represents a substantial drawback, since only a few carbocations are thermally stable under these conditions. In order to reduce the reaction temperature and still achieve a reasonable reaction rate, one has two options. The first of these is to increase the electrophilicity or electron demand of the substrate and dications should be useful in this regard. The ionic hydrogenation is then expected to involve a lower energy barrier and to be thermodynamically more favorable. The second option would be to use a more efficient hydride donor.

Promising substrates for ionic hydrogenation are the dications **36** and **40**, whose reactions

are is discussed in the following section. Hydride donors used for this reaction were hydrogen gas, sodium borohydride and isopentane. Dications have another attractive feature for studying ionic hydrogenation reactions. With a monocation, the product hydrocarbon is often not soluble in the superacid solution and is also subject to a re-oxidation by excess SbF_5, as mentioned above. With a dication, the monocation product is soluble in the acid solution, and the C-H center produced is not subject to re-oxidation by the SbF_5.

2.2.4.2 Ionic Hydrogenation of the Bicyclo[3.3.3]undecyl and Tricyclo[5.3.1.1^{3,9}]dodecyl dications

As discussed in Section 2.2.3, page 91 the high electrophilicity of the dications **36** and **40** should facilitate the ionic hydrogenation to form monocations. In addition to that, the LUMO orbital of the two dications **36** and **40**, which are the acceptor orbitals in the usual HOMO-LUMO treatment, show that the largest lobes of these orbitals are in the cavity of the multicyclic framework, which might then support an attack of the hydride into the cavity as opposed to an outside position. Thermodynamic considerations, as already discussed, suggest that the classical monocations **78** and **34** are of similar energy to the μ-H bridged cations, and the formation of the μ-H species should be possible on these grounds, if only to a small extent. The formation of only a small amount of the μ-H bridged cation is expected to be easily detectable, since experimental data of similar μ-H compounds, as well as the results of high level *ab initio* calculations, indicate that the μ-hydrogen should possess an unusually high field ^{1}H NMR chemical shift (i. e. no competing peaks expected in the same region).

Addition of isopentane to a solution of the dications **36** and **40** however, only formed a clean solution of the monocations **78** and **34** and isopentyl cation, and the excess isopentane is also seen in the NMR spectra. No high field peak could be observed in the hydrogen NMR spectrum, indicating that no detectable μ-H bridged cation had formed.

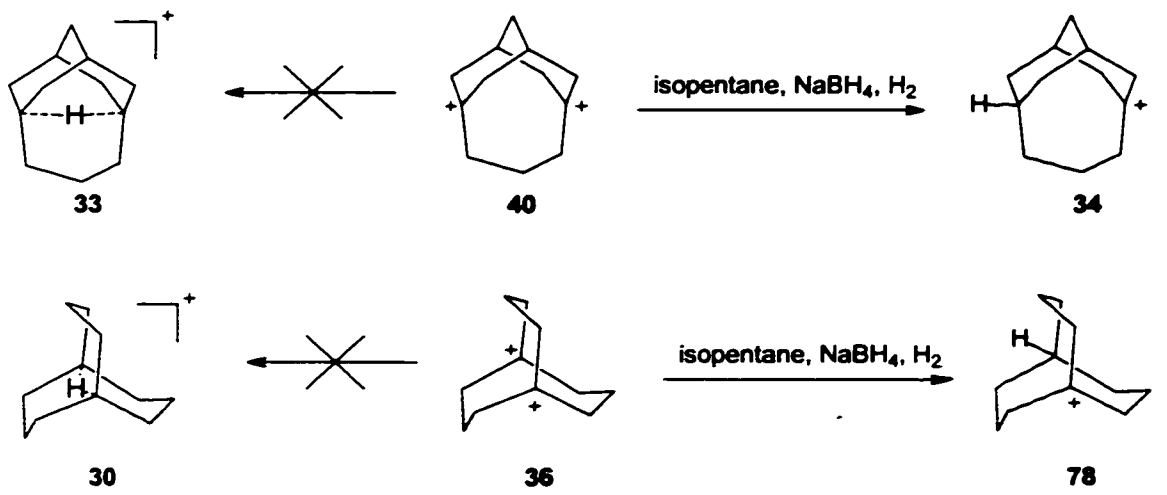

33 40 34

30 36 78

The individual compounds were identified by comparing the NMR data with that of the independently prepared species (see also Section 2.2.3, page 91). The reduction of the dications **36** and **40** with isopentane occurred instantly at temperatures of -116°C. For the tricyclic system, this reduction was found to be the best way to obtain the monocation **34** without any of its rearrangement products (compare Section 2.2.3, page 91).

The preference of these reduction reactions to form only the classical *out*-cations **78** and **34** can be attributed to a significantly larger steric hindrance in the transition state for the delivery of the hydride into the cavity, as compared to the corresponding outside delivery (see Figure 66).

Figure 66: Possible transition states for the *in*-delivery (left) or the *out*-delivery (right) of a hydride by isopentane to the bicyclo[3.3.3]undecyl dication **36**.

The use of the hydride donor sodium borohydride yielded similar results and again no high field hydrogen signal in the ^1H NMR could be observed. The reaction however proceeded significantly slower than the reaction with isopentane. This could be attributed to a limited solubility of the $NaBH_4$ in a solution of SbF_5 and SO_2ClF at low temperatures. At -105°C (168 K) the progress of the reduction could be conveniently followed by NMR spectroscopy, which showed that 47 % of the dication was reduced to the classical monocation **78** within a time period of 3 h (see Figure 67). In a similar way, 3.5 hours were required at -84°C (189 K) to completely reduce the tricyclo dication **40**, forming a solution of the monocation **35** (which results from a rearrangement reaction of the expected monocation **34**) (see Section 2.2.3.2, page 129) .

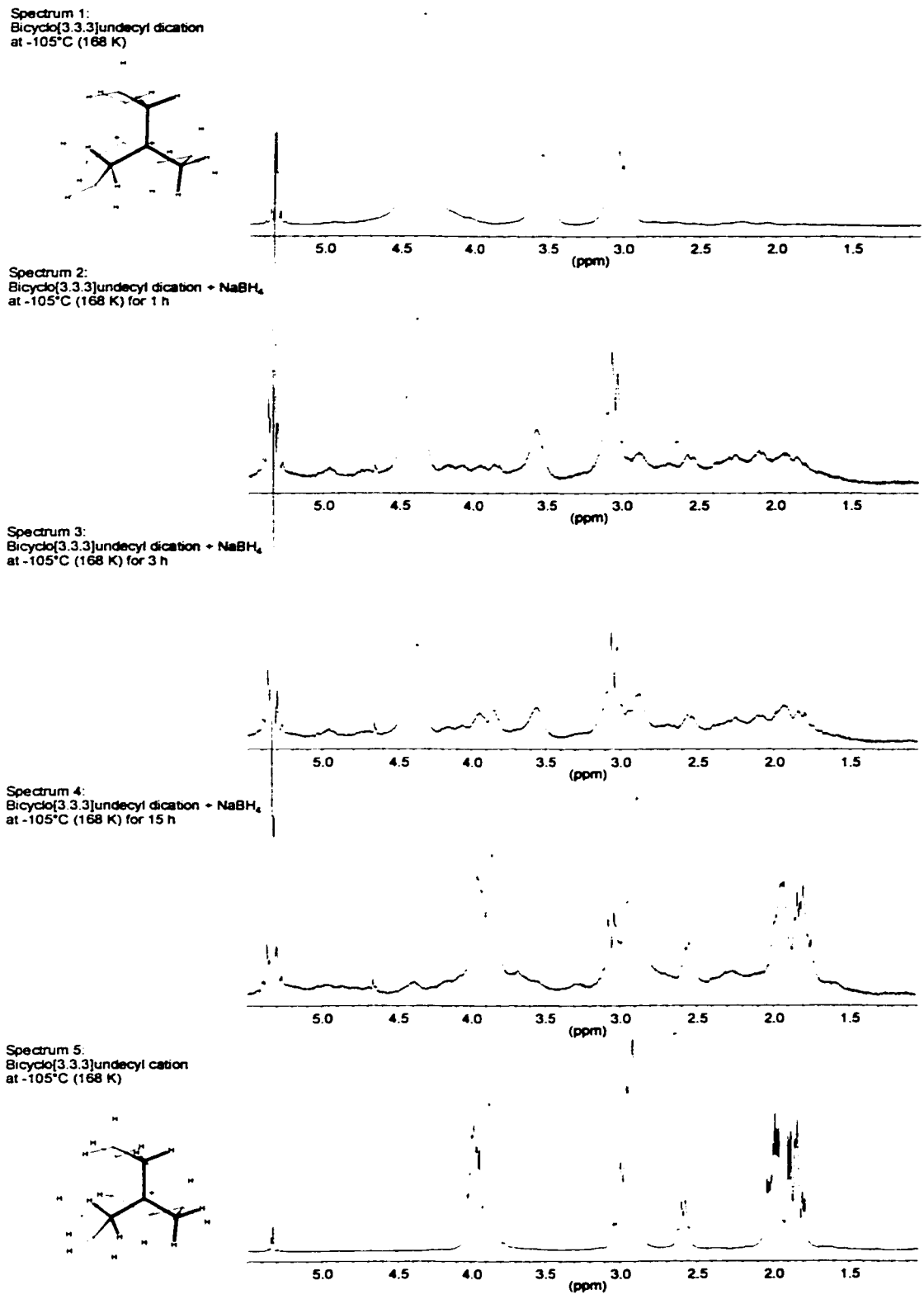

Figure 67: Reduction of the bicyclo[3.3.3]undeca-1,5-diyl dication **36** with sodium borohydride at -105°C (168 K).

Finally, hydrogen gas was used as a reducing reagent, in the hope that the small size of the H_2 molecule would cause less steric hindrance for the introduction of a hydride into the cavity of these multicyclic dications, and therefore result in the formation of a detectable amount of the μ-H bridged species. However, the reduction reactions were again relatively slow, and once again, none of the desired μ-H bridged cation could be observed. A solution of the bicyclic dication **36** was 69 % reduced at -116°C within a time period of 6 hours at a hydrogen pressure of 8 bars. Similarly, approximately 66 % of tricyclic dication **40** was reduced at a temperature of -126°C over 12 hours with a hydrogen pressure of 8 bars.

Nevertheless, the reduction of these dications with hydrogen at temperature as low as -126°C has demonstrated that these dications have a considerably higher reactivity towards ionic hydrogenation compared to monocations, which are reported to require temperatures higher than -10°C. In the reactions described here, there was no indication that the monocations produced in the hydride transfers were being further reduced to the hydrocarbon, which is also evidence that there is a distinct break in the reactivity of the mono and dications. It is also significant that an excess of isopentane transfers only one hydride in these reactions.

2.3 Internal Delivery of a Hydride

The external hydride delivery attempts discussed in the previous section showed that the outside position of the multicyclic dications **36** and **40** is attacked by various hydride donors in preference to the inside. This selectivity can be attributed to a larger steric hindrance for hydride delivery to the inside position (see Figure 66, Section 2.2.4.2, page 162). The transport of a hydride to the outside position (e.g. shift 1 in Figure 68) in the multicyclic dications **36** or **40** should be prevented by fixing the location of the hydride donor closer to the inside than to the outside of the multicyclic framework. In principle, this could be done by introducing substituents at positions in the bicyclo[3.3.3]undecyl and tricyclo[5.3.1.$1^{3,9}$]dodecyl systems, which would allow an internal delivery of the hydride, and where this reaction would favor hydride transfer to the *in*-location as shown in Figure 68.

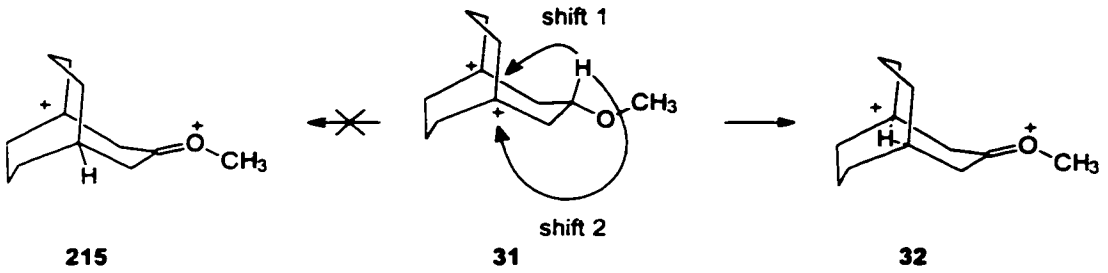

Figure 68: Preference for the inside delivery of a hydride (shift 1) over the outside delivery (shift 2) by having a fixed donating group in an appropriate position.

Preliminary *ab initio* calculations of bicyclic and tricyclic systems possessing a variety of substituents showed that an isobutyl or a methoxy substituent at the 3 position of the bicyclic system, or the 7 position of the tricyclic system were the most promising candidates for forming a μ-H bridged cation by this route (see Section 2.1, page 72). The first approach attempted was to try and prepare the methoxy substituted bicyclo[3.3.3]undecyl system, which is discussed in Section 2.3.1, page 165.

However, problems with a late stage bridgehead functionalization in the synthetic pathway blocked a preparation of the desired cation precursor and a different approach had to be considered. The second synthetic attempt was to prepare an isobutyl-substituted tricyclo[5.3.1.$1^{3,9}$]dodecyl system (discussed in Section 2.3.2, page 171). The isobutyl substituent was chosen for two reasons; first, the methoxy substituent was found to prevent an

efficient functionalization of the bridgehead positions in the bicyclo[3.3.3]undecyl system. Secondly, a methoxy substituent might itself be protonated by the superacid, and the C-$O^-(H)CH_3$ substituent formed would then actually disfavor the H^- transfer shown in Figure 68. An isobutyl group would not have this problem. The tricyclic skeleton was chosen because the inner dication opening is calculated to be somewhat larger than in the [3.3.3] bicyclic system, and there should therefore be slightly more room for the internal hydride delivery process (Figure 69).

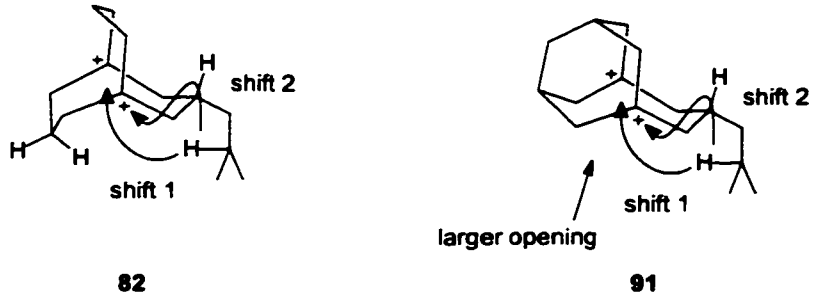

82 **91**

Figure 69: A larger opening of the cavity of the tricyclic system **91** (right) should provide a structure for a more facile hydride shift than in the bicyclic structure **82** (left).

At the same time as the synthetic preparation of the tricyclic structure was in progress, more sophisticated *ab initio* calculations at the B3LYP / 6-31G* level of theory were performed, which are discussed in Section 2.3.3, page 178.

2.3.1 Synthesis of the 3-Methoxybicyclo[3.3.3]undecyl system

3-Methoxybicyclo[3.3.3]undecane was synthesized by following the synthetic strategy used by Leonard[172] and coworkers for preparing the parent system, by introducing the methoxy substituent in the first stages of the overall sequence. At the time this synthesis was performed, the more recent variation of Wayne and Snyder[176] for preparing the parent system had not yet been published.

4-Methoxyphenol is a cheap and readily available starting material for the preparation of 4-methoxycyclohexanone on a large scale. Catalytic hydrogenation at 135°C and 35 bars hydrogen pressure using palladium on activated charcoal as catalyst produced the alcohol **217**

in high yield. Attempts to only partially reduce the phenol **216** directly to the ketone **218** were found to be sluggish and could not be driven to completion without further reduction of the ketone **218** to the alcohol **217**. Since the separation of a mixture of the phenol **216** and the ketone **218** by distillation was troublesome, the ketone **218** was generated by exhaustive reduction of the phenol to the alcohol, followed by Jones oxidation to form **218** in a two step procedure. The morpholino enamine **219** was prepared according to the method of Stork[167], and this was reacted with acrolein in ether to form the adduct **220**. This addition reaction could be monitored by ^{1}H NMR spectroscopy, focusing on the alkene hydrogens, and was found to be complete within 12 h at room temperature. Formation of the bicyclic alcohol **221** was performed in water via an acid catalyzed aldol reaction using a cation exchanger as the proton source. The alcohol **221** was found to be soluble in water, and water insoluble polymeric side reaction products formed during the aldol condensation could be conveniently separated by filtration. Removal of the alcohol group was achieved by preparing the mesylate derivative **222** followed by a zinc reduction according to the method of Fujimoto and coworkers.[171]

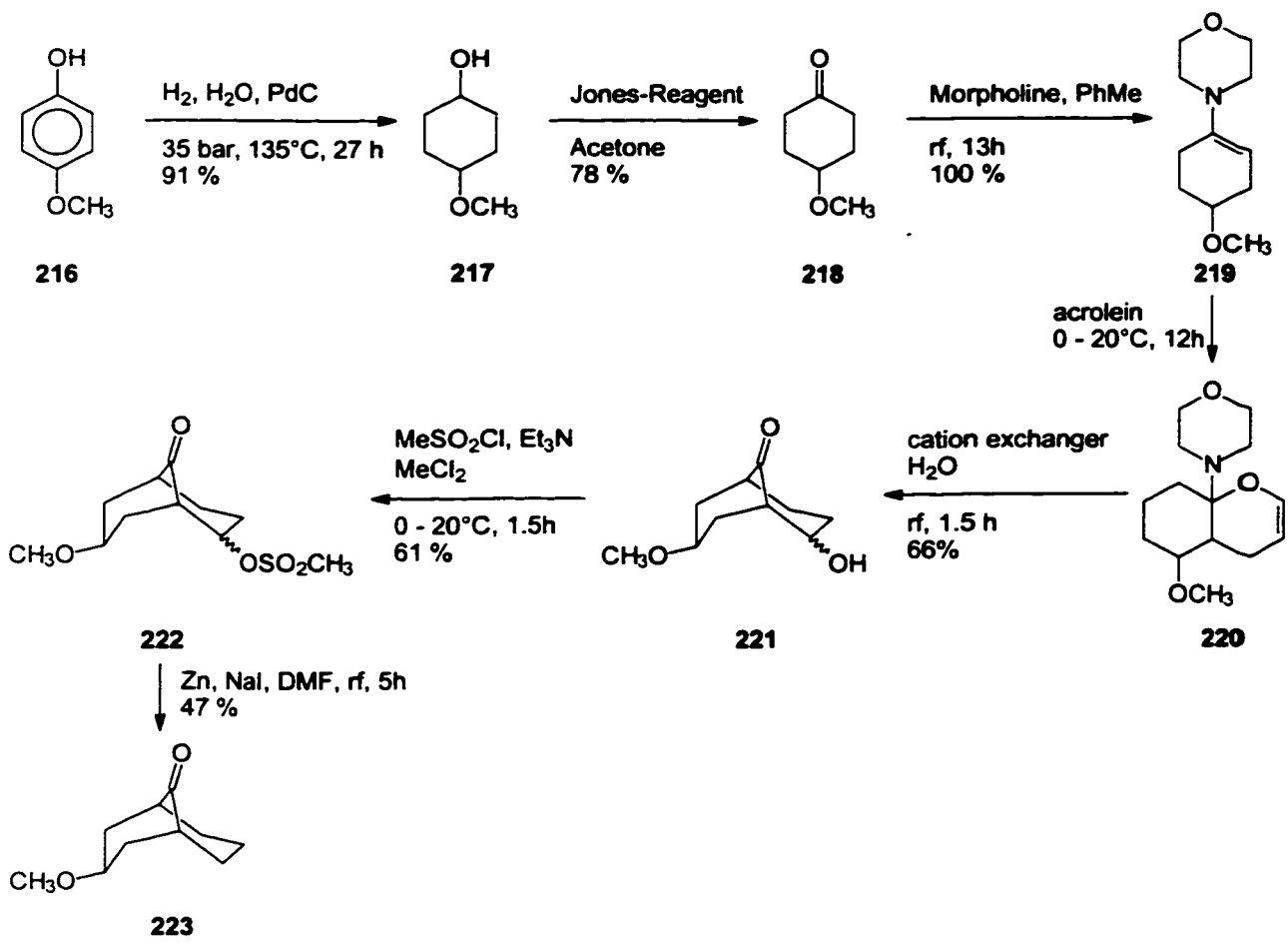

A ring expansion reaction with *in situ* generated diazomethane from Diazald® produced the bicyclo[3.3.2]decyl ketone **224** in a reaction which was found to be slightly faster for the methoxy substituted substrate **223** than for the unsubstituted parent system (compare Section 2.2.1, page 77). The second ring expansion of the ketone bridge was accomplished by a variation of the synthesis employed by Leonard. Ketone **224** was unusually unreactive towards nucleophiles (see also Section 2.2.3.3, page 142) but it could be converted into the exocyclic alkene **225** in 76 % yield using the acidic Lombardo reagent.[189]

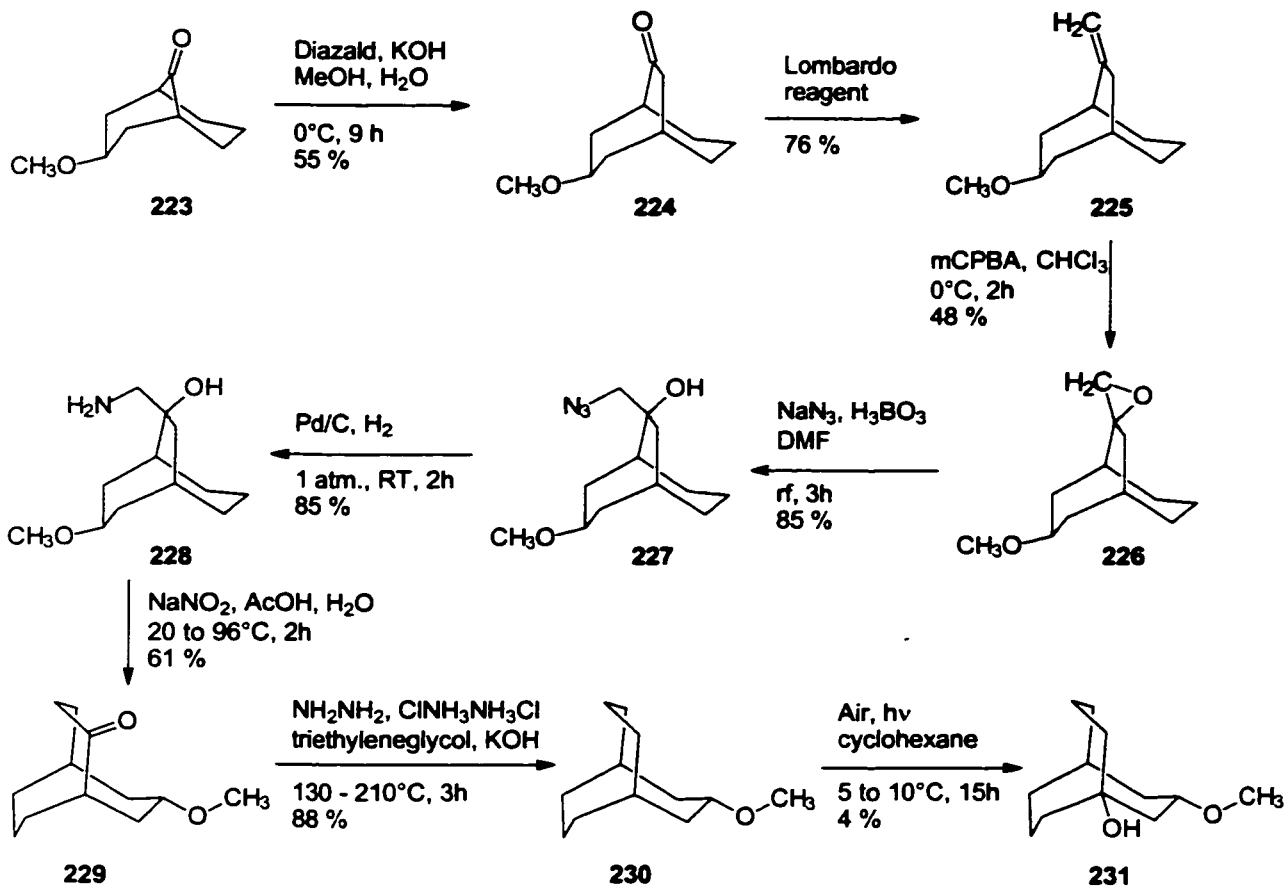

Epoxidation with mCPBA was critically dependent on the reaction time and the reaction temperature. The best results were achieved at 0°C with a reaction time of 2 hours. However, the formation of the aldehyde side product **233** could not be completely suppressed.

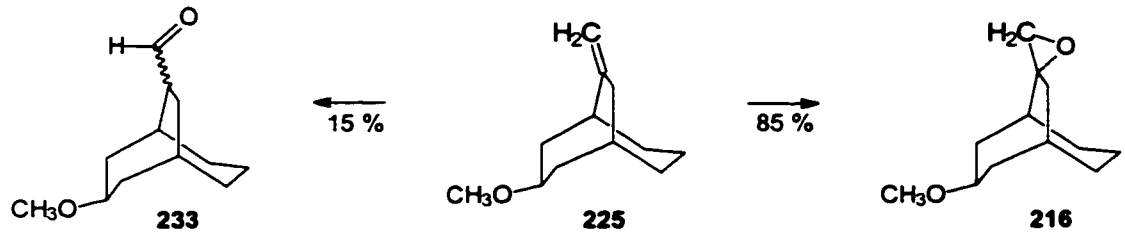

Nucleophilic attack by azide anion on refluxing the epoxide in DMF with sodium azide and boric acid formed the azide **227** which was reduced by catalytic hydrogenation at room temperature and atmospheric pressure. The resulting amino alcohol was then dissolved in acetic acid and addition of sodium nitrite solution induced a second ring expansion to form 3-methoxybicyclo[3.3.3]undecan-6-one. Wolff Kishner reduction using the method of Nagata

and Itazaki[177] yielded the ether **230**. The stereochemistry associated with the various intermediates was of no concern, since the final ether **230** has no stereochemical isomers.

Attempts to oxidize the bridgehead positions according to the procedure of Parker and coworkers[179] involved a sluggish reaction , which yielded in the best case the mono alcohol **231** in 4 % yield. Longer exposure to air formed a complex mixture containing only traces of the 3-methoxybicyclo[3.3.3]undecane-1,5-diol **232,** according to GC-MS analysis.

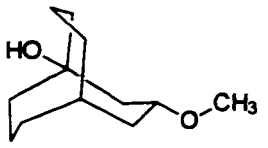

231

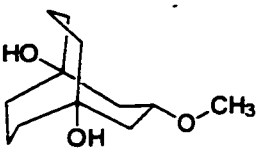

232

Attempts to brominate the bridgehead positions using Br_2 under irradiation (sunlamp) or using NBS with the initiators AIBN or dibenzoylperoxide were not successful and resulted in the formation of complex mixtures.

This distinctly different oxidation behavior compared to the unsubstituted parent system can be explained by the facile formation of a radical adjacent to the methoxy group, resulting in the formation of an ether peroxide, which could lead to cleavage of the bicyclic framework (see Scheme 14).

Scheme 14: Possible mechanism for the fragmentation of the bicyclo[3.3.3]undecyl framework.

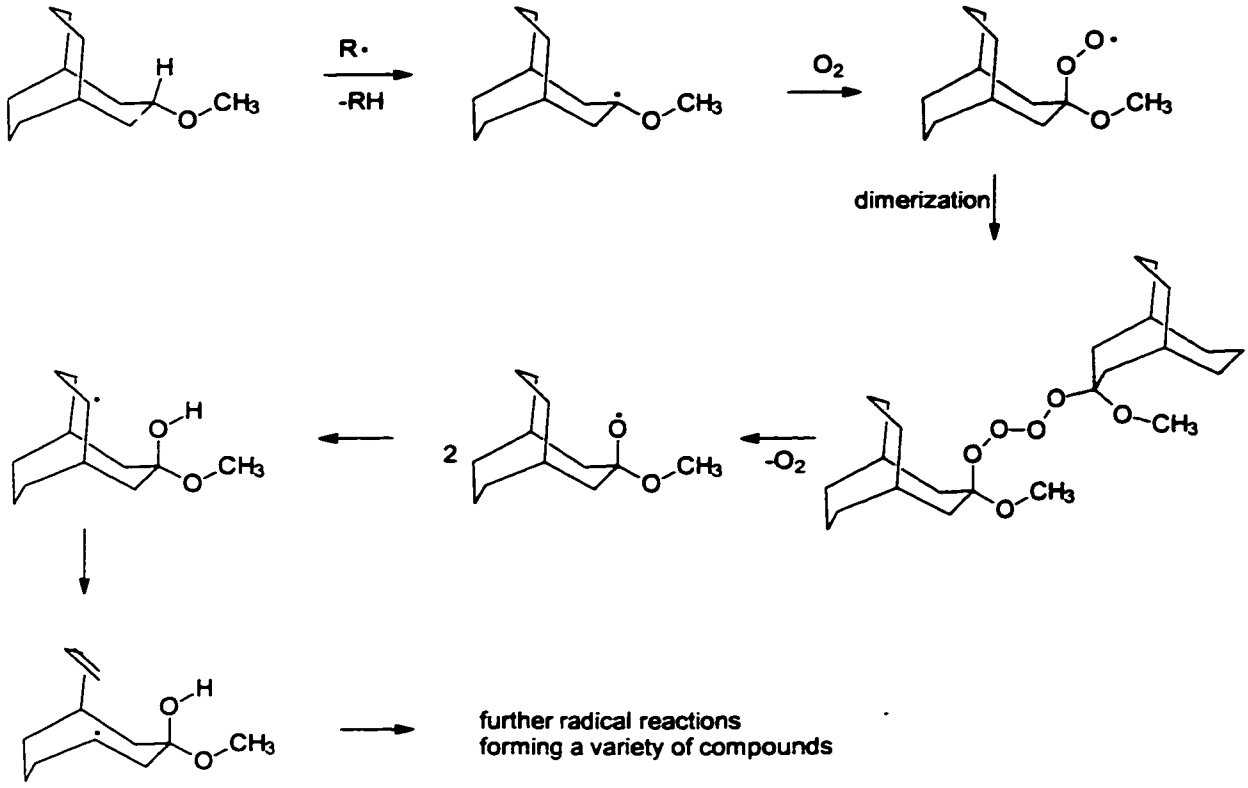

Ab initio calculations support this proposal, showing that the bridgehead radical **234** is only 2.2 kcal/mol more stable than the oxygen stabilized radical **235**.

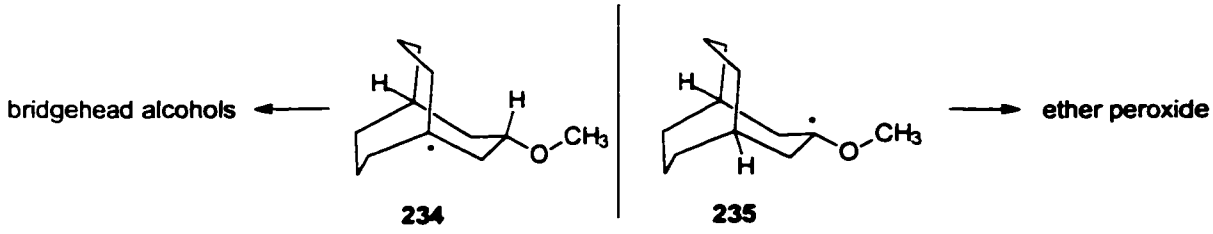

An alternative way to functionalize the bridgehead positions would involve the formation of a cation intermediate by a hydride abstraction route. An appropriate hydride acceptor would be formaldehyde activated with a Lewis acid such as aluminum chloride, as illustrated below.

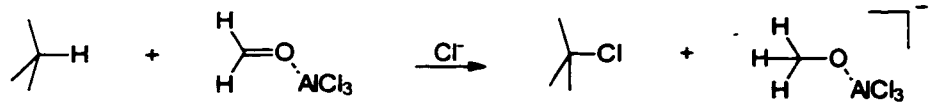

However, the ether substituted carbon is also expected to form a highly stabilized cation

which would also then lead to undesired products.

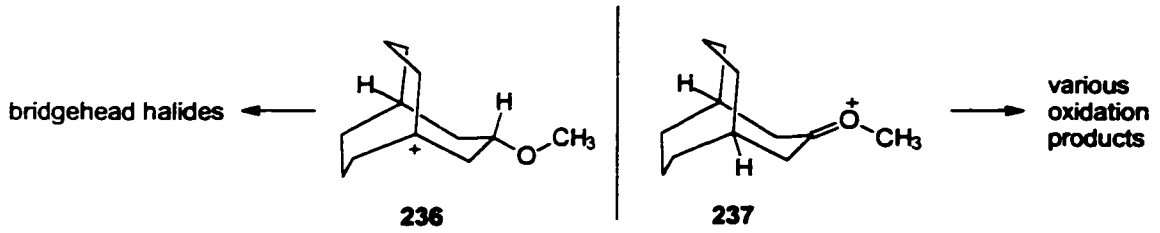

236 237

Furthermore, this functionalization method would produce the bridgehead halide, which would most likely be thermally rather unstable, and probably decompose into a complex mixture similar to what was found for known halides **111, 112** and **129**.

Ab initio calculations at a B3LYP / 6-31G* level of theory predict the oxocation **237** to be 11.7 kcal/mol more stable than the bridgehead cation **236**. For the details of the *ab initio* calculations, see Table 32.

Table 32: B3LYP / 6-31G* calculation results of methoxy substituted bicyclo[3.3.3]undecyl derivatives.

Structure	B3LYP / 6-31G* [hartrees]	ZPE [kcal/mol]	$H°_0$-$H°_{298}$ [kcal/mol]	S [cal/mol K]	G_{298} [hartrees][a]	rel. free energy (ref.)[b]
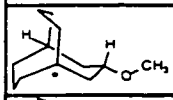 **234**	-545.071541926	197.15	8.43	108.67	-544.803328260	
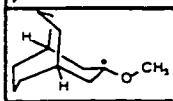 **235**	-545.071541926	197.64	8.33	107.25	-544.799808304	2.21 (**234**)
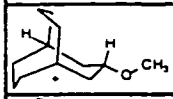 **236**	-544.858443839	197.65	8.41	106.75	-544.586327192	
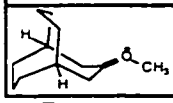 **237**	-544.879639805	199.08	8.27	105.55	-544.604964688	-11.70 (**236**)

[a]Free energy values were calculated by using a scale factor of 0.98 for the ZPE, the thermal correction of the enthalpy from 0 K to 298 K and the entropy. [b]relative free energy in kcal/mol.

2.3.2 Synthesis of a 5-substituted tricyclo[5.3.1.$1^{3,9}$]dodecyl system

The large ring strain of the bicyclo[3.3.3]undecyl or the tricyclo[5.3.1.$1^{3,9}$]dodecyl system is substantially reduced by introducing an sp^2 center at the bridgehead positions (see also Section 2.2.3, page 91). This property is unusual for most multicyclic frameworks, which often show the opposite trend. It is therefore surprising that the formation of an enolate of the

tricyclic ketone **118** forms the bridgehead isomer using LDA or LiHMDS.

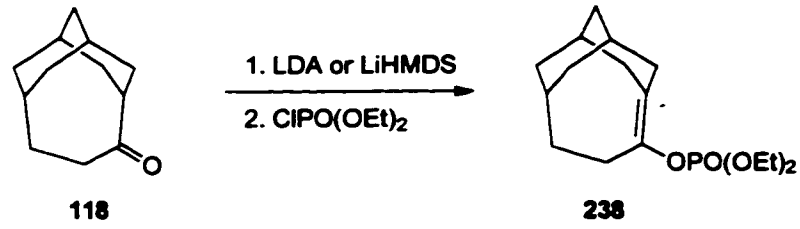

118 **238**

Ward and Murray found that the use of HMDS and TMSI directed the enolate towards the bridge to form a promising precursor for 7-substituted tricyclo[5.3.1.$1^{3,9}$]dodecane derivatives.

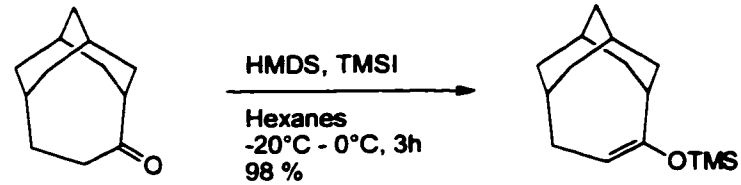

118 **239**

Using the silyl enolether **239**, four different electrophiles were found to attack it at the 7-position to form substitution products.

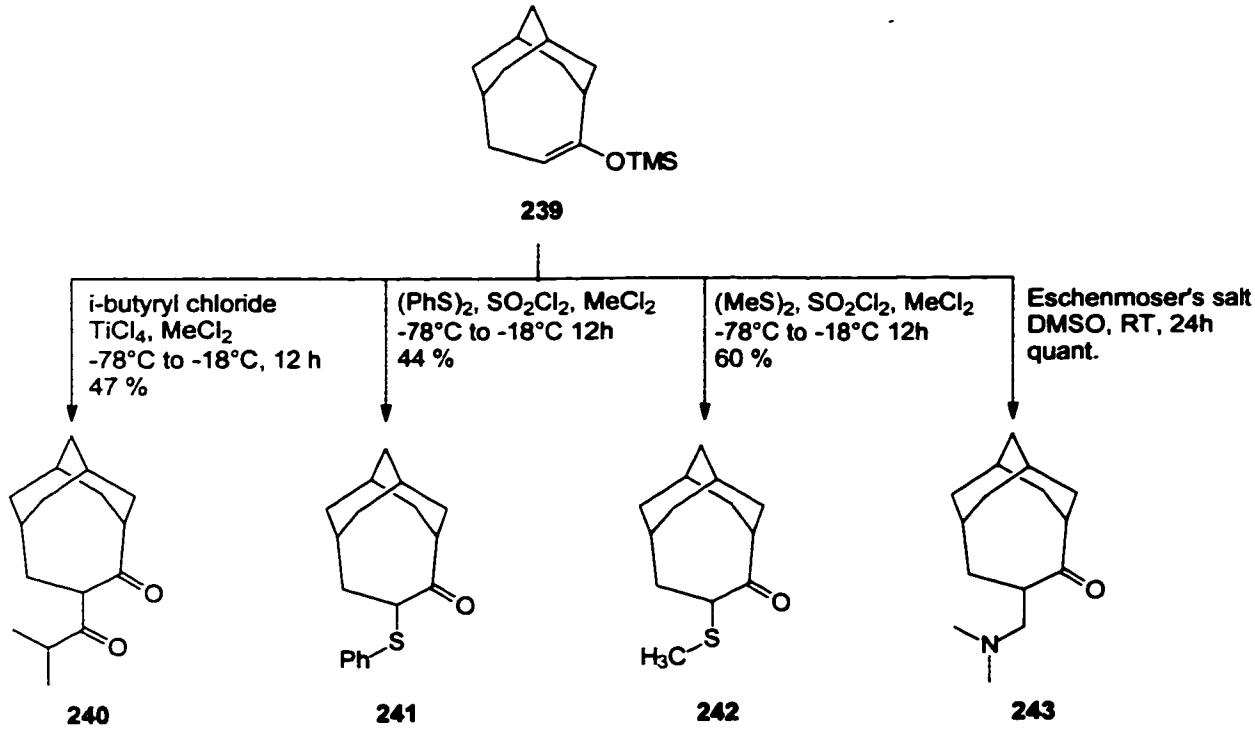

239

240 **241** **242** **243**

Treatment of the silyl enol ether **239** with isobutyryl chloride and titanium tetrachloride introduced an isobutyryl substituent directly at the desired 7-position in a moderate yield of 47 %.

Sulfur electrophiles such as benzenesulfenyl chloride or methanesulfenyl chloride were also found to react with the silyl enol ether **239** over a 12 hour period at room temperature to produce the sulfur-substituted tricyclic products **241** and **242** in 44 % and 60 % yield respectively.

The most efficient method to introduce a substituent at the 7-position was the use of Eschenmoser's salt in DMSO at room temperature, producing **243** in quantitative yield.

The formation of a double bond in the C_3 bridge of the tricyclic framework would increase the already high ring strain of this multicyclic structure. Hence, the formation of the enolate of **240** is expected to be less favourable than in "normal" 1,3-diketones, which usually exist in the enol form to a significant extent. NMR experiments confirm this supposition, showing no low field signal for the enol hydrogen in the solution spectrum of the diketone **240**.

240 **244**

The unfavorable formation of an enolate of the diketone **240** suggested that the two ketone groups could be considered as isolated carbonyl groups, hence a Wolff-Kishner reduction was attempted despite the usual formation of a pyrazole derivative in such cases. However, the increase of ring strain in the C_3 bridge on forming a double bond was not large enough to prevent the formation of a pyrazole unit and the sole product of the attempted Wolff Kishner reduction was the heterocyclic derivative **245** .

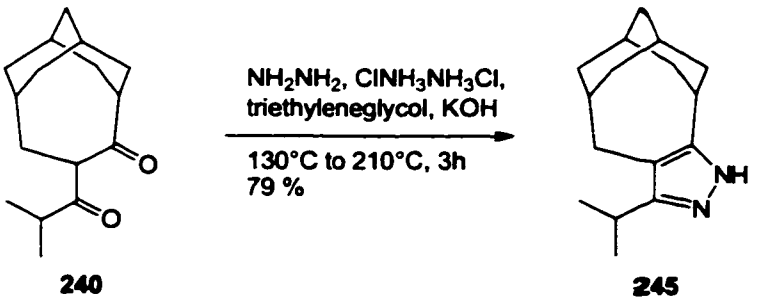

240 245

A variation of the Wolff Kishner reduction is the use of tosylhydrazine to form the corresponding hydrazone derivative, which can then either be reduced with sodium borohydride or sodium cyanoborohydride to form the corresponding alkane. Attempts to form the *bis*tosylhydrazone **246** by refluxing the diketone **240** with tosylhydrazine in methanol for several hours was not successful.

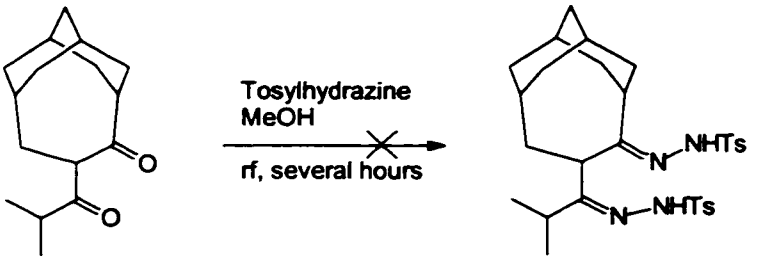

240 246

Another way to reduce the ketone groups in **240**, would be the use of ethanedithiol to form the bisdithiane derivative **247** followed by a nickel reduction using nickel chloride and sodium borohydride.

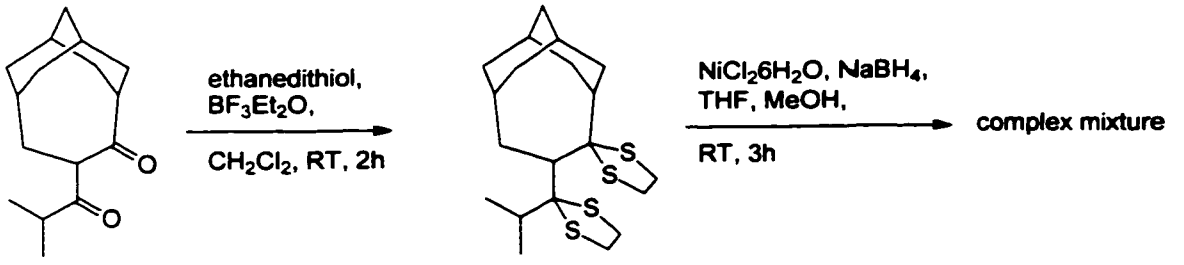

240 247

However, the reduction reaction of the bisdithiane **247** with *in situ* generated nickel did not result in the formation of any detectable amount of the desired alkane.

Reduction of the diketone **240** with lithium aluminum hydride in ether resulted in the formation of the diol **248**, which was converted into the dichloride **249** using thionyl chloride in dichloromethane. However, the zinc reduction method of Fujimoto and coworkers[171] left the dichloride **249** unchanged, even after 18 h of reflux.

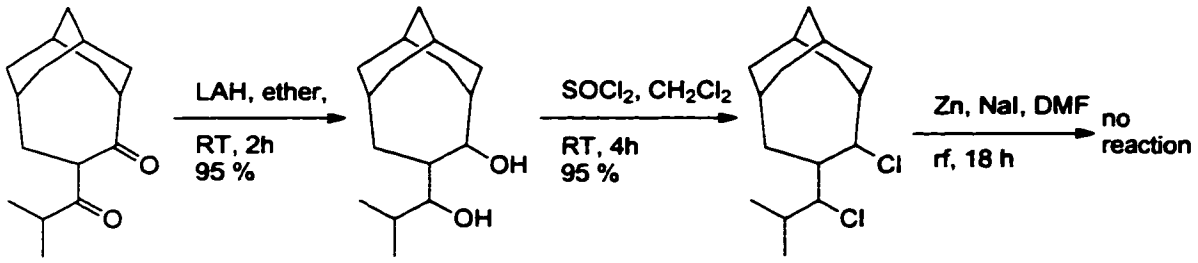

240 **248** **249**

The diol was then converted into the diphosphate ester **250**, and the reduction of this was attempted via a Birch type reaction using lithium in liquid ammonia in the presence of tertiary butyl alcohol as the proton source. However the material obtained contained no alkane **251**.

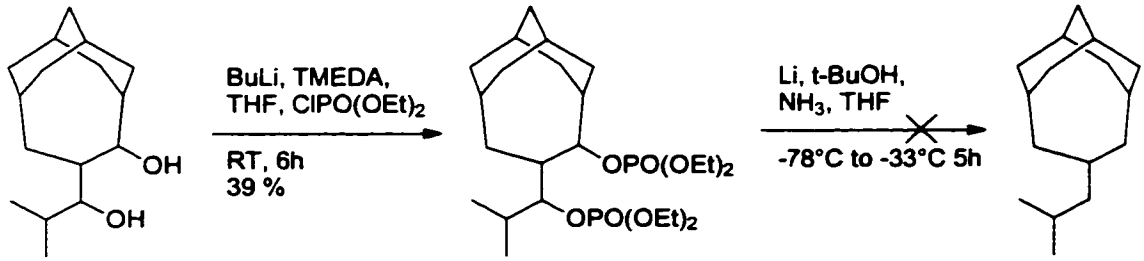

248 **250** **251**

After the unsuccessful attempts to reduce the diketone **240**, a carbonyl transposition of the ketone **118** to the ketone **119** was attempted, since the latter would be a valuable precursor for 7-substituted derivatives of the tricyclo[5.3.1.$1^{3,9}$]dodecyl system.

A conventional sequence for a carbonyl transposition using the α phenylthio ketone **241**, consists of the reduction of the ketone to the alcohol, converting the alcohol into a leaving group followed by an elimination to form an enol thioether, which can be converted into the new ketone on hydrolysis with aqueous mercuric salts.

The thio ketone **241** was reduced to the alcohol **252** using lithium aluminum hydride in ether and the resulting alcohol converted to the chloride **253** by refluxing it with a solution of thionyl chloride in benzene. This chloride however, proved inert to an elimination reaction

using potassium tertiary butoxide.

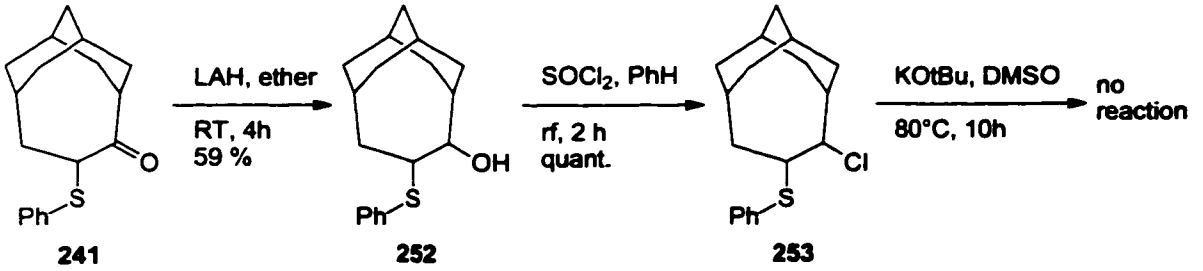

241 252 253

Attempts to reduce the ketone group of the thio ketone **241** using a Wolff Kishner reaction resulted in the formation of a mixture of the tricyclic alkane **61** and alkene **254** in about 20 % yield. The alternative method for this reduction, using the tosylhydrazone and sodium cyanoborohydride, was also not successful since the hydrazone **255** could not be formed.

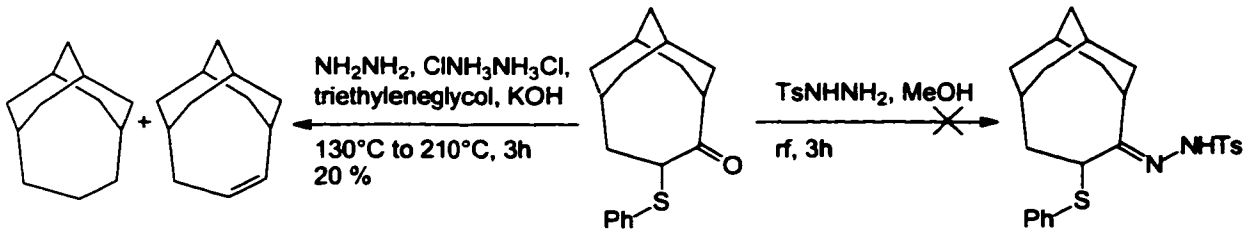

61 254 241 255

A third series of experiments was then performed, using a different strategy to try to achieve a carbonyl transposition. It was found that deprotonation of the ketone **242** with LiHMDS in ether formed the bridge enolate, which could be trapped by quenching the enolate solution with diethylchlorophosphate to form the enol phosphate **256** in 65 % yield. Birch reduction of the phosphate ester **256** in liquid ammonia not only reduced the phosphate group, but also the methyl sulfide group, forming the alkene **254** in 89 % yield. Fortunately, hydroboration followed by an oxidative workup with sodium hydroxide and hydrogen peroxide formed the 7-substituted alcohol **257** in a reasonable yield of 74 %.

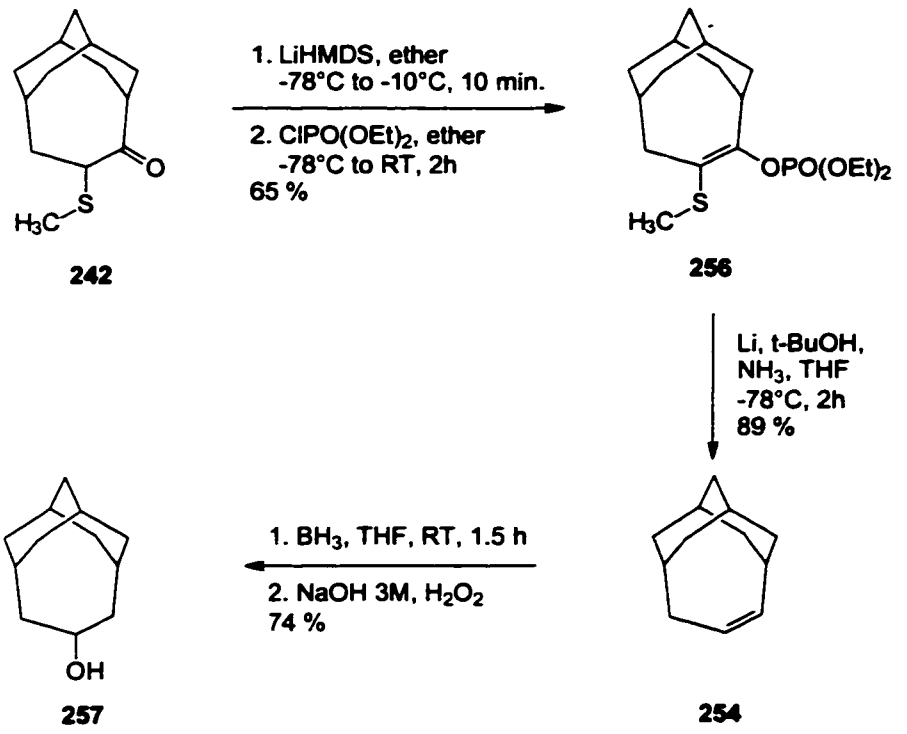

Although a route to 7-substituted alcohol **257** was found, which potentially opens a way to the formation of a variety of 7-substituted tricyclo[5.3.1.$1^{3,9}$]dodecyl derivatives, the project involving an isobutyl substitued tricyclo[5.3.1.$1^{3,9}$]dodecyl derivative was canceled, for two reasons:

1. The synthesis of the desired isobutyl substituted tricyclic dichloride **261** would involve several more steps from the alcohol **257**.

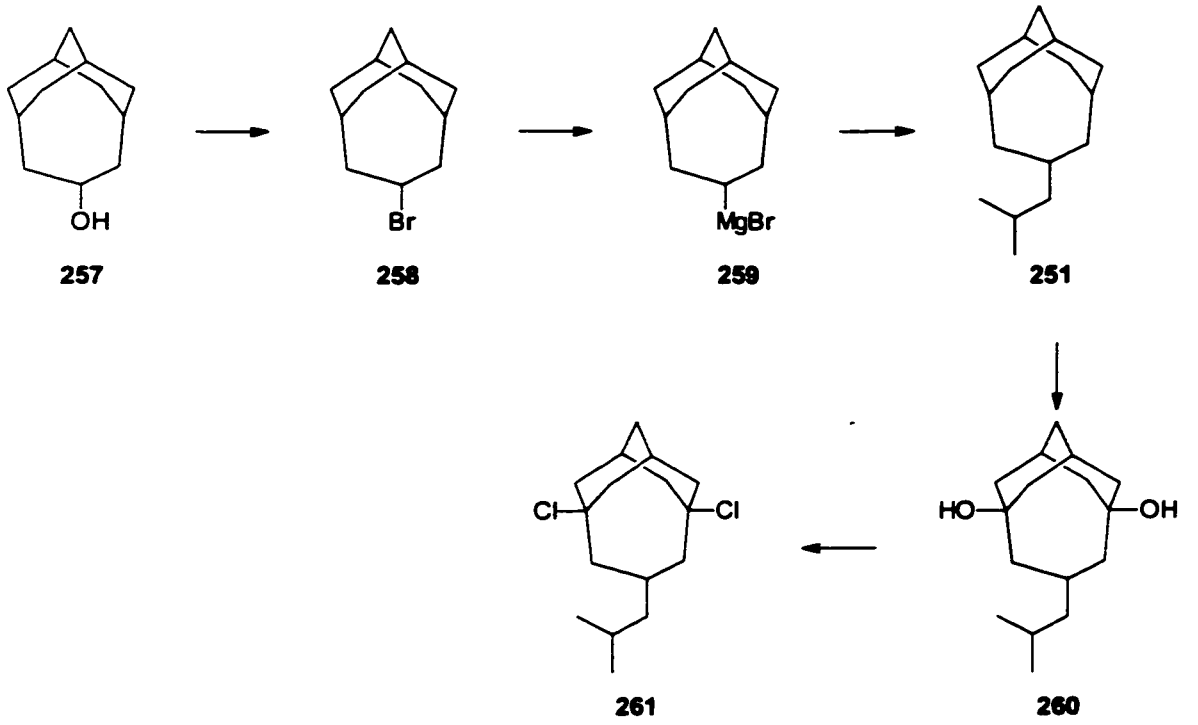

257 258 259 251

261 260

At this point, more starting material was needed and in order to obtain a reasonable amount of the dication precursor **261**, a significant amount of time would have been required.

2. High level *ab initio* calculations indicated that despite a thermodynamically favorable rearrangement of the classical dication **91** into the desired μ-H bridged dication **92**, the transition state involved was predicted to be extremely high, suggesting that this rearrangement was very unlikely to occur.

2.3.3 *Ab initio* Calculations of the transition-states for internal hydride shifts in the bicyclo[3.3.3]undecyl and tricyclo[5.3.1.$1^{3,9}$]dodecyl systems

At the same time as the preparation of the isobutyl substituted tricyclo[5.3.1.$1^{3,9}$]dodecyl system was in progress, more sophisticated *ab initio* calculations at a B3LYP / 6-31G* level of theory were carried out to determine the calculated transition-state barriers for the hydride shift reactions.

The ground state calculations comparing the classical bridgehead dication with the corresponding nonclassical μ-H bridged dication revealed that the methoxy and isobutyl

substituents were the most promising candidates (see Tables 33 and 34).

Table 33: Calculated energy (B3LYP / 6-31G*) differences between the classical dications and the corresponding μ-H bridged species in the bicyclic and tricyclic systems containing methoxy or isobutyl substituents.

Substituent	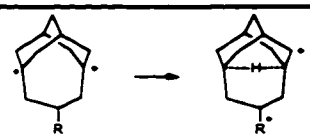	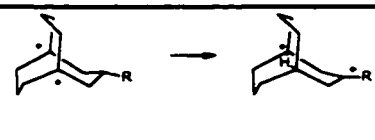
R = OCH_3	-2.5	-7.9
R = i-butyl	-5.4	-11.8

The transition-states of these four reactions were then calculated, and they revealed that these barriers had unreasonably high values of at least 50 kcal/mol.

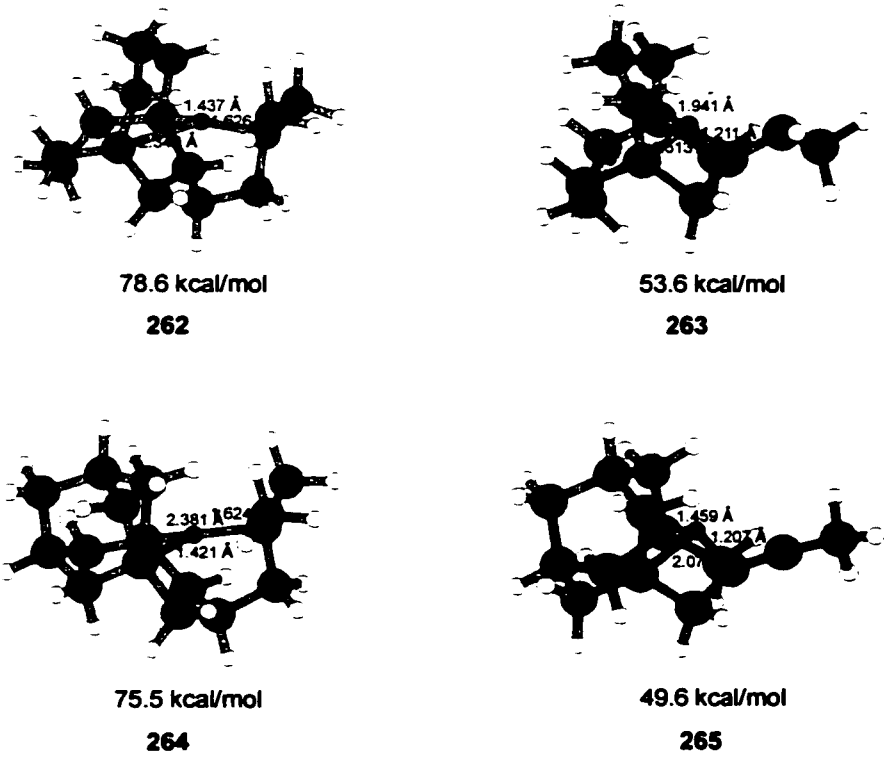

Figure 70: Calculated transition states (B3LYP / 6-31G*) of isobutyl- and methoxy-substituted bicyclo[3.3.3]undecyl and tricyclo[5.3.1.$1^{3,9}$]dodecyl systems. Energy values are free energy activation energies.

In order to have reactions which would occur at a reasonable rate at a temperature of -80°C, energy barriers of less than 18 kcal/mol are necessary. Calculated energies at the B3LYP / 6-31G* level of theory, involving highly nonclassical transition states such as **262** through **265** usually overestimate the experimental values. However, the discrepancy typically does not exceed 15 kcal/mol. Since the calculated energy values are over 50 kcal/mol, an experimental value of at least 35 kcal/mol is expected in the best case, and this is still far beyond a value that would allow the rearrangement to proceed.

The reason for the unusually high energy barriers for these hydride shifts is found in the relatively long bond distances in the transition states. In the methoxy derivatives **263** and **265**, this is due to the geometrical arrangement of the bridgeheads in question and the 3- or the 7-position in the bicyclic or the tricyclic system, respectively. The approach of the tertiary hydrogen of the isobutyl substituent into the cavity of the bicyclic or tricyclic structures **262** and **264** is limited by a steric interaction of the methyl groups of the isobutyl substituent and the nearby bridge hydrogen of the multicyclic structure, as indicated in Figure 70.

Table 34 summarizes calculation details on the four transition states **262** through **265**.

Table 34: Calculation results for the (B3LYP / 6-31G*) transition states of methoxy and isobutyl substituted bicyclo[3.3.3]undecyl and tricyclo[5.3.1.$1^{3,9}$]dodecyl systems.

Structure	B3LYP 6-31G* [hartrees] img. freq.[a]	ZPE [kcal/mol]	$H°_0$-$H°_{298}$ [kcal/mol]	S [cal/mol K]	G_{298} [hartrees][b]	rel. free energy (ref.)[c]
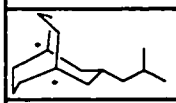 **82**	-586.565323229	239.23	10.26	120.79	-586.231929315	
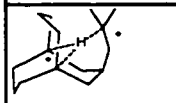 **262**	-586.44040394 -1487	237.52	9.34	111.08	-586.106598469	78.65 (**31**)
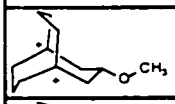 **31**	-543.823394827	188.63	8.49	106.91	-543.565319640	
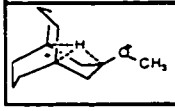 **263**	-543.734776634 -911	186.32	8.22	105.22	-543.479958847	53.56 (**82**)

Structure	B3LYP 6-31G* [hartrees] img. freq.[a]	ZPE [kcal/mol]	$H°_0$-$H°_{298}$ [kcal/mol]	S [cal/mol K]	G_{298} [hartrees] [b]	rel. free energy (ref.) [c]
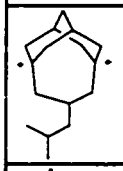 **91**	-624.683296009	243.60	10.14	120.88	-624.343293819	
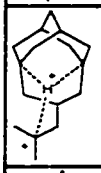 **264**	-624.564311484 -1420	242.18	9.14	110.00	-624.223038739	75.46 (**91**)
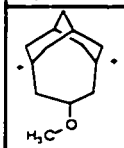 **93**	-581.94033684	192.83	8.46	107.09	-581.675831260	
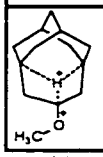 **265**	-581.860026007 -755	191.37	7.95	103.23	-581.596805712	49.59 (**93**)

[a] Single imaginary frequency in cm^{-1}. [b] Free energy calculated by using a scale factor of 0.98 for the ZPE, the thermal correction of the enthalpy from 0 K to 298 K and the entropy. [c] relative free energy in kcal/mol.

Chapter III

Theoretical Aspects of the μ-Hydrido Bond

3.1 Molecular Orbital Diagrams

The μ-hydrido bond can best be described as a 3-center-2-electron (3c-2e) bond. The H_3^+ molecule can be considered the prototype of this bonding mode, which results from the interaction between the normal 2-center-2-electron bond of dihydrogen and a proton (see Figure 71).

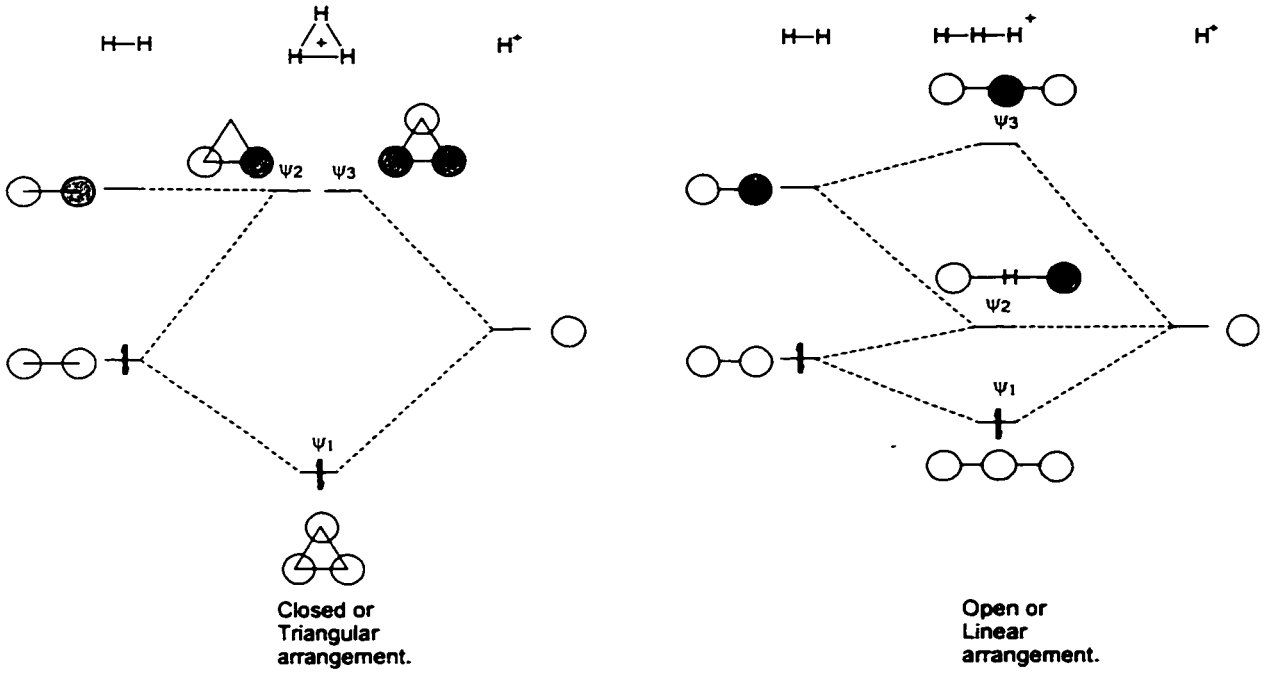

Figure 71: Molecular orbital diagrams for closed and open geometries of H_3^+.

The closed form of H_3^+ has one occupied and a pair of degenerate unoccupied antibonding orbitals, and the linear form of H_3^+ possesses one occupied bonding orbital, a nonbonding and an antibonding orbital. Various intermediate "bent" geometries can be constructed and gradually changing from the linear form to the closed or triangular form causes the HOMO (ψ_1) to become lower in energy due to more efficient overlap of all three hydrogens. The energy gap between the two unoccupied orbitals (ψ_2 and ψ_3) vanishes as the angle of the center

hydrogen approaches 60°. This is due to the increasing antibonding interaction of ψ_2 and bonding interaction of ψ_3 as the angle between the terminal hydrogens decreases (see Figure 72). Since the occupied orbital experiences greater stabilization with this change, the triangular or closed form of H_3^+ is preferred over the linear one. This is in agreement with high level *ab initio* calculations as well as spectroscopic gas phase measurements.[200]

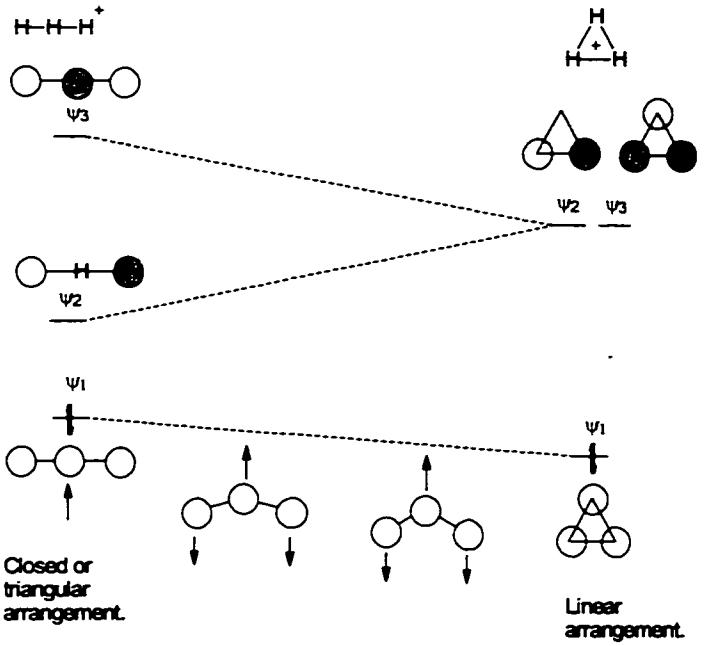

Figure 72: Walsh diagram for the linear to triangular form of H_3^+.

In a similar way, a proton can interact with a C-C single bond to form a μ-H bridged species. This process can also be regarded as the protonation of an alkane (Figure 73).

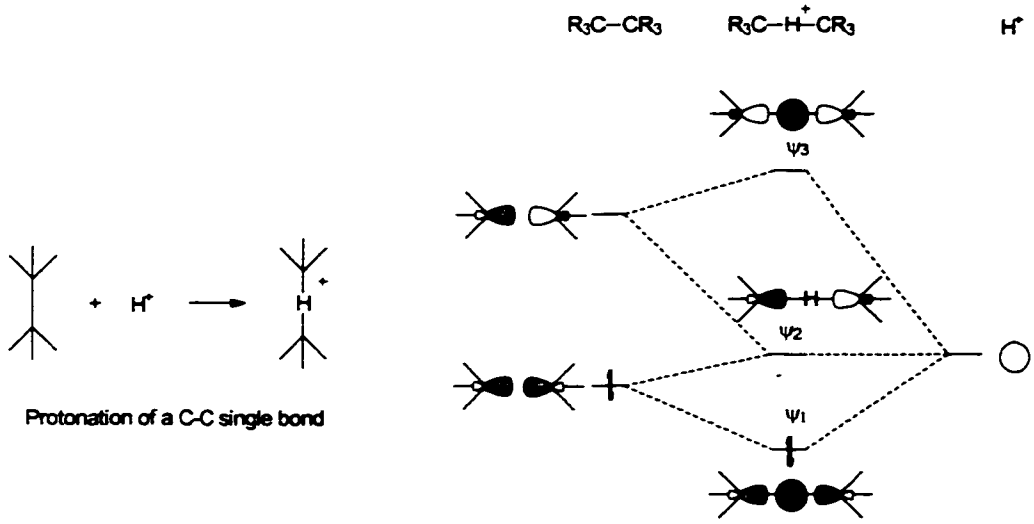

Figure 73: Protonation of a C-C single bond to form a μ-hydrido bridged carbocation.

The arrangement of the 3 atoms in question again can vary from a bent to a linear structure. However, the carbon atoms possess additional substituents, which experience increasing steric hindrance with an increasingly bent C-H-C bond. This effect opposes the electronic effects, which would favor a bent structure. Since the electronic effect is considerably weaker than the steric effect, most of the observed μ-hydrido bridged carbocations are calculated to have a linear or slightly bent structure as illustrated in Figure 74.

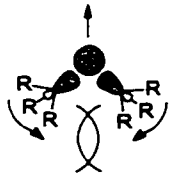

Figure 74: Increasing steric interaction of the substituents R with decreasing C-H-C angle.

3.2 NMR Properties of the μ-Hydrogen

Considering the HOMO orbital of a μ-H bond, one finds that most of the electron density is located close to the μ-hydrogen. Therefore, it is better described as a hydride than as a proton. Since hydrogen chemical shifts depend mostly on diamagnetic shielding factors, the

large electron density around the μ-hydrogen explains its exceptionally high field NMR shift (down to -7.7 ppm in the cyclooctyl cation (see Section 1.8, page 53).

Attempts by Cioslowsky[160b] to predict corresponding NMR shifts using high level *ab initio* calculations did not result in a good agreement with experimentally measured values (compare Section 1.8, page 55). Cioslowsky[160b] suggested that large vibrational motions of the μ-hydrogen as a result of a very flat potential energy surface (PES) were responsible for the discrepancy. *Ab initio* calculations at the Becke3LYP / 6-31G* level of theory were used to explore this PES and the associated chemical shifts of the μ-hydrogen (this work). The known bicyclo[4.4.4]tetradecyl-1,6-μ-H bridged cation **28** was calculated, since the availability of experimental data allowed a comparison with the theoretically predicted values. The geometry of **28** was optimized at a B3LYP / 6-31G* level of theory and the structure obtained modified by changing the relative location of the μ-hydrogen in both a horizontal or a vertical direction (see Figure 75), but keeping all other geometrical parameters constant.

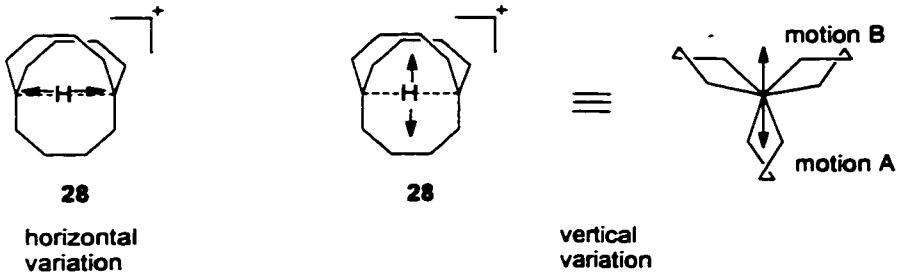

Figure 75: Exploration of the potential energy surface (PES) by varying the relative location of the μ-hydrogen.

This simplified treatment is expected to closely resemble the real situation in the μ-H cation, for two reasons. First, the carbon atoms are considerably heavier than the hydrogen, hence the vibrations of these are expected to be of a much slower frequency and can therefore be approximated by a static carbon framework. Second, the μ-hydrogen is expected to possess a much flatter PES than all other hydrogens in the molecule. Therefore the amplitude of the vibrations are expected to be much larger for the μ-hydrogen than for all other hydrogens.

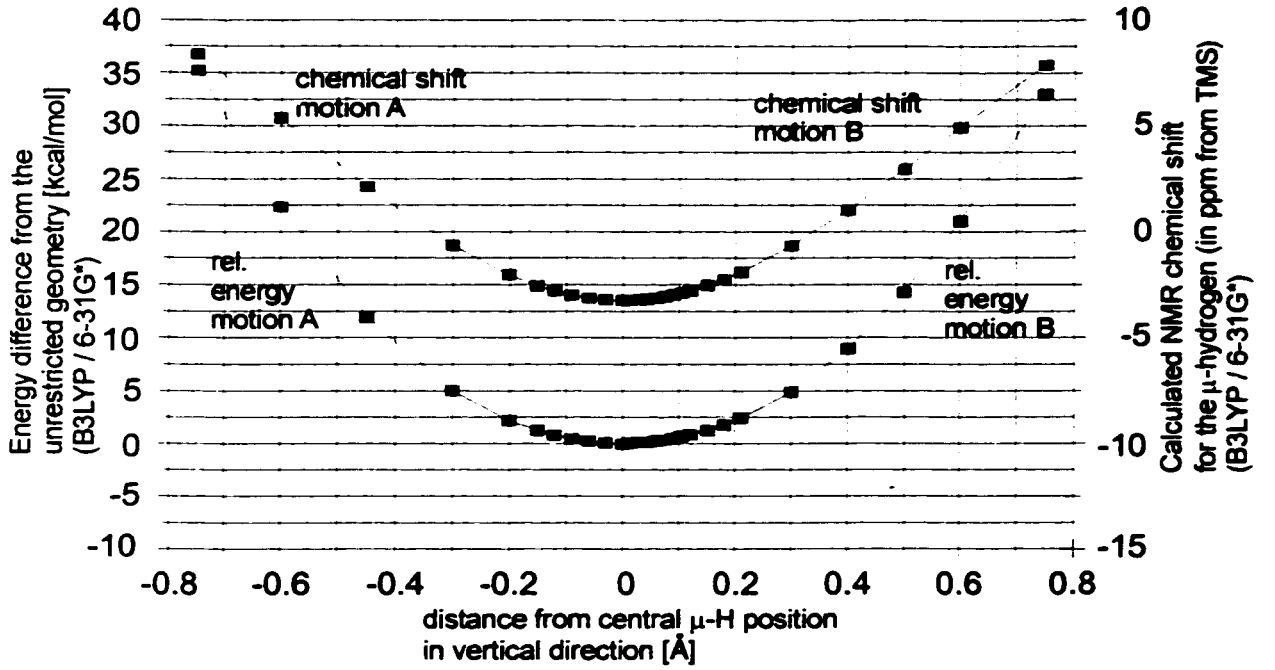

Figure 76: Dependence of the calculated energy and the ^{1}H NMR shift of the μ-hydrogen on vertical variation of the μ-hydrogen in the bicyclo[4.4.4]tetradecyl μ-H bridged cation **28**.

Variation of the μ-H cation location in the vertical direction (see Figure 76) indicates a very flat energy profile within the first 0.2 Å. At room temperature 95 % of the molecules would reside in a vibrational energy potential of *ca.* 1.8 kcal/mol, which corresponds to a vertical variation of no more than 0.18 Å, involving an associated chemical shift change of the μ-hydrogen of 0.98 ppm ranging from -2.94 to -1.96 ppm.

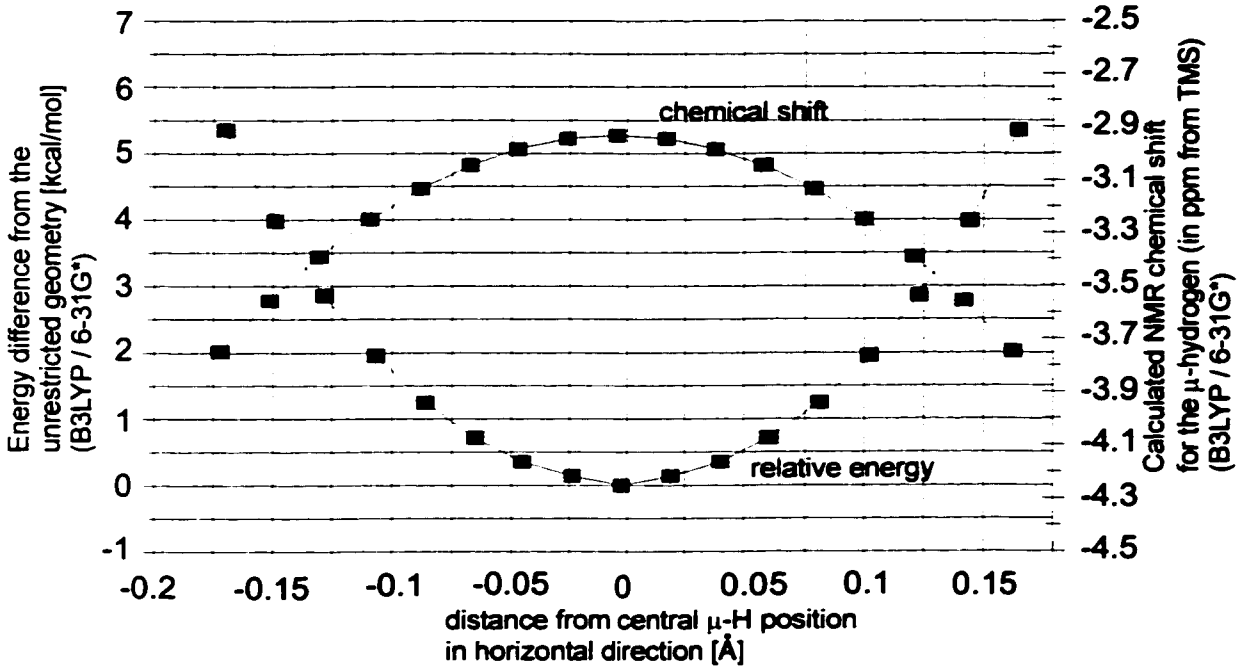

Figure 77: Dependence of the calculated energy and the ^{1}H NMR shift of the μ-hydrogen on horizontal variation of the μ-hydrogen in the bicyclo[4.4.4]tetradecyl μ-H bridged cation **28**.

The other principal vibrational direction of the μ-hydrogen is in the horizontal direction (termed horizontal effect) (see Figure 77). Calculations at a B3LYP / 6-31G* level of theory using the GIAO method for the chemical shift computation, predicts that a change of the μ-H location away from the center of the 3c-2e bond in a horizontal direction, leads to a high field shift of the μ-hydrogen.

For relatively large vibrational motions of the μ-hydrogen, the effect of the horizontal variation (horizontal effect) opposes the effect of the variation in vertical direction (vertical effect). The magnitude of the horizontal effect is slightly smaller than the vertical effect and would partially cancel out the latter. Assuming vibrational motions corresponding to an energy of 2 kcal/mol, which would account for more than 96 % of the "vibrational" population at room temperature, the chemical shift change of the μ-hydrogen is expected to be only 0.32 ppm, ranging from -2.94 to -3.26 ppm, numbers which are reasonably close to the experimentally measured value of -3.46 ppm. Hence, the explanation for the large chemical shift discrepancy between MP2 (Full) / 6-31G** // HF / 6-31G** GIAO-CHPF NMR calculations (-10.06 ppm) [160b] and the experimentally measured value (-3.46 ppm) **cannot** be

attributed to large vibrational motions of the μ-hydrogen. Furthermore, GIAO NMR calculations using the packages Gaussian 94 and Gaussian 98[201] at the B3LYP / 6-31G* level have agreed much better with the corresponding experimental values than these reported by Cioslowski.[160b]

The chemical shift of the μ-hydrogen was found to be very sensitive to the separation of the terminal carbons of the C-H-C bond and a shorter distance is associated with much higher field chemical shifts for the μ-hydrogen. An accurate calculation of this distance was difficult due to the relatively flat energy surface and the distance varied significantly at different levels. In general, low level calculations underestimated the strength of the μ-H bond, and the calculated terminal carbon separation is predicted to be too large. Reasonable agreement between calculations and the NMR experiment is only obtained with relatively large basis sets and methods which include electron correlation, such as B3LYP or the various Møller-Plesset methods (MP2, MP3, MP4 etc.). The difficulties in calculating an accurate terminal carbon separation of the μ-H bond are therefore proposed to be the reason for the large discrepancy between the theoretically calculated and the experimentally measured chemical shift of the μ-hydrogen, as reported by Cioslowski.[160b]

The good to excellent agreement of calculated and experimentally measured chemical shifts of a variety of different carbocations at a B3LYP / 6-31G* or MP2 (Full) / 6-31G* level of theory suggests that the prediction of the NMR shift is very accurate if the geometrical structure of the molecule in question is close to reality. Hence, the high sensitivity of the μ-hydrogen to the distance of the terminal carbons in the μ-H bond allows one to use the NMR parameter as an experimental measure of this distance, which turn out to be quite close to the calculated distance if high level *ab initio* calculations with electron correlation are used.

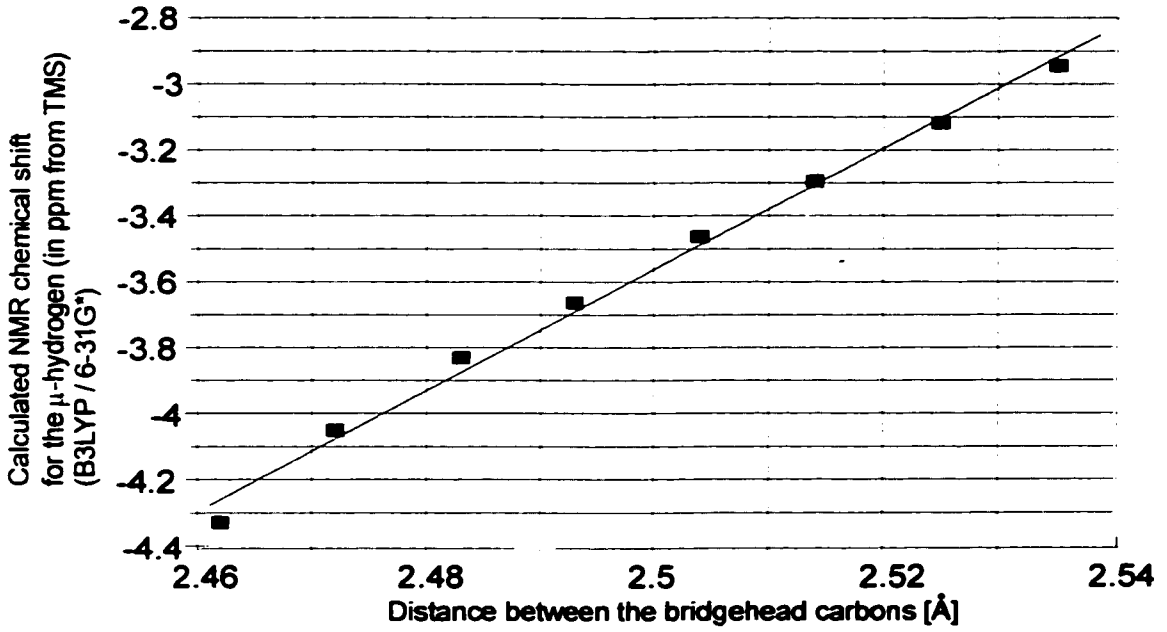

Figure 78: Dependance of the chemical shift of the μ-hydrogen in the bicyclo[4.4.4]tetradecyl μ-H bridged carbocation on the terminal carbon separation of the μ-H bond.

Using B3LYP / 6-31G* calculations, a match of the theoretical and experimental chemical shift of the μ-H hydrogen was found at a distance of the terminal carbons of the μ-H bond of 2.493 Å (see Figure 78). This result suggests that the calculations at MP2 / 6-31G** (terminal carbon separation: 2.462 Å)[160b] overestimate the bond strength of the μ-H bonds, which then results in a smaller distances between the two carbons in question. On the other hand, the B3LYP / 6-31G* calculations appear to slightly underestimate this bond strength and predict a value of 2.535 Å for the terminal carbon separation. Nevertheless, the calculated value of -2.95 ppm for the μ-hydrogen at the B3LYP / 6-31G* level, compared to the experimental value of -3.46 ppm, is in the range of the commonly observed accuracy for this type of calculation and this method is therefore considered to be adequate for further investigations into μ-H bridged carbocations and their properties.

Exploring the potential energy surface of the μ-hydrogen of the bicyclic system **33** (see Figure 79), similar trends to those found for the bicyclo[4.4.4]tetradecyl μ-H bridged cation were noted. The chemical shift, however, of the μ-hydrogen was calculated to be -12.02 ppm versus the -2.94 ppm of the bicyclo[4.4.4]tetradecyl system (see Figures 80 and 81). Another

difference between these two bicyclic systems is the steeper potential energy surface of the smaller bicyclo[3.3.3]undecyl system. Both of these differences indicate a much more distinct μ-H bond character in the smaller system, which can be attributed as a direct consequence of the closer proximity of the two bridgehead centers.

Vibrational motions of the μ-hydrogen in the [3.3.3] system, corresponding to a 2 kcal/mol energy difference, would involve a chemical shift change of 0.32 ppm, ranging from -12.02 ppm to -12.34 ppm. The vertical effect again opposes the horizontal effect and a 2 kcal/mol energy difference would imply a chemical shift change of 0.81 ppm ranging from -12.02 ppm to -11.21 ppm. Adding the two effects, the B3LYP / 6-31G* calculations predict a chemical shift for the μ-hydrogen to be in the range of -11.78 ppm to -12.02 ppm (see Figures 79 through 81).

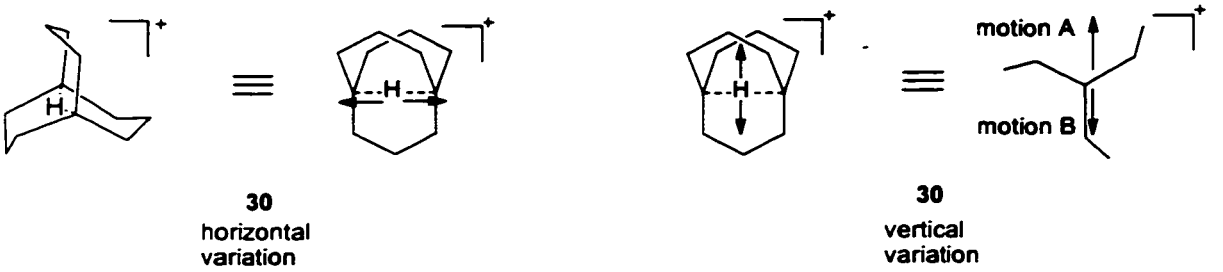

Figure 79: Horizontal and vertical variation of the location of the μ-hydrogen in the bicyclo[3.3.3]undecyl μ-H bridged carbocation **30.**

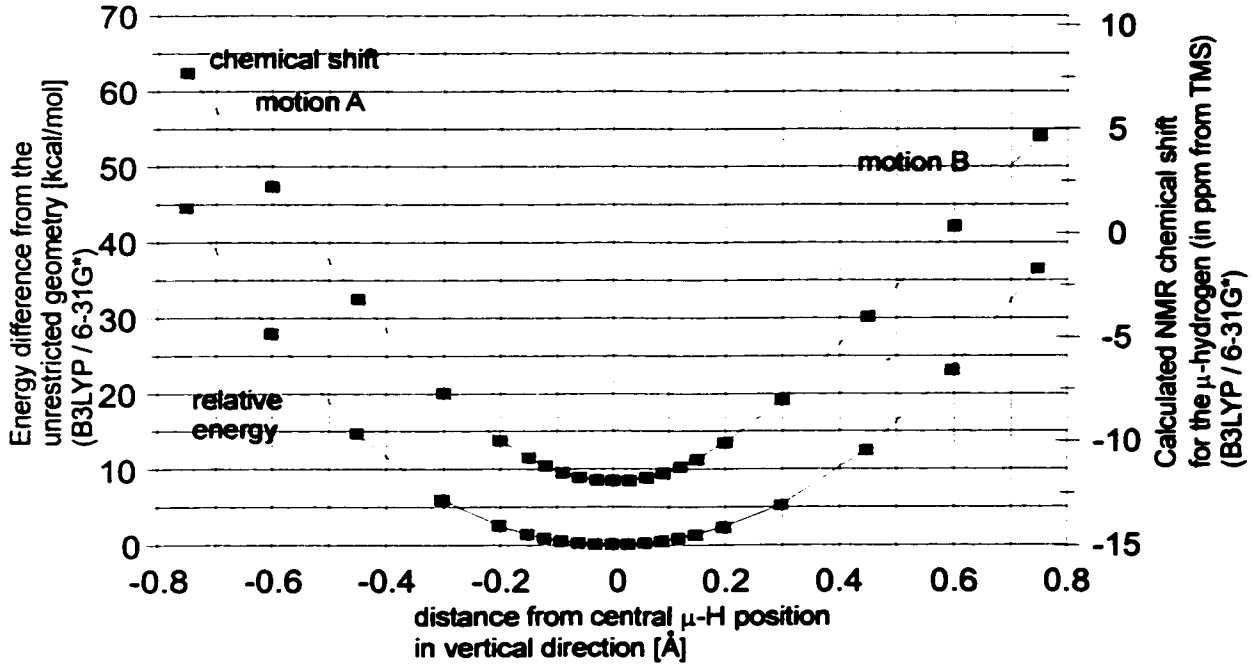

Figure 80: Dependence of the calculated energy and the ^{1}H NMR shift of the μ-hydrogen on vertical variation of the μ-hydrogen in the bicyclo[3.3.3]undecyl μ-H bridged cation.

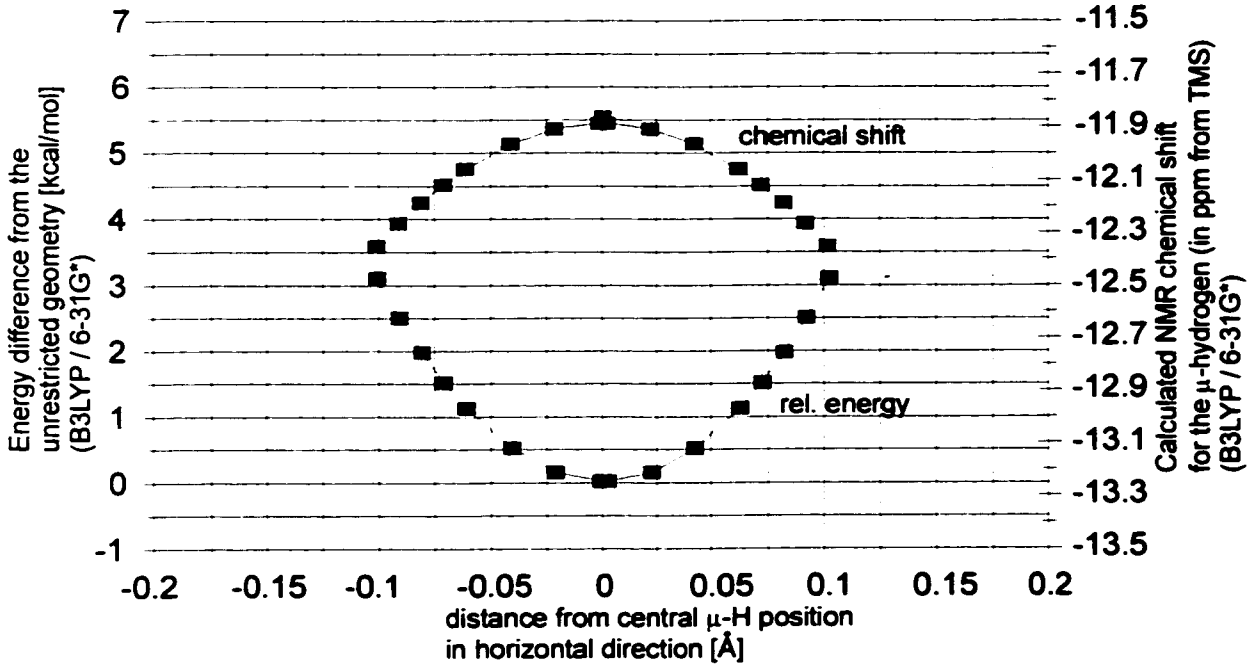

Figure 81: Dependence of the calculated energy and the ^{1}H NMR shift of the μ-hydrogen on horizontal variation of the μ-hydrogen in the bicyclo[3.3.3]undecyl μ-H bridged cation.

The motions of the μ-hydrogen in the tricyclic system **33** can also be divided into a horizontal and in a vertical variation. However, the tricyclic system has a Cs symmetry and the orientation of the vertical motion is no longer degenerate.

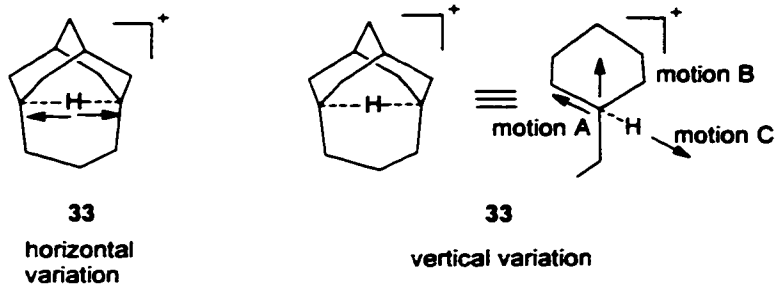

Figure 82: Different motions of the μ-hydrogen of the tricyclo[5.3.1.1^{3,9}]dodecyl μ-H bridged cation **33**.

Three different orientations (motions A, B, and C in Figure 82) were calculated and are illustrated in Figures 83 and 84.

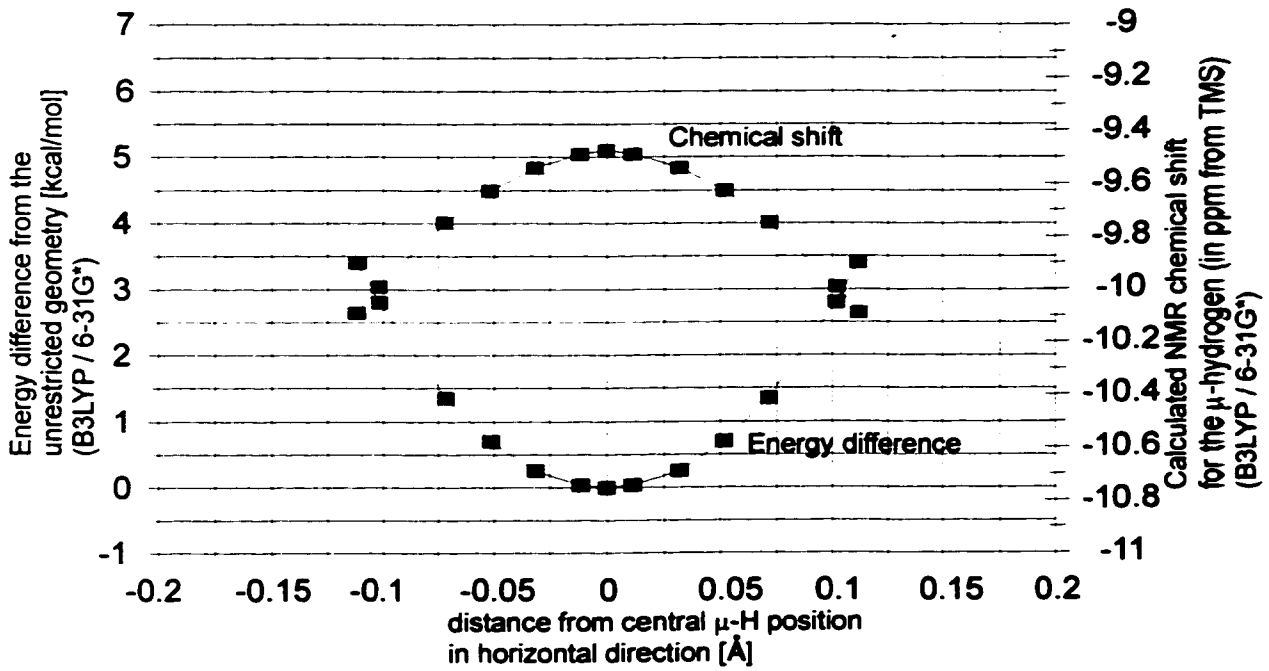

Figure 83: Dependence of the calculated energy and the ^{1}H NMR shift of the μ-hydrogen on horizontal variation of the μ-hydrogen in the tricyclo[5.3.1.1^{3,9}]dodecyl μ-H cation **33**.

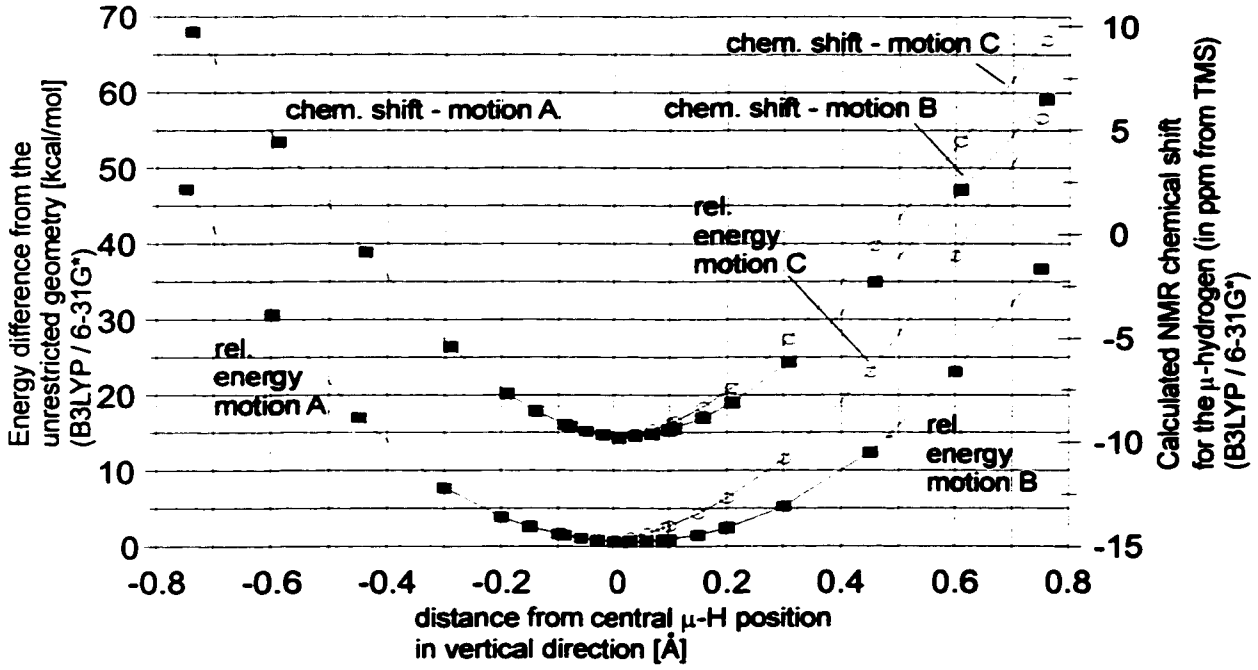

Figure 84: Dependence of the calculated energy and the ^{1}H NMR shift of the μ-hydrogen on vertical variation of the μ-hydrogen in the tricyclo[5.3.1.1^{3,9}]dodecyl μ-H cation **33**.

Similar to the bicyclo[3.3.3]undecyl system, the potential energy surface is steeper compared to the bicyclo[4.4.4]tetradecyl μ-H bridged cation **28**, however the qualitative trends are the same. Assuming vibrations corresponding to a 2 kcal/mol energy difference, the horizontal variation involves a chemical shift change of 0.34 ppm in the range of -9.47 ppm to -9.81 ppm. The vertical changes corresponding to the same 2 kcal/mol, were found to be most significant for the motions A and C, involving a chemical shift change of 1.27 ppm ranging from -9.47 ppm to -8.20 ppm. Averaging the two opposing effects, the expected change of the chemical shift of the μ-H hydrogen ranges from -9.01 to -9.47 ppm.

3.3 1,2-Hydrido Bridged Cations

An exception to the distinct NMR property of the μ-H hydrogens are the 1,2-hydrido bridged cations, such as the ethyl and the *sec*-butyl cations **266** and **269**. The absence of a distinct high field hydrogen can be explained by two effects.

1. Having a relatively steep angle for the μ-hydrogen, the HOMO orbital is dispersed over a larger area compared to the linear μ-H bridged protonated ethane (see Figure 85). The

associated electron charge is therefore more spread out and the diamagnetic shielding effects on the μ-H hydrogen are not as effective as in the linear case.

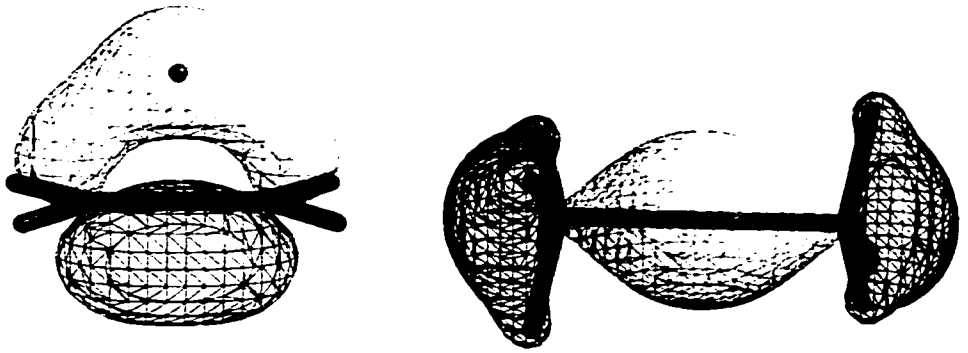

266 **267**

Figure 85: HOMO orbitals of the 1,2-hydrido bridged ethyl cation **266** and a linear $C_2H_7^+$ cation **267**.

Calculation of the NMR chemical shift of the μ-hydrogen at an MP(Full) / 6-311+G** level of theory yielded a value of -1.19 ppm for the ethyl cation **266** and -15.6 ppm for the linear μ-H bridged protonated ethane **267**.

2. The μ-hydrogen sits in a shallow energy minimum with respect to the "classical" structure. For the *sec*-butyl cation, an energy difference of only 1.5 kcal/mol (MP2(Full) / 6-31G*) was calculated between the symmetrical μ-hydrido bridged structure **269** and either of the "classical" structures **268** or **270** (these "classical" structures still have partial bridging of one of the α hydrogens).

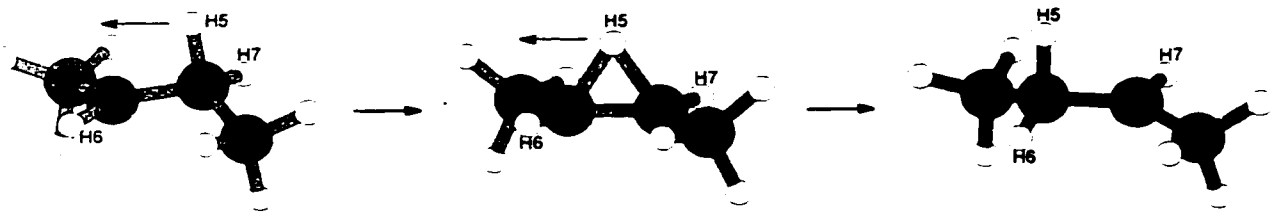

268 **269** **270**

MP2 (Full) / 6-31G* calculations of the energy and the NMR chemical shift of the μ-hydrogen with varying distances to C2 or C3 reveal the flat energy profile for this motion (see Figure 86). The chemical shift of the μ-hydrogen and H6 (same value as H7 due to symmetry) were calculated to possess values of -2.3 ppm and 7.4 ppm respectively in the symmetrically bridged structure **269**.

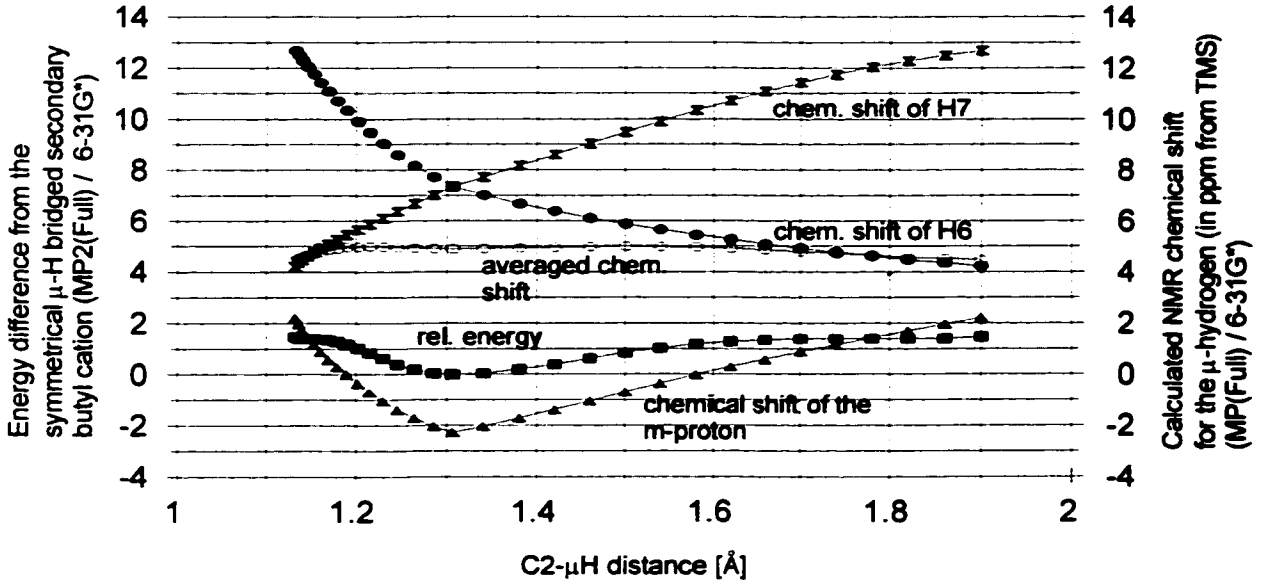

Figure 86: Calculated (B3LYP / 6-31G*) relative energy and chemical shift of the μ-hydrogen depending on the relative location of the "μ-hydrogen" of the *sec*-butyl cation.

Moving H5 gradually closer to C2 (or C3; these are degenerate pathways, however one should note that the lengthening of the H5-C2 distance has a different step size than the corresponding H5 - C3 distance and the curves in Figure 86 are therefore not symmetric) increases the classical carbocation character. The chemical shifts of H5 (still partially bridged), H7 and H6 in **268** were calculated as 2.2, 4.2 and 12.7 ppm, respectively.

The facile 1,2 hydrogen shift causes rapid scrambling of the hydrogens H5, H6 and H7, and the experimental NMR spectra show only an averaged signal for these three hydrogens (see Figure 87). Interestingly, the averaged signal at different μ-H - C2 distances is relatively constant and varies only from 4.5 ppm in the "classical" structure **268** or **270** to 5.0 ppm for the symmetrically bridged structure **269**. Hence, the theoretically predicted averaged NMR shift (MP2(Full) / 6-31G*) for the hydrogens H5, H6 and H7 is 4.8 ppm.

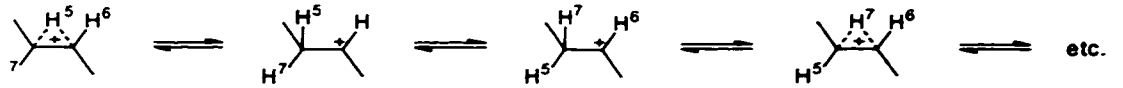

Figure 87: Scrambling of the secondary hydrogens of the *sec*-butyl cation.

Experimental measurements by Saunders and coworkers in the condensed phase have shown, that this scrambling process has a barrier of less than 2.4 kcal/mol and the averaged hydrogen shift for the three "secondary" hydrogens was measured as *ca.* 6.8 ppm.[202] Despite the relatively large discrepancy between this and the calculated value of 4.8 ppm, the absence of an unusually high field hydrogen is shown both experimentally and theoretically.

3.4 Interaction of a Carbocation with a C-H Bond

Another way to describe a μ-H bond is the interaction of a carbocation and a normal 2c-2e C-H bond, which has the possibility of being a transition state process or a reactive intermediate in an overall hydride shift reaction. The electrophilicity or electron demand of the cationic center has a strong influence on the energy profile for an overall hydride shift. The more electrophilic (less stabilized cation) the cationic center that is involved, the greater is the stabilization experienced through the interaction with a C-H bond and the more likely it is that an intermediate will be formed as one moves along this reaction pathway. To recap, the likelihood of forming a μ-H bridged intermediate increases with the electrophilicity of the involved cation.

In the gas phase, primary, secondary and tertiary carbocations form adducts with alkanes and these are thought to contain μ-H bonding structures. The extremely electrophilic methyl cation and methane form an adduct in a rather exothermic reaction (36 kcal/mol).[203] The more stabilized ethyl cation, isopropyl cation and *tert*-butyl cation show gradually decreasing exothermic reactions with their corresponding alkanes (see Table 35).

Table 35: Reaction enthalpies of primary, secondary and tertiary carbocations with hydrocarbons on forming μ-H bridged adducts.

Reaction	exp. $\Delta H°_R$ [kcal/mol]	calc. $\Delta H°_R$ [kcal/mol]
	-36	-37.7[a]
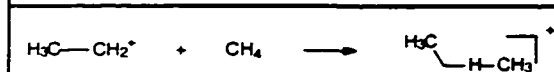	-6.6	
	-3.4	
		-13.06[a]
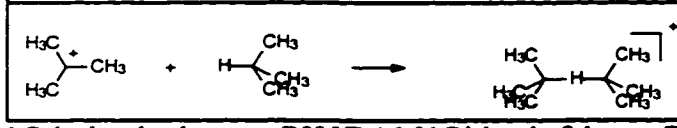		-6.98[b]

[a] Calculated values at a B3LYP / 6-31G* level of theory. The ZPE and the thermal correction for the enthalpy were scaled by 0.98. [b] The reaction enthalpy was calculated from the absolute energies.

Low level calculations (molecular mechanics or semiempirical calculations) or *ab initio* calculation without electron correlation are known to underestimate the bond strength of the μ-bond, which is also associated with longer calculated C-H-C distances. In order to compare the influence of different calculation methods and different basis sets for these μ-H bridged carbocation calculations, three of the reactions shown in Table 35 were calculated at the B3LYP / 6-31G*, B3LYP / 6-311+G**, MP2(Full) / 6-31G* and MP2(Full) / 6-311+G** levels of theory (see Table 36).

Table 36: Reaction enthalpies for selected alkyl cation-alkane adducts.

	Reaction		B3LYP / 6-31G*	B3LYP / 6-311+G**	MP2(Full) / 6-31G*	MP2(Full) / 6-311+G**
1	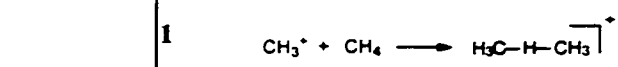	$H°_{298}$[a]	-37.70	-38.39	-34.66	-38.58
		ΔE[b]	-40.41	-41.20	-37.56	-41.46
2	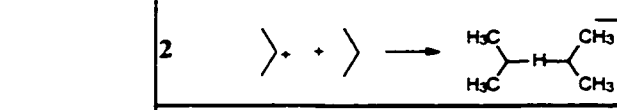	$H°_{298}$[a]	-13.02	-11.05	-14.16	-16.69
		ΔE[b]	-13.44	-12.13	-15.63	-18.43
3	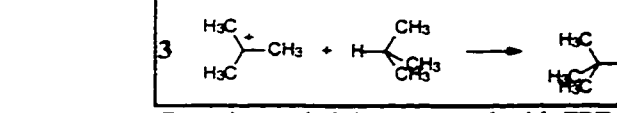					
		ΔE[b]	-6.98	-5.36	-13.39	-16.82

[a]Reaction enthalpies corrected with ZPE and thermal correction from 0K to 298 K. For the ZPE and the thermal correction enthaly, a scale factor of 0.98 [188] was used for B3LYP calculations and 0.93 [188] for MP2(Full) calculations. [b]Reaction energies without ZPE corrections.

All the molecules involved in the three alkyl cation - alkane reactions were optimized at the indicated calculation level and analytical frequencies were then obtained on the optimized geometries except for reaction 3 in Table 36 for which only geometry optimizations were performed (analytical frequencies at these levels, using large basis sets such as 6-311+G** require massive computer resources, which were not available)

The smallest differences between the various computation levels was found for the reaction of the primary methyl cation with methane. Consideration of the ZPE as well as the thermal energy correction for the enthalpy, decreased the reaction enthalpy *ca.* 2.8 kcal/mol at all four levels. The use of larger basis sets for a specific method (B3LYP, MP2(Full)) resulted in a larger reaction enthalpy, which can be attributed to a greater stability of the μ-H bridged reaction product. This effect was considerably larger for the MP2(Full) level than for the B3LYP level. Nevertheless, rather good agreement with the experimental value was achieved in the case of reaction 1 in Table 36.

Considering the reaction of the secondary cation (reaction 2 in Table 36) the differences between the B3LYP and the MP2(Full) calculations were considerably larger than for the primary reaction 1. A possible explanation for these findings would be the need for a more sophisticated electron correlation method to properly calculate the μ-H bond which results from the interaction of a more stabilized cation and a C-H bond, compared to the extremely

electrophilic methyl cation interaction with a C-H bond. This effect is even larger for the tertiary case involving the highly stabilized *tert*-butyl cation.

Comparing the geometries of a particular μ-H bridged species as a function of the calculation method, the distance between the terminal carbons of the μ-H bond was consistently calculated to be smaller with the MP2(Full) method compared to the B3LYP method. Similarly, the use of the larger basis set, 6-311+G** compared to 6-31G*, also resulted in a smaller C-H-C distance; however, this effect was considerably smaller than that caused by the B3LYP *vs.* MP2(Full) method variation (see Table 37).

Table 37: Geometrical parameters for the μ-H bond in primary, secondary and tertiary μ-H cations.

Structure		B3LYP / 6-31G*	B3LYP / 6-311+G**	MP2(Full) / 6-31G*	MP2(Full) / 6-311+G**
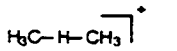 **267**	C-H-C dist. [Å]	2.071	2.028	1.953	1.923
	C-H-C angle [°]	113.1	109.5	105.7	102.7
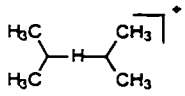 **271**	C-H-C dist. [Å]	2.554	2.543	2.468	2.402
	C-H-C angle [°]	170.8	169.3	164.5	151.1
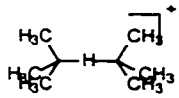 **272**	C-H-C dist. [Å]	2.603	2.597	2.521	2.504
	C-H-C angle [°]	180.0	178.4	180.0	180.0

In the primary and secondary μ-H bridged cations **267** and **271**, the C-H-C angle becomes smaller, as the C-H-C distance is reduced in the higher calculation levels, and this can be attributed to a more effective interaction between the two terminal carbons of the μ-H bond. A stronger interaction between the two terminal carbons on forming a bent C-H-C structure also involves increasing steric interactions of the substituents on these carbons, which is significant smaller in the cation **267** than in **271** or **272** (see Figure 88).

Figure 88: Increased overlap of the terminal carbons of the μ-H bond and a decreasing C-H-C angle.

Summarizing the results of these calculations, it becomes clear that MP2(Full) methods generally predict a stronger μ-H bond for a particular system than the corresponding B3LYP method. A similar trend also exists for the use of larger basis sets, however this effect is significantly smaller than for the change of the calculation method.

For most of the calculations conducted in this thesis work the B3LYP / 6-31G* level of theory was used, since the use of a larger basis set, or more importantly the use of MP2(Full) methods, would require a much larger amount of computer resources. Knowing what kind of change in energy and geometry is brought about by the use of these higher methods then allows one to make better decisions about which system should be treated with the better procedures.

The calculations shown in Table 35 predict that virtually all alkyl cation-alkene interactions should lead to stable μ-H bridged cations. However, solvent effects play a significant role in stabilizing carbocations and one would expect that the formation of a μ-H cation would be less favorable in solution than in the gas phase, due to stronger stabilization of the carbocation compared to the μ-H bridged structure. Brownstein, and Olah, showed that the hydride transfer reaction between *tert*-butyl cation and butane has an energy barrier of 4.3 ± 0.6 kcal/mol and does not form any observable adduct containing a μ-H bond.[204] Similarly, the interaction of the secondary solution-phase isopropyl cation and propane involves a very rapid hydride shift, but there is no evidence for any observable μ-H bridged adduct. More electrophilic cations such as primary carbocations are not observable in the condensed phase and the adduct reactions with alkanes remain reserved for the gas phase.

Internal hydride transfers in secondary and tertiary carbocations show a large dependance

on the geometrical features of the system under consideration. If one fixes the distance between the two carbons involved in the exchange, then one can evaluate two factors: 1. at what C-C distances are μ-H structures formed and 2. for what distances does the H-transfer (hydride shift) involve a transition state process, and how does the size of the transition-state barrier depend on the C-C distance?

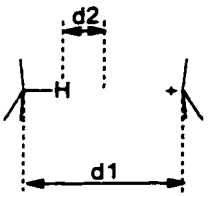

Figure 89: Theoretical model consisting of a *tert*-butyl cation and *tert*-butane where d1 is fixed at set values, and d2 is then varied.

An illustrative example is the model shown in Figure 89, which consists of a tertiary carbocation and an isobutane unit, where the C-C tertiary centers are artificially fixed at the set distances (d1 = 2.60 to 3.3 Å) and where the tertiary hydrogen is gradually moved from one *tert*-butyl system to the other (d2).

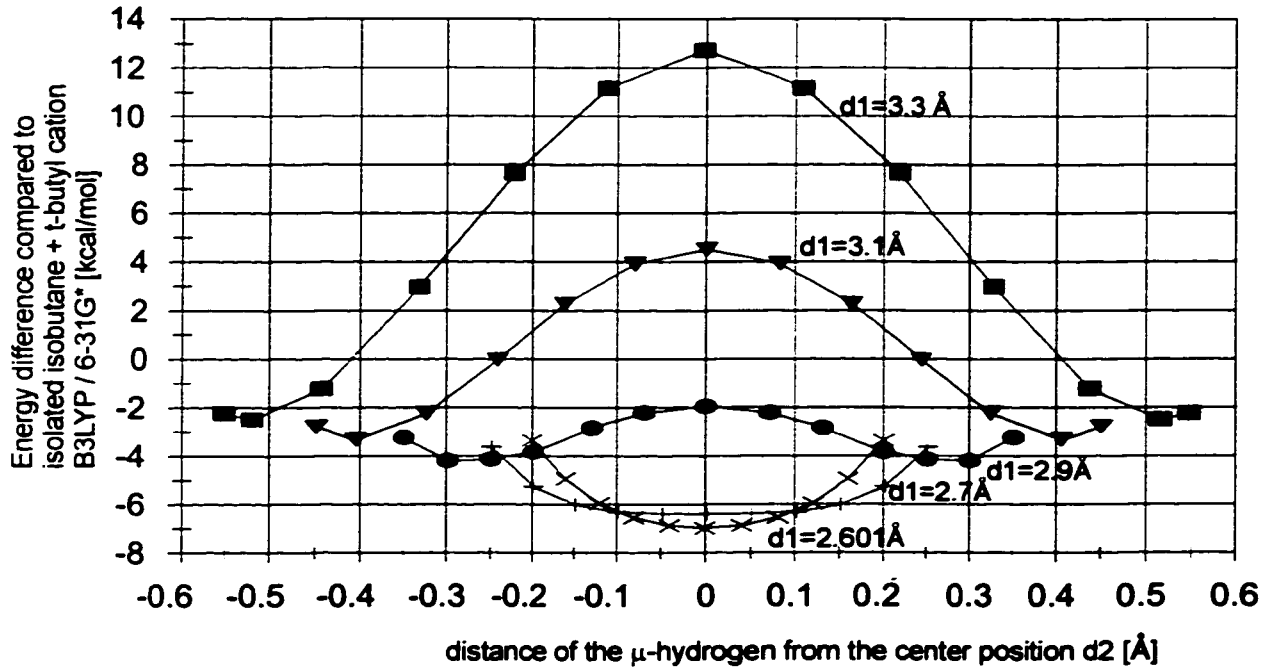

Figure 90: Energy changes according to B3LYP / 6-31G* calculations for the hydride transfer reaction between two *tert*-butyl species as a function of the separation of the tertiary centers.

The energy changes involved in these hydride shifts are illustrated in Figure 90. The reference energy of this system is the sum of the energies of *tert*-butyl cation and isobutane calculated as separate molecules at B3LYP / 6-31G*. As the two molecules approach in a face to face fashion (Figure 89) the corresponding ground states show a gradual increase of the tertiary C-H bond length, which is 1.101 Å in isobutane, 1.132 Å with a d1 = 3.3 Å, 1.145 Å with a d1 = 3.1 Å and 1.179 Å with a d1 = 2.9 Å. In addition to that, the energy barrier gradually decreases from 15.2 kcal/mol (d1 = 3.3 Å) to 7.8 kcal/mol (d1 = 3.1 Å) to 2.2 kcal/mol (d1=2.9 Å). With even smaller separations, d1 = 2.7 Å or 2.6 Å, no energy barrier in the hydride shift process is involved, but an intermediate is formed. The calculated ground state (B3LYP / 6-31G*) of this adduct without any geometrical restriction is found to be a symmetrical μ-hydrido bridged species with a terminal carbon separation of the μ-bond of 2.6025 Å, and an angle at the μ-H of 180°. The two *tert*-butyl units are in a slightly skewed arrangement with respect to each other (torsion angle = 64.7°) (see Figure 91 and Table 37).

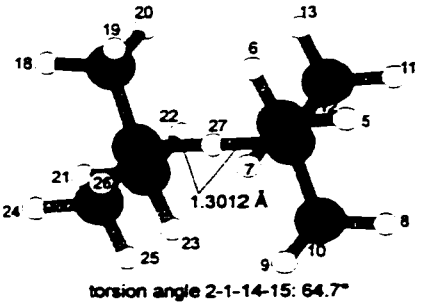

Figure 91: Adduct of isobutane and *tert*-butyl cation.

3.5 pK_a Estimation of μ-H Bridged Carbocations

As discussed in the Introduction (see Section 1.4.1, page 11), the pK_a of a carbocation is one measure of stability, since this quantity relates to the strength of the acid-solvent needed to prepare the cation. As indicated previously, the μ-H cations **30** and **33**, the targets of this thesis work, were expected to be very weakly acidic, probably stable in aqueous solution at pH = 7. In this section the calculations used to arrive at an approximate pK_a value for **30** and **33** are described.

The experimental measurement of a carbocation pK_a is almost impossible, because at the point where pH (or H_o) = pK_a, the equal concentration of alkene and cation react rapidly with each other.

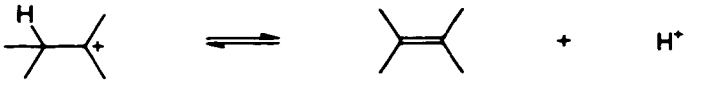

It is quite easy however to calculate accurate gas-phase energies for the cations and alkenes. If one makes some estimates for the pK_a's of some known systems, then a working relationship between experimental pK_a and alkene-carbocation energy differences can be set up.

Ranging from the cyclooctyl to cycloundecyl structures, secondary μ-H bridged-carbocations are thermally very unstable. One needs typical superacid conditions to prepare these so their pK_a values are not very different from *tert*-butyl cation (see also Section 1.8, page 54). Tertiary monocyclic μ-H cations are also not very thermally stable, and in addition

require superacid conditions for their preparation. They are expected to be a little less acidic than *tert*-butyl because of the extra bond energy of the μ-H bridge.

More promising are the known series of bicyclic and tricyclic systems (see Section 1.4.1, page 11). The weakest cation acids among this group can be prepared in CF_3COOH solvent and are estimated to have pK_a values in the -1 to +5 range. A minimum value of -13 was used for *tert*-butyl cation, since this species is not stable in 100 % sulfuric acid (H_o = -11.9). Some 1,2-dimethyl-2-norbornyl cations are stable in 100 % sulfuric acid, so these are assigned the very rough estimate of -7, on the assumption that the $\frac{[\text{alkene}]}{[\text{cation}]}$ ratio for stability should be at least 10^{-4} or 4 units on the log scale. Figure 92 shows the relationship between these pK_a estimates and the calculated energy difference between alkene and carbocation. Extrapolating the data to cations **30** and **33** produces estimated pK_a values of +18 and +17. Even the tricyclo[6.3.1.$1^{3,10}$]tridecyl μ-H bridged cation has an estimated pK_a of +12.

The isomeric *out*- and μ-H bridged bicyclo[3.3.3]undecyl cations make an interesting comparison. From calculations, these two cations are almost equal in energy, but in a pKa sense one would expect the *out*-cation to have a value close to *tert*-butyl cation (-13), while the μ-H cation estimate is +18.

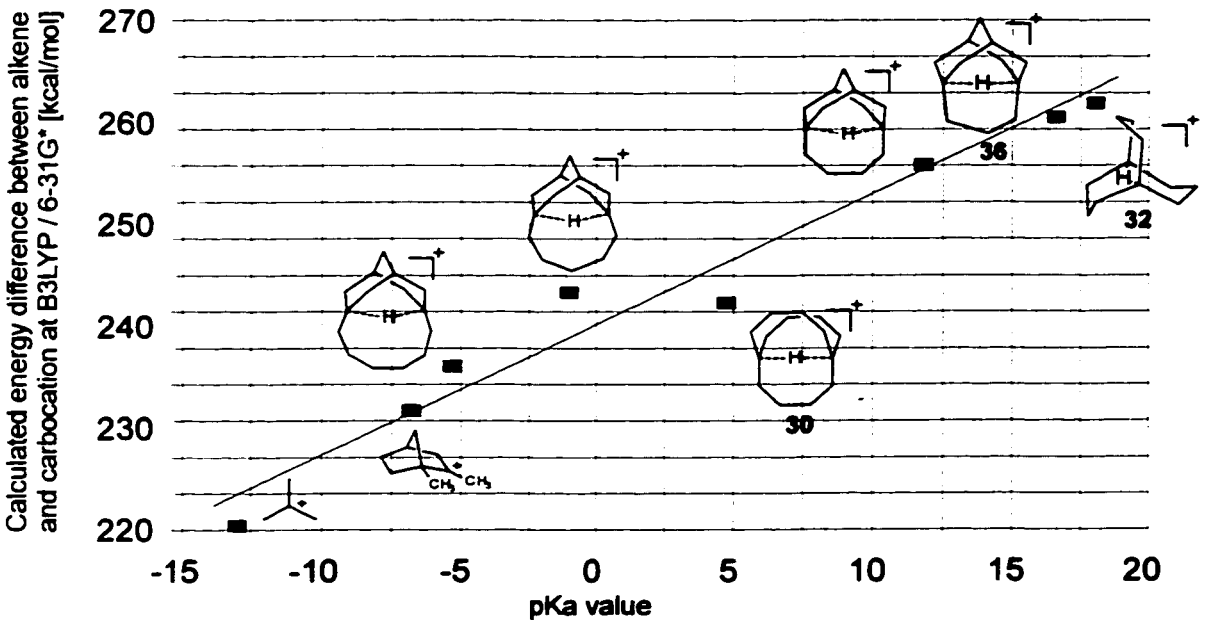

Figure 92: pKa estimation of the two target molecules **30** and **33** using various "known"pKa values for constructing a working curve.

All of the calculation data for Figure 92 are given in Table 38.

Table 38: B3LYP 6-31G* energies and pK_a values.

Structure	E at B3LYP 6-31G* [hartrees]	ZPE [hartrees]	$H°_0 - H°_{298}$ [kcal/mol]	$S°_{298}$ [cal/mol K]	$G°_{298}$ [hartrees]	pK_a ΔG^a
30	-430.3284435	176.55	6.45	91.67	-430.08532595	18.0 (calc.) 258.64
41	-429.9047970	169.19	6.49	91.76	-429.67315692	
33	-468.435649632	181.16	6.21	90.07	-468.18496735	16.6 (calc.) 256.68
43	-468.01556014	174.10	6.24	90.21	-467.77592436	
273	-507.767800562	199.07	6.97	95.77	-507.49061082	11.8 (calc.) 250.12
53	-507.359036873	192.82	7.12	97.11	-507.09201241	

Structure	E at B3LYP 6-31G* [hartrees]	ZPE [hartrees]	$H°_0 - H°_{298}$ [kcal/mol]	$S°_{298}$ [cal/mol K]	$G°_{298}$ [hartrees]	pK_a ΔG^a
 **28**	-548.28680110	230.47	8.60	106.48	-547.96302962	+4.75 (exp) 231.25
 **51**	-547.907998661	224.22	8.75	108.15	-547.69451733	
 **67**	-547.088676565	216.79	7.75	101.20	-546.7851137	-1 (exp) 232.69
 **53**	-546.708796227	211.00	7.75	101.24	-546.41430606	
 **274**	-586.396330884	235.11	8.77	109.01	-586.06621259	-5.3 (exp) 222.49
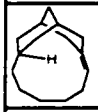 **275**	-586.032318473	229.02	8.60	108.32	-585.71165893	
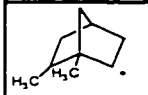 **276**	-351.719699851	138.06	6.22	90.06	-351.536305862	-6.8 (exp) 216.40
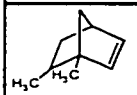 **277**	-351.365145459	131.36	5.82	87.08	-351.191444338	
	-157.554082113	73.65	4.47	76.25	-157.467588	-13 (exp) 200.73
	-157.227288051	68.09	3.92	70.58	-157.14769758	

[a]Calculated free energy difference between alkene and carbocation at B3LYP / 6-31G*.

Chapter IV

Summary, Overall Conclusions and Future Work

4.1 Summary

The preliminary analysis of the bicyclo[3.3.3]undecyl and tricyclo[5.3.1.$1^{3,9}$]dodecyl ring systems showed that the most promising approach for the preparation of the corresponding μ-H bridged carbocations would be the reduction of the bicyclo[3.3.3]undecyl or tricyclo[5.3.1.$1^{3,9}$]dodecyl bridgehead dications with a hydride (Section 2.1, page 58). This hydride delivery can in principle be made to occur in two different ways - internal or external hydride delivery.

Aspects on the external hydride delivery are described in Section 2.2.4, page 157. The preparation of the dication precursors **112** and **129** was accomplished in twelve and eight step procedures, respectively, mostly following known syntheses. However, most of the literature procedures were modified or changed to give a shorter and more efficient synthesis in both cases (Section 2.2.1, page 77).

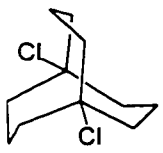

112

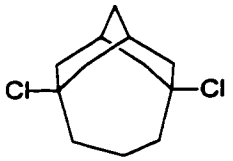

129

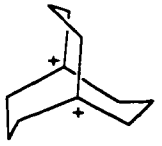

36

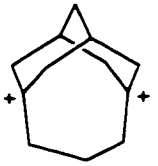

40

The dications **36** and **40** were then generated by reacting the 1,5-dichlorobicyclo[3.3.3]undecane **112** and the 5,9-dichlorotricyclo[5.3.1.$1^{3,9}$]dodecane **129** with SbF_5 at -116°C (the bicyclo[3.3.3]undecyl mono and dications had already been reported by Olah [183]). In order to ensure complete ionization of the dications, the NMR spectra were compared to those of the bicyclo[3.3.3]undec-1-yl cation **78** and to tricyclo[5.3.1.$1^{3,9}$]dodec-5-yl cation **34**. In addition to that, the ^{13}C NMR chemical shifts of the mono and dications were also compared to theoretically calculated (B3LYP / 6-31G*) NMR shifts, which showed excellent agreement with most of the experimentally obtained values. The C^+ peaks showed the biggest differences, which can be attributed to solvent effects. The NMR spectra of the

bicyclo[3.3.3]undecyl system showed NMR line-broadening and the conformational change causing this was attributed to a ring flipping process. The associated energy barrier for the bicyclic alkane **59** was measured as 11.0 ± 0.2 kcal/mol, the monocation **78** as 10.5 ± 0.3 kcal/mol and the dication **36** as 9.4 ± 0.5 kcal/mol. The tricyclic system was also found to undergo this ring flipping process, and the associated energy barrier was measured as 13.1 ± 0.1 kcal/mol for the hydrocarbon **61**. Measuring the corresponding energy barriers in the tricyclic mono or dication was not possible with NMR spectroscopy, since complete rearrangement or decomposition, respectively, was noted, before any dynamic NMR behavior could be observed (Section 2.2.3, page 104).

The stabilization of these cations was shown to be a result of angle strain relief and effective C-H and C-C hyperconjugation, the latter being most important in the tricyclic system, leading to exceptionally low field NMR chemical shifts for the β carbons. The combination of these stabilization factors was found to be the reason that it was possible to even generate the dications **40** and **36**, given the exceptionally close proximity of the cation centers. Both system show a lower field NMR chemical shift for the cationic carbon(s) in the monocations than in the dications, which was rationalized on the basis of a more localized charge in the monocation.

The preparation of these cations led to the discovery of the rearrangement reactions **(34)** to **(36)**

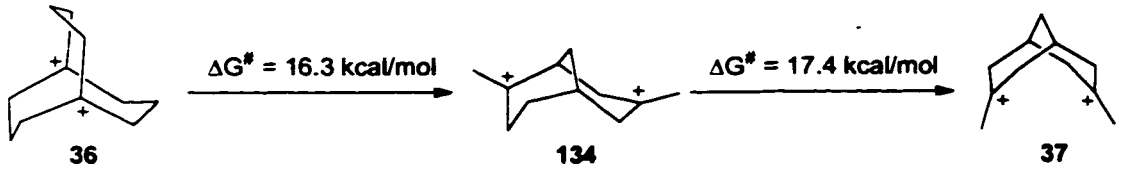

(34)

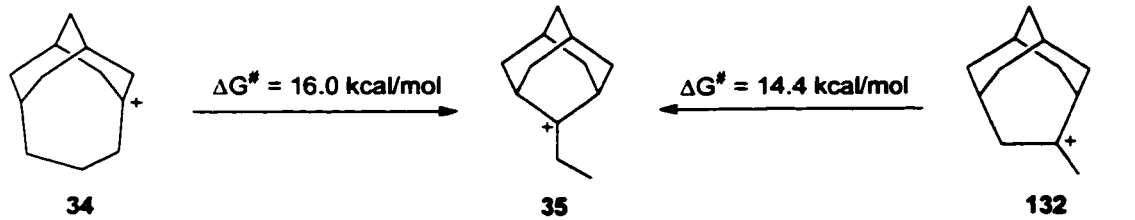

(35)

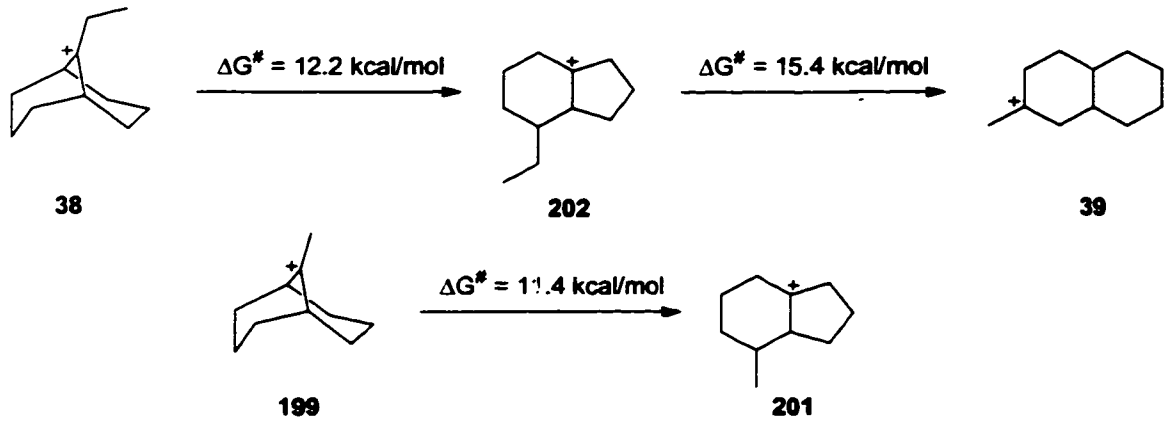

The bicyclo[3.3.3]undeca-1,5-diyl dication was found to rearrange into the 3,7-dimethylbicyclo[3.3.1]nona-3,7-diyl dication **37** via the observable 2,7-dimethyl-bicyclo[3.3.1]nona-2,7-diyl dication **134**, and the associated energy barriers were measured as 16.3 ± 0.4 kcal/mol and 17.4 ± 0.4 kcal/mol (see reaction **(34)**). The two rearrangement products were also investigated by *ab initio* calculations, and the theoretical results agreed with the experimental ones in terms of energy and NMR chemical shift predictions. A plausible mechanism for the overall rearrangement was proposed and *ab initio* calculations were used to estimate the energy of all intermediates involved (Section 2.2.3.1, page 110).

The second rearrangement reaction involved a twofold ring contraction of the tricyclic monocation **34**. The "intermediate" **132** could not be directly observed in the rearrangement reaction of the cation **34** into **35**, which involved an energy barrier of 16.0 ± 0.7 kcal/mol. However, this homoadamantyl cation **132** , prepared by a separate route, rearranged into **35** upon warming the cation solution to -73°C, corresponding to an energy barrier of 14.4 ± 0.3 kcal/mol (see Equation **(35)**). A plausible mechanism was investigated in detail with *ab initio* calculations and two transition states leading to the products observed were found at a B3LYP / 6-31G* level of theory, yielding values of 23.5 kcal/mol and 15.3 kcal/mol, respectively. Single point calculations of these B3LYP / 6-31G* optimized structures at MP2(fc) / 6-311++G** resulted in somewhat different values of 14.8 and 12.3 kcal/mol, which were in reasonably good agreement with the experimental values (Section 2.2.3.2, page 129).

The third rearrangement involved the 9-ethylbicyclo[3.3.1]non-9-yl cation, which was

found to also undergo a multi-step reaction to form the 2-methyl-2-decalyl cation **39** via the observable intermediate **202**. The latter structure is related to a rearrangement product derived from 9-methylbicyclo[3.3.1]non-9-yl cation and first observed by Sorensen and Kirchen, however the structure of this rearrangement product was not known before this work was conducted. Using 2D-NMR techniques (C-H HETCOR, COSY) as well as *ab initio* calculations at the B3LYP / 6-31G* and the MP2(Full) / 6-31G* levels of theory, the two products in question were identified with high certainty as the 5-ethylbicyclo[4.3.0]non-1-yl cation and the 5-methylbicyclo[4.3.0]non-1-yl cation. In the ethyl substituted case, energy barriers of 12.2 ± 0.6 and 15.4 ± 0.6 kcal/mol were measured, and in the methyl case a barrier of 11.4 ± 0.6 kcal/mol was found (see Equation 36). A plausible mechanism for these rearrangements was proposed, which was also investigated using *ab initio* calculations, and the relative energies of all proposed intermediates were evaluated (Section 2.2.3.3, page 142).

The tricyclic and the bicyclic systems show distinctly different behavior in these rearrangement reactions, which was explained by different relative energies for the intermediates involved. The lack of a defined rearrangement reaction in the tricyclic dication **40** was attributed to a smaller flexibility of the carbon frame, which inhibits the necessary Wagner Meerwein shifts.

Ionic hydrogenation of the dications **36** and **40** was conducted using the hydride donors isopentane, sodium borohydride and hydrogen gas. However, in all cases only the corresponding classical monocations were formed and no μ-hydrido bridged species could be observed. In the case of the tricyclic system, the ionic hydrogenation of the dication **40** with isopentane was the "cleanest" way to generate the monocation **34**, without any of its rearrangement products (Section 2.2.4, page 157).

Attempts at the synthesis of appropriate precursors for the internal hydride delivery route are described in Section 2.3, page 164. The first precursor target molecule was the 3-methoxybicyclo[3.3.3]undecane-1,5-diol. After a fourteen step synthesis, the last step was ultimately unsuccessful and a different target molecule had to be found. The second attempt involved the precursor 7-isobutyltricyclo[5.3.1.$1^{3,9}$]dodeca-5,9-diol **260**. The synthesis was completed up to the advanced stage of tricyclo[5.3.1.$1^{3,9}$]dodecan-5-ol **257**. However, the

synthesis was stopped due to results of more detailed *ab initio* calculation at the B3LYP / 6-31G* level, which were performed simultaneously. These results predicted that possible transition states for the internal hydride delivery reaction would have activation energies between 49.6 and 75.5 kcal/mol.

Chapter III describes theoretical aspects of the μ-hydrido bond. The unusually high field NMR chemical shift of the μ-hydrogen was investigated with *ab initio* calculations at the B3LYP / 6-31G* and the MP2(Full) / 6-31G* levels of theory. Using these, the potential energy surface of the μ-hydrogen was examined and the chemical shift change brought about by varying the relative location of the μ-H was evaluated, focusing on the bicyclo[3.3.3]undecyl, tricyclo[5.3.1.1.^{3,9}]dodecyl and bicyclo[4.4.4]tetradecyl μ-H bridged carbocations. The results of these calculations show that a very flat energy potential exists in all three cations if the μ-hydrogen experiences a displacement of less than *ca.* 0.2 to 0.3 Å. A possible large vibrational motion of the μ-H hydrogen would cause a chemical shift change of no more than ca. 0.5 ppm. Using B3LYP / 6-31G* calculations, the chemical shift of the μ-hydrogen was calculated as -12.02 ppm for the bicyclo[3.3.3]undecyl μ-H cation **30**, -9.47 ppm for the tricyclo[5.3.1.1^{3,9}]dodecyl μ-H cation **33** and -2.94 ppm for the bicyclo[4.4.4]tetradecyl μ-H cation **28** (exp. -3.46 ppm). Because of the large dependence of the chemical shift of the μ-H on the distance between the terminal carbons of the μ-H bond (C-H-C separation) this distance could be calibrated with the calculated NMR chemical shifts, and a value of 2.493 Å was obtained for the bicyclo[4.4.4]tetradecyl μ-H bridged carbocation **28**.

The absence of an unusually high field chemical shift for the μ-H in the bridged 2-butyl cation was rationalized by *ab initio* calculations, showing that a smaller electron density is located near the hydrogen in question, compared to that in a typical linear μ-H bond. A calculated NMR chemical shift of +4.8 ppm was derived for the averaged peak of the three -CH_2-$^+$CH- hydrogens, somewhat higher field than the experimental value of +6.8 ppm.

Calculations were also used to demonstrate the greater tendency of a carbocation with a large electron demand to form μ-H bridged structures compared to more stabilized cation species. Furthermore, using primary, secondary and tertiary examples of a carbocation-alkane adduct possessing a μ-H bond, the results of *ab initio* calculations at four different theoretical

levels were compared, which revealed that MP2 calculations seem to slightly overestimate and B3LYP calculations slightly underestimate the strength of the μ-H bond.

The critical parameter of the terminal carbon separation in a μ-H carbocation was explored using an adduct of the *tert*-butyl cation and isobutane. The results show that a symmetrically bridged μ-H cation is an intermediate if the C-H-C separation is less than *ca.* 2.8 Å.

Finally, the pK_a stability of the two target molecules **30** and **33** was estimated by calculating the free energy difference between the μ-H cation and the corresponding alkene, and then placing these cations on a pK_a *vs.* calculated profile for a series of "known" pK_a values involving other cations. The pK_a value of bicyclo[3.3.3]undecyl μ-H bridged cation was predicted to be + 18, and the value for tricyclo[$5.3.1.1^{3,9}$]dodecyl μ-H bridged cation, +17.

4.2 Overall Conclusion - Future Work

Various attempts to prepare the target molecules **30** and **33** by introducing a hydride into the cavity of a bicyclic or tricyclic dication using external hydride donors were unsuccessful, and *ab initio* calculations show that internal hydride delivery involves transition states with very high energy barriers; hence, this type of approach, introduction of the "*in*-" hydrogen after the carbon framework of the molecule has been assembled, has little hope for success.

Considering the analysis of possible approaches discussed earlier for the preparation of μ-H cations (Section 2.1, page 58), most of these require a starting material which has an *in*-hydrogen in place. The direct preparation of these starting materials is not very feasible due to the very high strain energies involved. The protonation of a C-C single bond has also been shown in this thesis to be almost impossible to achieve.

The remaining possible method to introduce the "*in*-" hydrogen is to synthesize a relatively large carbocyclic framework, possessing an *in*-hydrogen and to then ring contract this system to form the smaller homologs. One possible example is outlined in Scheme 15.

15 Possible approach to a tricyclo[5.3.1.1^{3,9}]dodecyl μ-H bridged carbocation.

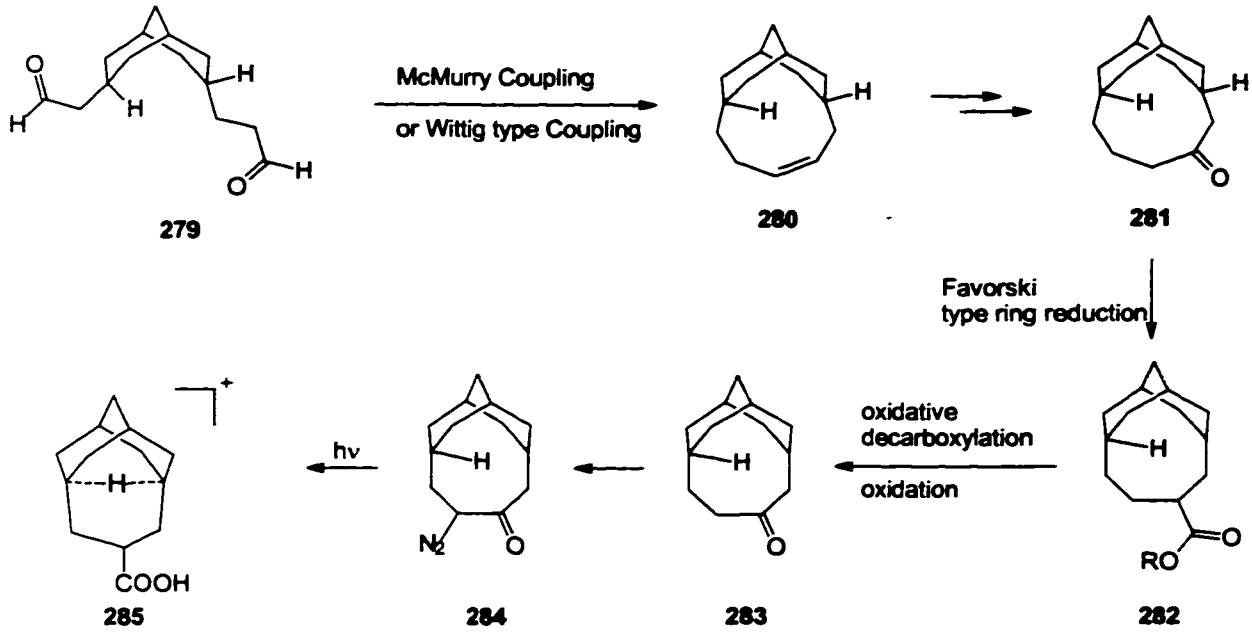

Despite the potential difficulties involved in preparing these strained carbocyclic systems, this type of approach (involving ring contractions) appears at this stage to be the most promising route to small μ-hydrido bridged carbocations.

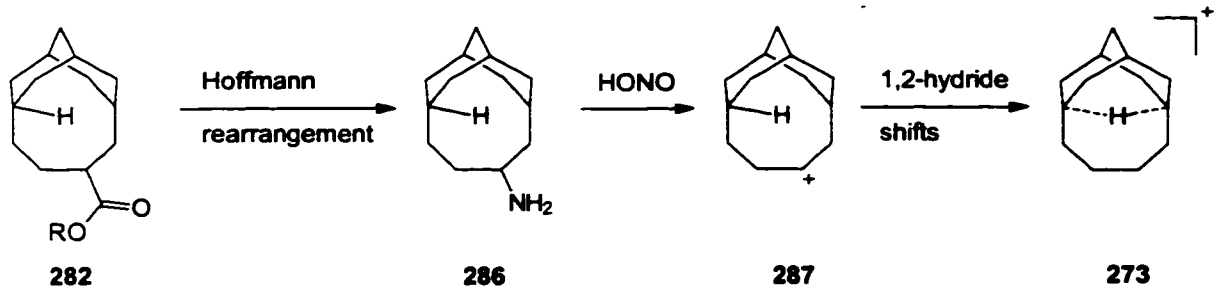

The preparation of cation **273** would involve a less strained structure intermediate between known μ-H bridged cations and the very strained systems discussed in this thesis.

Chapter V

Experimental Section

5.1 General Information

NMR spectra were recorded on either a Bruker ACE 200 (^{1}H 200 MHz), AMX 300 (^{1}H 300 MHz), AM 400 (^{1}H 400 MHz) or DRX 400 Avance (^{1}H 400 MHz) spectrometer. Proton chemical shifts were referenced to the residual $CHCl_3$ (δ 7.27 ppm) in $CDCl_3$, $CHDCl_2$ (δ 5.32 ppm) in CD_2Cl_2, HDO (δ 4.80 ppm) in D_2O and CD_3OH (δ 4.78 ppm) in CD_3OD unless otherwise stated. The carbon signals of $CDCl_3$ (δ 77.00 ppm), CD_2Cl_2 (δ 54.00 ppm) and CD_3OD (49.30 ppm) were used to reference the carbon chemical shifts. Unlocked samples were referenced using the spectrometer SR value, measured with locked samples under identical conditions. The coupling constants were measured with an accuracy of ± 0.5 Hz. Variable temperature NMR (VT NMR) experiments were calibrated using 100 % methanol.[205] The assignment of carbons types (Cq), (CH), (CH_2), or (CH_3) was determined using DEPT 135 and DEPT 90 experiments.

X-ray crystallographic data were measured and solved by Dr. M. Parvez.

GC-MS data were obtained on an HP 5890 Series II GC / HP 5974 mass selective detector MS spectrometer. High and low resolution MS spectra were measured on a Kratos MS80 or a Micromass VG7070 spectrometer by Dr. Q. Wu and Ms. D. Fox. IR data were collected on Mattson 4030 spectrometer and mp. obtained from a Gallenkamp Melting Point Apparatus MF 370.

GC spectra were recorded on a HP 5890 GC, using a wide bore 3% OV-1 1mm x 15m column and an FID detector. Purification of volatile analytical samples was performed on a HP 5890 GC using a 3 % OV-1 4mm x 8' column and TCD detector. Merck 0.2mm silica gel 60 F254 on aluminum plates were used for analytical TLC analysis. The visualization of the corresponding spots was accomplished by spraying the plates with a solution of potassium permanganate and sodium carbonate (10 g $KMnO_4$ and 20 g Na_2CO_3 in 250 mL water). Column chromatography was conducted using a 30 to 50 fold mass ratio of silica gel 60 (20 -

63 μm from Merck, cat. nr. 9385-9) to the compound being purified. The solvent mixture and other details are given in the individual experimental description.

All of the chemicals used were purchased from either Aldrich, Sigma, Fisher-Scientific or BDH and were used without additional purification unless stated otherwise. Antimony pentafluoride was purified by heating the commercial product with silicon dioxide in a thick wall Schlenk flask to 120°C for 20 hours (Caution, the developing pressure from the reaction $4\ HF + SiO_2 = SiF_4 + 2\ H_2O$ has to be considered) and triply distilling the resulting mixture in high vacuum at room temperature. Fluorosulfonic acid was double distilled in high vacuum at approx. 50°C. The sulfuryl chloridefluoride was prepared by a fluoride exchange of sulfuryl chloride [206] and purified by double distilling over antimony pentafluoride. THF and ether were dried with sodium using benzophenone ketyl as indicator. Dichloromethane was distilled over phosphorus pentoxide under a stream of nitrogen. DMF, DMSO and diisopropylamine were dried with 4 Å molecular sieves. Dried hexanes, distilled from lithium aluminum hydride under a nitrogen atmosphere, were used for the formation of 4-trimethylsilyloxy-tricyclo[5.3.1.$1^{3,9}$]dodec-4-ene. In all other cases, hexanes were used as obtained from BDH.

The following known compounds are reported here because the published characterization data were unavailable or incomplete: N-cyclohex-1-enyl-morpholine **95**, 2-hydroxybicyclo[3.3.1]nonan-9-one **97**, 2-chlorobicyclo[3.3.1]nonan-9-one **99**, bicyclo[3.3.1]non-2-en-9-one **98**, bicyclo[3.3.1]nonan-9-one **100**, vicyclo[3.3.2]decan-9-one **101**, 9-aminomethylbicyclo[3.3.2]decan-9-ol **105**, bicyclo[3.3.3]undecan-2-one **106**, bicyclo[3.3.3]undecane **59**, bicyclo[3.3.3]undecan-1-ol **109**, bicyclo[3.3.3]undecane-1,5-diol **110**, 1,5-dichlorobicyclo[3.3.3]undecane **112**, 9-ethylbicyclo[3.3.1]nonan-9-ol **195**, 9-methylbicyclo[3.3.1]nonan-9-ol **197**, 9-methylenebicyclo[3.3.2]decane **102**, 1,3-Dichloroadamantane **164**, 3-methylenebicyclo[3.3.1]nonan-7-one **165**, 3-methylbicyclo[3.3.1]non-2-en-7-one **166**, 3,7-dimethylbicyclo[3.3.1]nona-2,6-diene **158**, 3,7-dimethylbicyclo[3.3.1]nona-2,7-diene **167**, bicyclo[3.3.3]undec-1-yl cation **78**, bicyclo[3.3.3]undeca-1,5-diyl dication **36**, 9-methylbicyclo[3.3.1]non-9-yl cation **199**, 1-dichloromethyladamantane **114**, tricyclo[4.3.1.$1^{3,8}$]undec-6-one **115**, 6-(aminomethyl)tricyclo[4.3.1.$1^{3,8}$]undecan-6-ol **117**, tricyclo[5.3.1.$1^{3,9}$]dodecan-6-one **118**,

tricyclo[5.3.1.1^{3,9}]dodecane **61** and 2-ethyl-2-adamantanol **180**.

The reported yields correspond to isolated yields for products of high purity (stated as pure compound). In some cases, the isolation of the pure product was difficult, and the yield was calculated from the amount of the product and a purity estimation via ^{1}H NMR or GC.

5.2 General Procedures for Carbocation generation

A special apparatus, illustrated in Figure 95, was designed for the generation of the carbocations in NMR tubes.

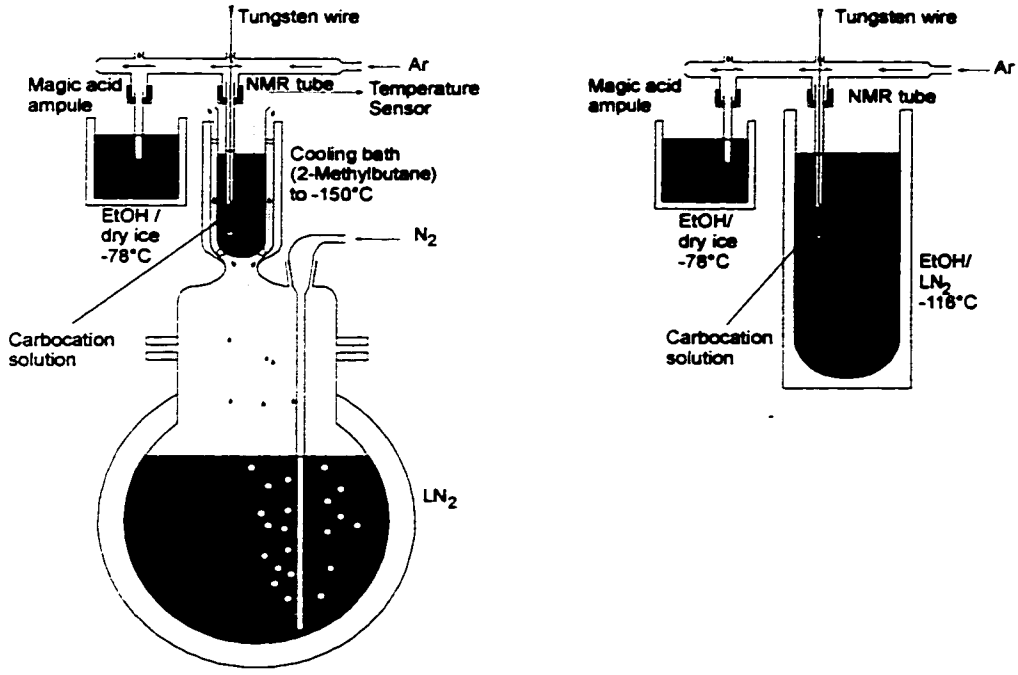

Figure 95: Apparatus for the generation of carbocations a) with a cold stream of nitrogen and 2-methylbutane (left) as cooling bath or b) with a slush of frozen ethanol as cooling bath.

Depending on the thermal stability of the carbocation, either a slush of liquid nitrogen (LN_2) and ethanol (-116°C), or a stream of cold nitrogen to cool 2-methylbutane (down to -150°C), was used to cool the NMR tube in which the cation was generated. The open ends on top of the argon stream line allowed physical access to the magic acid solutions and to the subsequent carbocation precursor solutions (mixing of solutions was carried out by stirring with a tungsten wire), while a constant flow of argon prevented the samples from being contaminated with

moisture. The advantage of this technique was that one could handle moisture and temperature sensitive reaction solutions requiring physical stirring and that the corresponding reactions could be carried out within a relatively short time period.

Different starting materials required slightly different methods for the generation of the corresponding carbocations, and these are described in the detailed descriptions.

5.3 3-Methoxybicyclo[3.3.3]undecyl system

5.3.1 4-Methoxycyclohexanol (217)

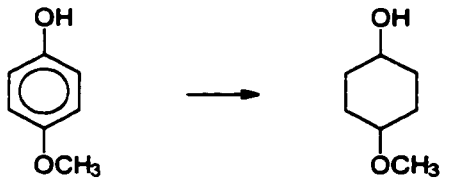

217

4-Methoxyphenol (36.4 g, 0.293 mol), 10 % palladium on activated charcoal (2 g) and water (600 mL) were hydrogenated at 135°C and 35 bar (500 psi) for 27 h. The resulting reaction mixture was continuously extracted with dichloromethane for 2 days and the organic layer was filtered, dried with magnesium sulfate, filtered again and concentrated on the rotavapor to yield 49.7g of crude material. Vacuum distillation at 19 mmHg and 105°C to 108°C yielded 34.76 g (yield: 91 %) of the pure (mixture of cis and trans from ^{1}H NMR) 4-methoxy-cyclohexanol **217**. Spectral data were in accordance with the literature.[207]

GC-MS m/z (rel. intensity): 41 (13), 58 (23), 72 (100), 81 (8), 98 (7, M^+ - MeOH), 112 (24, M^+ - H_2O), 130 (2, M^+). ^{1}H NMR (200 MHz, $CDCl_3$) δ (ppm): mixture of cis and trans; total of 28 protons (OH not visible), 3.72 (p, J = 5.4 Hz, 2H), 3.33 (s, 3H), 3.31 (s, 3H), 3.28 (tt, J_1 = 5.7, J_2 = 2.8 Hz, 1H), 3.17 (p, J = 4.6 Hz, 1H), 1.99 (m, 3H), 1.83 (m, 3H), 1.63 (m, 8H), 1.31(m, 2H). ^{13}C NMR (50 MHz, $CDCl_3$) δ (ppm): 78.0 (CH), 75.6 (CH), 69.2 (CH), 67.9 (CH), 55.6 (CH_3), 55.2 (CH_3), 32.4 (CH_2), 30.2 (CH_2), 28.8 (CH_2), 26.9 (CH_2).

5.3.2 4-Methoxycyclohexanone (218)

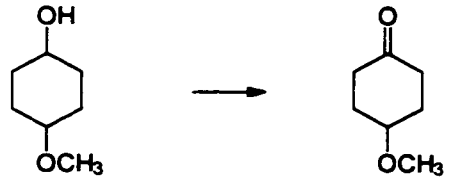

217 **218**

4-Methoxycyclohexanol **217** (134 g, 1.03 mol) was dissolved in acetone (400 mL) and cooled to 10 - 15°C before Jones reagent (103 g CrO_3, 87 mL H_2SO_4, 300 mL water) was added dropwise until the yellowish color persisted for 5 *min.* (280 mL of the Jones reagent was required). The excess of Cr(VI) was destroyed by adding a few drops of 2-propanol. The clear colorless top layer of the reaction mixture was separated and the remaining green slurry washed twice with acetone (50 mL). The combined acetone layers were stirred with sodium bicarbonate (20 g) for 5 h before they were filtered and concentrated on the rotavapor to yield 161.55g of the oily crude material. Vacuum distillation at 17 mmHg (86°C to 93°C) afforded 104.0 g (yield: 78 %) of the pure (from ^{1}H NMR) oily liquid 4-methoxycyclohexanone **218**. Spectral data agreed with literature values.[208]

GC-MS m/z (rel. intensity): 41 (45), 58 (46), 68 (59), 74 (100), 87 (12), 96 (13), 113 (14), 128 (74). ^{1}H NMR (200 MHz, $CDCl_3$) δ (ppm): 3.62 (tt, J_1 = 5.7 Hz, J_2 = 2.85 Hz, 1H), 3.42 (s, 3H), 2.65 - 2.48 (m, 2H), 2.33 - 1.84 (m, 6H). ^{13}C NMR (50 MHz, $CDCl_3$) δ (ppm): 210.8 (Cq), 74.2 (CH), 55.9 (CH_3), 36.9 (CH_2), 30.0 (CH_2).

5.3.3 N-(4-Methoxycyclohex-1-enyl)morpholine (219)

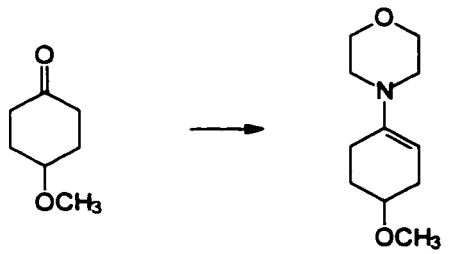

218 **219**

4-Methoxycyclohexanol **218** (29.0 g, 0.226 mol), morpholine (34.8 g, 0.404 mol) and p-

toluenesulfonic acid (0.3 g) were dissolved in 150 mL of toluene and refluxed with azeotropic removal of water for 13 h. The toluene of the resulting orange solution was removed on the rotavapor and the residual oily liquid distilled at 0.4 mmHg and 102 to 104°C to yield 46.6g (yield: quant.) of the pure (from ^{1}H NMR) 4-(4-methoxycyclohex-1-enyl)-morpholine **219**. The measured boiling point was in agreement with the literature value (Literature 99.5°C at 0.5 mmHg).[209]

GC-MS m/z (rel. intensity): 41 (15), 54 (16), 67 (10), 81 (19), 94 (31), 108 (100), 124 (31), 139 (58), 166 (20), 197 (36). ^{1}H NMR (200 MHz, $CDCl_3$) δ (ppm): 4.58 (t, J = 3.2 Hz, 1H), 3.79 (dd, J_1 = 4.6 Hz, J_2 = 3.2 Hz, 4H), 3.46 (m, 1H), 3.37 (s, 3H), 2.79 (ddd, J_1 = 4.6 Hz, J_2 = 3.2 Hz, J_3 = 1.2 Hz, 4H), 2.42 (dt, J_1 = 13.6 Hz, J_2 = 8.2 Hz, 1H), 2.31 - 1.88 (m, 4H), 1.72 (m, 1H).^{13}C NMR (50 MHz, $CDCl_3$) δ (ppm): 144.8 (Cq), 96.7 (CH), 75.4 (CH), 66.8 (2 x CH_2), 55.6 (CH_3), 48.3 (2 x CH_2), 30.2 (CH_2), 27.4 (CH_2), 24.6 (CH_2).

5.3.4 exo- and endo-2-Hydroxy-7-methoxybicyclo[3.3.1]nonan-9-one (exo-221) and (endo-221)

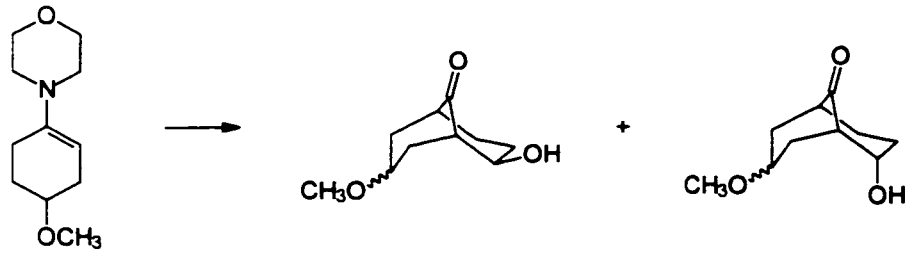

219 **exo-221** **endo-221**

N-(4-Methoxycyclohex-1-enyl)morpholine **219** (63.3 g, 0.321 mol) was dissolved in dry ether (400 mL) under an Ar atmosphere and cooled to 0°C. At this temperature, acrolein (16.2 g, 0.289 mol)[a] was added and the reaction mixture was stirred for 12 h. Within the first 3 h, the reaction solution was allowed to warm to room temperature. After completion of the

[a]The acrolein purchased from Aldrich, cat. no. 11,022-1, was distilled into a trap cooled to 0°C. Hydroquinone (100 ppm) was added in the trap prior the distillation.

stirring period, ion exchanger (400 mL) [a] and water (500 mL) were added and the resulting mixture stirred intensely for 1.5 h. The ether was then distilled off and the resulting aqueous mixture refluxed for 2.5 h. After the reaction suspension was cooled to room temperature, the solution was filtered and concentrated on the rotavapor to yield 39.1 g of a viscous pale yellowish oil consisting of an endo-exo alcohol mixture in a ratio of 1.43:1. This crude material was used for the subsequent steps without further purification. An analytical sample was prepared by flash chromatography (silica gel, hexanes-ether 1:1) for characterization purposes.

exo-2-Hydroxy-7-methoxybicyclo[3.3.1]nonan-9-one **(exo-221)**: GC-MS m/z (rel. intensity): 41 (79), 55 (100), 67 (40), 79 (56), 97 (34), 107 (18), 138 (23), 152 (15), 184 (6). High res. MS (IE): (M^+): calc. 184.109945 found 184.1098 (-0.6 ppm), $M^+ - CH_3OH$: calc. 152.083730 found 152.0835 (-1.3 ppm). IR neat (NaCl) cm^{-1}: 3428 s, 2930 s, 1724 s, 1452 m, 1094 s. ^1H NMR (200 MHz, $CDCl_3$) δ (ppm): 4.36 (s, br, 1H), 3.30 (s, 3H), 2.62 (s, br, 1H), 2.51 (m, br, 2H), 2.42 - 1.70 (m, 8H). ^{13}C NMR (50 MHz, $CDCl_3$) δ (ppm): 217.6 (Cq), 76.8 (CH), 72.7 (CH), 56.0 (CH_3), 52.2 (CH), 44.2 (CH), 37.7 (CH_2), 34.6 (CH_2), 29.9 (CH_2), 26.9 (CH_2).

endo-2-Hydroxy-7-methoxybicyclo[3.3.1]nonan-9-one **(endo-221)**: GC-MS m/z (rel. intensities): 41 (99), 55 (100), 67 (36), 79 (43), 95 (42), 108 (29). 134 (12), 152 (14), 166 (28), 184 (10). High res. MS (IE): M^+: calc. 184.109945 found 184.1091 (-4.4 ppm), $M^+ - H_2O$: calc. 166.099380 found 166.0994 (+0.0ppm), $M^+ - CH_3OH$: calc. 152.083730 found 152.0830 (-4.6 ppm). IR neat (NaCl) cm^{-1}: 3401 s, 2933 s, 1715 s, 1453 m, 1095 s, 1057 s. ^1H NMR (200 MHz, $CDCl_3$) δ (ppm): 4.00 - 3.76 (m, 2H), 3.28 (s, 3H), 3.03 (s, br, 1H), 2.71 - 2.60 (m, 1H), 2.53 (dt, J_1 = 13.5 Hz, J_2 = 3.0 Hz, 1H), 2.48 - 2.33 (m, 1H), 2.18 - 2.07 (m, 2H), 1.99 - 1.55 (m, 5H). ^{13}C NMR (50 MHz, $CDCl_3$) δ (ppm): 216.3 (Cq), 73.1 (CH), 72.7 (CH), 55.8 (CH_3), 52.3 (CH), 42.5 (CH), 37.0 (CH_2), 30.8 (CH_2), 28.0 (CH_2), 27.7 (CH_2).

---

[a]The cation exchanger Amberlite IR 120(plus), from Aldrich cat. nr. 21,653-4, was recycled from other reactions. The used ion exchanger was washed (methanol - HCl 1:1 to 2:1 solution), pure methanol and finally with deionized water until the washings were pH neutral.

5.3.5 exo- and endo-2-Mesyl-7-methoxybicyclo[3.3.1]nonan-9-one (exo-222) and (endo-222)

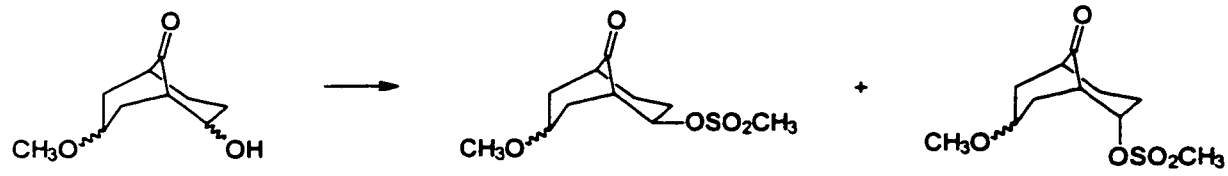

221 **exo-222** **endo-222**

A mixture of 2-hydroxy-7-methoxybicyclo[3.3.1]nonan-9-one **221** (37.1 g, 0.135 mol), triethylamine (60.7 g, 0.600 mol) and dichloromethane (500 mL) was cooled to 0°C and methanesulfonyl chloride (45.8 g, 0.400 mol) was added dropwise at a rate such that the temperature remained below 8°C. During the addition the initially clear, slightly yellow solution darkened to a brownish color and some triethylammonium chloride precipitated. After the addition, the reaction mixture was allowed to warm to room temperature and stirred for an additional 1.5 h. Water was then added until all the triethylammonium chloride had dissolved, then conc. hydrochloric acid was added to acidify the reaction mixture. The dichloromethane layer was separated and the aqueous layer extracted with dichloromethane (3 x 50 mL). The combined organic layers were filtered through a silica gel column (*ca.* 250 g silica gel), and then washed with ether (1.5 L). Concentration of the resulting yellowish solution yielded 45.2 g of a viscous yellow oil containing 71% (from ^{1}H NMR) of the desired product, as an endo : exo mixture in the ratio of 1.43 : 1 (yield: 61%). This mixture was used in the following step without further purification. An analytical sample was prepared (chromatography, silica gel, hexanes - ether 1:1) for the characterization of the pure isolated endo and exo isomers.

exo-2-Mesyl-7-methoxybicyclo[3.3.1]nonan-9-one **(exo-222)**: MS (EI) m/z (rel. intensity): 41 (53), 79 (73), 107 (67), 166 (100), 183 (2), 262 (15). High res. MS (IE): M^+: calc. 262.087499 found 262.0873 (-0.9 ppm), M^+ - $HOSO_2CH_3$: calc. 166.099380 found 166.0989 (-2.6 ppm). IR neat (NaCl) cm^{-1}: 2937 s, 1725 s, 1353 s, 1174 s, 1097 s, 952 s, 929 s, 863 m, 839 m.^{1}H NMR (400 MHz, $CDCl_3$) δ (ppm): 5.20 (q, J = 2.8 Hz, 1H), 3.84 (m, 1H), 3.25 (s, 3H), 2.99 (s, 3H), 2.74 - 2.67 (m, 1H), 2.55 - 2.48 (m, br, 1H), 2.31 - 1.98 (m, 4H), 2.14 - 1.98 (m, 3H), 1.95 - 1.86 (m, 1H). ^{13}C NMR (100 MHz, $CDCl_3$) δ (ppm): 213.7 (Cq), 85.4 (CH),

72.0 (CH), 56.0 (CH_3), 48.9 (CH), 43.4 (CH), 39.1 (CH_3), 37.6 (CH_2), 34.3 (CH_2), 29.0 (CH_2), 25.5 (CH_2).

endo-2-Mesyl-7-methoxybicyclo[3.3.1]nonan-9-one **(endo-222)**: MS (EI) m/z (rel. intensities): 43 (59), 55 (82), 79 (100), 97 (63), 123 (50), 135 (53), 151 (48), 166 (58), 183 (22), 230 (14), 262 (49). High res. MS (IE): M^+: calc. 262.087499 found 262.0865 (-3.8 ppm), M^+ - CH_3OH: calc. 230.061284 found 230.0613 (+ 0.0 ppm). IR neat (NaCl) cm^{-1}: 2936 m, 1727 s, 1357 s, 1175 s, 1097 s, 951 s, 927 s, 862 m, 836 m. ^1H NMR (400 MHz, $CDCl_3$) δ (ppm): 4.78 (dt, $J_1 = 11.4$ Hz, $J_2 = 5.7$ Hz, 1H), 3.88 (m, 1H), 3.31 (s, 3H), 3.04 (s, 3H), 3.00 - 2.93 (m, 1H), 2.58 - 2.47 (m, 2H), 2.30 - 1.99 (m, 5H), 1.97 - 1.88 (m, 1H), 1.76 - 1.63 (m, 1H). ^{13}C NMR (100 MHz, $CDCl_3$) δ (ppm): 212.2 (Cq), 81.0 (CH), 72.2 (CH), 56.0 (CH_3), 50.2 (CH), 42.3 (CH), 38.6 (CH_3), 37.0 (CH_2), 31.6 (CH_2), 27.2 (CH_2), 26.3 (CH_2).

5.3.6 3-Methoxybicyclo[3.3.1]nonan-9-one (223)

222 **223**

A mixture of exo- and endo-2-mesyl-7-methoxybicyclo[3.3.1]nonan-9-one **222** (45.2 g, 0.122 mol, 71 % purity from ^1H NMR), sodium iodide (128.9 g, 0.86 mol), and zinc dust (112.5 g, 1.72 mol) in dimethylformamide (1.8 L) was refluxed for 5 h. The cold reaction mixture was then filtered using a sintered glass filter funnel, concentrated on the rotavapor, and after the addition of water (500 mL), the resulting mixture was extracted with dichloromethane (3 x 100 mL). The combined organic layers were dried with magnesium sulfate, filtered and concentrated on the rotavapor to yield 16.3 g crude material. Distillation at 0.05 mm Hg and *ca.* 80°C afforded 11.49 g 3-methoxybicyclo[3.3.1]nonan-9-one **223**, with a purity of 84 % according to GC (yield: 47 %). This product was used for the subsequent steps without further purification. An analytical sample for characterization was purified using column chromatography (silica gel, hexanes - ether 95:5).

GC-MS m/z (rel. intensity): 41 (100), 55 (97), 67, (94), 79 (75), 95 (62), 108 (57), 121 (21), 136 (65), 153 (8), 168 (44). High res. MS (IE): M^+: calc. 168.115030 found 168.1139 (-6.6 ppm). IR neat (NaCl) cm^{-1}: 2928 s, 1726 s, 1440 m, 1100 s, 912 m, 732 s. ^1H NMR (200 MHz, $CDCl_3$) δ (ppm): 3.94 (tt, J_1 = 8.2 Hz, J_2 = 5.2 Hz, 1H), 3.22 (s, 3H), 2.43 - 2.29 (m, 2H), 2.25 - 2.08 (m, 2H), 2.05 - 1.73 (m, 7H), 1.61 - 1.41 (m, 1H). ^{13}C NMR (50 MHz, $CDCl_3$) δ (ppm): 219.2 (Cq), 73.0 (CH), 55.8 (CH_3), 44.5 (2 CH), 37.5 (2 CH_2), 34.9 (2 CH_2), 19.3 (CH_2).

5.3.7 3-Methoxybicyclo[3.3.2]decan-9-one (224)

223 **224**

A solution of 3-methoxybicyclo[3.3.1]undecan-9-one **223** (11.24 g, 56.1 mmol, 85 % purity from GC) in 20 mL of methanol was mixed with a solution of potassium hydroxide (45 g, 0.8 mol) in water (65 mL) and methanol (65 mL) at 0°C. Maintaining this temperature, a saturated solution of Diazald® (27.0 g, 127 mmol) in methanol (335 mL) was added dropwise over a period of 9 h. The resulting reaction mixture was then allowed to warm to room temperature and stirred for an additional 2 h. After filtration, water (200 mL) was added and the methanol removed using the rotavapor. Extraction of the resulting mixture with dichloromethane (3 x 60 mL) yielded 11.95 g crude product. Purification using column chromatography (silica gel, hexanes : ether - 95 : 5) afforded 7.48 g of the 3-methoxybicyclo[3.3.2]dodecan-9-one **224** with a purity of 76 % according to GC (yield: 55 %). The impurity was 3-methoxybicyclo[3.3.1]dodecan-9-one **223**. An analytical sample using preparative GC was prepared for the characterization.

GC-MS m/z (rel. intensities): 41 (100), 55 (63), 67 (49), 79 (50), 93 (25), 108 (22), 122 (14), 139 (6), 154 (6), 182 (6). High res. MS (IE): M^+: calc. 182.130680 found 182.1308 (+0.7 ppm), $M^+ - CH_3$: calc. 137.107205 found 167.1067 (-2.9 ppm), $M^+ - CH_3OH$: calc. 150.104465 found 150.1049 (+3.0 ppm). IR neat (NaCl) cm^{-1}: 2923 s, 1696 s, 1453 m, 1092 s. ^1H NMR

(200 MHz, $CDCl_3$) δ (ppm): 3.76 (tt, J_1 = 8.4 Hz, J_2 = 4.2 Hz, 1H), 3.31 (s, 3H), 2.85 (p, J = 4.7 Hz, 1H), 2.73 (dd, J_1 = 19.0 Hz, J_2 = 4.0 Hz, 1H), 2.48 (ddd, J_1 = 19.0 Hz, J_2 = 4.1 Hz, J_3 = 1.5 Hz, 1H), 2.33 (tt, J_1 = 9.0 Hz, J_2 = 4.5 Hz, 1H), 2.17 - 1.94 (m, 2H), 1.92 - 1.50 (m, 8H). ^{13}C NMR (50 MHz, $CDCl_3$) δ (ppm): 215.8 (Cq), 76.6 (CH), 56.0 (CH_3), 48.4 (CH), 47.3 (CH_2), 37.8 (CH_2), 32.4 (CH_2), 32.1 (CH_2), 27.6 (CH), 27.2 (CH_2), 22.2 (CH_2).

5.3.8 3-Methoxy-9-methylenebicyclo[3.3.2]decane (225)

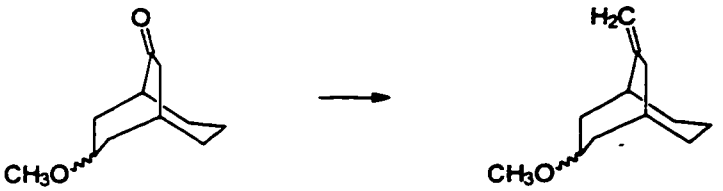

224 **225**

The Lombardo reagent[189] (130 mL) and dichloromethane (52 mL) were cooled to 0°C under an argon atmosphere. Within 10 min. a solution of 3-methoxybicyclo[3.3.2]dodecan-9-one **224** (4.29 g, 19.1 mmol, 81 % purity from GC) was added to the Lombardo reagent,[189] maintaining a reaction temperature of 0°C. The resulting slurry was allowed to warm to room temperature and stirred for a further 2 h before it was diluted with hexanes (130 mL). Portionwise addition of a slurry of sodium bicarbonate (78 g) and water (42 mL) caused the reaction mixture to separate into a gray, sticky precipitate and a clear colorless solution, after the evolution of carbon dioxide had ceased. The two phases were separated and the gray precipitate washed with 2 portions of hexanes (50 mL). The combined organic layers were dried with magnesium sulfate, filtered and concentrated on the rotavapor to yield 4.66 g of a yellow oil. Purification by column chromatography (silica gel, hexanes 100 %) afforded 3.24 g (yield: 94 %) 3-methoxy-9-methylenebicyclo[3.3.2]dodecane **225** (pure according to ^1H NMR) as a colorless oil.

GC-MS m/z (rel. intensity): 41 (73), 53 (33), 67 (29), 79 (100), 91 (86), 105 (39), 120 (26), 133 (38), 148 (19), 180 (2). High res. MS (IE): M^+: calc. 180.151415 found 180.1506 (-4.7 ppm), $M^+ - CH_3OH$: calc. 148.125200 found 148.1237 (-9.8 ppm). IR neat (NaCl) cm^{-1}: 2921 s, 1449 m, 1096 s, 879 m. ^1H NMR (200 MHz, $CDCl_3$) δ (ppm): 4.71 (q, br, J = 1.9 Hz, 1H),

4.58 (q, J = 2.0 Hz, 1H), 3.72 (tt, J_1 = 11.2 Hz, J_2 = 4.9 Hz, 1H), 3.30 (s, 3H), 2.86 - 2.72 (m, br, 1H), 2.67 - 2.38 (m, 2H), 2.26 - 2.09 (m, 3H), 1.79 - 1.21 (m, 8H). ^{13}C NMR (50 MHz, $CDCl_3$) δ (ppm): 153.5 (Cq), 109.7 (CH_2), 77.2 (CH), 56.0 (CH_3), 41.5 (CH), 40.3 (CH_2), 39.4 (CH_2), 39.1 (CH_2), 30.9 (CH_2), 30.4 (CH_2), 29.9 (CH), 24.1 (CH_2).

5.3.9 3-Methoxy-9-oxiranylbicyclo[3.3.2]decane (226)

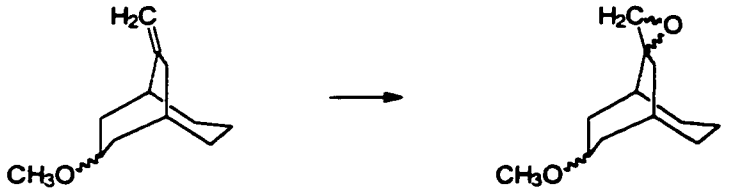

225 **226**

A solution of m-chloroperbenzoic acid (5.32 g, 30.8 mmol) in chloroform (150 mL) was cooled to 0°C and 3-methoxy-9-methylenebicyclo[3.3.2]decane **225** (3.05 g, 16.9 mmol) dissolved in chloroform (30 mL) was added within 10 min. The resulting reaction mixture was stirred at 0°C for 2 h before washing with a solution of sodium bicarbonate and sodium carbonate (1:1, 5 %). The organic layer was then dried with magnesium sulfate, filtered and concentrated on the rotavapor to afford 4.18 g of a colorless crude product. Purification on a silica gel column with hexanes - ether (95 : 5) yielded 1.87 g (yield: 48 %) of the 3-methoxy-9-oxiranylbicyclo[3.3.2]decane **226** with a purity of 85 % according to GC (main impurity 3-methoxybicyclo[3.3.2]decane-9-carbaldehyde **233**).

GC-MS m/z (rel. intensity): 41 (89), 55 (47), 67 (100), 79 (83), 93 (39), 107 (30), 121 (24), 136 (27), 164 (6), 196 (1). High res. MS (IE): M^+: calc. 196.146330 found 196.1475 (+6.2 ppm), M^+ - CH_3OH: calc. 164.120115 found 164.1197 (-2.6 ppm). IR neat (NaCl) cm^{-1}: 2917 s, 1457 m, 1094 s, 919 m, 733 m. ^{1}H NMR (200 MHz, $CDCl_3$) δ (ppm): 3.64 (tt, J_1 = 11.2 Hz, J_2 = 4.9 Hz, 1H), 3.24 (s, 3H), 2.51 (s, 2H), 2.34 - 2.07 (m, 2H), 2.06 - 1.21 (m, 12H). ^{13}C NMR (50 MHz, $CDCl_3$) δ (ppm): 76.6 (CH), 60.9 (Cq), 56.7 (CH_2), 55.9 (CH_3), 40.4 (CH), 40.3 (CH_2), 39.7 (CH_2), 35.1 (CH_2), 29.8 (CH_2), 29.7 (CH), 27.3 (CH_2), 24.2 (CH_2).

5.3.10 9-Azidomethyl-9-hydroxy-3-methoxybicyclo[3.3.2]decane (227)

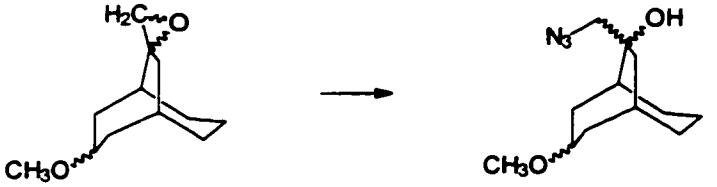

226 **227**

A solution of 3-methoxy-9-oxiranylbicyclo[3.3.2]decane **226** (1.39 g, 7.08 mmol), boric acid (2.40 g 38.8 mmol), sodium azide (2.40 g, 36.9 mmol) and dimethylformamide (70 mL) was refluxed for 3h. The DMF was removed *in vacuo* before water (100 mL) was added and the resulting mixture extracted with dichloromethane (3 x 25 mL). After drying, filtering and concentrating on the rotavapor, 2.15 g of a yellowish oil was isolated, and was purified on a silica gel column using hexanes : ether (1:1) to give 1.54 g of the pure (from ^{1}H NMR) 9-azidomethyl-9-hydroxy-3-methoxybicyclo[3.3.2]decane **227**.

MS (EI) m/z (rel. intensity): 41 (65), 67 (76), 81 (99), 108 (33), 123 (21), 133 (21), 151 (100), 211 (2). High res. MS (IE): $M^+ - N_2$: calc. 211.157229 found 211.1574 (+1.0 ppm), $M^+ - CH_2N_3$: calc. 183.138505 found 183.1387. IR neat (NaCl) cm^{-1}: 3427 s, 2924 s, 2099 s, 1454 m, 1288 m, 1094 m. ^{1}H NMR (200 MHz, $CDCl_3$) δ (ppm): 3.77 (p, J = 5.7 Hz, 1H), 3.67 (s, br, 1H), 3.38 (s, 3H), 3.33 (s, 2H), 2.37 - 2.11 (m, 3H), 2.10 - 1.10 (m, 11H). ^{13}C NMR (50 MHz, $CDCl_3$) δ (ppm): 78.7 (CH), 77.7 (Cq), 61.5 (CH_2), 56.1 (CH_3), 44.3 (CH_2), 39.9 (CH), 34.2 (CH_2), 33.6 (CH_2), 33.01 (CH_2), 30.2 (CH), 28.7 (CH_2), 22.2 (CH_2).

5.3.11 9-Aminomethyl-9-hydroxy-3-methoxybicyclo[3.3.2]decane (228)

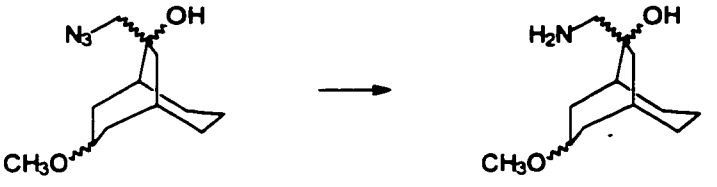

227 **228**

9-Azidomethyl-9-hydroxy-3-methoxybicyclo[3.3.2]decane **227** (1.54 g, 6.44 mmol) and 10 % palladium on activated charcoal (20 mg) in ethanol (40 mL) was hydrogenated at room

temperature and atmospheric pressure for 2 h. The ethanol was removed on the rotavapor after filtration and the residue dissolved in hydrochloric acid (30 mL, 5 %). The aqueous solution was washed with dichloromethane (3 x 20 mL) before sodium hydroxide solution (15 %) was added until the mixture became basic. This solution was then extracted with dichloromethane (3 x 25 mL) and the combined organic phases dried with magnesium sulfate, filtered and concentrated on the rotavapor to yield 1.42 g (yield: 85 %) of the 9-aminomethyl-9-hydroxy-3-methoxybicyclo[3.3.2]decanol **228** (82 % purity from ^{1}H NMR). This material was used directly for the next step. An analytical sample was prepared for characterization using column chromatography (silica gel, ether - methanol 90 : 10, trace of ammonium hydroxide).

MS (EI) m/z (rel. intensity): 41 (83), 67 (82), 81 (95), 91 (43), 109 (30), 151 (100), 183 (39), 238 (8), 239 (1). IR neat (NaCl) cm^{-1}: 3373 s, 2921 s, 1454 m, 1086 s, 1032 m, 980 m. ^{1}H NMR (200 MHz, $CDCl_3$) δ (ppm): 3.79 (tt, J_1 = 7.8 Hz, J_2 = 5.3 Hz, 1H), 3.33 (s, 3H), 2.76 (d, J = 12.8 Hz, 1H), 2.57 (d, J = 12.8 Hz, 1H), 2.33 - 1.82 (m, 10H), 1.81 - 1.41 (m, 7H). ^{13}C NMR (50 MHz, $CDCl_3$) δ (ppm): 78.5 (CH), 76.0 (Cq), 56.0 (CH_3), 51.9 (CH_2), 44.4 (CH_2), 39.5 (CH), 35.8 (CH_2), 33.5 (CH_2), 32.7 (CH_2), 30.5 (CH), 27.8 (CH_2), 23.4 (CH_2).

5.3.12 7-Methoxybicyclo[3.3.3]undecan-2-one (229)

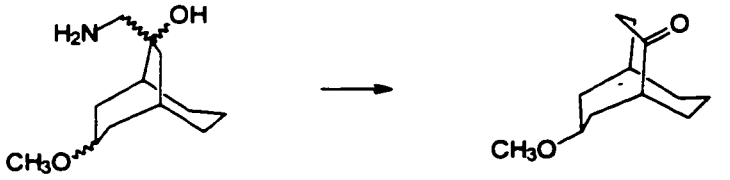

228 **229**

9-Aminomethyl-9-hydroxy-3-methoxybicyclo[3.3.2]decane **228** (0.320 g, 1.28 mmol) was dissolved in a solution of acetic acid (0.640 mL, 11.2 mmol) in water (10 mL). At room temperature a solution of sodium nitrite (0.64 g, 9.3 mmol) in water (2 mL) was added dropwise and the reaction mixture stirred for 2 hours and for a further hour at 96°C (steam bath). Extraction with ether (3 x 25 mL), drying, filtering and concentrating the combined extracts afforded 0.32 g of a waxy solid. Purification via column chromatography (silica gel, hexanes : ether 8 : 2) gave 0.18 g (yield: 61 %) of 7-methoxybicyclo[3.3.3]undecan-2-one **229** (87 % from ^{1}H NMR; impurity 3-methoxybicyclo[3.3.2]decan-9-one **224**). An analytical

sample for characterization was prepared using preparative GC.

GC-MS m/z (rel. intensity): 41 (100), 55 (69), 67 (47), 79 (29), 93 (13), 107 (9). 121 (6), 136 (7), 168 (4), 196 (1). High res. MS (IE): M^+: calc. 196.146330 found 196.1455 (-4.4 ppm). IR neat (NaCl) cm^{-1}: 2922 s, 1689 s, 1455 m, 1089 s. ^1H NMR (200 MHz, $CDCl_3$) δ (ppm): 3.52 (tt, J_1 = 11.4 Hz, J_2 = 4.1 Hz, 1H), 3.39 (s, 3H), 3.11 - 2.88 (m, 2H), 2.69 (q, br, J = 8.5 Hz, 2H), 2.33 - 2.03 (m, 4H), 1.93 - 1.41 (m, 8H). ^{13}C NMR (50 MHz, $CDCl_3$) δ (ppm): 218.9 (Cq), 76.6 (CH), 56.4 (CH_3), 46.6 (CH), 36.8 (CH_2), 35.1 (CH_2), 34.1 (CH_2), 29.4 (CH), 28.9 (CH_2), 28.3 (CH_2), 27.2 (CH_2), 21.2 (CH_2).

5.3.13 3-Methoxybicyclo[3.3.3]undecane (230)

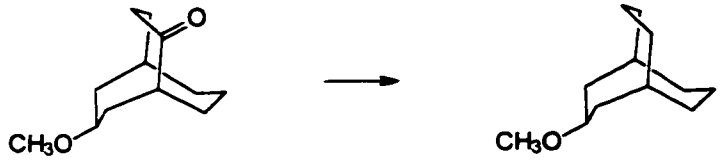

229 **230**

7-Methoxybicyclo[3.3.3]undecan-2-one **229** (141.7 mg, 0.628 mmol, purity 87 % by ^1H NMR), hydrazine (100 %, 9.80 g, 306 mmol), hydrazine dihydrochloride (2.57 g, 24.4 mmol) and triethylene glycol (17.2 g, 115 mmol) was heated to 130°C for 2h. Then, potassium hydroxide (85 %, 3.00 g, 45.5 mmol) was added portionwise before the temperature was gradually raised to 210°C and maintained there for 3 h. The cold reaction solution was then diluted with 50 mL water, extracted with ether (3 x 25 mL) and the combined ether extracts washed once with water, dried with magnesium sulfate, filtered and concentrated on the rotavapor to afford 191.8 mg of a crude material. Purification on a silica gel column using a hexane - ether mixture in the ratio 95 : 5 resulted in the isolation of 112.3 mg (yield: 88 %) 3-methoxybicyclo[3.3.3]undecane **230** with a purity of 90 % from GC (impurity 3-methoxybicyclo[3.3.2]decane). For characterization purposes, an analytical sample was prepared using preparative GC.

GC-MS m/z (rel. intensity): 41 (100), 55 (39), 67 (41), 79 (26), 91 (10), 107 (8). 122 (5), 135 (5), 150 (1), 182 (1). High res. MS (IE): M^+: calc. 182.167065 found 182.1655 (-8.4 ppm). IR neat (NaCl) cm^{-1}: 2916 s, 1457 m, 1161 m, 1094 s. ^1H NMR (400 MHz, $CDCl_3$) δ (ppm):

3.37 (tt, J_1 = 11.7 Hz, J_2 = 4.0 Hz, 1H), 3.35 (s, 3H), 2.52 (q, br, J = 9.3 Hz), 1.95 (dddd, J_1 = 13.9 Hz, J_2 = 10.2 Hz, J_3 = 3.9 Hz, J_4 = 1.1 Hz), 1.71 - 1.58 (m, 6H), 1.57 - 1.40 (m, 8H). ^{13}C NMR (100 MHz, $CDCl_3$) δ (ppm): 77.6 (CH), 56.2 (CH_3), 34.3 (2 x CH_2), 29.5 (2 x CH_2), 29.4 (2 x CH), 29.0 (2 x CH_2), 20.4 (CH_2), 20.0 (CH_2).

5.3.14 3-Methoxybicyclo[3.3.3]undecan-1-ol (231)

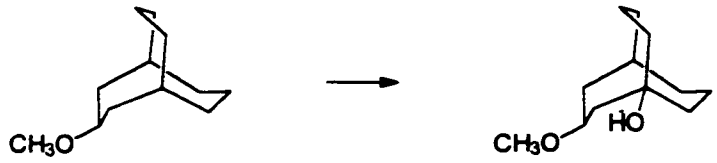

230 **231**

Air was bubbled through a solution of 3-methoxybicyclo[3.3.3]undecane (18.6 mg, 0.102 mmol) in cyclohexane (30 mL) for 15 hours. During this procedure, the solution was irradiated with light (Sunlamp) and cooled to 5 to 10°C (quartz vessels). Concentration and purification of the crude material on a silica gel column (hexanes - ether 1:1) yielded 0.9 mg (yield: 4%) of 3-methoxybicyclo[3.3.3]undecan-1-ol **231**. Attempts to further oxidize the reaction mixture to the diol formed only traces of the desired 3-methoxybicyclo[3.3.3]undecan-1,5-diol **232** (from ^{1}H NMR). All the other starting material decomposed into a complex mixture.

GC-MS m/z (rel. intensity): 41 (100), 55 (62), 67 (37), 79 (28), 97 (27), 109 (6), 123 (6), 137 (4), 155 (2), 166 (1), 198 (1). ^{1}H NMR (200 MHz, $CDCl_3$) δ (ppm): 3.40 (tt, J_1 = 10.8 Hz, J_2 = 4.4 Hz, 1H), 3.37 (s, 3H), 2.49 (q, br, J = 9.3 Hz, 1H), 2.02 - 1.87 (m, 4H), 1.84 - 1.53 (m, 9H), 1.52 - 1.39 (m, 3H). ^{13}C NMR (50 MHz, $CDCl_3$) δ (ppm): 74.9 (Cq), 56.4 (CH_3), 45.0 (CH_2), 40.5 (CH_2), 40.5 (CH_2), 34.8 (CH_2), 29.7 (CH_2), 29.6 (CH_2), 29.1 (CH), 29.0 (CH_2), 21.5 (CH_2), 21.0 (CH_2).

5.4 Bicyclo[3.3.3]undecyl system

5.4.1 N-Cyclohex-1-enylmorpholine (95)

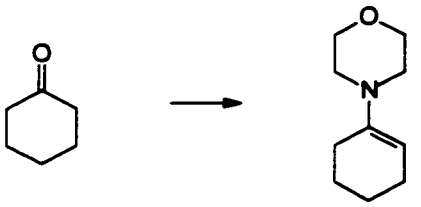

95

A solution of cyclohexanone (49.1 g, 0.500 mol), morpholine (52.3 g, 0.607 mol) and p-toluenesulfonic acid (2 g) in toluene (300 mL) were refluxed for 20 h with azeotropic removal of water. Concentration on the rotavapor yielded a orange oil, which was distilled in vacuum (0.3 mmHg) and the fraction at 85 to 90°C was collected to give 74.81 g (yield: 81 %) of N-cyclohex-1-enylmorpholine **95** (90 % purity ^{1}H NMR). The ^{1}H and ^{13}C-NMR data of the distillate was in accordance with the literature data.[166, 210]

^{1}H NMR (200 MHz, $CDCl_3$) δ (ppm): 1.61 - 1.72 (m, 4H), 2.00 - 2.10 (m, 4H), 2.76 (t, J = 4.8 Hz, 4H), 3.71 (t, J = 4.8 Hz, 4H). ^{13}C NMR (50 MHz, $CDCl_3$) δ (ppm): 145.41 (Cq), 100.36 (CH), 66.95 (CH_2), 46.43 (CH_2), 26.77 (CH_2), 24.37 (CH_2), 23.18 (CH_2), 22.72 (CH_2).

5.4.2 2-Hydroxybicyclo[3.3.1]nonan-9-one (97)

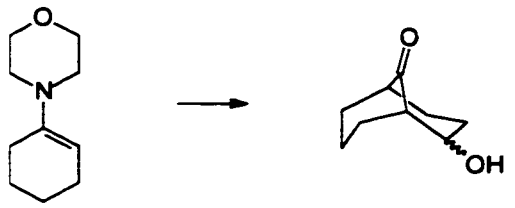

95 **97**

N-Cyclohex-1-enylmorpholine **95** (75.0 g, 0.448 mol) was dissolved in ether (400 mL), cooled to 0 °C in a 2 L RB flask, and acrolein (90 %, 33.3 mL, 27.9 g, 0.448 mol) was added. The resulting colorless solution was stirred for 12 h at 20 °C (^{1}H NMR signals at 6.06 (m) and 4.58 (m) for N-cyclohex-1-enylmorpholine). Water (300 mL) and then H_2SO_4 (98 %, 65.9 g) in water (150 mL) was added to the reaction mixture (*ca.* 12 % w/w H_2SO_4 in water). The ether was distilled off followed by about 50 mL of water. The resulting mixture was refluxed

for an additional 3 h. The cold reaction mixture was filtered (sintered glass funnel) and extracted with CH_2Cl_2 (4 x 150 mL). The organic layer was dried ($MgSO_4$) and concentrated to yield 59.0 g (yield: 85%) of the crude waxy solid 2-hydroxybicyclo[3.3.1]nonan-9-one **97** as a *ca.* 1:1.45 mixture of the exo and endo isomers, whose ^{13}C NMR shifts were in good agreement with the literature[211] values.

GC-MS m/z (rel. intensity): 39(72), 41(87), 55(100), 67(29), 83(34), 98(95), 111(10), 126(4), 135 (9), 154(9). ^1H NMR (200 MHz, $CDCl_3$) δ (ppm): 1.38 - 2.76 (m, 22H), 4.04 (p, J = 4.5 Hz, 0.689 H), 4.36 (s, br, 1H). ^{13}C NMR (50 MHz, $CDCl_3$) δ (ppm): 220.51 (Cq), 219.04 (Cq), 76.17 (CH), 72.74 (CH), 54.19 (CH), 54.07 (CH), 45.79 (CH), 44.88, (CH), 34.37 (CH_2), 33.76 (CH_2), 30.41 (CH_2), 29.10 (CH_2), 28.72 (CH_2), 28.09 (CH_2), 27.51 (CH_2), 26.96 (CH_2), 20.37 (CH_2), 19.24 (CH_2).

5.4.3 2-Chlorobicyclo[3.3.1]nonan-9-one and Bicyclo[3.3.1]non-2-en-9-one (99) and (98)

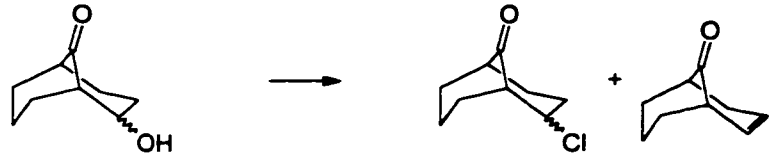

97 **99** **98**

2-Hydroxybicyclo[3.3.1]nonan-9-one **97** (5.00 g, 32.4 mmol) in pyridine (10 mL) was added with magnetic stirring to a pre-mixed solution of pyridine (21 mL, 0.26 mol) and phosphorus oxychloride (5.9 mL, 0.065 mol), cooled to 0 °C in an ice bath, at a rate such that the temperature remained between 0 and 5 °C. The mixture was allowed to warm to 20 °C and stirred an additional 3 h. Water was added cautiously at a rate such that the reaction mixture stayed below 50 °C. A slush formed during this addition making stirring difficult, and the mixture was manually shaken while the water was added. Eventually a clear brown solution formed. This was concentrated on the rotavapor to half the original volume. Acidification with aq. HCl (10 %) followed by extraction with dichloromethane (3 x 30 mL), drying with magnesium sulfate and concentration gave 5.27 g of residual solid (87 % 1-chlorobicyclo[3.3.1]undecan-9-one **99** and 12 % bicyclo[3.3.1]non-2-en-9-one **98** by GC), (combined yield: 95 %). Samples of separated endo- and exo-1-chloro-

bicyclo[3.3.1]undecan-9-one **99** and bicyclo[3.3.1]non-2-en-9-one **98** had ^{13}C NMR spectra in good agreement with published data.[211, 212]

Bicyclo[3.3.1]non-2-en-9-one **(98)**: GC-MS m/z (rel. intensity): 136(100), 108(11), 93(55), 79(70), 67(40), 39 (18). ^1H NMR (200 MHz, $CDCl_3$) δ (ppm): 5.92(dt, J_1 = 9.5Hz, 3.5Hz, 1H), 5.56(dddd, J_1 = 9.5Hz, J_2 = 5.9Hz, J_3 = 2.4Hz, J_4 = 1.5Hz, 1H), 2.64 - 2.90(m, 2H), 1.44 - 2.1(m, 6H), 2.35 - 2.61(m, 2H). ^{13}C NMR (50 MHz, $CDCl_3$) δ (ppm): 215.4 (Cq), 129.5 (CH), 126.7 (CH), 47.2 (CH), 45.1 (CH), 36.4 (2 x CH_2), 32.7 (CH_2), 16.4 (CH_2).

exo-1-Chlorobicyclo[3.3.1]undecan-9-one **(exo-99)**: GC-MS m/z (rel. intensity): 41(21), 55(24), 67(100), 79(33), 93(23), 109(61), 119(62), 137(42), 172(53), 174(16). ^1H NMR (200 MHz, $CDCl_3$) δ (ppm): 4.29 (ddd, J_1 = 12.5 Hz, J_2 = 5.9 Hz, J_3 = 5.5 Hz, 1H), 2.69 - 2.78 (m, 1H), 2.34 - 2.63 (m, 3H), 1.79 - 2.28 (m, 7H), 1.50 - 1.67 (m, 1H). ^{13}C NMR (50 MHz, $CDCl_3$) δ (ppm): 216.18 (Cq), 65.48 (CH), 54.78 (CH), 45.6 (CH), 34.86 (CH_2), 32.89 (CH_2), 30.04 (CH_2), 28.51 (CH_2), 19.81(CH_2).

endo-1-Chlorobicyclo[3.3.1]undecan-9-one **(endo-99)**: GC-MS m/z (rel. intensity): 41(16), 55(18), 67(100), 79(19), 93(8), 109(67), 119(27), 137(63), 172(42), 174(13). ^1H NMR (200 MHz, $CDCl_3$) δ (ppm): 4.60 - 4.70 (m, 1H), 2.60 - 2.80 (m, 2H), 2.36 - 2.55 (m, 2H), 1.91 - 2.22 (m, 7H), 1.50 - 1.67 (m, 1H). ^{13}C NMR (50 MHz, $CDCl_3$) δ (ppm): 216.18 (Cq), 65.48 (CH), 54.78 (CH), 45.61 (CH), 34.86 (CH_2), 32.89 (CH_2), 30.04 (CH_2), 28.51 (CH_2), 19.81 (CH_2).

5.4.4 Bicyclo[3.3.1]nonan-9-one (100)

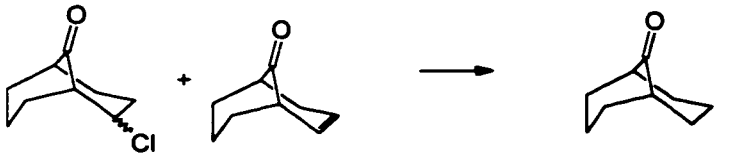

99 **98** **100**

A mixture of endo- / exo-1-chlorobicyclo[3.3.1]undecan-9-ones **99** and bicyclo[3.3.1]non-2-en-9-one **98** (29.9 g, 0.173 mol, based on 87 % 1-chlorobicyclo[3.3.1]undecan-9-one and 12 % bicyclo[3.3.1]non-2-en-9-one), sodium iodide (51.8 g, 0.346 mol) and zinc powder (45.2 g, 0.692 mol) was mixed with 250 mL of dimethylformamide and refluxed for 14 h. After

cooling, water (500 mL) was added and the mixture filtered. The filter residue was washed several times with hexanes and the aqueous filtrate was extracted with hexane (4 x 200 mL). The combined hexane solution was washed twice with water, dried with magnesium sulfate and concentrated on the rotavapor to give 20.1 g of solid product containing bicyclo[3.3.1]non-2-en-9-one **98** and bicyclo[3.3.1]non-9-one **100** (8 % and 89 % respectively by GC). This material was placed in a 250 mL RB flask, methanol (100 mL) and PtO_2 (20 mg) were added, and the flask was fitted with a septum and a syringe needle inlet. The flask was evacuated through the needle until the methanol began to boil and hydrogen was introduced from a cylinder using a very low back pressure; this process was repeated 2 times. The solution was then stirred at ambient temperature for 2 h. The platinum was filtered off and the methanol evaporated. The residue was taken up in acetone (100 mL) and Jones reagent (5 mL) was added. After stirring for 10 min., aqueous sodium bisulfite solution (10 %) was added until the solution color became green, the precipitate was filtered, washed with acetone, and the acetone evaporated. The residue was taken up in ether, washed with water and bicarbonate solution (5 %), dried with magnesium sulfate and concentrated to give 17.96 g of an off-white crystalline residue (yield: 75 %) m.p. 152 - 154 °C, lit.[213] 154 - 156 °C. The ^{1}H NMR spectrum of the crude product was identical to that of the recrystallized material (**100**), and GC. analysis gave a single peak.

GC-MS m/z (rel. intensity): 39 (100), 55 (48), 67 (93), 82 (61), 95 (12), 110 (20), 138 (14). ^{1}H NMR (200 MHz, $CDCl_3$) δ (ppm): 2.46 - 2.32 (m, 2H), 2.18 - 1.91 (m, 10H), 1.60 - 1.45 (m, 2H). ^{13}C NMR (50 MHz, $CDCl_3$) δ (ppm): 221.7 (Cq), 46.5 (2 x CH), 34.3 (4 x CH_2), 20.5 (2 x CH_2).

5.4.5 Bicyclo[3.3.2]decan-9-one (101)

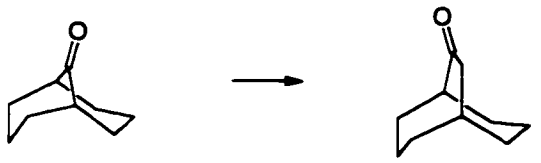

100 101

A solution of potassium hydroxide (80.0 g, 1.21 mol) in water (32 mL) and methanol (30 mL) was cooled to 0°C and mixed with bicyclo[3.3.1]nonan-9-one **100** (15.2 g, 0.110 mol) in methanol (30 mL). Maintaining a reaction temperature of 0°C a solution of Diazald® (58.0 g, 0.271 mol) in methanol (390 mL) was added dropwise over a time period of 17 h. The resulting suspension was then allowed to warm up to room temperature and then stirred for an additional 3h before it was concentrated on the rotavapor to half of the original volume. Filtration and extraction with ether (3 x 60 mL) yielded 14.89 g crude material, which was purified by column chromatography (silica gel, hexanes - ether, 95 : 5) to yield 13.47 g (yield: 72 %) bicyclo[3.3.2]decan-9-one **101** (89 % purity from GC; impurity bicyclo[3.3.1]nonan-9-one **100**). The MS and NMR data obtained were in accordance with the literature values.[214]

GC-MS m/z (rel. intensities): 41 (33), 55 (40), 67 (80), 81 (100), 96 (77), 109 (40), 123 (9), 152 (68). ^{1}H NMR (200 MHz, $CDCl_3$) δ (ppm): 2.82 (p, J = 4.9 Hz, 1H), 2.47 (d, J = 4.6 Hz, 2H), 2.18 (hept, J = 4.6 Hz, 1H), 1.93 - 1.34 (m, 12H). ^{13}C NMR (50 MHz, $CDCl_3$) δ (ppm): 217.1 (Cq), 51.0 (CH), 47.0 (CH_2), 31.9 (2 x CH_2), 28.1 (CH), 27.0 (2 x CH_2), 21.4 (2 x CH_2).

5.4.6 9-Trimethylsilanyloxybicyclo[3.3.2]decane-9-carbonitrile (108)

101 108

Bicyclo[3.3.2]decan-9-one **101** (0.784 g, 5.15 mmol) and dry zinc chloride (50 mg) were mixed with TMSCN (10 mL) and heated to 100°C for 12h. The excess TMSCN was then removed under vacuum (0.05 mmHg, RT) before the residue was dissolved in ether (60 mL). The ether solution was washed with cold (0°C) sodium bicarbonate solution (5%, 30 mL),

dried with magnesium sulfate, filtered and concentrated on the rotavapor to give 1.30 g (yield: 83 %) of a waxy solid (83 % **108** by GC). This material was used for the following steps without further purification. For characterization purposes, an analytical sample was prepared using column chromatography (silica gel, hexanes 100 %) and the MS and NMR data obtained were in accordance with literature values.[176]

GC-MS m/z (rel. intensity):67 (38), 75 (87), 82 (59), 95 (30), 110 (59), 133 (27), 155 (14), 168 (12), 209 (67), 236 (100), 251 (8). ^{1}H NMR (200 MHz, $CDCl_3$) δ (ppm): 2.62 (dd, J_1 = 15.3 Hz, J_2 = 4.4 Hz, 1H), 2.35 (p, J = 4.2 Hz, 1H), 2.20 (p, J = 4.2 Hz), 2.11 (dd, J_1 = 15.3 Hz, J_2 = 4.4 Hz, 1H), 2.17 - 1.91 (m. 2H, partial overlap, with H at 2.11 ppm), 1.90 - 1.45 (m. 10H), 0.24 (s, 9H). ^{13}C NMR (50 MHz, $CDCl_3$) δ (ppm): 124.1 (Cq), 75.3 (Cq), 48.3 (CH_2), 45.9 (CH), 32.6 (CH), 32.2 (CH_2), 30.7 (CH_2), 27.8 (CH_2), 26.8 (CH_2), 22.3 (CH_2), 22.2 (CH_2), 1.2 (3 x CH_3).

5.4.7 9-Aminomethylbicyclo[3.3.2]decan-9-ol (105)

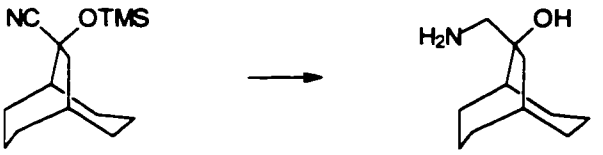

108 **105**

Lithium aluminium hydride (2.2 g, 58 mmol) was added to a solution of 9-trimethylsilanyloxybicyclo[3.3.2]decane-9-carbonitrile **108** (2.92 g, 84 %, 9.76 mmol) in ether (100 mL). The resulting reaction mixture was stirred overnight at room temperature, before a solution of potassium hydroxide (5 mL, 209 g/L) was added cautiously. Stirring for 20 min., filtration and concentration of the resulting solution yielded an oily substance, which was chromatographed (silica gel, ether 100% with traces of ammonium hydroxide solution) yielded 1.50 g (yield: 84 %) of the pure 9-aminomethylbicyclo[3.3.2]decan-9-ol **105**. The NMR data obtained agreed with the literature data.[176]

^{1}H NMR (200 MHz, $CDCl_3$) δ (ppm):2.84 (d, J = 12.8 Hz, 1H), 2.53 (d, J = 12.8 Hz, 1H), 2.26 - 2.03 (m, 3H), 1.97 (p, J = 4.4 Hz, 1H), 1.91 - 1.36 (m, 15H). ^{13}C NMR (50 MHz, $CDCl_3$) δ (ppm): 76.8 (Cq), 52.1 (CH_2), 44.3 (CH), 40.6 (CH), 32.1 (CH_2), 31.9 (CH_2), 31.2

(CH_2), 28.1 (CH_2), 28.0 (CH_2), 22.4 (CH_2), 22.3 (CH_2).

5.4.8 Bicyclo[3.3.3]undecan-2-one and Bicyclo[3.3.3]undecan-3-one (106) and (107)

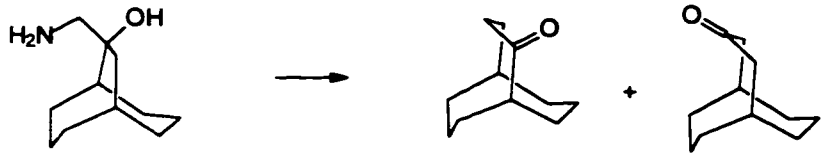

105 106 107

Sodium nitrite (3.6 g, 52.2 mmol) in water (20 mL) was added to a solution of 9-aminomethylbicyclo[3.3.2]decan-9-ol (1.50 g, 8.18 mmol) and acetic acid (3.6 mL, 62.9 mmol) in water (72 mL) at room temperature over a period of 30 min. The resulting solution was further stirred at room temperature for 4 h and then heated to 90°C for 3h. Neutralization with sodium carbonate solution (10 %), extraction with ether (3 x 25 mL) drying the combined ether extracts with magnesium sulfate, filtering and concentrating yielded 1.41 g of semisolid crude product. Purification using column chromatography (silica gel, hexanes - ether 95 : 5) afforded 1.23 g (yield: 87 %) bicyclo[3.3.3]undecan-2-one **106** containing about 3 % of the isomeric bicyclo[3.3.3]undecan-3-one **107**. The recorded MS and NMR data are in accordance with literature data.[176]

GC-MS m/z (rel. intensity): 41 (49), 55 (59), 67 (80), 81 (76), 96 (100), 109 (75), 122 (13), 137 (8), 138 (8), 166 (47). ^{1}H NMR (200 MHz, $CDCl_3$) δ (ppm): 2.64 (p, J = 4.8 Hz, 1H), 2.46 - 2.27 (m, 3H), 1.88 - 1.68 (m, 2H), 1.64 - 1.17 (m, 12H). ^{13}C NMR (50 MHz, $CDCl_3$) δ (ppm): 220.4 (Cq), 47.8 (CH), 36.4 (CH_2), 30.5 (CH), 28.7 (CH_2), 28.0 (CH_2), 26.8 (CH_2), 20.4 (CH_2).

5.4.9 Bicyclo[3.3.3]undecane (59)

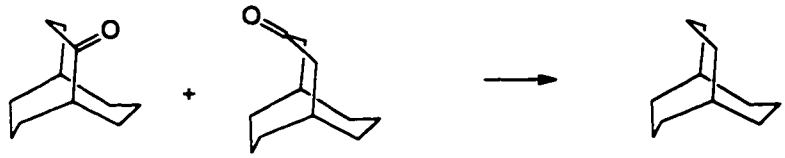

106 107 59

A mixture of the bicyclo[3.3.3]undecanones **106** and **107** (1.21 g. 7.28 mmol), hydrazine (80 %, 27.6, 710 mmol), hydrazine dihydrochloride (6.21 g, 59.2 mmol) and triethylene glycol

(147 mL, 1.10 mol) was heated to 130°C for 2 h. Then, potassium hydroxide (11.4 g, 173 mmol) was added portionwise before the temperature was gradually raised to 210°C and maintained there for another 3h. The cold reaction solution was then diluted with water (50 mL), extracted with ether (3 x 25 mL) and the combined ether extracts washed once with water, dried with magnesium sulfate, filtered and concentrated on the rotavator to give a waxy solid. Purification was accomplished by dissolving the solid crude material in hexanes (5 mL) and filtering it through a column (silica gel, 15 g). The column was washed with 150 mL of hexanes and the combined filtrates were concentrated on the rotavapor to afford 1.05 g (yield: 91 %) of the bicyclo[3.3.3]undecane **59** (96 % purity from GC). The recorded spectral data were in accordance with published results.[172, 215] Variable temperature ^{1}H NMR (400 MHz) experiments revealed a collapse of the axial-equatorial hydrogen signals at 231 K (coalescence), which corresponds to a "bridge-flip" barrier of 11.1 ± 0.2 kcal/mol.

GC-MS m/z (rel. intensity): 41 (57), 37 (100), 81 (98), 96 (99), 109 (46), 124 (26), 152 (63).^{1}H NMR (210 K, 400 MHz, $CDCl_3$) δ (ppm): 2.32 (q, J = 9.3 Hz, 2H), 1.64 - 1.44 (m, 9H), 1.43 - 1.13 (m, 9 H). ^{1}H NMR (303 K, 400 MHz, $CDCl_3$) δ (ppm): 2.40 (s, br, 2H), 1.73 - 1.29 (m, 18H). ^{13}C NMR (303 K, 100 MHz, $CDCl_3$) δ (ppm): no observable change with temperature: 30.8 (2 x CH), 29.0 (6 x CH_2), 20.2 (3 x CH_2).

5.4.10 Bicyclo[3.3.3]undecan-1-ol and Bicyclo[3.3.3]undecane-1,5-diol (109) and (110)

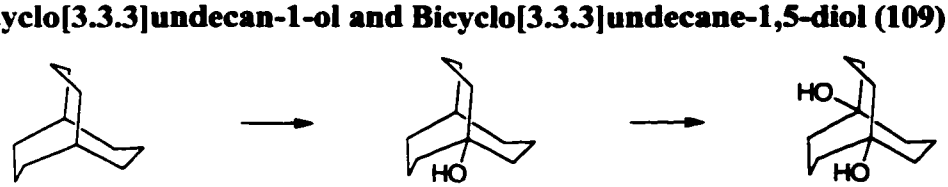

59 **109** **110**

Method a (partial oxidation): Bicyclo[3.3.3]undecane (250mg, 1.64 mmol) was dissolved in hexanes (20 mL) and placed in a 1 L RB flask. Evaporation of the hexanes formed a thin film on the wall of the flask, which was then exposed to oxygen. The atmosphere of the reaction flask was replaced every 12 h. After two days, the solid material was chromatographed (silica gel, ether 100 %) to give 97.8 mg (yield: 53 % based on consumed starting material) of the pure bicyclo[3.3.3]undecan-1-ol **109**, 42.0 mg of the monoperoxide,

50.6 mg diperoxide and 15.2 mg bicyclo[3.3.3]undecane-1,5-diol **110**.

Method b (exhaustive oxidation): Bicyclo[3.3.3]undecane **59** (340mg, 2.23 mmol) was dissolved in hexanes (20 mL) and placed in a 1 L round bottom flask. Evaporation of the hexanes formed a thin film on the wall of the flask, which was exposed to oxygen. The atmosphere of the reaction flask was replaced every 12 h. After 3 weeks, the solid material was dissolved in THF and sodium borohydride (0.5g, 13.2 mmol) was added and the resulting mixture stirred for 24 h. Evaporation of the THF, addition of ether, filtration and concentration on the rotavapor yielded white solid crude material, which was purified by column chromatography (silica gel, ether 100%) to yield 212.2 mg (yield 52 %) of the pure bicyclo[3.3.3]undecane-1,5-diol **110**. The spectral data obtained were in accordance with the literature.[178, 216]

Bicyclo[3.3.3]undecan-1-ol **(109)**: GC-MS m/z (rel. intensity): 41 (32), 55 (40), 67 (29), 79 (27), 97 (100), 107 (9), 126 (37), 140 (6), 150 (1). ^{1}H NMR (400 MHz, $CDCl_3$) δ(ppm): 2.26 (hept., J = 5.0 Hz, 1H), 2.97 (s, br, 1H), 1.66 - 1.49 (m, 12H), 1.48 - 1.34 (m, 6H). ^{13}C NMR (100 MHz, $CDCl_3$) δ (ppm): 76.4 (Cq), 39.8 (3 x CH_2), 30.3 (CH), 28.9 (3 x CH_2), 20.9 (3 x CH_2).

Bicyclo[3.3.3]undecan-1,5-diol **(110)**: GC-MS m/z (rel. intensity): 43 (50), 55 (100), 67 (91), 83 (71), 110 (59), 123 (57), 138 (24), 148 (6), 156 (18), 166 (1). ^{1}H NMR (200 MHz, $CDCl_3$) δ (ppm): 1.74 (s, br, 18H), 1.49 (s, 2H). ^{13}C NMR (50 MHz, $CDCl_3$) δ (ppm): 75.7 (2 x Cq), 40.2 (6 x CH_2), 21.5 (3 x CH_2).

5.4.11 1,5-Dichlorobicyclo[3.3.3]undecane (112)

110 **112**

Bicyclo[3.3.3]undecane-1,5-diol **110** (18 mg, 21.6 mmol) was dissolved in dichloromethane (3 mL) and cooled to 0°C. Hydrochloric acid (37 %, 3 mL) was added and the resulting suspension stirred vigorously for 15 min. The organic layer was separated and filtered through

a column of magnesium sulfate (1.5 g). Evaporation of the dichloromethane was performed by blowing nitrogen across the solution while keeping the temperature below 4°C, to afford 17.0 mg of the pure 1,5-dichlorobicyclo[3.3.3]undecane **112**, which was immediately used for the generation of the corresponding dication (dichloride **112** experiences significant decomposition at room temperature within 2 hours). NMR data were in agreement with the literature.[183]

^{1}H NMR (400 MHz, $CDCl_3$) δ (ppm): 4.23 (t, br, J = 6.4 Hz, 12H), 3.87 - 3.72 (m, 6). ^{13}C NMR (100 MHz, $CDCl_3$) δ (ppm): 78.5 (2 x Cq), 41.5 (6 x CH_2), 23.3 (3 x CH_2).

5.4.12 9-Ethylbicyclo[3.3.1]nonan-9-ol (195)

100 **195**

Lithium (200 mg, 28.8 mmol) was cut into small pieces (3 mm wire, 0.2 - 0.5 mm long) and added to ether (20 mL). One crystal of iodine (approx. 0.5 mg) and a few drops of ethyl bromide were added at room temperature. After the reaction had started (disappearance of the yellowish color, slight turbidness and shiny silvery surface of the Li) the reaction mixture was cooled to -10°C, the rest of the ethyl bromide (total 1.49 g, 13.7 mmol) was added over a period of 3 hours maintaining the temperature below -10°C and the resulting mixture was stirred overnight while allowing it to warm up to room temperature. The ethyllithium solution was added to bicyclo[3.3.1]nonan-9-one **100** (400 mg, 2.89 mmol) in ether (20 mL) at -78°C using a transfer needle, which allowed separation of the alkyllithium solution from the excess solid lithium. The reaction mixture was then allowed to warm to room temperature and stirred for an additional 2 h. The work up was conducted by pouring the reaction mixture into an aqueous ammonium chloride solution (5 %, 200 mL), followed by extraction with ether (3 x 30 mL). After drying ($MgSO_4$), filtration and concentration on the rotavapor gave 440 mg of a crude material. Purification on a silica gel column (hexanes - ether 95 :5) afforded 430 mg of the pure 9-ethylbicyclo[3.3.1]nonan-9-ol **195**. The recorded NMR and IR data were in

agreement with the literature.[217]

GC-MS m/z (rel. intensity): 41 (9), 55 (13), 67 (14), 79 (18), 111 (10), 121 (57), 139 (100), 150 (2), 168 (1). IR neat (NaCl) cm^{-1}: 3368 s, 2954 m, 2911 s, 2883 s, 1457 w, 1136 w, 1117 w, 973 w. ^1H NMR (400 MHz, $CDCl_3$) δ (ppm): 2.09 (tt, J_1 = 13.5 Hz, J_2 = 6.3 Hz, 2H), 1.88 - 1.67 (m, 4H), 1.64 (q, J = 7.7 Hz, 2H), 1.62 - 1.54 (s, br, 4H), 1.53 - 1.39 (m, 4H), 1.35 (s, br, 1H), 0.85 (t, J = 7.7 Hz, 3H). ^{13}C NMR (100 MHz, $CDCl_3$) δ (ppm): 73.0 (Cq), 36.4 (2 x CH), 30.5 (CH_2), 29.1 (2 x CH_2), 27.2 (2 x CH_2), 21.1 (CH_2), 20.4 (CH_2), 6.1 (CH_3).

5.4.13 9-Chloro-9-methylbicyclo[3.3.1]nonane (196)

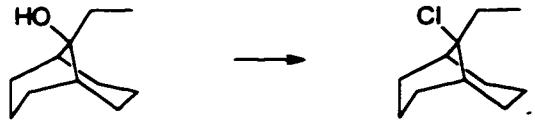

195 **196**

9-Ethylbicyclo[3.3.1]nonan-9-ol **195** (57.0 mg, 0.339 mmol) was dissolved in dichloromethane (5 mL), cooled to 0°C and hydrochloric acid (conc., 5 mL) was added. The resulting mixture was stirred vigorously for 15 min., maintaining the temperature at 0°C. The organic layer was then separated and filtered through a column of magnesium sulfate (approx. 2 g). Evaporation of the dichloromethane was carried out by blowing nitrogen onto the solution and keeping the solution temperature below 5°C, to yield 55 mg (yield: 87 %) of the pure 9-chloro-9-ethylbicyclo[3.3.1]nonane **196**. (This chloride was found to decompose into a complex mixture at room temperature within hours. Therefore, the characterization was conducted solely by NMR spectroscopy).

^1H NMR (400 MHz, $CDCl_3$) δ (ppm): 2.42 - 2.39 (m, 2H), 2.07 (q, J = 7.3 Hz, 2H), 2.02 - 1.93 (m, 3H), 1.86 (tq, J_1 = 19.8 Hz, J_2 = 5.2 Hz, 2H), 1.72 - 1.64 (m, 2H), 1.63 - 1.55 (m, 2H), 1.54 - 1.46 (m, 1H), 1.05 (t, J = 7.3 Hz, 3H). ^{13}C NMR (100 MHz, $CDCl_3$) δ (ppm): 84.3 (Cq), 37.9 (2 x CH), 33.1 (CH_2), 29.2 (2 x CH_2), 28.6 (2 x CH_2), 20.8 (CH_2), 19.8 (CH_2), 7.8 (CH_3).

5.4.14 9-Methylbicyclo[3.3.1]nonan-9-ol (197)

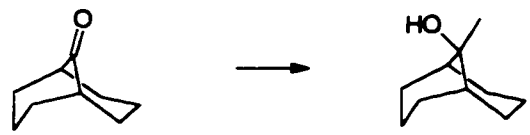

100 197

Methyllithium solution (1.5 M, 3.5 mL) was added to bicyclo[3.3.1]nonan-9-one **100** (322.4 mg, 2.33 mmol) in ether (20 mL) at -78°C. The reaction mixture was then allowed to warm to room temperature and stirred for an additional 2 h. The work up was conducted by pouring the reaction mixture onto an ammonium chloride solution (5 %, 200 mL), extraction with ether (3 x 30 mL), drying the combined organic layers with magnesium sulfate, filtering and concentrating on the rotavapor to give 359 mg (yield: quant) of the pure 9-methyl-bicyclo[3.3.1]nonan-9-ol **197**. The spectral data obtained were in accordance with literature values.[189]

GC-MS m/z (rel. intensity): 43 (100), 55 (43), 67 (52), 79 (32), 97 (40), 111 (11), 121 (15), 139 (16), 154 (13). ^{1}H NMR (200 MHz, $CDCl_3$) δ (ppm): 2.24 (m, 2H), 1.93 - 1.54 (m, 9H), 1.52 - 1.39 (m, 4H), 1.30 (s, 3H). ^{13}C NMR (50 MHz, $CDCl_3$) δ (ppm): 72.0 (Cq), 38.7 (2 x CH), 29.7 (2 x CH_2), 27.5 (CH_3), 27.0 (2 x CH_2), 20.7 (CH_2), 20.5 (CH_2).

5.4.15 9-Methylenebicyclo[3.3.2]decane (102)

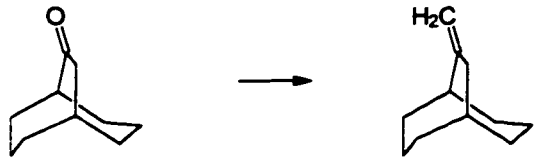

101 102

Bicyclo[3.3.2]docan-9-one **101** (12.4 g, 81.5 mmol) in dichloromethane (90 mL) was added to a slurry of the Lombardo reagent[189] (300 mL) at 0°C. The resulting reaction mixture was allowed to warm to room temperature and stirred for an additional 2 hours, after which hexanes (200 mL) and a slurry of sodium bicarbonate (185 g) and water (50 mL) were added and the resulting mixture was stirred until no gas development could be observed. The hexanes layer was decanted and the grey slurry washed with hexanes (2 x 50 mL). The combined organic

layers were dried with magnesium sulfate, filtered and concentrated on the rotavapor to give 13.17 g of a yellow oil. Purification using a silica gel column (hexanes 100%) yielded 9.9 g (yield: 81 %) of the pure 9-methylenbicyclo[3.3.2]decane **102**. The spectral data obtained were in accordance with literature values.[172, 218]

GC-MS m/z (rel. intensity): 41 (57), 67 (91), 79 (100), 93 (66), 107 (50), 121 (14), 135 (11), 150 (6). IR neat (NaCl) cm^{-1}: 3064 m, 2901 s, 1627 m, 1448 s, 881 s. ^1H NMR (200 MHz, $CDCl_3$) δ (ppm): 4.75 (p, J = 2.1 Hz, 1H), 4.62 (p, J = 2.1 Hz, 1H), 2.84 (p, J = 4.0 Hz, 1H), 2.59 (hex., J = 1.9 Hz, 2H), 2.18 (p, J = 4.0 Hz, 1H), 1.85 - 1.43 (m, 12 H). ^{13}C NMR (50 MHz, $CDCl_3$) δ (ppm): 154.6 (Cq), 109.3 (CH_2), 44.3 (CH), 38.7 (CH_2), 32.7 (CH_2), 32.2 (CH_2), 31.2 (CH), 22.0 (CH_2).

5.4.16 2-Methylbicyclo[3.3.3]undecan-2-ol (191)

106 **191**

Methyllithium solution (1.5 M, 1.5 mL) was added to bicyclo[3.3.3]nonan-2-one **106** (215 mg, 1.29 mmol) in ether (20mL) at -78°C. The reaction mixture was then allowed to warm to room temperature and stirred for an additional 2 h. The reaction mixture was poured into an ammonium chloride solution (5 %, 100 mL). Extraction with ether (3 x 25 mL) and concentration of the dried ($MgSO_4$) extracts on the rotavapor gave 180.1 mg (yield: 77 %) of the pure (by GC-MS) 2-methyl-bicyclo[3.3.3]nonan-2-ol **191**.

GC-MS m/z (rel. intensity):41 (22), 55 (29), 71 (100), 81 (50), 96 (76), 107 (11), 125 (22), 136 (11), 149 (8), 167 (13), 182 (1). High res. MS (IE): M^+ - CH_3: calc. 167.14359 found 167.14498 (-8.3 ppm). IR neat (NaCl) cm^{-1}:3395 m, 2904 s, 1459 m, 1371 w, 1099 w, 889 w. ^1H NMR (400 MHz, $CDCl_3$) δ (ppm): 2.38 (hept, J = 5.0 Hz, 1H), 2.14 (p, J = 4.9 Hz, 1H), 1.87 - 1.69 (m, 2H), 1.68 - 1.33 (m, 15H), 1.30 (s, 3H). ^{13}C NMR (100 MHz, $CDCl_3$) δ (ppm): 75.8 Cq, 44.5 (CH), 34,9 (CH_2), 31.0 (br, CH_3), 29.9 (CH), 28.7 (CH_2), 28.4 (CH_2), 27.6 (CH_2), 26.8 (CH_2), 24.0 (CH_2), 21.0 (CH_2), 21.0 (CH_2).

5.4.17 1,3-Dichloroadamantane (164)

164

Paraformaldehyde (12 g, 400 mmol) was added in portions to adamantane (12.0 g, 88.1 mmol) and aluminum chloride (24.0g, 180 mmol) in dichloromethane (72 mL) at 0°C. The reaction mixture was stirred for 1 h at 0°C and allowed to warm to room temperature before an additional portion of aluminum chloride (24.0 g, 180 mmol) and paraformaldehyde (12 g, 400 mmol) were added. After 3 hours of stirring of the resulting reaction mixture, it was poured onto ice (approx. 400 g). Extraction with ether (3 x 60 mL), drying of the combined organic layers with magnesium sulfate, filtering and concentration of the filtrates on the rotavapor yielded 18.0 g (yield: 89 %) of 1,3-dichloroadamantane **164** with a purity of 89 % (from GC). This material was used for the subsequent reactions without further purification. The spectral data were in agreement with literature values.[219]

GC-MS m/z (rel. intensity): 39 (17), 65 (14), 77 (25), 91 (32), 105 (9), 113 (16), 127 (6), 133 (16), 169 (100), 204 (2), 206 (1) $M^+ + 2$ - 56 % of M^+. ^1H NMR (200 MHz, $CDCl_3$) δ (ppm): 2.46 (s, 2H), 2.31 (hept, $J = 2.8$ Hz, 2H), 2.06 (d, $J = 3.0$ Hz, 8H), 1.60 (t, $J = 2.9$ Hz, 2H). ^{13}C NMR (50 MHz, $CDCl_3$) δ (ppm): 66.7 (Cq), 56.4 (CH_2), 45.6 (4 x CH_2), 33.5 (CH_2), 33.2 (2 x CH).

5.4.18 3-Methylenebicyclo[3.3.1]nonan-7-one and 3-Methylbicyclo[3.3.1]non-2-en-7-one (165) and (166)

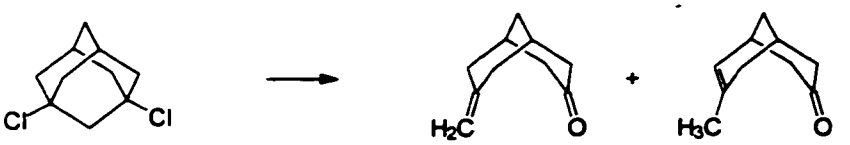

164 **165** **166**

1,3-Dichloroadamantane **164** (1.89 g, 9.21 mmol), dioxane (60 mL) and aqueous sodium hydroxide solution (1M, 60 mL) were heated in a pressure vessel to 185°C for 70 hours. After cooling the reaction mixture to room temperature, it was extracted with ether (3 x 35 mL) and the combined extracts were washed with water (3 x 20 mL). The ether extracts were then dried with magnesium sulfate, filtered and concentrated on the rotavapor to give the crude material, which was purified using column chromatography (silica gel, hexanes - ether 80 : 20) to afford 304.1 mg (yield: 22 %) of the pure (from ^{1}H NMR) 3-methylbicyclo[3.3.1]non-2-en-7-one **166** and 583.9 mg (yield: 42 %) of the pure (from ^{1}H NMR) 3-methylenebicyclo[3.3.1]nonan-7-one **165**. The recorded spectral data were in accordance with literature values.[220]

3-Methylbicyclo[3.3.1]non-2-en-7-one (**166**): GC-MS m/z (rel. intensity): 39 (5), 58 (8), 77 (14), 93 (100), 150 (32). ^{1}H NMR (400 MHz, $CDCl_3$) δ (ppm): 5.41 (dhept., J_1 = 4.7 Hz, J_2 = 1.2 Hz, 1H), 2.64 (s, br, 1H), 2.61 - 2.53 (m, 1H), 2.49 (ddd, J_1 = 14.9 Hz, J_2 = 6.1 Hz, J_3 = 1.2 Hz, 1H), 2.41 (dd, J_1 = 14.2 Hz, J_2 = 4.3 Hz, 1H), 2.37 - 2.19 (m, 3H), 1.97 (d, br, J = 12.7 Hz, 1H), 1.91 (ddq, J_1 = 12.7 Hz, J_2 = 3.2 Hz, J_3 = 2.5 Hz, 1H), 1.78 (d, J = 17.8 Hz, 1H), 1.57 (s, 3H). ^{13}C NMR (100 MHz, $CDCl_3$) δ (ppm): 212.3 (Cq), 132.8 (Cq), 124.6 (CH), 50.3 (CH_2), 49.1 (CH_2), 37.4 (CH_2), 31.1 (CH_2), 30.2 (CH_2), 30.2 (CH), 23.2 (CH_3).

3-Methylenebicyclo[3.3.1]nonan-7-one (**165**): GC-MS m/z (rel. intensity): 39 (11), 53 (6), 67 (18), 79 (21), 92 (100), 106 (31), 132 (3), 150 (41). ^{1}H NMR (200 MHz, $CDCl_3$) δ (ppm): 4.76 (t, J = 1.8 Hz, 2H), 2.42 (s, br, 2H), 2.40 - 2.30 (m, 6H), 2.24 (d, J = 13.6 Hz, 2H), 1.92 (d, br, J = 13.2 Hz, 1H), 1.88 (d, br, J = 13.2 Hz, 1H). ^{13}C NMR (50 MHz, $CDCl_3$) δ (ppm): 210.9 (Cq), 141.6 (Cq), 114.6 (CH_2), 47.3 (2 x CH_2), 41.3 (2 x CH_2), 32.0 (CH_2), 30.7 (2 x CH).

5.4.19 7-endo 7-Methyl-3-methylenebicyclo[3.3.1]nonan-7-ol (169)

165 169

Methyllithium solution (1.5 M, 3.5 mL) was added to 7-methylenebicyclo[3.3.1]nonan-3-one **165** (774 mg, 5.15 mmol) in ether (20mL) at -78°C. The reaction mixture was then allowed to warm to room temperature and stirred for an additional 2 h. The workup was conducted by pouring the reaction mixture onto an ammonium chloride solution (5 %, 100 mL), extraction with ether (3 x 25 mL), drying the combined organic layers with magnesium sulfate, filtering and concentrating on the rotavapor.

The resulting residue was dissolved in ether (20 mL), cooled to -78°C and methyllithium solution (1.5 M, 3.5 mL) was again added. This resulting reaction solution was worked up as mentioned above. The residue obtained was treated once more with methyllithium and worked up as previously described to give 650 mg of a crude material containing 495 mg starting material. Column chromatography (silica gel, ether - hexanes 5 : 95) yielded 153.4 mg (yield: 50 % based on consumed starting material) of the pure (from ^{1}H NMR) 7-endo 7-methyl-3-methylenebicyclo[3.3.1]nonan-7-ol **169**.[a]

GC-MS m/z (rel. intensity): 43 (10), 77 (12), 92 (100), 108 (108), 133 (4), 148 (21), 166 (2). High res. MS (IE): M^+ - H_2O: calc. 148.12520 found 148.12479 (+2.8 ppm). IR neat (NaCl) cm^{-1}: 3522 s, 2963 m, 2910 s, 1627 w, 1426 m, 1375 m, 1250 w, 1136 m, 1076 m, 889 m. ^{1}H NMR (200 MHz, $CDCl_3$) δ (ppm): 4.88 (t, J = 4.3 Hz, 2H), 3.53 (s, br, 1H), 2.52 - 2.24 (m, 4H), 2.11 (s, br, 2H), 1.86 - 1.42 (m, 6H), 1.14 (s, 3H). ^{13}C NMR (50 MHz, $CDCl_3$) δ (ppm): 148.5 (Cq), 112.3 (CH_2), 66.2 (Cq), 44.6 (2 x CH_2), 39.3 (2 x CH_2), 33.2 (CH_2), 32.9 (CH_3), 28.9 (2 x CH).

---

[a]The assignment of the endo configuration was based on the fact that the use of this starting material for the preparation of carbocations produced protonated cyclic ether products, which are not expected to form with the exo configuration of this starting material.

5.4.20 3-endo, 7-endo 3-Hydroxymethyl-7-methylbicyclo[3.3.1]nonan-7-ol (170)

169 **170**

7-Methyl-3-methylenebicyclo[3.3.1]nonan-7-ol **169** (148 mg, 0.891 mmol) was dissolved in THF (20 mL) under an argon atmosphere cooled to 0°C and a BH_3 - THF solution (1 M, 3 mL) was added. The resulting reaction solution was allowed to warm to room temperature and stirred for an additional 3h. After the stirring period, water (3 mL) was carefully added and after the hydrogen evolution had ceased, sodium hydroxide solution (5 mL) and hydrogen peroxide solution (30 %, 4 mL) were added. The resulting reaction mixture was stirred vigorously for 3 hours, then extracted with ether (3 x 15 mL). The combined organic layers were washed with sodium bisulfite (5 %, 10 mL), dried with magnesium sulfate, filtered and concentrated on the rotavapor. The solid residue was purified on a silica gel column (hexanes - ether 1:1) to yield 89.2 mg (yield: 54 %) of the pure 3-endo, 7-endo 3-hydroxymethyl-7-methylbicyclo[3.3.1]nonan-7-ol **170**.[a]

GC-MS m/z (rel. intensity): 43 (20), 55 (11), 67 (18), 79 (43), 93 (100), 108 (40), 123 (12), 135 (28), 148 (26), 166 (13), 184 (1). IR neat (NaCl) cm^{-1}: 3292 s, 2937 s, 2910 s, 2864 m, 1372 w, 1141 m, 1035 m, 1007 w, 907 w. ^1H NMR (400 MHz, $CDCl_3$) δ (ppm): 3.47 (d, J = 3.8 Hz, 2H), 2.23 - 2.08 (m, 2H), 1.99 - 1.73 (m, 6H), 1.71 - 1.40 (m, 7H), 1.17 (s, 3H). ^{13}C NMR (100 MHz, $CDCl_3$) δ (ppm): 71.5 (Cq), 67.5 (CH_2), 45.8 (2 x CH_2), 34.9 (CH_3), 31.5 (CH), 28.3 (CH_2), 28.3 (2 x CH_2), 24.8 (2 x CH).

---

[a]The assignment of the endo configuration was based on the fact that the use of this starting material for the preparation of carbocations produced protonated cyclic ether products, which are not expected to form with the exo configuration of this starting material.

5.4.21 3-endo 3,7-Dimethylbicyclo[3.3.1]non-6-en-3-ol (179)

166 179

Methyllithium solution (1.5 M, 1.5 mL) was added to 7-methylbicyclo[3.3.1]non-6-en-3-one **166** (254.6 mg, 1.69 mmol) in ether (20mL) at -78°C. The reaction mixture was then allowed to warm to room temperature and stirred for an additional 2 h. The work up was conducted by pouring the reaction mixture into an ammonium chloride solution (5 %, 100 mL), extraction with ether (3 x 25 mL), drying the combined organic layers with magnesium sulfate, filtering and concentrating on the rotavapor. The semi-solid residue was purified with column chromatography (silica gel, hexanes - ether 90 : 10) to afford 125.8 mg (yield: 67 % based on consumed starting material) of the 3-endo 3,7-dimethylbicyclo[3.3.1]non-6-en-3-ol **179**.[a]

GC-MS m/z (rel. intensities): 43 (6), 77 (8), 93 (100), 107 (9), 133 (2), 148 (26), 166 (1). High res. MS (IE): $M^+ - H_2O$: calc. 148.12520 found 148.12553 (-2.2 ppm). IR neat (NaCl) cm^{-1}: 3548 s, 2961 m, 2911 s, 1449 w, 1379 m, 1141 w, 1079 m, 912 w. ^1H NMR (200 MHz, $CDCl_3$) δ (ppm): 5.78 (d, br, J = 6.3 Hz, 1H), 3.50 (s, br, 1H), 2.46 - 2.13 (m, 3H), 2.03 (d, J = 17.9 Hz, 1H), 1.92 - 1.40 (m, 6H), 1.67 (s, 3H), 1.10 (s, 3H). ^{13}C NMR (50 MHz, $CDCl_3$) δ (ppm): 136.6 (Cq), 128.4 (CH), 70.0 (Cq), 45.7 (CH_2), 41.8 (CH), 37.1 (CH), 32.2 (CH_3), 31.5 (CH_2), 28.8 (CH), 26.9 (CH), 23.2 (CH_3).

---

[a]The assignment of the endo configuration of the alcohol group was based on the fact that the use of this starting material for the preparation of carbocations produced protonated cyclic ether products, which are not expected to form with the exo configuration of this starting material.

5.4.22 3,7-Dimethylbicyclo[3.3.1]nona-2,6-diene and 3,7-Dimethylbicyclo[3.3.1]nona-2,7-diene (158) and (167)

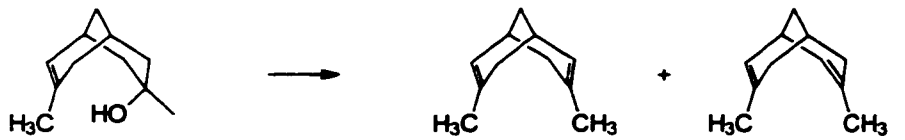

179 158 167

3,7-Dimethylbicyclo[3.3.1]non-6-en-3-ol **179** (200 mg, 1.20 mmol) in pyridine (5 mL) was added to a solution of pyridine (15 mL) and phosphorus oxychloride (1.00 mL, 10.9 mmol) at room temperature. The reaction solution was heated to 40°C for 3 hours before it was carefully poured onto ice (300 g). The ice was melted and the resulting mixture extracted with hexanes (3 x 25 mL). The combined organic layers were washed 3 times with water, dried with magnesium sulfate, filtered and concentrated on the rotavapor to give a yellow oil, which was purified using column chromatography (silica gel, hexanes 100 %) to give 153 mg (yield: 78 % based on consumed starting material) of a mixture of 3,7-dimethylbicyclo[3.3.1]nona-2,6-diene **167** and 3,7-dimethylbicyclo[3.3.1]nona-2,7-diene **158** in a ratio of 1 : 5. The recorded NMR data were in accordance with literature values.[221]

GC-MS m/z (rel. intensity): 40 (23), 80 (36), 91 (63), 93 (100), 105 (34), 133 (16), 148 (42). ^{1}H NMR (200 MHz, $CDCl_3$) δ (ppm): 5.42 (d, J = 5.4 Hz, 2H), 2.41 (s, br, 2H), 2.15 (dd, J_1 = 17.3 Hz, J_2 = 5.6 Hz, 2H), 1.69 (d, J = 17.3 Hz, 2H), 1.51 (s, 6H), 1.49 (t, J = 3.0 Hz, 2H). ^{13}C NMR (50 MHz, $CDCl_3$) δ (ppm): 132.0 (2 x Cq), 125.8 (2 x CH), 36.1 (2 x CH_2), 28.9 (CH_2), 28.6 (2 x CH), 23.6 (2 x CH_3).

5.4.23 Bicyclo[3.3.3]undec-1-yl cation (78)

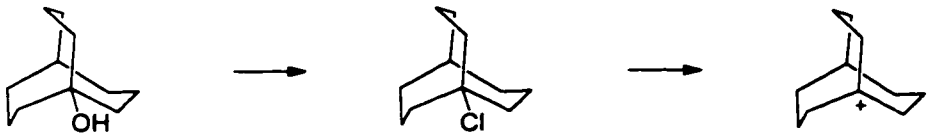

109 111 78

Bicyclo[3.3.3]undecan-1-ol **109** (20 mg, 0.119 mmol) was dissolved in dichloromethane (4 mL), cooled to 0°C and conc. hydrochloric acid was added. The resulting mixture was

intensely stirred for 15 min. before the dichoromethane layer was separated using a pipette, filtered through a magnesium sulfate column (approx. 2 g) and concentrated under a stream of nitrogen, keeping the temperature below 5°C. The resulting solid was dissolved in dichloromethane-d_2 (0.15 mL) and added to a solution of antimony pentafluoride (100 mg, 0.461 mmol) in sulfuryl chloridefluoride (total 1.8 mL) at -116°C. The antimony pentafluoride solution was prepared by dissolving the SbF_5 in a small portion of the sulfuryl chloridefluoride (approx. 0.4 mL), transferring it into a 10 mm NMR tube (0.8 mm wall), and condensing the rest of the sulfuryl chloridefluoride on top of the SbF_5 solution. The sample was kept still in order to avoid mixing of the SbF_5 with the sulfuryl chloridefluoride. Addition of the dichloromethane-d_2 solution of the 1-chlorobicyclo[3.3.3]undecane **111** to the cold sulfuryl chloridefluoride caused precipitation of the cation precursor, as well as partial freezing of the dichloromethane. Using a tungsten wire, the reaction solution was then quickly mixed to form a slightly yellowish, clear solution.

The ^{1}H NMR spectrum agreed well with a low field spectrum previously published by Olah,[183] although he was unable to see any line-broadening phenomena. In the present experiment at 189K, the ring flip of the C_3 bridges was clearly frozen out in the NMR spectrum. Warming the solution to 213 K caused collapse of two of the resolved doublets. Line shape analysis of the spectra at 211K, 221K, 232K revealed energy barriers of 10.5, 10.7 and 10.3 kcal/mol averaging to 10.5 ± 0.3 kcal/mol. At 232 K decomposition peaks of the monocation became apparent within 25 min., and warming the sample to 243 K for 25 min. caused approximately 70 % of the bicyclic cation **78** to rearrange into a complex mixture. The activation energy for decomposition was measured as 17.5 ± 0.3 kcal/mol.

^{1}H NMR (189K, 300 MHz) δ (ppm): 4.08 - 3.89 (m, 3H), 3.85 (s, br, 3H), 3.04 - 2.75 (m, 6H), 2.54 (q, J = 8.12 Hz, 1H), 2.02 - 1.88 (m, 3H), 1.78 (ddd, J_1 = 15.9 Hz, J_2 = 12.9 Hz, J_3 = 5.0 Hz, 3H). ^{13}C NMR (75 MHz) δ (ppm): 357.5 (C^+), 58.6 (3 x CH_2), 37.5 (3 x CH_2), 36.0 (CH), 33.2 (3 x CH_2).

5.4.24 Bicyclo[3.3.3]undeca-1,5-diyl Dication (36)

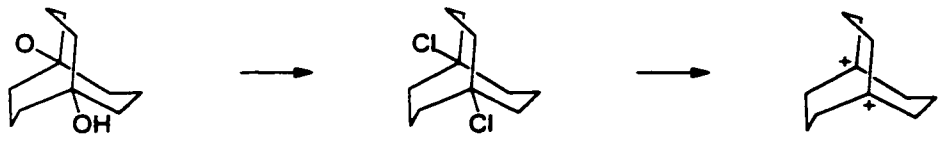

110 112 36

Bicyclo[3.3.3]undecane-1,5-diol **110** (12.6 mg, 0.0683 mmol) was dissolved in dichloromethane (4 mL) cooled to 0°C and conc. hydrochloric acid was added. The resulting mixture was stirred vigorously for 15 min. before the dichloromethane layer was separated using a pipette, filtered through a magnesium sulfate column (approx. 2 g) and concentrated under a stream of nitrogen, keeping the temperature below 5°C. The resulting solid 1,5-dichlorobicyclo[3.3.3]undecane **112** was dissolved in dichloromethane-d_2 (0.15 mL) and added to a solution of antimony pentafluoride (100 mg, 0.461 mmol) in sulfuryl chloridefluoride (total 1.8 mL) at -116°C. The antimony pentafluoride solution was prepared by dissolving the SbF_5 in a small portion of the sulfuryl chloridefluoride (approx. 0.4 mL), transferring it into a 10 mm NMR tube (0.8 mm wall), and condensing the rest of the sulfuryl chloridefluoride on top of the SbF_5 solution. The reaction mixture was then stirred with a tungsten wire to form a clear, slightly yellowish solution which was used directly for NMR analysis. This solution was found to be "metastable" in terms of solubility. Warming the reaction mixture to -78°C caused, to a large extent, irreversible precipitation of the dication. No precipitation was observed when the reaction solution was kept at -116°C over a period of several hours. Further warming of the precipitate-solution above -78°C brought about decomposition into a complex mixture within 20 min. At 221 K 80 % of the dication had decomposed within 20 min. The energy barrier for dication decomposition was determined to be about 15.4 ± 0.5 kcal/mol. Decomposition of this dication into a complex mixture only occurs in the presence of dichlormethane-d_2 in the reaction mixture. The absence of this solvent leads to a clean rearrangement of the bicyclo[3.3.3]undeca-1,5-diyl dication **36** into 3,7-dimethylbicyclo[3.3.1]nonyl dication **37** (see below). The hydrogen and carbon NMR data for dication **36** were in agreement with published values.[183]

^{1}H NMR (168 K, 300 MHz) δ (ppm): 4.39 (s, br, 12H), 3.52 (s, br, 3H), 3.17 - 2.90 (m, br,

3H). ^{13}C NMR (168 K, 75 MHz) δ (ppm): 347.0 (C^+), 58.1 (6 x CH_2), 23.6 (3 x CH_2).

Dication rearrangement:

36 **134** **37**

Bicyclo[3.3.3]undecane-1,5-diol **110** (20.0 mg, 0.109 mmol) was dissolved in dichloromethane (4 mL), cooled to 0°C and conc. hydrochloric acid was added. The resulting mixture was intensely stirred for 15 min. before the dichloromethane layer was separated using a pipette, filtered through a magnesium sulfate column (approx. 2 g) and concentrated under a stream of nitrogen, in a 5 mm NMR tube (0.5 mm wall) keeping the temperature below 5°C. The NMR tube was then cooled to -116°C , sulfuryl chloridefluoride (0.4 mL) was condensed into it and a precooled solution of antimony pentafluoride (300 mg, 1.38 mmol) in sulfuryl chloridefluoride (0.4 mL) was added. Stirring the reaction mixture with a tungsten wire produced a slightly yellowish, clear solution. Keeping this reaction mixture at -78°C for 10 hours caused partial rearrangement of the bicyclo[3.3.3]undeca-1,5-diyl dication **36** into 2,7-dimethylbicyclo[3.3.1]nona-2,7-diyl dication **134** and 3,7-dimethylbicyclo[3.3.1]nona-3,7-diyl dication **37**. The rate for the rearrangement into 2,7-dimethylbicyclo[3.3.1]nona-2,7-diyl dication **134** was measured at 216 K (9 % of the dication **36** rearranged within 5 min.) and at 221 K (36 % of the dication **36** rearranged with 30 min.) and gave an energy barrier of 16.4 ± 0.3 kcal/mol. Further warming to 232 K and maintaining this temperature for 30 min. converted 32 % of the 2,7-dimethylbicyclo[3.3.1]nona-2,7-diyl dication **134** into the 3,7-dimethylbicyclo[3.3.1]undeca-3,7-diyl dication **37** with an associated energy barrier of 17.3 ± 0.4 kcal/mol. This final dication proved to be thermally very stable and experienced only approximately 40 % decomposition into a complex mixture when kept at -18°C for 1 week. This corresponds to an activation barrier of 21.9 kcal/mol.

2,7-Dimethylbicyclo[3.3.1]nona-2,7-diyl dication (**134**): ^1H NMR (189 K, 300 MHz) δ (ppm): 4.91 - 4.72 (m, 3H), 4.65 - 4.45 (m, 2H), 4.10 (s, br, 2H), 4.00 (s, 3H), 3.94 (s, br, 3H), 3.48 - 3.23 (m, 3H), 3.06 - 2.93 (m, 1H), 2.86 (s, 1H). ^{13}C NMR (189 K, 75 MHz) δ (ppm):

329.3 (C^+), 323.6 (C^+), 65.4 (CH_2), 63.1 (CH), 59.1 (CH_2), 57.7 (CH_2), 54.0 (CH_2), 54.0 (CH_2), 46.8 (CH_3), 46.8 (CH_3), 32.8 (CH).

3,7-Dimethylbicyclo[3.3.1]undeca-3,7-diyl dication **(37)**: ^{1}H NMR (210 K, 300 MHz) δ (ppm): 4.63 (d, br, J = 18.8 Hz, 4H), 4.25 (dd, J_1 = 15.3 Hz, J_2 = 6.3 Hz, 4H), 3.66 (p, J = 3.4 Hz, 6H), 3.14 (s, 2H), 2.28 (s, 2H). ^{13}C NMR (210 K, 75 MHz) δ (ppm): 332.3 (2 x C^+), 64.0 (4 x CH_2), 45.3 (2 x CH_3), 26.3 (2 x CH), 25.7 (CH_2).

5.4.25 Ionic reduction of Bicyclo[3.3.3]undeca-1,5-diyl Dication (36)

5.4.25.1 Reduction with Isopentane

112 **36** **78**

Bicyclo[3.3.3]undecane-1,5-diol **110** (15.6 mg, 0.0847 mmol) was converted into the corresponding dichloride and subsequently ionized into the bicyclo[3.3.3]undeca-1,5-diyl dication **36** as described previously (see Section 5.4.24, page 250). To the clear dication solution isopentane (12 μL, 0.268 mmol) was added at -116°C and the resulting mixture was thoroughly stirred. Reduction of the dication **36** to the bicyclo[3.3.3]undec-1-yl cation **78** occurred instantly, and quantitatively. No further reduction of the bicyclo[3.3.3]undecyl system to the hydrocarbon could be observed. Warming the reaction mixture to 221 K caused line broadening of all signals due to rapid intermolecular hydride shifts between the excess isopentane and the various monocations present.

Isopentane: ^{1}H NMR (189K, 300 MHz) δ (ppm):1.45 (nonet, J = 6.7 Hz, 1H), 1.22 (p, J = 7.1 Hz, 2H), 0.92 (t, J = 7.1 Hz, 3H), 0.91 (d, J = 6.7 Hz, 6H). ^{13}C NMR (189 K, 75 MHz) δ (ppm): 32.1 (CH_2), 30.4 (CH), 22.4 (2 x CH_3), 12.3 (CH_3).

Isopentyl cation: ^{1}H NMR (189K, 300 MHz) δ (ppm): 4.19 (decuplet, J = 5.2 Hz, 2H), 3.72 (t, J = 5.2 Hz, 6H), 1.57 (t, J = 5.4 Hz, 3H). ^{13}C NMR (189 K, 75 MHz, $CDCl_3$) δ (ppm): 335.9 (C^+), 58.0 (CH_2), 45.5 (2 x CH_3), 9.9 (CH_3).

Bicyclo[3.3.3]undec-1-yl cation **(78)**: ^{1}H NMR (189K, 300 MHz) δ (ppm): 4.08 - 3.89 (m,

3H), 3.85 (s, br, 3H), 3.04 - 2.75 (m, 6H), 2.54 (q, J = 8.12 Hz, 1H), 2.02 - 1.88 (m, 3H), 1.78 (ddd, J_1 = 15.9 Hz, J_2 = 12.9 Hz, J_3 = 5.1 Hz, 3H). ^{13}C NMR (189 K, 75 MHz) δ (ppm): 357.2 (C^+), 58.5 (3 x CH_2), 37.4 (3 x CH_2), 35.8 (CH), 33.1 (3 x CH_2).

5.4.25.2 Reduction with Sodium Borohydride

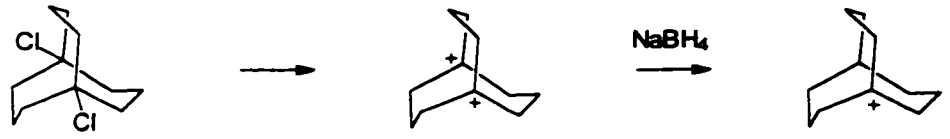

112 **36** **78**

Bicyclo[3.3.3]undecane-1,5-diol **110** (15.6 mg, 0.0847 mmol) was converted into the corresponding dichloride and subsequently ionized into the bicyclo[3.3.3]undeca-1,5-diyl dication **36** as previously described (see Section 5.4.24, page 250). To the clear dication solution, sodium borohydride (4.3 mg, 0.114 mmol) was added at -116°C and the resulting reaction mixture was observed by NMR spectroscopy. At 168 K within a 3 hour period 47 % of the dication was reduced. The reaction was complete after 15 h, leaving a solution of the relatively pure bicyclo[3.3.3]undec-1-yl cation **78**. The NMR data obtained were in accordance with the bicyclo[3.3.3]undec-1-yl cation **78** as previously described in this thesis.

^{1}H NMR (179 K, 300 MHz) δ (ppm): 4.08 - 3.84 (m, 6H), 3.04 - 2.75 (m, 6H), 2.54 (q, J = 7.8 Hz, 1H), 2.02 - 1.88 (m, 3H), 1.78 (ddd, J_1 = 16.0 Hz, J_2 = 12.4 Hz, J_3 = 4.6 Hz, 3H). ^{13}C NMR (179K, 75 MHz) δ (ppm): 357.1 (C^+), 58.3 (3 x CH_2), 37.3 (3 x CH_2), 35.7 (CH), 32.9 (3 x CH_2).

5.4.25.3 Reduction with Hydrogen

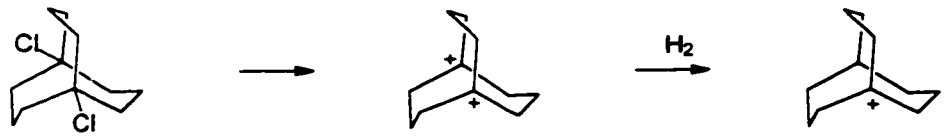

112 **36** **78**

Bicyclo[3.3.3]undecane-1,5-diol **110** (9.80 mg, 0.0532 mmol) was converted into the corresponding dichloride and subsequently ionized into the bicyclo[3.3.3]undeca-1,5-diyl

dication **36** (see Section 5.4.24, page 250) in a thick wall NMR tube, which was then attached to a pressure adapter, cooled to -116°C (slush of frozen EtOH), and the solution was hydrogenated at 8 bars for 6 hours. The argon atmosphere present from the cation generation was replaced by hydrogen, performing 5 vacuum-pressure cycles (evacuating the sample (12 mmHg) and pressurizing it again with 8 bars of hydrogen). The resulting solution consisted of a mixture of 69 % bicyclo[3.3.3]undec-1-yl monocation **78** and 31 % bicyclo[3.3.3]undeca-1,5-diyl dication **36**. ^{1}H and ^{13}C NMR data were consistent with values obtained for the pure mono **78** or dication **36** respectively.

^{1}H NMR (200 K, 300 MHz) δ (ppm): 4.08 - 3.84 (m, br, 6H), 3.04 - 2.75 (m, 6H), 2.54 (s, br, 1H), 2.02 - 1.78 (m, 6H). ^{13}C NMR (200 K, 75 MHz) δ (ppm): 357.4 (C^{+}), 58.8 (3 x CH_2), 37.6 (3 x CH_2), 36.0 (CH), 33.2 (3 x CH_2).

5.4.26 2-Methylbicyclo[3.3.3]undec-1-yl Cation (192)

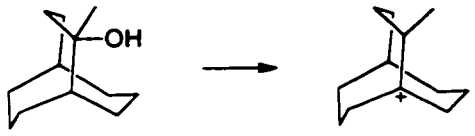

191 **192**

2-Methylbicyclo[3.3.3]undecan-2-ol **191** (17.2 mg, 0.0943 mmol) in dichloromethane-d_2 (0.15 mL) was added to a solution of antimony pentafluoride (100 mg, 0.461 mmol), fluorosulfonic acid (70.0 μL, 1.22 mmol) and sulfuryl chloridefluoride (1.8 mL) in a 10 mm NMR tube (0.8 mm wall) at -116°C. The super acid solution was prepared by dissolving the SbF_5 in an aliquot of the sulfuryl chloridefluoride (0.4 mL) and transferring it into the NMR tube followed by the addition of the fluorosulfonic acid, and then condensing sulfuryl chloridefluoride on top of the Magic acid solution. The addition of the dichloromethane solution of the bicyclic alcohol caused instant precipitation of the alcohol and partial freezing of the dichloromethane. This mixture was then vigorously stirred with a tungsten wire to form a slightly yellow, clear solution of the 2-methylbicyclo[3.3.3]undec-1-yl cation **192**. Warming the cation solution to 211 K for 25 min. caused 50 % of the cation to decompose into a complex mixture. The energy barrier for this decomposition was measured as 15.2 ± 0.7

kcal/mol.

^{1}H NMR (168 K, 300 MHz) δ (ppm): 4.64 (sestet, br, J = 3.3 Hz, 1H), 4.31 - 3.58 (m, 4H), 3.53 (s, 1H), 3.19 - 2.79 (m, 2H), 2.69 (s, br, 1H), 2.61 - 2.11 (m, 2H), 2.10 - 0.90 (m, 10H). ^{13}C NMR (168 K, 75 MHz) δ (ppm): 361.6 (C^+), 61.1 (CH), 58.7 (CH_2), 55.8 (CH_2), 45.0 (CH_2), 37.8 (CH_2), 36.9 (CH_2), 35.8 (CH), 33.4 (CH_2), 33.0 (CH_2), 30.6 (CH_2), 20.5 (CH_3).

5.4.27 9-Methylbicyclo[3.3.2]dec-9-yl cation (190)

102 **190**

A solution of antimony pentafluoride (100 mg, 0.461 mmol), fluorosulfonic acid (70.0 µL, 1.22 mmol) and sulfuryl chloridefluoride (0.4 mL) was transferred into a 10 mm NMR tube (0.8 mm wall) and cooled to -135°C. On top of the Magic acid, a sulfuryl chloridefluoride layer was condensed in such a way that no mixing occurred. At -135°C, a solution of bicyclo[3.3.2]undec-9-ene **102** in dichloromethane-d_2 (0.15 mL) was added and the resulting mixture was intensely mixed with a tungsten wire until a clear nearly colorless solution was obtained. NMR analysis revealed the presence of two rearranged carbocations, whose structures could not be determined solely with hydrogen, carbon and DEPT NMR spectra. Warming the solution to 211 K for 55 min. caused about 60 % decomposition of the two cations into a complex mixture, which corresponds to an energy barrier of 14.7 kcal/mol. However, no rearrangement into the 9-ethylbicyclo[3.3.1]non-9-yl (**38**) or methyldecalyl cation (**39**) could be observed.

^{1}H NMR (300 MHz) δ (ppm): 4.10 - 3.43 (m, 4H), 3.33 - 2.63 (m, 2H), 2.47 - 0.77 (m, 13H). ^{13}C NMR (75 MHz) δ (ppm): 327.0 (C^+), 315.4 (C^+), 76.0 (Cq), 67.0 (CH_2), 60.4 (CH), 51.0 (CH_2), 48.1 (CH_2), 44.4 (CH_2), 38.4 (CH_2), 36.5 (CH_3), 32.8 (CH_2), 29.8 (CH_2), 23.7 (CH_2), 22.7 (CH_2), 21.6 (CH_2), 17.9 (CH_3), 17.0 (CH_3), 14.5 (CH_3).

5.4.28 9-Methylbicyclo[3.3.1]non-9-yl Cation (199)

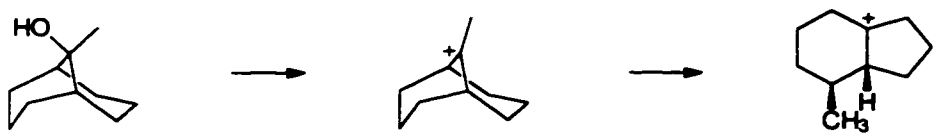

203 **205** **207**

A solution of antimony pentafluoride (100 mg, 0.461 mmol), fluorosulfonic acid (70.0 µL, 1.22 mmol) and sulfuryl chloridefluoride (1.8 mL) was cooled to -135°C and a solution of 9-methylbicyclo[3.3.1]nonan-9-ol **197** in dichloromethane d_2 (0.15 mL) was added. The resulting mixture was stirred with a tungsten wire until a clear, nearly colorless solution had formed. The resulting cation solution consisted of the 9-methylbicyclo[3.3.1]non-9-yl cation **199** with high purity. Rearrangement into the cis-5-methylbicyclo[4.3.0]non-1-yl cation **201** occurred to the extent of 49 % by warming the sample to 157 K for 15 min., corresponding to an activation energy of 11.3 ± 0.2 kcal/mol (the cis stereochemistry of **201** could be assigned using COSY and C-H HETCOR 2D NMR spectroscopy, see Figure 96 and 97). Further warming caused the cation solution to decompose into a complex mixture of at least 5 different classical and nonclassical carbocations. The 9-methylbicyclo[3.3.3]non-9-yl cation **199** was already known, and the spectral data was in agreement with the published data.[190]

9-Methylbicyclo[3.3.1]non-9-yl cation **199**: ^{1}H NMR (148 K, 300 MHz) δ (ppm): 4.34 (s, br, 2H), 3.60 (s, 3H), 2.93 (s, br, 4H), 2.74 (s, br, 4H), 2.13 - 1.89 (m, 2H), 1.47 - 1.15 (m, 2H). ^{13}C NMR (148 K, 75 MHz) δ (ppm): 326.4 (C^+), 68.8 (2 x CH), 49.4 (br, 4 x CH_2), 41.8 (CH_3), 20.6 (2 x CH_2).

cis-5-Methylbicyclo[4.3.0]non-1-yl cation **201**:

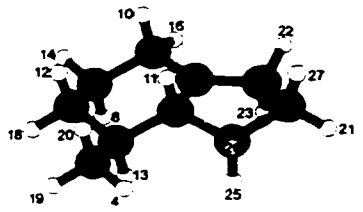

201

^{1}H NMR (179 K, 300 MHz) δ (ppm): 4.29 (**22**, dd, J_1 = 23.4 Hz, J_2 = 7.2 Hz, 1H), 4.16 (**16**, d, br, J = 19.6 Hz, 1H), 3.82 - 3.60 (**23**, m, 1H), 3.60 - 3.36 (**10**, m, 1H), 3.09 (**11**, m, 1H), 2.70

(**25**, s, br, 1H), 2.61 - 2.35 (**14, 21**, m, 2H), 2.24 (**13**, s, br, 1H), 2.13 - 1.93 (**8, 18, 27**, m, 3H), 1.93 - 1.77 (**26**, m, 1H), 1.76 - 1.58 (**12**, t, J = 12.7, 1H), 1.30 (**4, 19, 20**, d, J = 6.4 Hz, 3H). ^{13}C NMR (179 K, 75 MHz) δ (ppm): 331.3 (**15**, C^+), 80.6 (**6**, CH), 60.2 (**9**, CH_2), 48.5 (**5**, CH_2), 42.0 (**2**, CH), 31.4 (**3**, CH_2), 30.5 (**7**, CH_2), 27.6 (**17**, CH_2), 24.1 (**24**, CH_2), 20.2 (**1**, CH_3).

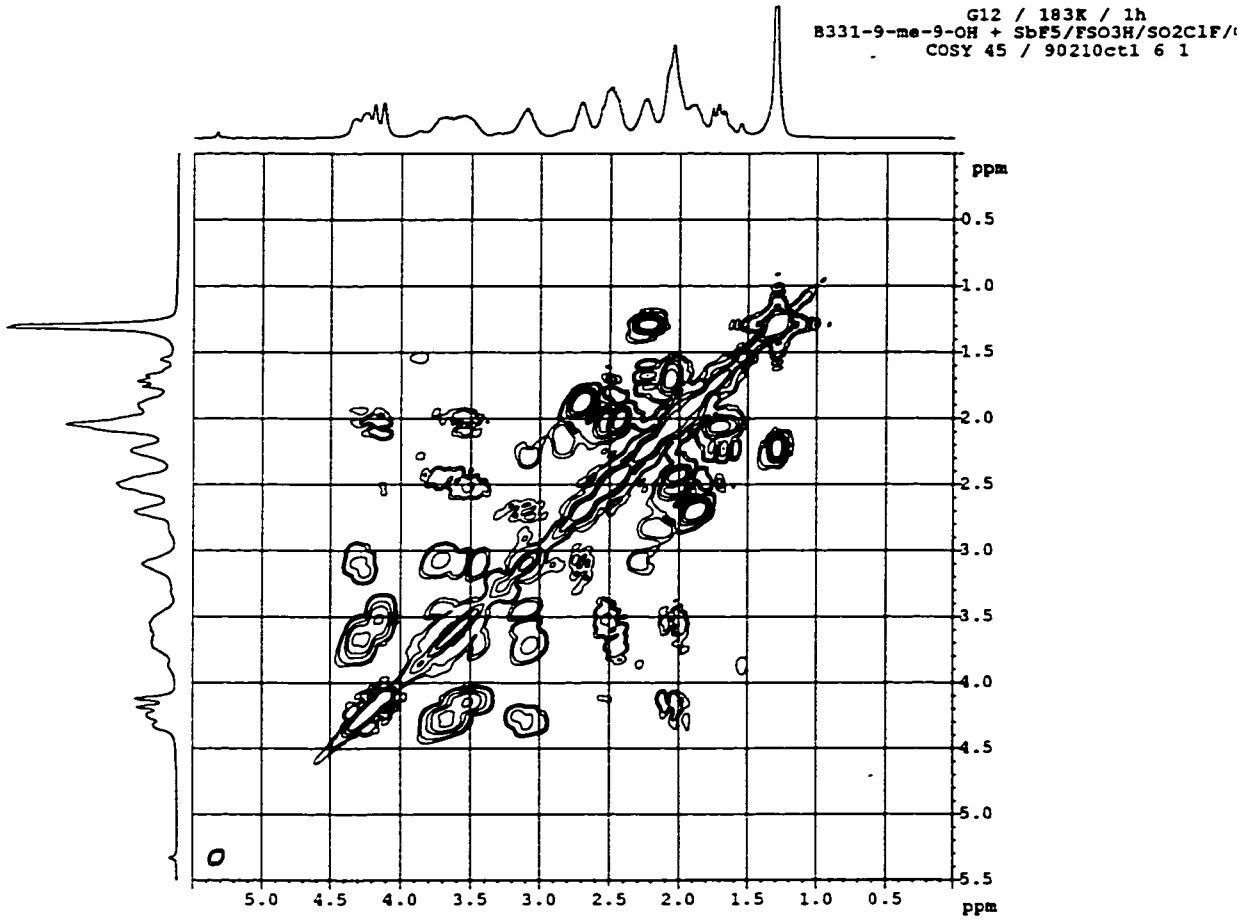

Figure 96: COSY NMR spectrum of the cis-9-methylbicyclo[4.3.0]non-1-yl cation at 179 K **201**.

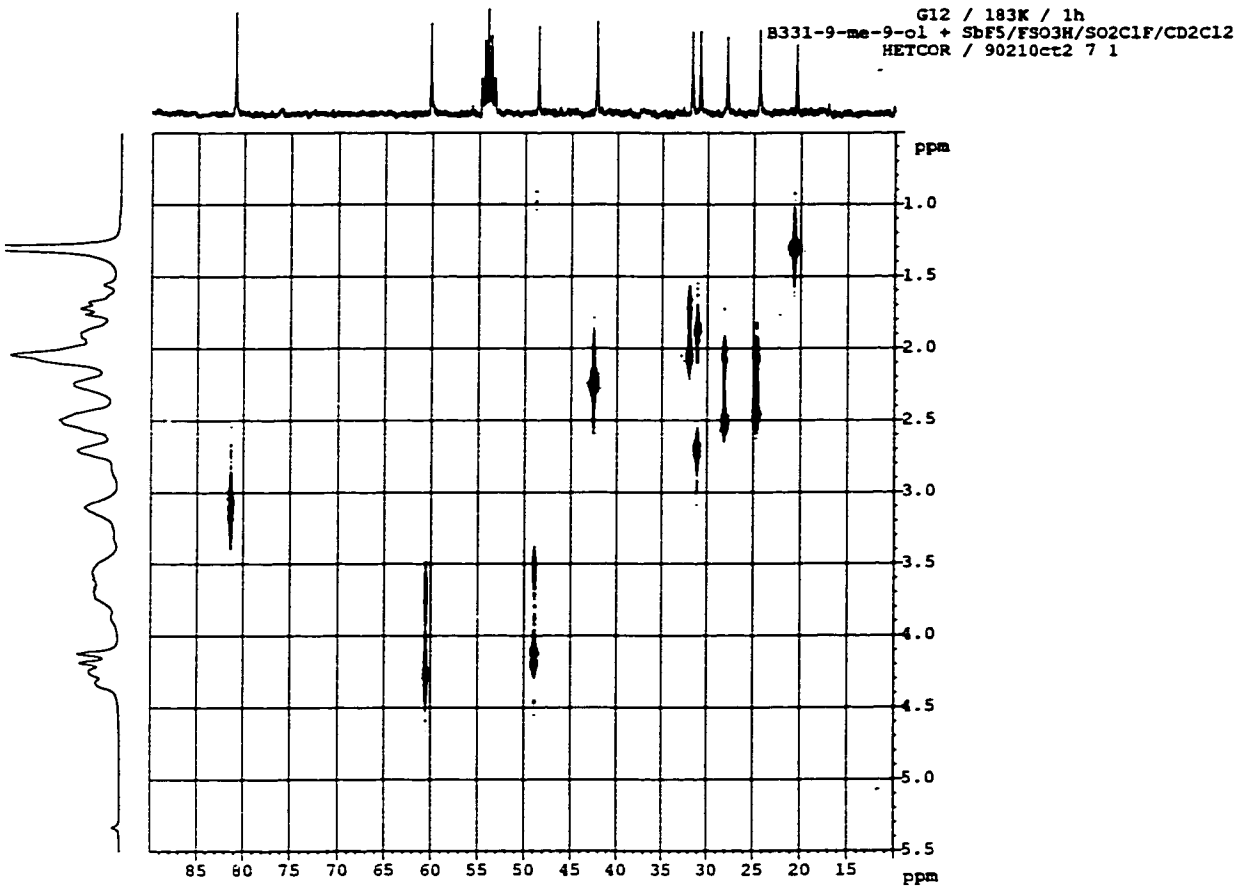

Figure 97: H-C HETCOR NMR spectrum of the cis-9-methylbicyclo[4.3.0]non-1-yl cation **201**.

5.4.29 9-Ethylbicyclo[3.3.1]non-9-yl Cation (38)

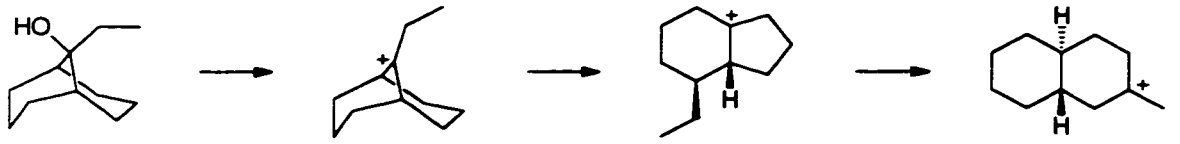

195 38 202 39

Method a: A solution of antimony pentafluoride (100 mg, 0.461 mmol), fluorosulfonic acid (70.0 μL, 1.22 mmol) and sulfuryl chloridefluoride (1.8 mL) was cooled to -130°C and a solution of 9-ethylbicyclo[3.3.1]nonan-9-ol **195** in dichloromethane-d_2 (0.15 mL) was added. The resulting mixture was stirred with a tungsten wire until a clear, nearly colorless solution had formed. This solution consisted of a mixture of the 9-ethylbicyclo[3.3.1]non-9-yl **38**, and the rearranged cis-5-ethylbicyclo[4.3.0]non-1-yl cation **202** (the cis stereochemistry of this rearrangement product could be assigned using COSY and C-H HETCOR 2D NMR spectroscopy, see Figures 98 and 99).

Method b: The 9-ethylbicyclo[3.3.1]nonan-9-ol **195** (17.1 mg, 0.102 mmol) was converted into the corresponding chloride by dissolving the alcohol in dichloromethane (4 mL), cooling the solution to 0°C and adding conc. hydrochloric acid (4 mL). The resulting mixture was stirred intensely for 15 min. before the layers were allowed to separate. The dichloromethane layer was then passed through a column of magnesium sulfate (2 g) and concentrated under a nitrogen stream in a 10 mm NMR tube (wall 0.8 mm) (the sample temperature was maintained below 5°C at all times). Sulfuryl chloridefluoride (1 mL) was added to the sample and the mixture cooled to -130°C, before a precooled (-78°C) solution of antimony pentafluoride (100 mg, 0.461 mmol) in sulfuryl chloridefluoride was added. Using a tungsten wire, the reaction mixture was stirred until a nearly colorless, clear solution had formed. This cation solution consisted of the 9-ethylbicyclo[3.3.1]non-9-yl cation **38** of high purity. Maintaining the sample for 1 hour at 168K induced 83 % of the initial cation to rearrange into the cis-5-ethylbicyclo[4.3.0]non-1-yl cation **202**. This corresponds to an activation barrier of 12.2 ± 0.1 kcal/mol.

Once rearranged into the cis-5-ethylbicyclo[4.3.0]non-1-yl cation **202** the solutions prepared either by method **a** or **b** behaved identically. Maintaining them at 200K for 1h induced further

rearrangement to the trans-2-methyldecalyl cation **39** to an approximate 67 % extent, which corresponds to a 15.4 ± 0.6 kcal/mol energy barrier.

9-Ethylbicyclo[3.3.1]undec-9-yl cation **38**: ^{1}H NMR (158 K, 300 MHz) δ (ppm): 4.28 (s, 2H), 3.96 (q, J = 5.1 Hz, 2H), 2.89 (s, br, 4H), 2.65 (s, br, 4H), 2.02 (m, 2H), 1.53 (t, J = 5.3 Hz, 3H), 1.32 (m, 2H). ^{13}C NMR (158K, 75 MHz) δ (ppm): 328.1 (C^{+}), 65.2 (2 x CH), 50.0 (CH_2), 48.4 (br, 4 x CH_2), 20.5 (CH_2), 9.06 (CH_3).

cis-5-Ethylbicyclo[4.3.0]undec-1-yl cation **202**:

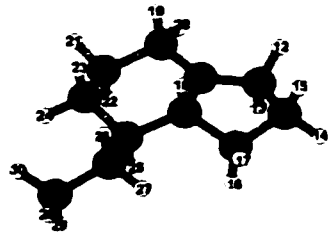

202

^{1}H NMR (179 K, 300 MHz, $CDCl_3$) δ (ppm): 4.25 (**12**, d, br, J = 24.1 Hz, 1H), 4.12 (**20**, d, J = 18.9 Hz, 1H), 3.79 - 3.62 (**13**, m, br, 1H), 3.61 - 3.48 (**19**, m, br, 1H), 3.30 - 3.11 (**18**, m, br, 1H), 2.80 - 2.52 (**21**, **24**, m, 2H), 2.45 (**14**, m, 1H), 2.29 - 1.76 (**15**, **17**, **22**, **23**, **25**, **27**, m, 6H), 1.71 - 1.38 (**16**, **26**, m, 2H), 1.06 (t, J = 13.2 Hz, 3H). ^{13}C NMR (179 K, 75 MHz, $CDCl_3$) δ (ppm): 326.7 (**5**, C^{+}), 82.9 (**4**, CH), 59.9 (**1**, CH_2), 49.8 (**9**, CH), 48.7 (**6**, CH_2), 31.1 (**7**, CH_2), 28.9 (**8**, CH_2), 28.1 (**10**, CH_2), 28.0 (**3**, CH_2), 24.4 (**2**, CH_2), 11.0 (**11**, CH_3).

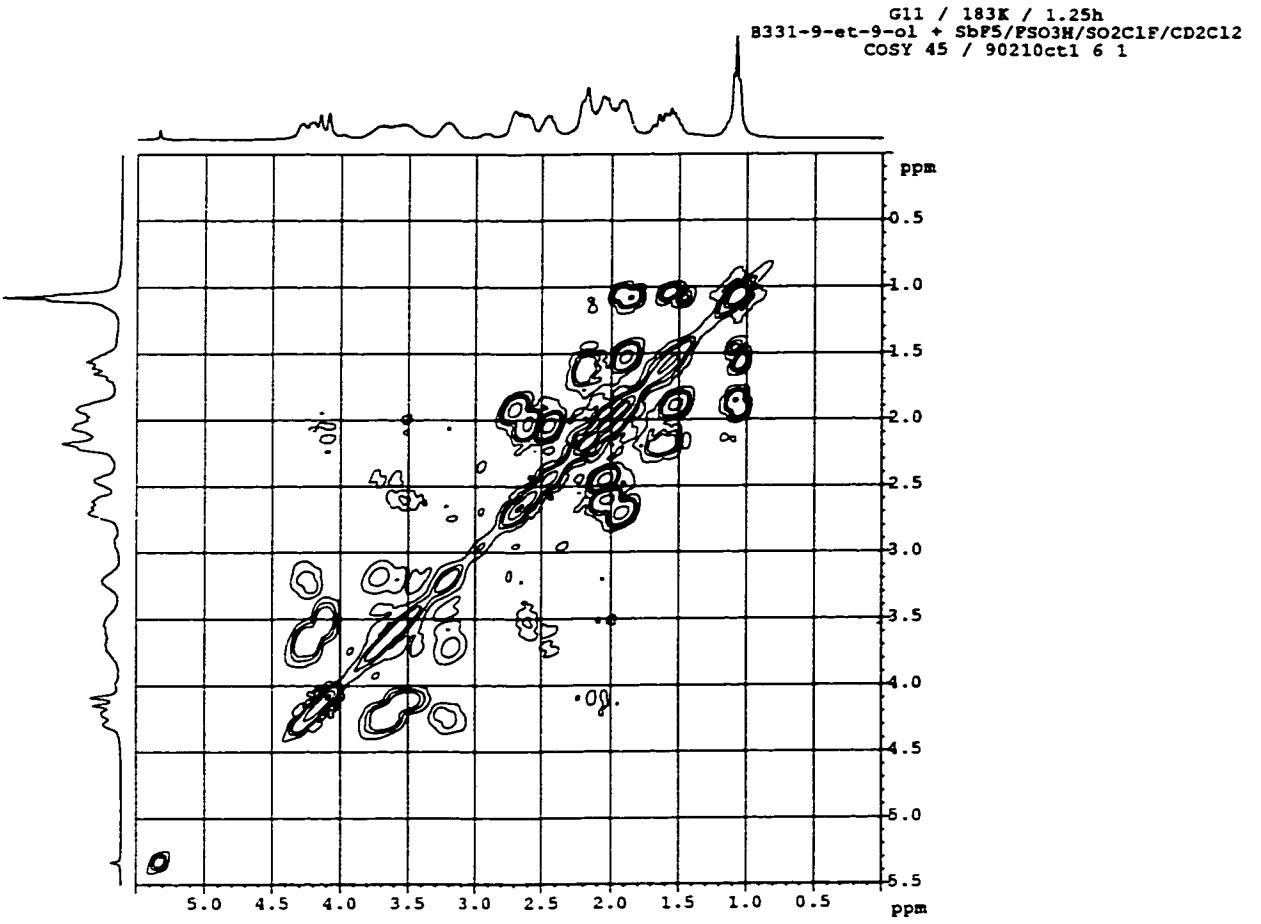

Figure 98: COSY NMR spectrum of the cis-9-ethylbicyclo[4.3.0]non-1-yl cation **202**.

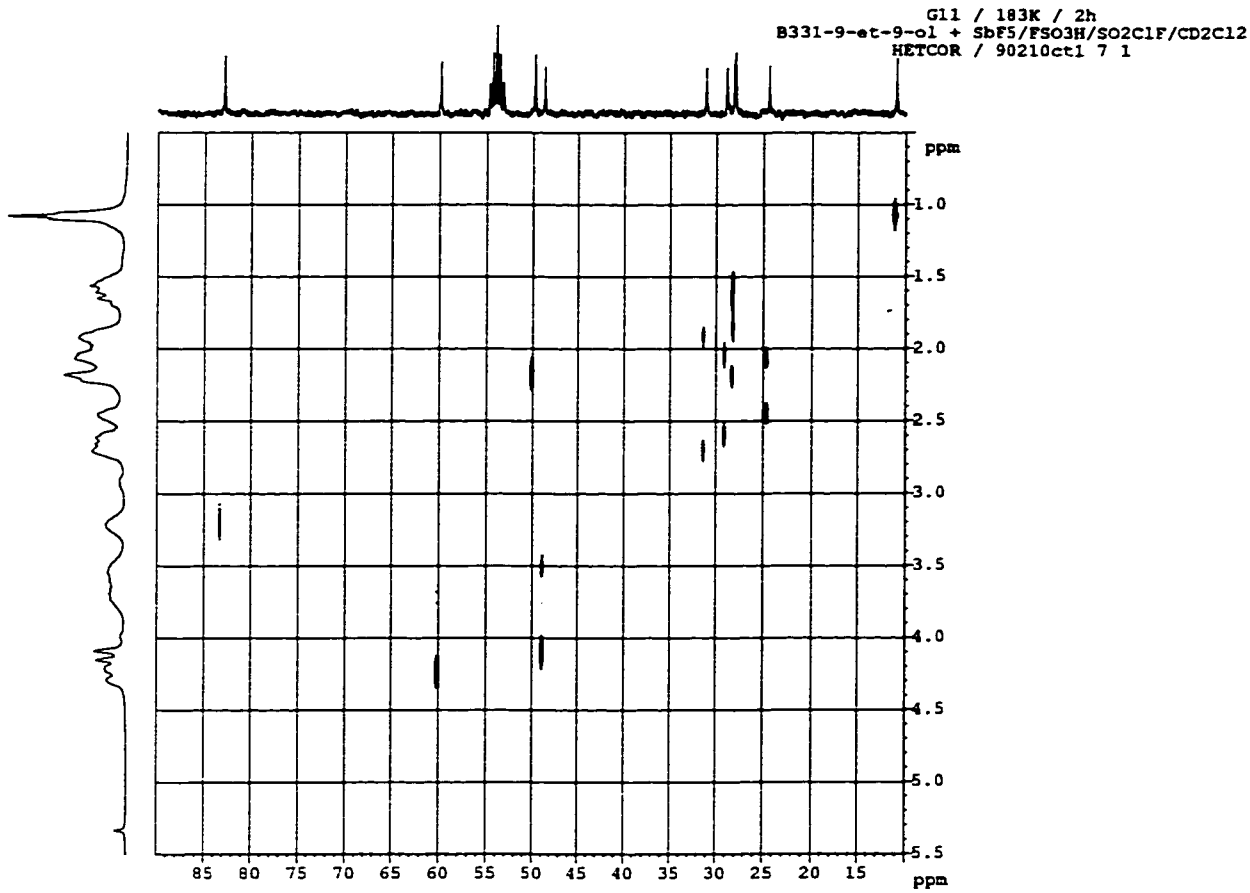

Figure 99: C-H HETCOR NMR spectrum of the cis-9-ethylbicyclo[4.3.0]non-1-yl cation **202**.

trans-2-Methyldecalyl cation **39**: ^{1}H NMR (221 K, 300 MHz) δ (ppm): 4.20 (d, J= 10.3 Hz, 2H), 3.67 (s, 3H), 3.49 (s, 2H), 2.74 - 2.59 (m, 1H), 2.16 - 1.81 (m, 6H), 1.55 (p, J= 12.7 Hz, 2H), 1.45 - 1.25 (m, 2H), 1.11 (t, J= 11.5 Hz, 1H). ^{13}C NMR (221 K, 75 MHz) δ (ppm): 325.7 (C^{+}), 65.7 (CH_2), 59.0 (CH_2), 53.6 (CH), 44.1 (CH_3), 42.2 (CH_2), 41.2 (CH), 35.8 (CH_2), 32.1 (CH_2), 26.5 (CH_2), 26.1 (CH_2).

5.4.30 Protonated 1,3-Dimethyl-2-oxatricyclo[3.3.1.1^{3,7}]decane (157)

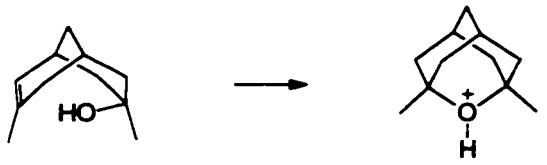

179 157

3-endo 3,7-Dimethylbicyclo[3.3.1]non-6-en-3-ol **179** (18.9 mg, 0.114 mmol) was added to a 10 mm NMR tube (wall 0.8 mm) cooled to -78°C and mixed with sulfuryl chloridefluoride (1 mL). The resulting solution was then cooled to -116°C before a precooled solution (-78°C) of antimony pentafluoride (100 mg, 0.461 mmol), fluorosulfonic acid (70.0 µl, 1.22 mmol) and sulfuryl chloridefluoride (0.8 mL) was added. The resulting solution was mixed with a tungsten wire to form a colorless, clear solution containing **157** as the sole product.

^{1}H NMR (168K, 300 MHz) δ (ppm): 7.87 (s, 1H), 2.69 (s, 2H), 2.45 (d, J = 14.5 Hz, 4H), 2.28 (d, J = 14.5 Hz, 4H), 2.19 (s, 1H), 1.91 (s, 6H). ^{13}C NMR (168K, 75 MHz) δ (ppm): 101.9 (2 x Cq), 40.0 (4 x CH_2), 32.3 (CH_2), 27.9 (2 x CH_3), 26.9 (2 x CH).

5.4.31 Protonated 3-Methyl-4-oxatricyclo[4.3.1.1.^{3,8}]undecane (173), and Protonated 7-endo 7-Hydroxymethyl-3-methylbicyclo[3.3.1]non-3-yl Cation (174)

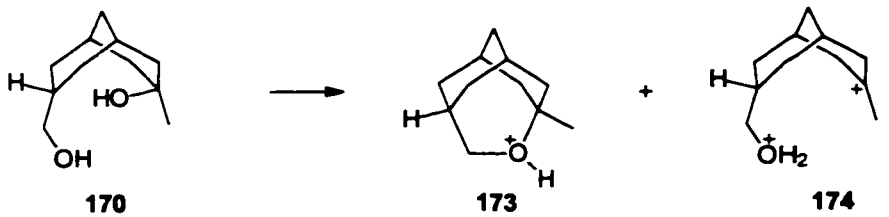

170 173 174

3-endo, 7endo 3-Hydroxymethyl-7-methylbicyclo[3.3.1]nonan-7-ol **170** (16.8 mg, 0.0912 mmol) was added to a 10 mm NMR tube (wall 0.8 mm) cooled to -78°C and mixed with sulfuryl chloridefluoride (1 mL). The resulting solution was then cooled to -116°C before a precooled solution (-78°C) of antimony pentafluoride (100 mg, 0.461 mmol), fluorosulfonic acid (70.0 µl, 1.22 mmol), and sulfuryl chloridefluoride (0.8 mL), was added. The resulting solution was mixed with a tungsten wire to form a nearly colorless, clear solution. This

solution consisted of protonated 3-methyl-6-oxatricyclo[4.3.1.1.^{3,8}]undecane **173**, and protonated 7-endo 7-hydroxymethyl-3-methylbicyclo[3.3.1]non-3-yl cation **174**, in a ratio of 1: 0.61 according to ^{1}H NMR.

^{1}H NMR (168 K, 300 MHz) δ (ppm): 2 cations combined: 9.51 (s, 1H), 8.27 (s, 0.61H), 4.82 (s, 1.59H), 4.74 - 4.31 (3.20H), 4.01 (s, br, 1.88H), 3.74 (s, br, 2.49H), 2.93 (s, 1.62H), 2.53 (s, br, 2.96 H), 2.43 - 2.07 (m, 7.79H), 2.06 - 1.49 (m, 6.70H), 1.15 - 0.62 (m, 1.43H). ^{13}C NMR (168 K. 75 MHz) δ (ppm): protonated 3-methyl-6-oxatricyclo[4.3.1.1.^{3,8}]undecane **173**: 110.3 (Cq), 88.1 (CH_2), 41.9 (2 x CH_2), 35.6 (2 x CH_2), 32.9 (CH_2), 32.7 (CH), 29.9 (CH_3), 26.8 (2 x CH), protonated 7-endo 7-hydroxymethyl-3-methylbicyclo[3.3.1]non-3-yl cation **174**: 334.5 (C^+), 81.0 (CH_2), 68.4 (2 x CH_2), 47.4 (CH_3), 31.4 (CH_2), 28.3 (CH), 26.3 (2 x CH), 24.2 (CH_2).

5.4.32 3,7-Dimethylbicyclo[3.3.1]nona-3,7-diyl Dication (37) (from 3,7-Dimethylbicyclo[3.3.1]nona-2,6-diene)

167 **37**

3,7-Dimethylbicyclo[3.3.1]nona-2,7-diene **167** (1.30 mg, 0.00877 mmol) was added to a 10 mm NMR tube (wall 0.8 mm) cooled to -78°C and mixed with sulfuryl chloridefluoride (1 mL). The resulting solution was then cooled to -135°C before a precooled solution (-78°C) of antimony pentafluoride (200 mg, 0.923 mmol), fluorosulfonic acid (70.0 µl, 1.22 mmol) and sulfuryl chloridefluoride (0.8 mL) was added. These were then mixed with a tungsten wire to form a yellowish solution. The spectral data obtained were in accordance with the same cation obtained by the rearrangement of the bicyclo[3.3.3]undeca-1,5-diyl dication **37**.

^{1}H NMR (179 K, 300 MHz) δ (ppm): 4.65 (d, br, J = 17.8 Hz, 4H), 4.27 (d, br, J = 15.1 Hz, 4H), 3.66 (s, 6H), 3.13 (s, 2H), 2.27 (s, 2H). ^{13}C NMR (179 K, 75 MHz) δ (ppm): 333.6, 64.0, 45.0, 26.1, 25.8.

5.5 Tricyclo[5.3.1.1^{3,9}]dodecyl System

5.5.1 1-Dichloromethyladamantane (114)

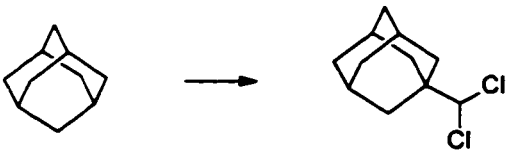

114

Adamantane (55.4 g, 0.407 mol), sodium hydroxide solution (50 % (w/w), 812 mL), benzene (82 mL) and triethylphenylammonium chloride (1.64 g) were heated to 40°C. Under vigorous stirring, chloroform (328 mL, 489 g, 4.09 mol) was added dropwise over a period of 36 h (formation of a brown-black suspension) followed by a 30 min. heating period at 40°C. To the resulting mixture, sulfuric acid (40 % in water) was added until the reaction mixture was acidic and then ether (300 mL) was added. The emulsion formed was filtered through a sintered glass filter funnel, and the residue was washed with ether (50 mL). The ether layer was separated, and the aqueous solution was extracted with two more 300 mL portions of ether. The combined organic layers were dried with magnesium sulfate and concentrated on the rotavapor, to produce a mixture of 49 % (^{1}H NMR) of 1-dichloromethyladamantane **114** and 48 % (^{1}H NMR) of unreacted adamantane (yield: 95 % based on consumed adamantane). This mixture was used for the following step without further purification. The NMR data obtained agreed with the literature values.[182]

GC-MS m/z (rel. intensity): 39 (79), 53 (30), 65 (33), 79 (89), 91 (100), 107 (29), 135 (61), 183 (0.14), 185(0.07), 218 (0.88), 219 (0.25), 220 (0.70), 221 (0.17), 222 (0.08) ^{1}H NMR (200 MHz, $CDCl_3$) δ (ppm):5.40 (s, 1H), 2.19 (t, br, 3H), 1.64 - 1.80 (m, 12H) ^{13}C NMR (50 MHz, $CDCl_3$) δ (ppm): 83.9 (CH), 37.7 (CH_2), 36.5 (Cq), 28.4 (CH_2), 28.17 (CH).

5.5.2 Tricyclo[4.3.1.1^{3,8}]undec-6-one (115)

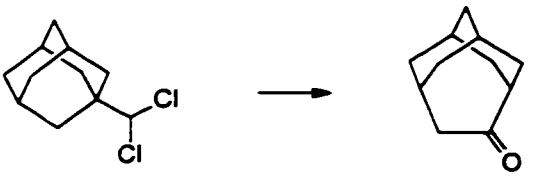

114 115

A mixture of adamantane and 1-dichloromethyladamantane **114** (4.98 g, 57 % 1-dichloromethyl adamantane) was heated with phosphoric acid (85 %, 100 mL) to 120°C for 24 h. After cooling the reaction mixture to room temperature, water (250 mL) was added and the mixture then extracted with ether (3 x 150 mL). The combined organic phases were washed with water (50 mL), sodium bicarbonate solution (5 %, 50 mL), dried with magnesium sulfate and concentrated on the rotavapor to give 4.10 g of a crude mixture. Column chromatography (silica gel 100 g, hexanes-ether 95:5) yielded 1.45 g of pure tricyclo[4.3.1.1^{3,8}]undecan-6-one **115** (yield: 94 % based on consumed starting material). The NMR spectra obtained were in accordance with the literature.[222]

GC-MS m/z (rel. intensity): 41 (100), 53 (41), 67 (31), 79 (74), 91 (43), 107 (10), 135 (14), 164 (17). ^{1}-H NMR (200 MHz, $CDCl_3$) δ (ppm):2.65 (t, J = 6.2 Hz, 1H), 2.51(d, J = 2.6Hz, 2H), 2.14 - 1.90(m, 5H), 1.87 - 1.76 (m, 2H), 1.76 - 1.68 (s, br, 2H), 1.67 - 1.49 (m, 4H). ^{13}C NMR (50 MHz, $CDCl_3$) δ (ppm): 217.9, 49.8, 49.0, 37.2, 34.9, 32.0, 27.0, 26.2.

5.5.3 6-Cyano-6-(trimethylsiloxy)tricyclo[4.3.1.1^{3,8}]undecane (116)

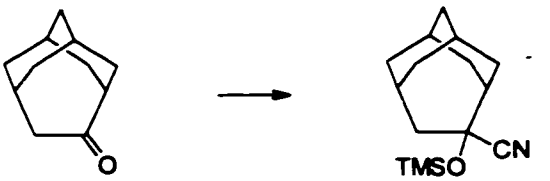

115 116

To a mixture of tricyclo[4.3.1.1^{3,8}]undec-4-one **115** (375 mg, 2.28 mmol) and zinc iodide (50 mg, 0.16 mmol) was added 1 mL TMSCN with cooling (water bath, 10°C). The resulting clear solution was stirred at ambient temperature for 12 h before the excess TMSCN was evaporated under vacuum (15 mmHg). The solid residue was dissolved in ether, washed twice

with a sodium bicarbonate solution (5 %), dried and concentrated on the rotavapor to give 653 mg of solid 6-cyano-6-(trimethylsiloxy)tricyclo[4.3.1.1^{3,8}]undecane **116** (93 % pure by GC, yield: quant.). This product was used for the following steps without further purification.

GC-MS m/z (rel. intensity): 45 (50), 53 (33), 67 (30), 75 (68), 84 (100), 91 (51), 105 (20), 119 (24), 127 (17), 151 (10), 221 (58), 222 (13), 248 (77), 263 (3.56, M^+), 264 (0.55), 265 (0.68). High res. MS found: $M^+ - CH_3$: calc. 248.159643 found 248.1580 (-6.4ppm). IR neat (cm^{-1}): 2953 (m), 2900 (s), 2850 (m), 2222 (w), 1446 (m), 1248 (s), 1088 (s), 841 (s). ^{1}H NMR (200 MHz, $CDCl_3$) δ (ppm): 2.68 (ddd, J = 15.3, 4.3, 1.4, 1H), 2.27 - 2.11 (m, 2H), 2.10 - 1.96 (m, 3H), 1.95 - 1.76 (m, 5H), 1.74 - 1.47 (m, 5H), 0.22 (s, 9H). ^{13}C NMR (200 MHz, $CDCl_3$) δ (ppm): 124.7 (Cq), 77.9 (Cq), 52.2 (CH_2), 43.8 (CH), 38.1 (CH_2), 36.9 (CH_2), 36.3 (CH_2), 33.1 (CH_2), 30.7 (CH), 30.1 (CH_2), 27.1 (CH_2), 1.4 (CH_3).

5.5.4 6-(Aminomethyl)tricyclo[4.3.1.1^{3,8}]undecan-6-ol (117)

116 **117**

A solution of 6-cyano-6-trimethylsiloxytricyclo[4.3.1.1^{3,8}]undecane **116** (2.65 g, 10.1 mmol) in ether (30 mL) was added dropwise to a mixture of lithium aluminum hydride (1.91 g, 50.0 mmol) and ether (20 mL). After completion of addition, the reaction mixture was refluxed for 4 h. Cautious addition of an aqueous solution of potassium hydroxide (200 g/L, 4 mL) produced a white precipitate, which was filtered off after 2 h of stirring. The resulting solution was concentrated to give 2.03 g of a waxy solid, 6-aminomethyltricyclo[4.3.1.1^{3,8}]undecan-6-ol **117** (95 % pure by ^{1}H NMR, yield: 98 %). The spectral data of the amino alcohol agreed with literature values.[181]

IR neat (cm^{-1}): 3363 (m, br), 2897 (s), 1652 (w), 1589 (w), 1446 (m), 960 (m). ^{1}H NMR (200MHz, $CDCl_3$) δ (ppm): 2.86 (d, J = 12.6, 1H), 2.55 (d, J = 13.2, 1H), 2.28 (d, br, J = 13.8, 1H), 2.07 - 1.95(m,2H), 1.94 - 1.79 (m, 7H), 1.79 - 1.48 (m, 8H), 1.42 (d, br, 11.5, 1H). ^{13}C

NMR (50MHz, $CDCl_3$) δ (ppm): 73.6 (Cq), 51.8 (CH_2), 48.2 (CH_2), 38.7 (CH_2), 38.7 (CH), 36.8 (CH_2), 36.6 (CH_2), 31.8 (CH_2), 31.4 (CH_2), 30.4 (CH), 27.7 (CH), 27.6 (CH).

5.5.5 Tricyclo[5.3.1.1^{3,9}]dodecan-6-one and Tricyclo[5.3.1.1^{3,9}]dodecan-7-one (118) and (119)

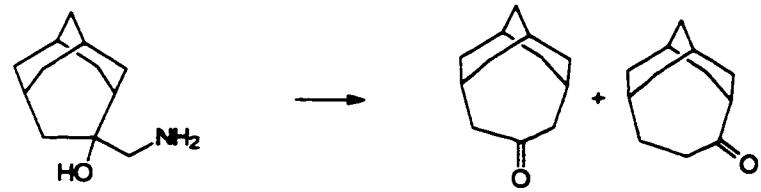

117 118 119

6-(Aminomethyl)tricyclo[4.3.1.1^{3,8}]undecane-2-ol **117** (22.8 g, 117 mmol) was dissolved in a mixture of water (710 mL) and acetic acid (26.7 mL, 467 mmol). At ambient temperature, a solution of sodium nitrite (24.2 g, 351 mmol) in water (210 mL) was added dropwise over a period of 2 h. After completion of the addition, the reaction mixture was heated to 90°C for 2h, then recooled and extracted with ether. The ethereal phase was washed with sodium bicarbonate solution, dried with magnesium sulfate and concentrated on the rotavapor. The waxy solid obtained was purified by column chromatography (silica gel, 500 g, hexanes:ether 95:5). Concentration of the major band eluant yielded 18.78 g product consisting of 96 % (GC) tricyclo[5.3.1.1^{3,9}]dodecane-6-one **118** and tricyclo[5.3.1.1.^{3,9}]dodecan-7-one **119** 3 % (GC) (yield: 90 %). The IR data were in accordance with the literature.[181, 223]

GC-MS m/z (rel. intensity): 41 (94), 53 (42), 67 (44), 79 (100), 91 (44), 107 (7), 115 (7), 122 (5), 135 (5), 147 (5), 149 (4), 166 (2), 178 (M^+, 6). High res. MS (EI): M^+ calc. 178.135765 found: 178.1343 (- 8.22 ppm). ^{1}H-NMR (200 MHz, $CDCl_3$) δ (ppm): 2.59 (t, 2H, J = 6.6Hz), 2.28 (t, 1H, J = 6.9Hz), 1.73 - 2.20 (m, 11H), 1.48 (t, 4H, J = 6.6 Hz). ^{13}C-NMR (50 MHz, $CDCl_3$) δ (ppm): 223.6, 43.2, 39.2, 36.2, 34.8, 34.6, 33.8, 26.5, 25.4.

5.5.6 Tricyclo[5.3.1.1^{3,9}]dodecane (61)

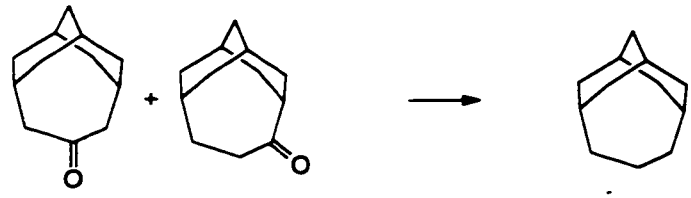

118 119 61

Using the procedure of Nagata *et. al.*[177] a mixture tricyclo[5.3.1.1^{3,9}]dodec-6-one **118** and tricyclo[5.3.1.1^{3,9}]dodec-7-one **119** (0.750 g, 4.21 mmol), hydrazine (55 %, 15.7 mL, 278 mmol), hydrazine dihydrochloride (3.53 g, 33.6 mmol) and triethylene glycol (84.0 mL, 632 mmol) was heated to 130°C for 3 h. The temperature was then increased to 215°C within 30 min., at which point it was kept for 3 h. After cooling the reaction mixture was cooled to room temperature, water (300 mL) was added and the resulting solution was extracted with ether (3 x 50 mL). The combined organic layers were dried with magnesium sulfate, filtered and concentrated on the rotavapor to give 0.87 g crude material. Purification on a column (silica gel, 50 g, hexanes 100 %) yielded 0.64 g of white waxy tricyclo[5.3.1.1^{3,9}]dodecane **61** (96 % pure by GC, yield: 89 %). The following MS and NMR data were in agreement with the published data of Sasaki[181] and Murray.[223]

GC-MS m/z (rel. intesity): 41 (20), 55 (13), 67 (32), 79 (6), 93 (70), 107 (13), 121 (67), 136 (20), 149 (7), 164 (100). ^{1}H NMR (400 MHz, $CDCl_3$) 233K δ (ppm): 2.12 - 1.93 (m, 4H), 1.91 - 1.53 (m, 9H), 1.51 - 1.29 (m, 5H), 1.18 (td, J = 13.8, 2.8, 2H). ^{1}H NMR (400 MHz, $CDCl_3$) 363K δ (ppm): 2.22 - 2.05 (s, br, 2H), 2.04 - 1.88 (m, 4H), 1.87 - 1.76 (s, br, 2H), 1.75 - 1.39 (m, 12H). ^{13}C NMR (100 MHz, $CDCl_3$) 233K δ (ppm): 39.3 (CH_2), 37.0 (CH_2), 35.4 (CH_2), 31.0 (CH_2), 26.2 (CH), 25.2 (CH), 24.9 (CH), 21.4 (CH_2). ^{13}C NMR (100 MHz, $CDCl_3$) 363K δ (ppm): 37.5 (CH_2), 36.0 (CH_2), 35.7 (CH_2), 26.5 (CH), 25.7 (CH), 21.7 (CH_2).

5.5.7 Tricyclo[5.3.1.1^{3,9}]dodecan-5-ol and Tricyclo[5.3.1.1^{3,9}]dodecane-5,9-diol (120) and (121)

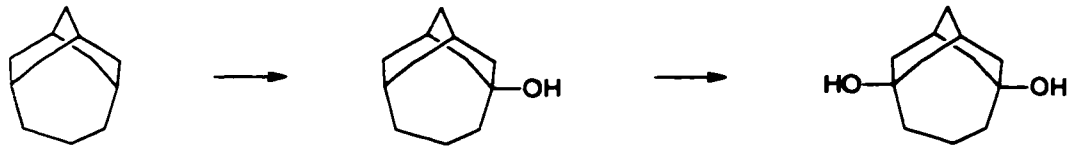

61 120 121

Method a - partial oxidation: Tricyclo[5.3.1.1^{3,9}]dodecane **61** (640 mg, 3.89 mmol) was dissolved in hexanes (40 mL), placed in a 1 L round bottom flask and the solvent was evaporated on a rotavapor to produce a fine solid film of the hydrocarbon on the glass wall. The flask was stoppered and stored at ambient temperature for 7 days. After 3 and 5 days, the air in the flask was replaced with fresh air. The resulting mixture of alkane, mono alcohol and diol was separated via column chromatography (silica gel, 30 g, hexanes-ether 80:20, followed by ether 100 %) yielding 130.0 mg starting material, 172.8 mg mono alcohol **120** and 322.6 mg diol **121**, all of which were white solids (84 % yield of **120** and **121** based on consumed alkane).

Method b - exhaustive oxidation: Tricyclo[5.3.1.1^{3,9}]dodecane **61** (180 mg, 1.10 mmol) was dissolved in hexanes (20 mL), placed in a 500 mL round bottom flask and the solvent was evaporated on a rotavapor to obtain a fine solid film of **61** on the glass wall. Oxygen was then passed into the flask at a rate of 1 to 3 mL/min. for 2 weeks. The solid was then dissolved in methanol and sodium borohydride (2 g, 52.8 mmol) was added in small portions over a period of 2 h. The reaction mixture was then concentrated on a rotavapor and the diol **121** extracted with warm chloroform (50°C, 3 x 20 mL). Purification of the diol with column chromatography (silica gel, 30 g, ether 100 %) yielded 69.2 mg of the pure solid diol **121** (32 % yield).

Tricyclo[5.3.1.1^{3,9}]dodecan-5-ol **120**: GC-MS m/z (rel. intensity): 40 (33), 53 (15), 67 (23), 79 (100), 91 (91), 105 (48), 119 (40), 133 (15), 147 (8), 162 (36), 180 (1). High res. MS (EI): M^+: calc. 180.151415 found 180.1514 (-0.1 ppm). IR neat (cm^{-1}): 3340 (m), 2905 (s), 2847 (m), 1450 (m), 1057 (m), 926 (m), 908(m), 732 (m). ^1H NMR (400MHz, 300K, $CDCl_3$) δ (ppm): 2.07 - 1.92 (m, 5H), 1.91 - 1.82 (s, br, 2H), 1.82 - 1.58 (m, 8H), 1.58 - 1.45 (m, 4H),

1.44 - 1.37 (m, 1H). ^{13}C NMR (100MHz, 300K, $CDCl_3$) δ (ppm): 71.1 (Cq), 46.1 (CH_2), 45.1 (br, CH_2), 37.1 (CH_2), 35.2 (CH_2), 34.5 (br, CH_2), 28.3 (br, CH), 24.8 (CH), 22.2 (CH_2).

Tricyclo[5.3.1.1^{3,9}]dodeca-5,9-diol **121**: GC-MS m/z (rel. intensity):41 (12), 55 (12), 67 (14), 79 (38), 95 (100), 105 (32), 117 (64), 135, (45), 145 (21), 160 (89), 178 (51). High res. MS (EI): M^+ - H_2O calc. 178.135765 found: 178.1347 (-6.0 ppm). ^{1}H NMR (300MHz, 230K, CD_3OH) δ (ppm): 2.27 - 2.13 (2s, br, 4H), 2.01 (dd, J = 13.9, 5.6, 2H), 1.98 (m, 1H), 1.94 (d, J = 13.6, 2H), 1.83 (m, 2H), 1.78 - 1.56 (m, 7H). ^{13}C NMR (75MHz, 240K, CD_3OH) δ (ppm): 71.5 (Cq), 49.3 (CH_2), 47.0 (CH_2), 43.1 (CH_2), 36.1 (CH_2) , 32.1 (CH), 31.1 (CH), 23.4 (CH_2). ^{1}H NMR (300MHz, 330K, CD_3OH) δ (ppm): 2.24 - 2.12 (s, br, 2H), 2.06 (d, J = 14.1, 4H), 1.88 (dd, J = 14.1, 5.6, 4H), 1.80 (s,6H), 1.64 (s, 2H). ^{13}C NMR (75MHz, 330K, CD_3OH) δ (ppm): 71.5 (Cq), 47.4 (CH_2), 46.6 (CH_2), 36.3 (CH_2), 31.9 (CH), 23.5 (CH_2).

5.5.8 5,9-Dichlorotricyclo[5.3.1.1^{3,9}]dodecane (129)

121 **129**

Tricyclo[5.3.1.1^{3,9}]dodeca-5,9-diol **121** (15.0 mg, 76.4 μmol) was dissolved in dichloromethane (3 mL) and the solution was cooled to 0°C. At this temperature, hydrochloric acid (conc., 2 mL) was added, and the heterogeneous mixture was stirred vigorously for 10 min. The organic layer was then separated and dried by passing it through a column containing magnesium sulfate (2 g). The dichloromethane of the filtrate was evaporated using a stream of nitrogen. The solid obtained **(129)** was directly used for the next step.

GC-MS m/z (rel. intensity): 39 (43), 53 (31), 67 (34), 79 (95), 91 (95), 106 (100), 119 (81), 196 (17), 197(2), 198(4) (elimination of HCl in the injector). ^{1}H NMR (400MHz, 0°C, $CDCl_3$) δ (ppm): 2.66 (dd, J = 14.6, 6.3, 2H), 2.60 - 2.45 (m, 4H), 2.37 (dd, J = 14.8, 5.5, 2H), 2.33 - 2.21 (m, 3H), 2.16 (s, br, 1H), 2.12 - 1.95 (m, 3H), 1.68 (s, br, 3H). ^{13}C NMR (100MHz, 0°C, $CDCl_3$) δ (ppm): 74.8 (Cq), 49.5 (CH_2), 47.5 (CH_2), 43.2 (CH_2), 33.8 (CH_2), 32.1 (CH), 31.1 (CH), 23.9 (CH_2).

5.5.9 6-Bis(dimethylamino)phosphatotricyclo[5.3.1.1^{3,9}]dodec-5-ene (278)

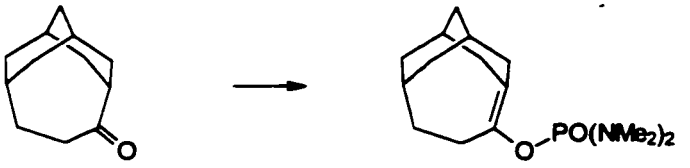

118 278

n-Butyllithium solution in hexane (2.5 M, 3.8 mL, 9.49 mmol) was added to a solution of diisopropylamine (1.52 mL, 10.7 mmol) in THF (30 mL) at -78°C. The resulting solution was allowed to warm up to 0°C and was stirred for 10 min. before it was cooled again to -78°C. A solution of tricyclo[5.3.1.1^{3,9}]dodecan-6-one **118** (404 mg, 2.27 mmol) in THF (4 mL) was added dropwise and again, the resulting solution was allowed to warm to 0°C and stirred at this temperature for 10 min. before it was cooled to -78°C. Then bis(dimethylamino)chlorophosphate (1.17 mL, 7.60 mmol) was added dropwise. The reaction mixture was then allowed to warm up to room temperature within a 2 hour time period and was stirred overnight. This reaction mixture was then poured into a solution of sodium bicarbonate (5 %, 150 mL) at 0°C. Extraction with dichloromethane yielded a crude product as a yellow oil, which was purified on a silica gel column (15 g, ether 100 % / MeOH 100 %) to yield 377.2 mg of the pure 6-bis(dimethylamino)phosphatotricyclo[5.3.1.1^{3,9}]dodec-5-ene **278** (yield: 53 %). The NMR data obtained were in agreement with the literature.[223]

GC-MS m/z (rel. intensity): 44 (55), 67 (9), 79 (21), 91 (20), 105 (11), 117 (17), 135 (45), 153 (100), 160 (24), 177 (0), 267 (0), 312 (1).^{1}H NMR (200MHz, $CDCl_3$) δ (ppm): 3.03 - 2.86 (m, 1H), 2.85 - 2.72 (1), 2.68 - 2.58 (4s, 12H), 2.38 - 2.17 (m, 3H), 2.17 - 1.96 (m, 4H), 1.95 - 1.74 (m, 4H), 1.74 - 1.47 (m, 2H), 1.47 - 1.13 (m, 2H). ^{13}C NMR (50MHz, $CDCl_3$) δ (ppm): 143.8 (Cq), 128.5 (Cq), 43.8 (CH_2), 39.8 (CH_2), 38.9 (CH), 36.8 (CH_2), 36.6 (CH_3), 35.7 (CH_2), 34.5 (CH), 33.5 (CH_2), 32.5 (CH_2), 28.7 (CH_2), 27.1 (CH).

5.5.10 Tricyclo[5.3.1.1^{3,9}]dodec-5-ene (62)

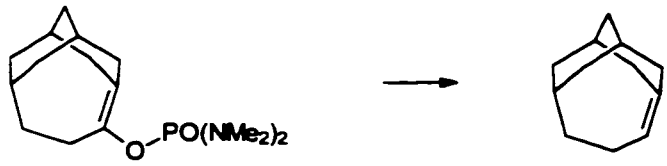

278 62

Sodium (198 mg, 8.63 mmol) was dissolved in a mixture of ammonia (20 mL) and *tert*-butyl alcohol (320 mg, 4.32 mmol) at -78°C. A solution of 6-bis(dimethylamino)phosphato-tricyclo[5.3.1.1^{3,9}]dodec-5-ene **278** in THF (2 mL) was added dropwise within 5 min. The reaction mixture was stirred for an additional 2 h, while the temperature was allowed to rise to -33°C (bp. NH_3 liq.). After cooling to -78°C, solid ammonium chloride was added until the blue color of the sodium disappeared. Diethyl ether (20 mL) was added and the reaction mixture was warmed up to room temperature allowing the ammonia to evaporate. Addition of water (50 mL) produced two phases, and after separation the aqueous layer was extracted with ether (2 x 20 mL). The combined organic layers were dried with magnesium sulfate and concentrated on the rotavapor to yield a yellowish oil. Purification on a column (silica gel, 15g, hexanes 100 %) yielded 130mg of the pure tricyclo[5.3.1.1^{3,9}]dodec-5-ene **62** (yield: 93 %). The MS and NMR data of this product were in accordance with literature values.[223]

GC-MS (rel intensity): 41 (38), 53 (22), 67 (22), 79 (100), 91 (89), 105 (51), 119 (36), 133 (13), 147 (10), 162 (39). ^{1}H NMR (400MHz, $CDCl_3$) δ (ppm): 5.44 (dd, J = 11.5, 4.4, 1H), 2.49 (dq, J = 12.1, 2.2, 1H), 2.44 (qd, J = 12.1, 5.0, 1H), 2.34 (s, br, 1H), 2.26 (d, J = 10.4, 1H), 2.17 - 2.07 (m, 2H), 2.06 - 1.81 (m. 5H), 1.72 (ddp, J = 12.6, 4.8, 2.2, 1H), 1.60 (dd, J = 13.3, 5.0, 1H), 1.56 - 1.43 (m, 3H), 1.05 (d, J = 12.6, 1H). ^{13}C NMR (100MHz, $CDCl_3$) δ (ppm): 142.0 (Cq), 124.8 (CH), 48.4 (CH_2), 46.2 (CH_2), 39.1 (CH), 36.1 (CH_2), 35.6 (CH_2), 34.1 (CH_2), 32.2 (CH), 29.7 (CH_2), 27.2 (CH), 26.7 (CH_2).

5.5.11 2-Ethyl-2-adamantanol (180)

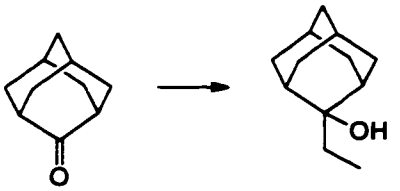

180

2-Adamantanone (194 mg, 1.29 mmol) was dissolved in ether (10 mL), cooled to -78°C before a solution of ethyllithium in hexanes (10 mL, 5.0 mmol) was added. The resulting solution was allowed to warm up to ambient temperature and was stirred for a further 2.5 h. Addition of the reaction mixture to cold ammonium chloride solution (5 %, 100 mL), extraction with ether (3 x 20 mL), drying ($MgSO_4$), filtration and concentration yielded 119.5 mg of 2-ethyl-2-adamantanol **180** (yield: 51 %), which was sufficiently pure for further use. The spectral data agreed with those from the literature.[224]

GC-MS m/z (rel intensity): 41 (3), 57 (3), 67 (4), 81 (7), 91 (10), 107 (5), 133 (4), 151 (100), 162 (4, $M^+ - H_2O$). ^1H NMR (200MHz, $CDCl_3$) δ (ppm): 2.17 (d, J = 11.7, 2H), 1.94 - 1.75 (s, br, 4H), 1.69 (q, J = 7.3, 2H), 1.75 - 1.61 (m, br, 4H), 1.54 (d, J = 11.7, 2H), 1.42 (s, br, 1H), 0.88 (t, J = 7.3, 3H). ^{13}C NMR (50MHz, $CDCl_3$) δ (ppm): 74.8 (Cq), 38.3 (CH_2), 36.5 (CH), 34.5 (CH_2), 33.0 (CH_2), 30.5 (CH_2), 27.5 (CH), 27.3 (CH), 6.4 (CH_3).

5.5.12 6-Methyltricyclo[4.3.1.1^{3,8}]undecan-6-ol (133)

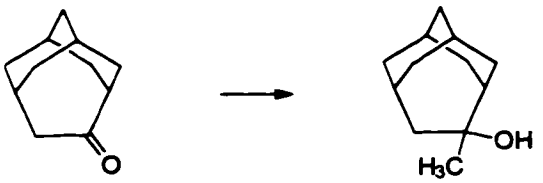

115 **133**

Tricyclo[4.3.1.1^{3,8}]undecan-6-one **115** (420 mg, 1.46 mmol) was dissolved in ether (20 mL) and cooled to -78°C. At this temperature, methyllithium (1.5 M, 3.4 mL, 5.1 mmol) was added, and the resulting solution was stirred for two more hours, while allowing it to warm to ambient temperature. The resulting reaction mixture was then poured onto an aqueous solution of ammonium chloride (5 %, 100 mL) at 0°C. Extraction with ether (3 x 30 mL), drying of the

combined organic layers with magnesium sulfate, filtration and concentration afforded a semi solid crude material, which was purified on a silica gel column using a mixture of hexanes and ether (95:5) to yield 439.3 mg of the pure, crystalline 6-methyltricyclo[4.3.1.1^{3,8}]undecan-6-ol **133** (yield: 95 %).

GC-MS m/z (rel. intensity): 43 (78), 59 (50), 67 (44), 79 (100), 93 (65), 105 (33), 122 (14), 147 (16), 162 (38), 180 (2). High res. MS (IE): M^+: calc. 180.15142 found 180.14961 (10 ppm). IR neat (NaCl) cm^{-1}: 3382 s, 2960s, 1444m, 1367 w, 1112w, 919 w, 740 w. ^{1}H NMR (200MHz, $CDCl_3$) δ (ppm): 2.24 (d, J = 13.2, 1H), 2.02 - 1.90 (m, 3H), 1.90 - 1.80 (m, 4H), 1.80 - 1.67 (m. 4H), 1.67 - 1.59 (m, 1H), 1.59 - 1.46 (m, 4H), 1.34 -1.28 (s, 3H). ^{13}C NMR (50MHz, $CDCl_3$) δ (ppm): 77.35 (Cq), 51.17 (CH_2), 45.03 (CH), 38.24 (CH_2), 37.14 (CH_2), 36.86 (CH_2), 33.85 (CH_3), 32.66 (CH_2), 31.42 (CH_2), 30.49 (CH), 27.89 (CH), 27.68 (CH).

5.5.13 Tricyclo[5.3.1.1^{3,9}]dodec-5-yl cation (34)

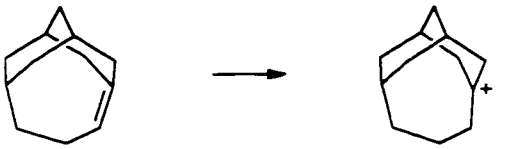

62 **34**

A mixture of antimony pentafluoride (50.0 mg, 231μmol), fluorosulfonic acid (100 mg, 1.00 mmol) and sulfuryl chloride fluoride (0.3 mL) was prepared and cooled to -140°C (the solution became very viscous). On top of this mixture, sulfuryl chloride fluoride (0.2 mL) was condensed, and then a solution of tricyclo[5.3.1.1^{3,9}]dodec-5-ene **62** (12.3 mg, 75.8 μmol) in dichloromethane d_2 (70 μL) was added. The dichloromethane solution immediately froze on contact with the sulfuryl chloride fluoride and only slowely dissolvrf upon stirring with a tungsten wire. A constant stream of argon over the sample was maintained at all times to keep the sample free of moisture. This procedure generated a mixture of the tricyclo[5.3.1.1^{3,9}]dodec-5-yl cation **34** and the rearranged 6-methyltricylo[4.3.1.1^{3,8}]undec-6-yl cation **132** and was the most successful attempt to obtain the tricyclo[5.3.1.1^{3,9}]dodec-5-yl cation **34** directly. Upon warming the reaction solution to 200 K for 8 min. 50 % of the cation mixture rearranged into the 2-ethyladamantyl cation **35**. This corresponds to an activation

energy of about 14.3 ± 0.7 kcal/mol.

Tricyclo[5.3.1.$1^{3,9}$]dodec-5-yl cation **34**: ^{1}H NMR (143 K, 400 MHz) δ (ppm): (signals from the two cations are not resolved) 4.40 - 3.55 (m, 6H), 3.02 - 0.85 (13H). ^{13}C NMR (143 K, 100 MHz) δ (ppm): 335.5 (C^+), 75.8 (CH), 71.0 (CH_2), 69.4 (CH), 59.9 (CH_2), 58.1 (CH_2), 43.8 (CH_2), 37.4 (CH_2), 36.0 (CH_2), 32.1 (CH_2), 31.9 (CH_2), 28.7 (CH).

6-Methyltricyclo[4.3.1.$1^{3,8}$]undec-6-yl cation **132**: 1H NMR (143 K, 400 MHz) δ (ppm): (the signals from the two cations are not resolved) 4.40 - 3.55 (m, 6H), 3.02 - 0.85 (13H). ^{13}C NMR (143 K, 100 MHz) δ (ppm): 322.6 (C^+), 67.3 (CH_2), 63.0 (CH), 44.0 (CH_3), 33.4 (2 x CH_2), 33.1 (2 x CH_2), 33.1 (CH_2), 27.7 (CH), 26.7 (2 x CH).

2-Ethyladamantyl cation **35**: ^{1}H NMR (195 K, 400 MHz) δ (ppm): 4.23 (s, 2H), 4.11 (q, J = 6.7 Hz, 2H), 3.00 (d, J = 12.8 Hz, 4H), 2.67 (d, J = 12.8 Hz, 4H), 2.26 (s, 2H), 2.22 (s, 2H), 1.59 (t, J = 6.7 Hz, 3H). ^{13}C NMR (195 K, 100 MHz) δ (ppm): 324.9 (C^+), 63.1 (2 x CH), 51.9 (4 x CH_2), 50.0 (CH_2), 36.6 (CH_2), 29.2 (2 x CH), 9.3 (CH_3).

5.5.14 Tricyclo[5.3.1.$1^{3,9}$]dodeca-5,9-diyl Dication (40)

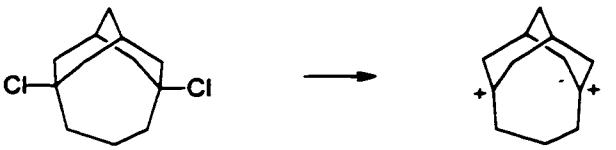

129 **40**

The 5,9-dichlorotricyclo[5.3.1.$1^{3,9}$]dodecane **129** (15 mg, 64 μmol) was dissolved in dichloromethane-d_2 (0.2 mL) and added to a solution of antimony pentafluoride (100 mg, 0.461 mmol), and sulfuryl chloridefluoride (1.8 mL) at -116°C. The sample was mixed with a tungsten wire while an argon stream prevented moisture contamination. Warming the cation solution to 210 K for 10 min. caused decomposition of the dication to an approximately 90 % extent. This corresponds to an activation energy of about 14.5 ± 0.4 kcal/mol.

^{1}H NMR (168K, 300MHz) δ (ppm): 4.90 - 4.10 (m, 13H), 3.76 (s, br, 1H), 3.41 (s, br, 1H), 2.70 (s, 2H). ^{13}C NMR (168K, 75MHz) δ (ppm): 327.8 (Cq), 72.1 (CH), 67.1 (CH), 65.9 (CH_2), 60.1 (CH_2), 57.5 (CH_2), 35.1 (CH_2), 27.6 (CH_2).

5.5.15 6-Methyltricyclo[4.3.1.1^{3,9}]undec-6-yl Cation (132)

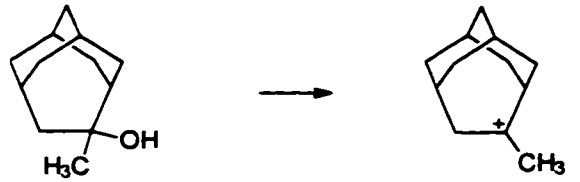

133 **132**

A solution of antimony pentafluoride (100 mg, 0.461 mmol), fluorosulfonic acid (100 mg, 1.00 mmol) and sulfuryl chloride fluoride (1.8 mL) were cooled to -135°C. At this temperature, a solution of 6-methyltricyclo[4.3.1.1^{3,8}]undecan-6-ol **133** (18.6 mg, 0.103 mmol) in dichloromethane-d_2 (0.15 mL) was added, and the solution was stirred with a tungsten wire until a clear slightly yellowish solution was formed, maintaining the sample under a constant stream of argon. At 168 K, the 6-methyltricyclo[4.3.1.1^{3,8}]undec-6-yl cation **132** could be observed (^{1}H NMR and ^{13}C NMR). At 211 K this quantitatively rearranged into the 2-ethyl-2-adamantyl cation **35** within 20 min. The corresponding energy barrier was estimated as 14.4 ± 0.3 kcal/mol.

6-Methyltricyclo[4.3.1.1^{3,8}]undec-6-yl cation **132**: ^{1}H NMR (168 K, 300MHz) δ (ppm): 4.27 (s, 2H), 4.16 (t, J = 6.9, 1H), 3.59 (s, 3H), 2.54 (s, br, 2H), 2.40 (s, 1H), 2.24 (s, 2H), 2.16 - 1.80 (m, 6H), 1.68 (d, J = 13.7, 2H). ^{13}C NMR (168 K, 75MHz) δ (ppm): 323.3 (Cq), 67.5 (1C, CH_2), 63.5 (1C, CH), 44.1 (1C, CH_3), 33.6 (2C, CH_2), 33.3 (3C, CH_2), 27.8 (1C, CH), 26.8 (2C, CH).

2-Ethyl-2-adamantyl cation **35**: ^{1}H NMR (200 K, 300MHz) δ (ppm): 4.20 (s; 2H), 4.08 (q, J = 6.1, 2H), 2.99 (d, J = 12.2, 4H), 2.62 (d, J = 12.2, 4H), 2.23 (s, 2H), 2.21 (s, 2H), 1.58 (t, J = 6.1, 3H). ^{13}C NMR (200 K, 75MHz) δ (ppm): 325.6 (Cq), 62.9 (CH), 51.6 (CH_2), 49.8 (CH_2), 36.3 (CH_2), 28.9 (CH), 8.8 (CH_3).

5.5.16 2-Ethyl-2-adamantyl Cation (35)

5.5.16.1 Method 1: Ionization of Tricyclo[5.3.1.1^{3,9}]dodecan-5-ol

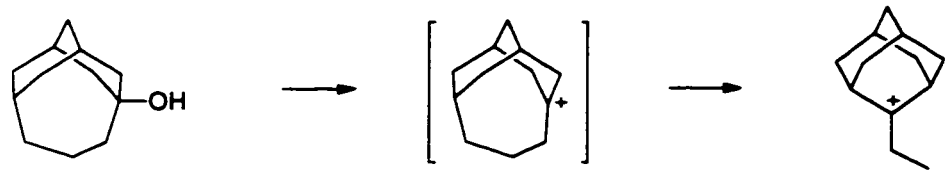

120 34 35

A mixture of antimony pentafluoride (25 mg, 0.12 mmol), trifluoromethanesulfonic acid (65 mg, 0.43 mmol) and sulfuryl chloridefluoride (0.3mL) was cooled to -126°C. At this temperature a solution of tricyclo[5.3.1.1^{3,9}]dodecan-5-ol **120** (10 mg, 0.056 mmol) in dichloromethane-d_2 (80 µl) was added, forming a white suspension. This mixture was stirred until a clear solution formed (a few minutes). Repeated experiments at -130°C to -135°C were not successful in trapping the tricyclo[5.3.1.1^{3,9}]dodec-5-yl cation **34**. In every case a clean solution of the 2-ethyl-2-adamantyl cation **35** was obtained. Attempts to prepare the 5-chlorotricyclo[5.3.1.1^{3,9}]dodecane **128** as a cation precursor resulted in the formation of a complex mixture.

^{1}H NMR (168 K, 400MHz) δ (ppm): 4.20 (s; 2H), 4.09 (q, J = 5.9, 2H), 2.97 (d, J = 12.8, 4H), 2.61 (d, J = 12.8, 4H), 2.22 (s, 2H), 2.22 (s, 2H), 1.58 (t, J = 5.9, 3H). ^{13}C NMR (168 K, 100MHz) δ (ppm): 324.8 (C^+), 62.9 (2 x CH), 51.7 (CH_2), 49.9 (4 x CH_2), 36.4 (CH_2), 29.0 (2 x CH), 9.1 (CH_3).

5.5.16.2 Method 2: Ionization of 2-Ethyladamantan-2-ol

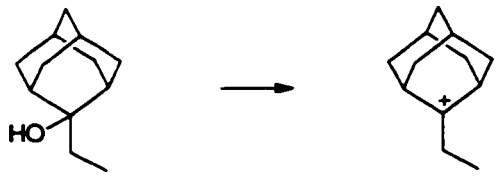

180 35

A solution of antimony pentafluoride (50 mg, 0.23 mmol), fluorosulfonic acid (50 mg, 0.50 mmol) and sulfuryl chloridefluoride (0.8 mL) was cooled to -126°C before a solution of 2-ethyladamantan-2-ol **180** (10 mg, 55 µmol) was added. The resulting mixture was stirred with a tungsten wire, under a constant stream of argon, until a clear solution of **35** was formed.

^{1}H NMR (153 K, 400MHz) δ (ppm): 4.19 (s; 2H), 4.06 (q, J = 6.1 Hz, 2H), 2.99 (d, J = 12.2 Hz, 4H), 2.63 (d, J = 12.2 Hz, 4H), 2.22 (s, 2H), 2.20 (s, 2H), 1.58 (t, J = 6.3 Hz, 3H). ^{13}C NMR (153 K, 100MHz) δ (ppm): 324.8 (C^+), 62.9 (2 x CH), 51.7 (4 x CH_2), 49.9 (CH_2), 36.4 (CH_2), 29.0 (2 x CH), 9.1 (CH_3).

5.5.17 Tricyclo[5.3.1.1^{3,9}]dodeca-5,9-diyl Dication + Isopentane

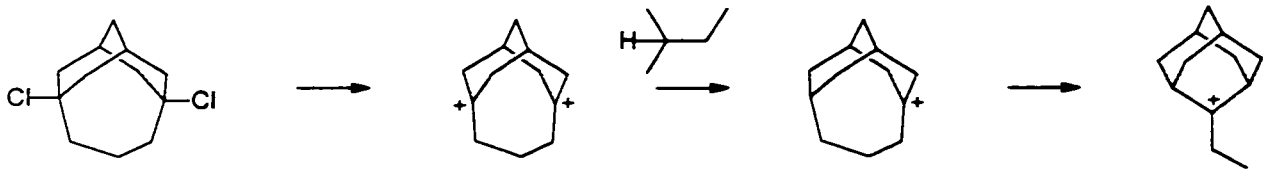

129 **40** **34** **35**

The 5,9-dichlorotricyclo[5.3.1.1^{3,9}]dodecane **129** (16.6 mg, 71.2 μmol) was dissolved in dichloromethane-d_2 (70 μL) and added to a frozen mixture of SbF_5 (50 mg) and sulfuryl chloridefluoride at -143°C. This mixture was then allowed to melt (*ca.* -135°C) before isopentane (15 μL) was added. Stirring with a tungsten wire then formed a clear, slightly yellow solution consisting of a clean mixture of tricyclo[5.3.1.1^{3,9}]dodec-5-yl cation **34**, isopentyl cation and isopentane. This method was the most successful way to prepare **34** indirectly without any of its rearrangement products. Warming the reaction solution to -52°C (221 K) for 10 min. caused 34 % of the monocation **34** to rearrange into the 2-ethyl-2-adamantyl cation **35**, corresponding to an energy barrier of 16.0 ± 0.7 kcal/mol.

Tricyclo[5.3.1.1^{3,9}]dodec-5-yl cation **34**: ^{1}H NMR (179K, 300MHz) δ (ppm): 4.30 - 4.10 (s, br, 2H), 4.10 - 3.70 (m, 4H), 2.87 (q, J = 12.3, 1H), 2.54 - 2.31 (m, 3H), 2.30 - 2.14 (m, 2H), 2.04 (t, J = 13.7, 2H), 1.92 (s, 1H), 1.90 - 1.63 (m, 4H). ^{13}C NMR (179 K, 75MHz) δ (ppm): 335.1 (Cq), 75.5 (CH), 70.9 (CH_2), 69.2 (CH), 60.0 (CH_2), 57.2 (CH_2), 43.7 (CH_2), 37.6 (CH_2), 36.1 (CH_2), 32.2 (2 x CH_2), 28.7 (CH).

Isopentyl cation: ^{1}H NMR (179 K, 300 MHz) δ (ppm): 4.19 (s, br, 2H), 3.68 (s, br, 6H), 1.56 (s, br, 3H). ^{13}C NMR (179 K, 75 MHz) δ (ppm): 335.7 (C^+), 57.1 (CH_2), 44.7 (2 x CH_3), 9.2 (CH_3).

Isopentane: ^{1}H NMR (179 K, 300 MHz) δ (ppm): 1.42 (nonet, J = 6.6 Hz, 1H), 1.19 (p, J = 6.9 Hz, 2H), 0.89 (t, br, J = 6.9 Hz, 6H). ^{13}C NMR (179 K, 75 MHz) δ (ppm): 31.4 (CH_2),

29.7 (CH), 21.7 (2 x CH_3).

5.5.18 Tricyclo[5.3.1.$1^{3,9}$]dodeca-5,9-diyl Dication + Sodium Borohydride

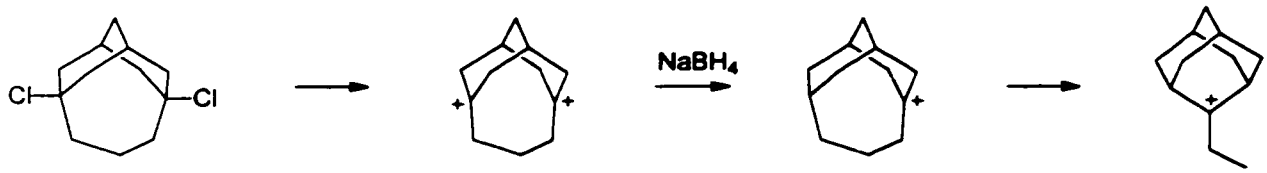

129 40 34 35

The 5,9-dichlorotricyclo[5.3.1.$1^{5,9}$]dodecane **129** (10.0 mg, 42.9 μmol) was dissolved in dichloromethane-d_2 (0.2 mL) and added to a solution of antimony pentafluoride (100 mg, 462 μmol), and sulfuryl chloridefluoride (1.8 mL) at -120°C. After stirring until a clear solution had formed the dication **40** was reacted with sodium borohydride (30.0 mg, 793 μmol). At 189 K (-84°C) the dication **40** was initially reduced to the monocation **34** accompanied by the formation of other unknown species, which both rearranged to the adamantyl cation **35**. The reduction was complete within a time period of 3.5 h, during which a substantial amount of the adamantyl cation **35** had formed. Raising the temperature to 221 K (-63°C) for 20 min. completed the rearrangement, forming a relatively pure solution of the cation **35**. The measured energy barrier for the monocation rearrangement was 15.8 ± 0.5 kcal/mol.

Tricyclo[5.3.1.$1^{3,9}$]dodeca-5,9-diyl dication **40**: ^{1}H NMR (168 K, 300 MHz) δ (ppm): 4.76 (s, br, 1H), 4.60 (s, br, 1H), 4.55 - 4.01 (m, 12H), 3.78 (s, br, 1H), 3.49 - 3.32 (m, 1H), 2.72 (s, 2H).^{13}C NMR (168 K, 75 MHz) δ (ppm): 327.8 (C^+), 72.1 (CH), 67.1 (CH), 65.8 (2 x CH_2), 60.1 (2 x CH_2), 57.5 (2 x CH_2), 35.1 (CH_2), 27.6 (CH_2).

2-ethyl-2-adamantyl cation **35**: ^{1}H NMR (200 K, 300 MHz) δ (ppm): 4.20 (s, br, 2H), 4.10 (q, J = 6.1 Hz, 2H), 2.98 (d, J = 12.0 Hz, 4H), 2.62 (d, J = 12.0 Hz, 4H), 2.22 (s, 2H), 2.20 (s, 2H), 1.57 (t, J = 6.1 Hz, 3H). ^{13}C NMR (200 K, 75 MHz) δ (ppm): 325.7(C^+), 62.9 (2 x CH), 51.6 (4 x CH_2), 49.9 (CH_2), 36.4 (CH_2), 29.0 (2 x CH), 8.9 (CH_3).

5.5.19 Tricyclo[5.3.1.1^{3,9}]dodeca-5,9-diyl Dication + Hydrogen

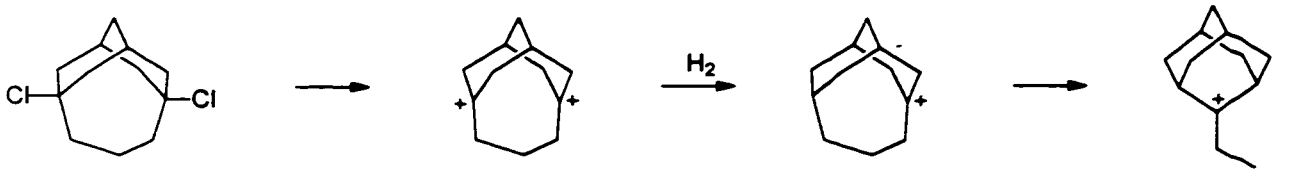

129 **40** **34** **35**

The 5,9-dichlorotricyclo[5.3.1.1^{3,9}]dodecane **129** (6.1 mg, 27 μmol) was dissolved in dichloromethane-d_2 (70 μL), placed into a 5 mm NMR tube and cooled to -78°C. At this temperature, sulfuryl chloridefluoride (0.2mL) was added to the sample solution and the reaction mixture was cooled to -126°C (n-pentane / liq. nitrogen slush). A precooled solution (-78°C) of antimony pentafluoride (50.0 mg, 231 μmol) in sulfuryl chloridefluoride (0.2 mL) was then added, before the NMR tube was placed into a stainless steel tube (cooled with n-pentane / liq. nitrogen slush; -126°C), which was pressurized with hydrogen. The argon atmosphere was replaced by hydrogen by repeated pressurizing (8 bars hydrogen) and depressurizing (releasing the hydrogen) cycles (8 times). Finally, the hydrogen pressure (8 bars) was maintained for 12 h, while the sample was kept at -126°C.

This procedure generated a mixture of mono- **34** and dication **40** (approx. 2:1 ratio), which was stable up to about 198 K (-75°C). Heating the sample to 213 K (-63°C) for 10 min. caused the monocation **34** to rearrange into the ethyladamantyl cation **35** to an extent of *ca.* 40 % and the dication **40** into a complex mixture. The associated energy barrier for this monocation **34** rearrangement was estimated as 15.3 ± 0.8 kcal/mol

Tricyclo[5.3.1.1^{3,9}]dodeca-5,9-diyl dication **40**: ^{1}H NMR (168 K, 300 MHz) δ (ppm): 4.76 (s, br, 1H), 4.60 (s, br, 1H), 4.55 - 4.01 (m, 12H), 3.78 (s, br, 1H), 3.49 - 3.32 (m, 1H), 2.72 (s, 2H).^{13}C NMR (168 K, 75 MHz) δ (ppm): 327.8 (C^+), 71.8 (CH), 66.8 (CH), 65.7 (2 x CH_2), 59.9 (2 x CH_2), 57.4 (2 x CH_2), 34.9 (CH_2), 27.6 (CH_2).

Tricyclo[5.3.1.1^{3,9}]dodec-5-yl cation **34**: ^{1}H NMR (168 K, 300 MHz) δ (ppm): (the signals for the tricyclo[5.3.1.1^{3,9}]dodec-5-yl cation **34** were partially overlapped with the other cations present) 4.93 - 3.69 (m, 6H), 3.48 - 1.36 (m, 13H).^{13}C NMR (168 K, 75 MHz) δ (ppm): 336.2 (C^-), 75.6 (CH), 71.0 (CH_2), 69.3 (CH), 60.0 (CH_2), 57.3 (CH_2), 43.7 (CH_2), 37.6 (CH_2), 36.1

(CH_2), 32.2 (CH_2), 32.2 (CH_2), 28.7 (CH).

2-Ethyl-2-adamantyl cation **35**: ^{1}H NMR (213 K, 300 MHz) δ (ppm): 4.19 (s, br, 2H), 4.08 (q, J = 6.8 Hz, 2H), 2.97 (d, J = 12.3 Hz, 4H), 2.62 (d, J = 12.3 Hz, 4H), 2.22 (s, 2H), 2.20 (s, 2H), 1.57 (t, J = 5.9 Hz, 3H). ^{13}C NMR (213 K, 75 MHz) δ (ppm): 325.3 (C^+), 62.6 (2 x CH), 51.4 (4 x CH_2), 49.6 (CH_2), 36.1 (CH_2), 28.7 (2 x CH), 8.8 (CH_3).

5.5.20 6-Trimethylsilyloxytricyclo[5.3.1.1^{3,9}]dodec-6-ene (239)

118 **239**

The procedure of Ward and Murray[223] was used: A solution of tricyclo[5.3.1.1^{3,9}]dodecan-6-one **118** (243mg, 1.36 mmol) and hexamethyldisilazane (0.891g, 5.52 mmol) was dissolved in hexanes and cooled to -20°C. At this temperature, trimethylsilyl iodide (1.09 g, 5.45 mmol) was added dropwise and the resulting reaction mixture was stirred for 30 min. at -20°C, allowed to warm to room temperature and stirred for a further 15 hours. The clear slightly yellowish solution was then washed with cold (0°C) sodium bicarbonate solution (5 %), dried with magnesium sulfate and concentrated on the rotavapor to give 327.7 mg (yield: 96 %) of a slightly yellow oil, which was essentially pure 6-trimethylsilyloxy-tricyclo[5.3.1.1^{3,9}]dodec-6-ene **239**. The spectral data obtained were in agreement with the literature.[223]

GC-MS m/z (rel. intensity): 45 (18), 55 (13), 73 (100), 91 (13), 105 (6), 117 (5), 129 (4), 155 (21), 168 (7), 181 (4), 235 (2), 250 (4). IR neat (NaCl) cm^{-1}: 2905 s, 1678 m, 1439 m, 1248 s, 1175 s, 1134 s, 929 s, 842 s, 751 m. ^{1}H NMR (200 MHz, $CDCl_3$) δ (ppm): 4.72 (td, J_1 = 5.9 Hz, J_2 = 1.6 Hz, 1H), 2.49 (t, J = 9.2 Hz, 1H), 2.27 - 2.13 (m, 2H), 2.11 - 1.74 (m, 7H), 1.71 - 1.35 (m, 6), 0.15 (s, 9H). ^{13}C NMR (50 MHz, $CDCl_3$) δ (ppm): 156.3 (Cq), 105.2 (CH), 37.8 (CH_2), 35.5 (2 x CH_2), 35.0 (CH), 34.8 (2 x CH_2), 33.5 (CH_2), 25.4 (CH), 24.9 (2 x CH), 0.5 (3 x CH_3).

5.5.21 7-(Isobutyryl)tricyclo[5.3.1.1.^{3,9}]dodecan-6-one (240)

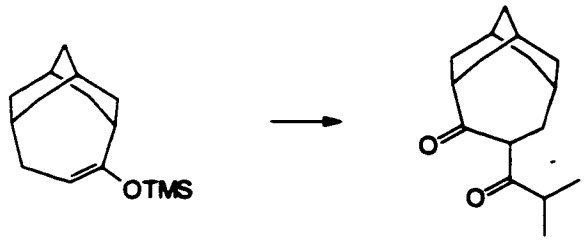

239 **240**

6-Trimethylsilyloxytricyclo[5.3.1.1^{3,9}]dodec-6-ene **239** (28.4 mg, 0.113 mmol) was dissolved in dichloromethane (5 mL) and cooled to -78°C. At this temperature isobutyryl chloride (23.7 µL, 0.245 mmol) and titanium tetrachloride (26.9 µL, 0.245 mmol) were added. The resulting reaction mixture was stirred at -78°C for 2 h and at -18°C for 12 h, before it was poured onto an ice cold sodium bicarbonate solution (5 %, 100 mL). Extraction with ether (3 x 25 mL), drying of the combined organic layers with magnesium sulfate, filtration and concentration afforded 27.7 mg of yellow crude material, which was purified by column chromatography (silica gel, hexanes - ether 95 : 5) to give 13.3 mg (yield: 47 %) of the pure 7-(isobutyryl)tricyclo[5.3.1.1.^{3,9}]dodecan-6-one **240**.

GC-MS m/z (rel. intensity): 43 (100), 55 (59), 79 (55), 91 (24), 107 (10), 117 (7), 135 (6), 160 (17), 178 (24), 205 (5), 248 (3). High res. MS (IE): M^+ calc. 248.177630 found 248.1782 (+2.2 ppm). IR neat (NaCl) cm^{-1}: 2910 s, 1718 s, 1684 s, 1449 s, 1364 m, 1331 m, 1086 m, 1047 m. ^{1}H NMR (200 MHz, $CDCl_3$) δ (ppm): 4.53 (dd, J_1 = 10.6 Hz, J_2 = 6.5 Hz, 1H), 2.62 - 2.48 (m, 2H), 2.42 - 2.21 (m, 3H), 2.20 - 1.77 (m, 9H), 1.68 - 1.53 (m, 2H), 1.36 - 1.22 (m, 1H), 1.08 (d, J = 2.0 Hz, 3H), 1.04 (d, J = 2.0 Hz, 3H). ^{13}C NMR (50 MHz, $CDCl_3$) δ (ppm): 219.3 (Cq), 210.0 (Cq), 54.8 (CH), 44.1 (CH), 41.7 (CH_2), 40.9 (CH), 38.1 (CH_2), 34.7 (CH_2), 34.1 (CH_2), 33.9 (CH_2), 31.7 (CH_2), 27.2 (CH), 26.1 (CH), 24.5 (CH), 18.9 (CH_3), 18.0 (CH_3).

5.5.22 7-Thiomethyltricyclo[5.3.1.1^{3,9}]dodecan-6-one (242)

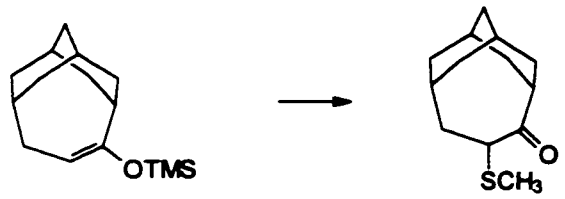

239 **242**

A solution of dimethyl disulfide (1.05 mL, 11.8 mmol) and sulfuryl chloride (0.960 mL, 11.8 mmol) in dichloromethane (200 mL) was stirred at room temperature for 2 hours before it was cooled to -78°C and 6-trimethylsilyloxytricyclo[5.3.1.1^{3,9}]dodec-6-ene **239** (1.40 g, 5.59 mmol) in dichloromethane (50 mL) was added. This solution was allowed to warm to room temperature and was stirred for a further 12 h. The workup was accomplished by pouring the reaction mixture onto ice (400 g) extracting it with dichloromethane (3 x 50 mL), drying the combined organic phases with magnesium sulfate, filtering and concentrating it on the rotavapor to yield 1.27 g (yield: 60 %) of a crude product containing 60 % 7-thiomethyltricyclo[5.3.1.1^{3,9}]dodecan-6-one **242** and 21 % tricyclo[5.3.1.1^{3,9}]dodecan-6-one **118** (by GC). Purification of the crude product proved difficult and it was therefore directly used for subsequent steps. An analytical sample was prepared using a silica gel column (hexanes - ether 95 : 5) for characterization.

GC-MS m/z (rel. intensity): 41 (40), 55 (41), 74 (89), 93 (45), 105 (31), 119 (26), 135 (35), 149 (64), 177 (43), 191 (33), 224 (100). High res. MS (IE): M^+: calc. 224.12349 found 224.12404 (-2.5 ppm). IR neat (NaCl) cm^{-1}: 2909 s, 1694 s, 1447 s, 1356 w, 1067 m, 810w, 780w. ^1H NMR (400 MHz, $CDCl_3$) δ (ppm): 4.27 (dd, J_1 = 12.6 Hz, J_2 = 5.0 Hz, 1H), 2.36 (t, J = 7.6 Hz, 1H), 2.28 - 2.13 (m, 4H), 2.10 - 1.96 (m, 3H), 2.01 (s, 3H), 1.95 - 1.77 (m, 4H), 1.67 (t, J = 12.1 Hz, 1H), 1.56 - 1.43 (m, 2H), 1.22 (d, J = 15.5 Hz, 1H). ^{13}C NMR (100 MHz, $CDCl_3$) δ (ppm): 219.2 (Cq), 49.9 (CH), 46.5 (CH_2), 43.9 (CH), 38.2 (CH_2), 34.5 (CH_2), 34.0 (CH_2), 33.8 (CH_2), 33.4 (CH_2), 30.8 (CH_2), 27.0 (CH), 25.8 (CH), 25.8 (CH).

5.5.23 Diethyl-7-thiomethyltricyclo[5.3.1.1^{3,9}]dodec-6-en-6-yl Phosphate (256)

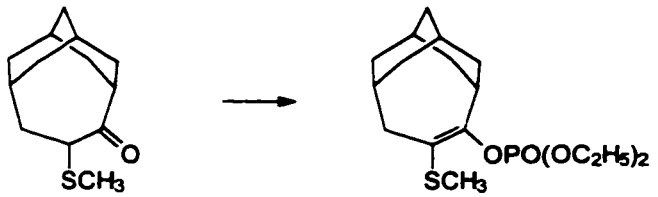

242 **256**

n-Butyllithium (2.5 M, 0.36 mL, 0.90 mmol) was added to a solution of hexamethyldisilazane (0.188 mL, 146 mg, 0.902 mmol) in ether (15 mL), cooled to -78°C. The resulting solution was warmed up to 0°C for 10 min. before it was cooled again to -78°C. At this temperature, 7-thiomethyltricyclo[5.3.1.1^{3,9}]dodecan-6-one **242** (100 mg, 0.446 mmol) in ether (3 mL) was added. The reaction mixture was then allowed to warm to -10°C for 10 min. before it was cooled again to -78°C and diethyl chlorophosphate in ether (2 mL) was added. This reaction mixture was stirred at -78°C for 30 min. and at room temperature for 2 h. The workup was conducted by pouring the reaction mixture into an ice cold sodium bicarbonate solution (5 %, 50 mL), extraction with ether (3 x 25 mL), drying with magnesium sulfate, filtering and concentrating on the rotavapor. The crude material obtained was purified on a silica gel column (hexanes - ether 1 : 1) to give 95.9 mg (yield: 65 %) of the pure diethyl 7-thiomethyltricyclo[5.3.1.1^{3,9}]dodec-6-en-6-yl phosphate **256**.

GC-MS m/z (rel. intensity): 55 (58), 67 (52), 81 (100), 91 (66), 99 (63), 117 (57), 131 (56), 149 (58), 159 (65), 191 (68), 206 (67), 131 (66), 346 (18), 360 (5). High res. MS (IE): M^+: calc. 360.152424 found 360.1511 (-3.8 ppm). IR neat (NaCl) cm^{-1}: 2909 m, 1443 w, 1272 m, 1029 s, 972 m. ^1H NMR (200 MHz, $CDCl_3$) δ (ppm): 4.28 (dqd, J_1 = 7.3 Hz, J_2 = 7.1 Hz, J_3 = 3.2 Hz, 2H), 4.17 (p, J = 7.3 Hz, 2H), 3.15 (dp, J_1 = 11.4 Hz, J_2 = 2.2 Hz, 1H), 2.39 (dd, J_1 = 12.7 Hz, J_2 = 2.2 Hz, 1H), 2.31 (s, br, 1H), 2.23 - 2.06 (m, 4H), 2.19 (s, 3H), 2.05 - 1.79 (m, 5H), 1.73 (d, br, J = 12.6 Hz, 1H), 1.66 (d, J = 14.9 Hz, 1H), 1.51 (dh, J_1 = 12.6 Hz, J_2 = 1.9 Hz, 1H), 1.44 (d, br, J = 16.0, 1H), 1.34 (td, J_1 = 7.3 Hz, J_2 = 1.1 Hz, 3H), 1.33 (td, J_1 = 7.3 Hz, J_2 = 1.1 Hz, 3H). ^{13}C NMR (50 MHz, $CDCl_3$) δ (ppm): 141.5 (Cq), 132.9 (Cq), 64.4 (CH_2), 63.9 (CH_2), 50.2 (CH_2), 46.2 (CH), 41.5 (CH_2), 39.0 (CH), 37.0 (CH_2), 35.7 (CH_2), 34.3 (CH_2), 34.0 (CH), 32.3 (CH_2), 28.1 (CH), 16.1 (CH_3), 16.1 (CH_3), 15.1 (CH_3).

5.5.24 7-Thiophenyltricyclo[5.3.1.1^{3,9}]dodecan-6-one (241)

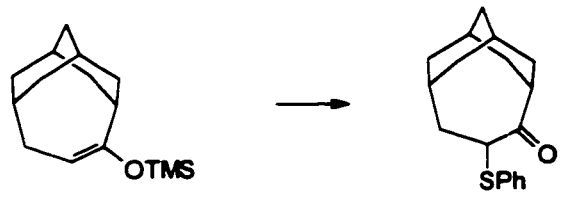

239 **241**

Diphenyl disulfide (174 mg, 0.797 mmol) was dissolved in dichloromethane (10 mL) before the addition of sulfuryl chloride (108 mg, 0.800 mmol). The resulting solution was stirred for 30 min. at room temperature and then cooled to -78°C. At this temperature 6-trimethylsilyloxytricyclo[5.3.1.1^{3,9}]dodec-6-ene **239** (118 mg, 0.471 mmol) in dichloromethane (10 mL) was added and stirred for 2 h at -78°C and 12 h at -18°C. The workup of the reaction mixture was accomplished by pouring it onto an ice cold aqueous sodium bicarbonate solution (5%, 50 mL), extraction, drying with magnesium sulfate, filtering and concentration on the rotavapor to yield the crude material. Purification was accomplished by column chromatography (silica gel, hexanes - ether 95 : 5) to yield 87.1 mg of the pure 7-thiophenyltricyclo[5.3.1.1^{3,9}]dodecan-6-one **241**.

GC-MS m/z (rel. intensities): 41 (80), 55 (64), 65 (56), 79 (100), 91 (79), 109 (76), 135 (64), 149 (47), 177 (5), $M^{+\cdot}$: 286 (32), $M^{+\cdot}$ + 2: 288 (2) 6% of $M^{+\cdot}$. High res. MS (IE): $M^{+\cdot}$: calc. 288.154789 found 288.1545 (-1.0 ppm). ^{1}H NMR (200 MHz, $CDCl_3$) δ (ppm): 7.38 - 7.31 (m, 2H), 7.30 - 7.22 (m, 2H), 7.21 - 7.16 (m, 1H), 7.80 (dd, J_1 = 12.4 Hz , J_2 = 4.7 Hz, 1H), 2.43 (t, J = 7.4 Hz, 1H), 2.32 - 2.16 (m, 3H), 2.14 - 1.72 (m, 9H), 1.63 - 1.39 (m, 2H), 1.34 - 1.22 (m, 1H). ^{13}C NMR (50 MHz, $CDCl_3$) δ (ppm): 218.5 (Cq), 136.8 (CH), 135 (Cq), 131.1 (CH), 128.8 (CH), 126.8 (CH), 52.0 (CH), 47.0 (CH_2), 39.6 (CH), 38.2 (CH_2), 34.5 (CH_2), 34.0 (CH_2), 33.4 (CH_2), 30.9 (CH_2), 28.4 (CH), 27.0 (CH), 25.8 (CH).

5.5.25 7-Thiophenyltricyclo[5.3.1.1^{3,9}]dodecan-6-ol (252)

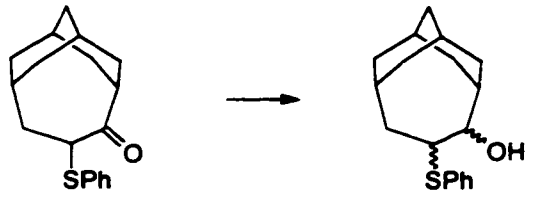

239 **252**

Lithium aluminum hydride (57.7 mg, 0.139 mmol) was mixed with ether (15 mL) under an Ar atmosphere, and a solution of 7-thiophenyltricyclo[5.3.1.1^{3,9}]dodecan-6-one **241** (87.1 mg, 0.304 mmol) in ether (15 mL) was added dropwise. The resulting reaction mixture was stirred at room temperature for 4 h, before potassium hydroxide solution (209 g / L, 3 mL) was cautiously added and the resulting mixture stirred until the grey color changed to white. Filtration, and concentration on the rotavapor yielded 93.8 mg crude material, which was purified using column chromatography (silica gel, hexanes - ether 80 : 20) to afford 52.0 mg (yield: 59 %) of the pure 7-thiophenyltricyclo[5.3.1.1^{3,9}]dodecan-6-ol **252**.

GC-MS m/z (rel. intensity): 41 (41), 65 (43), 79 (57), 91 (49), 110 (100), 119 (20), 135 (25), 161 (8), 178 (8), M^-: 288 (8), M^- + 2: 290 (1, 3 % of M^+). IR neat (NaCl) cm^{-1}: 2903 s, 1473 m, 1448 m, 1419 m, 1093 m, 920 s. High res. MS (EI): M^+: calc. 288.154789 found 288.1545 (-1.0 ppm). ^{1}H NMR (200 MHz, $CDCl_3$) δ (ppm): 7.48 - 7.41 (m, 2H), 7.37 - 7.25 (m, 3H), 3.83 (dt, J_1 = 12.0 Hz, J_2 = 4.9 Hz, 1H), 3.56 (d, J = 8.5 Hz, 1H), 2.65 (s, br, 1H), 2.43 - 2.09 (m, 3H), 2.05 - 1.55 (m, 10 H), 1.54 - 1.21 (m, 3H). ^{13}C NMR (50 MHz, $CDCl_3$) δ (ppm): 134.2 (Cq), 132.1 (CH), 129.1 (CH), 127.3 (CH), 70.7 (CH), 50.7 (CH), 40.6 (CH_2), 35.9 (CH_2), 33.2 (CH_2), 31.0 (CH_2), 30.6 (CH_2), 30.3 (CH), 25.9 (CH), 25.8 (CH), 25.5 (CH_2), 25.2 (CH).

5.5.26 Tricyclo[5.3.1.1^{3,9}]dodec-6-ene (254)

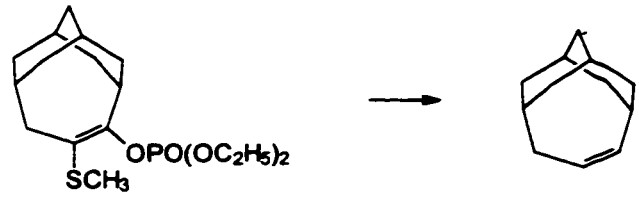

256 **254**

Lithium (23.7 mg, 3.41 mmol) was dissolved in liquid ammonia (15 mL) at -78°C before the addition of *tert*-butyl alcohol (127 mg, 1.71 mmol). The reaction temperature was kept at -78°C while diethyl 7-thiomethyltricyclo[5.3.1.1^{3,9}]dodec-6-en-6-yl phosphate **256** (123.9 mg, 0.344 mmol) in tetrahydrofuran (3 mL) was added. The resulting reaction mixture was stirred for 2 h at -78°C before solid ammonium chloride (ca. 5 g) was added until the blue colour of the reaction mixture disappeared. Ether (10 mL) was then added, and the mixture allowed to warm to room temperature (allowing the liquid ammonia to evaporate). Water (50 mL) was added and the resulting mixture was extracted with ether (3 x 25 mL), dried with magnesium sulfate, filtered and concentrated on the rotavapor. The oil obtained was purified using a silica gel column and pure hexanes to give 49.6 mg (yield: 89 %) of the desired tricyclo[5.3.1.1^{3,9}]dodec-6-ene **254**.

GC-MS m/z (rel. intensity): 41 (31), 53 (15), 79 (100), 91 (64), 105 (35), 119 (31), 133 (23), 147 (16), 162 (31). ^{1}H NMR (200 MHz, $CDCl_3$) δ (ppm): 5.89 (ddt, J_1 = 13.1 Hz, J_2 = 10.9 Hz, J_3 = 2.3 Hz, 1H), 5.36 (dt, J_1 = 13.1 Hz, J_2 = 4.5 Hz, 1H), 2.57 (t, J = 9.2 Hz, 1H), 2.26 - 2.00 (m, 3H), 1.99 - 1.74 (m, 3H), 1.62 - 1.18 (m, 9H). ^{13}C NMR (50 MHz, $CDCl_3$) δ (ppm): 134.0 (CH), 126.8 (CH), 40.2 (CH_2), 2 x 35.7 (CH), 2 x 35.3 (CH_2), 33.7 (CH_2), 29.7 (CH), 27.1 (CH), 24.6 (2 x CH).

5.5.27 Tricyclo[5.3.1.1^{3,9}]dodecan-7-ol (257)

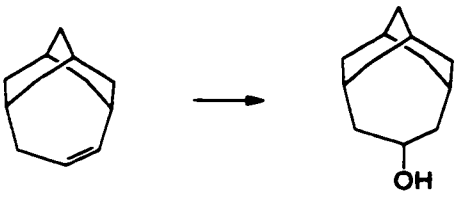

254 **257**

Tricyclo[5.3.1.1^{3,9}]dodec-6-ene **254** (10.9 mg, 0.0674 mmol) was dissolved in THF (10 mL) and cooled to 0°C. At this temperature, borane in THF (1M, 0.34 mL) was added and the solution was stirred for 1.5 h. After the stirring period, NaOH solution (3 M, 2 mL) and hydrogen peroxide (30 %, 2 mL) were added and the resulting mixture stirred vigorously for 2 h. Extraction of this reaction mixture with ether (3 x 25 mL), washing the combined organic layers with aqueous sodium bisulfite solution (5 %, 20 mL), followed by drying with magnesium sulfate, filtration and concentration on the rotavapor, gave the crude material, which was purified on a silica gel column (hexanes - ether 95 : 5) to afford 9.5 mg (yield: 74 %) of the tricyclo[5.3.1.1^{3,9}]dodecan-7-ol **257**.

GC-MS m/z (rel. intensity): 41 (69), 55 (54), 67 (58), 79 (97), 93 (100), 105 (34), 119 (29), 136 (69), 147 (12), 162 (27), 180 (4). IR neat (NaCl) cm^{-1}: 3401 m, 2904 s, 1460 m, 1372 w, 1099 w, 891 w. ^{1}H NMR (200 MHz, $CDCl_3$) δ (ppm): 3.92 (tt, J_1= 11.5 Hz, J_2= 3.9 Hz, 1H), 2.29 - 2.03 (m, 6H), 1.90 - 1.67 (m, 6H), 1.54 - 1.43 (m, 4H), 1.37 - 1.25 (m, 3H). ^{13}C NMR (50 MHz, $CDCl_3$) δ (ppm): 68.4 (CH), 46.4 (2 x CH_2), 39.5 (2 x CH_2), 35.6 (CH_2), 31.8 (2 x CH_2), 26.1 (CH), 25.5 (CH), 24.9 (2 x CH).

5.5.28 7-Dimethylaminomethyltricyclo[5.3.1.1^{3,9}]dodecan-6-one (243)

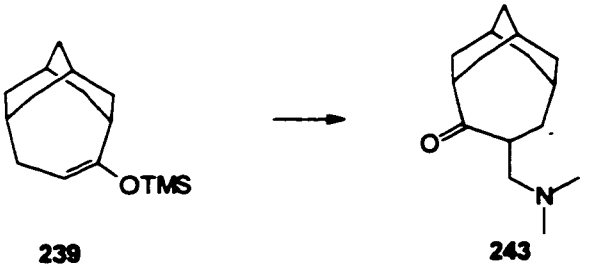

239 243

N,N-Dimethylmethylenimmoniumiodide (Eschenmoser's salt) (235 mg, 1.27 mmol) was dissoved in DMSO (15 mL) followed by the addition of 6-trimethylsilyloxy-tricyclo[5.3.1.1^{3,9}]dodec-6-ene **239** (106 mg, 0.423 mmol) in DMSO (3 mL) at room temperature. The resulting reaction mixture was stirred for 24 hours before it was poured onto water (200 mL). Extraction with ether (3 x 30 mL), drying the combined organic layers with magnesium sulfate, filtering and concentration on the rotavapor yielded the crude product, which was purified on a silica gel column (hexanes - ether 1:1) to afford 99.4 mg (yield: quant.) of the pure 7-dimethylaminomethyltricyclo[5.3.1.1^{3,9}]dodecan-6-one **243**.

GC-MS m/z (rel. intensities): 42 (9), 58 (100), 67 (4), 79 (10), 91 (5), 105 (1), 107 (1), 235 (1). High res. MS (IE): M^+ calc. 235.193614 found 235.1941 (+2.0 ppm) IR neat (NaCl) cm^{-1}: 2905 s, 1692 s, 1453 s, 1382 m, 1261 m, 1095 m, 1040 m, 1009 m. ^{1}H NMR (200 MHz, $CDCl_3$) δ (ppm): 3.49 (ddt, J_1 = 12.3 Hz, J_2 = 7.6 Hz, J_3 = 4.7 Hz, 1H), 2.79 (dd, J_1 = 12.0 Hz, J_2 = 7.9 Hz, 1H), 2.41 - 2.21 (m, 3H), 2.17 (s, 6H), 2.15 - 1.78 (m, 9H), 1.65 - 1.43 (m, 2H), 1.42 - 1.14 (m, 3H). ^{13}C NMR (50 MHz, $CDCl_3$) δ (ppm): 223.2 (Cq), 61.1 (CH_2), 45.9 (2 x CH_3), 45.8 (CH_2), 43.9 (CH), 41.7 (CH), 38.3 (CH_2), 35.0 (CH_2), 34.2 (CH_2), 33.9 (CH_2), 31.0 (CH_2), 27.3 (CH), 26.3 (CH), 25.5 (CH).

References

(1) Angelini, G.; Hanack, M.; Vermehren, J.; Speranza, M., *J. Am. Chem. Soc.*, **1988**, *110*, 1298.

(2) Bremer, M.; Schleyer, R. v. R.; Schötz, K.; Kausch, M.; Schindler, M., *Angew. Chem. Int. Ed. Engl.*, **1987**, *26*, 761.

(3) Olah, G. A., *Angew. Chem. Int. Ed. Engl.*, **1973**, *12*, 173.

(4) Brown, H. C., *The Nonclassical Ion Problem*, Plenum Press, New York, **1977**,

(5) Nenitzesçu, C. D., *Carbonium Ions*, Olah, G. A.; Schleyer, P. v. R., Eds., vol. 1, p. 1, Wiley-Interscience, New York, **1968**.

(6) a) Fischer, E.; Fischer, O., *Chem. Ber.*, **1878**, *11*, 195. b) Fischer, E.; Fischer, O., *Chem. Ber.*, **1878**, *11*, 612. c) Fischer, E. ; Fischer, O., *Chem. Ber.*, **1902**, *35*, 1189. d) Meth-Cohn, O.; Travis, A. S., *Chem. Brit.*, **1995**, 547.

(7) a) Arrhenius, S., *Z. Phys. Chem.*, **1887**, *1*, 631. b) Lorenz, R., *Angew. Chem.*, **1927**, *40*, 1461.

(8) a) Stieglitz, J., *Am. Chem. J.*, **1899**, *21*, 101. b) Tarbell, D. S.; Tarbell, A. T., *Essays on The History of Organic Chemistry in the United States, 1875 - 1955*, Folio Publishers, Nashville, TN, **1986**, p. 65.

(9) *Nobel Laureates in Chemistry 1902 - 1992*, James, L. K., Ed., American Chemical Society and Chemical Heritage Foundation, **1993.**

(10) a) Norris, J. F., *Am. Chem. J.*, **1901**, *25*, 117. b) Norris, J. F., *Chem. Zentr.*, **1901**, *1*, 699. c) Norris, J. F.; Sanders, W. W., *Am. Chem. J.*, **1901**, *25*, 54. d) Norris, J. F.; Sanders, W. W., *Chem. Zentr.*, **1901**, *1*, 463.

(11) a) Norris, J. F.; Sanders, W. W., *Am. Chem. J.*, **1901**, *34*, 3815. b) Norris, J. F., *Am. Chem. J.*, **1901**, *25*, 117. c) Kehrmann, F.; Wentzel, F., *Chem. Ber.*, **1901**, *34*, 3815.

(12) Hammett, L. P.; Deyrup, A. J., *J. Am. Chem. Soc.*, **1933**, *55*, 1900.

(13) Hantzsch, A., *Physik. Chem.*, **1907**, *61*, 257.

(14) Meerwein, H.; Van Emster, K., *Chem. Ber.*, **1922**, *55*, 2500.

(15) Wagner, G.; Brickner, W., *Chem. Ber.*, **1899**, *32*, 2303.

(16) Hughes, E. D.; Ingold, C. K., *J. Chem. Soc.*, **1935**, 244.

(17) Freudenberg, K., *Sitzber. Heidelberg. Akad. Wiss.*, **1927**, 3.

(18) a) Whitmore, F. C., *J. Am. Chem. Soc.*, **1932**, *54*, 3274. b) Whitmore, F. C., *Chem. Eng. News*, **March 8, 1948**, 668.

(19) Nevell, T. P.; Salas, E. de; Wilson, C. L., *J. Chem. Soc.*, **1939**, 1188.

(20) Meerwein, H., *Methoden der Organischen Chemie, Houben-Weyl*, Müller, E., Ed., vol. 6/3, Thieme, Stuttgart, **1965**.

(21) Seel, F., *Z. Anorg. Allgem. Chem.*, **1943**, *250*, 331. b) Seel, F., *Z. Anorg. Allgem. Chem.*, **1943**, *252*, 24.

(22) Brown, H. C.; Pearsall, H. W.; Eddy, L. P., *J. Am. Chem. Soc.*, **1950**, *72*, 5347.

(23) Wetyporoch, E.; Firla, T., *Ann. Chim.*, **1933**, *500*, 287.

(24) Olah, G. A.; Kuhn, S. J.; Olah, J. A., *J. Chem. Soc.*, **1957**, 2174.

(25) Fairbrother, F., *J. Chem. Soc.*, **1945**, 503.

(26) a) Rosenbaum, J.; Symons, M. C. R., *Proc. Chem. Soc. (London)*, **1959**, *92*, 1959. b) Rosenbaum, J.; Rosenbaum, M.; Symons, M. C. R., *Mol. Phys.*, **1960**, *3*, 205. c) Rosenbaum J.; Symons, M. C. R., *J. Chem. Soc.*, **1961**, *1*, 1961.

(27) Finch, A. C. M.; Symons, M. C. R., *J. Chem. Soc.*, **1965**, 378.

(28) McLafferty, F. W., *Mass Spectrometry of Organic Ions*, Academic Press, New York, **1963**.

(29) Pearson, D. E., *J. Am. Chem. Soc.*, **1950**, *72*, 4169.

(30) a) Olah, G. A.; Kuhn, S., *Acta Chim. Acad. Sci. Hung.*, **1956**, *10*, 233. b) Olah, G. A.; Kuhn, S., *Chem. Ber.*, **1956**, *89*, 866. c) Olah, G. A.; Kuhn, S., *J. Am. Chem. Soc.*, **1960**, *82*, 2380.

(31) a) Olah, G. A.; Kuhn, S.; Togyesi, W. S.; Baker, E. B., *J. Am. Chem. Soc.*, **1962**, *84*, 12733. b) Olah, G. A., *Rev. Chim.*, **1962**, *1*, 1139. c) Olah, G. A.; Toglyesi, W. S.; Kuhn, S. J.; Moffatt, M. E.; Bastien, J. J; Baker, E. B., *J. Am. Chem. Soc.*, **1963**, *85*, 1328.

(32) Olah, G. A.; Baker, E. B.; Evan, J. C.; Togyesi, W. S.; McIntyre, J. S.; Bastien, I. J., *J. Am. Chem. Soc.*, **1964**, *86*, 1360.

(33) a) Hogeveen, H.; Brouwer, D. M., *Chem. Commun.*, **1964**, b) Brouwer, D, M.; Mackor, E. L., *Proc. Chem. Soc.*, **1964**, 147.

(34) a) Gillespie, R. J., *Acc. Chem. Res.*, **1968**, *1*, 202. b) Gillespie, R. J.; Peel, T. E., *Adv. Phys. Org. Chem.*, **1972**, 9, 1. c) Gillespie, R. J.; Peel, T. E., *J. Am. Chem. Soc.*, **1973**, *95*, 5173.

(35) Hall, N. R.; Conant, J. V., *J. Am. Chem. Soc.*, **1927**, *49*, 3047.

(36) a) Saunders, M.; Kates, M. H., *J. Am. Chem. Soc.*, **1980**, *102*, 6867. b) Myhre, P. C.; Webb, G. G.; Yannoni, C. S., *J. Am. Chem. Soc.*, **1990**, *112*, 8991. c) Koch, C. W.; Liu, B.; De Frees, D. J.; Sunko, D. E.; Vančik, H., *Angew. Chem. Int. Ed. Engl.*, **1990**, *19*, 183.

(37) Schleyer, P. v. R.; Sieber, S., *Angew. Chem. Int. Ed. Engl.*, **1993**, *32*, 1606.

(38) a) Hogeveen, H.; Kwant, P. W., *Acc. Chem. Res.*, **1975**, *8*, 413. b) Hogeveen, H.; Kwant, P. W., *Tetrahedron Lett.*, **1973**, 1665. c) Hogeveen, H.; Kwant, P. W., *J. Am. Chem. Soc.*, **1974**, *96*, 2208.

(39) Prelog, V.; Traynham, T. J., *Molecular Rearrangements*, vol. 1, De Mayo, P., Ed., Wiley-Interscience, New York, **1963**, 593.

(40) Cope, A. C.; Martin, M. M.; McKervey, M. A., *Quart. Rev. Chem. Soc.*, **1966**, *20*, 119.

(41) Kirchen, R. P.; Sorensen, T. S.; Wagstaff, K., *J. Am. Chem. Soc.*, **1978**, *100*, 6761.

(42) Paquette, L. A.; Ternansky, R. J.; Balogh, D. W.; Kentgen, G., *J. Am. Chem. Soc.*, **1983**, *105*, 5446. b) Paquette, L. A.; Weber, J. C.; Kobayashi, T., *J. Am. Chem. Soc.*, **1988**, *110*, 1303.

(43) a) Olah, G. A.; Prakash, G. K. S.; Fessner, W.-D.; Kobayashi, T. Paquette, L. A., *J. Am. Chem. Soc.*, **1988**, *110*, 8599. b) Olah, G. A.; Prakash, G. K. S.; Kobayashi, T. Paquette, L. A., *J. Am. Chem. Soc.*, **1988**, *110*, 1304.

(44) For example see: Lenoir, D.; Siehl, H. U., *Methoden der Organischen Chemie, Houben-Weyl*, vol. E19c, p. 302ff, Georg Thieme Verlag, Stuttgart, **1990**.

(45) a) Sorensen, T. S., *Adv. Carbocation Chem.*, **1995**, *2*, 123. b) Schleyer P. v. R.; Maerker, C.; Buzek, P.; Sieber, S., *Stable Carbocation Chemistry*, Prakash, G. K. S.; Schleyer, P. v. R., Eds., p. 19, Wiley-Interscience, New York, **1997**. c) Sorensen, T. S., *Stable Carbocation Chemistry*, Prakash, G. K. S.; Schleyer, P. v. R., Eds., p. 75, Wiley-Interscience, New York, **1997**. d) Saunders, M.; Jiménez-Váaquez, H. A.; Kronja, O., *Stable Carbocation Chemistry*, Prakash, G. K. S.; Schleyer, P. v. R., Eds., p. 297, Wiley-Interscience, New York, **1997**.

(46) a) Reichardt, C., *Solvent Effects in Organic Chemistry*, VCH-Verlag, Weinheim, **1989**. b) Amis, E. S. ; Hinton, J. F., *Solvent Effects on Chemical Phenomena*, Academic Press, New York, **1973**. c) Hammett, L. P., *Physical Organic Chemistry*, second ed., McGraw, Hill, New York, **1970**.

(47) Gold. V., *J. Chem. Soc.*, **1956**, 4633.

(48) a) Gold, V., *J. Chem. Soc. Faraday Trans.I*, **1972**, 1611. b) Abraham, M. H., *J. Chem. Soc., Perkin Trans. II*, **1973**, 1893.

(49) Bingham, R. C.; Schleyer, P. v. R., *J. Am. Chem. Soc.*, **1971**, *93*, 3189.

(50) Staley, R. H. ; Wietling, R. D.; Beauchamp, J. L., *J. Am. Chem. Soc.*, **1977**, *99*, 5964. b) Houriet, R.; Schwarz, H., *Angew. Chem. Int. Ed. Engl.*, **1979**, *18*, 951.

(51) Olah, G. A.; Prakash, G. K. S.; Sommer, J., *Superacids*, p. 67, Wiley-Interscience, New York, **1985.**

(52) For thermodynamic data on carbocations in the gas phase see: a) Aue, D. H.; Bowers, M. T., *Gas Phase Ion Chemistry*, Bowers, M. T., Ed., vol. 2, ch. 9, Academic Press, New York **1979**. b) Ausloos, P., *Interactions Between Ions and Molecules*, Plenum Press, New York **1975**. c) Taft, R. W., *Prog. Phys. Org. Chem.*, **1982**, *14*, 247. For thermochemical data of carbocations in condensed phase see: d) Arnett, E. M.; Petro, C., *J. Am. Chem. Soc.*, **1978**, *100*, 5402. e) Arnett, E. M.; Hofelich, T. C., *J. Am. Chem. Soc.*, **1983**, *105*, 2889.

(53) Hammett, L. P.; Deyrup, A. J., *J. Am. Chem. Soc.*, **1932**, *54*, 2721.

(54) Ryabova, R. S.; Medvetskaya, I. M.; Vinnik, M. I., *Russ. J. Phys. Chem.*, **1966**, *40*, 82.

(55) a) Gillespie, R. J.; Peel, T. E.; Robinson, E. A., *J. Am. Chem. Soc.*, **1971**, *93*, 5083. b) Gillespie, R. J.; Peel, T. E., *J. Am. Chem. Soc.*, **1973**, *95*, 5173.

(56) Olah, G. A.; Prakash, G. K. S.; Sommer, J., *Superacids*, p. 33, Wiley-Interscience, New York, **1985**.

(57) Sommer, J. Canivet, P.; Schwartz, S.; Rimmelin, P., *Nouv. J. Chim.*, **1981**, *5*, 45.

(58) Gold, V.; Laali, K.; Morris, K. P.; Zduneck, L. Z., *Chem. Commun.*, **1981**, 769.

(59) Devynck, J.; Fabre, P. L.; Tremillon, B.; Ben Hadid, A., *J: Electroanal. Chem.*, **1978**, *91*, 93. b) Brouwer, D. M.; Van Doorn, J. A., *Rec. Trav. Chim. Pays-Bas.*, **1970**, *89*, 553. c) Brouwer, D. M.; Van Doorn, J. A., *Rec. Trav. Chim. Pays-Bas.*, **1972**, *91*, 895.

(60) Deno, N. C.; Jaruzelski, J.; Schriesheim, *J. Am. Chem. Soc.*, **1955**, *77*, 3044.

(61) Deno, N. C.; Schriesheim, A., *J. Am. Chem. Soc.*, **1955**, *77*, 3051.

(62) a) H_m: Arnett, E. M.; Mach, G. W., *J. Am. Chem. Soc.*, **1964**, *86*, 2471. b) H_I: Hinman, R. L.; Lang, J., *J. Am. Chem. Soc.*, **1964**, *86*, 3796. c) H_A: Yates, K.; Stevens, J. B.; Katritzky, A. R., *Can. J. Chem.*, **1964**, *42* 1957. d) H_C: Reagan, M. T., *J. Am. Chem. Soc.*, **1969**, *91*, 5506.

(63) Field, F. H.; Franklin, J. L., *Electron Impact Phenomena*, Academic Press, New York, **1957**.

(64) a) Henderson, W. G.; Taagepera, M.; Holtz, D.; McIver, R. T. jr.; Beauchamp, J. L.; Taft, R. W., *J. Am. Chem. Soc.*, **1972**, *94*, 4729. b) Staley, R. H.; Beauchamp, J. L., *J. Am. Chem. Soc.*, **1974**, *96*, 6252. c) Bowers, M. T.; Aue, D. H.; Webb, H. M.; McIver, R. T. jr., *J. Am. Chem. Soc.*, **1971**, *93*, 4314. d) Briggs, J. P.; Yamdagni, R.; Kebarle, P., *J. Am. Chem. Soc.*, **1972**, *94*, 5128. e) for review see: Aue, D. H.; Bowers, M. T., *Gas Phase Ion Chemistry*, Bowers, M. T., Ed., vol. 2, ch. 9, Academic Press, New York **1979.**

(65) a) Ausloss, P., *Interactions Between Ions and Molecules*, Plenum Press, New York, **1975**. b) Lias, S. G.; Shold, D. M.; Ausloos, P., *J. Am. Chem. Soc.*, **1980**, *102*, 2540. c) Kebarle, P., *Ann. Rev. Phys. Chem.*, **1977**, *28*, 445. d) Almoster Ferreira, M. A., *Ionic Processes in the Gas Phase*, Reidel, Dordrecht, **1984**. e) Sharma, R. B.; Sharma, D. K. S.; Hiraoka, K.; Kebarle, P., *J. Am. Chem. Soc.*, **1985**, *107*, 3747.

(66) Arnett, E. M.; Larsen, J. W. *Carbonium Ions*, Olah, G. A.; Schleyer, P. v. R, Eds., vol. 1, p. 441, Wiley-Interscience, New York **1968.** b) Arnett, E. M.; Petro, C., *J. Am. Chem. Soc.*, **1978**, *100*, 5402. c) Arnett, E. M.; Hofelich, T. C., *J. Am. Chem. Soc.*, **1983**, *105*, 2889.

(67) a) Arnett, E. M.; Burke, J. J., *J. Am. Chem. Soc.*, **1966**, *88*, 4308. b) Arnett, E. M.; Bushick, R. D., *J. Am. Chem. Soc.*, **1964**, *86*, 1564.

(68) a) Streitwieser, A. Jr. *Sovolytic Displacement Reactions*, McGraw-Hill, New York, **1962.** b) Thornton, E. R. *Solvolysis Mechanisms*, Ronald Press, New York **1964.**

(69) Raber, D. J.; Harris, J. M.; Schleyer, P. v. R., *Ion and Ion Pairs in Organic Reactions*, Szwarc, M., Ed., vol. 2, p. 247, Wiley-Interscience, New York, **1974.** b) Bentley, T. W.; Schleyer, P. v. R., *Adv. Phys. Org. Chem.*, **1977**, 14, 2. c) Harris, J. M., *Prog. Phys. Org. Chem.*, **1974**, 11, 89. d) Kessler, H.; Geigel, M., *Acc. Chem. Res.*, **1982**, 15, 2.

(70) Amis, E. S.; Hinton, J. F., *Solvent Effects on Chemical Phenomena*, Academic Press, New York, **1973**.

(71) a) Lancelot, C. J.; Cram, D. J.; Schleyer, P. v. R., *Carbonium Ions*, Olah, G. A.; Schleyer, P. v. R., Eds., vol. 3, p. 1347., Wiley-Interscience, New York, **1972.** b) Müller, P.; Mareda, J., *Helv. Chim. Acta*, **1985**, *68*, 111. c) Schneider, H.-J.; Becker, N.; Schmidt, G.; Thomas, F., *J. Org. Chem.*, **1986**, *51*, 3602.

(72) a) Stirling, C. J. M., *Acc. Chem. Res.*, **1979**, *12*, 198. b) Stang, P. J., *Acc. Chem. Res.*, **1978**, *11*, 107.

(73) Parker, W.; Tranter, R. L.; Watt, C. I. F.; Chang, L. W. K.; Schleyer, P. v. R., *J. Am. Chem. Soc.*, **1974**, *96*, 7172.

(74) a) Olah, G. A.; White, A. M., *J. Am. Chem. Soc.*, **1969**, *91*, 5801. b) Olah, G. A.; Donovan, D. J. J., *J. Am. Chem. Soc.*, **1977**, *99*, 5026. c) Saunders. M.; Hagen, E. L., *J. Am. Chem. Soc.*, **1968**, *90*, 6881. d) Olah, G. A.; Baker, E. B.; Evans, J. C.; Tolgyesi, W. S.; McIntyre, J. S.; Bastien, I. J., *J. Am. Chem. Soc.*, **1964**, *86*, 1360.

(75) Lias, S. G.; Bartmess, J. E.; Liebman, J. F.; Holmes, J. L; Levin , R. D.; Mallard, N. G., *J. Phys, Chem. Ref. Data*, **1988**, *17*, Suppl. 1.

(76) Olah, G. A., *Acc. Chem. Res.*, **1976**, *9*, 41.

(77) Myhre, P. C.; Kruger, J. D.; Hammond, B. L.; Lok, S. M.; Yannoni, C. S.; Macho, V.; Limbach, H. H.; Vieth, H. M., *J. Am. Chem. Soc.*, **1984**, *106*, 6079.

(78) a) Olah, G. A.; Bollinger, J. M.; Cupas, C. A.; Lukas, J., *J. Am. Chem. Soc.*, **1967**, *89*, 2692. b) Arnett, E. M.; Petro, C., *J. Am. Chem. Soc.*, **1978**, *100*, 5408. c) Vancik, H.; Percac, K.; Sunko, D. E., *J. Am. Chem. Soc.*, **1990**, *112*, 7418.

(79) a) Attina, M.; Cacace, F.; Giacomello, J., *J. Am. Chem. Soc.*, **1981**, *103*, 4711. b) Attina, M.; Cacace, F.; Cipollini, R.; Speranza, M., *J. Am. Chem. Soc.*, **1985**, *107*, 4824.

(80) a) Saunders, M.; Rosenfeld, J. C., *J. Am. Chem. Soc.* **1969**, *91*, 7756. b) Saunders, M.; Vogel, P.; Hagen, E. L.; Rosenfeld, J. C., *Acc. Chem. Res.*, **1973**, *6*, 53. c) Saunders, M.; Jimenez-Vazquez, H. A., *Chem. Rev.*, **1991**, *91*, 375.

(81) Hewett, A. P. W., *Ph. D. Thesis*, Yale, University, New Haven, Connecticut, **1975**.

(82) Sorensen, T. S.; Whitworth, S. M., *J. Am. Chem. Soc.*, **1990**, *112*, 8135.

(83) Brownstein, S.; Bornais, J., *Can. J. Chem.*, **1971**, *49*, 7.

(84) a) Brouwer, D. M.; Hogeveen, H., *Prog. Phys. Org. Chem.*, **1971**, *9*, 179. b) Brouwer, D. M., *Rec. Trav. Chim. Pays-Bas*, **1968**, *87*, 210.

(85) Franklin, J. L., *Carbonium Ions*, Olah, G. A.; Schleyer, P. v. R., Eds., vol. 1, p. 77, Wiley-Interscience, New York **1968.** b) Bowen, D. R.; Williams, D. H.; De Mayo, P., *Rearrangements in Ground and Excited States*, vol. 1, ch. 2, Academic Press, New York **1980**.

(86) a) Chupka, W. A., *J. Chem. Phys.*, **1959**, *30*, 191. b) Wallington, M., *J. Phys. E.*, **1971**, 1.

(87) Brayford, J. R.; Wyatt, P. A. H., *J. Chem. Soc.*, **1955**, 2453.

(88) Lehmann, T. A.; Bursey, *Ion Cyclotron Resonance Spectrometry*, Wiley-Interscience, **1976**.

(89) Franklin, J. L., *Ion-Molecule Reactions*, Plenum Press, New York, **1972**.

(90) Hyman, K., *Non-Aqueous Solvent Systems*, Waddington, T. C., Ed., p. 47, Academic Press, New York, **1965**.

(91) Olah, G. A., *J. Am. Chem. Soc.*, **1978**, *100*, 5163.

(92) Jache, A. W., *Adv. Inorg. Chem. Radiochem.*, **1974**, *16*, 177.

(93) Barr, J.; Gillespie, R. J.; Thompson, R. C., *Inorg. Chem.*, **1964**, *3*, 1149.

(94) Olah, G. A.; Prakash, G. K. S.; Sommer, J., *Superacids*, p. 25,Wiley-Interscience, New York, **1985**.

(95) Fabre, P. L.; Devynck, J.; Tremillon, B., *Chem. Rev.*, **1982**, *82*, 591.

(96) Olah, G. A.; Kuhn, S.; Olah, J., *J. Chem. Soc.*, **1957**, 2174.

(97) a) Olah, G. A., *Friedel-Crafts and Related Reactions*, Wiley-Interscience, New York, **1963**. b) Olah, G. A., *Friedel and Crafts Chemistry*, Wiley-Interscience, New York, **1973**.

(98) Olah, G. A., Bruce, M. R.; Edelson, E. H.; Husain, A., *Fuel*, **1984**, *63(8)*, 1130.

(99) McCauley, D. A., unpublished results, see Olah, G. A.; Prakash, G. K. S.; Sommer, J., *Superacids*, p. 51, Wiley-Interscience, New York, **1985**.

(100) Olah, G. A.; Prakash, G. K. S.; Sommer, J., *Superacids*, p. 217ff, Wiley-Interscience, New York, **1985**.

(101) Gillespie, R. J., unpublished results; see in Olah, G. A.; Prakash, G. K. S.; Sommer, J., *Superacids*, p. 51, Wiley-Interscience, **1985**.

(102) Farcasiu, D., *Acc. Chem. Res.*, **1982**, *15*, 46.

(103) Krespan, C. G., Petrov, V. A., *Chem. Rev.*, **1996**, *96*, 3269.

(104) Gmelin-Handbuch der Anorganischen Chemie, syst. No. 18, vol. 13, p. 401, Verlag Chemie, Weinheim, **1943**.

(105) Hoffman, G. J.; Holder, B. F.; Lolly. W. L., *J. Phys. Chem.*, **1958**, *62*, 364.

(106) Brunel, D.; Germain, A.; Commeyras, A., *Nouv. J. Chim.*, **1967**, *40*, 675.

(107) "JANAF Thermchemical Tables", **1971**, *Natl. Stand. Ref. Data Ser., Nat. Bur. Stand.*, NSRDS-NBS 37, 2nd. Ed., U.S. Gov. Print. Off., Washington, D.C.

(108) Hogness, T. R.; Lunn, E. G., *Phys. Rev.*, **1925**, *26*, 44.

(109) Olah, G. A.; Prakash, G. K. S.; Sommer, J., *Superacids*, p. 69, Wiley-Interscience, New York, **1985**.

(110) Kelly, D. P.; Brown, H. C., *Aust. J. Chem.*, **1976**, *29*, 957.

(111) Ahlberg, P.; Engdahl, C., *J. Am. Chem. Soc.*, **1979**, 101, 3940.

(112) a) Saunders, M.; Cox, D.; Ohlmstead, W., *J. Am. Chem. Soc.*, **1973**, *95*, 3018. b) Saunders, M.; Lloyd, J. R., *J. Am. Chem. Soc.*, **1977**, *99*, 7090.

(113) Saunders, M.; Cox, D.; Lloyd, J. R., *J. Am. Chem. Soc.*, **1979**, *101*, 6656.

(114) a) for CPMAS NMR see: Myhre, P. C.; Yannoni, C. S.; *J. Am. Chem. Soc.*, **1981**, *103*, 203. b) for the apparatus see: Vančik, H.; Sunko, D. E., *J. Am. Chem. Soc.*, **1989**, *111*, 3742.

(115) Lichtin, N. N., *Carbonium Ions*, Olah, G. A., Schleyer, P. v. R., Eds., vol. 1, ch. 4., Wiley-Interscience, New York, **1968**.

(116) Gillespie, R. J., Robinson, E. A., *Carbonium Ions, Olah*, G. A., Schleyer, P. v. R., Eds., vol. 1, ch. 3., Wiley-Interscience, New York, **1968**.

(117) Gillespie, J.; Milne, J. B.; Thompson, C., *Inorg. Chem.*, **1966**, *5*, 468.

(118) Olah, G. A.; Pittman, C. U.; Symons, M. C. R., *Carbonium Ions*, Olah, G. A., Schleyer, P. v. R., Eds., vol. 1, ch. 5, Wiley-Interscience, New York, **1968**.

(119) Saunders, M.; Hagen, E. L., *J. Am. Chem. Soc.*, **1968**, *90*, 6881.

(120) Olah, G. A.; Spear, R. J., *J. Am. Chem. Soc.*, **1975**, *97*, 1539. b) Spiesecke, H.; Schneider, W. G., *Tetrahedron Lett.*, **1961**, 468. c) Nelson. G. L.; Levy, G. C.; Cargioli, J. D., *J. Am. Chem. Soc.*, **1972**, *94*, 3089.

(121) a) Olah, G. A.; Prakrash, G. K. S.; Schleyer, P. v. R., *Superacids*, ch. 3, Wiley-Interscience, New York, **1985**. and references therein. b) Lenoir, D.; Siehl, H.-U., *Methoden der Organischen Chemie, Houben-Weyl*, p. 249ff, Georg Thieme Verlag, Stuttgart, **1990**. and references therein. c) Olah, G. A.; Prakash, G. K. S.; Kobayashi, T.; Paquette, L. A., *J. Am. Chem. Soc.*, **1988**, *110*, 8599. d) Olah, G. A.; Kelly, D. P, Jeuell, C. L.; Porter, R. D., *J. Am. Chem. Soc.*, **1970**, *92*, 2544.

(122) Lenoir, D.; Siehl, H.-U., *Methoden der Organischen Chemie, Houben-Weyl*, vol. 19c, p. 38, Georg Thieme Verlag, Stuttgard, **1990**.

(123) a) for the allyl and the benzyl cations see: Olah, G. A.; Prakrash, G. K. S.; Schleyer, P. v. R., *Superacids*, ch. 3, Wiley-Interscience, **1985**. and references therein. b) Lenoir, D.; Siehl, H.-U., *Methoden der Organischen Chemie, Houben-Weyl*, vol 19c, p. 249ff, Georg Thieme Verlag, Stuttgart, **1990**. and references therein. c) for the halide substituted cations see: Olah, G. A.; Liang, G.; Mo, Y. K., *J. Org. Chem.*, **1974**, *39*, 2394. d) for the oxygen and sulfur containing adamantyl cations see: Olah, G. A.; Nakajima, T.; Prakash, G. K. S., *Angew. Chem. Int. Ed. Engl.*, **1980**, *19*, 811.

(124) Schleyer, P. v. R.; Lenoir, D.; Mison, P.; Liang, G.; Prakash, G. K. S., *J. Am. Chem. Soc.*, **1980**, *102*, 683.

(125) Newton, M. D.; Schulman, J. M.; Manus, M. M., *J. Am. Chem. Soc.*, **1981**, *103*, 17.

(126) Binsch, G., *Dynamic Nuclear Magnetic Resonance Spectroscopy*, Jackman, L. M.; Cotton, F. A., Eds., p. 45ff, Academic Press, London, **1975**. b) Steigel, A., *NMR, Basic Principles and Progress*, Diehl, P., Fluck, E.; Kosfeld, R., Eds., vol. 15, p. 1, Springer Verglag, Berlin, **1978**.

(127) a) Saunders. M.; Chandrasekhar, J.; Schleyer, P. v. R., *Rearrangements in Ground and Excited States*, De Mayo, P., Ed., vol. 1, p. 1, Academic Press, New York, **1980**. b) Saunders, M.; Jaffe, M. H.; Vogel, P., *J. Am. Chem. Soc.*, **1971**, *93*, 2558. c) Saunders, M.; Vogel, P., *J. Am. Chem. Soc.*, **1971**, *93*, 2559, 2561.

(128) Myhre, P. C.; Yannoni, C. S., *J. Am. Chem. Soc.*, **1981**, *103*, 230. b) Yannoni, C. S., *Acc. Chem. Res.*, **1982**, *15*, 201. c) Lyerla, J.; Yannoni, C. S.; Fyfe, C. A., *Acc. Chem. Res.*, **1982**, *15*, 208.

(129) Yannoni, C. S.; Kendrick, R. D., *J. Chem. Phys.*, **1981**, *74*, 747. b) Horne, D.; Kendrick, R. D.; Yannoni, C. S., *J. Magn. Res.*, **1983**, *52*, 299. c) Yannoni, C. S.;

Clarke, T. C., *Phys. Rev. Lett.*, **1983**, *51*, 1191.

(130) Yannoni, C. S.; Kendrick, R. D.; Myhre, P. C.; Bebout, D. C.; Petersen, B. L, *J. Am. Chem. Soc.*, **1989**, *111*, 6440.

(131) Olah, G. A.; Baker, E. B.; Evans, J. C.; Tolgyesi, W. S.; McIntire, J. S.; Bastien, J. J., *J. Am. Chem. Soc.*, **1964**, *86*, 1360.

(132) for a review see: Evans, J. C., *Carbonium Ions*, Olah, G. A., Schleyer, P. v. R., Eds., vol. 1, ch. 6, Wiley-Interscience, New York, **1968**.

(133) Craig, N. C.; Lai, R. K.-Y.; Matus, L. G.; Miller, J. H.; Palfrey, S. L., *J. Am. Chem. Soc.*, **1980**, *102*, 38.

(134) Sunko, D. E., *Stable Carbocation Chemistry*, Prakash, G. K. S.; Schleyer, P. v. R., Eds., ch. 11, Wiley-Interscience, New York, **1997**.

(135) Henis, J. M. S., *Ion-Molecule Reactions*, Franklin, J. L., Ed., vol.2, ch. 9., Plenum Press, New York, **1972**.

(136) a) Hollander, J. M.; Jolly, W. L., *Acc. Chem. Res.*, **1970**, *3*, 1931. b) Betteridge, D.; Baker, A. D., *Anal. Chem.*, **1970**, *42*, 42A.

(137) Olah, G. A.; Mateescu, G. D.; Wilson, L. A.; Goss, M. H., *J. Am. Chem. Soc.*, **1970**, *92*, 7231.

(138) Olah, G. A.; Svoboda, J. J.; Ku. A. T., *Synthesis*, **1973**, 492.

(139) Olah, G. A.; Olah, J. A.; Svoboda, J. J., *Synthesis*, **1973**, 490.

(140) Hollenstein, S., Laube, T., *J. Am. Chem. Soc.*, **1993**, *115*, 7240.

(141) Laube, T., *Angew. Chem. Int. Ed. Engl.*, **1986**, *25*, 349.

(142) Laube, T., *Angew. Chem. Int. Ed. Engl.*, **1987**, *26*, 560. b) Laube, T., *Helv. Chim. Acta*, **1994**, *77*, 943.

(143) Pulay, P., *Mol. Phys.*, **1969**, *17*, 197.

(144) Berkert, U.; Allinger, N. L., *Molecular Mechanics*, American Chemical Society Monograph 177, Washington, D. C., **1982**.

(145) Stewart, J. J. P., *Reviews of Computational Chemistry*, Lipkovitz, K.; Boyd, D. B., Eds., VCH Publishers, New York, **1990**.

(146) Hehre, W. J.; Radom, L; Schleyer, P. v. R.; Pople, J. A., *Ab initio Molecular Orbital Theory*, Wiley-Interscience, New York, **1986**.

(147) Møller, C.; Plesset, M. S., Phys. Rev., **1934**, *46*, 618.

(148) Hohenberg, P.; Koh, W., *Phys. Rev. B*, **1964**, *136*, 864.

(149) Becke, A. C., *J. Chem. Phys.*, **1993**, *98*, 5648.

(150) Hehre, W. J.; Radom, L; Schleyer, P. v. R.; Pople, J. A., *Ab initio Molecular Orbital Theory*, ch. 4, Wiley-Interscience, New York, **1986**.

(151) For a discussion on basis sets and the use of different calculation methods see: Hehre, W. J.; Radom, L; Schleyer, P. v. R.; Pople, J. A., *ab initio Molecular Orbital Theory*, ch. 3, Wiley-Interscience, New York, **1986**.

(152) a) Cope, A. C.; Fenton, S. W.; Spencer, C. F., *J. Am. Chem. Soc.*, **1952**, *74*, 5884. b) Prelog, V.; Schenker, K., *Helv. Chim. Acta*, **1952**, *35*, 2044.

(153) a) Cope, A. C.; Berchtold, G. A.; Peterson, P. E.; Sharmen, S. H., *J. Am. Chem. Soc.* **1960**, *82*, 6366. b) Roberts, A. A.; Anderson. C. B., *Tetrahedron Lett.*, **1969**, 3883.

(154) a) Dunitz, J. D.; Prelog, V., *Angew. Chem.*, **1960**, *72*, 896. b) Allinger, N. L.; Szkrybalo, W., *Tetrahedron*, **1968**, *24*, 4699. c) Allinger, N. L.; Greenberg, S., *J. Am. Chem. Soc.* **1962**, *84*, 2394.

(155) For reviews on 3c-2e bonds, see a) Olah, G. A.; Prakash, G. K. S.; Field, L. D.; Wade, K., *Hypercarbon Chemistry*, Wiley-Interscience: New York, **1987.** b) DeKock, R. L.; Bosma, W. B., *J. Chem. Educ.*, **1988**, *65*, 194. c) McMurry, J. E.; Lectka, T., *Acc. Chem. Res.*, **1992**, *25*, 47.

(156) Sorensen, T. S., *Stable Carbocation Chemistry*, Prakash, G. K. S., Schleyer, P. v. R., Eds., ch. 3, Wiley-Interscience, New York, **1997**.

(157) McMurry, J. E.; Hodge, C. N., *J. Am. Chem. Soc.*, **1984**, *106*, 6450. b) McMurry, J. E.; Lectka, T.; Hodge, C. N., *J. Am. Chem. Soc.*, **1989**, *111*, 8867.

(158) Wolinski, K., Hinton, J. F., Pulay, P., *J. Am. Chem. Soc.*, **1990**, *112*, 8251.

(159) a) Schindler, M.; Kutzelnigg, W., *J. Chem. Phys.*, **1982**, *76*, 1919. Schindler, M., *J. Am. Chem. Soc.*, **1987**, *109*, 1020. b) Cioslowski,J., *J. Am. Chem. Soc.*, **1993**, *115*, 5177.

(160) McMurry, J. E.; Lectka, T., *J. Am. Chem. Soc.* **1990**, *112*, 869.

(161) Benson, S. W., *Thermochemical Kinetics*, p. 272, Wiley-Interscience, New York, **1976**.

(162) a) Olah, G. A.; Prakash, G. K. S.; Williams, R. E.; Field, L. D.; Wade, K., *Hypercarbon Chemistry*, p. 148f., Wiley-Intersciance, New York, **1987**. b) Olah, G. A.; Prakash, G. K. S.; Sommer, J., *Superacids*, p. 125f., Wiley-Interscience, New York, **1985**. c) Vogel, P., *Carbocation Chemistry*, p. 63, 103, 167, Elsevier, Amsterdam, **1985**.

(163) Alder, R. W.; Casson, A.; Session, R. B., *J. Am. Chem. Soc.* **1979**, *101*, 3652.

(164) Carlson, B.A.; Brown, H.C., *Org. Synth.*, **1978**, *58*, 24.

(165) Fell, B.; Seide, W.; Asinger, F., *Tetrahedron Lett.*, **1968**, 1003.

(166) Foote, C.S.; Woodward, R.B., *Tetrahedron*, **1964**, *20*, 687.

(167) Stork, G.; Brizzolara, A.; Landesman, H.; Szmuszkovicz, J.; Terrell, R., *J. Am. Chem. Soc.* **1963**, *85*, 207

(168) Schut, R.N.; Liu, T.M.H., *J. Org. Chem.*, **1965**, *30*, 2845.

(169) Cope, A.C.; Nealy, D.L.; Scheiner, P.; Wood, G., *J. Am. Chem. Soc.*, **1965**, *87*, 3130.

(170) Allan, R.D.; Cordiner, B.G.; Wells, R.J., *Tetrahedron Lett.*, **1968**, 6055.

(171) Fujimoto, Y.; Tatsuno, T., *Tetrahedron Lett.*, **1976**, *37*, 3325.

(172) Coll, J. C.; Crist, DeL., R.; Barrio, M. del C.; Leonard, N. J., *J. Am. Chem. Soc.*, **1972**, *94*, 7092.

(173) Gutsche, G. D.; Redmore, D., *Advan. Alicycl. Chem.*, **1968**, *2*, 81.

(174) Parker, W.; Steele, W. V.; Stirling, W.; Watt, I., *J. Chem. Thermodynamics*, **1975**, *7*, 795.

(175) Spartan Version 4.0, on IBM PowerPC 250 AIX UNIX 3.0.2.

(176) Wayne, G. S.; Snyder, G. J., *Synth. Comm.*, **1995**, *25*, 3267.

(177) Nagata, W.; Itazaki, H., *Chem. Ind.*, **1964**, 1194.

(178) Doyle, M.; Parker, W.; Gunn, P. A.; Martin, J.; MacNicol, D. D., *Tetrahedron Lett.*, **1970**, 3519. b) Engler, E. M.; Andose, J. D.; Schleyer, P. v. R., *J. Am. Chem. Soc.* **1973**, *95*, 8005.

(179) Parker, W.; Tranter, R. L.; Watt, I. F.; Chang, L. W. K.; Schleyer, P. v. R., *J. Am. Chem. Soc.* **1974**, *96*, 7121.

(180) a) Geluk, H. W.; Schlatmann, J. L. M. A., *J. Chem. Soc., Chem. Commun.*, **1967**, 426. b) Schleyer, R. v. R.; Funke, E.; Liggero, S. H., *J. Am. Chem. Soc.*, **1969**, *91*, 3965. c) Nordlander, J. E.; Wu, F.Y-H.; Jindal, S. P., *J. Am. Chem. Soc.*, **1969**, *91*, 3962. d) Schlatmann, J. L. M. A.; Korsloot, J, G. ; Schut, J., *Tetrahedron*, **1970**, *26*, 949.

(181) Sasaki, T.; Eguchi, S.; Toru, T.; Itoh, K., *J. Am. Chem. Soc.*, **1972**, *94*, 1357.

(182) Tabushi, I.; Yoshida, Z.-i.; Takahashi, N., *J. Am. Chem. Soc.*, **1970**, *92*, 6670.

(183) Olah, G. A.; Liang, G.; Schleyer, P. v. R.; Parker, W.; Watt, C. I. F., *J. Am. Chem. Soc.*, **1977**, *99*, 966.

(184) Stetter, H.; Gaertner, J., *Chem. Ber.*, **1966**, *99*, 925.

(185) Hamill, H.; Karim, A.; McKervey, M. A., *Tetrahedron*, **1971**, *27*, 4317.

(186) Stepanov, F. N.; Martynova, É. N.; Zosim, L. A.; Yurchenko, A. G., *J. Org. Chem. USSR (Engl. Transl.)*, **1971**, *7*, 2632.

(187) Kimoto, K.; Imagawa, T.; Kawanisi, M., *Bull. Chem. Soc. Jpn.*, **1972**, *45*, 3698.

(188) Scott, A. P.; Radom, L., *J. Phys. Chem.*, **1996**, *100*, 16502.

(189) Lombardo, L.; Uchiyama, M.; Noyori, R., *Org. Synthesis*, **1986**, coll. vol. VIII, 386.

(190) Kirchen, R. P.; Sorensen, T. S., *J. Am. Chem. Soc.* **1978**, *100*, 1487.

(191) Kirkbride, P. K., Sorensen, T. S., *J. Phys. Org. Chem.*, **1991**, *4*, 492.

(192) a) Marvell, E. N.; Seubert, J., Sturmer, D.; Federici, W., *J. Org. Chem.*, **1970**, *35*, 396. b) Heumann, A.; Kraus, W., *Tetrahedron*, **1978**, *34*, 411.

(193) D. N. Kursanov, Z. N. Parnes and N. M. Loim, *Synthesis*, **1974**, 633.

(194) Kursanov D.N.; Parnes, Z.N. Kalinkin, M.I; Loim, N.M., *Ionic Hydrogenation and Related Reactions*, Harwood, Chur, **1985**

(195) Kursanov, D.N.; Parnes, Z.N., *Russ. Chem. Rev. (Engl. Transl.)*, **1969**, *38*, 812.

(196) Kursanov D.N.; Parnes, Z.N.; Bassova, G.I.; Loim, N.M.; Zdanovich, V.I., *Tetrahedron*, **1967**, *23*, 2235.

(197) Sommer, J.; Bukala, J.; Hachoumy, M.; Jost, R., *J. Am.Chem.Soc.*, **1997**, 119, 3274.

(198) a) Olah, G.A.; Schlosberg, R.H., *J. Am. Chem. Soc.*, **1968**, *90*, 2726. b) Hogeveen, H.; Bickel, G.F., *J. Chem. Soc., Chem. Commun.*, **1967**, 635. c) Corma, A.; Miguel, R.J.; Orchillès, V.A., *J. Catal.*, **1994**, *145*, 171. d) Corma, A.; Planelles, J.; Sandoz-Marin, J.;Thomas, F., *J. Catal.*, **1985**, *93*, 30. e) Olah, G.A.; Prakash, S.K.; Sommer, J., *Superacids*; Wiley-Interscience, New York, **1985**.

(199) Hogeveen, H.; Gaasbeek, C. J.; Bickel, A. F., *Rec. Trav. Chim.*, **1969**, *88*, 353. b) Hogeveen, H.; Gaasbeek, C. J., *Rec. Trav. Chim.*, **1969**, *88*, 719. c) Hogeveen, H.; Bickel, A. F., *Rec. Trav. Chim.*, **1967**, *86*, 1313.

(200) Salmon, L.; Poshusta, R. D., *J. Chem. Phys.*, **1973**, *59*, 3497.

(201) a) Gaussian 94, Revision D.2, Frisch, M. J.; Trucks, G. W.; Schlegel, H. B.; Gill, P. M. W.; Johnson, B. G.; Robb, M. A.; Cheeseman, J. R.; Keith, T.; Petersson, G. A.; Montgomery, J. A.; Raghavachari, K.; Al-Laham, M. A.; Zakrzewski, V. G.; Ortiz, J. V.; Foresman, J. B.; Cioslowski, J.; Stefanov, B. B.; Nanayakkara, A.; Challacombe, M.; Peng, C. Y.; Ayala, P. Y.; Chen, W.; Wong, M. W.; Andres, J. L.; Replogle, E. S.; Gomperts, R.; Martin, R. L.; Fox, D. J.; Binkley, J. S.; Defrees, D. J.; Baker, J.; Stewart, J. P.; Head-Gordon, M.; Gonzalez, C.; Pople, J. A., Gaussian, Inc., Pittsburgh PA, **1995**. b) Gaussian 98, Revision A.3, Frisch, M. J.; Trucks, G. W.; Schlegel, H. B.; Scuseria, G. E.; Robb, M. A.; Cheeseman, J. R.; Zakrzewski, V. G.; Montgomery, J. A. Jr.; Stratmann, R. E.; Burant, J. C.; Dapprich, S.; Millam, J. M.; Daniels, A. D.; Kudin, K. N.; Strain, M. C.; Farkas, O.; Tomasi, J.; Barone, V.; Cossi, M.; Cammi, R.; Mennucci, B.; Pomelli, C.; Adamo, C.; Clifford, S.; Ochterski, J.; Petersson, G. A.; Ayala, P. Y.; Cui, Q.; Morokuma, K.; Malick, D. K.; Rabuck, A. D.; Raghavachari, K.; Foresman, J. B.; Cioslowski, J.; Ortiz, J. V.; Stefanov, B. B.; Liu, G.; Liashenko, A.; Piskorz, P.; Komaromi, I.; Gomperts, R.; Martin, R. L.; Fox, D. J.; Keith, T.; Al-Laham, M. A.; Peng, C. Y.; Nanayakkara, A.; Gonzalez, C.; Challacombe, M.; Gill, P. M. W.; Johnson, B.; Chen, W.; Wong, M. W.; Andres, J. L.; Gonzalez, C.; Head-Gordon, M.; Replogle, E. S.; Pople, J. A., Gaussian, Inc., Pittsburgh PA, **1998**.

(202) Saunders, M.; Kates, M. R., *J. Am. Chem. Soc.* **1978**, *100*, 7082. b) Saunders, M.; Hagen, E. L.; Rosenfeld, J., *J. Am. Chem. Soc.* **1968**, *90*, 6882.

(203) Hiraoka, K.; Kebarle, P., *J. Am. Chem. Soc.* **1976**, *98*, 6119.

(204) a) Brownstein, S.; Bornais, J., *Can. J. Chem.*, **1971**, *49*, 7. b) Olah, G. A.; Mo. Y. K.; Olah, J. A., *J. Am. Chem. Soc.*, **1973**, *95*, 4939.

(205) Amman, C.; Meier, P.; Merbach, A. E., *J. Magn. Res.*, **1982**, *46*, 319.

(206) Private communication, Siehl, H. U., Universität Ulm, **1995**.

(207) Baeckvall, J.-E.; Nordberg, R. E.; Bjoerkman, E. E.; Moberg, C., *J. Chem. Soc. Chem. Commun.*, **1980**, *20*, 943.

(208) Majewski, M.; Mackinnon, J., *Can. J. Chem.*, **1994**, *72*, 1699.

(209) a) Paquette, L.A.; Stucki, H., *J. Org. Chem.*, **1966**, *31*, 1232. b) Stork, G.; Briozzolara, A.; Landesman, H. ; Szmuskovicz, J.; Terrell, R., *J. Am. Chem. Soc.*, **1963**, *85*, 207.

(210) Stork, G.; Landesman, H.K., *J. Am. Chem. Soc.*, **1956**, *78*, 5129.

(211) Heumann, A.; Kolshorn, H., *Tetrahedron*, **1975**, *31*, 1571.

(212) Erman, W.F.; Kretschmar, H.C., *J. Org. Chem.*, **1968**, *33*, 1545.

(213) Knights, E.F.; Brown, H.C., *J. Amer. Chem. Soc.*, **1968**, *90*, 5283.

(214) Doyle, M.; Parker, W., *J. Chem. Soc. Perkin Trans. 1*, **1977**, 858. b) Tian, J.; Yan, Y.; Gong, B.; Valente, E. J.; Zubkowski, J. D., *Synth. Commun.*, **1998**, *28*, 1907.

(215) Craciun, L.; Jackson, J. E., *J. Amer. Chem. Soc.*, **1996**, *118*, 48.

(216) Murray, R. P.; Murray, R. J.; Watt, C. I. F., *Tetrahedron*, **1980**, *36*.

(217) Bestmann, H. J.; Roeder, T.; Suehs, K., *Chem.Ber.*, **1988**; *121*, 1509.

(218) Leonard, L., *J. Am. Chem. Soc.*, **1970**, *92*, 6685.

(219) Slobodin, Y. M.; Ashkinazi, L. A..; Klimchuk, G. N., *J. Org. Chem. USSR (Engl.Transl.)*, **1984**, *20*, 1125.

(220) a) Yurchenko, A.G. et al., *J. Org. Chem. USSR (Engl.Transl.)*, **1974**, *10*, 1195. b) Denmark, S. E.; Henke, B. R. *J. Am. Chem. Soc.*, **1991**, *113*, 2177. c) Mink, L.; Rettig, M. F.; Wing, R. M., *J. Am. Chem. Soc.*, **1991**, *113* 2065. d) Senda, Y.; Ishiyama, J.-I.; Imaizumi, S., *J. Chem. Soc. Perkin Trans. 2*, **1981**, 90. e) Bishop, R., *Aust. J. Chem.*, **1984**, *37*, 319.

(221) Krasutskii, P. A.; Rodionov, V. N.; Khotkevich, A. B.; Serguchev, Yu. A.; Yurchenko, A. G; Bubnov, Y. N.; Grandberg, A. I.; Averina, N. V.; Zefirov, N. S., *J. Org. Chem. USSR (Engl.Transl.)*, **1985**, *21*, 1452.

(222) a) Gill, G.B.; Black, R.M., *J. Chem. Soc. C*, **1970**, 671. b) Schleyer, R. von R.; Funke, E.; Liggero, S. H., *J. Am. Chem. Soc.*, **1969**, *91*, 3965.

(223) Ward, Harry D.; Murray, Roger K., *J. Org. Chem.*, **1990**, *55*, 81.

(224) Landa, S.; Vais, J.; Burkhard, J., *Coll. Czech. Chem. Commun.*, **1967**, *32*, 570.

Appendix A

Calculation Data

1 Bicyclo[3.3.3]undecyl system

1.1 Bicyclo[3.3.3]undec-1-yl cation (78)

N-N= 6.870949049607D+02 E-N=-2.353789415132D+03 KE= 4.260061817611D+02
1\1\UOFC-OXYGEN\FOpt\RB3LYP\6-31G(d)\C11H19(1+)\CTAESCHL\15-Oct-1996\0
\\#BECKE3LYP 6-31G* OPT FREQ\\Bicyclo[3.3.3]undecyl monocation out sym
metric\\1,1\C,-1.2677271433,-1.1355643135,-1.0072039847\C,0.0436437795
,-1.0523297445,-1.8024390257\C,1.372033373,-1.1075078313,-0.9584367054
\C,-1.621468634,0.0010416346,0.0000685003\C,-1.2674635957,1.4421066099
,-0.4793251956\C,0.0435312768,2.088246602,-0.0087198176\C,1.3716737066
,1.384824878,-0.4794343487\C,1.4141297177,0.0004383042,0.0004068722\C,
-1.2677714811,-0.3051515984,1.4879094017\C,0.0432766476,-1.037501772,1
.8096836115\C,1.3716087843,-0.276318364,1.4389605481\H,-1.3291819848,-
2.1042582635,-0.4949894885\H,-2.0584933696,-1.1652865048,-1.7671662279
\H,0.0599218258,-0.1491071343,-2.41965898\H,0.1046323699,-1.8982954373
,-2.4947105788\H,2.1936403357,-0.9668936628,-1.6779319898\H,1.48582142
8,-2.0811737652,-0.4763367841\H,-1.3299274302,1.48480326,-1.57403077\H
,-2.0584054879,2.1143246038,-0.1237649905\H,0.1048962201,3.1113228215,
-0.3936757922\H,0.0595035898,2.1694379588,1.082136467\H,1.4846663421,1
.4548990852,-1.5637252711\H,2.193496111,1.937401268,0.0018921812\H,-2.
0587977617,-0.9490047076,1.8923703978\H,-1.3285914752,0.621164473,2.07
3015282\H,0.0593248703,-2.0197269681,1.3284053329\H,0.1045806017,-1.22
11603996,2.8872071481\H,2.193676965,-0.9690346711,1.6771941108\H,1.483
372263,0.6271769197,2.0426065869\H,-2.7188598446,0.0011337192,-0.00032
64899\\Version=SGI-G94RevD.2\HF=-430.3387498\RMSD=9.594e-09\RMSF=5.721
e-05\Dipole=1.1285438,0.0002231,0.0003946\PG=C01 [X(C11H19)]\\@

1.2 Bicyclo[3.3.3]undeca-1,5-diyl dication (36)

N-N= 6.753269365945D+02 E-N=-2.313255048462D+03 KE= 4.250193847724D+02
1\1\UOFC-OXYGEN\FOpt\RB3LYP\6-31G(d)\C11H18(2+)\CTAESCHL\07-Oct-1996\0
\\#BECKE3LYP 6-31G* OPT\\Bicyclo[3.3.3]undecyl dication symmetric\\2,1
\C,-0.9556603129,1.1221131059,1.3367215957\C,-0.7781310742,1.939958379
3,0.0000056563\C,-0.9556377836,1.1221304427,-1.3367238293\C,0.00026770
94,0.0002977162,1.3979177894\C,1.4500554919,0.267016643,1.335589209\C,
2.0670734354,-0.298459461,0.0000158115\C,1.4500779647,0.2670341718,-1.
3355607251\C,0.0002912167,0.0003158167,-1.3979178702\C,-0.4933999247,-
1.3887338662,1.3362643253\C,-1.2905624072,-1.6419974019,-0.0000215288\
C,-0.4933774829,-1.3887165857,-1.3362907062\H,-1.9909013602,0.79491649
77,1.4600092989\H,-0.7138414041,1.8271431008,2.1496912165\H,0.18198140
23,2.4590137326,0.0000170847\H,-1.563224666,2.7016834458,0.0000039544\
H,-0.7138049719,1.8271708265,-2.1496803065\H,-1.9908767171,0.794935285
3,-1.4600331839\H,1.6845406409,1.3273401534,1.4571019613\H,1.939827222
9,-0.2933767302,2.1496060101\H,3.121065249,-0.0056358676,0.0000266476\
H,2.0299146327,-1.3891811384,0.0000084449\H,1.6845650928,1.3273593541,
-1.4570552451\H,1.9398639264,-0.2933483635,-2.1495764171\H,-1.22385674
19,-1.5329755434,2.1498972396\H,0.3083266598,-2.1211599599,1.457913985
\H,-2.2189809097,-1.0685524956,-0.0000256006\H,-1.5601258406,-2.702200
4757,-0.0000306646\H,-1.2238203893,-1.5329478418,-2.1499379372\H,0.308
3513411,-2.1211409409,-1.4579362157\\Version=SGI-G94RevD.2\HF=-429.294
3933\RMSD=6.062e-09\RMSF=4.093e-05\Dipole=-0.0009945,0.0015839,0.\PG=C
01 [X(C11H18)]\\@

1.3 Bicyclo[3.3.3]undecyl μ-H bridged cation (30)

N-N= 6.922536058538D+02 E-N=-2.363668335731D+03 KE= 4.260340799728D+02
1\1\ UOFC-OXYGEN\FOpt\RB3LYP\6-31G(d)\C11H19(1+)\CTAESCHL\05-Oct-1995\
0\\# BECKE3LYP 6-31G* OPT\\trial on mumanxcat\\1,1\C,-1.1212446571,-1.
297839371,-1.0232135561\C,-2.0032771568,-0.0090007449,-0.9813262074\H,
-2.7081711042,-0.0122560481,-1.8169003732\C,-1.1326433968,1.2875485958
,-1.0236632857\H,-2.6049945387,-0.0114951977,-0.0650816269\H,-0.708301
9481,-1.4399263082,-2.0273035659\H,-1.7513865572,-2.1666206132,-0.7966
708317\H,0.00029283,0.000005663,0.0006113871\H,-1.7704181598,2.1508208
135,-0.7974212122\H,-0.7209682208,1.4329213549,-2.0278034662\C,-0.0051
35477,1.1916813566,-0.0004741506\C,1.4551551099,-1.2870300602,-0.46481
08886\C,-0.3174046397,-1.2941505009,1.4873092863\C,1.4437537421,1.2996
47095,-0.4652655341\C,-0.3288007068,1.291821609,1.4868600802\C,1.85521
87755,0.0079611363,-1.2420339889\H,1.5782482174,-2.1513667876,-1.12884
34868\H,2.1183874234,-1.4316437238,0.3942769095\H,1.3688272478,0.00564
40214,-2.2244482242\H,1.5592215625,2.1648035171,-1.1296001045\H,2.1056
847189,1.4504034461,0.3937698958\H,2.9323203078,0.0126740051,-1.428532
5137\H,0.1805094019,2.1599288819,1.9229153693\H,-0.2257456391,-0.00042
97515,3.2534090743\H,-1.4052036395,1.4318108247,1.6302239436\H,0.19953
7826,-2.1575812976,1.9236683125\H,-1.3925320466,-1.4435722329,1.630723
2648\C,0.1492179586,0.001046464,2.2265566188\H,1.2434365387,0.00587943
56,2.2937271993\C,0.0053697447,-1.1916855801,-0.0000583657\\Version=SG
I-G94RevB.3\HF=-430.3284435\RMSD=6.652e-09\RMSF=7.865e-05\Dipole=0.000
2473,-0.0000148,0.0000568\PG=C01 [X(C11H19)]\\@

1.4 Transition-state of the 3-methoxybicyclo[3.3.3]undecyl dication (263)

N-N= 8.999575442601D+02 E-N=-3.026897941330D+03 KE= 5.385455017559D+02
1\1\UOFC-OXYGEN\FTS\RB3LYP\6-31G(d)\C12H20O1(2+)\CTAESCHL\24-Apr-1998\
0\\#BECKE3LYP 6-31G* OPT(CALCFC, TS, NOEIGENTEST) GEOM=CHECKPOINT GUES
S=READ\\3-Methoxy-bicyclo[3.3.3]undecyl-1,5-dication\\2,1\C,1.57919408
73,1.4650114731,-0.334492974\C,0.0951425431,1.3280163479,-0.0596700295
\H,-3.5777157978,0.7858234875,-0.1889935286\H,-1.3698983885,1.40570727
08,1.5620274886\C,-0.7946865946,1.0825892753,-1.2745093281\H,2.0933076
219,1.7786080891,0.5768935394\H,1.6319808243,2.3090201889,-1.043881408
8\C,2.3518126958,0.285049509,-0.9691456413\C,2.3557774196,-1.008605804
2,-0.0537886205\H,3.3974345167,0.5801543695,-1.0932979322\H,1.96666640
3,0.039293645,-1.9610234481\H,2.9851109889,-0.8703231434,0.8284085979\
H,2.7650955251,-1.822322571,-0.674773427\C,0.9586508477,-1.2804520256,
0.2699153755\H,0.4952251474,-1.5975691146,-1.8609486164\C,0.4409196825
,-1.1024521743,1.6629429145\H,-4.2616446204,-0.8171980597,-0.565122357
4\C,0.4957388145,0.3995646627,2.2395679778\H,1.0914732297,-1.681458746
5,2.3364553272\H,-0.583270031,-1.4830301364,1.7481070299\H,0.064908024
1,0.3444120924,3.2428655053\C,-0.2894015118,1.4852700702,1.4064674436\
H,1.5401620708,0.6930629638,2.3617150887\H,0.0282569915,2.4742608118,1
.7680658075\H,-1.7242153878,1.6572244074,-1.2737001542\C,-1.0174223728
,-0.3601906663,-0.7663249608\H,-0.2927102793,1.203843336,-2.236048633\
H,-0.513232609,-0.0147430634,0.2793131953\C,0.0016281086,-1.5246527186
,-0.8895195096\O,-2.2437575647,-0.8260111208,-0.4696284778\H,-0.550866
6446,-2.4611314529,-0.7212207363\C,-3.4691372061,-0.1100932137,-0.8073
695739\H,-3.4853061494,0.1301261782,-1.8722519572\\Version=SGI-G94RevD
.2\HF=-543.7347766\RMSD=6.926e-09\RMSF=3.615e-06\Dipole=0.6047322,0.14
2294,-0.101571\PG=C01 [X(C12H20O1)]\\@

1.5 Transition-state of the 3-isobutylbicyclo[3.3.3undecyl dication (262)

N-N= 1.153424022398D+03 E-N=-3.625741347253D+03 KE= 5.806102566841D+02
1\1\UOFC-OXYGEN\FTS\RB3LYP\6-31G(d)\C15H26(2+)\CTAESCHL\01-Apr-1998\0\
\#BECKE3LYP 6-31G* OPT(CALCFC, TS, NOEIGENTEST) GEOM=CHECKPOINT GUESS=
READ\\3-isobutyl-bicyclo[3.3.3]undecyl-1,5-dication TS\\2,1\C,1.138135
0827,1.5188769751,-0.9831432601\C,0.2720268626,1.1881958294,0.23961084
92\H,-0.6271389769,-1.7241644603,2.1584895455\H,0.3254826386,0.2157034
838,3.1073997072\C,-1.1177566027,1.2833519646,0.8582777882\H,1.7459722
375,2.4143474589,-0.8057248749\H,0.5752874003,1.6771177086,-1.90004304

63\C,2.1083397918,0.2705395151,-1.1010283567\C,1.5664292016,-1.1389149
441,-0.5291848517\H,3.0626874439,0.4911588795,-0.6214777629\H,2.334141
348,0.0771113626,-2.1529512933\H,2.4657309503,-1.7678213508,-0.4673894
333\H,0.90028951,-1.5705476375,-1.2717644679\C,0.9166667513,-1.1747096
165,0.821506854\H,-0.8927080754,-2.2167610249,0.4947163732\C,1.7660194
917,-1.0509638956,2.022948022\C,-2.4134580398,-0.442591286,-0.37844822
63\C,1.2995196442,0.3129496093,2.6211333375\H,2.8331434493,-1.03227977
21,1.7892510827\H,1.5660664857,-1.865061375,2.7328242414\H,2.012435251
8,0.6396671694,3.383720441\C,1.2978607132,1.2893263395,1.4464228263\H,
2.3150327453,1.3376211526,1.0623848146\H,1.0524216188,2.309197648,1.78
17971405\H,-1.0522550646,1.7209754205,1.8568618324\C,-1.6525410574,-0.
1983095918,0.9422814485\H,-1.8338171654,1.88323459,0.294127294\H,-2.34
57305986,-0.2991981901,1.7814214012\C,-0.5511194983,-1.3851120028,1.12
34298262\H,-2.7848550847,-1.4739216255,-0.3976922834\C,-1.5443721401,-
0.1943654847,-1.5909446586\H,-3.2716728419,0.2398155222,-0.3962421463\
C,-1.1544023679,-1.3801194601,-2.4219121317\H,-0.2845842062,0.20044835
01,-0.6425051584\C,-1.7760693127,1.0559048033,-2.3868779269\H,-2.77094
57507,0.9227206846,-2.8490208462\H,-1.0715322842,1.180154852,-3.212703
6295\H,-1.844847546,1.9743748382,-1.8004803083\H,-0.9802801437,-2.2973
957124,-1.855586915\H,-0.3289150656,-1.1784136993,-3.1103485818\H,-2.0
310793974,-1.5824368018,-3.0634923653\\Version=SGI-G94RevD.2\HF=-586.4
404039\RMSD=5.854e-09\RMSF=8.765e-06\Dipole=-0.2002673,-0.3610748,-0.1
626959\PG=C01 [X(C15H26)]\\@

1.6 3,7-dimethylbicyclo[3.3.1]nona-3,7-diyl dication (37)

N-N= 6.560357083367D+02 E-N=-2.276133623951D+03 KE= 4.250385873251D+02
1\1\GINC-ALPHA23\FOpt\RB3LYP\6-31G(d)\C11H18(2+)\ROOT\08-Oct-1998\0\\#
BECKE3LYP 6-31G* OPT GEOM=CHECKPOINT GUESS=READ\\3,7-dimethyl-bicyclo[
3.3.1]nonanyl-3,7-dication\\2,1\C,-0.5438592431,-0.6372053774,1.615827
782\C,0.6208211366,-1.3604291008,1.0753064685\C,1.6712791899,-0.637169
7272,0.3369773135\C,1.3456399404,0.7915517864,-0.1618267752\C,0.517680
1004,1.5386914983,0.8967333461\C,-0.8130294107,0.7915170612,1.08442281
51\C,-1.61500383,0.8044359426,-0.2394962749\C,0.6001346046,0.804471403
,-1.5183467585\C,-0.8639207763,0.6378681013,-1.4964074293\C,0.77042581
3,-2.7961237308,1.3344015397\C,-1.5852227708,0.3743171559,-2.745805378
3\H,-0.287602105,-0.5695503024,2.6978913453\H,-1.4271504453,-1.2940714
213,1.6333649965\H,2.128159184,-1.2940142171,-0.4191971996\H,2.4802123
826,-0.5695058129,1.0999682607\H,2.3017546193,1.298175566,-0.320164273
9\H,0.3388281416,2.5745850315,0.5869669377\H,1.0648262672,1.5974724842
,1.8444645999\H,-1.4282538047,1.2981155424,1.8332556541\H,-2.060601144
6,1.8167089096,-0.3731111752\H,-2.5090162126,0.1619994083,-0.240529182
5\H,1.0462932916,0.1620562029,-2.2930912729\H,0.707213489,1.8167531151
,-1.9710346774\H,0.2769772411,-3.3054560283,0.4796706416\H,1.811486234
5,-3.1356861678,1.3226412603\H,0.2396834577,-3.1357111772,2.2300804565
\H,-1.6352743726,-0.7317794543,-2.8325285442\H,-2.6245040921,0.7191677
417,-2.7309648407\H,-1.0527006558,0.7191905033,-3.638402878\\Version=D
EC-AXP-OSF/1-G98RevA.3\HF=-429.3290158\RMSD=3.650e-09\RMSF=3.625e-05\D
ipole=-0.2978235,-0.8852147,-0.5158938\PG=C01 [X(C11H18)]\\@

1.7 9-ethylbicyclo[3.3.1]non-9-yl cation (38)

N-N= 6.780978819942D+02 E-N=-2.335690987246D+03 KE= 4.260384013297D+02
1\1\GINC-AURORA\FOpt\RB3LYP\6-31G(d)\C11H19(1+)\MACI10\07-Mar-1999\0\\
#BECKE3LYP 6-31G* OPT\\9-ethylbicyclo[3.3.1]non-9-yl cation conformer
c\\1,1\C,1.0169908002,-1.4079228279,-1.0235917494\C,1.4208369546,-1.70
93474343,0.4235400601\C,0.3007554805,0.0205806903,-1.2059707684\C,0.29
46653839,-1.4035933728,1.4167252222\C,-0.4042625412,0.0246345327,1.175
0912065\C,1.2324079411,1.241425131,-0.9721669059\C,-0.7841812781,-0.08
71660133,-0.232136886\C,0.5054400165,1.2457908543,1.4822911355\C,-2.15
71911771,-0.4228619167,-0.6380710445\C,1.6602778435,1.4538660701,0.489
0800436\C,-2.9039260959,0.941059267,-0.8608983573\H,-0.0876866293,0.03
30674995,-2.2298901305\H,1.6697927469,-2.7753368134,0.4991178666\H,0.3
30963262,-2.1765705226,-1.3974355757\H,-1.287577614,0.0399339076,1.822

3747538\H,2.0394122644,2.4756871765,0.599545207\H,2.3307456365,-1.1705
726686,0.6918830521\H,-0.1450164726,2.1292739161,1.4827969377\H,-2.436
5240652,1.5312205768,-1.6532867981\H,0.6474936786,-1.3831930328,2.4534
038329\H,0.6881302502,2.1243459155,-1.3297268602\H,2.1071972652,1.1371
561484,-1.622521397\H,-0.484983884,-2.1717590327,1.3594797794\H,0.8848
410438,1.1446144736,2.5044981414\H,2.5002610074,0.80201582,0.739047735
4\H,-2.6824259251,-0.9815822448,0.1433995054\H,-2.1729268855,-0.983936
3171,-1.5781090614\H,1.8772398494,-1.3906419937,-1.7012967237\H,-2.942
5453278,1.5335403542,0.0567662497\H,-3.9272701699,0.7039469548,-1.1633
982542\\Version=SGI-G94RevD.3\HF=-430.3540878\RMSD=7.917e-09\RMSF=5.62
1e-06\Dipole=-0.6488784,-0.2614418,-0.1918007\PG=C01 [X(C11H19)]\\@

1.8 9-methylbicyclo[3.3.1]non-9-yl cation (199)

N-N= 5.823920354264D+02 E-N=-2.054469347484D+03 KE= 3.871217532834D+02
1\1\GINC-ALPHA29\FOpt\RB3LYP\6-31G(d)\C10H17(1+)\ROOT\05-Feb-1999\0\\#
BECKE3LYP 6-31G* OPT\\9-methylbicyclo[3.3.1]nonyl 1 cation / chair-cha
ir\\1,1\C,0.4987684026,1.2023868448,-0.1170618082\C,-0.2907925835,1.28
04477155,-1.4520482242\H,-0.8767331181,2.2053734926,-1.451259047\C,-1.
186609402,0.0657395555,-1.7417942679\H,0.4543912425,1.3903421299,-2.24
96206864\H,1.2275204839,2.0173511295,-0.058223429\H,0.2524129006,1.466
9812213,2.0628076615\C,-0.4159660697,1.3348931163,1.2045829594\H,-1.44
56919763,0.0665261313,-2.8061384161\C,-0.505226767,-1.2693342005,-1.40
17933406\H,-2.1363875927,0.1562360686,-1.2098754444\H,-1.2379229793,-2
.0820931541,-1.3642089597\C,0.2943141799,-1.2717650496,-0.0705393079\H
,0.2063729449,-1.5346133388,-2.1934500897\H,-0.9659726716,2.2734020185
,1.0780848851\C,-1.3461285023,0.1378359605,1.4251508701\C,1.1315671943
,-0.0916173909,0.1193430019\H,-2.2142290397,0.1952297876,0.7671803898\
H,-1.7400773715,0.1902088575,2.4480982353\H,0.0204829326,-1.4049461284
,2.118810886\C,-0.6224591725,-1.2014752137,1.255124515\C,2.4896549243,
-0.1931793843,0.6772489866\H,0.8791729472,-2.1928239631,0.020298465\H,
-1.3169703597,-2.0434861118,1.1658432986\H,2.7992795262,0.6995167914,1
.2290080751\H,3.1582364211,-0.260104604,-0.2032945656\H,2.6533824862,-
1.1066920497,1.2566584358\\Version=DEC-AXP-OSF/1-G98RevA.3\HF=-391.038
4299\RMSD=9.936e-09\RMSF=3.364e-05\Dipole=0.9157955,-0.0700237,0.35738
2\PG=C01 [X(C10H17)]\\@

1.9 5-ethylbicyclo[4.3.0]non-1-yl cation (202)

N-N= 6.537473048040D+02 E-N=-2.287376602943D+03 KE= 4.260348914995D+02
1\1\GINC-OZONE5\FOpt\RB3LYP\6-31G(d)\C11H19(1+)\CTAESCHL\09-Mar-1999\0
\\#BECKE3LYP 6-31G* OPT\\2-ethylbicyclo[4.3.0]undec-6-yl cation\\1,1\C
,-1.4293537738,-2.2513280644,-0.3203701827\C,-0.1395661082,-2.81409299
44,-0.9552898747\C,0.7077534507,-1.5493367354,-1.1995834856\C,0.328018
2476,-0.6086588599,-0.0254507658\C,-1.0266160513,-1.0201746298,0.37192
57974\C,-1.8418117714,-0.249562708,1.3132407153\C,-1.6622795233,1.2851
132319,1.1161378119\C,-0.1868288632,1.6716096409,0.9744129225\C,0.5159
043946,0.938905278,-0.1821239153\C,2.0116898051,1.2816538913,-0.315019
0838\C,2.2864656097,2.7515625934,-0.6527461498\H,-2.0508932263,-2.9219
909731,0.2859609064\H,-2.1158583411,-1.8740728722,-1.111853732\H,-0.33
84397437,-3.3831146849,-1.8654069955\H,0.3539942466,-3.4864990993,-0.2
448306624\H,0.4276344276,-1.0707067207,-2.1462747837\H,1.778446235,-1.
756090121,-1.2395981096\H,0.9275916943,-0.9013403304,0.8669443799\H,-1
.4388673139,-0.5133852568,2.3109110256\H,-2.887084723,-0.5753779954,1.
3113813208\H,-2.1245179827,1.7918320785,1.9678002773\H,-2.2242331359,1
.5874547705,0.2244503325\H,0.3463878381,1.4743572385,1.9157159123\H,-0
.1238456978,2.7513272544,0.8060999084\H,0.0147343616,1.213965303,-1.12
26039502\H,2.5220063848,1.0102603188,0.6208726051\H,2.4506578524,0.651
9976328,-1.0987631808\H,3.3583745688,2.9078339118,-0.8067891914\H,1.77
32333822,3.0526263953,-1.5735715343\H,1.9704266734,3.4267792883,0.1487
527358\\Version=DEC-AXP-OSF/1-G98RevA.3\HF=-430.3548341\RMSD=6.561e-09
\RMSF=6.345e-06\Dipole=-1.1830075,-1.187672,0.4075948\PG=C01 [X(C11H19
)]\\@

1.10 5-methylbicyclo[4.3.0]non-1-yl cation (208)

N-N= 5.636484142335D+02 E-N=-2.017155495884D+03 KE= 3.871235181187D+02
1\1\GINC-ALPHA20\FOpt\RB3LYP\6-31G(d)\C10H17(1+)\ROOT\13-Feb-1999\0\\#
BECKE3LYP 6-31G* OPT\\b430-2-me-6-cation\\1,1\C,0.8606204178,0.3897745
109,-2.6139373384\C,0.9253426528,0.3787441044,-1.0833216722\C,1.175326
9046,1.7789796121,1.0428090922\H,0.7373337028,-0.6176872336,-3.0236172
986\C,-0.119966811,1.1630648237,1.6501067261\C,-0.3585020599,-0.272801
5736,-0.4745911912\C,1.1391017689,1.7815703228,-0.4888046816\H,2.03479
02919,1.2022158521,1.4045016686\C,-1.0642505317,-1.2775274893,1.613625
7467\H,-0.9568899019,1.8612783373,1.4487928883\H,-1.2218237086,0.31014
36497,-0.871357441\H,0.3504010688,2.4591173503,-0.8458643424\H,1.76586
47543,-0.2599626636,-0.7749960671\H,1.2861834383,2.7923297056,1.438390
5947\C,-0.5123034486,-0.0762628966,0.9755835433\H,-0.0832328857,1.0426
464627,2.7378225565\C,-0.643089882,-1.7795307919,-0.7109806494\H,2.084
4750641,2.185426142,-0.8684503898\H,1.7868145059,0.801631332,-3.026899
1884\H,0.0285029074,1.0085540834,-2.9714246489\H,-1.5220701224,-3.2339
116084,0.7084494732\H,-1.7408818452,-1.0707991575,2.4521019748\H,-0.16
4277044,-1.7328469392,2.0865288748\C,-1.5668639147,-2.1719135037,0.459
9603476\H,0.3021861153,-2.3346750584,-0.6638599176\H,-1.0887406143,-1.
9706361673,-1.6886508623\H,-2.611126303,-1.9274067994,0.2358325854\\Ve
rsion=DEC-AXP-OSF/1-G98RevA.3\HF=-391.0414295\RMSD=8.891e-09\RMSF=5.06
8e-06\Dipole=-0.5322642,-0.0835127,1.0548553\PG=C01 [X(C10H17)]\\@

1.11 2-methyl-2-decalyl cation (39)

N-N= 6.617171672733D+02 E-N=-2.303462405327D+03 KE= 4.260432974463D+02
1\1\GINC-ALPHA22\FOpt\RB3LYP\6-31G(d)\C11H19(1+)\ROOT\14-Nov-1998\0\\#
BECKE3LYP 6-31G* OPT\\3-methyl-bicyclo[4.4.0]decyl-3-cation\\1,1\C,-2.
2624143278,-1.878044301,0.2018510252\C,-1.2843210103,-2.4152683918,-0.
8498326377\C,-2.1470913246,-0.3533953456,0.3574108607\C,-0.6928022233,
0.0664773511,0.6822337289\C,0.2545291734,-0.4797990294,-0.3956200954\C
,0.1704257292,-2.0066764337,-0.5433711456\C,-0.5519683183,1.5809565223
,0.8155498427\C,0.9663734194,1.9921787721,1.0959754368\C,1.7121277205,
1.3819374754,-0.0054008408\C,1.7834681318,-0.0660075144,-0.0441575502\
C,2.184920625,2.199837687,-1.1359774536\H,-2.0652579012,-2.3595229671,
1.1694726715\H,-1.3370734133,-3.5087898876,-0.9002331717\H,-1.56498465
74,-2.0424569046,-1.8443345583\H,-2.4659522779,0.141342925,-0.57101828
49\H,-2.8131191487,0.0038390219,1.1508964319\H,-0.4167765236,-0.396418
6881,1.642301593\H,-0.000723749,-0.021268366,-1.3615493397\H,0.8400991
674,-2.3517670972,-1.339061952\H,0.504125665,-2.4781678041,0.390849553
3\H,-0.8982234858,2.0880371852,-0.0929214616\H,-1.1301325708,1.9821421
666,1.653958161\H,1.0534598629,3.0806847694,1.1255902449\H,1.242882113
2,1.5593795647,2.0627887471\H,-3.2901896058,-2.139523824,-0.0726300728
\H,2.4468500838,-0.4572858058,-0.8182229847\H,2.0040205921,-0.51396932
16,0.9288660279\H,2.2878945135,1.6360706444,-2.0670499349\H,1.60051500
74,3.1144628055,-1.2776244599\H,3.2031007581,2.5300308312,-0.852044236
\\Version=DEC-AXP-OSF/1-G98RevA.3\HF=-430.3622879\RMSD=4.074e-09\RMSF=
2.209e-05\Dipole=1.5678844,1.4621502,-0.0447325\PG=C01 [X(C11H19)]\\@

2 Tricyclo[5.3.1.1^{3,9}]dodecyl system

2.1 Tricyclo[5.3.1.1^{3,9}]dodec-5-yl cation (34)

1\1\GINC-OZONE7\FOpt\RB3LYP\6-31G(d)\C12H19(1+)\CTAESCHL\26-Aug-1998\0
\\#BECKE3LYP 6-31G* OPT\\t5311m-2c\\1,1\C,0.3749060776,-1.2351560357,1
.331510011\C,-0.1426989051,-1.4501650774,-0.022837989\C,0.8206750953,-
1.4546159998,-1.115448989\C,1.4944649774,0.0082710545,-1.096485989\C,2
.1796989627,0.1898731098,0.258754011\C,1.1154169628,0.188856024,1.3586
97011\C,0.1726918655,1.395319948,1.194492011\C,-0.4531531496,1.5834278
975,-0.217156989\C,0.504856885,1.1536159748,-1.376631989\C,-1.58981890
36,-1.4686321941,-0.283987989\C,-2.337059003,-0.2359792543,0.300701011
\C,-1.9283221105,1.0977387786,-0.338415989\H,1.156101137,-1.9722419727
,1.555227011\H,-0.3976169187,-1.280905098,2.101144011\H,0.3682161116,-
1.6570810363,-2.088007989\H,1.6448011515,-2.1525179333,-0.928655989\H,
2.2279429809,-0.0360538863,-1.908627989\H,2.7062138851,1.1527481522,0.

268714011\H,2.9349910253,-0.5862458293,0.429400011\H,1.5770509593,0.23
20290612,2.350561011\H,0.7825077945,2.2765279971,1.429576011\H,-0.6125
821329,1.3757958847,1.959323011\H,-0.550332237,2.6674788897,-0.3501819
89\H,1.1294538154,2.0175380251,-1.635670989\H,-0.0790510975,0.93734592
77,-2.279541989\H,-1.9766508317,-2.3607482253,0.241166011\H,-1.8029418
938,-1.5897492113,-1.349558989\H,-2.2012420055,-0.2039032434,1.3863710
11\H,-3.4052579891,-0.4072813404,0.133362011\H,-2.5658221719,1.8600457
272,0.126855011\H,-2.20573411,1.0918927563,-1.400581989\\Version=DEC-A
XP-OSF/1-G94RevE.2\HF=-468.4551061\RMSD=5.292e-09\RMSF=1.152e-05\Dipol
e=0.0799589,-1.0086002,0.0509105\PG=C01 [X(C12H19)]\\@

2.2 Tricyclo[5.3.1.1^{3,9}]dodeca-5,9-diyl dication (40)

1\1\ UOFC-OXYGEN\FOpt\RB3LYP\6-31G(d)\C12H18(2+)\CTAESCHL\19-Oct-1995\
0\\# BECKE3LYP 6-31G* OPT\\test on 5311dicat\\2,1\H,1.9545303893,0.,-2
.1783674848\C,0.3120893961,1.3208856322,1.7625325967\H,1.3666079537,1.
4177916325,2.0323354412\C,-0.297427116,0.,2.3572061834\H,-0.2464527271
,2.1492597637,2.2324144312\C,0.3120893961,-1.3208856322,1.7625325967\H
,2.2147288688,1.3756000668,-0.1172314983\C,0.1097319554,1.4065505775,0
.303578142\H,1.1983567667,2.1569553206,-1.3559345833\H,-0.2464527271,-
2.1492597637,2.2324144312\C,0.1097319554,-1.4065505775,0.303578142\H,-
0.0659695231,0.,3.4261121531\H,-1.3843803756,0.,2.2583115433\H,1.36660
79537,-1.4177916325,2.0323354412\C,-1.2471781921,-1.3318763389,-0.2716
352122\C,1.24918222,-1.3349677045,-0.6265297875\C,-1.2471781921,1.3318
763389,-0.2716352122\C,1.24918222,1.3349677045,-0.6265297875\H,-2.0357
02903,-1.3763815541,0.4831261017\H,-1.3967471848,-2.1590006213,-0.9807
082381\C,-1.3496661571,0.,-1.1428178104\C,-0.248356708,0.,-2.197930677
\H,-1.3967471848,2.1590006213,-0.9807082381\H,-2.035702903,1.376381554
1,0.4831261017\H,-2.3572622118,0.,-1.5688109742\H,1.1983567667,-2.1569
553206,-1.3559345833\H,2.2147288688,-1.3756000668,-0.1172314983\C,1.10
2971692,0.,-1.4914562301\H,-0.3397673229,-0.880713745,-2.8453031051\H,
-0.3397673229,0.880713745,-2.8453031051\\Version=SGI-G94RevB.3\State=1
-A'\HF=-467.4122173\RMSD=7.187e-09\RMSF=3.274e-05\Dipole=0.0217448,0.,
0.2648887\PG=CS [SG(C4H4),X(C8H14)]\\@

2.3 Tricyclo[5.3.1.1^{3,9}]dodecayl μ-H bridged cation (33)

N-N= 7.942535109597D+02 E-N=-2.655341797868D+03 KE= 4.638130519272D+02
1\1\GINC-ZINC10\FOpt\RB3LYP\6-31G(d)\C12H19(1+)\UNKNOWN\23-Jun-1998\0\
\#BECKE3LYP 6-31G* OPT\\Tricyclo[5.3.1.1]dodecyl-1,5-mu-H-cation\\1,1\
H,-2.2266875056,2.1590873385,0.2969464399\C,-1.8381741774,1.3084260109
,-0.2757119053\C,-2.5306357703,0.000000195,0.2496575853\C,-0.324684824
6,1.1962167932,-0.1059848574\H,-2.0831626891,1.4695274238,-1.330261828
3\H,1.2806778531,2.1721896644,-1.1843906839\C,0.3236557101,1.256878901
3,1.2664593811\H,-3.5841631413,0.0000007145,-0.0418883057\H,-2.5109451
576,-0.0000011648,1.3457829426\C,-1.8381748137,-1.3084247472,-0.275715
0819\H,-2.2266880847,-2.1590871041,0.2969418425\C,-0.3246855678,-1.196
2160963,-0.1059881266\H,-2.083163968,-1.4695238292,-1.3302651723\C,0.6
633755005,-1.269631954,-1.2622638049\H,-0.422814505,-1.2768415515,2.06
68613401\H,0.927205862,-2.1683429421,1.3522170683\H,1.2806765913,-2.17
21873345,-1.1843965132\C,1.5794282738,0.0000009682,-1.1416976848\H,0.1
4899355,-1.295446818,-2.2280508323\H,2.3208427049,0.0000019933,-1.9456
700203\H,2.9301480182,-0.8775595007,0.3238920743\C,0.663375902,1.26963
51085,-1.2622603098\H,0.1489939914,1.2954529125,-2.2280472845\H,0.9272
076348,2.1683391024,1.352222586\C,1.2445044425,-0.0000022121,1.3879395
854\H,-0.4228134178,1.2768372039,2.0668648682\H,1.7526530896,-0.000003
3253,2.3564969842\C,2.2788022956,-0.0000011088,0.2377139877\C,0.323654
9829,-1.2568818149,1.2664562197\H,-0.4097610828,0.0000004079,-0.180779
866\H,2.9301485359,0.877556546,0.3238944301\\Version=DEC-AXP-OSF/1-G94
RevD.2\HF=-468.4356497\RMSD=5.946e-09\RMSF=1.307e-05\Dipole=-0.2288771
,0.0000004,-0.0249992\PG=C01 [X(C12H19)]\\@

2.4 Transition-state of the 7-methoxytricyclo[5.3.1.1^{3,9}]dodecyl dication (265)

N-N= 1.009033758257D+03 E-N=-3.331998613219D+03 KE= 5.763427020885D+02
1\1\UOFC-OXYGEN\FTS\RB3LYP\6-31G(d)\C13H20O1(2+)\CTAESCHL\15-Feb-1998\
0\\#BECKE3LYP 6-31G* OPT(CALCFC, TS, NOEIGENTEST) GEOM=CHECKPOINT GUES
S=READ\\3-Methoxy-tricyclo[5.3.1.1]dodecyl mu H bridged dication trans
ition state\\2,1\C,-0.3009977539,-1.8891141208,-0.3877912447\C,0.11666
29839,-1.017161061,0.7869863909\C,-1.3092810529,-1.0227378512,-1.23223
33225\H,-0.8212796277,-2.7884544329,-0.0305487605\H,0.5563097701,-2.22
44767664,-0.9804641716\C,-1.0479627327,-0.4012745367,1.5508099299\C,-2
.5830318483,-0.7526049201,-0.4300553667\C,-0.7082008706,0.4387508819,-
1.6469226575\C,1.4679195617,-0.6919022761,1.393616675\H,-1.5139309506,
-1.536784542,-2.1743787584\H,0.6550352826,-0.2263394974,-0.3141079106\
C,-2.2324862759,0.1662257208,0.7357443866\C,-0.6721973689,1.3601482551
,-0.4694744171\C,1.5043259873,0.3890651981,0.2828357676\H,-0.702401080
6,0.3103674913,2.3050961069\H,-1.4186399485,-1.2707284676,2.1258281043
\H,-3.3701317101,-0.319931487,-1.0551379877\H,-2.9856054073,-1.6949807
548,-0.0343867901\H,-1.4112886603,0.8317606087,-2.3904819729\H,0.27335
87189,0.3251626429,-2.1220420118\H,2.2407401061,-1.4436703246,1.224150
1382\H,1.457207991,-0.3773992293,2.4365998264\C,-1.9286173654,1.689389
6518,0.14474796\C,0.6262418967,1.6741914729,0.2556670526\O,2.543976938
2,0.485766191,-0.5694188309\H,-3.0734032093,0.3551568109,1.410581788\C
,3.8060801858,-0.2120488212,-0.350142824\H,-2.7544538938,1.9079906461,
-0.5345782695\H,-1.8779209756,2.4036812132,0.968285967\H,1.1575866031,
2.4308596133,-0.3471117313\H,0.4573341504,2.1256511791,1.2369362028\H,
4.1622746559,-0.0439759221,0.668248221\H,3.7004590704,-1.2780005912,-0
.5702030147\H,4.4862015285,0.2424167199,-1.0696643086\\Version=SGI-G94
RevD.2\HF=-581.860026\RMSD=4.996e-09\RMSF=9.949e-06\Dipole=-0.3573489,
0.0460874,0.4607411\PG=C01 [X(C13H20O1)]\\@

2.5 Transition-state of the 7-isobutyltricyclo[5.3.1.1^{3,9}]dodecyl dication (264)

N-N= 1.009033758257D+03 E-N=-3.331998613219D+03 KE= 5.763427020885D+02
1\1\UOFC-OXYGEN\FTS\RB3LYP\6-31G(d)\C13H20O1(2+)\CTAESCHL\15-Feb-1998\
0\\#BECKE3LYP 6-31G* OPT(CALCFC, TS, NOEIGENTEST) GEOM=CHECKPOINT GUES
S=READ\\3-Methoxy-tricyclo[5.3.1.1]dodecyl mu H bridged dication trans
ition state\\2,1\C,-0.3009977539,-1.8891141208,-0.3877912447\C,0.11666
29839,-1.017161061,0.7869863909\C,-1.3092810529,-1.0227378512,-1.23223
33225\H,-0.8212796277,-2.7884544329,-0.0305487605\H,0.5563097701,-2.22
44767664,-0.9804641716\C,-1.0479627327,-0.4012745367,1.5508099299\C,-2
.5830318483,-0.7526049201,-0.4300553667\C,-0.7082008706,0.4387508819,-
1.6469226575\C,1.4679195617,-0.6919022761,1.393616675\H,-1.5139309506,
-1.536784542,-2.1743787584\H,0.6550352826,-0.2263394974,-0.3141079106\
C,-2.2324862759,0.1662257208,0.7357443866\C,-0.6721973689,1.3601482551
,-0.4694744171\C,1.5043259873,0.3890651981,0.2828357676\H,-0.702401080
6,0.3103674913,2.3050961069\H,-1.4186399485,-1.2707284676,2.1258281043
\H,-3.3701317101,-0.319931487,-1.0551379877\H,-2.9856054073,-1.6949807
548,-0.0343867901\H,-1.4112886603,0.8317606087,-2.3904819729\H,0.27335
87189,0.3251626429,-2.1220420118\H,2.2407401061,-1.4436703246,1.224150
1382\H,1.457207991,-0.3773992293,2.4365998264\C,-1.9286173654,1.689389
6518,0.14474796\C,0.6262418967,1.6741914729,0.2556670526\O,2.543976938
2,0.485766191,-0.5694188309\H,-3.0734032093,0.3551568109,1.410581788\C
,3.8060801858,-0.2120488212,-0.350142824\H,-2.7544538938,1.9079906461,
-0.5345782695\H,-1.8779209756,2.4036812132,0.968285967\H,1.1575866031,
2.4308596133,-0.3471117313\H,0.4573341504,2.1256511791,1.2369362028\H,
4.1622746559,-0.0439759221,0.668248221\H,3.7004590704,-1.2780005912,-0
.5702030147\H,4.4862015285,0.2424167199,-1.0696643086\\Version=SGI-G94
RevD.2\HF=-581.860026\RMSD=4.996e-09\RMSF=9.949e-06\Dipole=-0.3573489,
0.0460874,0.4607411\PG=C01 [X(C13H20O1)]\\@

2.6 6-Methyltricyclo[4.3.1.1^{3,8}]undec-6-yl cation (132)

1\1\GINC-ALPHA14\FOpt\RB3LYP\6-31G(d)\C12H19(1+)\ROOT\25-Nov-1998\0\\#
BECKE3LYP 6-31G* OPT\\2-methyl-bicyclo[4.3.1.1]undecyl-2-cation\\1,1\C
,1.0553798797,1.1232419968,-1.2719540879\C,0.3585058593,1.6503999699,0

.0023829121\C,1.0392938799,1.1179949962,1.2832819121\C,1.2925709386,-0
.402267994,1.2568859121\C,2.1127709528,-0.7696029623,0.0082319121\C,1.
3077339384,-0.3970569934,-1.2486810879\C,0.0205719708,-1.2349420432,-1
.3070420879\C,-0.8834760318,-1.1666160781,-0.0108630879\C,0.0057569711
,-1.2410120437,1.2971719121\C,-1.1594911311,1.4024299112,-0.0065030879
\C,-1.7096730784,0.0377338899,-0.0060450879\C,-3.1782390725,-0.1150661
668,0.0011079121\H,0.453468869,1.3983609736,2.1694079121\H,2.007485860
4,1.6217600337,1.3872309121\H,1.8607589489,-0.668564972,2.1569519121\H
,2.3532149942,-1.840333953,0.0075309121\H,3.067322932,-0.2308039254,0.
0151679121\H,1.8864529486,-0.660183971,-2.1428930879\H,0.2781530119,-2
.2959260332,-1.3988530879\H,-0.5798070388,-0.9850900664,-2.1898830879\
H,-1.5442559981,-2.0392531037,-0.0159530879\H,0.2619710121,-2.30361803
38,1.3857109121\H,-0.6045250384,-0.9960130673,2.1745869121\H,2.0248498
602,1.6273590343,-1.3614270879\H,0.4807858687,1.4075169746,-2.16415708
79\H,0.453454817,2.7429319736,0.0052059121\H,-1.6418981504,1.900880892
6,-0.8711980879\H,-1.6548031509,1.9127238921,0.8430259121\H,-3.7297871
089,0.8264538119,0.0030959121\H,-3.4765200488,-0.7262691784,-0.8655500
879\H,-3.466553049,-0.722350178,0.8741559121\\Version=DEC-AXP-OSF/1-G9
8RevA.3\HF=-468.4615108\RMSD=4.768e-09\RMSF=1.786e-05\Dipole=-1.915440
6,-0.0265835,-0.0024308\PG=C01 [X(C12H19)]\\@

2.7 2-Ethyl-2-adamantyl cation (35)

N-N= 7.808128307971E+02 E-N=-2.628841622743E+03 KE= 4.638302801092E+02
1|1|GINC-UNK|FOpt|RB3LYP|6-31G(d)|C12H19(1+)|PCUSER|21-Jun-1998|0||#BE
CKE3LYP 6-31G* OPT GEOM=CHECKPOINT GUESS=READ||2-ethyl-adamantyl-2-cat
ion||1,1|C,-2.3535777143,-0.481109044,-0.0991156304|C,-1.2193252714,-1
.5236523511,-0.0283835649|C,-0.4017819351,-1.321308503,1.2573275421|C,
0.2395104616,0.0963252196,1.2576050175|C,-0.9404574907,1.1779565621,1.
1812821319|C,-1.7508942695,0.9386982727,-0.097122857|C,-0.826656601,1.
1331463914,-1.3039155057|C,0.3535653953,0.051410575,-1.2331614269|C,1.
004336304,0.3761106932,0.0391812696|C,-0.2874170056,-1.3663442026,-1.2
404782107|C,2.3159981111,1.0390051384,0.0872941398|C,3.3970728408,-0.0
990451207,0.1575534867|H,-1.6442352497,-2.5339054273,-0.0296236971|H,0
.3853597902,-2.0787153499,1.3477084781|H,-1.0328445666,-1.4077919687,2
.1487683484|H,0.8321245429,0.284835575,2.157996385|H,-0.5290429333,2.1
927572729,1.2159164017|H,-1.5325087128,1.0316402062,2.0914246939|H,-2.
5536138006,1.6860422747,-0.147357933|H,-0.4121261945,2.1467201475,-1.3
373004357|H,-1.3333199727,0.9532099382,-2.2584875803|H,1.0262670465,0.
208382982,-2.0818449849|H,-3.0326523999,-0.6003682515,0.7534083162|H,0
.5034332681,-2.1252231373,-1.2312805748|H,-0.8345534558,-1.485864477,-
2.1821482975|H,-2.9521296949,-0.6320816369,-1.0052641648|H,2.497104839
6,1.6339465089,-0.8138249941|H,2.414876553,1.6665095458,0.97905305|H,4
.3762589519,0.3854124246,0.1935989188|H,3.2788731362,-0.7101168164,1.0
560263728|H,3.3604919008,-0.7425515978,-0.7251666547||Version=x86-Win3
2-G94RevE.1|HF=-468.4733243|RMSD=4.495e-009|RMSF=1.037e-005|Dipole=0.8
250162,0.4326797,0.0299773|PG=C01 [X(C12H19)]||@

2.8 Transition state 1 (181) in the Tricyclo[5.3.1.1^{3,9}]dodec-5-yl cation rearrangement

N-N= 7.922822040352D+02 E-N=-2.651758740343D+03 KE= 4.637795159543D+02
1\1\GINC-ZINC10\FTS\RB3LYP\6-31G(d)\C12H19(1+)\UNKNOWN\13-Jul-1998\0\\
#BECKE3LYP 6-31G* OPT(CALCFC, TS, NOEIGENTEST) GEOM=CHECKPOINT GUESS=R
EAD\\tricyclo[5.3.1.1]dodecyl-1-cation TS to 2-cation\\1,1\C,-0.283571
0835,-1.0578009459,-1.3958938013\C,0.6738620873,-1.4846634912,-0.21952
93095\C,-0.0086119134,-1.4353372615,1.1779107222\C,-1.4712580073,-0.098
0272398,-1.0997033003\C,-1.0792965271,-0.3401173862,1.3604303462\C,-1.
0761501105,1.4228416721,-1.0819879897\C,-2.1289490826,-0.454342339,0.2
430298895\C,-0.4975821912,1.1063935371,1.3778282349\C,-0.0207319714,1.
4746389301,-0.0122897935\C,1.3153243293,1.3246263927,-0.4238697506\C,2
.3376327151,0.5835004409,0.3211446924\C,2.1061528154,-0.8809873216,-0.
2474000382\H,-2.1983215592,-0.2068528212,-1.912295812\H,-0.742826094,-
1.976445585,-1.7782298572\H,-1.5551356126,-0.4919131025,2.3355782125\H

,0.3110572555,-0.6739757776,-2.2371233513\H,0.8844008806,-2.5434279511
,-0.411368525\H,-2.5243725412,-1.4763469242,0.2095462373\H,-1.94941836
71,2.0318571301,-0.8324723327\H,-0.6937613755,1.735580821,-2.058884779
6\H,-0.5146293726,-2.3925085332,1.3490630107\H,0.2936889584,1.19830188
52,2.1268138413\H,-1.2948208203,1.803772713,1.658699971\H,2.4937394884
,-0.9206970822,-1.2719132732\H,0.6803434536,2.5301474101,0.0248686202\
H,0.7521357728,-1.3621866924,1.9662055467\H,2.7693461741,-1.5098221714
,0.3584701601\H,1.5327803609,1.594110501,-1.4588800241\H,-2.9821248654
,0.2074182728,0.4368100107\H,2.1791323024,0.5873826473,1.4002059147\H,
3.3578599944,0.9012553337,0.0968870179\\Version=DEC-AXP-OSF/1-G94RevD.
2\HF=-468.4213264\RMSD=8.140e-09\RMSF=1.340e-05\Dipole=0.8135475,1.154
9155,-0.1782895\PG=C01 [X(C12H19)]\\@

2.9 Transition state 2 (183) in the Tricyclo[5.3.1.$1^{3,9}$]dodec-5-yl cation rearrangement

N-N= 7.848699517871D+02 E-N=-2.637887292623D+03 KE= 4.637417174610D+02
1\1\UOFC-OXYGEN\FTS\RB3LYP\6-31G(d)\C12H19(1+)\CTAESCHL\22-Jul-1998\0\
\#BECKE3LYP 6-31G* OPT(CALCFC, TS, NOEIGENTEST) GEOM=CHECKPOINT GUESS=
READ\\TS2 from T5311msc to t4311mtc\\1,1\C,1.0157974148,1.0779679909,-
1.2754398556\C,0.2254719133,1.6535627217,-0.0791272489\C,0.8190546177,
1.232162955,1.2794668645\C,1.4314285785,-0.4014855134,-1.1241187214\C,
1.1661028052,-0.2633061762,1.366862713\C,0.252074628,-1.3884965485,-1.
2278174313\C,2.1372877266,-0.6193444259,0.226273999\C,-0.0695034684,-1
.186313138,1.3075877703\C,-0.7696453771,-1.25279134,-0.0732789728\C,-1
.7533560747,-0.0918970821,-0.3189346797\C,-3.0807763881,-0.2762140742,
0.1148295285\C,-1.3026440971,1.4545443934,-0.1628396027\H,2.1248578963
,-0.6363833483,-1.9403607126\H,1.9306701257,1.6741741244,-1.3845101449
\H,1.6558330034,-0.4388613246,2.3320190085\H,0.4532720204,1.2286247996
,-2.2083470818\H,0.2943234943,2.7518649086,-0.1345692367\H,3.035656522
5,0.0064731743,0.2926832367\H,0.6498170126,-2.4100000775,-1.1979784887
\H,-0.2541391471,-1.2879892931,-2.1988916639\H,1.7426157703,1.80366914
02,1.4373506362\H,-0.7934826029,-0.9102570428,2.0881033681\H,0.2593537
595,-2.2066239737,1.5406069611\H,-1.7080974896,2.011596029,-1.01201995
21\H,-1.3934298773,-2.1580170135,-0.0875325756\H,0.1406612669,1.526385
1833,2.092034993\H,-1.7617196674,1.8538128219,0.7456994994\H,2.4708231
976,-1.6609832186,0.3137833488\H,-3.8373152424,0.4868643935,-0.0762464
267\H,-3.4218268868,-1.1823566749,0.6212076619\H,-2.0156268283,-0.0823
311843,-1.4238186081\\Version=SGI-G94RevD.2\HF=-468.3981207\RMSD=7.293
e-09\RMSF=3.155e-06\Dipole=-2.9521789,0.014315,-0.1757922\PG=C01 [X(C1
2H19)]\\@

2.10 Transition state 3 (185) in the Tricyclo[5.3.1.$1^{3,9}$]dodec-5-yl cation rearrangement

N-N= 7.962576776580D+02 E-N=-2.659964839365D+03 KE= 4.637947509319D+02
1\1\GINC-ALPHA12\FTS\RB3LYP\6-31G(d)\C12H19(1+)\SFANG\15-Aug-1998\0\\#
BECKE3LYP 6-31G* OPT(CALCFC, TS, NOEIGENTEST) GEOM=CHECKPOINT GUESS=RE
AD\\t5mcts5a second trial\\1,1\C,-1.2759639621,1.2742810147,-0.2131877
118\C,0.1187532543,1.5133557381,0.4060905609\H,1.3502857865,1.07997583
49,2.162390825\C,1.2397668278,1.3317919394,-0.647777842\H,0.1495439489
,2.5540349955,0.7544183826\H,-1.4884225286,2.138840453,-0.8536872234\H
,-2.0624068609,1.2915853167,0.5542632823\C,-1.3791384347,0.0046353078,
-1.0813227006\C,-0.2969735464,0.0496078714,-2.1747298316\H,-2.37121537
07,0.0027018645,-1.5480064075\C,-1.2460484397,-1.3110584897,-0.2881421
047\H,1.213690918,2.1985687739,-1.3187520606\C,1.0896833771,0.05713264
91,-1.5069626874\H,2.2231480829,1.3556890608,-0.1588566311\H,1.8654900
639,0.0929863299,-2.281155832\H,-0.39455546,-0.8152393761,-2.842822515
9\C,1.2881382791,-1.2644019637,-0.734614511\H,-0.4247441095,0.94507537
83,-2.7948615956\C,0.1626121468,-1.5817951313,0.2861249683\H,-1.470078
802,-2.1423117322,-0.9671039263\H,-2.0056788273,-1.3745287325,0.505312
554\H,2.2673341651,-1.2856996054,-0.2377043901\H,1.3001423172,-2.09025
07579,-1.4566864055\H,0.2211057622,-2.6464179617,0.5416573199\C,0.4958
930978,-0.8513215666,1.6038781563\H,-0.374964037,-1.2163276843,2.34168

09117\H,1.3527437561,-1.2315253106,2.1630282508\C,-0.5562051049,0.2103
711135,2.5970492694\H,-0.3434984052,0.1415960894,3.662314665\H,-1.6019
999554,0.2009046374,2.300513388\C,0.4584957641,0.7007919217,1.66593733
56\\Version=DEC-AXP-OSF/1-G94RevE.2\HF=-468.4177442\RMSD=9.709e-09\RMS
F=5.300e-06\Dipole=-0.0577196,-0.387484,2.3863769\PG=C01 [X(C12H19)]\\
@

2.11 Transition state 4 (184) in the Tricyclo[5.3.1.1^{3,9}]dodec-5-yl cation rearrangement

N-N= 7.857864159227D+02 E-N=-2.638852341407D+03 KE= 4.637960029147D+02
1\1\GINC-ZINC10\FTS\RB3LYP\6-31G(d)\C12H19(1+)\UNKNOWN\18-Jul-1998\0\\
#BECKE3LYP 6-31G* OPT(CALCFC, TS, NOEIGENTEST) GEOM=CHECKPOINT GUESS=R
EAD\\2-methyl-tricyclo[4.3.1.1]undecyl-2-cation to 3-cation ts\\1,1\C,
1.0977181016,1.1351462471,-1.261990416\C,0.3423963168,1.6829101548,-0.
0129384899\C,0.9411695516,1.0910570101,1.32133096\C,1.2093972056,-0.42
59789789,1.2607716808\C,2.1162320092,-0.7440098572,0.0588808588\C,1.37
57782968,-0.3786728278,-1.2396996261\C,0.105789992,-1.2418289727,-1.37
06238744\C,-0.8443733729,-1.1552208716,-0.1533519317\C,-0.0682697198,-
1.2934544386,1.1848351871\C,-1.1051914994,1.385345244,0.0407402629\C,-
1.7100249684,0.1161146744,-0.1130804384\C,-3.1695876913,-0.0644520688,
0.2843088535\H,0.3049733194,1.3479228791,2.1779658852\H,1.8859762963,1
.6260329337,1.475128396\H,1.7294445801,-0.6886548459,2.1897130203\H,2.
3799862688,-1.8082034861,0.0568941432\H,3.0569209059,-0.1844508843,0.1
313126035\H,2.0179725728,-0.5974981669,-2.1009034661\H,0.4131822763,-2
.2893885592,-1.4691139368\H,-0.4395152444,-0.9999924559,-2.2937606938\
H,-1.5541184348,-1.9858654729,-0.2250955768\H,0.2277244543,-2.34415143
93,1.2837934971\H,-0.7327717823,-1.0825799781,2.0333537365\H,2.0539974
925,1.6695069145,-1.2897976342\H,0.5555162806,1.4278769594,-2.17043594
76\H,0.4534552607,2.770642433,0.0044984758\H,-1.7122371045,0.658432887
2,-1.1909917687\H,-1.7923541222,2.2219968753,0.1949956134\H,-3.7218951
75,0.8792118965,0.307346806\H,-3.6728393265,-0.7555761706,-0.396507045
4\H,-3.1996238488,-0.5069942087,1.2865057339\\Version=DEC-AXP-OSF/1-G9
4RevD.2\HF=-468.4370509\RMSD=9.749e-09\RMSF=1.599e-05\Dipole=-1.272769
,0.9075161,-0.0811456\PG=C01 [X(C12H19)]\\@

2.12 Transition state 5 (187) in the Tricyclo[5.3.1.1^{3,9}]dodec-5-yl cation rearrangement

N-N= 7.854149080324D+02 E-N=-2.638029548017D+03 KE= 4.637891167312D+02
1\1\GINC-ALPHA13\FTS\RB3LYP\6-31G(d)\C12H19(1+)\CTAESCHL\10-Aug-1998\0
\\#BECKE3LYP 6-31G* OPT(CALCFC, TS, NOEIGENTEST) GEOM=CHECKPOINT GUESS
=READ\\TS 1 from T4311 ti T3311\\1,1\C,-0.0134016813,-1.819684935,-0.2
634693054\C,0.8029562939,-0.904348433,0.6537359549\C,-0.1099530276,-0.
210863376,1.7034521548\C,-1.2266453757,-1.0936278933,-0.8786260769\C,-
2.1590615463,-0.6591208835,0.2682002283\C,-0.833217234,0.1283550448,-1
.7480729918\C,-1.4317083125,0.3806857999,1.1418063628\C,-1.207944173,1
.6475036646,0.3077210449\C,-0.2813918062,1.318938016,-0.9333531023\C,1
.0550088661,1.1761417936,-0.3567220806\C,3.268169293,0.1406901812,0.25
34238668\C,1.8655500557,0.016922415,-0.3285204508\H,0.6224806661,-2.27
08586228,-1.0334219551\H,0.4440283248,0.5368011066,2.2852224278\H,-2.0
594817196,0.6513440259,1.9987168962\H,-3.086694112,-0.2280730923,-0.12
73805521\H,1.8321436309,-0.5546600237,-1.2582642213\H,-2.4469818836,-1
.5323923942,0.8657977276\H,1.5873331174,-1.4439864065,1.1940735124\H,-
1.7269308064,0.4825485678,-2.2735155341\H,-0.1192778992,-0.1622377458,
-2.5296394666\H,-0.7800659207,2.4620082209,0.9042010617\H,-2.157345284
3,2.0116606314,-0.098547335\H,-0.2489302917,2.2458694923,-1.5325372806
\H,1.3804356188,2.0225011645,0.2564097563\H,3.7229037797,-0.84717083,0
.3691275934\H,-1.7498093891,-1.8036143697,-1.5283188125\H,-0.380967828
9,-2.6492186571,0.3572516038\H,3.9102790306,0.7238412457,-0.4145145397
\H,3.2587757605,0.6298263912,1.2333860247\H,-0.3720629055,-1.003737069
2,2.4144994656\\Version=DEC-AXP-OSF/1-G94RevE.2\HF=-468.4376388\RMSD=4
.067e-09\RMSF=8.108e-06\Dipole=0.8472223,0.6029998,-0.1190283\PG=C01 [
X(C12H19)]\\@

2.13 Transition state 6 (189) in the Tricyclo[5.3.1.1^{3,9}]dodec-5-yl cation rearrangement

N-N= 7.824243651822D+02 E-N=-2.632806135921D+03 KE= 4.637859547628D+02
1\1\GINC-OZONE6\FTS\RB3LYP\6-31G(d)\C12H19(1+)\FSUN\20-Aug-1998\0\\#BE
CKE3LYP 6-31G* OPT(CALCFC, TS, NOEIGENTEST) GEOM=CHECKPOINT GUESS=READ
\\t4mcts2g\\1,1\C,-0.4346719424,0.9325746621,1.4626942117\C,-0.0360511
996,1.4386649169,0.0587951565\H,2.6909130808,1.6698437066,0.0452535754
\C,-1.2542999292,1.427412685,-0.8812918589\C,2.3773417171,0.6237122746
,-0.0316224305\H,-1.1754094422,1.6272571385,1.8774734749\H,0.432555629
1,0.9495854167,2.138916168\C,-1.0288143413,-0.4880232308,1.3687109989\
C,-2.2594312615,-0.4701304136,0.4360461997\H,-1.3261745651,-0.82089864
33,2.3694884765\C,0.0309990938,-1.4554893048,0.8045711868\H,-2.0028341
248,2.1203272719,-0.4776591502\C,-1.8399874886,0.0021364956,-0.9719389
567\H,-0.9783336591,1.8025389031,-1.875466937\H,-2.710620838,0.0140737
726,-1.6365340517\H,-2.7016580521,-1.4724584235,0.3814624472\C,-0.7754
422952,-0.9558507033,-1.5449752784\H,-3.0310749927,0.1946726603,0.8436
788502\C,0.4581885138,-1.0019357682,-0.6138374183\H,-0.3716922321,-2.4
730215062,0.746522114\H,0.9008519637,-1.501777054,1.4757538339\H,-0.47
76761577,-0.6421827027,-2.5550494079\H,-1.1847861266,-1.9680631744,-1.
6400902524\H,1.2018476036,-1.6937793575,-1.0277657962\H,1.2452928323,0
.8563907353,-1.5379630812\H,4.3487675335,-0.1163701351,-0.1537463188\C
,1.0460100235,0.4158800078,-0.5162145515\C,3.3878985231,-0.3638860294,
0.3230932213\H,3.5961173333,-0.2147258518,1.4020848383\H,3.1035407247,
-1.4006469914,0.1488246942\H,0.4099370072,2.4388406845,0.1106336402\\V
ersion=DEC-AXP-OSF/1-G94RevE.2\HF=-468.4392183\RMSD=5.717e-09\RMSF=1.6
67e-05\Dipole=2.7037989,0.5602374,-0.0477837\PG=C01 [X(C12H19)]\\@

3 Bicyclo[4.4.4]tetradecyl μ-H bridged cation (28)

N-N= 1.026110052758D+03 E-N=-3.301363666929D+03 KE= 5.427637239087D+02
1\1\GINC-OZONE5\FOpt\RB3LYP\6-31G(d)\C14H25(1+)\CTAESCHL\12-Apr-1999\0
\\#BECKE3LYP 6-31G* OPT(CALCFC)\\bicyclo[4.4.4]tetradecyl 1,6-mu-H cat
ion\\1,1\C,-0.0000711114,-0.0014980435,-1.2666283919\C,-0.0838301998,1
.4866395818,-1.5792408658\C,1.330108829,-0.6743204937,-1.5803114496\C,
-1.2480464896,-0.8173896124,-1.579326434\H,-0.0011217716,-0.0036691786
,-0.0002931456\C,-1.081273277,2.3187103971,-0.7465526633\C,0.001328691
2,0.0012008998,1.2671119892\C,2.5501589095,-0.2265092835,-0.7489310622
\C,-1.4716497658,-2.0946670099,-0.7431836641\H,0.9112998256,1.93838733
09,-1.5082111574\H,-0.3699308051,1.5395650758,-2.641318286\H,1.5173959
375,-0.4570345052,-2.643469431\H,1.2215645181,-1.7613626346,-1.5046441
672\H,-1.1522380534,-1.093589816,-2.6409964926\H,-2.1351137755,-0.1790
773371,-1.5080111875\C,-0.7331342974,2.4530827274,0.7456514278\C,-0.92
44887722,1.1692743644,1.5799155246\C,1.4764174305,0.21989375,1.5765177
291\C,2.4911939822,-0.5909656934,0.7441031825\C,-1.7578403962,-1.85833
9679,0.7491912461\C,-0.5478326134,-1.3844619023,1.5819033117\H,-2.0999
666838,1.92540977,-0.8563144857\H,-1.1004596734,3.3221157008,-1.185127
706\H,3.4275575348,-0.7146224374,-1.1864490701\H,2.7225602727,0.851700
6702,-0.8613300644\H,-2.3333621745,-2.6114593002,-1.1789780144\H,-0.62
42857602,-2.7829472467,-0.8536867806\H,0.2890299821,2.8376167705,0.854
7979246\H,-1.3864987246,3.2154078779,1.183013943\H,-1.9681263583,0.844
96738,1.5087072974\H,-0.7462816378,1.3988925777,2.6421287449\H,1.58781
94009,-0.0461127174,2.6392881987\H,1.7162983028,1.2855661998,1.5012629
04\H,3.4784585938,-0.4066248218,1.1808251857\H,2.3123227428,-1.6679600
267,0.8566832417\H,-2.0930476367,-2.8043961248,1.1874029607\H,-2.59990
14,-1.1632020151,0.8604021134\H,0.254477066,-2.1262753306,1.5086456088
\H,-0.834695239,-1.3451958788,2.644352586\\Version=DEC-AXP-OSF/1-G98Re
vA.3\HF=-548.2868011\RMSD=3.475e-09\RMSF=1.156e-04\Dipole=0.0001811,-0
.0005238,0.0026636\PG=C01 [X(C14H25)]\\@

4 Tricyclo[6.3.1.1^{3,10}]tridecyl μ-H bridged cation (273)

N-N= 9.027099663575D+02 E-N=-2.962334745891D+03 KE= 5.027363148118D+02
1\1\UOFC-OXYGEN\FOpt\RB3LYP\6-31G(d)\C13H21(1+)\CTAESCHL\09-Jan-1998\0
\\#BECKE3LYP 6-31G* OPT GEOM=CHECKPOINT GUESS=READ\\Tricyclo[6.3.1.1]t
ridecyl mu H cation\\1,1\C,-0.7396574927,-1.1112814477,-1.3859052188\C
,0.0960701421,-1.2132399883,-0.1242669807\C,-0.7306601824,-1.366065746
9,1.1378945003\C,-1.6646826502,-0.1304249107,1.261512357\C,-2.54541553
53,-0.001220162,-0.0003396504\C,-1.6644569279,0.1288197669,-1.26194872
54\C,-0.7316565121,1.3653725884,-1.1380657728\C,0.0948275903,1.2134222
11,0.1243340199\C,-0.7411168163,1.1105893487,1.3857282906\C,1.53314189
87,-1.7205365403,-0.1872066314\C,2.5751378511,-0.6928995102,0.34609590
96\C,2.5745072305,0.6953351287,-0.3455121411\C,1.5314203745,1.72195766
75,0.1876364361\H,-1.3429703051,-2.0235565993,-1.4837889305\H,-0.10462
11211,-1.0449814168,-2.2756056153\H,-0.0927267286,-1.4718463026,2.0222
981329\H,-1.3279362571,-2.2834425604,1.054579278\H,-2.2864827159,-0.22
2921069,2.1565018315\H,-3.2019960611,0.8719226095,0.0905955754\H,-3.20
11260506,-0.8749971941,-0.0914561642\H,-2.2860971518,0.2207596642,-2.1
57106626\H,-1.3298604906,2.2821645223,-1.0549280929\H,-0.0935660299,1.
4717737784,-2.0222794686\H,-1.345366203,2.0222646337,1.483449564\H,-0.
1062543682,1.044911694,2.2755968876\H,1.7778331744,-1.9676532272,-1.22
59528061\H,1.6092011588,-2.6448464857,0.3989445391\H,3.5597479806,-1.1
481338093,0.2014946446\H,2.4570113161,-0.5679601769,1.4312120012\H,2.4
566860444,0.5702994773,-1.4306488089\H,3.5586330657,1.151557471,-0.200
7337276\H,1.6067485863,2.6463773893,-0.3984422439\H,1.7756555973,1.969
2292248,1.226452683\H,0.3927327365,0.0001079479,0.0000789895\\Version=
SGI-G94RevD.2\HF=-507.7678006\RMSD=5.777e-09\RMSF=7.482e-06\Dipole=-0.
0097338,0.0003932,0.0000331\PG=C01 [X(C13H21)]\\@

5 Tricyclo[7.3.1.1^{3,11}]tetradecyl μ-H bridged cation (67)

N-N= 1.013987682941D+03 E-N=-3.274980432873D+03 KE= 5.416509324746D+02
1\1\ UOFC-OXYGEN\FOpt\RB3LYP\6-31G(d)\C14H23(1+)\SORENSEN\30-Sep-1995\
0\\# BECKE3LYP 6-31G* OPT\\trial on ad5cat\\1,1\C,-1.4580636697,1.6038
759682,0.142642135\C,-0.2408425712,1.5340267527,1.094111738\H,-0.51085
01703,1.0713294062,2.0485496765\H,0.1245752652,2.5453309376,1.31720996
86\C,0.8809842364,0.7796392567,0.4061862933\H,-2.2730878477,2.15505459
22,0.6206755425\H,-1.1362913558,-2.1973689216,1.5169798428\C,-1.054640
2403,2.2772388581,-1.1857180139\H,-0.7452954381,3.3129627484,-1.003211
3391\H,-1.9172468808,2.323655965,-1.8606121109\C,0.0950251639,1.491444
4614,-1.8505537458\C,1.3138326164,1.424487301,-0.8968077377\C,-0.64052
62575,-2.1031399532,-0.6083923722\C,-0.3413411529,0.0275124632,-2.1076
6722i\H,2.144574171,0.8738442082,-1.3514241252\C,1.9050071523,0.045419
8188,1.2541179638\H,1.6768122566,2.4373960456,-0.6775292323\H,0.459654
1315,-0.5482372804,-2.5840586813\H,0.135918437,-2.4916156382,-1.277488
4034\H,0.3879200758,1.9618036158,-2.7936715527\C,-1.8907928428,0.14125
55326,-0.1129627292\H,-1.2048941729,0.0052630398,-2.7856483769\H,-2.75
54067284,0.1143620128,-0.7895506368\H,0.2468901197,-0.2427294925,-0.05
73099027\H,2.7178481097,-0.3124620794,0.6117157342\C,1.3861198438,-1.1
146826573,2.1287089579\H,2.3425570638,0.8147752423,1.9100831385\H,2.18
72896135,-1.3382402874,2.8413647214\C,1.0322590653,-2.4349561969,1.398
2803109\H,0.5368503169,-0.7844007928,2.7411879746\C,-0.3956803571,-2.6
190195983,0.8247532126\H,1.1710997024,-3.2359313751,2.1325881667\H,1.7
746483214,-2.6325273816,0.611813486\H,-0.6030203133,-3.6942325455,0.79
88359747\H,-1.597242834,-2.5104481156,-0.9723447014\H,-2.1941414307,-0
.3497941839,0.8169822704\C,-0.7528677219,-0.5994002936,-0.7892016973\\
Version=SGI-G94RevB.3\HF=-547.0886766\RMSD=4.086e-09\RMSF=1.033e-05\Di
pole=-0.0363652,0.2332125,-0.2197838\PG=C01 [X(C14H23)]\\@

Appendix B

X-Ray Crystal Structure of
Tricyclo[5.3.1.1.^{3,9}]dodeca-5,9-diol

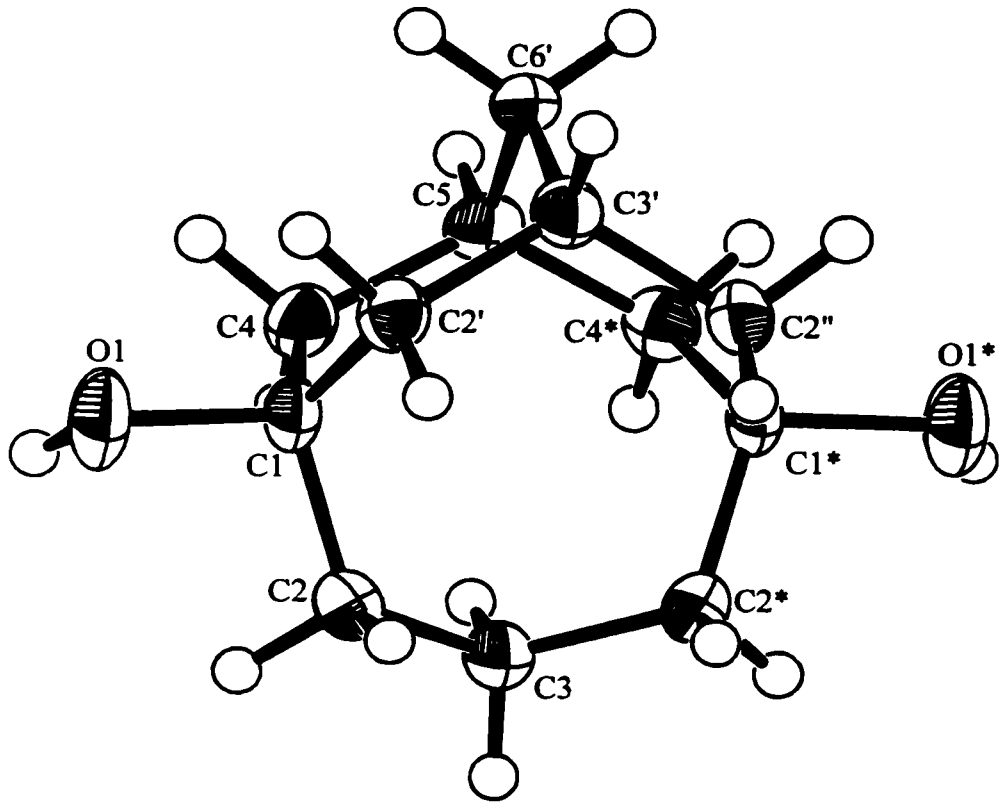

Experimental

Data Collection

A colourless prismatic crystal of $C_{12}H_{20}O_2$ having approximate dimensions of 0.45 x 0.40 x 0.20 mm was mounted on a glass fiber. All measurements were made on a Rigaku AFC6S diffractometer with graphite monochromated Mo-Kα radiation.

Cell constants and an orientation matrix for data collection, obtained from a least-squares refinement using the setting angles of 25 carefully centered reflections in the range $19.42 < 2\theta < 23.12°$ corresponded to an I-centered tetragonal cell (laue class: 4/mmm) with dimensions:

a = 10.058(4) Å
c = 20.599(7) Å
V = 2083.8(7) Å

For Z = 8 and F.W. = 196.29, the calculated density is 1.261 g/cm^3. The systematic absences of:

hkl: $h+k+l \neq 2n$
hk0: $h \neq 2n$
hhl: $2h+l \neq 4n$

uniquely determine the space group to be:

$I4_1/amd$ (#141)

The data were collected at a temperature of -113 ± 1°C using the ω-2θ scan technique to a maximum 2θ value of 55.2°.Omega scans of several intense reflections, made prior to data collection, had an average width at half-height of 0.25° with a take-off angle of 6.0°. Scans of (1.31 + 0.34 tan θ)° were made at a speed of 4.0°/min (in omega). The weak reflections ($I < 10.0\sigma(I)$) were rescanned (maximum of 4 scans) and the counts were accumulated to ensure good counting statistics. Stationary background counts were recorded on each side of the reflection. The ratio of peak counting time to background counting time was 2:1. The diameter of the incident beam collimator was 1.0 mm, the crystal to detector distance was 400 mm, and the detector aperture was 9.0 x 13.0 mm (horizontal x vertical).

Data Reduction

A total of 674 reflections was collected. The intensities of three representative reflection were measured after every 200 reflections. No decay correction was applied.
The linear absorption coefficient, μ, for Mo-Kα radiation is 0.83 cm^{-1}. Azimuthal scans of several reflections indicated no need for an absorption correction. The data were corrected for Lorentz and polarization effects.

Structure Solution and Refinement

The structure was solved by direct methods[1] and expanded using Fourier techniques[2]. The non-hydrogen atoms were refined anisotropically. Hydrogen atoms were included but not refined. C5 and C6 were disordered for which allowance was made. Hydroxyl H was also located over two sites with half occupancy factors at each location. The

final cycle of full-matrix least-squares refinement using F^2 coefficients with the aid of SHELX97[3] was based on 350 observed reflections ($I > 2.00\sigma(I)$) and 47 variable parameters and converged (largest parameter shift was 0.000 times its esd) with unweighted and weighted agreement factors: R = 0.0506 and wR = 0.1403. The standard deviation of an observation of unit weight was 1.006. The weighting scheme was based on counting statistics. The maximum and minimum peaks on the final difference Fourier
map corresponded to 0.278 and -0.328 $e^-/Å^3$, respectively.

Neutral atom scattering factors were taken from Cromer and Waber[4]. Anomalous dispersion effects were included in Fcalc[5]; the values for $\Delta f'$ and $\Delta f''$ were those of Creagh and McAuley[6]. The values for the mass attenuation coefficients are those of Creagh and Hubbel[7]. All calculations for data reduction were performed using the teXsan[8] crystallographic software package of Molecular Structure Corporation.

References

(1) SIR92: Altomare, A., Cascarano, M., Giacovazzo, C., Guagliardi, A. (1993). J. Appl. Cryst., 26, 343.

(2) DIRDIF94: Beurskens, P.T., Admiraal, G., Beurskens, G., Bosman, W.P., de Gelder, R., Israel, R. and Smits, J.M.M.(1994). The DIRDIF-94 program system, Technical Report of the Crystallography Laboratory, University of Nijmegen, The Netherlands.

(3) SHELXL97: Sheldrick, G. M. (1997). Program for the Refinement of Crystal Structures. University of Gottingen, Germany.

(4) Cromer, D. T. \& Waber, J. T.; "International Tables for X-ray Crystallography", Vol. IV, The Kynoch Press, Birmingham, England, Table 2.2 A (1974).

(5) Ibers, J. A. \& Hamilton, W. C.; Acta Crystallogr., 17, 781 (1964).

(6) Creagh, D. C. \& McAuley, W.J .; "International Tables for Crystallography", Vol C, (A.J.C. Wilson, ed.), Kluwer Academic Publishers, Boston, Table 4.2.6.8, pages 219-222 (1992).

(7) Creagh, D. C. \& Hubbell, J.H..; "International Tables for Crystallography", Vol C, (A.J.C. Wilson, ed.), Kluwer Academic Publishers, Boston, Table 4.2.4.3, pages 200-206 (1992).

(8) teXsan: Crystal Structure Analysis Package, Molecular Structure Corporation (1985 \& 1992).

EXPERIMENTAL DETAILS

A. Crystal Data

Empirical Formula	$C_{20}H_{20}O_2$
Formula Weight	196.29
Crystal Color, Habit	colourless, prism
Crystal Dimensions	0.45 X 0.40 X 0.20 mm
Crystal System	tetragonal
No. of Reflections Used for Unit Cell Determination (2θ range)	25 (19.4 - 23.1°)
Omega Scan Peak Width at Half-height	0.25°
Lattice Parameters	a = 10.058(4) Å c = 20.599(7) Å V = 2083.8(7) Å^3
Space Group	$I4_1/amd$ (#141)
Z value	8
D_{calc}	1.251 g/cm^3
F_{000}	864
μ(MoKα)	0.83 cm^{-1}

B. Intensity Measurements

Diffractometer	Rigaku AFC6S
Radiation	MoKα (λ = 0.71069 Å) graphite monochromated
Temperature	-113.0°C
Scan Type	ω-2θ
Scan Rate	4.0°/min (in ω) (up to 4 scans)
Scan Width	(1.31 + 0.34 tan θ)°
$2\theta_{max}$	55.2°
No. of Reflections Measured	Unique: 674
Corrections	Lorentz-polarization

C. Structure Solution and Refinement

Structure Solution	Direct Methods (SIR92)
Refinement	Full-matrix least-squares
Function Minimized	$\Sigma\omega(\|Fo\| - \|Fc\|)^2$
Least Squares Weights	$\sqrt{\Sigma\omega(\|Fo\| - \|Fc\|^2 / \Sigma\omega Fo^2)}$
ω	$1/(\sigma^2(Fo)+(0.0904P)^2+0.951P$
P-factor	$(Fo^2+ 2Fc^2/3$
Anomalous Dispersion	All non-hydrogen atoms
No. Observations (I>2.00σ(I))	350
No. Variables	47
Coefficients Used	F^2
Residuals: R; wR	0.0506 ; 0.1403
Goodness of Fit Indicator	1.006
Max Shift/Error in Final Cycle	0.000
Maximum peak in Final Diff. Map	0.278 $e^-/Å^3$
Minimum peak in Final Diff. Map	-0.328 $e^-/Å^3$

Table 1. Atomic coordinates (x 10^4) and equivalent isotropic displacement parameters (A^2 x 10^3) for b.
U(eq) is defined as one third of the trace of the orthogonalized Uij tensor.

Atom	x	y	z	U(eq)	S.O.F
O(1)	3152(2)	2500	1475(1)	45(1)	0.50
C(1)	1709(3)	2500	1427(2)	28(1)	0.50
C(2)	1287(2)	3779(2)	1777(1)	31(1)	1.00
C(3)	0	4458(3)	1568(2)	30(1)	0.50
C(4)	1330(3)	2500	703(2)	32(1)	0.50
C(5)	0	1845(7)	534(3)	30(1)	0.25
C(6)	0	4562(7)	818(3)	33(2)	0.25

Table 2. Bond lengths [A] and angles [deg] for b.

O(1)-C(1)	1.454(4)
C(1)-C(2)	1.535(3)
C(1)-C(2)#1	1.536(3)
C(1)-C(4)	1.539(5)
C(2)-C(3)	1.526(3)
C(3)-C(6)	1.548(8)
C(4)-C(5)#1	1.531(5)
C(5)-C(5)#1	1.318(14)
C(5)-C(6)#1	1.531(10)
C(5)-C(4)#2	1.531(5)
C(6)-C(5)#1	1.531(10)
O(1)-C(1)-C(2)	104.12(17)
O(1)-C(1)-C(2)#1	104.12(17)
C(2)-C(1)-C(2)#1	113.8(3)
O(1)-C(1)-C(4)	108.3(3)
C(2)-C(1)-C(4)	112.78(16)
C(2)#1-C(1)-C(4)	112.78(16)
C(3)-C(2)-C(1)	118.5(2)
C(2)-C(3)-C(2)#2	116.0(2)
C(2)-C(3)-C(6)	108.2(2)
C(5)#1-C(4)-C(1)	115.9(3)
C(5)#1-C(5)-C(6)#1	157.5(3)
C(5)#1-C(5)-C(4)#2	64.5(2)
C(6)#1-C(5)-C(4)#2	108.1(3)
C(5)#1-C(6)-C(3)	108.6(5)

Symmetry transformations used to generate equivalent atoms:
#1 x,-y+1/2,z #2 -x,y,z

Table 3. Anisotropic displacement parameters (A^2 x 10^3) for b.
The anisotropic displacement factor exponent takes the form:
-2 pi^2 [h^2 a*^2 U11 + ... + 2 h k a* b* U12]

Atom	U11	U22	U33	U23	U13	U12
O(1)	19(1)	69(2)	48(2)	0	2(1)	0
C(1)	16(2)	36(2)	31(2)	0	1(1)	0
C(2)	26(1)	33(1)	33(1)	-2(1)	-3(1)	-3(1)
C(3)	27(2)	29(2)	36(2)	-1(1)	0	0
C(4)	30(2)	36(2)	30(2)	0	6(1)	0
C(5)	36(4)	38(4)	15(2)	-6(3)	0	0
C(6)	25(3)	31(4)	42(4)	13(3)	0	0

Table 4. Hydrogen coordinates (x 10^4) and isotropic displacement parameters (A^2 x 10^3) for b.

Atom	x	y	z	U(eq)	S.O.F
H(1)	3458	3074	1235	68	0.50
H(2A)	1211	3576	2236	46	1.00
H(2B)	2002	4419	1731	46	1.00
H(3A)	0	5339	1738	46	0.25
H(3B)	0	4509	1103	46	0.25
H(4A)	2027	2049	463	48	0.50
H(4B)	1307	3414	553	48	0.50
H(5)	0	1737	68	44	0.50
H(6)	781	5030	673	49	0.50

Table 5. Torsion angles [deg] for b.

O(1)-C(1)-C(2)-C(3)	151.5(2)
C(2)#1-C(1)-C(2)-C(3)	-95.8(3)
C(4)-C(1)-C(2)-C(3)	34.3(3)
C(1)-C(2)-C(3)-C(6)	-47.7(4)
O(1)-C(1)-C(4)-C(5)#1	-151.4(3)
C(2)-C(1)-C(4)-C(5)#1	-36.7(4)
C(2)#1-C(1)-C(4)-C(5)#1	93.9(3)
C(2)-C(3)-C(6)-C(5)#1	63.2(2)

Symmetry transformations used to generate equivalent atoms:
#1 x,-y+1/2,z #2 -x,y,z

Table 6. Cartesian Coordinates [Å]

O1	3.1701	2.5144	3.0384
C1	1.7192	2.5144	2.9387
C2	1.2941	3.8008	3.6613
C3	0.0000	4.4841	3.2291
C4	1.3375	2.5145	1.4477
C5	0.0000	1.8556	1.0992
H1	3.4781	3.0918	2.5442
H2A	1.2184	3.5968	4.6066
H2B	2.0136	4.4443	3.5653
H3B	0.0000	4.5347	2.2717
H3A	0.0000	5.3696	3.5791
H4A	2.0387	2.0608	0.9537
H4B	1.3146	3.4337	1.1391
H5	0.0000	1.7470	0.1390
C2*	1.2941	1.2281	3.6613
C2*	-1.2941	3.8008	3.6613
C4*	-1.3375	2.5145	1.4477
C6*	0.0000	0.4408	1.6840
C3*	0.0000	0.5448	3.2291
H2A*	1.2184	1.4321	4.6066
H2B*	2.0136	0.5846	3.5653
C1*	-1.7192	2.5144	2.9387
H2A*	-1.2184	3.5968	4.6066
H2B*	-2.0136	4.4443	3.5653
H4A*	-2.0387	2.0608	0.9537
H4B*	-1.3146	3.4337	1.1391
H6*	0.7856	-0.0305	1.3855
H6*	-0.7856	-0.0305	1.3855
C2*	-1.2941	1.2281	3.6613
H3A*	0.0000	-0.3407	3.5791
O1*	-3.1701	2.5144	3.0384
H2A*	-1.2184	1.4321	4.6066
H2B*	-2.0136	0.5846	3.5653
H1*	-3.4781	3.0918	2.5442